The role of subchondral bone in osteoarthritis

Dr Andrew James Barr

Submitted in accordance with the requirements for the degree of
Doctor of Philosophy

The University of Leeds

School of Medicine

Leeds Institute of Rheumatic and Musculoskeletal Medicine

January 2016

Intellectual Property and Publication Statements

The candidate confirms that the work submitted is his own, except where work which has formed part of jointly-authored publications has been included. The contribution of the candidate and the other authors to this work has been explicitly indicated below. The candidate confirms that appropriate credit has been given within the thesis where reference has been made to the work of others.

The publications are listed on page iv

Acknowledgements

There are many people who I need to thank for their help and support with this thesis. First I would like to thank my supervisors Prof. Philip Conaghan and Dr Sarah Kingsbury for their guidance and support for the work that has been undertaken. Secondly I would like to thank Arthritis Research UK for the clinical research fellowship grant that funded the research for this PhD.

For the systematic literature review in Chapter 3, I would like to thank Jenny Makeham in Leeds General Infirmary NHS library for helping me with my literature search, Dr Mark Campbell and Devan Hopkinson for helping extract the data and quality scoring. I would also like to thank Professor Conaghan, Dr Sarah Kingsbury and Dr Mike Bowes for helping design the study and writing of the manuscript.

For the work in Chapter 4 addressing the construct validity of OA-attributable bone area I would like to thank Professor Conaghan, Sarah Kingsbury, Mike Bowes, Professor George Peat, Elizabeth Hensor and Bright Dube for assisting in the design of the study and writing the manuscript.

For the work in Chapters 5 and 6 I would like to thank Professor Conaghan, Sarah Kingsbury, Mike Bowes, George Peat, Professor Linda Sharples, Elizabeth Hensor and Bright Dube for assisting in the design of the study and writing the manuscript.

For Chapters 4, 5 and 6, I would like to thank Elizabeth Hensor and Bright Dube for assisting in the statistical analysis.

Provision of the bone shape biomarkers is courtesy of Mike Bowes at Imorphics, Manchester.

List of publications/presentations arising from this thesis

Original articles

Barr A, Dube B, Hensor EMA, Kingsbury SR, Peat G, Bowes MA, Sharples LD, Conaghan PG The relationship between three-dimensional knee MRI bone shape and total knee replacement – a case control study: data from the Osteoarthritis Initiative. *Rheumatology* 2015

Barr A, Campbell TM, Hopkinson D, Kingsbury SR, Bowes MA, Conaghan PG. A systematic review of the relationship between subchondral bone features, pain and structural pathology in peripheral joint osteoarthritis. *Arthritis Research & Therapy;2015*

Barr AJ, Dube B, Hensor EMA, Kingsbury SR, Peat G, Bowes MA, Conaghan PG. 2014. The relationship between clinical characteristics, radiographic osteoarthritis and 3D bone area: data from the Osteoarthritis Initiative. *Osteoarthritis & Cartilage, vol. 22(10), 1703-1709*

Barr A, Conaghan P. Osteoarthritis: recent advances in diagnosis and management. *Prescriber Nov 05, 2014 p26-34*

Barr A, Conaghan P. Disease-Modifying osteoarthritis drugs (DMOADs): what are they and what can we expect from them? *Medicographia 2013; 35(2):189*

Book Chapter

Barr A, Conaghan P. Chapter Osteoarthritis Oxford Textbook of Medicine (6 ed.) Oxford University Press; 2015: ISBN

Co-author contribution

Relationship between 3D knee MRI bone shape & total knee replacement:

AB formulated the provisional analysis with supervision from PC, MB and K. The specific details of the analysis design were formulated by AB with statistical support from LS, BD and EH and methodology support from SK, GP, MB, and PC. AB drafted the article and BD, EH, SK, GP, MB, LS and PC, revised the article.

A systematic review of the relationship….

AB carried out conception and design, eligibility assessment, extraction of data, quality assessment, along with drafting and revising of the manuscript content. DH carried out design, eligibility assessment and extraction of data. TC carried out conception and design, quality assessment and revising manuscript for content. MB carried out conception and design along with revising the manuscript for content. SK carried out conception and design eligibility assessment and revising the manuscript for content. PC carried out conception and design, quality assessment and revising the manuscript for content.

The relationship between clinical characteristics, radiographic osteoarthritis:

AB formulated the provisional analysis with supervision from PC, MB and SK. AB developed the design of the analysis with statistical support from BD and EH and methodology support from, PC, GP, SK and MB. AB performed the analysis. AB & BD drafted the article and MB, PC, SK, GP and EH revised the article.

All other papers were review articles published where AB drafted the article and PC revised it.

International Conference Presentation

European League Against Rheumatism Annual Conference 2015 Rome

1. Oral Presentation:

Three-dimensional magnetic resonance imaging knee bone shape predicts total knee replacement: data from the Osteoarthritis Initiative

2. Poster Presentation:

The relationship between 3D MRI knee bone shape and prevalent and incident knee pain: data from the osteoarthritis initiative

Abstract

Osteoarthritis (OA) is the most common form of arthritis. Affected individuals commonly suffer with chronic pain, joint dysfunction, and reduced quality of life. OA also confers an immense burden on health services and economies. Current OA therapies are symptomatic and there are no therapies that modify structural progression. The lack of validated, responsive and reliable biomarkers represents a major barrier to the development of structure-modifying therapies.

MRI provides tremendous insight into OA structural disease and has highlighted the importance of subchondral bone in OA. The hypothesis underlying this thesis is that novel quantitative imaging biomarkers of subchondral bone will provide valid measures for OA clinical trials. The Osteoarthritis Initiative (OAI) provided a large natural history database of knee OA to enable testing of the validity of these novel biomarkers.

A systematic literature review identified independent associations between subchondral bone features with structural progression, pain and total knee replacement in peripheral joint OA. However very few papers examined the association of 3D bone shape with these patient-centred outcomes.

A cross-sectional analysis of the OAI established a significant association between 3D bone area and conventional radiographic OA severity scores, establishing construct validity of 3D bone shape.

A nested case-control analysis within the OAI determined that 3D bone shape was associated with the outcome of future total knee replacement, establishing predictive validity for 3D bone shape.

A regression analysis within the OAI identified that 3D bone shape was associated with current knee symptoms but not incident symptoms, establishing evidence of concurrent but not predictive validity for new symptoms.

In summary, 3D bone shape is an important biomarker of OA which has construct and predictive validity in knee OA. This thesis, along with parallel work on reliability and responsiveness provides evidence supporting its suitability for use in clinical trials.

Table of Contents

List of Tables

List of Figures

List of Abbreviations

2D - two dimensional

3D - three dimensional

ACL - anterior cruciate ligament

BMD - bone mineral density

BML - bone marrow lesion

Cam – a resemblance to a camshaft

CT – computed tomography

DMOAD – disease-modifying osteoarthritis drug

DXA - dual-energy X-ray absorptiometry

EMBASE - Excerpta Medica database

KL – Kellgren Lawrence

MRI – magnetic resonance imaging

NA – no association

NC – no conclusion

OA - osteoarthritis

PET – positron emission tomography

PRISMA - Preferred Reporting Items for Systematic Reviews and Meta-Analyses

qCT – quantitative CT

THR – total hip replacement

TKR – total knee replacement

WOMAC - Western Ontario and McMaster Universities arthritis index

Chapter 1 Introduction

1.1 Background

Osteoarthritis (OA) is the commonest arthritis and is one of the leading causes of chronic pain, disability and socioeconomic burden in the world. In the United Kingdom and United States of America OA affects 8.5 million[1] and 26.9 million[2] people respectively. The prevalence of OA increases with age and obesity and is therefore expected to increase in prevalence in our ageing and increasingly obese population. The prevalence amongst Individuals aged 45 and older of any OA is estimated to increase from 26.6% currently to 29.5% by 2032. During the same interval, the number of individuals seeking a clinical review for peripheral OA is estimated to increase by 26,000 per million by 2032[3].

In adults above the age of 45 years, the individual prevalence of both knee [4] and hip [5] OA is as high as 28%. Together knee and hip OA are currently the eleventh greatest contributor to global disability, and it is highly likely that this is an underestimate of the true burden of OA. OA accounted for 10% of disability-adjusted life-years (DALYs) due to musculoskeletal conditions[6]. Approximately 2% of all sick days are attributable to knee OA and amongst individuals of working age, those with knee OA have twice the risk of sick leave and a 50% increased risk of disability pension compared with the general working population[7]. The pain and dysfunction of OA confers a substantial socioeconomic burden in developing countries of 1.0-2.5% gross domestic product[8]. Therefore OA represents a massive and rapidly increasing burden on individuals on health services and on society as a whole.

While the majority of patients report chronic pain, the burden of OA is intensified by the limitations of current non-surgical therapy with only 30% of people with OA reporting satisfaction with their analgesia[1, 9]. The mainstay of current non-surgical therapy involves a patient-centred package of non-pharmacological and pharmacological therapies for reducing pain and

improving function before considering surgery. These are limited to a moderate effect size at best[10] and may have significant toxicities. For example oral paracetamol[11] and non-steroidal anti-inflammatory drugs(NSAIDs)[12] are commonly prescribed and are associated with greater risk of cardiovascular, gastro-intestinal and renal adverse events[13]. This is of particular significance to a population of OA which tends to be older with more prevalent comorbidity

Attempts to develop a disease modifying osteoarthritis drug (DMOAD) have been hindered by the failure to demonstrate a substantive improvement in symptoms whilst also inhibiting structural deterioration of the OA joint. While recent trials report inhibition of structural progression, there are methodological limitations with these. Therefore there are currently no licensed structural-modifying therapies although these are highly desirable.

This may in part reflect the insensitivity and limitations of existing measures of structural progression. These are used to determine eligibility for, and as primary outcome measures in DMOAD trials[14]. These structural severity and progression measures have primarily been based upon two-dimensional projection images of conventional radiography which rely upon surrogate measures of cartilage loss. Therefore while the need for prevention and novel effective treatment strategies for OA is of vital importance, the demand for better biomarkers for determining the effectiveness of prospective DMOADs is of equal importance.

OA has traditionally been considered to be primarily a disease of cartilage and hence the focus has been on modifying this tissue. Historic attempts at developing DMOADs have focused primarily on preventing hyaline articular cartilage loss, in an attempt to provide “chondroprotective” therapies. However typical clinical OA is a pathology of multiple tissues and therefore more recently, other tissues have been targeted including the subchondral bone which is the bone that supports the articular cartilage and which plays an integral role in the pathogenesis of OA[15].

Although the diagnostic criteria for OA developed by in 1957 incorporated osteophytosis and subchondral sclerosis as a distinctive feature of OA, the subchondral bone is relatively understudied compared to cartilage. However

there is an increasing acknowledgement that it is involved in the pathogenesis of early and late-OA through both biomechanical and biochemical pathways. SCB is a dynamic structure which adapts to increased applied load by homeostatic remodelling of the trabecular SCB, changes in SCB mass and expansion of the SCB surface area, to name three examples. However SCB changes may also herald deterioration in nearby joint tissues especially the articular cartilage which highlights the importance of biomechanics and SCB in the aetiopathogenesis of OA.

SCB has a well-connected population of osteocytes that perceive load and respond to microdamage through mechanotransduction of load and apoptosis resulting in a biochemical orchestration of osteoblasts (bone forming cells) and osteoclasts (bone resorbing cells) that carry out homeostatic ‘reparative’ remodelling which occurs in a biphasic response. There is an initial increase in bone turnover in response to microfractures with a net bone resorption with associated loss of bone volume and increased porosity in the junction between the cartilage and bone which permits pathological ‘cross-talk’. As further SCB accumulates the bone remodelling cells and their biochemical signalling fail to achieve repair and become maladaptive. A subsequent reparative net bone formation response occurs but this is with hypomineralised osteoid with a reduced stiffness relative to the bone volume formed and this is associated with an alteration in bone shape. This biomechanical deterioration in SCB drives deterioration in adjacent joint tissues especially cartilage and OA develops. A better understanding of what represents pathological change in SCB and the biomechanical and biochemical pathways involved in the pathogenesis of OA may permit the identification of individuals most at risk of OA but also targets for bone-modifying therapies.

Conventional radiography (CR) is unable to capture the severity of the multi-tissue involvement in joints with OA joints. This is particularly important because many of the trials of prospective disease modifying agents in OA have attempted to recruit a homogenous population that are likely to exhibit structural progression by selecting people with CR-defined OA. Unfortunately these patients may lack uniformity in terms of joint tissue involvement because CR is insensitive to tissue pathology like bone marrow

lesions (BMLs) which have important prognostic implications and are associated with worse structural and symptomatic outcomes.

MRI-determined quantitative and semi-quantitative measurements of joint tissue in OA have started to be used as clinical outcome measures in structure-modification trials. This reflects the opinion of the Osteoarthritis Research Society International working group that recommended MRI cartilage morphology assessment be used as a primary structural end point in clinical trials which also acknowledged the rapid evolution of quantitative MRI assessments of subchondral bone and synovium. Therefore using MRI biomarkers of joint structure in OA represents a significant improvement in sensitivity to clinically significant structural pathology, responsiveness and in its correlation with pain compared with CR biomarkers. However we have not yet harnessed the full potential of MRI biomarkers and utilised all MRI has to offer.

There are several examples of 2D and 3D imaging biomarkers that have been described for bone and cartilage which highlight the importance of SCB. The SCB is important in the pathogenesis of OA including SCB shape. 3D bone imaging biomarkers have not been formally investigated as part of a biomarker validation process. The importance of modelling the shape of the knee bones with statistical shape modelling, active shape modelling and active appearance modelling is the analysis of bone shape may permit the validation of novel bone imaging biomarkers with improved responsiveness profile than existing imaging biomarkers for prospective use in OA modification trials.

The hypothesis underlying this thesis was that MRI evaluation of the SCB would provide a number of unique biomarkers of patient-centred OA outcomes for future therapeutic trials of disease modifying OA drugs. The 3D knee *bone shape* was examined in large cohorts for its construct validity by comparing it with conventional radiographic measures and for its criterion validity by examining it’s association with knee replacement and current and incident knee symptoms.

This thesis describes the independent association of imaging-defined OA subchondral bone biomarkers with patient-centred outcomes of OA and then

more specifically describes the validity of 3D bone shape. The association of 3D bone shape with knee replacement provided evidence of predictive validity. The association of 3D bone shape with current but not with incident persistent knee symptoms provided evidence of concurrent but not predictive validity. The association of 3D knee bone structure of OA with conventional radiographic OA measures provided evidence of construct validity. This work further underpins the value of quantitative bone measures in future therapeutic trials of disease modifying osteoarthritis drugs.

1.2 Structure of the thesis

The hypothesis underlying this thesis was that MRI evaluation of the SCB would provide a number of unique biomarkers of patient-centred OA outcomes for future therapeutic trials of disease modifying OA drugs

1.2.1 Chapter 2: Literature review

This was a narrative literature review covering OA and focussing on bone the osteoarthritis initiative (OAI) and semi-quantitative and quantitative imaging analysis. The unique resources of this thesis are the OAI and quantitative imaging of bone shape.

1.2.2 Chapter 3 A systematic review of the relationship between subchondral bone features, pain and structural pathology in peripheral joint osteoarthritis.

This was a systematic literature review of the relationship between imaging-assessed subchondral bone features, pain and structural pathology in peripheral joint osteoarthritis. This highlights that subchondral bone plays an integral role in the pathogenesis of OA and that subchondral bone shape is independently associated with structural progression, joint replacement and pain incidence in knee OA. This highlights that bone shape is important but understudied and bone represents a valid target in the prospective treatment of OA.

1.2.3 Chapter 4 The relationship between clinical characteristics, radiographic osteoarthritis and 3D bone area

This is a cross-sectional analysis of the relationship between clinical characteristics, CR measures of OA and OA-attributable 3D bone area. This identifies construct validity of bone area as it is significantly associated with CR measures such as osteophytes. However these CR measures do not substantively explain the variance in the OA-attributable 3D bone area which may reflect the additional information provided by 3D MRI when describing subchondral bone shape.

1.2.4 Chapter 5 The relationship between three-dimensional knee MRI bone shape and total knee replacement – a case control study

This is a nested case-control analysis within the OAI, of the relationship between 3D bone shape and the outcome of TKR. This identifies that a more advanced structural severity in 3D bone shape is associated with the outcome of TKR. This provides evidence of predictive validity of bone shape in regards to the outcome of TKR which reflects both pain and structural progression of OA.

1.2.5 Chapter 6 The relationship between 3D MRI bone shape and knee osteoarthritis symptoms in knees with and without radiographic knee osteoarthritis.

Chapter 6 is an analysis of the relationship between 3D bone shape and the outcomes of prevalent frequent knee symptoms (PFKS) and incident persistent knee symptoms (IPKS). This analysis incorporates knees without ROA but at risk of OA and all knees within the OAI. There was no association of 3D bone shape vectors with either PFKS or IPKS in knees without radiographic OA. However 3D bone shape vectors are associated with concurrent frequent knee symptoms of OA but not with incident persistent symptoms amongst all knees within the OAI that include those with radiographic OA. This provides evidence of concurrent validity for the association between 3D bone shape and knee symptoms.

1.2.6 Chapter 7 Discussion, future directions and conclusions

This chapter discusses the results of this thesis, the conclusions that can be drawn, an update on the literature review and the future directions in this field.

Chapter 2 Literature Review

This chapter reviews the current epidemiology of OA, the natural history and definitions of OA. The description of OA and historic trials of prospective therapies in OA previously relied on X-ray and focussed on cartilage measurement. MRI is better but we still have not utilised all of the 3D information provided by MRI. The best personalised biomarkers in OA are currently imaging biomarkers and the process of validation of biomarkers and the use of MRI is discussed. Finally the chapter also describes two novel resources, the Osteoarthritis Initiative[16] and automated statistical shape modelling. This explains the resource and technology used with modern quantitative analysis to develop novel imaging biomarkers of bone that may provide novel valid measures for clinical OA trials.

2.1 Introduction

Osteoarthritis (OA) is the most common arthritis and is a leading cause of global chronic pain, disability and socioeconomic burden. OA affects 8.5 million people in the United Kingdom[1]. In adults above the age of 45 years, radiographic and symptomatic knee OA have a prevalence of 19-28% and 7-17% respectively. The epidemiology and natural history differ between joints and individuals. The prevalence of OA increases with age and obesity..

2.2 Defining OA and subtypes

OA refers to structural deterioration of synovial joints that in early stages may initially involve individual tissues, which in the context of appropriate risk factors may evolve, by a complex cascade of biomechanical and biochemical pathologies, into the typical whole joint multi-tissue pathologies seen in typical painful clinical OA. This includes changes to the hyaline articular cartilage, the underlying subchondral bone, the meniscal fibrocartilages (in the knee) and the synovium.

2.2.1 The problems with defining OA

Definitions of OA have derived from epidemiological studies and clinical trials where OA may be defined using clinical findings (joint symptoms and examination findings) alone, the presence of imaging-assessed pathology, or a combination of the two. Only 50% of knees with radiographic OA (ROA) have symptoms[17] and activity-related pain of OA may occur in a prodromal phase before the incidence of ROA[18]. Therefore in research studies of OA, a more specific definition of OA can be achieved by any combination of joint imaging-assessed structural pathology (e.g. Kellgren Lawrence grade 2, a definite radiographic osteophyte –Figure 1)[19] and clinical findings and laboratory tests (e.g.Table 3)[20-22].

While conventional radiography (CR) is feasible, it is limited in its utility by its relatively insensitive detection of structural pathology in tissues other than bone (Figure 1).

Amongst individuals within the Framingham cohort above the age of 50 years, with no pain and normal knee radiography, 88% of individuals had at least one OA tissue lesion in the knee on magnetic resonance imaging (MRI) [23]. MRI can visualise the true three dimensional multi-tissue joint pathology of OA[24, 25] and these MRI-detected structural changes (Figure 2), which are more closely associated with patient reported pain[26]. Ultrasound (US) also has the capacity to acquire 3D images and, for example, has been shown to detect many more osteophytes than CR in hand OA[27, 28]. These modern imaging studies highlight that many of our concepts and definitions of OA have been based on an inaccurate imaging phenotype. Therefore there is currently no generally agreed-upon ‘gold standard’ for defining cases of OA, and the epidemiology of OA varies according to the definition of OA for any specified joint.

Figure 1 Conventional knee radiography

Table 1 The Kellgren Lawrence grade

Grade	Features of Osteoarthritis
Grade 0	No radiographic features
Grade 1	Doubtful joint space narrowing, possible osteophytic lipping
Grade 2	Possible joint space narrowing, definite osteophytes
Grade 3	Multiple osteophytes, definite joint space narrowing, some sclerosis, possible deformity of bone contour
Grade 4	Large osteophytes, marked joint space narrowing, severe sclerosis, definite bone deformity

This was first described by Kellgren and Lawrence[19]

Figure 2 Knee MRI demonstrating multi-tissue involvement

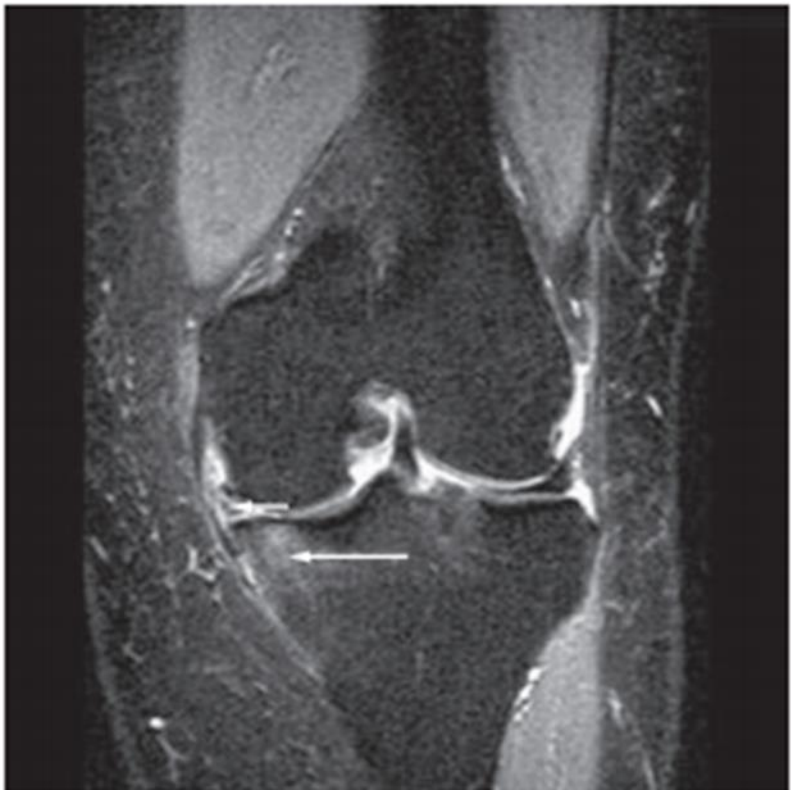

Medial tibial bone marrow lesion (long arrow) and macerated medial meniscus (short arrow). (Reprinted by permission from Macmillan Publishers Ltd: Nature Clincal Reviews [29] Copyright 2009.)

Table 2 The prevalence of MRI-detected knee lesions and crepitus

	General	MTF	LTF	PF
Presence of crepitus	180 (70.5%)	44 (17.3%)	48 (18.7%)	173 (67.9%)
Cartilage damage	221 (86.5%)	178 (69.8%)	151 (59.1%)	179 (70.1%)
Osteophytes	133 (52.0%)	95 (37.1%)	90 (35.3%)	102 (39.9%)
Medial meniscal damage	111 (43.7%)	95 (37.3%)	–	–
Lateral meniscal damage		–	30 (11.9%)	–
Cruciate pathology	23 (9.2%)	–	–	–
MCL pathology	48 (18.7%)	48 (18.7%)	–	–
LCL pathology	0 (0%)	–	0 (0%)	–

MCL / LCL – medial and lateral collateral ligaments of the knee

MTF / LTF /PF – medial tibiofemoral / lateral tibiofemoral / patellofemoral

(Reprinted by permission from Elsevier Ltd: Osteoarthritis and cartilage [30])

2.2.2 Early OA

The concept of early OA is imprecisely defined. Incident ROA has provided one operational concept of early OA. However both structural changes and symptoms of OA precede the incidence of ROA. As mentioned, at least one structural lesion of knee OA is present on MRI of people over 50 years without ROA or knee pain [23]. By the time knee ROA is detectable, 10% of knee hyaline articular cartilage is lost [31]. Incident knee ROA is preceded by prodromal symptoms of pain on twisting or pivoting and pain on standing by 39 and 25 months respectively[18]. Pain on stair climbing appears to be the first mechanical symptom to manifest amongst knees with ROA and at risk of ROA[32].

It is very likely that problems such as isolated cartilage defects and meniscal tears are early structural lesions that progress to clinical OA, though these are not currently classified as early OA. Compositional measures using special MRI sequences can also demonstrate glycosaminoglycan loss before MRI can detect morphological changes [33, 34]. So substantial evolution of the concept and alternative definitions of “early” OA are required.

2.2.3 Inflammatory OA

OA is not considered to be a classical inflammatory arthritis because of features including a relative paucity of neutrophils in synovial fluid, a lack of subchondral bone erosions and no evidence of systemic inflammation or features of autoimmunity; these features were used to distinguish OA from the archetypal inflammatory arthritis, rheumatoid arthritis (RA). Clinicians may refer to inflammatory OA as the discrete very swollen joints seen in some patients with hand OA. But it is likely that there is much more widespread synovitis than is appreciated clinically. Modern imaging with its more accurate detection of synovial hypertrophy and effusion has changed our understanding of the frequency of inflammation in OA joints[35]. Using contrast-enhanced MRI, extensive synovitis is prevalent in most knees (>85%)[36-38] and hands (68%)[39] with established OA that met the respective OA joint criteria (Table 3).

Erosive OA refers to a group of patients with radiographic erosions, and the term is often used synonymously with inflammatory OA (though not all OA inflammation is associated with erosions). The overall prevalence of erosive OA is unclear, and the prevalence of erosions varies somewhat according to their definition and the imaging modality employed for detection. In two cohorts of women selected for erosive hand ROA, erosions were identified in 17-18%, 35% and 61% of small joints using CR, ultrasonography and MRI respectively[28, 40]. When defined radiographically, erosive hand OA appears to have a greater association with obesity, hypertension, dyslipidaemia and the metabolic syndrome relative to non-erosive hand OA[41, 42].

2.2.4 Generalised OA

An imprecisely defined phenotype is where multiple OA joints are present in an individual, that may referred to as generalised or also polyarticular OA. It is well recognised that a history of hand OA confers an increased risk of hip and knee OA, a history of knee OA confers a higher risk of hip OA and vice versa. These associations are independent of confounding factors of age, gender and BMI[43]. Generalised OA also conferred a greater risk of knee OA structural progression[44]. Generalised OA has been more frequently observed in women than men and with increasing age and is associated with poorer function, disability, quality of life and mortality than OA involving fewer joints[45]. Whether generalised OA reflects an accumulation of adverse biomechanical environments in adjacent joints or load compensation from other joints or systemic factors such as genetic tendency or obesity is not well understood [45].

2.3 Epidemiology and risk factors

The epidemiology of OA is complex which reflects the variation in the applied definition[46], the specific joint involved and the heterogeneity of the OA phenotype[47]. Epidemiological studies, particularly analyses of large prospective cohorts, provide important information about risk factors that in turn provide insight into the aetiology of OA. This is supported by several well recognised associations with the prevalence and incidence of OA in

peripheral joints. These include both non-modifiable (e.g. age, gender, trauma, alignment and genetic predisposition) and modifiable risk factors (e.g. obesity, occupational injury). Modifiable risk factors are prospective interventional targets for treatment and prevention.

2.3.1 Prevalence

The knee, hip and hand are most frequently affected joints and the prevalence of OA increases with age, which is the most important risk factor for OA prevalence[2]. This may represent a senescent impairment of tissue regeneration in addition to a cumulative effect of other risk factors associated with ageing. Approximately 14% of adults older than 25 years and 34% of adults older than 64 years have clinical OA of one joint or more[2]. Symptomatic OA of the knee, hip and hand are more prevalent in females[4, 48-51]. The population prevalence of OA of the hip and knee in the UK is also greater with than without obesity (Figure 3)[52]. However in a meta-analysis of OA prevalence studies in adults older than 55 years, women have higher knee and hand OA prevalence but there is no significant gender difference for hip OA. In the same meta-analysis no significant gender differences were observed in the prevalence of knee, hip or hand OA amongst adults below 55 years of age[53]. Women tended to have greater prevalence of OA when non-radiographic (e.g. clinical) methods were used for defining OA.

Figure 3 Population prevalence of Hip and knee OA with and without obesity

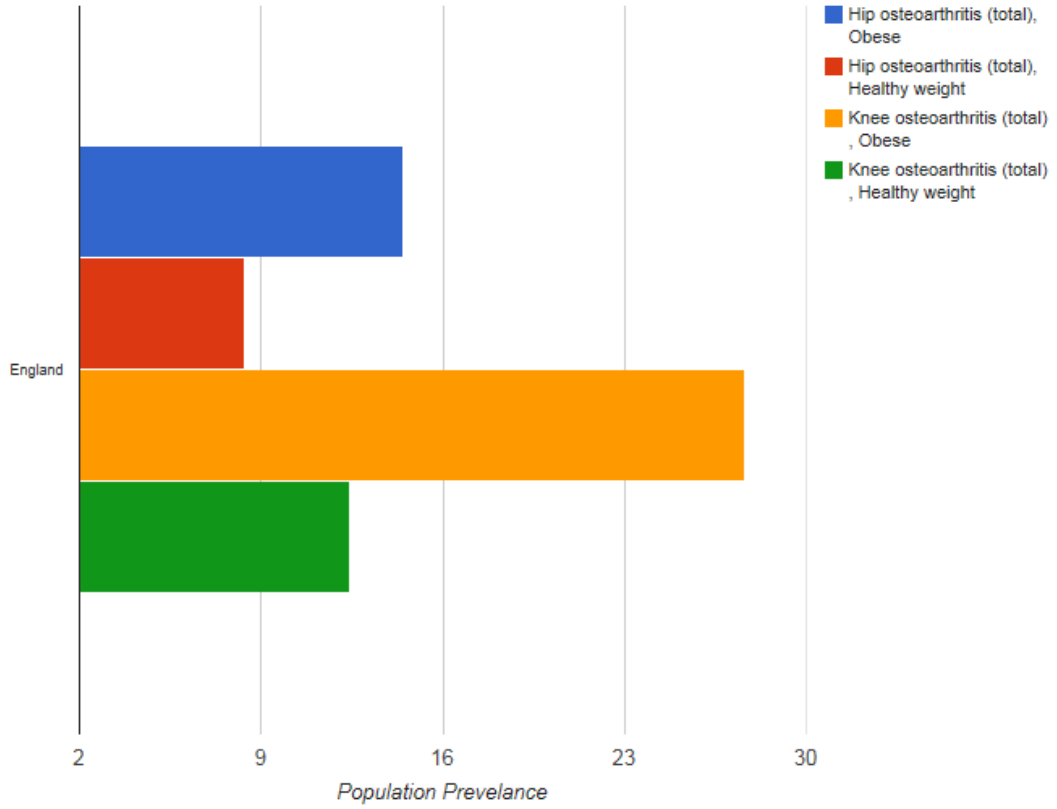

The population prevalence is expressed as percentage of the population above the age of 45. The English Longitudinal Study of Ageing (ELSA) - a large multicentre and multidisciplinary study of people aged 50 and over and their younger partners, living in private households in England – was chosen as the basis for the prevalence models. Sample members are drawn from respondents to the Health Survey for England (HSE). Study members have a face-to-face interview (a computer-assisted personal interview followed by a self-completion questionnaire) every two years of the study and a nurse assessment every four years. This particular survey was chosen because the sample used in ELSA was designed to be nationally representative and since osteoarthritis is rare under 50 years of age.

Reproduced (with permission) from the Arthritis research UK website

(http://www.arthritisresearchuk.org/arthritis-information/data-and-statistics/musculoskeletal-calculator/analysis.aspx?ConditionType=1,2&ChartType=1&AgeBracket=2,4,3&Bmi=1,2,3,4)

In adults aged 45 years and older in the American Johnston County project and Framingham cohorts, the prevalence of knee ROA was 28% and 19% respectively, whereas the symptomatic knee OA prevalence was 17% and 7% respectively[4, 51]. In adults aged 60 years and older 37% and 12% had knee ROA and symptomatic knee OA respectively[48]. In the UK 18% of adults above the age of 45 have self-reported knee OA. In a meta-analysis, a history of prior knee injury increased the risk of prevalent knee OA four fold[54].

In adults of 45 years or more in the USA Johnston County project the prevalence of hip ROA was 28% whilst symptomatic OA was 9%. In adults in the UK over 45 years 11% have self-reported hip OA. In adults over the age of 60 years the clinical ACR criteria for hand OA (Table 3) was met by 8%[49], whilst typical hand OA symptoms were reported by 22% of adults over 70 years of age[50]. Amongst adults above the age of 50 the prevalence of symptomatic foot and ROA was 17%[55].

2.3.2 Incidence

Generic risk factors for the incidence of the knee, hip and hand OA include age and female gender[43]. Occupational exposure to increased biomechanical stresses increases the risk of hip and knee (after adjusting for age, gender, body mass index and previous trauma)[56, 57]. Participation in sporting activities [58, 59] and the presence of OA in other joints increases the risk of incident hip and knee OA[43].

2.3.2.1 Age and Gender

The age and sex-standardized incidence rates of symptomatic OA in adults of 20 years and older are quoted as per 100,000 person years: these are 240, 88 and 100 for the knee, hip and hand respectively[60].

The incidence of symptomatic OA of the knee, hip and hand increases with age, with women having higher rates than men, particularly after 50 years of age. Amongst women the incidence of clinical OA of the hip and knee increases rapidly between 50 and 75 years and then decreases thereafter. However incident clinical hand OA peaks in women in peri- and post-menopausal years between 55 and 60 years and decreases thereafter[43].

Amongst men the incidence of clinical OA of the knee, hip and hand increases from 50 to 75 years and then decreases. A meta-analysis and large primary care database reported a greater risk of OA incidence amongst women for the knee, hip [53] and hand[43] respectively (Figure 4).

Table 3 American College of Rheumatology radiological and clinical criteria for osteoarthritis of the knee and hip

Hand (clinical)	
Osteoarthritis if 1, 2, 3, 4 or 1, 2, 3, 5 are present:	
1	Hand pain, aching, or stiff ness for most days of previous month
2	Hard tissue enlargement of two or more of ten selected joints*
3	Swelling in less than three metacarpophalangeal joints
4	Hard tissue enlargement of two or more distal interphalangeal joints
5	Deformity of two or more of ten selected hand joints*
Hip (clinical and radiographic)	
Osteoarthritis if 1, 2, 3 or 1, 2 ,4 or 1, 3, 4 are present:	
1	Hip pain for most days of previous month
2	Erythrocyte sedimentation rate of less than 20 mm in the first hour
3	Femoral or acetabular osteophytes on radiographs
4	Hip joint space narrowing on radiographs
Knee (clinical)	
Osteoarthritis if 1, 2, 3, 4 or 1, 2, 5 or 1, 4, 5 are present:	
1	Knee pain for most days of previous month
2	Crepitus on active joint motion
3	Morning stiff ness lasting 30 min or less
4	Age 38 years or older
5	Bony enlargement of the knee on examination
Knee (clinical and radiographic)	
Osteoarthritis if 1, 2 or 1, 3, 5, 6 or 1, 4, 5, 6 are present:	
1	Knee pain for most days of previous month
2	Osteophytes at joint margins on radiographs
3	Synovial fluid typical of osteoarthritis (laboratory)
4	Age 40 years or older
5	Crepitus on active joint motion
6	Morning stiff ness lasting 30 min or less
*Ten selected joints include bilateral second and third interphalangeal proximal joints, second and third proximal interphalangeal joints, and first carpometacarpal joint.	

Figure 4 The incidence of OA

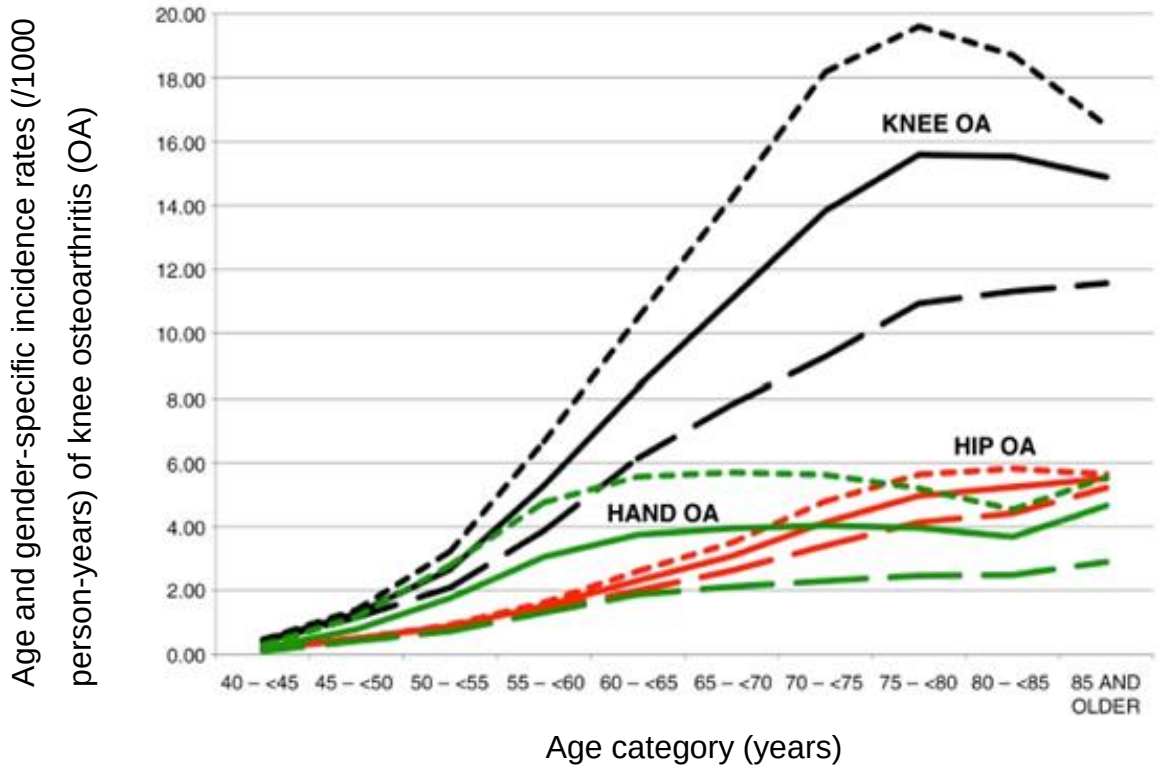

Age and gender-specific incidence rates (/1000 person-years) of knee osteoarthritis (OA) (black), hip OA (red), and hand OA (green). Solid, All population; short dash line, women; long dash line, men

SIDIAP (http://www.sidiap.org) is anonymised primary care

electronic medical records of a highly representative sample of patients attending GPs in Catalonia (North-East Spain), covering a population of about 5 million patients. SIDIAP contains primary care records for>5

million people from Catalonia (Spain). Participants aged ≥40 years with an incident diagnosis of knee, hip or hand OA between 2006 and 2010 were identified using International Classification of Diseases (ICD)-10 codes

.Reproduced from Annals of Rheumatic disease, Prieto-Alhambra D, et al. 79, 1659-64 2014; with permission from BMJ Publishing Group Ltd.[43].

2.3.2.2 Obesity

Obesity increases the biomechanical load upon weight-bearing joints which may explain its independent association with the incidence of knee ROA[61]. Obesity is the strongest potentially modifiable risk factor in meta-analyses and confers more than a three-fold greater risk of incident knee OA [62-64] and a greater risk of knee OA pain incidence[65] and structural progression[66]. Obesity is associated with incident hand OA[67] and self-reported knee OA but interestingly not hip OA[68, 69]. There is conflicting evidence as to whether obesity is associated with structural progression of the hip or knee but there is no association between body mass index and hand OA pain or structural progression[70]. Obesity directly increases the biomechanical load in weight-bearing joints that may also promote the production of proinflammatory cytokines (including adipokines) that mediate the catabolic processes of OA[71, 72].

2.3.2.3 Joint injury

Joint injury can cause damage to articular cartilage, bone, meniscus and rupture of the anterior cruciate ligament, all of which can cause a biomechanically adverse environment within the joint that predisposes to further deterioration of the joint tissues. Joint injury is associated with subsequent incident knee pain in a systematic review and meta-analysis of cohort studies[65] and also a nine-fold greater odds of progression to end-stage knee ROA in 48 months, amongst knees without baseline knee OA[73].

2.3.2.4 Bone shape and malalignment

There is increasing evidence that OA is a consequence of the failure to effectively dissipate adverse biomechanical forces within a susceptible joint. Bone shape within joints has long been recognised as a predisposing factor for adverse biomechanics. The presence of an aspherical femoral head (a cam-deformity) is associated with femoro-acetabular impingement and is associated with delamination of the acetabular cartilage and confers up to a ten-fold greater risk of end-stage hip OA within 5 years[74]. Similarly the expansion of the three-dimensional shape of tibial and femoral bones is associated with incident knee ROA[75]. Malalignment of the knees unequally

distributes load across the medial and lateral femoro-tibial joint compartment which results in a varus (bow-legged) or valgus (knock knees) deformity. The compartment with the greater load as a consequence of the malalignment is more likely to develop ROA and structural progression of cartilage damage[76, 77].

2.3.2.5 Genetics and epigenetics

Genetic studies within family-based studies and extreme OA phenotypes have confirmed the strength of genetic predisposition to OA. The identification of genes associated with OA through association studies confer only small effect sizes [78] but single-nucleotide polymorphisms (SNP) have been associated with established risk factors such as obesity (*FTO* [78, 79]) and hip bone shape (*FRZB* [80]). One SNP near the NCOA3 gene reached genome-wide significance level[81]. The *NCOA3* gene is clinically important because it is expressed in articular cartilage and its expression was significantly reduced in damaged cartilage compared to normal cartilage in femoral heads removed at the time of hip replacement[81]. As OA is likely a complex polygenic problem, genomics alone will be unlikely to stratify individuals into who will or will not develop OA, but may lead to the development of new therapeutic targets for individual joints[82].

Epigenetic studies have indicated the disruption of cartilage homeostasis may reflect environmental factors promoting abnormal expression of genes that disrupt the anabolic and catabolic processes that regulate cartilage integrity. The alteration in gene expression of anti-inflammatory or pro-inflammatory cytokines, articular cartilage proteins, matrix proteases and transcription factors may be involved in the pathogenesis of OA and represent important novel therapeutic targets [83].

2.3.3 Structural progression

Structural progression is usually defined as imaging evidence of structural deterioration in a joint, though soluble biomarkers may also reflect this process. Conventionally these have been surrogate measures of cartilage

damage from CR. Radiographic structural progression can be assessed by measuring joint space narrowing (JSN) using semi-quantitative tools like the OARSI atlas [84, 85] or quantitative tools. The Kellgren Lawrence grade[19] is a composite measure of JSN, osteophytes, subchondral sclerosis that is described on an ordinal scale (Figure 1,Table 1). Joint space width is used as a surrogate for assessing cartilage thickness but in the knee it reflects a construct of reduction in hyaline articular cartilage thickness along with meniscal extrusion and degeneration[86]. The Kellgren Lawrence scoring does not represent an interval variable where individual categories are equidistant from each other. Therefore it is important to recognise that the proportion of knees that progress from one grade to the next are not comparable for all starting points in the scale.

With its three dimensional visualisation of joint tissues, MRI has broadened concepts of structural progression. The quantification of MRI cartilage volume affords advantages over CR because structural loss of cartilage can be detected in the pre-ROA phase[87] and in end-stage OA, after the total loss of joint space width (‘bone on bone’ or Kellgren Lawrence grade 4)[88]. As well, MRI demonstrates structures other than cartilage (Table 2,Figure 2) that might be used to measure structural progression such as bone marrow lesions (BMLs) or bone shape.

The structural progression measured by ROA of knee, hip and hand OA is typically slow and takes place over several years but can also remain stable over years [89-92]. Structural progression varies by joint affected. In knees the mean annual risk of progression of KL grade is 5.6% ± 4.9% and mean rate of joint space narrowing is 0.13 ± 0.15mm/year, with change occurring in only a small group of “progressors” in a 12-month observational study and a 30 month randomised controlled trial[93, 94]. The same observation was made when structural progression was analysed in the OAI.

It is important to understand the inertia of the trajectory of radiographic structural progression in knee OA that has been described by Felson and colleagues. A nested case control analysis within the OAI described case knees as those with incident ROA (KL=2, a combination of incident JSN and osteophytosis) by the end of the first year of follow up and control knees

which maintained a stable KL grade of 2 during the first year. This was an elderly obese population. Both incident ROA (KL 2) and stable ROA (KL 2) knees were examined subsequently for progression of JSN (OARSI grade) or KL grade in the following (2^{nd}) year. 13.7% and 4.1% of knees developed a higher KL grade in the incident and stable groups respectively. 25.8% and 6.1% of knees developed progression in JSN in the incident and stable group (with JSN grade 0 or 1) respectively(Table 4)[92].

After adjustment for sex, race, baseline age, BMI, clinic site, physical activity survey of the elderly, quadriceps strength and alignment the incidence group had a four and five fold greater odds of KL grade and JSN grade progression than the stable group. This suggests that in adults with a mean age of 61 years and mean BMI of ~29, radiographic structural progression is not phasic but an inciting event precipitates a trajectory of structural deterioration with inertia.

Table 4 The inertia of knee osteoarthritis radiographic progression

	Incident JSN and KL 2 N=167	Stable JSN (grade 0-1) N=4979	Incident KL2 N=139	Stable KL2 and JSN N=3173
% with JSN progression	25.8%	6.1%	13.7%	4.1%
% without JSN progression	74.2%	93.9%	86.3%	95.9%

JSN – joint space narrowing, KL – Kellgren Lawrence

Data collected from the Osteoarthritis Initiative (OAI)

MRI-determined cartilage volume loss in knee OA progresses at a mean rate of 4% per annum and more than half of all knees are “progressors”[95]. Loss of cartilage volume occurs more rapidly with increasing age, body mass index, lower limb muscle weakness but also with co-existing structural changes such as BMLs and meniscal damage[95, 96] (Figure 2). Muscle

weakness has not been considered to be a risk factor for structural progression based upon a systematic review of studies using CR and not MRI[44].

2.3.4 Symptom progression

Studies that refer to OA ‘progression’ generally refer to structural progression, though sometimes progression to joint replacement is used as a surrogate for presumed worsening of pain and structure. OA symptom progression is not well defined and could refer to progression of pain severity or the new incidence of pain within individuals usually in cohort studies. Pain can be serially measured using numeric rating or visual analogue scales or using standardised questionnaires that ask patients to quantify pain severity. Amongst knees with ROA, little change is observed in knee pain over six years [97] except when large increases in radiographic structural severity are observed[98]. BMLs and bone shape are independently associated with future increases in knee pain severity[99-101] and incident knee pain[102] respectively. The probability of joint replacement is increased by increasing severity of joint pain[103], increasing ROA severity[104] and MRI-demonstrated BMLs, cartilage and meniscal damage and synovitis that indicate joint failure[103, 105].

2.3.5 Secondary osteoarthritis

The term ‘primary’ or idiopathic OA is less frequently used now, perhaps because we understand the frequency of pre-OA lesions (like meniscal damage) that would often not be detected in routine clinical practice and for which patients often have no knowledge (probably arising from minor or forgotten trauma). However OA does occur secondary to other diseases. Congenital or developmental causes include bone dysplasias such as epiphyseal dysplasia, localised diseases such as Perthe’s disease of the hip, congenital hip dislocation and slipped femoral epiphysis. Endocrinological predisposing diseases include acromegaly, diabetes mellitus, hyperparathyroidism and hypothyroidism. Metabolic predisposing diseases include haemochromatosis, ochronosis (alkaptonuria), Gaucher’s disease and Wilson’s disease. Finally neuropathic (Charcot joints), calcium

deposition diseases (primary pseudogout), haemoglobinopathies and other bone and joint diseases may also cause secondary OA.

2.3.6 Impact of osteoarthritis

Individuals with OA suffer pain which is associated with disability and reduced quality of life. The impact of OA on an individual's function, mood, relationships, occupation and leisure activities may be extensive. Workers with OA reported more frequent pain, greater use of healthcare resources and costs, reduced productivity and poorer quality of life as self-rated OA severity increased[106].

One in eight individuals with OA suffer self-reported unbearable pain and one in five give up holidays, hobbies and leisure activities. One third of people with OA retire early, give up work or reduce the number of hours they work because of their condition. Those who retire early do so an average of 8 years early. Furthermore two thirds of people with OA report an increase in their own costs including travel and treatment which in total equates to a mean of £480 per person each year[1].

OA is the most common worldwide cause of mobility disability and it is increasingly accountable as a cause for years lived with disability and limitation of quality of life[6].

The lived experiences of people with OA can be influenced for better or for worse by one or a combination of the following: functional impairment, attitudes towards OA symptoms, personal perceptions of OA and perceived perceptions of other people towards OA. Favourable changes in any of these may improve the lives of those living with OA[107] (Figure 5). A systematic review of generalised OA indicates this is associated with poorer quality of life, function and increased disability compared to an OA monoarthritis[45]. Increasing OA joint burden is also associated with increasing risk of depression[108].

Figure 5 The factors affecting lived experiences of OA

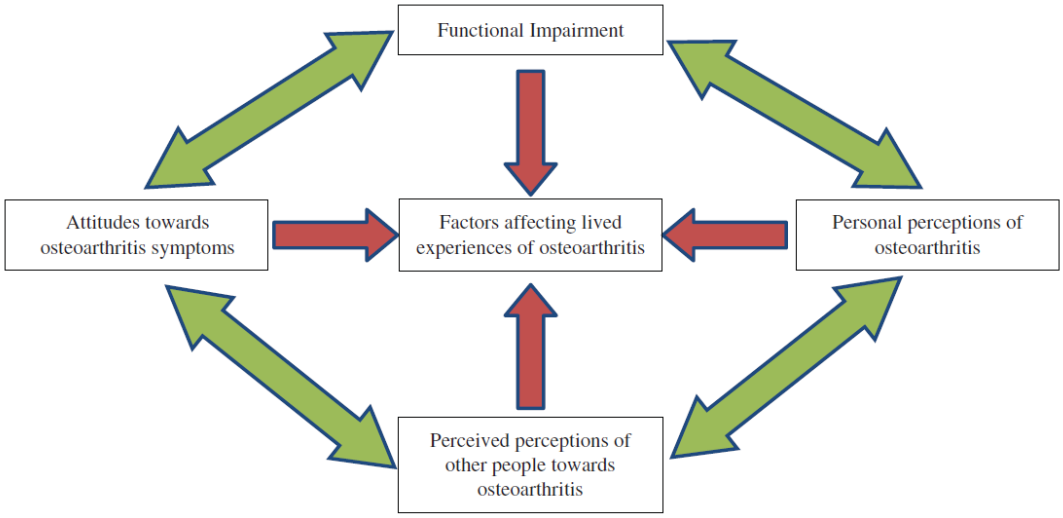

A line of argument diagram. Four concepts can act in isolation or in combination to influence the experiences perceived by the person with OA. Reprinted with permission of Taylor and Francis [107].

2.3.7 Health economic impact

OA is associated with pain, disability, absenteeism and early retirement. The socioeconomic burden ranges from one to two-and-a-half per cent of gross domestic product in developed countries[8]. The economic burden of OA on society and health services is tremendous. This is generated through a combination of direct and indirect costs. Individuals with OA have double the rate of absenteeism compared with controls in North American [109] and Swedish population based cohorts [7]. The mean total direct and indirect costs are two to three fold higher [109] and there was a 40–50% increased risk of disability pension in comparison with the general population[7].

In the UK between 1991 and 2006, 25845 hips and 23260 knees underwent total joint replacement[110]. The estimated mortality-adjusted lifetime risk of total hip replacement (THR) at age 50 was 11.6% for women and 7.1% for men. For total knee replacement (TKR) the risks were 10.8% for women and 8.1% for men[110]. OA represents more than 93% of all joint replacement indications and the total annual cost of joint replacements is estimated at £852 million in the UK in 2010[111].

2.3.8 Mortality

Case series of individuals with OA have utilised different methods to describe the effect of a diagnosis of OA on mortality. Conflicting results have been reported by two different analyses, reporting an increased mortality and normal mortality rates conferred by a diagnosis of OA compared with national statistics of the general population[112, 113]. Symptomatic OA of the hip and knee was reported to confer approximately a two-fold greater risk of cardiovascular (CV) and dementia-associated deaths compared with the general population. While this association did not adequately adjust for the confounding effects of disability and comorbidity in the general population, walking disability was found to be a major risk factor for mortality amongst individuals with OA[112]. A subsequent population cohort reported that OA did not confer a greater risk of CV events but disability was independently associated with this outcome after adjusting for the presence of symptomatic and asymptomatic ROA[114]. An analysis of the Framingham population cohort reported that hand OA did not confer a greater risk of mortality but symptomatic hand ROA conferred a greater risk of CV events than asymptomatic hand ROA. A cohort in North America, designed to describe osteoporotic fractures and recruited from secondary care, described a greater risk of all cause and CVD mortality conferred by the presence of hip ROA compared to the absence of ROA of the hip. This effect was independent of poor physical function but the causal effect was significantly explained by poor physical function [115]. Therefore a greater burden of OA and subsequent disability may be important risk factors for mortality.

2.4 Pathogenesis and pathological features

There are multiple tissues that are essential components of diarthrodial (synovial) joints. Each tissue has its own composition and structure which plays an important functional role in effectively dealing with mechanical loads encountered during life. The hyaline articular cartilage is a tissue capable of distributing and transferring impressive load across diarthrodial joints without sustaining significant structural deterioration[116]. This cartilage affords a gliding surface for the joint which is almost frictionless and which permits load transmission during dynamic activity. It is the unique

mechanical and morphological properties of hyaline cartilage that permit it to fulfil its complex functional demands[116-118]. Subchondral bone is also integral to the maintenance of the integrity of articular cartilage and works in concert with this cartilage to effectively dissipate load by a process of load-sensitive remodelling (see Section 2.6).

OA is a syndrome of deterioration of synovial joints that is characterised by focal and progressive loss of the hyaline articular cartilage of joints, bone changes beneath the cartilage, synovial inflammation and debilitating pain.

There is no single pathway of pathogenesis but in order for a structurally normal joint to become osteoarthritic, this requires a sufficient burden of joint tissue structural damage, biomechanical adversity along with a varying combination of risk factors (see epidemiology). These inflammatory, metabolic and genetic contributory factors may drive a subsequent heterogenous cascade of biomechanical and biochemical pathologies that overwhelm normal repair processes and establish the joint ‘failure’ that presents as clinical OA.

This pathogenesis is likely to progress through a sequence of stages that can be described macroscopically using MRI studies and microscopically using histological studies.

2.4.1 Macroscopic

In early asymptomatic stages only individual tissues are likely to be involved and cartilage defects[119], meniscal degeneration[120] and BMLs[121] are all known to be present amongst individuals without knee OA symptoms. These lesions (see Figure 2, Table 2) are associated with incident knee ROA[122] and structural progression of cartilage volume or thickness loss[123-125]. It is likely that a ‘domino effect’ occurs where an inciting event such as a meniscal tear predisposes to cartilage loss, adjacent bone marrow lesions, meniscal extrusion and malalignment which establishes a progressive biomechanical adverse environment within the joint.

2.4.2 Microscopic

OA represents whole-joint ‘failure’. Normal joint structure and function depend upon the ability of constituent tissues to perceive and respond to stress, strain and load. This is particularly true of the articular cartilage and subchondral bone. The cells within these tissues ensure the joint’s ability to receive and dissipate stress is maintained by homeostatic reparative processes. This includes the chondrocytes that maintain a substantial extracellular matrix. Chondrocytes synthesise molecules to restore the cartilage matrix, but also produce pro-inflammatory cytokines (e.g. interleukin-1) and tissue destructive enzymes (e.g. metalloproteinases) which decrease anabolic matrix synthesis (Figure 6)[126]. This matrix consists of a collagenous extracellular matrix, that consists of proteoglycan and elastin fibres. Cartilage and joint structural integrity and function are lost as a net catabolic process is established during the OA process. An extension of the calcified cartilage zone increases biomechanical forces across the cartilage and adjacent bone. Biomechanical derangements within the joint can stimulate the production of further catabolic enzymes. In parallel with these cartilage derangements the cellular activity in subchondral bone changes, probably to attempt to adjust to biomechanical forces. This results in resorption and the production of an increased volume of immature unmineralised bone. This may compromise the biomechanical support for the overlying cartilage which may augment the biomechanical forces transmitted through cartilage resulting in further damage. Furthermore an increased permeability at the junction between the articular cartilage and bone (osteochondral junction), driven by microcracks in the cartilage and subchondral angiogenesis, exposes the cartilage to an abnormal biochemical environment (Figure 7)[15]. Synovial inflammation is precipitated by cartilage debris and catabolic mediators entering the synovial cavity. Synovial macrophages produce some of the chemokines and metalloproteinases that degrade cartilage (Figure 6). This in turn amplifies synovial inflammation, creating a potentially vicious cycle between these tissues.

Figure 6 Pathogenesis of OA

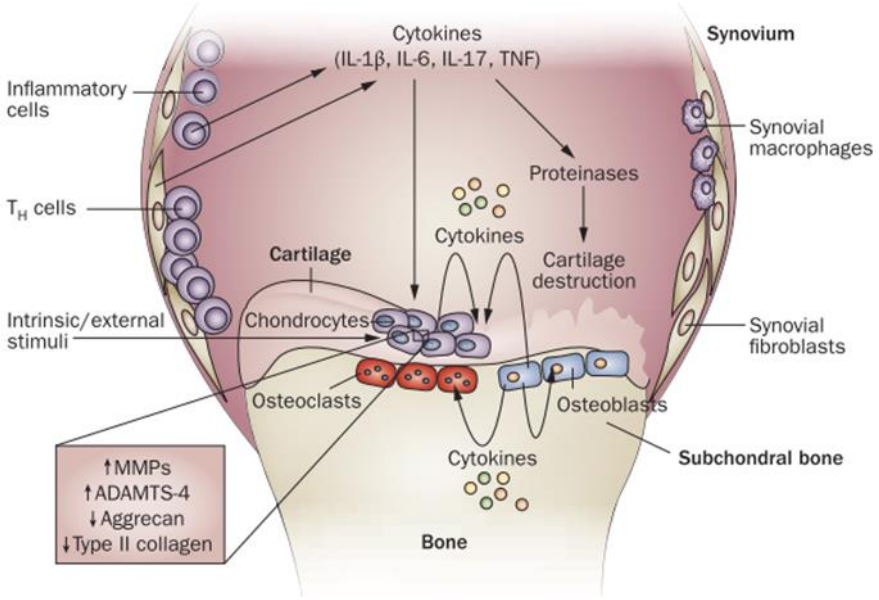

The role of proinflammatory cytokines in the pathophysiology of OA. The levels of cytokines are elevated in OA and downregulate anabolic events and upregulation of catabolic and inflammatory responses. This results in structural damage. Reprinted by permission from Macmillan Publishers Ltd: Nat. Rev. Rheumatol. [126], copyright (2011).

Figure 7 Pathogenesis of OA – osteochondral disruption

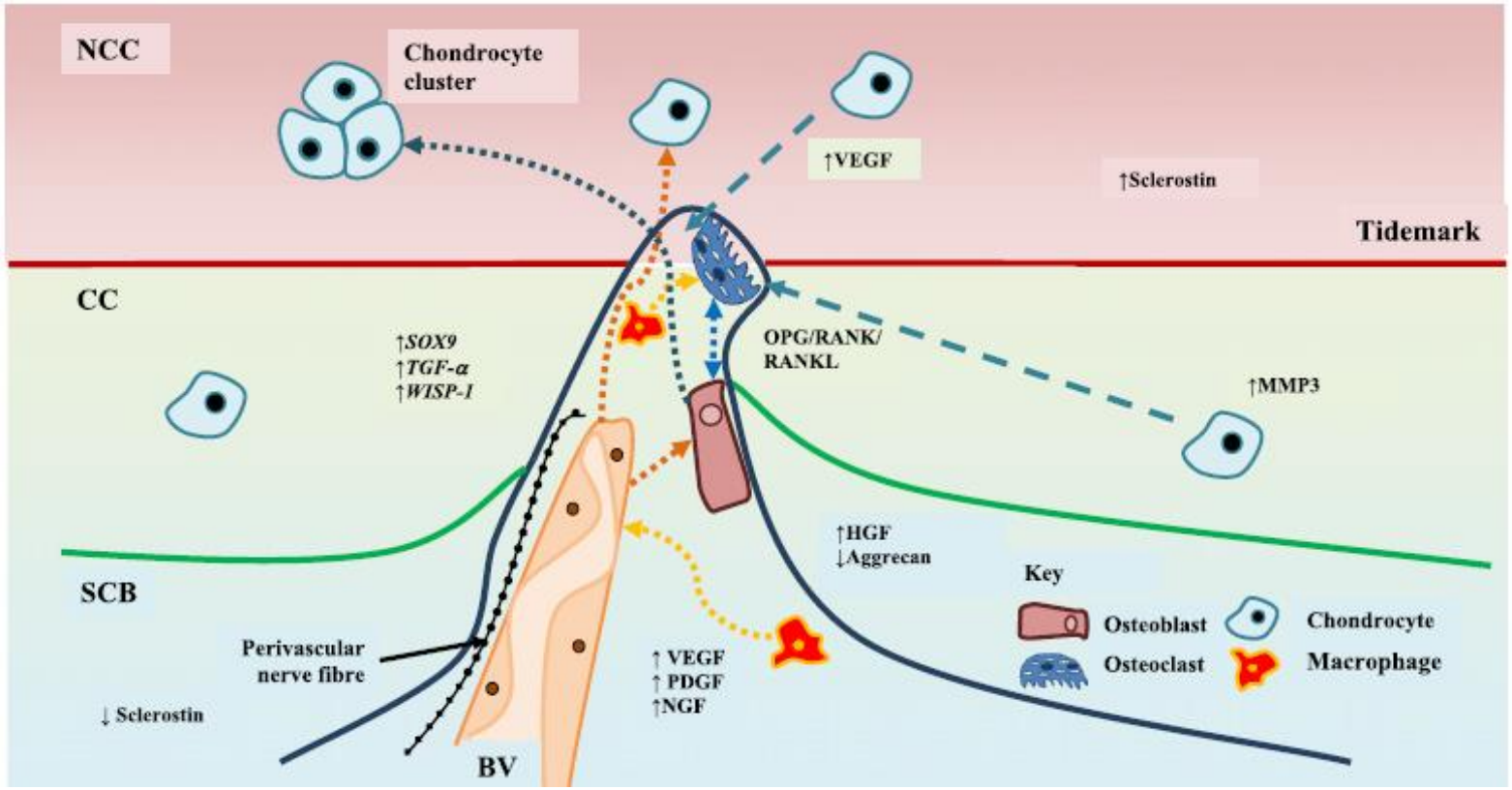

Molecular cross-talk at the osteochondral junction. A vascular channel is shown breaching from the subchondral bone (SCB), through the calcified cartilage (CC) into the non-calcified cartilage (NCC). Channel contents include macrophages, osteoclasts, osteoblasts and a blood vessel (BV). Cells within the channel interact through cytokines, growth factors and other signals that stimulate angiogenesis, nerve growth and sensitisation, osteoclastic activity and new bone formation. Importantly, these local interactions are enhanced in OA by signals across the osteochondral junction. With disruption of the tidemark, subchondral tissues become exposed to factors produced by articular chondrocytes nearer the joint surface, such as vascular endothelial growth factor (VEGF), and potentially to influences from the synovium. (Reprinted by permission from Elsevier Ltd: Bone [15])

2.4.3 Pain and measuring pain in OA

OA is one of the most common causes of chronic pain and pain is the most common symptom of OA. Pain is the primary reason for patients seeking medical help with OA and involves peripheral and central nociceptive mechanisms. Pain is important to recognise for its characteristics to accurately diagnose OA but also to appreciate its likely origin as any successful treatment must ideally target the source of pain. This section describes the origin of pain in OA, the characteristic pain of OA, the structural associations and likely determinants of pain and finally attempts to treat pain.

2.4.3.1 The pathogenesis of pain

OA pain is generated from damaged joint tissues where irritative chemical, mechanical or thermal stimuli precipitate afferent nociceptive neurons to depolarise and send nociceptive signals to the sensory cortex via the dorsal horn of the spinal cord.

Nociceptors within a joint vary by joint tissue and by stage of OA. Healthy diarthrodial joints have nociceptive fibres richly innervating the synovium and subchondral bone. These fibres also innervate the joint capsule and ligaments and the outer edge of the menisci in the knee but the cartilage is aneural and avascular in normal joints[127]. Therefore in normal joints and in early OA, the cartilage is unlikely to be the source of pain. However as OA progresses there is neurovascular invasion which provides cartilage with the potential for nociception[15](2.6.1.2 Subchondral bone and the osteochondral junction).

Activity-related pain of OA is typically present in a prodromal phase of ‘early’ OA before the incidence of ROA[18]. This pain in early OA is typically mechanical [128]and may reflect the increased load upon SCB denuded of shock-absorbing cartilage and increased intra-articular pressure with a joint effusion. Cartilage degradation products also promote a secondary synovitis and joint inflammation which involves the release of cyclooxygenases, lipo-

oxygenases, leukotrienes, phospholipases and nitrous oxide that are involved in pain mechanisms.

In acute pain, a peripheral nociceptor receives a stimulus and transduces this into an afferent sensory neurone action potential that relays with a spinal neurone for onward transmission to the thalamus and thereafter the sensory cortex. There are serotonergic and noradrenergic pathways within the central nervous system that provide descending inhibition to modulate and reduce the signal that is conveying the acute pain. However in chronic pain, greater sensitivity in the peripheral nociceptor can increase this signal and this is called peripheral sensitisation. Examples of mediators of peripheral sensitisation include neuronal growth factor (NGF), substance P, calcitonin gene-related peptide (CGRP), neuropeptide Y (NPY) and vasoactive intestinal peptide (VIP).

Central pain neurological mechanisms play an important role in the perception of pain. Increased nociceptive transmission from the spine to the sensory cortex can be increased due to inhibition of the inhibitory central descending pathways and this is called central sensitisation. Central sensitisation has many determinants and can be influenced by comorbidities including mood disorders, loneliness and sleeping problems in OA.

The enhanced pain experienced in response to a given stimulus reflects neural plasticity in the chronic pain of OA which involves both peripheral and central sensitisation. This is demonstrated by saline injections into the tibialis anterior muscle of patients with OA causing more intense pain than individuals without OA[129].

In more advanced forms of OA neuropathic pain may be involved whereby altered spontaneous and evoked activity from peripheral neuronal injury results in pain without the typical mechanical stimulus of OA pain. This unpredictable intense pain[128] is perhaps the most debilitating of OA[130].

2.4.3.2 OA pain and its structural associations

OA pain is well known to be poorly associated with conventional radiographic structural knee OA severity. Only 50% of knees with radiographic OA (ROA) have symptoms[17]. Little change in pain is

observed in knees with ROA over six years[97] except when large increases in ROA structural severity are observed[98].

CR is not as sensitive or specific in detecting structural pathology and progression as magnetic resonance imaging (MRI)[23, 86]. The OA joint tissue lesions detected by MRI (e.g. cartilage defects, meniscal tears, bone marrow lesions - see Figure 2) are prevalent in knees without ROA [23] and these are associated with incident symptoms [131] which highlights the importance of peripheral joint structural lesions in the pathogenesis of nociception. In particular a recent systematic literature review highlighted the important associations of MRI-detected synovitis and bone marrow lesions (BMLs) with knee OA pain[132]. An increase in the number or size of BMLs was associated with increasing knee pain, whilst a decrease in BMLs was associated with reduced knee pain[26]. BMLs are consistently associated with knee pain [26, 100, 133-135]. The pathophysiology by which BMLs may cause pain is unknown but this might include ischaemia from a decreased blood supply, subchondral microfractures, and raised intraosseous pressure[136-138].

Numerous other structural associations with pain have been demonstrated including SCB attrition (see 2.6.3) [135, 139], synovitis [135] and meniscal tears[135].

Demonstrating the longitudinal role of BMLs and synovitis in pain pathogenesis is more feasible because these lesions appear and disappear or regress. Meniscal tears and SCB attrition do not reverse.

2.4.3.3 OA pain and measuring pain

Pain is a characteristic feature of OA and is typically activity-related or mechanically-exacerbated and is relieved by rest. OA pain is characteristically intermittent in large OA knee cohort observational studies[140] but as OA becomes more advanced, patients report pain with different qualities (such as “a burning sensation”) which may reflect neuropathic pain, and central pain mechanisms including sensitisation may reduce pain thresholds.

Pain can be quantified using different methods and these include the visual analogue scale for pain (VAS), the numeric rating scale for pain (NRS), the

McGill pain questionnaire (MPQ), the Intermittent and Constant Osteoarthritis Pain (ICOAP) and the Western Ontario and McMaster Universities Arthritis Index (WOMAC).

Pain severity can be described using the pain VAS, NRS, pain quality can be assessed with the MPQ and the time course of pain can be described by the ICOAP. The WOMAC is used to evaluate the pain, stiffness, and physical functioning of the joints of patients with OA of the hip and knee.

The pain VAS is a unidimensional continuous measure comprised of a horizontal or vertical line which is usually 10 centimetres in length and anchored by two descriptors, one for each symptom extreme.

The NRS is a segmented numeric version of the VAS where a respondent must select integers (0–10) that reflects the intensity of their pain. There are also anchoring terms describing pain severity at the extremes of the 11-point numeric scale.

The MPQ identifies qualities of pain associated with distinct nociceptive disorders and neuropathic pain disorders like OA and also can measure the effectiveness and efficacy of pain interventions. This is a multidimensional pain questionnaire designed to measure pain intensity as well as the sensory, affective and evaluative aspects of pain in adults with chronic pain such as in OA. Four subscales evaluate the sensory, affective and evaluative, and miscellaneous aspects of pain

The ICOAP is another multidimensional OA-specific measure for comprehensively evaluating pain in people with hip or knee OA. This includes the impact of pain on mood, sleep, and quality of life pain as well as measuring the intensity and frequency of pain. It is an 11-item scale evaluating 2 pain domains: a 6-item scale evaluates intermittent pain while a 5-item scale evaluates constant pain.

The WOMAC is another multidimensional OA-specific measure for comprehensively evaluating the pain, stiffness, and physical functioning of the joints of patients with OA of the hip and knee. The WOMAC measures five items for pain (score range 0–20), two for stiffness (score range 0–8), and 17 for functional limitation (score range 0–68). Physical functioning questions cover activities of daily living[141].

2.4.3.4 Novel approaches to measuring and treating pain in OA

While structural joint pathology and inflammation are recognised as important contributing factors to pain, OA pain pathophysiology is relatively poorly understood. The mechanisms of peripheral and central sensitisation and neuropathic pain contribute to OA pain severity are important in the maintenance of pain and facilitate the conversion of acute pain into chronic pain. The role of the central nervous system in pain is highlighted by the observation that 10-20% of people with knee OA have persistent severe pain after total knee replacement[142-144]. Pain may therefore be a consequence of multiple mechanisms and this may explain why the response to conventional OA pain treatments, which often target one specific pain mechanism, is often inadequate.

Quantitative sensory testing (QST) is an example of a mechanism that assesses the mechanisms of pain involved and a phenotyping of pain. This evaluates somatosensory evoked responses to innocuous or noxious stimuli using several modalities including controlled chemical, thermal, mechanical and/or electrical. These stimuli are applied by an examiner to an anatomical test site such as a joint until the subject indicates pain. The subject's responses to the stimuli locally can be used to assess peripheral sensitisation. The subject may also report pain at a nearby or distant location from the applied stimulus which may imply central sensitisation. These methods are being used to develop strategies for measuring the pain mechanisms involved in OA pain perception and the relative impact of peripheral and central sensitisation, descending pain control, and referred pain. This may permit patient phenotyping for targeted therapy directed at the underlying pain mechanism.

One of the major mediators of peripheral sensitisation and pain in animal models of OA is nerve growth factor (NGF). The monoclonal antibody tanezumab provides a blockade of the NGF mechanism and in a randomised controlled trial in humans a sustained improvement in knee pain was demonstrated and therapy was essentially well tolerated. Unfortunately, trials were suspended due to increased rates of joint replacement[145] but investigation is now underway again.

In summary OA pain is a complex construct of tissue damage, peripheral sensitisation, central sensitisation and neuropathic pain. While OA pain has important structural associations with MRI-determined structural pathology these other mechanisms must be acknowledged as important determinants of OA pain.

2.5 Management

2.5.1 Clinical features

NICE and EULAR guidelines advise that appropriate symptoms, clinical findings and age at onset can be used to clinically diagnosed OA[146-148]. Activity related joint pain reported in patients over the age of 45 with less than 30 minutes of morning joint stiffness can be considered to have OA without further investigation. The likelihood is increased further by risk factors (see Epidemiology and risk factors) and joint-specific examination findings of pathology including knee crepitus or Heberden's nodes in the hands.

2.5.2 Investigation

X-rays and laboratory analysis of blood and synovial fluid are not necessary for the clinical diagnosis of OA. However in the presence of atypical features that suggest the presence of diagnoses other than OA, these tests may be used for differential diagnosis of inflammatory arthritis, septic arthritis or malignant bone pain[148]. These features include, rapid progression of symptoms, a hot swollen joint or prolonged morning stiffness of more than one hour

2.5.3 Treatment

Recent years have seen the emergence of a large number of evidence-based guidelines from important musculoskeletal organisations. These are based on the published literature, expert opinion and, to a lesser extent, patient opinion (all three sources are valid for comprehensive guidelines). There is generally broad agreement across these guidelines in which therapies they recommend, though some discrepancies are obvious.

2.5.3.1 Nonpharmacological interventions

Guidelines for the management of OA unanimously recommend the provision of health education and to encourage self-management. All individuals with OA should comprehend their arthritis reflects a failed repair process usually arising due to several joint insults, their personal risk factors (e.g obesity) and their prognosis. This information should be reinforced at subsequent consultations and with both electronic and written resources.

All patients with OA should be offered advice on exercise that initially focusses on local muscle strengthening and then general aerobic fitness thereafter. A Cochrane review finds that land based knee and hip exercise programmes can reduce pain and improve physical function[149, 150]. Exercise programmes must be tolerable and realistic to promote adherence and should therefore be tailored to the severity of the OA at presentation. It is unlikely that a patient with painful knee OA, that cannot perform a straight leg raise, will significantly benefit from walking without quadriceps strengthening first. Exercise programmes for individuals with significant muscle weakness should begin with low-impact exercises such as cycling on exercise bikes and walking laps in a swimming pool. Depending upon each individuals capability, the ‘dose’ of exercise should be titrated up.

Overweight or obese individuals should be offered a dietician’s review or dietary advice because weight loss is associated with reduction in pain and better function (though there is little evidence for benefits on structural progression)[151, 152]. Aids and devices (for example, splints for base of thumb OA and devices for opening jars) help with everyday activities. Recommended footwear for individuals with OA includes shoes with no heel elevation, thick shock-absorbing soles and adequate plantar arch support.

In summary, the multi-disciplinary patient-centred combination of exercise self-management and education should set realistic goals with regular reassessment and encouragement to maintain the required lifestyle changes[153].

2.5.3.2 Pharmacological interventions

The first-line pharmacological treatments are topical NSAIDs and oral paracetamol due to their favourable risk:benefit ratio. However recent evidence suggests that paracetamol may have greater toxicity than is generally appreciated, and be a less effective analgesic in OA than previously thought[10, 154](Table 6)

In one study, after 13 weeks of regularly taking either ibuprofen or paracetamol three times a day for knee OA, one in five participants lost more than 1g per decilitre of haemoglobin[13]. A systematic review identified a dose-response effect on cardiovascular, gastrointestinal and renal adverse events[11]

Topical capsaicin is a chilli pepper extract that depletes neurotransmitters in sensory terminals and attenuates the central transmission of peripheral pain impulses from the joint. It is generally recommended as supplementary analgesic for hand and knee OA and is again safe.

Treatments may vary in efficacy according to the anatomical location of OA; most of the published evidence derives from knee OA trials, both nonpharmacological and pharmacological interventions are used, separately but more commonly in combination, in the treatment of OA(Table 5).

Should further analgesia be required, practitioners should consider oral NSAIDS, selective COX-2 inhibitors and then opiates, acknowledging the greater risk of toxicity particularly with increasing age and co-morbidities. Nutraceuticals, including glucosamine sulphate and chondroitin sulphate products, are natural compounds consisting of glycosaminoglycan unit components and glycosaminoglycans respectively. Despite the substantial volume of published evidence, they are often not recommended due to the lack of certainty of clinically important analgesic or structural benefits. However nutraceuticals have been reported to afford small benefits in pain-relief in low quality trials[155, 156].

Table 5 Summary of the latest evidence based guidelines for OA treatments

Guideline	NICE 2014	OARSI 2014	OARSI 2014	EULAR 2013	ACR 2012	ACR 2012	ACR 2012
Site of OA	**all sites**	**knee**	**multijoint**	**knee and hip**	**hand**	**knee**	**hip**
exercise/physiotherapy (water and land based)	+	+	+	+	NE	+	+
education, self-management	+	+	+	+	(+)	(+)	(+)
weight loss in obesity	+	+	+	+	NE	+	+
thermotherapy (eg hot packs/spa)	+	NR	(+)	NE	(+)	(+)	(+)
acupuncture	-	NR	NR	NE	NE	(+)	NE
transcutaneous electrical nerve stimulation	+	NR	-	NE	NE	(+)	NE
aids, adaptations, braces, footwear (site specific)	+	(+)	(+)	+	(+)	(+)	(+)
paracetamol	+	(+)	+	NE	NE	(+)	(+)
topical NSAIDs	+	+	NR	NE	(+)	(+)	NR
oral NSAIDs (lowest possible dose)	+	(+)	(+)	NE	(+)	(+)	(+)
topical capsaicin	+[a]	(+)	NR	NE	(+)	-	NE
opioids (for refractory pain)	(+)	NR	NR	NE	-	(+)	NR
glucosamine and chondroitin sulphate	-	NR	NR	NE	NE	-	-
duloxetine	NE	NR	+	NE	NE	(+)	NR
risedronate	NE	-	-	NE	NE	NE	NE
strontium	-	NE	NE	NE	NE	NE	NE
intra-articular corticosteroids	+	(+)	+	NE	-	(+)	(+)
intra-articular hyaluronans	-	NR	-	NE	-	(+)	NR
surgery – lavage/debridement	-[b]	NE	NE	NE	NE	NE	NE
surgery – TJR/arthroplasty (site specific)	(+)	+	NE	NE	NE	NE	NE

this is not a head-to-head comparison of the guidelines but a summary of the recommendations; each guideline addresses different anatomical sites + treatment is unconditionally recommended; (+) treatment is conditionally recommended; - treatment is not recommended; [a] excluding hip osteoarthritis; [b] unless there is a clear history of mechanical knee locking; NR = no recommendation for treatment despite reviewing the evidence; NE = treatment not evaluated; TJR = total joint replacement

Reprinted by permission from John Wiley & Sons Ltd: Prescriber, Table reproduced from [157]

Table 6 Relationship between effect size for pain relief and quality of randomized controlled trial

	All trials ES (95% CI)	High quality trials (Jaded = 5), ES (95% CI)
Acupuncture	0.35 (0.15, 0.55)	0.22 (0.01, 0.44)
Acetaminophen	0.14 (0.05, 0.23)	0.10 (−0.03, 0.23)
NSAIDs	0.29 (0.22, 0.35)	0.39 (0.24, 0.55)
Topical NSAIDs	0.44 (0.27, 0.62)	0.42 (0.19, 0.65)
IAHA	0.60 (0.37, 0.83)	0.22 (−0.11, 0.54)
GS	0.58 (0.30, 0.87)	0.29 (0.003, 0.57)
CS	0.75 (0.50, 1.01)	0.005 (−0.11, 0.12)
ASU	0.38 (0.01, 0.76)	0.22 (−0.06, 0.51)
Lavage/debridement	0.21 (−0.12, 0.54)	−0.11 (−0.30, 0.08)

NSAIDs – non-steroidal anti-inflammatory drugs

IAHA – intra-articular hyaluronic acid

GS – glucosamine

CS – chondroitin sulphate

ASU -Avocado soybean unsaponifiables

Jaded - a procedure to independently assess the methodological quality of a clinical trial

ES – effect size. This is a standard mean difference between groups (e.g., treatment vs placebo). ES is calculated by dividing the mean difference between treatments by the standard deviation of the difference. It is, therefore, a number without units that can be used for cross-study comparisons. Clinically ES >0.2 is considered small, ES>0.5 is moderate and ES> 0.8 is a large effect.

(Reprinted by permission from Elsevier Ltd: Osteoarthritis and Cartilage [10]

The intra-articular injection of corticosteroids is a useful short-term adjunct in the treatment of moderate to severe OA pain, which may facilitate muscle strengthening and exercise. Hyaluronan (HA, or hyaluronic acid) is a high molecular-weight glycosaminoglycan, a naturally occurring synovial fluid and

cartilage component. It provides the visco-elastic properties of synovial fluid that may provide lubricating and shock absorbing properties. Intra-articular HA is not recommended for OA by the NICE guideline[148]; in contrast the ACR guideline conditionally recommends its use in individuals older than 74 years with knee OA pain that is refractory to conventional pharmacological therapies[158].

2.5.3.3 Joint surgery

Surgical intervention in OA may include arthroscopic surgery or partial or complete joint replacement. Arthroscopic debridement and lavage are not recommended as treatment for OA, except when there is a clear history of true mechanical locking of an osteoarthritic knee. However joint surgery should be considered if a patient with OA suffers persistent symptoms despite adequate use of the non-pharmacological and pharmacological interventions described above. In this circumstance clinicians should consider an orthopaedic referral to primarily consider joint replacement.

2.5.4 Conclusions

OA represents a process of joint failure with a great variety of risk factors and complex pathogenic pathways. OA confers a huge burden on individuals and health economies alike which is expected to increase in ageing and increasingly obese populations. Current treatments for OA consist of moderately effective non-pharmacological and pharmacological pain-relieving therapies. There are currently no licensed structure-modifying therapies. Joint replacement reduces pain but joint prostheses have a finite life expectancy and revision surgery offers less favourable outcomes.

2.6 Subchondral bone in OA

The subchondral bone (SCB) is the bone tissue adjacent to the hyaline articular cartilage of diarthodial (synovial) joints. The SCB can be divided into two regions, the SCB plate and the subchondral trabecular bone (Figure 10). The osteochondral junction (OCJ) is the interface between the rigid skeleton and the articular cartilage [159] and consists of the deeper calcified and non-calcified cartilage, the tidemark, the cement line and SCB plate

which is cortical bone (Figure 8,Figure 9,Figure 10). The OCJ is an important interface between the subchondral and synovial compartments and plays an integral role in maintaining normal joint physiology but also in the pathogenesis of OA.

Beneath the plate is the subchondral trabecular bone of the epiphysis which contains sensory nerves, blood vessels, endothelium and haemopoeitic bone marrow. The bone and cartilage form an osteochondral functional unit which is responsible for effectively dissipating forces associated with joint movement in order to maintain the integrity of the joint.

Figure 8 The structure of articular cartilage and subchondral bone

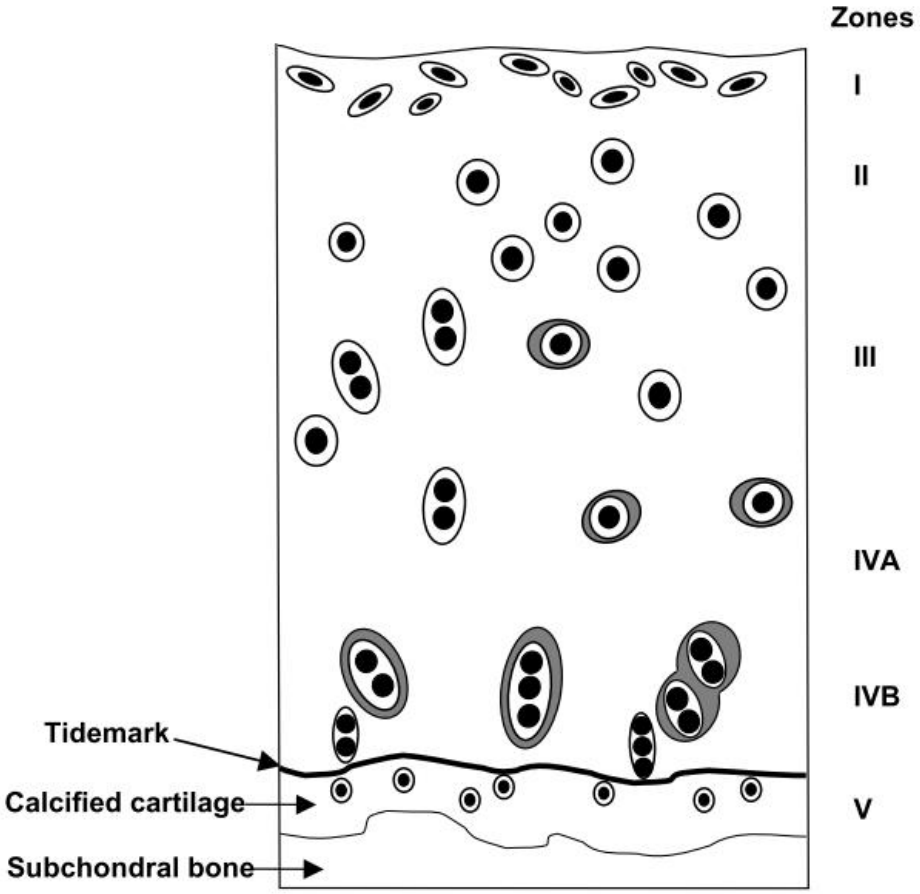

Diagrammatic representation of the zones of articular cartilage and subchondral bone. Reprinted by permission from BioMed Central: BMC Musculoskeletal Disorders, Lyons et al [159].

Figure 9 The anatomy and histology of joint tissues

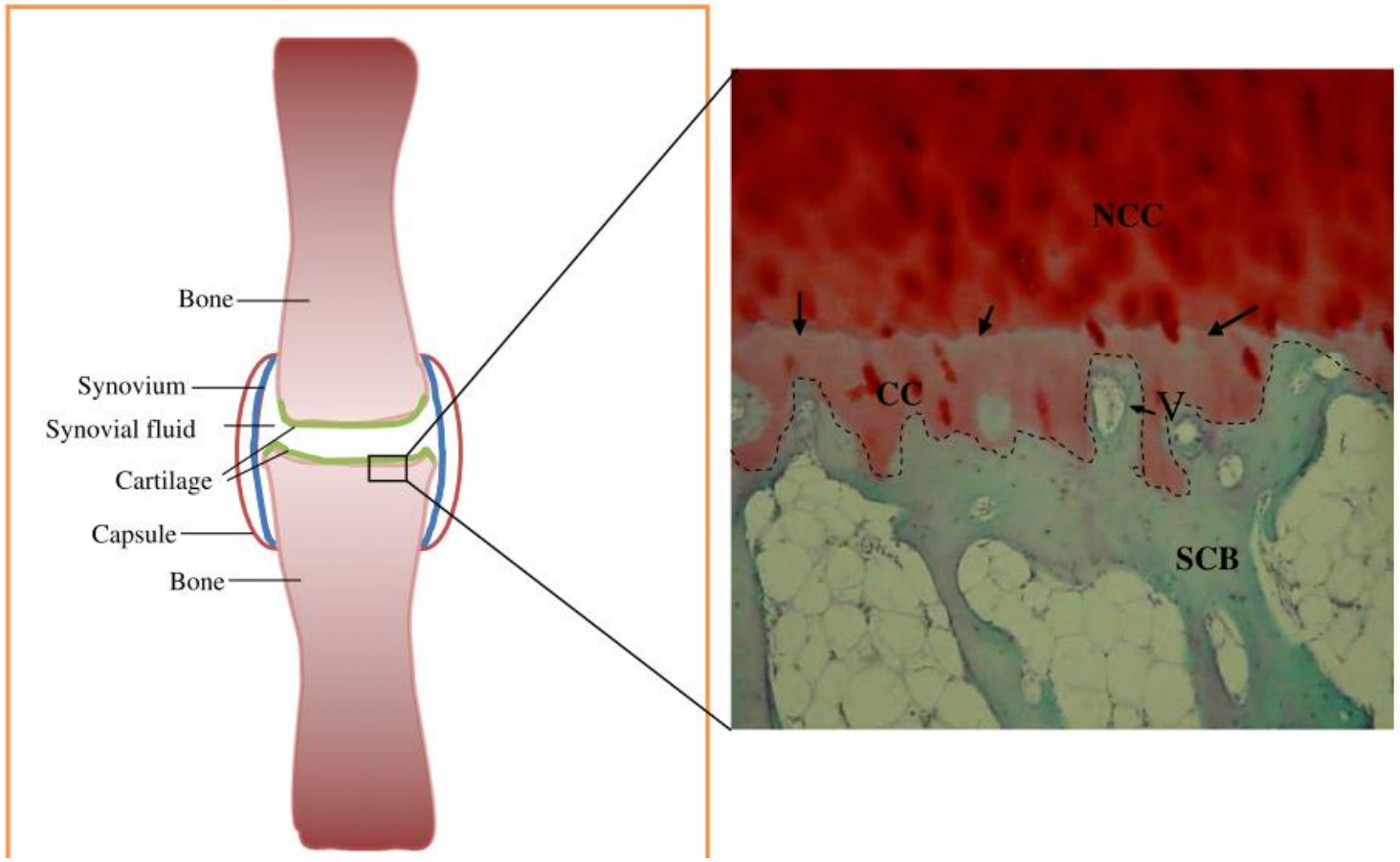

Normal joint structure and osteochondral junction. Photomicrograph showing osteochondral junction in a medial tibial plateau from a patient without arthritis. Scale bars represent 100 μm. NCC — non-calcified cartilage; CC — calcified cartilage; SCB — subchondral bone; Sp — subchondral bone space; V — vascular channel. Arrows denote tidemark; dotted line indicates the osteochondral junction. (Reprinted by permission from Elsevier Ltd: Bone [15])

Figure 10 The structure of articular cartilage and subchondral bone in a normal human joint.

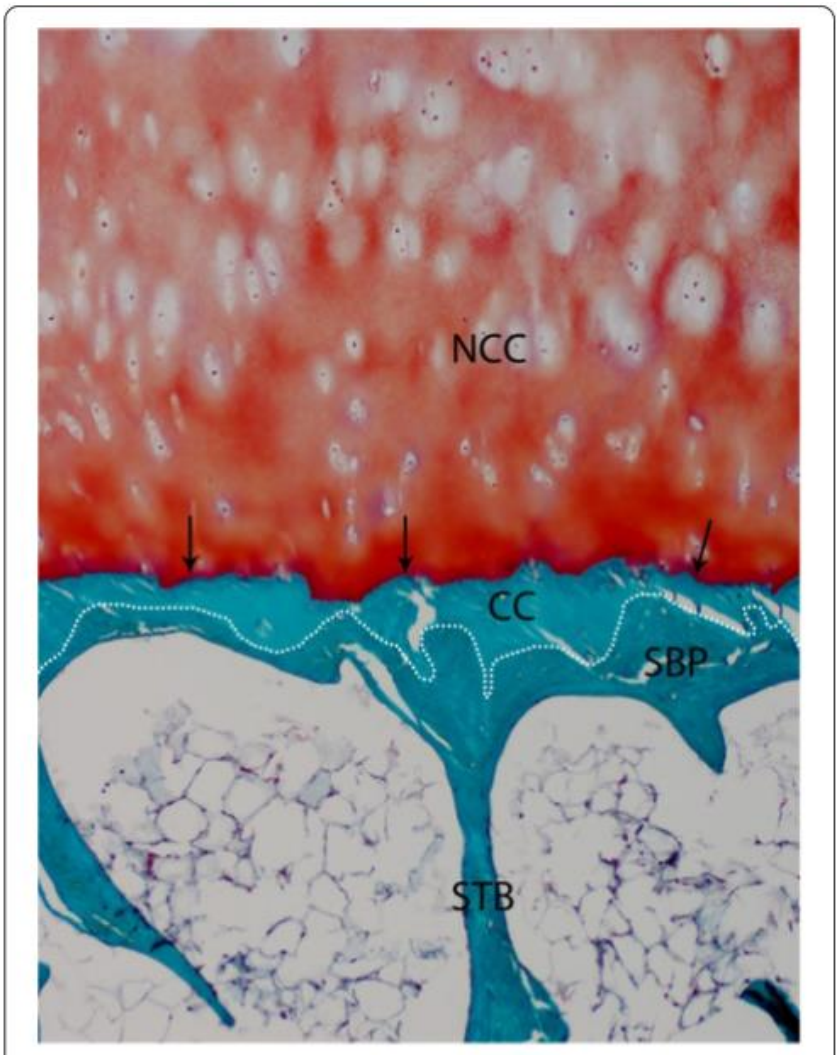

The structure of articular cartilage and subchondral bone in a normal human joint. CC, calcified cartilage; NCC, non-calcified cartilage; SBP, subchondral bone plate; STB, subchondral trabecular bone. Arrows denote the tidemark; the dotted line indicates the cement line. Reprinted by permission from BioMed Central: Arthritis Research & Therapy, Li et al[160].

SCB plays a supportive physiological role in maintaining and sustaining the viability of hyaline articular cartilage through biomechanical and biochemical pathways[161]. The SCB provides biomechanical support through shock-absorbing and supportive functions for protecting the cartilage. SCB physiologically undergoes continuous bone remodelling as part of an adaptive mechanism to appropriately dissipate load through bone. This

involves a tightly regulated homeostatic process of bone matrix formation and resorption, which is driven by osteoblasts and osteoclasts respectively with no overall change in the shape of the bone. Change in shape, architecture and integrity of the subchondral bone is associated with ineffective dissipation of load and subsequent biomechanically driven structural deterioration of the SCB and cartilage and the onset of OA.

In healthy joints there is convincing evidence that the vascular SCB provides biochemical support by the delivery of nutrients to the avascular cartilage through small channels that span the OCJ[161, 162]. The limited permeability for biochemical ‘cross-talk’ afforded by the integrity of the OCJ in healthy joints [163] is characteristically compromised in OA where osteochondral junction channels form which are associated with increased biochemical and cellular ‘cross-talk’ between SCB and cartilage[164]. This interaction is associated with important biochemically driven pathological deterioration of the SCB and cartilage and the onset of OA.

The role of the SCB in the biomechanical and biochemical pathogenesis of OA will be discussed below in terms of change in macroscopic SCB shape, SCB architecture and SCB cellular and biochemical effectors on a microscopic level.

2.6.1 Subchondral bone cellular changes in OA

The evidence describing the role of the SCB in OA pathogenesis at a cellular level is discussed here.

2.6.1.1 Subchondral bone remodelling

In the healthy joint bone turnover is a continuous process of modelling and remodelling carried out by bone forming osteoblasts and bone resorbing osteoclasts. These cells are not ‘permanent’ residents of the bone and are recruited and derived from their prospective progenitor cells when ‘demand’ requires the remodelling of bone. This is a carefully balanced homeostatic process intended to maintain the integrity of the osteochondral unit.

Remodelling involves resorption of ‘old bone’ by osteoclasts and the replacement with new osteoid secreted by osteoblasts. The first stage involves osteoclastic recruitment and activation which causes bone

resorption. Subsequently osteoblast precursors are recruited which proliferate and mature into osteoblasts before producing new bone matrix (osteoid). This matrix is then mineralised to produce new bone which finalises the bone remodelling (Figure 11).

Osteocytes are a third cell type and are the most abundant cell type in bone and are ‘permanent’ residents of bone, derived from osteoblasts. They have a dendritic morphology with extensive connectivity throughout the mineralized matrix of bone. They reside within the mineralised bone matrix in lacunae where they are integrated into the bone structure, able to perceive mechanical load and are connected to other osteocytes in a multicellular network via the lacunar-canalicular system. This is believed to represent the means by which osteocytes act as bone mechanosensors and respond to mechanical stimuli to maintain the integrity of SCB by coordinating osteoblastic and osteoclastic activity (Figure 16). These physiological pathways carefully balance catabolism and anabolism of the osteochondral unit to repair damaged tissue. When the extent of damage exceeds the capacity to repair it, the imbalance in the anabolic and catabolic molecular and cellular pathways leads to the pathogenesis of OA.

Figure 11 Physiological subchondral bone remodelling

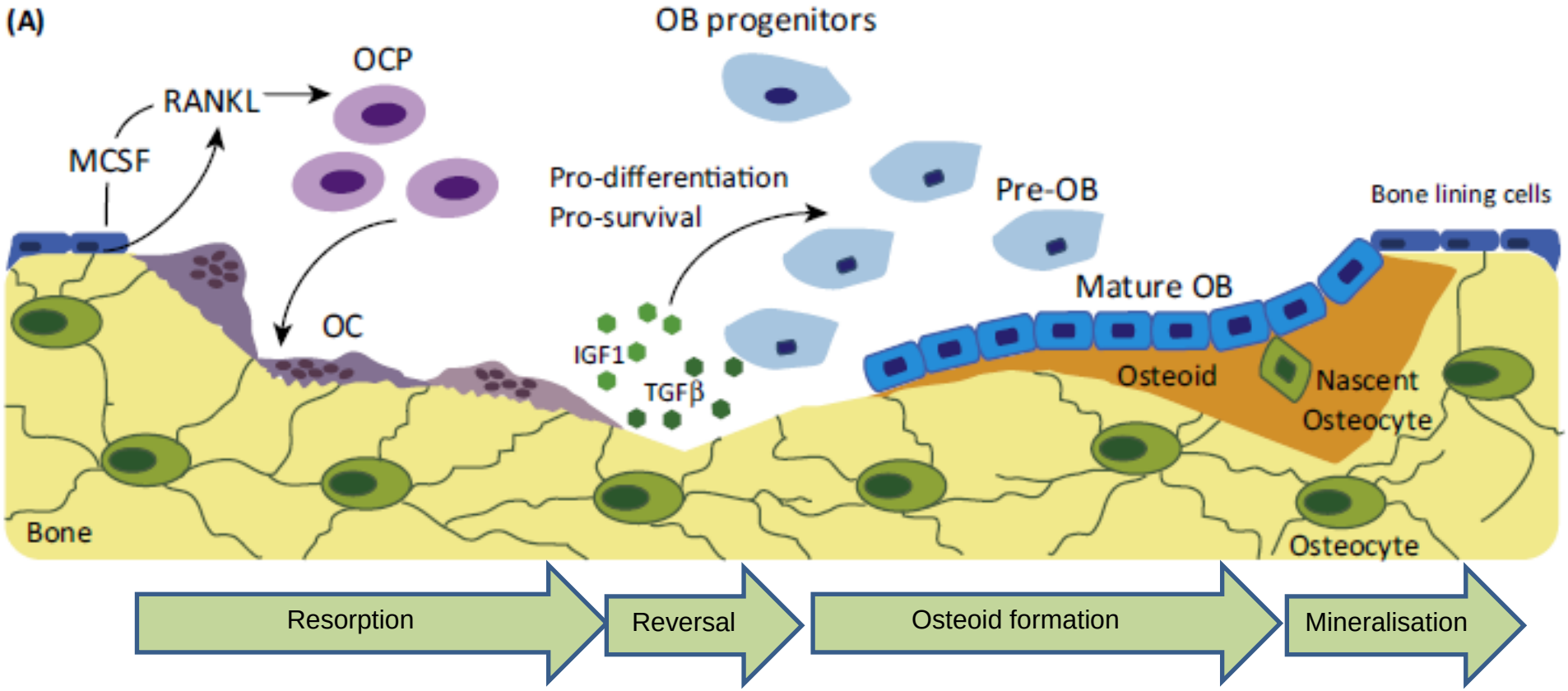

Osteoclasts–osteoblast interactions in the basic multicellular unit (BMU). (A) Osteoclasts (OC) differentiate from OC precursors (OCP) under the influence of MCSF and RANKL produced by osteoblast (OB) lineage cells including osteocytes. As OCs create a resorption pit, growth factors, including TGFb and IGF1, are released from the bone matrix. These growth factors may recruit mesenchymal osteoblast progenitors and promote their differentiation into mature cells that secrete osteoid to fill the area of resorbed bone. Some OBs differentiate further into matrix-embedded osteocytes. IGF1, insulin-like growth factor 1; MCSF, macrophage colony stimulating factor; RANKL, receptor activator of NF-kB ligand; TGFb, transforming growth factor b. Reprinted by permission from Elsevier Ltd: Trends Mol Med, Charles et al [165]

Subchondral bone is a dynamic structure and mechanical stimulation is a major environmental regulator of SCB, which remodels in response to load. Wolff's law describes this concept by stating SCB responds and adapts to repeated load. Increased load is associated with SCB microfractures which are repaired by homeostatic remodelling to maintain the integrity of the SCB[166]. Similarly SCB also remodels with decreased load such that in zero gravity, cosmonauts in space for six months experience significant reduction in tibial cortical and trabecular bone mass measured by quantitative computerised tomography[167] and dual-energy X-ray absorptiometry[168].

Osteocytes are the putative mechanosensors[169] that coordinate the remodelling. This is supported by a study where ablation of osteocytes (but not osteoblasts) in mice resulted in a resistance to disuse-induced bone resorption when the hind limbs are unloaded[170]. The pathway of mechanotransduction is not clearly described but in-vitro studies report osteocyte vesicular ATP release is proportional to the magnitude of loading and may be an acute mediator of mechanical signalling[171].

Osteocytes may promote osteoclastic resorption through the same biochemical mechanisms used by osteoblasts (Figure 12).

Osteoclastic differentiation and activation is promoted when receptor activator of nuclear factor kappa Beta ligand (RANKL) binds to its receptor (RANK) on osteoclasts and their precursors. Osteoprotegerin (OPG) is a decoy receptor of RANKL and hence inhibits osteoclastic activity and bone resorption. Osteocytes in vitro respond to unloading with a greater expression of RANKL than OPG[172] which is likely to increase osteoclastic resorption[173, 174].

Figure 12 The RANKL and OPG system

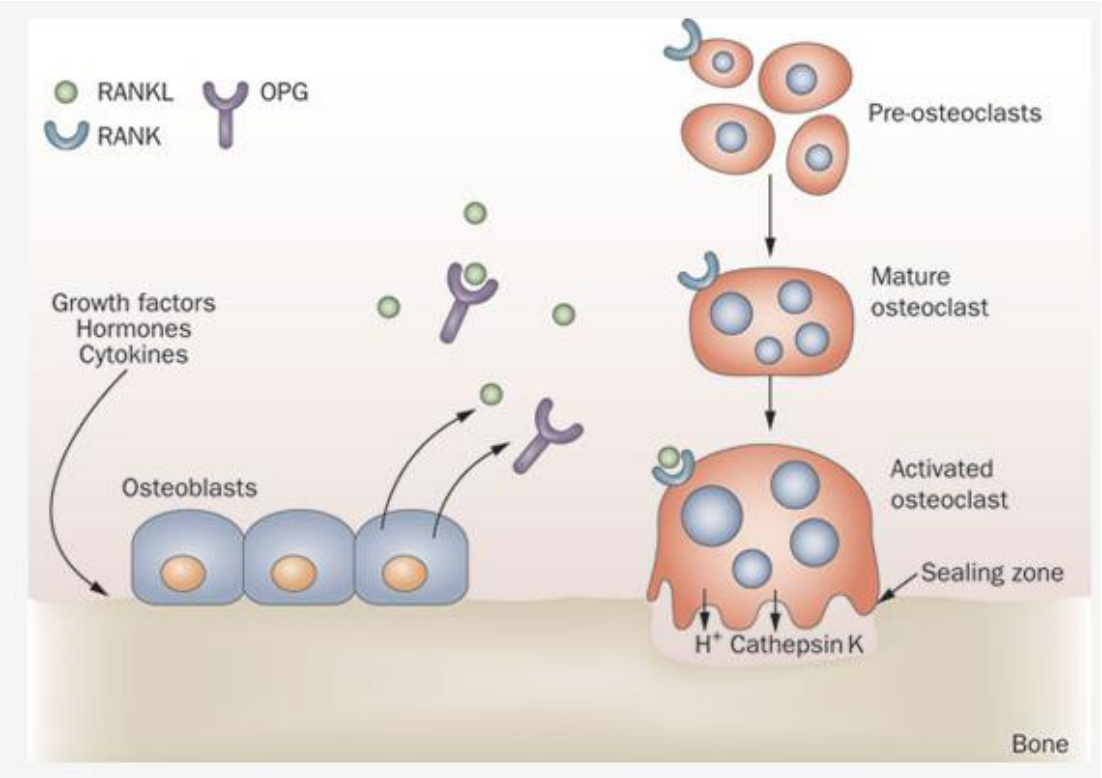

RANKL expressed by osteoblast lineage cells binds to RANK on the surface of pre-osteoclasts and mature osteoclasts, resulting in increased bone resorption via an increase in osteoclast differentiation, activity, and survival. OPG is a 'decoy receptor', also produced by osteoblasts, that binds to RANKL, preventing RANKL binding to RANK and thereby inhibiting osteoclastic bone resorption. It is the balance of RANKL and OPG that determines the ultimate rate of bone resorption. A high rate of bone remodeling may be due to an excess of RANKL over OPG. (Reprinted by permission from Macmillan Publishers Ltd: Nature Reviews Rheumatology [175]. Copyright 2011).

Figure 13 The osteocytic response to microdamage in SCB

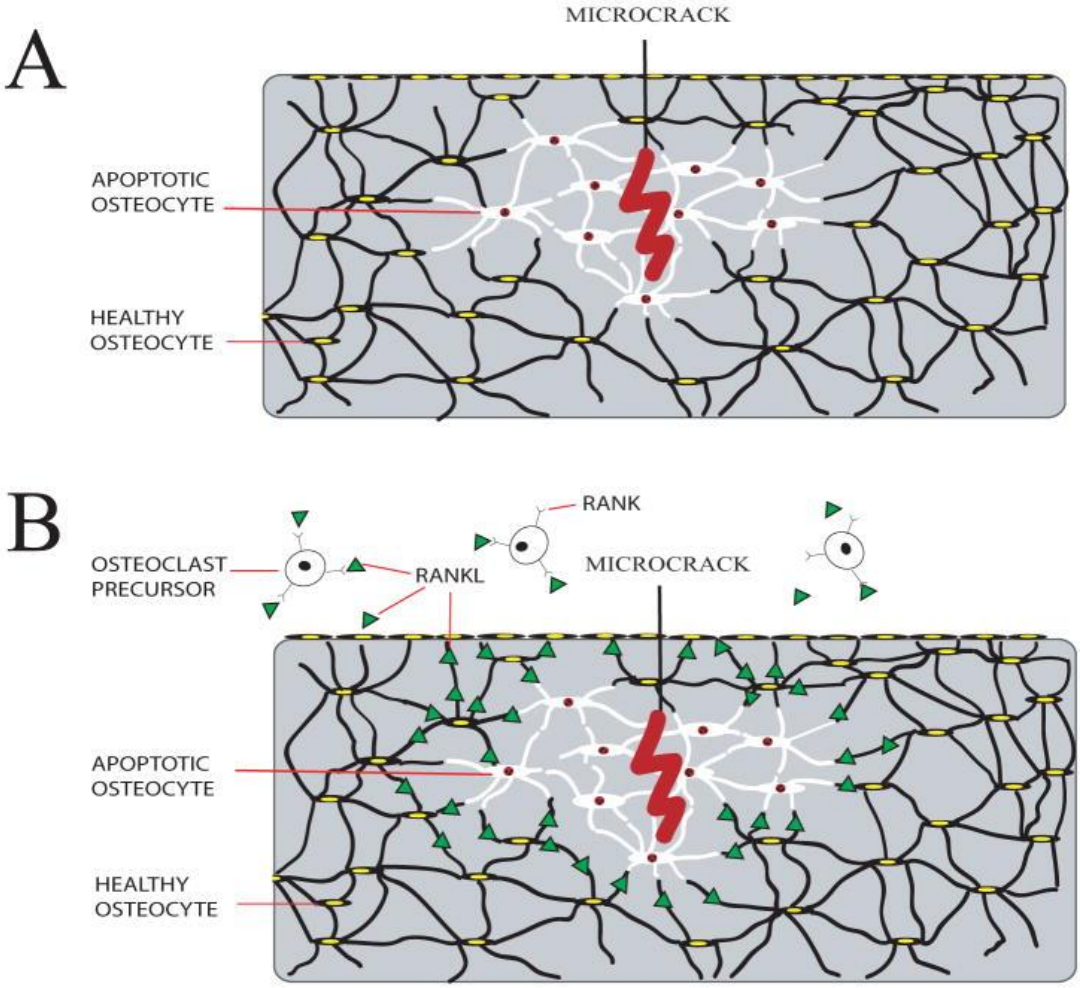

Schematic summary of the role of osteocytes in triggering bone resorption. A) Microcracks in bone caused by fatigue loading lead to highly localized osteocyte apoptosis (shown in white) surrounding the microcrack. B) Recent studies show that surviving osteocytes immediately neighboring the region of apoptosis upregulate production of pro-osteoclastogenic signals (i.e. RANKL, and others). Springer Calcif Tissue Int, Osteocytes: master orchestrators of bone, 2014 Schaffler et al, reprinted with permission of Springer [169].

Microfractures, microcracks or microdamage are well recognised and prevalent features of OA which involves the trabecular bone, the SCB plate and the calcified cartilage.[176, 177] They are observed after overloading[178] and may be linear or diffuse[166]. Typically there is local osteocyte apoptosis in the region of the microcrack (Figure 13).

The osteocytes that survive in the adjacent regions to the region of apoptosis then upregulate osteoclastogenic signals including RANKL. Osteocytes that are unaffected and at a significant distance from the microcrack do not upregulate osteoclastogenic signals. Therefore there is focal osteoclast recruitment and bone resorption as part of a microdamage repair process (Figure 13). Osteocytes appear to respond to the linear form of microcracks by promoting remodelling with osteoclastic bone resorption of the compromised tissue followed by the formation of new osteoid by osteoblasts (Figure 13). However osteocytes do not promote remodelling to diffuse areas of microdamage[166]. This supports the concept that OA represents a failure to meet the demands for ‘repair’ of the joint tissues. SCB microdamage is considered to be involved in the pathogenesis of OA both at initiation and progression stages as the accumulation of SCB microdamage exceeds the rate of repair[176]. Repeated loading of canine femurs was associated with an accumulation of such microdamage. A threshold effect was observed whereby the elastic modulus (stiffness) decreased after a sufficient accumulation of microdamage in the trabecular bone was accrued which implicates microdamage in biomechanical model of OA pathogenesis[179].

Another pathway that may permit osteocytes to coordinate remodelling is via the canonical Wnt signalling pathway, which promotes osteblastic maturation and bone formation[180]. Sclerostin is an inhibitor of a co-receptor low-density lipoprotein receptor-related protein 5 (LRP5) of the canonical Wnt signalling pathway and hence it inhibits bone formation[181]. Osteocytes produce Wnts and sclerostin[172]. In vivo experiments in rat ulnar bones indicate that sclerostin is produced in abundance in unloaded states which inhibits new bone formation. When ulnar load increases mechanotransduction by osteocytes dramatically reduces sclerostin

production which disinhibits the osteoblastic bone formation and hence new bone formation commences (Figure 14)[181].

Immobility and zero gravity in humans are well-recognised risk factors for net bone loss[167, 168]. Amongst postmenopausal women with and without immobility , sclerostin levels were significantly greater amongst immobile women and conferred significantly reduced bone formation biomarker and quantitative bone volume of the calcaneum[182].

Human femoral head specimens, from joints with OA undergoing arthroplasty, had significantly reduced bone osteocyte expression of sclerostin and increased osteoblast activity compared to normal controls. This highlights the importance of sclerostin and its potential role in the osteocyte-coordinated pathogenesis of OA [183]. Therefore osteocytes have the potential to sense and adapt to the mechanical demands upon the SCB by coordinating bone formation and resorption via osteoblastic and osteoclastic regulation with RANKL/OPG and Wnt/sclerostin(Figure 15, Figure 16). However these homeostatic processes fail in OA.

Figure 14 Sclerostin mediation of LRP5 signalling during mechanical loading

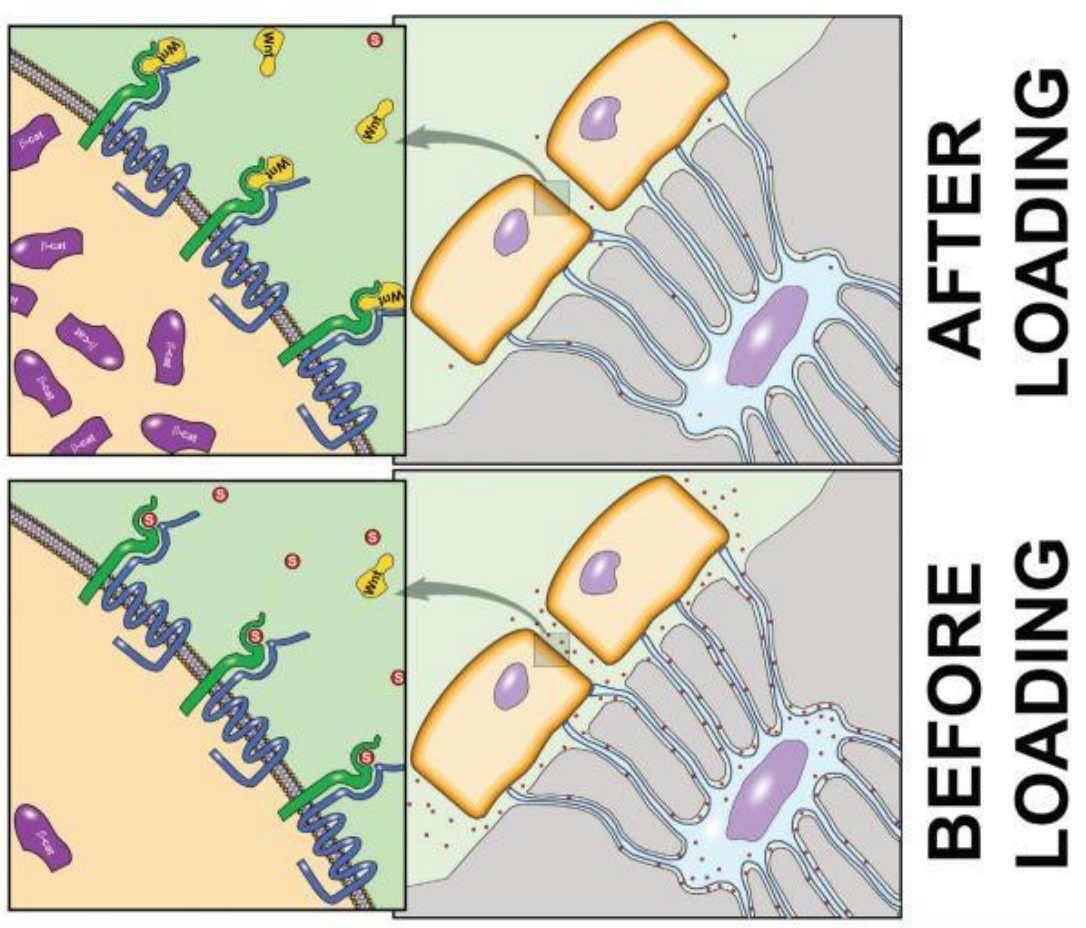

The role of sclerostin in Lrp5 signalling before and after mechanical loading. (Bottom) Before loading in the unstimulated state, dendritic osteocytes secrete plenty of sclerostin (purple circles). This inhibits Wnt signalling in the overlying osteoblasts by LRP5 receptor antagonism.

(Top) After mechanical loading, in the stimulated state, there is a substantial reduction in sclerostin levels which increases LRP5 availability for Wnt binding, which disinhibits the canonical Wnt intracellular signalling pathway that promotes bone formation. Reprinted with permission of American Society for Biochemistry and Molecular Biology, Journal of Biological Chemistry [181]

Figure 15 The mechanism by which osteocytes may coordinate bone remodelling

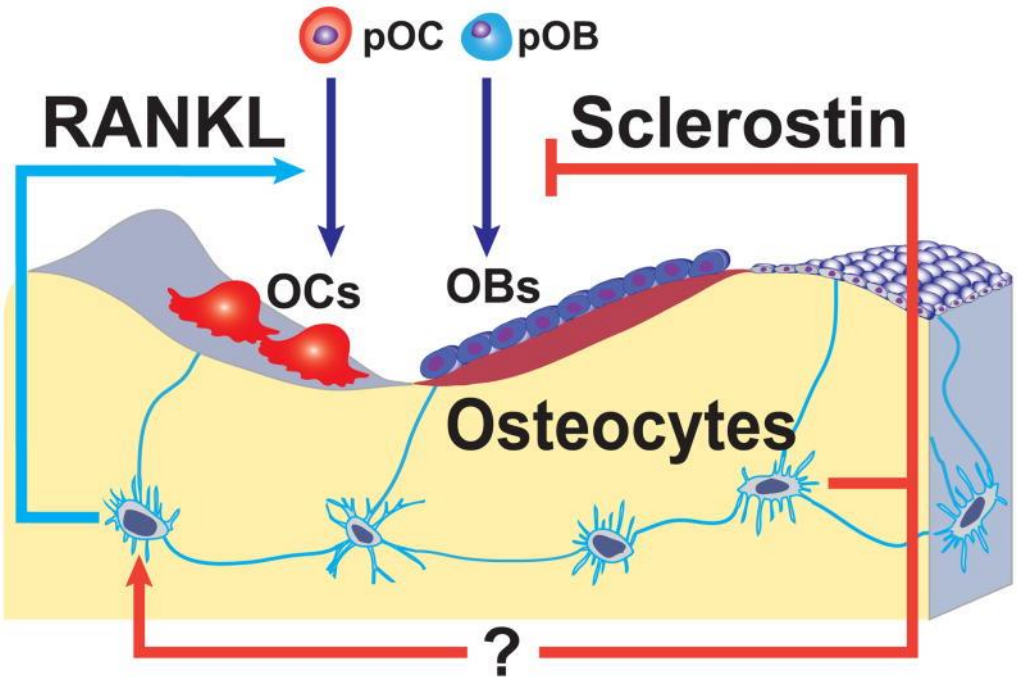

Osteoclasts (OCs) and osteoblasts (OBs) within a cancellous BMU are shown as being derived from precursors (pOC and pOB). (?) sclerostin may also stimulate RANKL expression by osteocytes. Reprinted by permission from John Wiley & Sons Ltd: J Bone Miner Res, [184]

Figure 16 The mechanism by which osteocytes may coordinate bone homeostais through mechanotransduction.

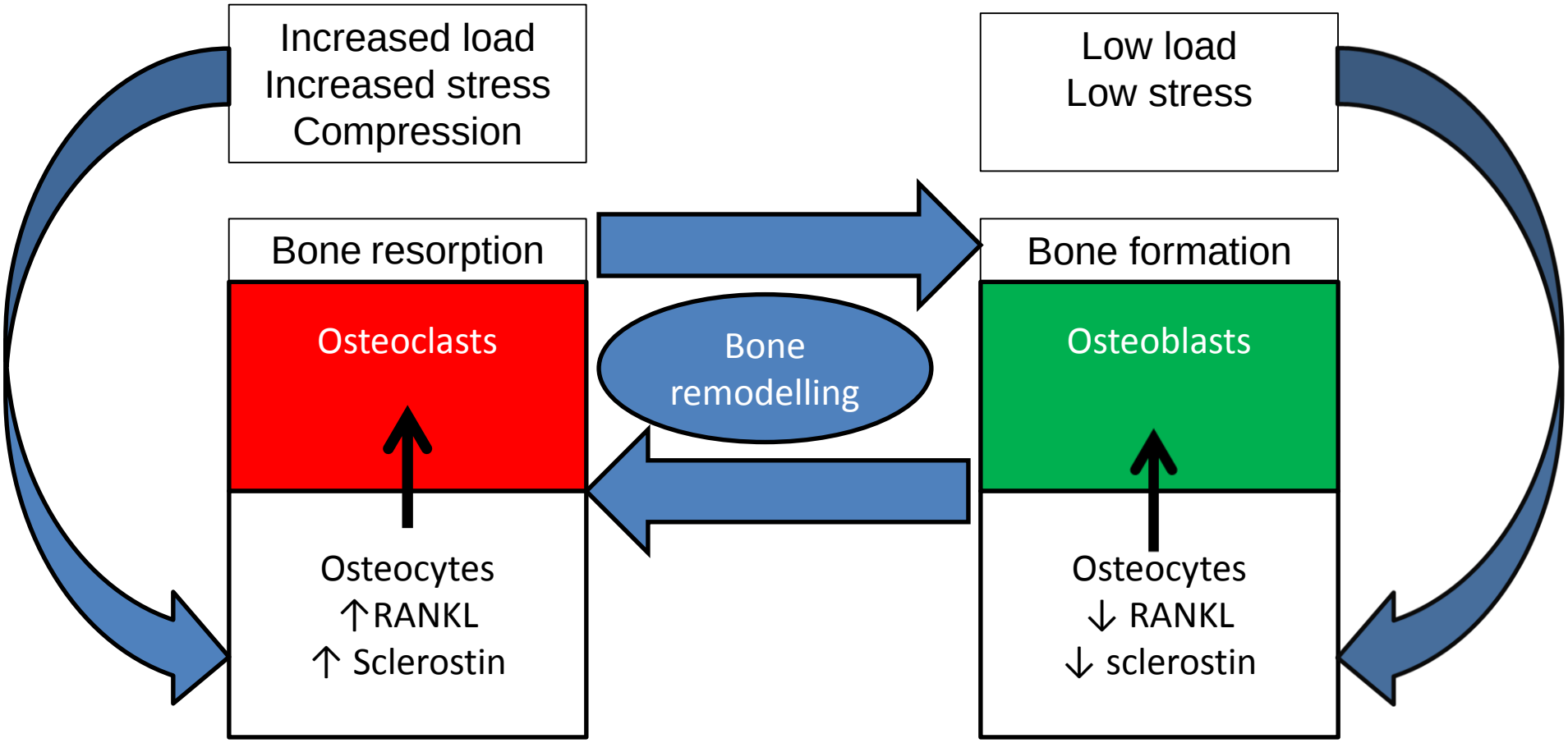

Osteocytes may orchestrate functional adapation in the subchondral bone by a process of mechanotransduction. This image summarises the role of osteocytes in bone homeostasis and is a summary of evidence described in the following articles [169, 181, 185]

2.6.1.2 Subchondral bone and the osteochondral junction

In early knee OA SCB remodelling involves a net osteoclastic resorption (2.6.2.2 Early OA). This includes an initial thinning of and channel formation through the SCB plate in early OA in canine [186, 187] and rabbit cruciate ligament transection models[188]. Channels within the SCB plate can be seen extending towards the cartilage with osteoclasts at the advancing edge in human tibial plateau explants at the time of knee replacement for OA[189]. This SCB plate resorption ultimately compromises the selective porosity of the normal OCJ after the OCJ channels completely traverse the OCJ [164, 176].

When intact the OCJ only permits the passage of nutrients but the presence of OCJ channels permits pathogenic biochemical ‘cross-talk’ between SCB and the cartilage and synovial compartment. This ‘cross-talk’ heralds the cartilage catabolism associated with a neurovascular invasion of the cartilage from the SCB. Osteoclasts and catabolic biochemical agents from the SCB also pass into the cartilage through the OCJ channels. This process results in cartilage fibrillation and fissuring which may progress so that fissuring occurs down to these OCJ channels. This permits biochemical and cellular interaction of the synovial compartment with the SCB and vice versa which promotes further catabolism within the osteochondral unit (Figure 17). These processes may increase the failure of the osteochondral unit to effectively dissipate load. This may increase loading within the joint, driving further SCB microdamage and SCB remodelling which may promote a vicious cycle of structural deterioration within the osteochondral unit.

The incursion of these neurovascular structures may extend into the non-calcified articular cartilage, osteophytes and even inner regions of menisci[190, 191]. Typically there is calcification and ossification of the cartilage around these channels which in part drives extension of the calcified cartilage region and the tidemark which may cause further biomechanical adversity, loading and microdamage for the SCB. Therefore the vascular incursion of cartilage heralds structural progression.

Figure 17 The pathological changes in the osteochondral unit in OA

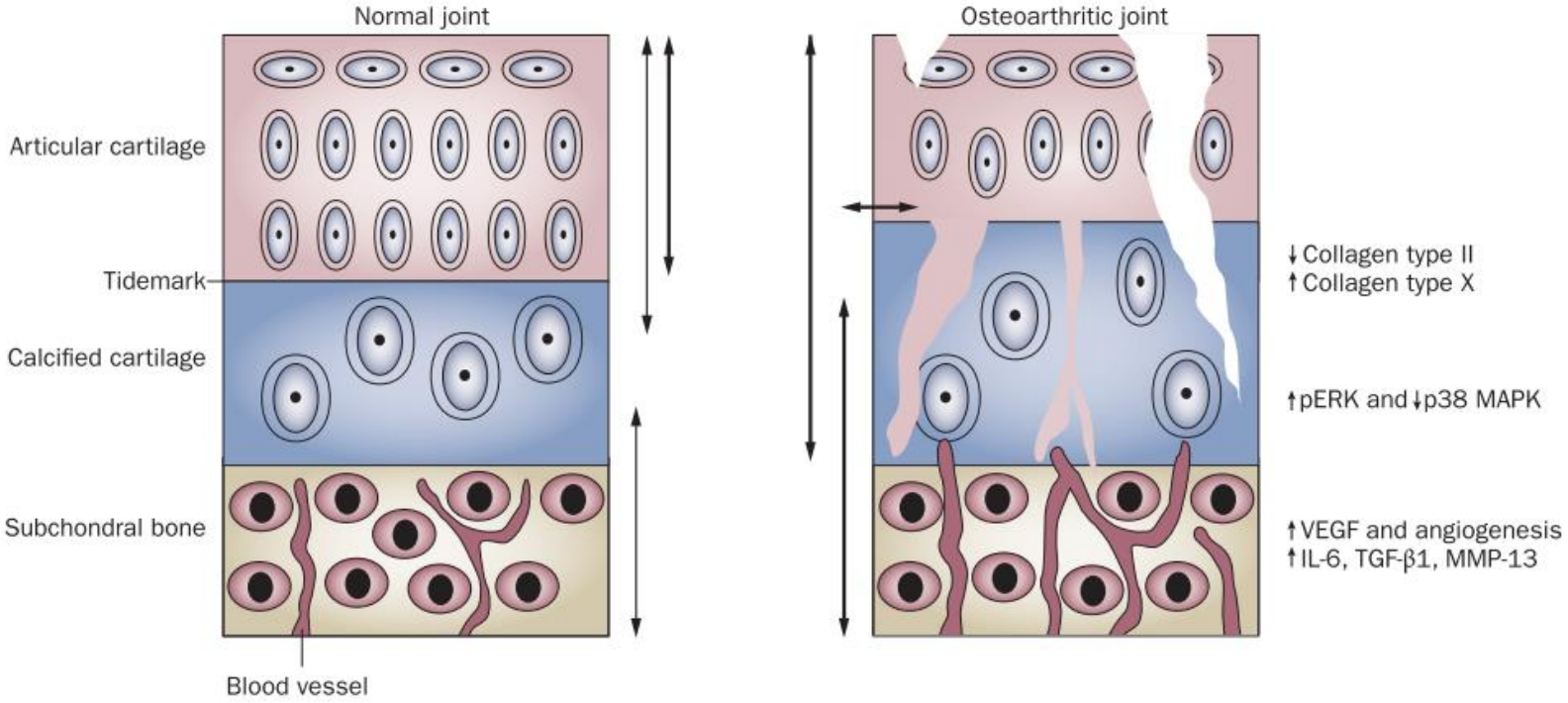

Complex changes in the bone–cartilage unit increase the flow of fluid and solutes in osteoarthritic joints. In OA, the permeability of the bone–cartilage unit is increased, through subchondral angiogenesis and the development of cartilaginous cracks and fissures, and patches of uncalcified cartilage that extend into the calcified layer. An increase in hydraulic conductance also leads to fluid exudation and further damage to the articular cartilage. OA subchondral bone osteoblasts have an activated phenotype characterized by production of IL-6, MMPs and angiogenic factors. Articular chondrocytes lose their stable phenotype and express markers of terminal differentiation. The tidemark—the demarcation line between calcified and articular cartilage—shifts upwards, representing a thinning of the articular cartilage, thereby increasing strain in the bone–cartilage unit. Reprinted by permission from Macmillan Publishers Ltd: Nat Rev Rheumatol [164], copyright 2011.

The role of the SCB in the pathogenesis of OCJ channel formation and the neurovascular incursion is discussed here.

Osteoclastic activity is increased in OA SCB and may be responsible for the migration of osteoclasts into the cartilage from subchondral pits[192], through the SCB plate OCJ channels towards the joint surface. These osteoclasts release multiple matrix metalloproteinases (MMPs) and cathepsin K which may degrade the articular cartilage matrix and promote the incursion of neurovascular channels into the articular cartilage[193, 194].

The formation of OCJ channels is typically associated with an infiltration of inflammatory cells (e.g. macrophages) into the SCB marrow spaces[189] which is likely to promote osteoclastic activity along with catabolic ‘cross-talk’ that drives cartilage degradation[164].

Osteoblasts in osteoarthritic SCB plates may also remotely promote the degeneration of articular cartilage by ‘cross talk’. Firstly OA osteoblasts may promote the vascular invasion of articular cartilage by SCB because they have an upregulated expression of the angiogenic growth factor hepatocyte growth factor which appears to cross the OCJ from the SCB into cartilage in early OA (before significant cartilage damage is present)[195]. Secondly in vitro experiments of osteoblasts, isolated from bones affected by OA, express cytokines that promote remodelling that appeared to inhibit the expression of chondroprotective genes (e.g. aggrecan) in chondrocytes whilst promoting the expression of genes for MMPs[196]. This indirectly promotes cartilage catabolism.

Chondrocytes are also capable of responding to increased load and by mechanotranduction release several pathogenic molecules including vascular endothelial growth factor (VEGF) which drives osteoclastogenesis in the SCB and migration of osteoclasts into the cartilage where they express MMPs[189]. However the capacity of chondrocytes to repair and remodel the extracellular matrix that surrounds them is comparatively limited relative to the bone matrix and its cellular components[197].

Both angiogenesis and neurogenesis are linked by common pathways that are stimulated by the release of proangiogenic factors like VEGF and beta-nerve growth factor (beta-NGF) in response to chondrocyte loading. This

drives the incursion of sensory and sympathetic nerves along with new blood vessels into a previously avascular and aneural cartilage[189, 198]. There is increased nerve growth factor expression within these vascular channels which drives sensory nerve growth.

Sensory innervation and vascular incursion of hyaline articular cartilage has been observed across a spectrum of early to advanced OA[198]. This provides a plausible mechanism for nociception and biochemically mediated progression in structural degeneration of the articular cartilage.

The formation of osteophytes and normal skeletal development have remarkably analogous mechanisms which are discussed here to explain the rationale for the SCB representing a treatment target in OA (2.6.4 Can the OA Subchondral Bone be therapeutically targeted?).

In-vitro studies indicate chondrocytes mediate physiological skeletal development by conversion of cartilage into skeleton (endochondral ossification). These mechanisms are in many ways analogous with pathogenic mechanisms in OA which includes signalling via Wnt pathway[180]. For endochondral ossification in the developing skeleton to occur chondrocytes produce MMPs which degrade cartilage and promote an invasion of healthy cartilage, by new blood vessels along with osteoclasts and osteogenic cells, mediated by vascular endothelial growth factor (VEGF). The activation of osteoclasts appears to be essential for subsequent endochondral ossification[199, 200].

Osteophyte formation occurs by an analogous process of endochondral ossification, initiated by vascular invasion of cartilage along with osteoclastogenesis [201-203] and concomitant increased bone turn over. However the notable exception to this analogy is that osteophytosis occurs in the mature skeleton (Figure 18).

Figure 18 Osteophyte formation in the mature skeleton

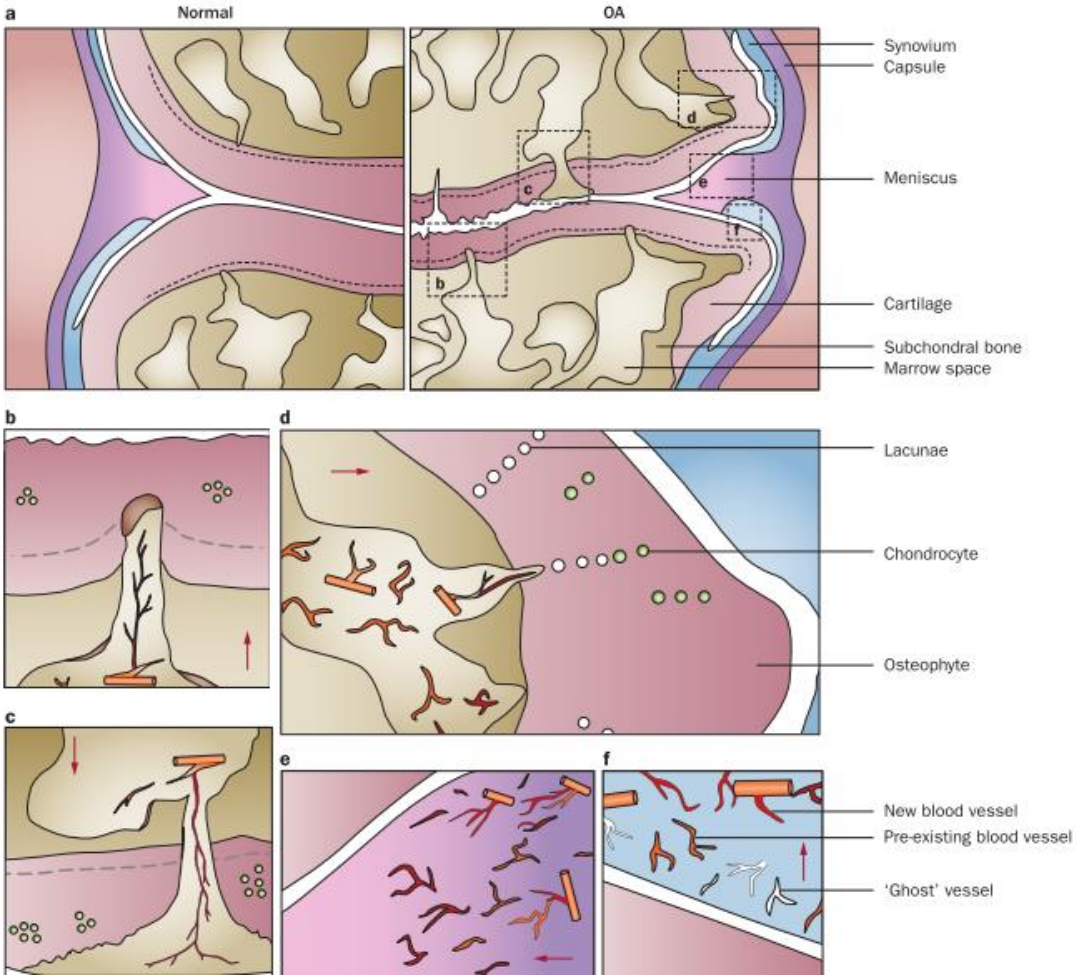

Sites of angiogenesis in the OA knee. a | The structure of the normal knee (left) and sites of angiogenesis in OA (right). The synovium is continuous with the periosteum and apposed to cartilage. The meniscus merges with the collagenous capsule. Subchondral bone contains marrow spaces. The tidemark between calcified and noncalcified cartilage is indicated by a dashed line. b | Osteoclasts and chondroclasts (brown) cut channels through the tidemark at the osteochondral junction and invade the normally avascular cartilage. Channels are occupied by vascularized mesenchymal tissue and endochondral ossification results in a bone cuff surrounding the channel. Pre-existing blood vessels are shown in orange, neovasculature in red, and chondrocytes as green circles. c | A fissure from the articular surface communicates with subchondral bone spaces. Vascularized mesenchymal tissue extends from the subchondral bone through the fissure and over the articular surface forming pannus. d | Osteophyte formation resulting from cartilage deposition. Reprinted by permission from Macmillan Publishers Ltd: Nat Rev Rheumatol.[190], copyright 2012

2.6.2 Subchondral bone architecture and remodelling in OA

The supporting trabeculae of the subchondral trabecular bone, arise from the SCB plate and provide important shock-absorbing function to the overlying cartilage by dissipating force across the joint surface with a gradual transition of strain and stress. The trabecular bone is a dynamic structure and, through the process of bone remodelling, adapts to the applied mechanical forces. Julius Wolff, a surgeon and anatomist from Berlin, described the relationship between bone geometry and mechanical influences on bone in 1892. Wolff's hypothesis states that the material properties and distribution of bone are determined by the direction and magnitude of applied load so that it is a better structure to resist such loads [197]. He similarly hypothesised that a reduction in applied load to a bone will result in a bone catabolism such that bone structure is intended to only withstand the loads applied to it.

Functional adaptation of bone, as proposed by Wollf, is mediated by the cells in bone. This includes osteocytes that are putative mechanosensors (along with chondrocytes), osteoclasts and their progenitors that resorb bone and osteoblasts that deposit bone matrix (see 2.6.1 Subchondral bone cellular changes in OA). The remodelling adaptation within the SCB ensures that biomechanical load is effectively dissipated through the osteochondral functional unit. Any alteration to the material properties of either the articular cartilage or the SCB that sufficiently impairs the ability to effectively dissipate load, is associated with the synchronous structural degeneration in cartilage and SCB[197, 204] involving biomechanical and biochemical pathways. Controversy remains over whether the bone or the cartilage is the first structure to 'fail' in the natural history of human OA. This section describes the pathological changes in SCB architecture in both early and established OA and highlights a biphasic response in SCB observed in animal models with significant similarities in humans. This section also describes the potential for SCB as an early target in the prevention of OA and previous attempts at targeting the bone as a treatment in OA.

2.6.2.1 Established OA and structural progression

The diagnostic criteria of ROA published in 1957 by Kellgren & Lawrence identifies subchondral sclerosis and osteophyte formation as pathognomonic of OA[19]. The Altman atlas also recognises subchondral sclerosis as a dichotomous outcome[84]. The architectural changes of this change will be discussed here.

Sclerosis implies a hardening or stiffening of the subchondral bone which has been hypothesised to represent a failure of SCB to dissipate load which promote cartilage degeneration.

In knee OA with established subchondral sclerosis, trabecular bone microarchitecture, mass and density can be measured using dual-energy x-ray absorptiometry (DXA), fractal signature analysis (FSA) [205], quantitative computed tomography[187], magnetic resonance imaging [206] and histologically [207] to determine the correlation with this pathognomonic feature. Joint tissue samples have also be assessed mechanically [207].

Amongst 3048 knees in the Framingham OA cohort, radiographic subchondral sclerosis was independently and strongly associated with ipsilateral increase in bone mineral density(BMD)[208]. A greater BMD was independently associated with subsequent joint space narrowing in the medial compartment[208, 209] and cartilage defect development[210].

FSA characterises the complicated histomorphometry of SCB by providing a description of trabecular SCB microarchitecture and directional physical properties from trabecular size, number, spacing and cross-linking on radiographic images[211, 212].

Buckland-Wright and colleagues observed that increasing severity of knee ROA and JSN was associated with thicker trabeculae with less space between trabeculae[212] (Figure 19)

Figure 19 Thicker and less well spaced trabeculae

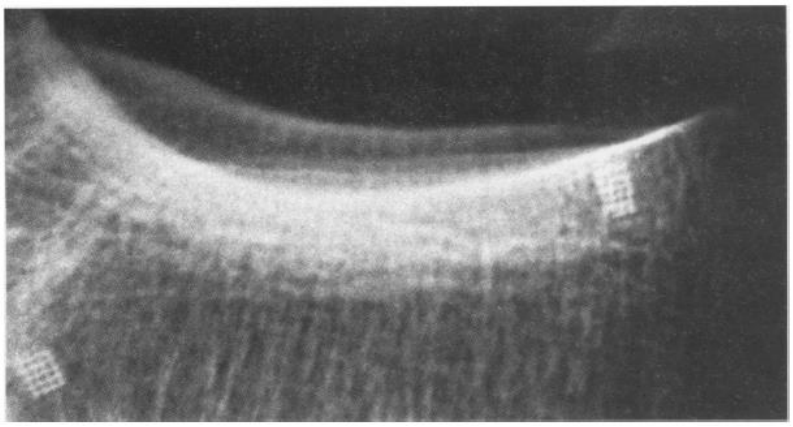

Part of a macroradiograph of an OA knee joint showing subchondral sclerosis showing trabeculae. These are thicker and less well spaced than in normal bone. Reproduced from Annals of Rheumatic diseases, Buckland-Wright et al, 55,1996, [212]. with permission from BMJ Publishing Group Ltd

In 138 knees with symptomatic and ROA, a higher baseline vertical or lower baseline horizontal trabecular fractal signature was strongly and independently associated with progression in JSN over three years[211]. Furthermore amongst knees awaiting joint replacement, increased SCB sclerosis, as represented by decreased trabecular spacing was independently associated with a lower minimum JSW [213].

Lo and colleagues examined the MRI knee scans of 482 participants of the Osteoarthritis Initiative. Increasing JSN grade was associated with increasing proximal tibial SCB BMD, trabecular thickness, trabecular number, bone volume fraction (a measure of SCB sclerosis) and reducing inter-trabecular spacing [206]. Bone volume fraction is the proportion of trabecular tissue volume within a defined volume of bone (Figure 20). Similar observations are made using volumetric computed tomography of knee and hips with OA[214, 215].

A longitudinal study by Dieppe and colleagues observed an association between increasing signal in the subchondral bones of knees (a surrogate of bone turnover) with established OA and subsequent increasing JSN (a surrogate of cartilage loss)[216].

Figure 20 Increasing bone volume fraction of OA SCB

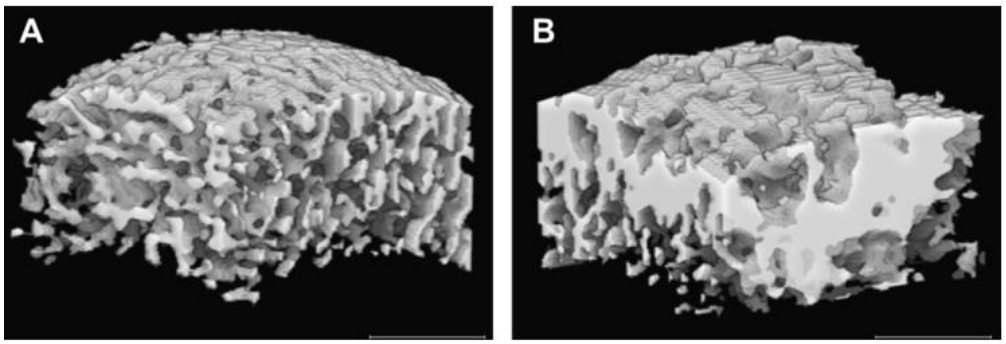

These are 3D reconstructed images of the subchondral bone in a normal (A) and OA (B) femoral heads. Reprinted by permission from Elsevier Ltd: Osteoarthritis and cartilage [215].

Radin and Rose in 1973 identified that increasing load placed through rabbit knees was associated with SCB trabecular microfracture[217], reversible stiffening of the SCB[218] accompanied by the earliest osteoarthritic changes in chondrocyte metabolism. Radin and Rose hypothesised but never proved that the increased volume and thickness of the SCB in OA was associated with increased stiffness which increased shear forces in the overlying cartilage which led to cartilage degeneration [219].

Radin and Rose assumed that bone volume is the only determinant of SCB stiffness. However other physical properties of SCB such as apparent density (reflecting the mineralized bone structural density in g/cm3) and the extent of microdamage accumulation are also major determinants of the mechanical properties and stiffness of SCB [179] (see 2.6.1.1 Subchondral bone remodelling).

Subsequent studies, that are described below, demonstrated that a greater volume of hypomineralised bone conferred a lower SCB stiffness after adjusting for bone volume fraction.

In humans the SCB of femoral heads removed at the time of total hip replacement for end stage OA were compared with normal autopsy controls using histological and biomechanical analyses.

Amongst femoral heads with OA, a significantly increased bone volume density with a reduction in mineralisation is observed [220, 221]. A significant excess of type I collagen is synthesised in the OA SCB, and the deposited collagen was significantly less mineralised with a substantially reduced calcium to collagen ratio [222]. While femoral heads with OA have significantly more hypomineralised SCB than controls, this appears to confer a significantly lower SCB stiffness only after adjusting for bone volume fraction[207]. This implies that the stiffness per unit of the hypomineralised bone volume is reduced. Apparently conflicting results were published by Pugh and colleagues who described significantly increased stiffness in SCB adjacent to subtle (histochemical) cartilage damage in cadaveric femoral heads compared to cadaveric femoral heads. However it is important to note that there was no adjustment for bone volume fraction and none of the femoral heads had subchondral sclerosis or macroscopic OA with ages ranging from 20-66 years[223].

Finally Day[224] and colleagues and Ding[225] collectively observed that amongst proximal tibia removed from cadavers micro-computed tomography, those with cartilage damage had increased bone volume fraction, trabecular thickness and reduced trabecular spacing compared to those without cartilage damage. Ding ensured those with and without OA were age- and gender-matched. Day mechanically tested the proximal tibiae of cadavers and despite the increase in bone volume fraction, the stiffness (tissue modulus) was reduced by 60% compared to SCB without overlying cartilage damage[224, 226]. This was attributed to the hypomineralisation of the SCB as a consequence of increased bone turnover and remodelling. Similar findings have been observed by Burr and Li and colleagues[227, 228].

An association between increasing histological SCB turnover, bone volume fraction and trabecular thickness with increasing severity of overlying cartilage degeneration was described in end-stage human OA by Matsui and colleagues in tibial condyles and Klose-Jensen and colleagues in femoral heads removed at the time of joint replacement [229, 230].

In summary these analyses highlight the typical changes of established and progressive OA as being increased BMD, bone volume fraction, trabecular thickness, trabecular number and decreasing trabecular spacing. The mechanical stiffness per unit of bone volume fraction is significantly reduced.

2.6.2.2 Early OA

While the SCB architectural changes of established and end-stage OA are well described in humans, the early changes of OA in humans are less well described. Identifying and studying humans at the point when the cartilage and subchondral bone begin to 'fail' or deteriorate is challenging and obtaining tissue for histological analysis is unethical. Therefore there has been significant reliance on animal models and comparison with in vivo studies in crude and imprecise but practical definitions of 'early' OA. These analyses highlight the importance of SCB changes in the initiation of OA. In contrast to the net osteoblastic expansion of bone volume fraction, the initial response is a net osteoclastic resorption of bone which correlates with the initial bone response to damage as part of the homeostatic repair mechanism (see 2.6.1.1 Subchondral bone remodelling). However this and subsequent formation of abnormal bone is associated with cartilage deterioration and OA initiation.

Animal models

Surgically induced cartilage 'groove' damage on the femoral condyles of Beagle dogs whilst avoiding damage to the underlying SCB caused OA pathology to develop in both the femoral and tibial tissues [231, 232]. Anterior cruciate ligament transection (ACLT) in the same animals caused a an unstable joint with similar OA-pathology consequences. ACL injury is a well-recognised risk factor (see 2.3.2.3 Joint injury) for knee OA and may result in increased joint loading. When the two dog models were compared with micro computed tomography of the tibial plateau, both models reported increased thinning and porosity of the SCB plate as well as the onset of cartilage damage[233]. This implies that irrespective of mechanism of induction , the net bone resorption and onset of cartilage damage is intrinsic to the process of OA [234].

In mice models knees were injected with collagenase or iodoacetate to cause cartilage deterioration[235-237] or they underwent ACLT to induce an unstable joint[238]. The tibiae were subsequently analysed using micro-computed tomography and histology to examine the bone changes during the follow up. In the early stages of the OA models a similar SCB resorption occurred [235, 237, 238]. Similar results are observed in ACLT of rats[239] rabbits [188] and cats[240] with thinning of the SCB plate. It is important to note that in the cat ACLT model, the SCB plate remained thin[240], however that rats, rabbits and in meniscectomised guinea pigs a subsequent recovery and thickening of SCB bone was observed [188, 239, 241] indicating a biphasic response in the SCB.

Finally invasive ACLT in mixed-breed dog- [187] and non-invasive ACLT in mice- [242] models of knee OA have been used for the longitudinal analysis of SCB BMD measured using quantitative computed tomography. These models identified that the BMD significantly decreases in the initial period after ACLT. In the mouse ACLT model, trabecular bone loss was evident after seven days but there was partial recovery by 28 days and by 56 days significant new (non-native) bone formation was evident with a new steady state [242]. This biphasic response in SCB with initial resorption may also reflect the period after injury where antalgic disuse may reduce load and induce net bone resorption as well (see 2.6.1.1 Subchondral bone remodelling)

In summary these models of early OA bone resorption and reduced bone volume fraction are distinguished from the sclerotic appearances seen in later stages of OA described above and in human femoral heads[222, 230] and canine ACLT knees [243].

Humans

Observational studies of human ‘early’ OA have identified comparable initial SCB resorption with a suggestion of second phase of net bone formation in the SCB.

Bolbos and colleagues reported a significantly lower bone volume fraction in the SCB of knees with early OA (KL grade 1-2) compared to healthy controls (KL grade 0) using high-resolution MRI[244].

Klose-Jensen and colleagues analysed the bone volume fraction, bone turnover in SCB regions with varying degrees of overlying cartilage damage in femoral heads removed at the time of hip replacement for OA or from controls without a history or evidence of joint disease. The analysis identified that in regions with no or mild cartilage deterioration, the SCB had significantly increased bone turnover and a lower mean bone volume fraction (which did not meet clinical significance) than controls while the most advanced cartilage loss had both significantly increased bone turnover and bone volume fraction than controls[230].

Van Meer and colleagues observed that BMD significantly decreases in the SCB of the tibia and femur of knees after ACLT in humans. There is a subsequent significant increase in the BMD after the second year but this does not exceed baseline[245]. Although these knees did not have OA ACLT is a known risk factor for OA (see 2.3.2.3 Joint injury).

The presence of increased bone turnover in early OA is supported by soluble biomarkers as well. Petersson and colleages identified a significantly higher serum level of a bone turnover marker (bone sialoprotein) amongst knees with than without incident ROA[204].

2.6.2.3 Does subchondral bone failure precede cartilage failure?

The osteochondral unit represents a functional unit of interdependent joint tissues. In established OA, these tissues each play a role in the biomechanical and biochemical pathways of pathogenesis. However an unanswered question is whether the deterioration or failure to repair in one tissue precede deterioration in the other as part of the cascade of OA pathogenesis.

Radin and colleagues observed that increased load in rabbit knees caused increased stiffness in SCB before substantial changes in the adjacent cartilage[218]. This led Radin and colleagues to hypothesise that SCB pathology and increased stiffness caused increased shear forces in the overlying cartilage which led to cartilage degeneration[219]

A number of human studies supports the theory that SCB pathology precedes cartilage degeneration. A cross-sectional study of knee MRI scans of post-menopausal women without knee OA symptoms, indicated that meniscal tears were associated with increased tibial bone area but not cartilage volume[246]. Tibial total bone area (tAB) has been discussed earlier(2.6.3 Bone shape and subchondral bone MRI features in OA). The major limitation of this study is that it assesses cartilage in cross-section which does not exclude a preceding period of cartilage loss.

A longitudinal study of adults with a mean age of 45 years without symptoms of knee OA had serial knee MRI measurements. An increasing baseline tibial bone area was associated with subsequent greater loss of cartilage volume on follow up[247]. This study also does not exclude a preceding period of cartilage loss which may have preceded MRI-detectable changes in tibial bone area.

However the most convincing evidence addressing whether bone pathology may precede cartilage damage is from animal models where histological assessment of the SCB and cartilage tissues is more accurate in early OA.

The following three models using Beagle canine knees illustrate that a common osteochondral degeneration of OA occurs after different initial joint insults including ACLT or isolated damage to either the articular cartilage or SCB.

The primary cartilage damage model involved small superficial grooves being surgically made on the weight-bearing region of the femoral condyles without damaging the SCB (Figure 21). Joint reassessment occurred after 10 weeks of forced joint loading[231, 232].

The ACLT model involved the surgical transection of the ACL in the same aged dogs to increase loading in both SCB and cartilage .

Figure 21 Primary Cartilage injury model

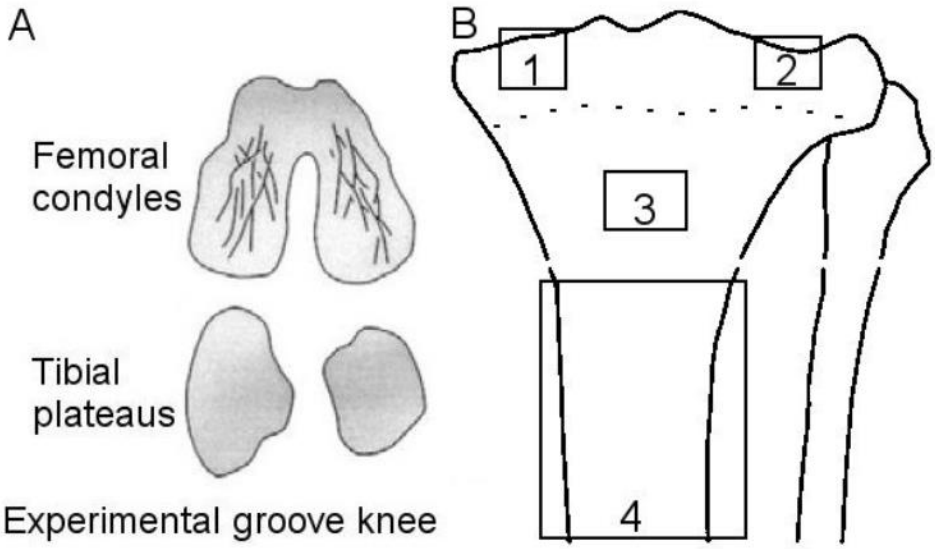

Schematic clarification of methods used. A: Localization of grooves made exclusively in the femoral condyles in the groove model. B: Selected regions that were analysed in the tibia using micro-CT. 1: cylinder in medial epiphysis; 2: cylinder in lateral epiphysis; 3: cylinder in metaphysis; 4: diaphysis. Reprinted by permission from BioMed Central: BMC Musculoskeletal Disorders, Sniekers et al [233].

For ACLT and primary cartilage damage knees, micro-computed tomography of the tibiae identified increased SCB plate thinning and porosity[233]. However the ACLT knees formed osteophytes from 10 weeks onwards whilst the primary cartilage damage knees first formed osteophytes at 20 weeks. Both models had histological evidence of cartilage degeneration in the tibia at 20 weeks. Bone resorption and incident cartilage damage are common consequences of the two OA models[234].

There are two OA models of initial ‘isolated’ SCB damage. The first used Beagle dogs of the same age as the ACLT and cartilage damage models. They received a patellofemoral impact inducing a trochlear bone marrow lesion but no cartilage damage on MRI of the knee was detected. Subsequent osteochondral biopsies from the femoral trochlea at six months identified cartilage degeneration[248]. The authors acknowledge that the MRI may have been insensitive to structural early cartilage damage.

The second ‘isolated’ SCB damage model involved tibial osteotomy, in significantly younger Beagle dogs, that conferred a valgus abnormality or a sham operation and a control group. Macroscopic and histologic analyses were made at seven and 18 months follow up which confirmed primarily medial femoral condyle cartilage degeneration.

Models of spontaneous OA in guinea pigs identified that SCB BMD in the medial tibia reduced before histological evidence of adjacent cartilage degeneration occurred[249].

In summary this evidence identifies that a common pathway to OA can be achieved by an initial failure of either SCB or cartilage. However while there remains controversy about whether bone or cartilage OA pathology represents the inciting event in human OA, cartilage is likely to deteriorate at the same time as SCB (see Figure 22).

2.6.2.4 Architectural associations with OA risk factors

The association of architectural changes of the SCB with OA risk factors is described here.

There are no studies in humans describing the association of obesity with trabecular architecture. However amongst humans with established knee OA, the BMD of the medial and lateral plateau is significantly greater on the side with greatest biomechanical load as a consequence of malalignment[250, 251] or meniscal damage[252]. Injury and anterior cruciate ligament transection are definitely associated with changes in SCB BMD in animal models as described above [187, 242]. In humans similar changes are seen after ACLT[245].

In summary OA SCB architectural changes are associated with OA risk factors.

Figure 22 An evidence-based hypothetical sequence of SCB OA pathology

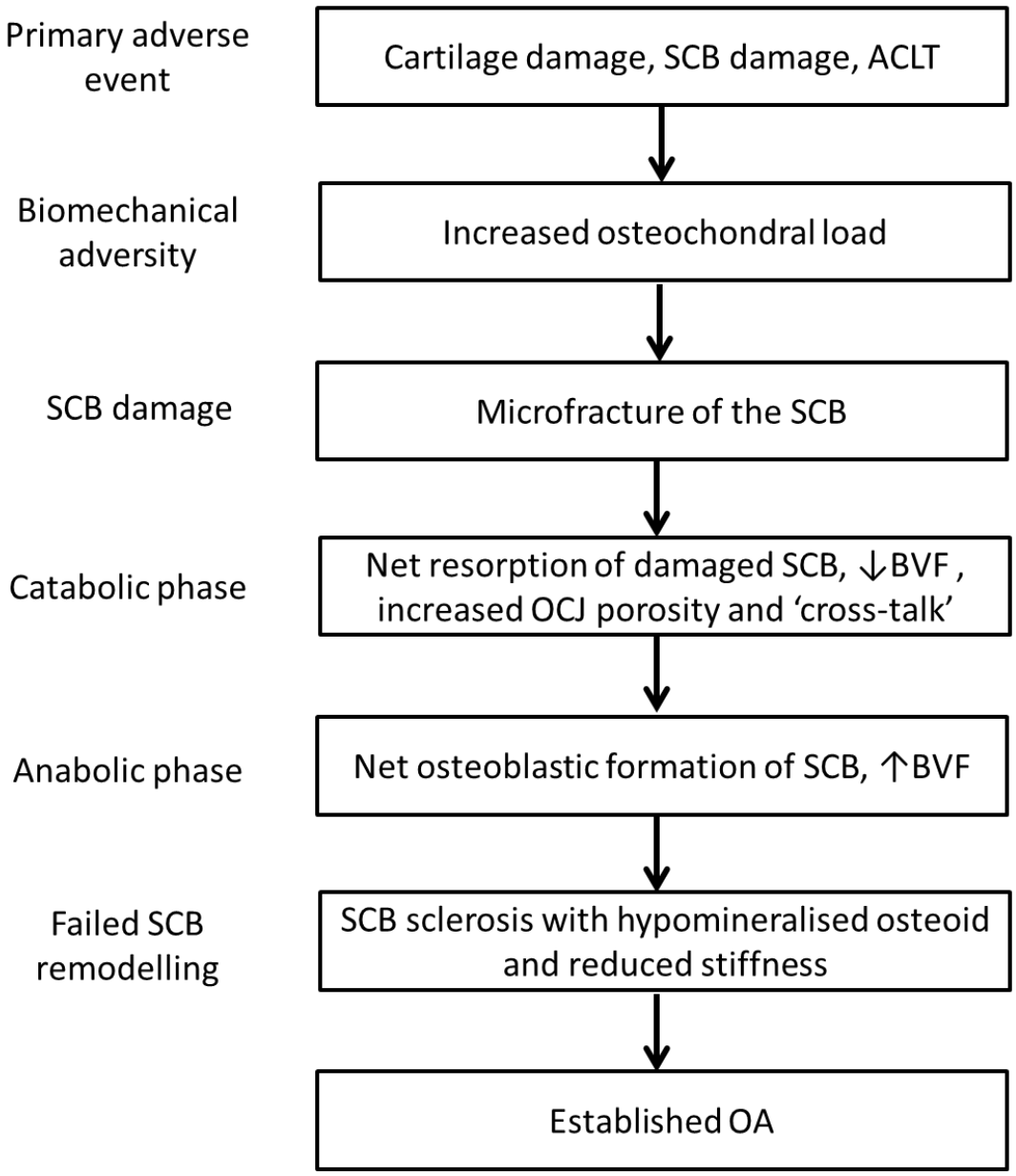

Anterior cruciate ligament (ACLT), bone volume fraction (BVF), osteochondral junction (OCJ). This sequence was formulated using the literature from the animal models and human evidence on OA, described in this chapter.

2.6.3 Bone shape and subchondral bone MRI features in OA

Change in bone shape such as flattening of the SCB (attrition) on conventional radiography has long been known to clinicians to be associated with OA symptom and structural progression[253]. Changes to the bone and joint geometry can adversely affect the congruity of the joint surfaces and impair the effective dissipation of load through the joint tissues which may overload the articulating tissues and promote their deterioration as part of the pathogenesis of OA (2.6.1.1 Subchondral bone remodelling, 2.6.1.2 Subchondral bone and the osteochondral junction).

Bone shape changes can now be quantified on two-dimensional conventional radiographic imaging as well as on three-dimensional tomographic imaging such as magnetic resonance imaging (MRI). MRI therefore provides a three-dimensional evaluation of SCB pathology in OA which includes shape, bone marrow lesions, osteophytes, cysts and attrition. These will all be discussed here including their association with OA risk factors and OA structural severity.

2.6.3.1 Bone shape of the knee

2.6.3.1.1 Knee subchondral bone cross-sectional area

While bone shape has been less studied than BMLs due to quantification issues, the area of subchondral cortical bone that constitutes the articulating region of the bone on one side of a diarthrodial joint can be quantified from tomographic imaging such as MRI using laborious manual segmentation techniques (2.10 Statistical Shape modelling). The formal nomenclature used to describe the total subchondral bone area is tAB[254].The bone most frequently segmented for bone area in the literature is the tibial plateau, due to its relatively flat shape and distinct cartilage margins. This bone area, measured as a cross-sectional bone area of an axial image of the tibia (Figure 23) has been described by Jones and colleagues in observational studies amongst the healthy population and those with and at risk of knee OA[31]. It can be divided into medial and lateral tAB (Figure 23)

Figure 23 Segmented axial medial and lateral tibial plateaus

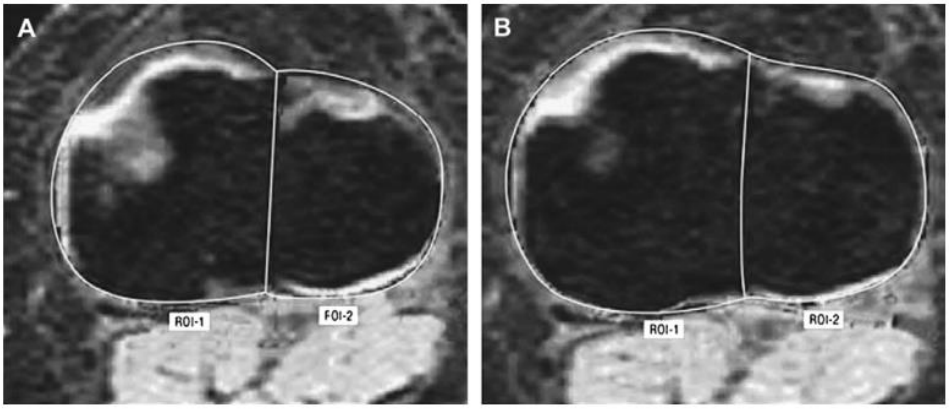

Tibial plateau bone area measurement by taking the mean of the area at different axial levels [255].

Bone area is associated with body size but also OA risk factors and these are discussed here. It is important to note that height and gender are determinants of bone area in healthy knees [256, 257]. In particular height accounts for 70% of the variance in tAB in knees indicating an allometric relationship between height and tAB[257]. This is a logical relationship as the greater the height, the larger the area will be required to dissipate the greater load. Furthermore, while there are gender differences in tAB, the majority of the variance in the difference in tAB between genders is explained by difference in height[256].

Amongst older adults tAB increases in size to a smaller extent than in developing children. The tibial tAB in healthy women, with a mean age of 57 years, increases by 0.8-1.2% per annum over 2.5 years [258]. Amongst male and female adults with a mean age of 64 years and with OA knee the medial and lateral tAB increase by a mean of 2.2% and 1.5% in two years respectively[259]. The significance of these differences should be considered in the context of the coefficient of the variance (measurement error) quantified as 2.3% for the medial tibia tAB, and 2.4% for the lateral tibia tAB. Amongst healthy knees only 18-21% had an increase in tAB above measurement error[258].

Obesity is independently prospectively associated with the incidence of ROA knee in the Framingham cohort and is therefore an established risk factor for knee OA[61]. Obesity may cause OA incidence (see 2.3.2.2 Obesity) as a result of increased joint loading. Obesity is associated with the medial and lateral tAB of the tibia [260]. Individuals with obesity (body mass index>30kg/m^2) also had greater medial tibial tAB in comparison with individuals with normal body mass index (18.5-24.9kg/m^2). Furthermore obesity was independently associated with an increase in medial tibial tAB[259] and a longitudinal increase in cartilage defects[261]. Body mass index explained 7.3% of the variance in the mean annual percentage change in the medial and lateral tAB as described above[259] which implies obesity is a significant determinant of tAB change. However while the mean magnitude of tAB change is of a similar order of magnitude as the measurement error (2.3%) further evidence is required to confirm obesity is a determinant of tAB. While a biomechanical cause for an association between obesity and tAB would be logical in the context of Wolff's law, both tAB and obesity may also share the same determinants such as a genetic aetiology.

In support of Wolff's law is the observation that tibial bone area appears to expand in response to increased applied load. The loss of integrity of the meniscal tissue within the knee impairs the capacity for the knee to effectively dissipate load. As a consequence the adjacent structures, including the articular cartilage and SCB are subject to increased load. It is therefore fitting that tibial tAB is highly correlated with ipsilateral meniscal surface area[262]. Furthermore ipsilateral meniscal extrusion and tears are independently associated with a larger tAB in cross-sectional observational studies[246, 263-265]. In a two year longitudinal study of 117 patients with knee OA, baseline extrusion of the medial meniscus was independently associated with a longitudinal expansion of the medial tibial tAB[265]. A limitation of this longitudinal analysis include the actual changes in tAB being small relative to the coefficient of the variance (measurement error) and the longitudinal model used height as a ratio (body mass index) not a metric measure which may result in inadequate adjustment of a major confounding factor.

Individuals with anterior cruciate ligament (ACL) tears have an independent association with larger tibial tAB than those without ACL tears in cross-sectional analysis [266]. Furthermore malalignment is independently associated with a larger tibial tAB change in the compartment with greater biomechanical load conferred by the malalignment[267, 268]. For example the medial tibial tAB was 10% larger in varus than neutrally aligned knees with OA[267]. Acknowledging the limitations of the existing literature, these findings support the role of load in SCB remodelling in the pathogenesis of OA.

A statistically independent association of tAB has been described with the severity of radiographic OA[259, 269]. Subsequent medial cartilage volume loss[210] and knee replacement[270] has been described independent of age, gender and body mass index. Therefore expansion of axial tibial cross-sectional bone area (tAB) is associated with knee OA severity, risk factors for structural progression and with structural progression itself but limitations conferred by a relatively large coefficient of the variance (measurement error) confirm the requirement for further validation of tAB as a biomarker of OA and a potential target for disease modification.

2.6.3.1.2 Three-dimensional knee bone shape

Eckstein and colleagues in chondrometrics have also utilised a different method of quantifying bone area over the tibia but also the femur and patella using manual segmentation derived from serial magnetic resonance (MR) images. This employs image segmentation and analysis algorithms[271] and is described later(2.10.2 The two- and three dimensional shape modelling for determining joint shape). Using this method similar gender differences in tibial bone area are also observed[262]. This segmentation method for measuring tAB describes a similar expansion in tAB seen in the medial tibia in varus malalignment but the same expansion is observed in the medial femur[267].

Imorphics have developed an automated segmentation method for defining the three dimensional shape of knee bones using the next generation of statistical shape modelling called active appearance models. This permits the quantification of the undulating three dimensional surfaces of the tibia,

femur and patella tibial based upon three-dimensional MRIs. As such the tAB can be quantified for each of the articulating surfaces of bones and the three dimensional shape of bones can be quantified on a continuous vector scale that describes the difference in shape between OA and no OA. The methods describing this are below (2.10.2 The two- and three dimensional shape modelling for determining joint shape).

Hunter and colleagues in Imorphics identified that changes in tAB in the femur, tibia and patella over 24 months all predicted incident knee ROA in the Osteoarthritis Initiative. Admittedly the limitations of this analysis include it was a nested case-control study without matching for body mass index.

Neogi and colleagues in Imorphics described the baseline three dimensional bone shape vector values for the tibia, femur and patella predicted incident knee ROA in the Osteoarthritis Initiative. Admittedly the limitations of this analysis include it was a nested case-control study but it did adjust for important covariate determinants of OA.

2.6.3.1.3 Two-dimensional proximal tibial shape

Nakamura and colleagues identified that stratifying tibial osteophyte morphology on conventional knee radiography (normal, horizontal, upward and downward -Figure 24) was significantly correlated with MRI-determined medial meniscal extrusion and degeneration. This association was not significant in the lateral compartment. While bone shape was associated with joint degeneration, only 8 knees had downward osteophytes, there was no adjustment for confounding factors and the analysis was cross-sectional which restricts any inferences about a causal role of bone shape[272].

Figure 24 Medial tibial osteophyte morphology

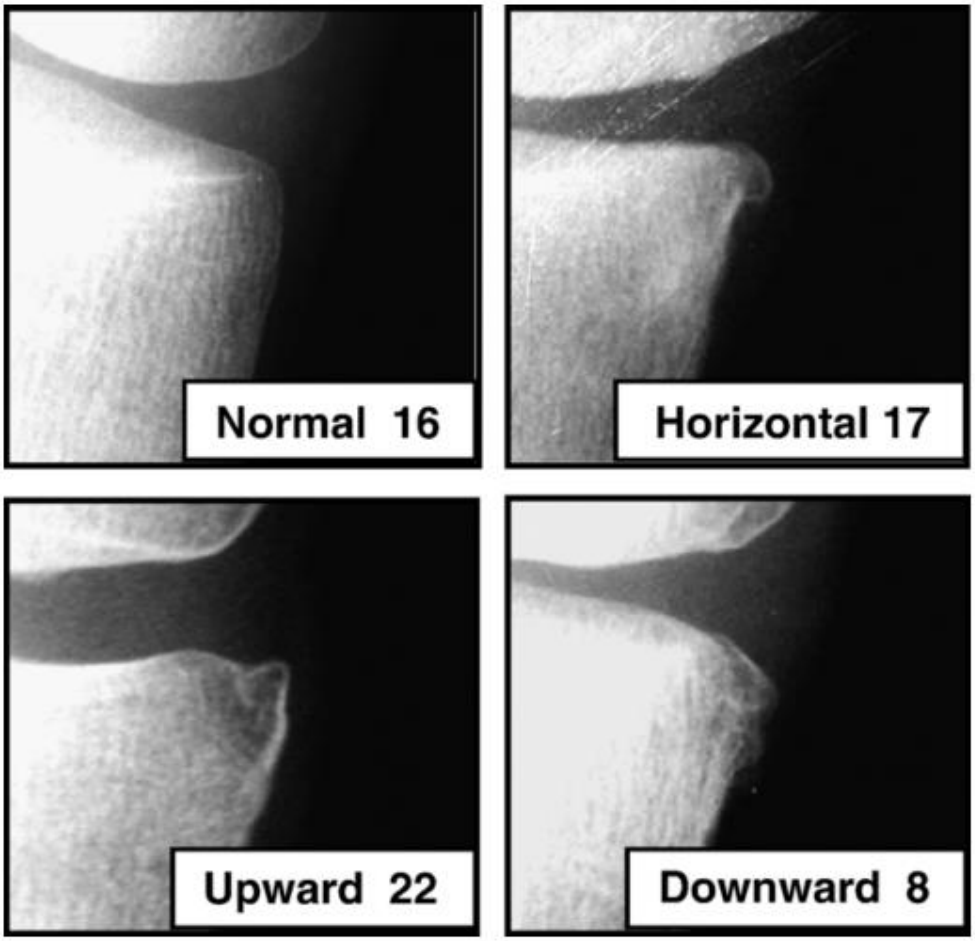

Medial tibial spur classification on X-ray. The shapes of the medial tibial spurs on X-ray were classified into four types. (Reprinted by permission from Elsevier Ltd: Magn Reson Imaging [272]).

2.6.3.1.4 Two-dimensional distal femoral shape

The shape of the distal femur, in particular a shallow femoral trochlear groove, has been associated with ‘premature’ OA in the context of a case series of 31 individuals with multiple epiphyseal dysplasia[273]. Stefanik and colleagues examined the shape of the femoral trochlea in 881 knees from the Multicenter Osteoarthritis Study (MOST) study. Knees with a flatter lateral trochlea (a shallower femoral trochlear grove) had an independent association with patellofemoral joint bone marrow lesions and cartilage damage[274].

Amongst knees with OA and normal, varus or valgus alignment, the femoral condyle shape varied most obviously in valgus malalignment when examining the geometry (angles, axes and tangents) of conventional radiographic images and axial MRI slices of distal femurs. The shape difference between knees with OA and controls was most noticeable in the lateral femoral condyle of valgus knees. There was no significant difference in shape of the femoral condyles between controls and varus knees with OA. This implies increased biomechanical load may cause shape change[275].

2.6.3.1.5 Two-dimensional shape of the tibiofemoral joint

Haverkamp and colleagues used statistical shape modelling to describe the shape of the distal femur and proximal tibia on conventional knee radiography in a cross-sectional sample of 609 women's knees in the Rotterdam cohort. The femoral and tibial width and the elevation of the lateral tibial plateau was independently associated with the presence of knee ROA and the bone widths were associated with diffuse cartilage defects[276].

Bredbenner and colleagues analysed the surface geometry of the tibia and femur in 12 individuals who were considered to have no risk of knee OA and 12 individuals with risk of OA from the Osteoarthritis Initiative. The surface geometry was segmented using statistical shape modelling and differences in surface geometry of the tibiae and femurs were found to be significantly different between those at and those not at risk without adjustment for confounders[277]. This analysis involved very small numbers and it should be noted that some individuals within the control arm of the OAI have evidence of knee ROA at baseline which limits any inferences from this analysis.

2.6.3.1.6 Patellar shape

Patella shape itself has not been associated with patellofemoral OA. However a medial tilt of the patella upon the femoral trochlea was associated with a reduction in WOMAC pain score severity amongst adults aged 25 to 60 in a community-based cross-sectional sample[278].

2.6.3.2 Bone shape of the hip

While risk factors for hip OA include a history of increased hip loading[279] or injury[280], increasing age[43], being female[43] and inherited genes[281], the geometric shape of the hip is now recognised to be an independent prospective risk factor for the development of ROA hip rather than being a consequence of OA itself. The evidence-base for this is described here.

2.6.3.2.1 Femoroacetabular impingement

Femoroacetabular impingement (FAI) is a pathological condition where there is impingement between the acetabulum and the femoral head during movement of the hip. The first of two types is where the presence of an aspherical femoral head (a cam-deformity) creates an abnormally shaped junction between the femoral head and neck and this additional material causes the impingement upon the acetabulum (Figure 25,Figure 26). As the asphericity of the femoral head increases so does the alpha angle which can be measured on conventional radiography of the hip (Figure 26). This impingement is associated with delamination of the acetabular cartilage and confers up to a ten-fold greater risk of end-stage hip OA within 5 years[74]. ‘Pistol grip’ deformity described by Doherty and colleagues also refers to similar asphericity of the femoral head and a risk factor for FAI[282]. A second possible form of FAI is the ‘pincer’ form the labrum of the acetabulum covers more of the femoral head than usual and causes impingement.

Figure 25 Radiographs of a normal hip and a hip with cam lesion

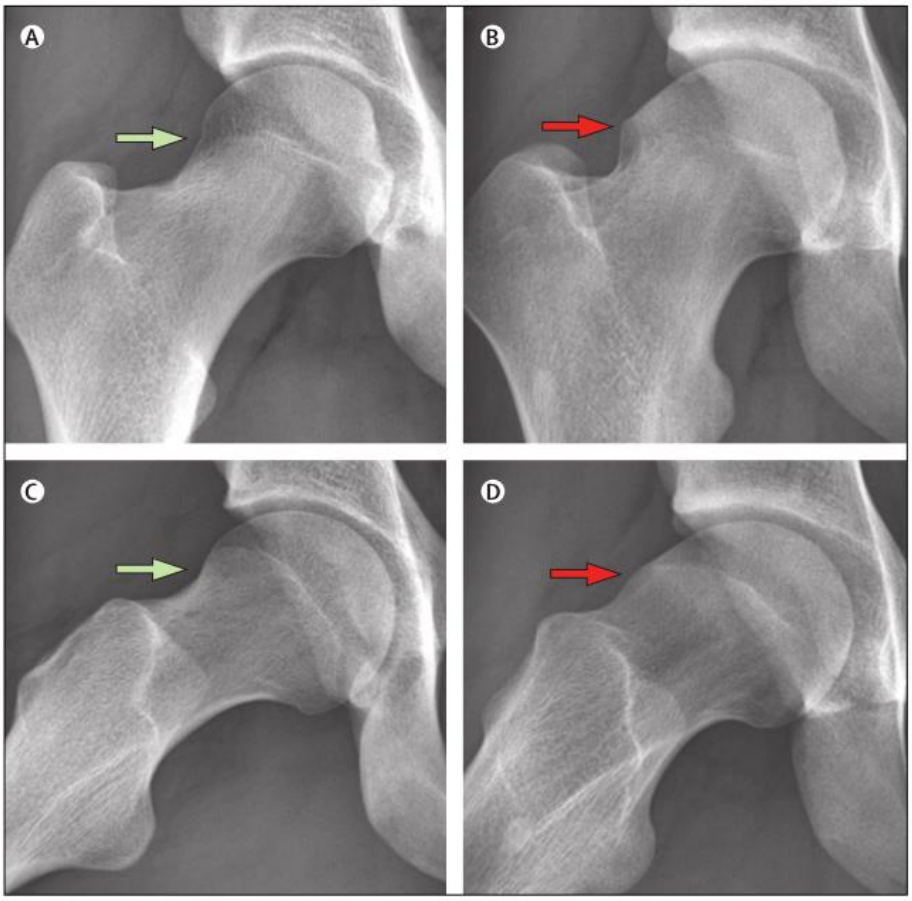

In a normal hip, the concavity of the femoral head-neck junction (green arrow) allows an extensive range of hip movement without impingement of the femur against the acetabular rim. In cam lesion femoroactebular impingement, the loss of this concavity at the anterosuperior head-neck junction (red arrow) results in impaction of the femur against the acetabular rim. (Reprinted by permission from Elsevier Ltd: Lancet [283]).

Figure 26 Mechanisms of cam impingement

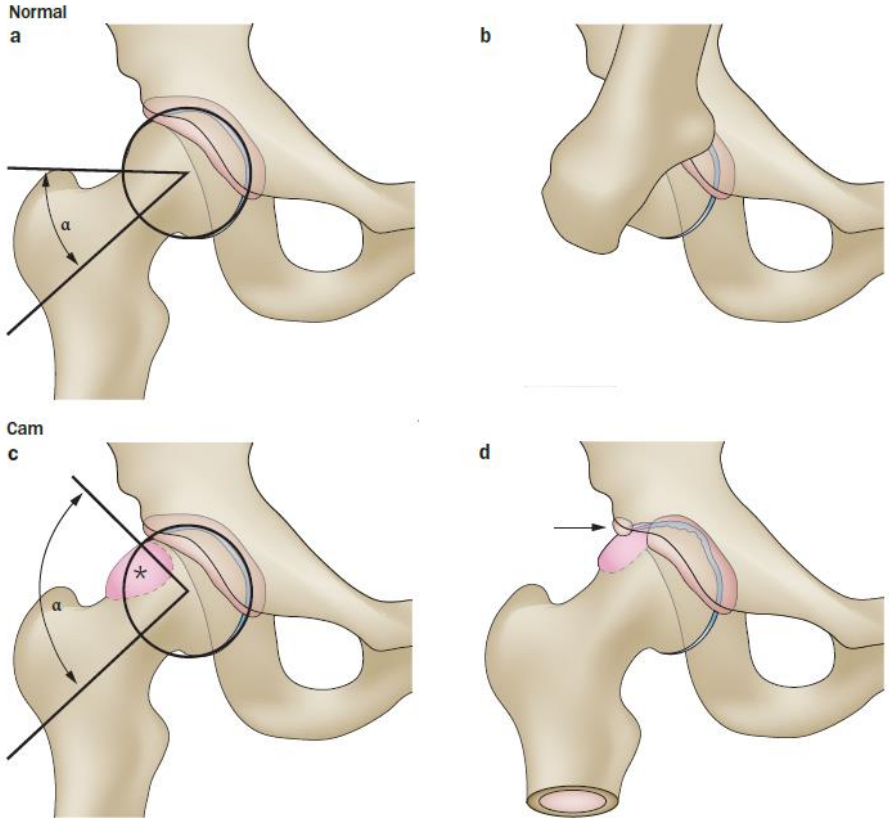

Mechanism of cam impingement. a,b | A spherical femoral head provides the hip with a wide range of motion. c,d | A cam abnormality (asterisk) can cause impingement (arrow) against the acetabular rim, especially during flexion and internal rotation of the hip. The α angle is indicated in a and c. (Reprinted by permission from Macmillan Publishers Ltd: Nat Rev Rheumatol [284] copyright 2013)

2.6.3.2.2 Acetabular dysplasia

Acetabular dysplasia has a European prevalence of 3.4% [285] and is also associated with prevalent hip OA. In the left panel (Figure 27) an incongruent type I hip has a shallower acetabulum than normal which increases the freedom of movement of the femoral head which may overload the labrum, which can shear from the acetabular bony rim[286]. In the right panel (Figure 27) a congruent type II hip has a ‘short roof’ acetabulum which does not cover the femoral head sufficiently. This may confer increased load upon a reduced area of the articular surface and cause possible ‘fatigue’ fracture.[286].

A prospective longitudinal study by Reijman and colleagues within the Rotterdam study identified that over a mean of 6.6 years follow up, 9.3% developed incident hip ROA. The presence of baseline acetabular dysplasia conferred a 4.3 fold greater odds of incident hip ROA than those without dysplasia and this association was independent of OA risk factors[287]. Lane and colleagues also observed an association of mild acetabular dysplasia with subsequent incident hip ROA during approximately nine years of follow up in a cohort of post-menopausal females[288].

Figure 27 Acetabular dysplasia and its association with OA hip

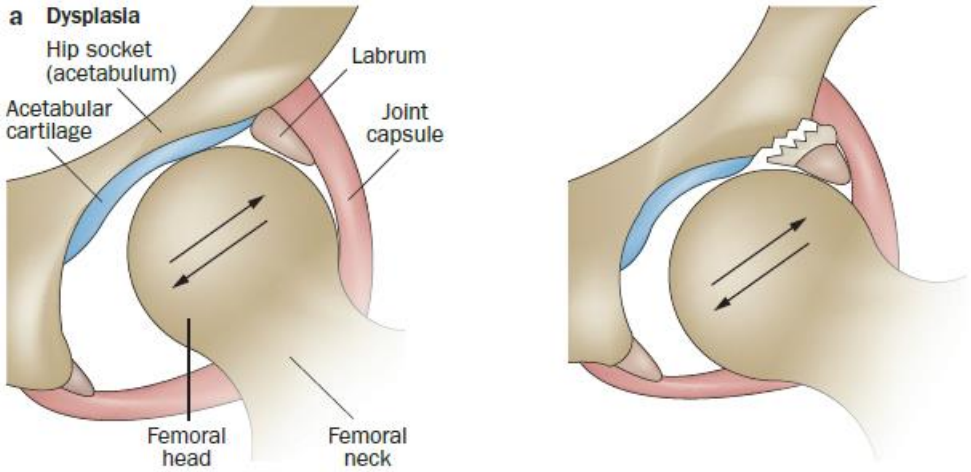

Schematic diagram of the hip joint architecture. a | Hip dysplasia pathophysiology of the acetabular rim in the incongruent type I hip (left panel). In this configuration, the hip has a shallower, more vertical acetabulum and a greater radius of curvature than normal. This architecture increases the freedom of movement of the femoral head, leading to overloading of the labrum, which can shear from the acetabular bony rim. (Reprinted by permission from Macmillan Publishers Ltd: Nat Rev Rheumatol [286], copyright 2012).

2.6.3.2.3 Two dimensional modelling of the femoral head

Shape recognition is an important function of statistical shape modelling and was first used for practical purposes for automated facial recognition. This involves a computer programme being trained to precisely and reliably recognise the edges of similar structures presented as images. Once trained, an automated statistical shape model of shape and shape change[289] can be used to capture subtle shape changes based on conventional radiography.

Gregory and colleagues analysed a subgroup of the Rotterdam study with 110 hips without hip ROA (KL grade <2) at baseline that were followed up after six years. This consisted of 55 cases of hips that progressed by 3 or more KL grades during the follow up and these were matched with controls based upon age and gender but not body mass index. Statistical shape modelling of the proximal femur identified significant subtle shape changes between cases and controls[290]. The inadequate matching or adjustment for BMI remained a major confounding factor.

Lynch and colleagues examined the proximal femoral shape from conventional hip radiography over eight years amongst approximately 350 elderly caucasian women without hip ROA at baseline. Using active shape modelling some subtle shape features were independently associated with incident hip ROA amongst 100 cases and 250 controls that did not develop hip ROA in a case-control analysis[291].

Waarsing and colleagues examined serial DXA images of hip joints in 161 individuals with established hip OA (ACR criteria), taken two years apart. A statistical shape model identified various features of the two-dimensional shape of the femur and acetabulum that were independently associated with structural progression and severity of the hip ROA[292]. This is the most convincing evidence of the three studies of an association between shape and structural progression. Therefore shape change of the hip joint is relevant in OA hip

2.6.3.4 Subchondral bone marrow lesions

Bone marrow lesions (BMLs) are the most studied SCB pathology to date. These are not detectable on conventional radiography and are best detected on T2-weighted (proton-density-weighted) fast spin echo images on MRI where they are non-cystic ill-defined hyperintensities (Figure 28)[293]. They are most frequently identified at sites of greater mechanical load, such as where malalignment loads the joint[294], where meniscal degeneration exists[295], in association with ACL tear [245, 266] [296] and with obesity [99, 121]. BMLs are histologically described as regions of 'localised infarction reaction'[297] with active and chronic remodelling processes[298, 299]. The increased turnover within BMLs reflects typical trabecular remodelling of OA. This is confirmed by the SCB histomorphometric changes within BMLs including a hypomineralised region of increased bone volume fraction with increased thickness of trabeculae but with reduced trabecular number and spacing[297, 298]. This makes areas of SCB affected by BML more susceptible to attrition where the bone becomes flattened or depressed[300] and the overlying cartilage more susceptible to degeneration. BMLs are typically found to be topographically adjacent to regions of histological cartilage degradation[299] and this correlates with the in-vivo imaging findings. BMLs in-vivo are common findings on MRI knee scans in the SCB of moderate to severe OA where their incidence increases with greater knee ROA severity[294] and they are associated with adjacent cartilage damage[301]. Clinical studies have identified that larger BMLs are more common in painful than non-painful knees[134]. The development of new BMLs has been associated with new onset knee pain[121]. BMLs, unlike bone attrition, can regress over time and can be found in individuals without structural ROA[121, 302].

Figure 28 Subchondral bone marrow lesions in the femoral trochlea

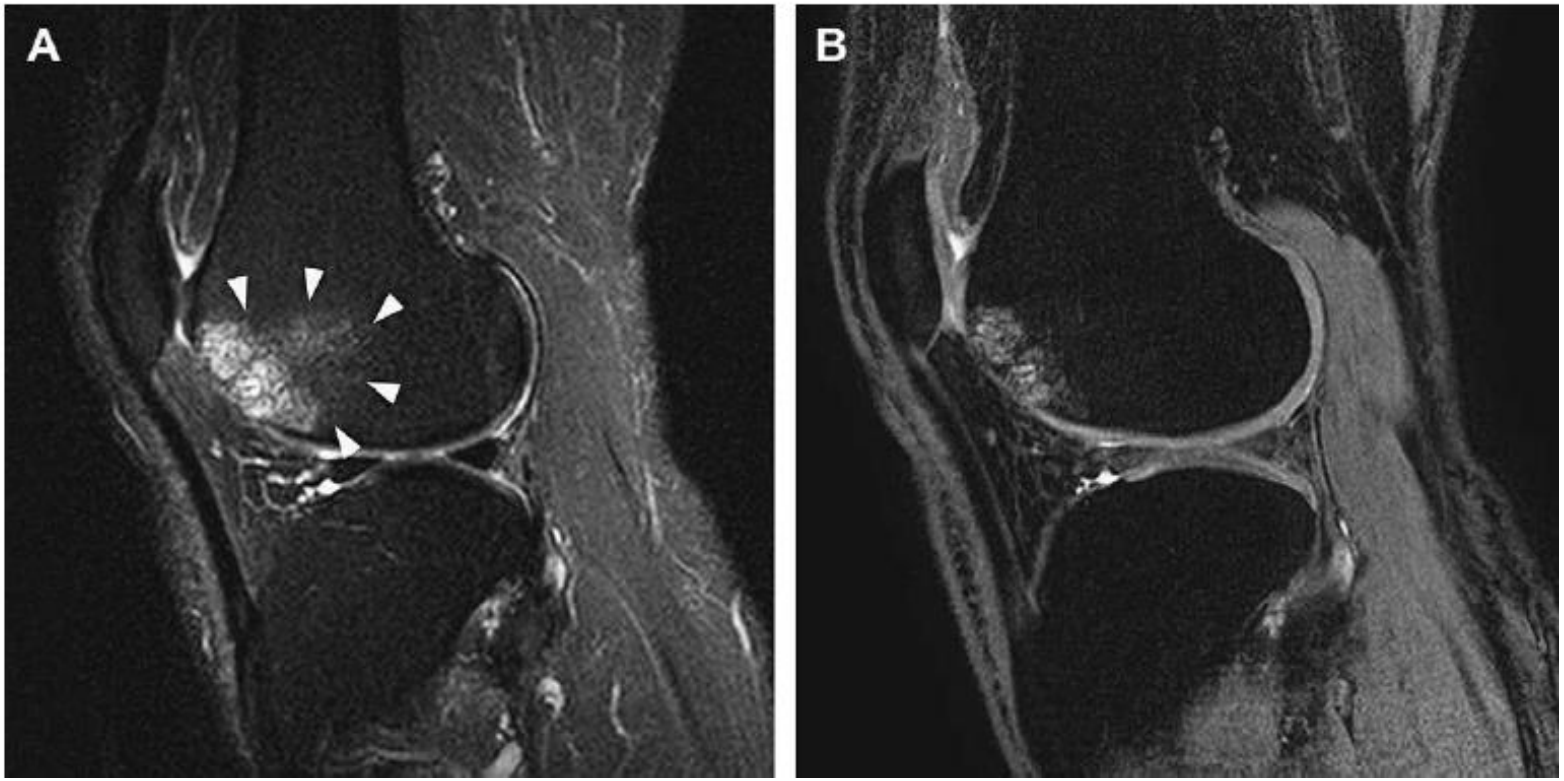

The bright white changes identified by the arrows are bone marrow lesions. (Reprinted by permission from Elsevier Ltd: Radiologic Clinics of North America [303]).

2.6.3.5 Subchondral bone attrition

SCB attrition is the flattening or depression of the SCB adjacent to the joint surface(Figure 29). The evidence suggests that MRI SCB attrition may be a reflection of tibiofemoral compartment-specific mechanical load. This is because the tibiofemoral compartment receiving the greatest biomechanical load from malalignment[304, 305] and meniscal extrusion and degeneration [305] is significantly more frequently affected by MRI-determined SCB attrition. BMLs share these same load-associations and it is fitting that BMLs are highly associated with and predict incident bone attrition longitudinally[300]. SCB with BMLs may be more susceptible to this 'collapse' and flattening because of the reduction in stiffness afforded by the hypomineralised SCB found within BMLs[297, 298](2.6.2.1 Established OA and structural progression). The prevalence of SCB attrition increases with greater Kellgren Lawrence grade radiographic structural severity of OA[306] and is independently associated with greater overlying cartilage loss[307].Bone attrition is independently associated with knee pain[139].

There is inconclusive evidence describing whether MRI-determined attrition is associated with obesity or not and there is no evidence describing MRI-determined attrition incidence after ACL rupture.

Figure 29 Subchondral bone attrition and osteophytosis

Subchondral bone attrition in the lateral tibiofemoral compartment. (Reprinted by permission from Elsevier Ltd: Radiologic Clinics of North America [303]).

2.6.3.6 Osteophytes

The term osteophyte may refer to three kinds of ‘osteophyte’. The first is a traction spur or enthesophyte, formed where tendons and ligaments insert. The second is an inflammatory spur or syndesmophyte formed where ligaments and tendons insert to bone as seen in ankylosing spondylitis. The third is the osteochondrophyte of OA which can form at the margins of diarthrodial joints, apophyseal joints and vertebral bodies. From hence forth osteophyte refers to an osteochondrophytes of OA. Osteophytes are a

characteristic feature of OA and are fibrocartilage-capped bony outgrowths originating from the periosteum of the cortical bone at the joint margins[308](Figure 29). They form as a consequence of stressors such as mechanical load and the process is driven by cytokines and growth factors. These promote the proliferation of mesenchymal stem cells in the periosteum to differentiate into chondrocytes as part of chondrogenesis[308]. Hypertrophic mature chondrocytes are subsequently replaced with osteoblasts that mediate bone formation by endochondral ossification(2.6.1.2 Subchondral bone and the osteochondral junction).

Like the other SCB pathologies, the presence of osteophytes are associated with increased mechanical load as a consequence of ACL tear[309], malalignment[305, 310] and meniscal damage[272, 311]. Osteophytes are also associated with x-ray severity[312] and cartilage damage[313]. The evidence describing an association with pain is inconclusive. There is no evidence describing the presence or absence of an association with obesity and MRI-determined osteophytes.

2.6.3.7 Subchondral bone cysts

SCB cysts are frequently found in knees with OA and are recognised as one of the hall-mark features on conventional radiography. They are considered to represent bone trauma. Their typical appearance on unenhanced MRI is a well-defined rounded area of fluid-like intensity[293]. However these are strictly cyst-like lesions and not pure cysts because the histological findings of these lesions do not include an epithelial lining[314] and they enhance on contrast enhanced MRI.[315]

The histological features are of bone trauma containing increased bone turnover, necrotic bone fragments which and are lined by a nonepithelial fibrous wall[314, 316]. The histomorphometric changes within these SCB cysts include a hypomineralised region of increased bone volume fraction which is similar to BMLs[316]. Femoral heads excised at the time of joint replacement had higher bone volume fractions with higher total SCB cyst volume[317]. Accordingly, SCB cysts are most frequently found adjacent to or within BMLs[315] and they develop longitudinally within BMLs amongst

patients with or at risk of knee osteoarthritis[318]. They may form as a consequence of increased load as they are more prevalent in knees with ACL tears[296] and their prevalence increases with increasing severity of knee OA[319]. Degeneration of articular cartilage is associated with the presence of adjacent SCB cysts[315, 316]. There is no evidence describing the association of MRI-determined SCB cysts with obesity, malalignment or meniscal damage.

In summary MRI-detected SCB lesions are associated with the histological and histomorphometric features of OA, risk factors for OA and OA structural severity and pain.

2.6.4 Can the OA Subchondral Bone be therapeutically targeted?

The collective evidence described above (2.6 Subchondral bone in OA) indicates the importance of subchondral bone in the pathogenesis of OA at a macroscopic level with bone shape, in terms of bone architecture and at cellular level.

2.6.4.1 Anti-resorptive drugs

SCB is an attractive treatment target given the known pathology of increased bone turnover associated with an excess of bone resorption initially and a subsequent increase in hypomineralised bone volume fraction with reduced stiffness and associated cartilage degradation.

2.6.4.1.1 Bisphosphonates

Anti-resorptive agents such as bisphosphonates inhibit osteoclasts and bone remodelling process[320] and may subsequently be chondroprotective. Animal models of OA in rats and dogs have identified a beneficial effect of several bisphosphonates in the context of high bone turnover through their impact on subchondral bone which includes inhibition of remodelling, osteophyte formation along with decreased vascular invasion of calcified cartilage, cartilage degradation and pain[239, 321-324]. This appears to be a class effect and zoledronic acid has also been shown to have a chondroprotective effect in rabbits[325].

In humans the effects of bisphosphonates on symptoms and structural progression have varied. The Knee OA Structural Arthritis (KOSTAR) study tested the efficacy of 5mg/day, 15mg/day or 50mg/week of risedronate in its effect on symptoms (WOMAC and patient global assessment) and structural progression (JSN using fluoroscopically positioned, semiflexed-view radiography) in patients with medial knee OA (determined by radiographic JSN) over two years. This was a phase III randomised placebo-controlled trial which found no significant difference in symptoms or structural progression between risedronate at any dose and placebo. This study did not account for the heterogeneity of the OA population regarding subchondral bone abnormalities because patients were selected on the basis of conventional radiography which is insensitive to the detection of SCB pathology like BMLs (2.9 Magnetic resonance imaging). Furthermore an evaluation of the sensitivity to change of JSN as an outcome measure for structural change suggests that these studies were significantly underpowered to show a response[326]. However some potentially beneficial effects have been noted. A dose-dependent reduction in biomarkers of cartilage degradation at 6 months of therapy was noted (C-terminal cross-linking telopeptide of type II collagen) which was associated with a slower knee OA structural progression based upon JSN[327]. On trabecular analysis of the SCB on conventional radiography in individuals with significant JSN during KOSTAR, there was loss of trabeculae in the placebo and 5mg/day groups while there was preservation of vertical trabeculae with 15mg/week of risedronate and an increase in vertical trabeculae with 50mg/week indicating a dose-dependent preservation of SCB integrity[328].

The British study of risedronate in structure and symptoms of knee OA (BRISK) investigated risedronate at a dose of 5mg/day or 15mg/day in a 1-year prospective, double-blind, placebo-controlled study. Symptoms were measured with WOMAC and patient global assessment and structural progression was measured with radiographic JSN. This trial included knees with medial knee OA[329]. This was a significant improvement in the patient’s global assessment and a trend towards attenuation of JSN and improvement in WOMAC but this was not significant.

Cartilage degradation and bone resorption markers were significantly decreased in the risedronate arms. Similar criticism applies to BRISK and KOSTAR for inadequate powering for the sensitivity to change of the outcome measure JSN. No study has examined cartilage volume as an endpoint in a bisphosphonate OA trial.

The only randomised placebo-controlled trial using MRI, that investigated symptomatic knee OA with concurrent BMLs, identified that zoledronic acid reduced the size of BMLs and knee pain at 6 months. However the pain reduction was not maintained at 1 year and BML size had a trend towards a smaller size[330].

The Fracture Intervention Trial (FIT) was a randomised placebo-controlled trial of alendronic acid for osteoporosis. The effect of alendronic acid on anterior vertebral radiographic osteophyte progression was described. Alendronic acid significantly reduced osteophyte progression but there was no data on pain[331].

Carbone and colleagues performed a cross-sectional study of the Women in the Health, Aging and Body Composition Study. Postmenopausal women with and without knee OA symptoms (n=818), underwent MRIs of their knees and 214 were taking anti-resorptives. Overall anti-resorptive use was not associated with pain but alendronic acid use was associated with significantly less severe pain (WOMAC). Alendronic acid and oestrogen therapy were associated with significantly less SCB attrition and BML prevalence in the knee on MRI in comparison with women not

receiving these medications[332].

Amongst participants of the Osteoarthritis Initiative cohort with moderate knee OA (Kellgren Lawrence 2-3) and a numeric rating scale (NRS) of pain of four or more out of ten, individuals taking bisphosphonates received a significant reduction in pain NRS at follow up at years two and three but not four. There was also a trend towards reduced JSN at year four follow up ($p=0.06$).

Cauley and colleagues described a large randomised placebo-controlled trial of annual zoledronic acid for the treatment of pain owing to back pain or fracture in postmenopausal women with osteoporosis. Zoledronic acid

significantly reduced the number of days with patient-reported back pain over a 3-year period which was independent of incident fracture[333]. This may indirectly reflect the capacity of zoledronate to reduce OA pain.

Koivisto and colleagues describe a randomised placebo-controlled trial of zoledronic acid for the treatment of lower back pain (LBP) in individuals with modic changes which are bone marrow pathologies associated with the presence and persistence of LBP. Zoledronate significantly reduced LBP at one month and NSAID use at one year[334]. This may indirectly reflect the capacity of zoledronate to reduce OA pain.

Furthermore there have been improvements in symptoms and progression of disease at certain locations and reduction in subchondral bone lesions[328-331].

In summary there is evidence supporting the potential for bisphosphonate being disease modifiers of symptoms and structural change in specific phenotypes of OA with SCB pathology. However more robust assessment with better outcome measures (e.g. MRI measures) in adequately powered trials are still required to establish the efficacy of bisphosphonates in OA.

2.6.4.1.2 Strontium

More recently the effect of strontium ranelate on structural progression (JSN) and knee pain (WOMAC) in knee OA was assessed in a randomised placebo-controlled trial over three years. This is the Strontium Efficacy in Knee OsteoarthrItis trial (SEKOIA). This identified a small reduction in both JSN and total WOMAC and WOMAC pain with 2g/day[335].

Pelletier and colleagues published an analysis of a subgroup of the SEKOIA that had MRI scans. This analysis concluded that at 36 months, there was a significant reduction in BML size score in 25-40% (similar to the effect of zoledronate) which also correlated with reduced cartilage volume loss in the medial compartment[336].

A post-hoc analysis of pooled data from two strontium trials for osteoporosis was performed to determine the efficacy of strontium in treating structural progression and symptoms of patients with spinal OA. The TReatment Of

Peripheral OSteoporosis (TROPOS) and Spinal Osteoporosis Therapeutic Intervention (SOTI) trials. After three-years there was no significant difference in vertebral osteophyte scores but an improvement in back pain. An improvement of one point or more on a likert scale, was significantly more frequent with strontium therapy[337].

Strontium has also demonstrated a reduction in cartilage defects and subchondral bone thickening in a randomised placebo-controlled trial in an ACLT model of OA in dogs[338].

The evidence supporting the potential for strontium to modify structural progression and pain in OA suggests strontium may be an effective therapy for OA knee. However strontium is associated with increased cardiovascular risk which limits its future utility.

2.6.4.2 Calcitonin

Calcitonin is a hormone that antagonises the effect of parathyroid hormone (PTH) in its bone resorptive effects. It has demonstrated the potential to improve symptoms and structural progression in OA in humans and animals.

18 Rabbits having surgically induced knee OA (e.g. ACLT) were randomised to receive calcitonin IM or placebo. The structural progression of OA based on histological and imaging was attenuated in the calcitonin group compared to placebo[339]. In ACLT models of OA in dogs, calcitonin inhibited the SCB trabecular resorption compared with the placebo arm. The preservation of SCB integrity was associated with a significant reduction in cartilage defects[340].

In humans intranasal calcitonin was administered in an open-label study of 220 women who fulfilled the criteria of having post-menopausal osteoporosis, with at least moderate regular pain in a knee with moderate radiographic OA (Kellgren Lawrence two or three). After three months of therapy there was significant improvement in WOMAC pain perception, stiffness and function and these were maintained to the end of the trial at one year. How much of this was placebo effects is unknown[341]. A small randomised placebo-controlled trial of oral calcitonin reported an

improvement in function and reduced cartilage degradation biochemical biomarkers[342].

2.6.4.3 Parathyroid hormone

Parathyroid hormone (PTH) is considered to promote matrix synthesis and inhibit the maturation of chondrocytes[343] that have been associated with endochondral ossification (the process of osteophyte formation). There are no human studies of parathyroid hormone in OA but in animal models after meniscal or ligament injuries in mice, a placebo controlled trial of teriparatide (recombinant human PTH) demonstrated less chondral damage and increased bone volume fraction in the teriparatide arm[344]. Similar improvements in trabecular thickness accompanied by chondroprotective effects have been demonstrated in rabbit OA models[345].

2.6.4.4 Vitamin D

Vitamin D is known to be important in bone metabolism and previous observational studies have suggested increasing levels above 36 ng/mL was associated with beneficial effect[346, 347]. Therefore a 2-year randomized, placebo-controlled trial of supplementing vitamin D levels in symptomatic knee OA to elevate serum levels to more than 36 ng/mL was performed. There was no significant difference between vitamin D and placebo groups for change in symptoms, bone marrow lesion size, cartilage thickness or radiographic JSW[348].

2.6.5 Summary

SCB plays an integral role in the pathogenesis of OA from the earliest through to the most advanced stages of OA. The likely sequence of events in SCB that lead to OA have been summarised (Figure 22). SCB pathologies are associated with conventional OA risk factors that over load joints but SCB shape and imaging abnormalities are independent risk factors for OA themselves before clinical OA develops and as it progresses (Table 7). Therefore SCB represents an important tissue in OA and potentially an important biomarker and target for prospective disease modification.

Table 7 The association of subchondral bone changes with knee & hip OA risk factors

	Age	Gender	Obesity	Injury or ACL tear	Malalignment	Meniscal damage	X-ray Severity	Cartilage damage
Trabecular bone mass, BMD or BVF. (CR/DXA/qCT or MRI)			n/a	+[245]	+[250, 251]	+[252]	+ [208, 215] [349]	+ [210] [350]
BML (MRI)	Not associated [121] [23]		+[99, 121]	+[245, 266] [296]	+[294]	+[295]	+ [294]	+ [301]
Osteophytes (MRI)	+[23]		n/a	+[309, 351]	+[305, 310]	+[272, 311]	+[312]	+[313]
Attrition (MRI)			Not associated [352]	n/a	+[304, 305]	+[305]	+[306]	+[307]
Cyst (MRI)	+[23]	n/a	n/a	+[296]	n/a	n/a	+[319]	+[315]
tAB (MRI)	+ [258]	+[256, 257]	+ [260] [259]	+ [266]	+ [267, 268]	+ [246, 263-265]	+ [269]	[353]
2D Shape			n/a	n/a	+[275]	+[272]	+[276]	+[74]

Bone mineral density (BMD), bone volume fraction (BVF), conventional radiography (CR), dual-energy X-ray absorptiometry (DXA), quantitative computed tomography (qCT), not available (n/a), an association is present with positive correlation (+).

2.7 Biomarkers validation and surrogate measures

2.7.1 Biomarkers and surrogate measures

A biomarker is something that can be measured (relatively) easily which tells us information about the presence, severity or progress of a disease process. This can include a chemical that can be measured in blood or urine, a genetic marker or in the case of this research a quantifiable imaging feature such as bone area or bone shape. An example of a biomarker used in rheumatology is C-reactive protein. As inflammation increases, the blood concentration increases. Many biomarkers provide at most a rough indication of the process that they are being used to measure, and very few are effective at predicting the future progress of disease. Biomarkers are therefore disease-centred variables and represent one end of a spectrum. At the other end of the spectrum are patient-centred variables which are variables that reflect how a patient 'feels, functions or survives'. These guide clinical decision making and are primary endpoints in clinical trials. For example in knee OA the end-stage of OA is treated with a total knee replacement which is a measure of 'joint survival'. However the time from the onset of OA to the time of a joint replacement may be more than three decades which is too long for any clinical trial. Therefore surrogate measures of the patient-centred outcome are required and these are referred to as surrogate outcome measures.

In order to be used as a surrogate outcome measure, a biomarker must demonstrate sufficient validity. Validation of a biomarker is a continuous incremental process and demonstrating validity is not all or nothing event. Validation requires certain domains to be assessed and once a threshold is exceeded then the biomarker may be used as a surrogate measure of how a patient feels, functions or survives[354]. One strategy used for biomarker validation is the Outcome Measures in Rheumatology (OMERACT) filter described by Boers and colleagues which will be described here[355].

2.7.2 Validation of biomarkers using the OMERACT filter

The OMERACT filter encapsulated the concepts of validity by requiring truth, discrimination and feasibility and this is described in the OMERACT hand book[356].

Truth requires that the biomarker measures the patient centred outcome it is intended to measure in an unbiased and relevant way. Truth summarises the concepts of face, content, construct, and criterion validity. Truth may also be referred to as internal validity.

Discrimination requires that the biomarker should be able to discriminate between situations of interest or different groups at one time point such as prognosis, or states at different times by measuring change. This discrimination summarises the demonstration of reliability and sensitivity to change or responsiveness respectively. This incorporates the concept of precision. This is important because precision errors should be sufficiently low in relation to the magnitude of expected change for a given marker during the natural history of change in the biomarker of a disease. If the measurement noise or error is high relative to the actual change in the biomarker (signal) being measured then a poor noise to signal ratio limits the utility of the biomarker.

Feasibility requires that the biomarker can be applied easily, acknowledging the constraints of time, money, and interpretability. Feasibility summarises an important stage in the selection of biomarkers, that may determine a biomarkers success. For imaging biomarkers this should evaluate the practicalities of using a biomarker including cost, burden upon the patient being imaged, equipment requirement, and overall ease of use are appraised. The feasibility has to be balanced against the need for a comprehensiveness and adequate coverage of the OA outcome. The challenge is to maximize feasibility by reducing the demands of the biomarker to the minimum required for validity.

The following defines the components of validation with a specific focus on imaging biomarkers for OA.

2.7.2.1. Face and Content validity

Face validity requires that the biomarker of OA should on the face of it reflect the OA outcome of interest. In order to demonstrate content validity, there should be evidence from qualitative research demonstrating that the biomarker measures the OA outcome or concept of interest. This should include evidence that the domain(s) of the OA biomarker are appropriate and comprehensive relative to its intended measurement of OA outcome and the population of OA that this is intended to apply to. For imaging biomarkers of OA (and their proposed scoring system or scale) they should capture the intended pathophysiologic features of OA such as pain. A review of the evidence for validation should consider this association from all perspectives including the researcher, clinician and patient.

2.7.2.2 Construct validity

In order to demonstrate construct validity, there should be evidence that the concept of the OA biomarker(s) should conform to *a priori* hypotheses regarding logical relationships that should exist with other measures or characteristics of OA and OA patient groups. Construct validity requires that the biomarker is a measure of the OA domain it is intended to measure. This is generally assessed by comparing the prospective OA biomarkers measure with other measures of the same OA domain. For example for a structural imaging biomarker of OA to have construct validity it should correlate or be associated with another structural measure of OA such as the KL grade or JSN or provide similar results. The judgement of the strength of association determines the strength of evidence of construct validity along with the number of measures of OA that it correlates with. This differs from criterion validity for OA biomarkers because criterion validity reflects the strength of association between an OA biomarker and an OA gold standard or ‘criterion’. However with constructs, there is no gold standard.

2.7.2.3 Criterion validity

Criterion validity reflects the extent to which a biomarker directly predicts a patient outcome or the existing gold standard biomarker of the patient outcome.

For example if total knee replacement (TKR) is the OA patient outcome of interest and computed tomographic (CT) measurement of bone width is the gold standard for predicting TKR, an OA MRI biomarker can demonstrate criterion validity if it correlates well with the CT bone measurement (the *gold standard* or ‘criterion’). However for many OA patient outcomes criterion validity cannot be measured because there is no gold standard.

Therefore criterion validity can also be demonstrated if the MRI biomarker is directly predictive of TKR which becomes the ‘criterion’.

Criterion validity can be divided into concurrent validity and predictive validity. Concurrent validity describes cross-sectional associations between OA biomarkers and the outcome of interest such as joint replacement. Predictive validity reflects a longitudinal relationship where an OA biomarker measurement at baseline is associated with a subsequent or future outcome of joint replacement.

2.7.2.4 Responsiveness

The capacity of an OA biomarker to validly detect or measure a significant change over time is described as responsiveness. In order to demonstrate responsiveness the biomarker should first be expected to change in a way that is concordant with other OA biomarkers of the same process.

Thereafter estimates of the standardised change in the biomarker over time such as the effect size or the standardised response mean, can be used to describe and quantify responsiveness. Furthermore the correlation between change in a validated biomarker and change in the new biomarker can be assessed by measuring the area under the curve (AUC) of the Receiver Operator Characteristic (ROC) curve if the validated biomarker can be dichotomised.

2.7.2.5 Reliability

This may be referred to as stability whereby the day-to-day variability of the measurement of the biomarker as a consequence of actual variation in the tissue structure being imaged or the measurement error of the biomarker

may contribute to measurement noise. One way of testing this is to use a test-retest reliability of the biomarker. If the biomarker will be measured by one individual only then the reliability can be expressed as an intra-observer reliability or intra-rater agreement. If the biomarker is measured by several observers then the reliability should also be expressed as an inter-observer reliability or inter-rater agreement. The level of agreement can be expressed as intra-class correlation coefficient (ICC) or a weighted Kappa coefficient (Kw). It can also be expressed as a coefficient of the variance of the same measure (CoV) which is a relative standard deviation and is expressed as a percentage and reflects the noise to signal ratio. This is particularly relevant when automated measurements of the biomarker are made.

In summary there are many components that are required to validate a biomarker as a surrogate measure of a patient-centred outcome. Validity is not binary but is a continuous process and therefore appraisal of evidence is required to suitably validate biomarkers.

2.8 Biochemical biomarkers

Biochemical biomarkers of OA have the potential to contribute to the diagnosis of OA, the delineation of phenotypes, the quantification of tissue burden and prognosis and to measure the efficacy of therapeutic interventions. However even the best described biochemical biomarkers (cartilage markers) lack sufficient discriminative capacity and validity to be used to facilitate the clinical trial design, diagnosis and estimation of prognosis in individuals with OA or to be used as surrogate outcome measures in intervention trials[357].

Important molecules in joint tissue metabolism and pathogenesis of OA have potential as biochemical biomarkers of OA. These include enzymes, cytokines and the constituents of the extracellular matrix that include collagen and proteoglycan precursors and degradation products that are released into biological fluids. These may first be released locally into the synovial fluid of the joint with OA and then systemically into the blood and urine. The concentration in these compartments may reflect cartilage, subchondral bone and synovial metabolism which may be used as a

measure of joint tissue degradation and formation. The advantages and disadvantages of this approach are now discussed.

The majority of connective tissue components of joints are frequently present in many other tissues in the body and therefore the systemic measurement of concentrations of these components in the blood and urine will reflect the healthy tissue turn-over of the whole body (systemic metabolism) and not specific joint pathology of OA. This may be particularly relevant when the pathologic turnover in small joints of the hand is less than the physiologic turnover in all of the other larger joints. Furthermore systemic biochemical marker concentrations are subject to systemic distribution, metabolism and excretion. The volume of distribution may vary with body mass index and the metabolism and excretion may vary with varying degrees of renal and hepatic dysfunction that are prevalent amongst people with OA. Systemic concentrations may also vary with food intake, physical activity, and when multiple joints and other connective tissues are involved. Therefore these systemic biomarkers may not accurately capture the specific local tissue pathology when only a few joints are affected by OA and their utility may be greater in generalised OA.

Measuring biomarker concentrations in synovial fluid may offer a more accurate representation of OA pathology within specific joints. However variation in joint movement and intermittent synovitis may cause concentrations of biomarkers to vary over time.

The National Institutes of Health-funded OA biomarkers network has classified specific biomarker definitions into five categories to improve the development and analysis of OA biomarkers; Burden of disease, Investigative, Prognostic, Efficacy of intervention and Diagnostic (BIPED) [358]. A recent systematic review classified 26 biochemical markers of cartilage, bone or synovial metabolism by the BIPED categories[357]. The best performing, most frequently and broadly described biochemical biomarkers are in the context of knee and hip OA and are considered to be a measure of collagen degradation (urinary C-terminal telopeptide II, serum cartilage oligomeric protein). There is evidence of predictive validity of these two biomarkers for incidence of knee ROA [359, 360] and progression of hip

and knee ROA[361] in longitudinal cohort studies having adjusted for age, gender and BMI. However biochemical markers have little ability to predict symptoms[360]. The performance of the other biomarkers e.g. serum hyaluronic acid and urine/serum N-terminal peptide 1, could not be adequately evaluated due to a lack of evidence. Despite the considerable research efforts made to determine if they can be used for as surrogate measures for diagnostic purposes or to reflect how a patient feels, functions or survives, the authors of the systematic review [357] concluded that none of the available biomarkers had sufficient discriminative properties to be used for these purposes. The same conclusions have been drawn by the European Society for Clinical and Economic Aspects of Osteoporosis and Osteoarthritis also draw the same conclusion[362].

Currently none of these biochemical markers, are sufficiently discriminating to be used as surrogate outcome measures[363].

2.9 Magnetic resonance imaging

Conventional radiography (CR) is unable to capture the severity of the multi-tissue involvement in joints with OA joints. This is particularly important because many of the trials of prospective disease modifying agents in OA (DMOADs) have attempted to recruit a homogenous population that are likely to exhibit structural progression by selecting people with knee Kellgren-Lawrence grades ≥2. Unfortunately these patients may lack uniformity in terms of joint tissue involvement because CR is insensitive to tissue pathology like bone marrow lesions (BMLs) which have important prognostic implications and are associated with worse structural and symptomatic outcomes (2.4.3.2 OA pain and its structural associations). Amongst individuals within the Framingham cohort above the age of 50 years, with no pain and normal knee radiography, 88% of individuals had at least one OA tissue lesion in the knee on magnetic resonance imaging (MRI) [23]. This included an osteophyte, cartilage damage and BML prevalence of 72%, 68% and 50% respectively. MRI is more sensitive to osteophytes and cartilage damage than conventional radiography[364]. Therefore appropriate

stratification and monitoring of these tissue pathologies among patients with OA requires MRI.

MRI offers several advantages including the ability to examine the presence and extent of tissue pathology in each of the joint tissues in OA[25]. The quantification of MRI cartilage morphometry in knee OA has demonstrated good evidence of reliability and responsiveness and there is some evidence of its predictive and construct validity[365, 366]. This includes loss of quantitative cartilage volume being a potential predictor of total knee replacement (TKR). The measurement of subchondral BMLs and synovitis in knee OA has also demonstrated good responsiveness for semiquantitative MRI assessment[366]. Further data is required to accurately quantify the BMLs and synovitis and to determine whether these demonstrate predictive validity of outcomes such as TKR.

The disadvantages of MRI include that the acquisition is more time-consuming and expensive than plain radiography. However in terms of clinical trials, the greater responsiveness of tissue measures might mitigate the additional costs because fewer patients may be required to demonstrate a structure-modifying effect.

MRI-determined quantitative and semi-quantitative measurements of joint tissue in OA (2.11Imaging biomarkers in OA) have started to be used as clinical outcome measures in structure-modification DMOAD trials. This reflects the opinion of the Osteoarthritis Research Society International (OARSI) working group that recommended MRI cartilage morphology assessment be used as a primary structural end point in clinical trials which also acknowledged the rapid evolution of quantitative MRI assessments of subchondral bone and synovium[367].

Therefore using MRI biomarkers of joint structure in OA represents a significant improvement in sensitivity to clinically significant structural pathology, responsiveness and in its correlation with pain compared with CR biomarkers. However we have not yet harnessed the full potential of MRI biomarkers and utilised all of the three dimensional tomographic information that MRI has to offer.

2.10 Statistical Shape modelling, active shape modelling and active appearance modelling

Man-made or manufactured shapes are relatively easy to describe and identify in two or three-dimensions. However describing the shape of naturally occurring organs like joints that adapt to their environment is much more challenging but represents an important source of in vivo information. This is because the shapes are often complex, asymmetrical structures and there is significant variation between individuals at a population level.

Historically defining the shape of similar tissues or organs has been achieved by the process of manual segmentation. This is a labour-intensive and time-consuming process which requires that the edge of the structure of interest (e.g. a cartilage plate or SCB area seen on an MRI slice) be drawn around to define the shape of it. However computers can be trained to recognise shape using ‘machine vision’. If the geometric properties of the target tissue are manually segmented in a substantial population of training set images, the segmented regions of interest can be analysed for their geometric (shape) properties using statistical analysis to create a statistical shape model (SSM). This ‘trained’ SSM is a shape-recognition model that has learnt what shape to look for in a subsequent target image. This process involves the analysis of geometric shape identifying landmarks on the edge of the target tissue that are consistent at a population level. These are referred to as consistent landmarks and their automated application to subsequent target images can automate the segmentation and substantially reduce the labour-intensive approach of manual segmentation. One of the first applications for this shape recognition was in the application of facial recognition in 1998. How well the training set represents the variation in shape in the target image population is one of the determinants of how well the model can segment the shape accurately. Where multiple MRI slices are available for one joint, the cartilage plate or SCB area can be segmented on serial adjacent slices which permit a 3D shape reconstruction to be made (2.10.2.3 Segmented three dimensional bone area, cartilage thickness and volume).

The next generation of shape recognition involved an additional statistical model that incorporates the variation in characteristics in the target images. These are called active shape models(ASM)[289]. An ASM involves a local search algorithm which relies upon the same pure edge-based approach of the SSM. However the model actively seeks to update the fit of the model to the target image (without using the grey-scale texture) to ensure the best fit is achieved which brings the model closer to the correct solution (Figure 30). Hutton and colleagues used this for the purposes of detecting cephalometric landmarks[368].

Figure 30 Active shape model and local searching

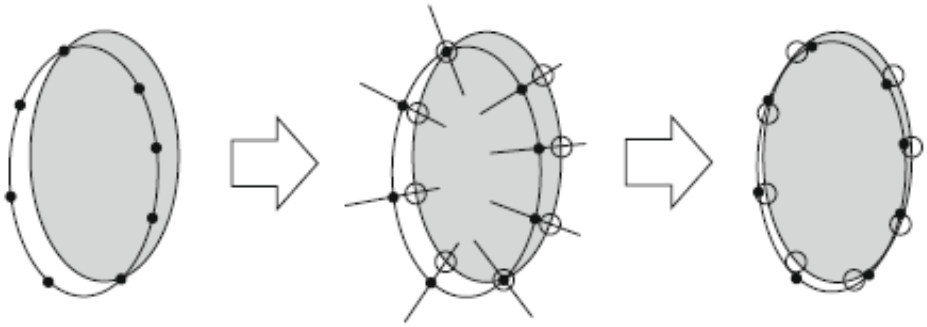

In the first image the model at the beginning has been synthesised by the ASM. The model then attempted to constrain the edge of the shape using learned consistent landmarks. However local searches for all landmarks are evaluated at different positions perpendicular to the model surface in the second image and the new best landmark positions are identified . The ASM model parameters and landmarks are then updated to minimise the distances between the model landmarks and the actual shape. Reprinted by permission from Elsevier Ltd: Medical Image Analysis [369] - 2009)

Finally the latest generation of shape modelling is the active appearance model (AAM). These also actively seek to keep to a minimum the difference between the actual shape of a new target image and one synthesised by the AAM. This is achieved not only by local searches of the shape (as in ASM) but also by using a model of grey-scale texture on either side of the edge of the shape. The model learns, from training sets, what grey-scale texture to expect on either side of the learned edge by analysing the greyscale

changes in a rim of 5-6mm spanning either side of the learned edge in a perpendicular manner to the edge. This ensures the appearance of the grey-scale texture is actively searched to optimise the shape automated segmentation. In the tissues of the knee, for example, the MRI signal provides a grey-scale variation which may have darker signal in the cartilage overlying the SCB and brighter signal in the bone. By learning from training samples, the AAM can actively define shape more accurately. This is the technology that has been applied in defining bone shape and bone area in the subsequent Chapters 4-6.

2.10.1 The applications of shape modelling

The advantages of analysing the shape, or the change in shape of tissues based on imaging is that this can provide three-dimensional morphological data that can be used non-invasively to describe human physiology and pathophysiology in vivo. Tissue shape can indeed be a directly involved in the pathogenesis of disease(2.6.3.2.1 Femoroacetabular impingement). In states of disease shape may be particularly important when planning interventions with narrow therapeutic windows such as surgical resection of cancer or radiotherapy. It may also be useful when creating prostheses. Finally shape and volume can be determined by shape models and these may provide important prognostic information if suitably validated. Examples of how statistical shape modelling, active shape models and active appearance models have all contributed to these are described below.

The physiological shape changes in the tracheobronchial tree[370] and liver [371] during breathing have been modelled in order to better understand the changes in these organs during bronchoscopy and surgery. The shape change in the levator ani during straining[372] has also been modelled. The shape change in mandibles during development has also been measured with models longitudinally to describe growth of bone[373]. The shape of the larynx has also been modelled to describe the association of shape with pitch of voice as part of natural variation[374]. The variation in the shape of brains during development[375] and during ageing[376] have also been performed to describe these physiological processes.

The left atrium is known to remodel and dilate in atrial fibrillation. This shape change in the left atrium in atrial fibrillation is believed to be associated with the outcome of cerebrovascular accident. Therefore shape modelling has been used by Cates and colleagues to describe the shape changes in the chambers of the heart[377].

Echocardiographic imaging of the fetal heart is an important component of screening for congenital abnormalities. In order to improve the sensitivity of screening it has been proposed that active appearance models of the heart chambers may add important diagnostic information to the screening process and these models have been trained.

Vertebral fractures are important causes of morbidity. However while conventional radiography is inexpensive and accessible it is relatively insensitive to detecting osteoporotic fractures compared to computed tomography which is more expensive and less accessible. The shape change of vertebrae seen on conventional radiography may be subtle but the detection of a fracture affects clinical management and may prevent morbidity. The shape change associated with small fractures may be subtle and therefore active appearance models are being trained upon conventional radiographs to try to improve the sensitivity of fracture detection.[378, 379].

Brain tissue shape has also been used to identify associations between brain tissue shape and conditions like attention-deficit hyperactivity disorder[380], schizophrenia[381, 382] and psychiatric disorders[383].

Planning radiotherapy is very important. Irradiation of noncancerous tissue may cause significant iatrogenic comorbidity. Shape models may improve the anatomical spatial awareness and minimise complications of therapy in head and neck malignancy[384] as well as prostate malignancy[385]. Tumour pathology can also be detected focally within an organ using shape modelling for more targeted therapy[385].

Training for surgical interventions such as hysteroscopy can be provided by modelling the shape of multiple real uterine cavities and converting this information into a simulator or virtual hysteroscopy for trainee surgeons[386]. Planning surgical interventions with computer-assisted surgery is an

evolving area of research. Pre-operative planning in neurosurgery with segmented brain images may be improved with 3D models of the brain, that provide localization, targeting, and visualization of tumours that can be used to simulate planned interventions[387] (Figure 31). Pre-operative shape modelling from ultrasound can also be used to assist planning in hip replacement[388, 389], for anterior cruciate ligament reconstruction[390, 391].

Figure 31 3D Segmentation of tissues of the brain

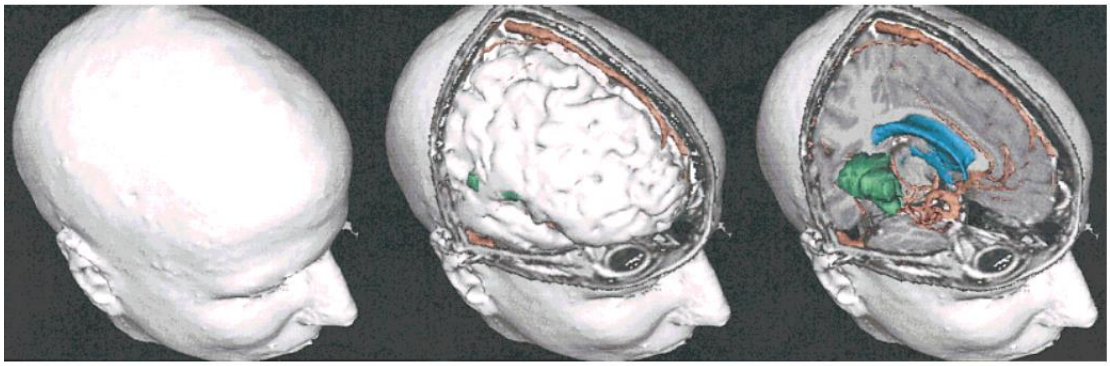

A model of a patients head and segmented brain regions. Reprinted by permission from John Wiley & Sons Ltd: Journal of Magnetic Resonance Imaging [387].

In order to improve the fit and comfort of hearing aids, a better shape fit in the external auditory meatus is required. Designing custom-made hearing aids to fit the external auditory meatus using shape models has been described.[392]

Prognostic information may be obtained from shape modelling of medical images. For example the volume of the prostate in prostate cancer is a strong predictor of treatment outcome especially if this volume is combined with a baseline prostate-specific antigen level[393]. Cam deformity of a femoral head on conventional radiography is also predictive of ten-fold greater risk of end-stage hip OA within 5 years[74].

In summary the field of shape modelling has already identified important applications in medical practice in terms of improving our understanding of

physiology and pathophysiology in humans. Shape models may also improve prognostic accuracy and interventional precision and permit personalised medicine by making custom-made prostheses. This technology and its application in the field of OA will be described in the next section.

2.10.2 The two- and three dimensional shape modelling for determining joint shape, cartilage volume and bone area

The shape of the subchondral bone has been identified as being associated with risk factors for OA, the structural progression of OA and it is an independent risk factor for incident OA and joint replacement (2.6.3 Bone shape and subchondral bone MRI features in OA, 2.11.1.2.5 Quantitative bone area and three-dimensional bone shape). However most of the assessments of bone shape used to demonstrate these associations have been based upon two-dimensional images alone or with reconstruction into three-dimensional shapes. While imaging biomarkers are the best personalised biomarkers (2.11 Imaging biomarkers in OA), more responsive biomarkers are required for the purposes of clinical trials, and three dimensional shape may provide novel imaging biomarkers of cartilage and subchondral bone shape, this section discusses the existing imaging shape biomarkers.

2.10.2.1 Segmented bone shape on conventional radiography

Agricola and colleagues have used SSM to describe the 2D shape of the SCB in the hip joint including the femoral head and acetabular shape to describe the association with OA progression in a nationwide prospective hip OA cohort study [394].

Waarsing and colleagues described the association of knee bone 2D shape, determined by SSM, with the presence or absence of cartilage defects[276].

Lynch and colleagues examined the association of incident hip OA with variations in 2D proximal morphology, assessed by ASM [291].

2.10.2.2 Segmented two dimensional tibial bone area

Jones and colleagues have described the cross-sectional bone area of the tibia described in observational studies amongst the healthy population and those with and at risk of knee OA [31]. Bone area was calculated from axial

MRI slices of the tibial bone plateau (Figure 23) that were closest to the joint. The medial and lateral tibial bone areas were then measured from these directly using manual segmentation to provide the cross-sectional bone areas. An average of the three areas was used as an estimate of the tibial plateau bone area (tAB)[263, 395, 396].

2.10.2.3 Segmented three dimensional bone area, cartilage thickness and volume

Eckstein and Chondrometric's colleagues have also quantified cartilage volume, cartilage thickness and bone area over the tibia but also the femur and patella using laborious manual segmentation derived from serial magnetic resonance (MR) images, and analysis algorithms[271]. This Cartilage thickness has also been segmented (

Figure 32) which can be used to provide a reconstruction of the femoral and tibial cartilage plates in three dimensions. Eckstein and colleagues have defined the different regions (Figure 33,Figure 34), and subregions within the knee (Figure 33,Figure 34). For bone area (tAB), the medial and lateral femur, tibia and patella are consistently divided into different subregions that can be appreciated below for the femur and tibia. Notably the central region of the femur is identified as the 'weight bearing' region which is distinct from the femoral trochlea of the patellofemoral joint or the posterior femur (Figure 33,Figure 34). The tibia is divided into medial and lateral regions and these two are further subdivided into five subregions (Figure 34).

Figure 32 Measuring cartilage thickness

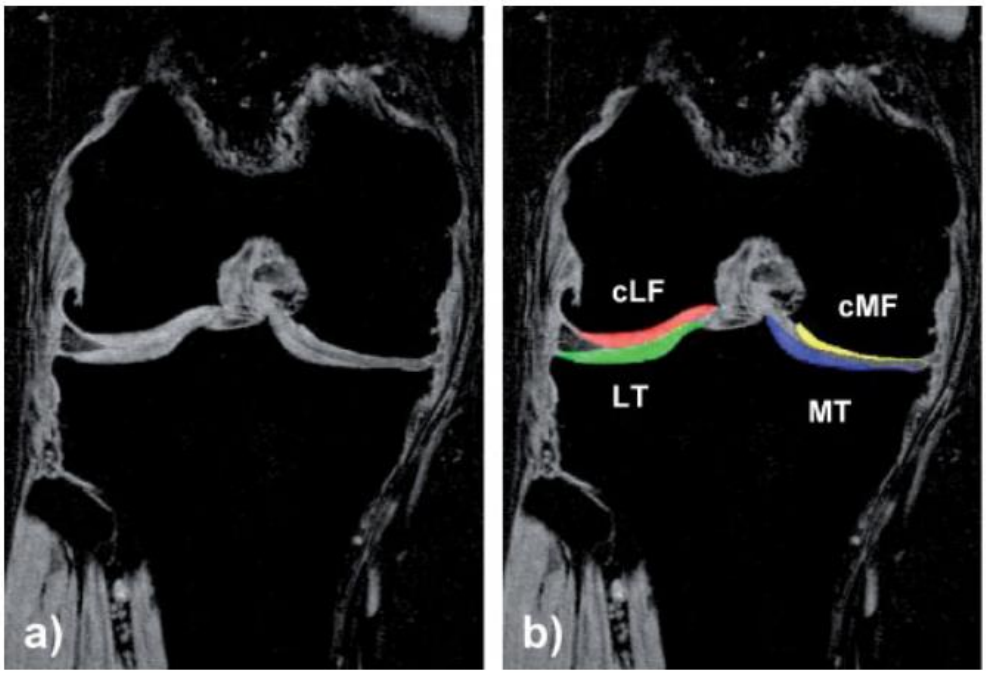

Examples of the coronal measurement of cartilage thickness using segmentation. cLF (central lateral femur), cMF (central medial femur). Reprinted by permission from John Wiley & Sons Ltd: NMR Biomed from [397]

Figure 33 Reconstruction of tAB of the medial and lateral tibia and femur

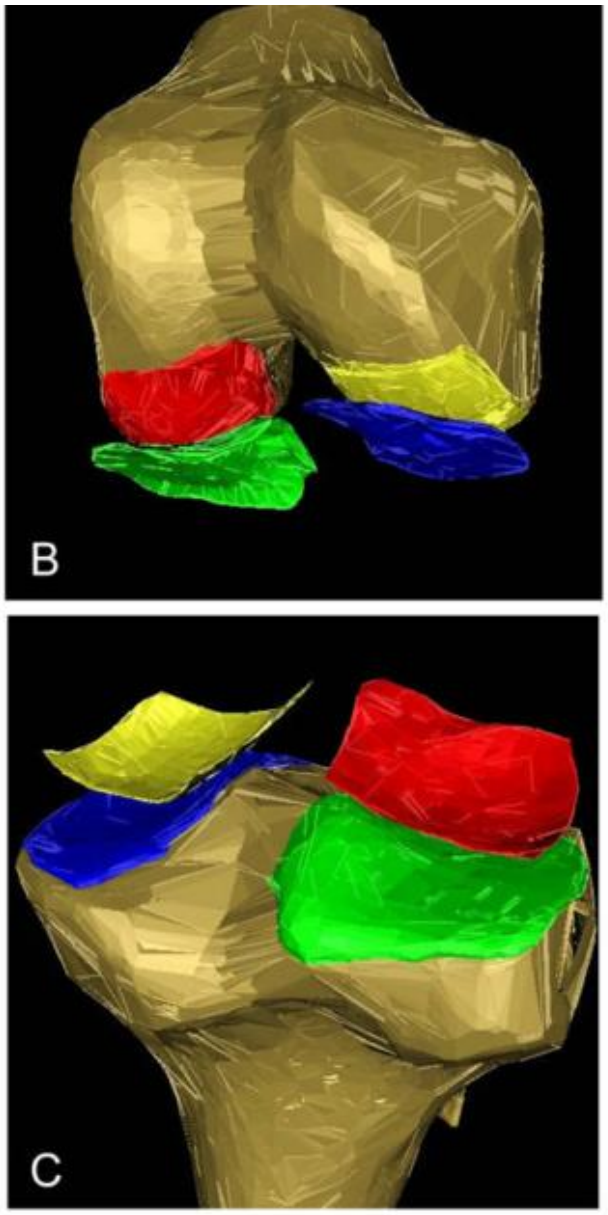

b) Reconstruction of the femoral bone only and of the tAB of the above cartilages

c) Reconstruction of the tibial bone only and of the tAB of the above cartilages

Springer Calcif Tissue Int, Medial-to-lateral ratio of tibiofemoral subchondral bone area is adapted to alignment and mechanical load, 2009 Eckstein et al, reprinted with permission of Springer Reproduced from [267]

Figure 34 Regions and subregions of the knee - chondrometrics

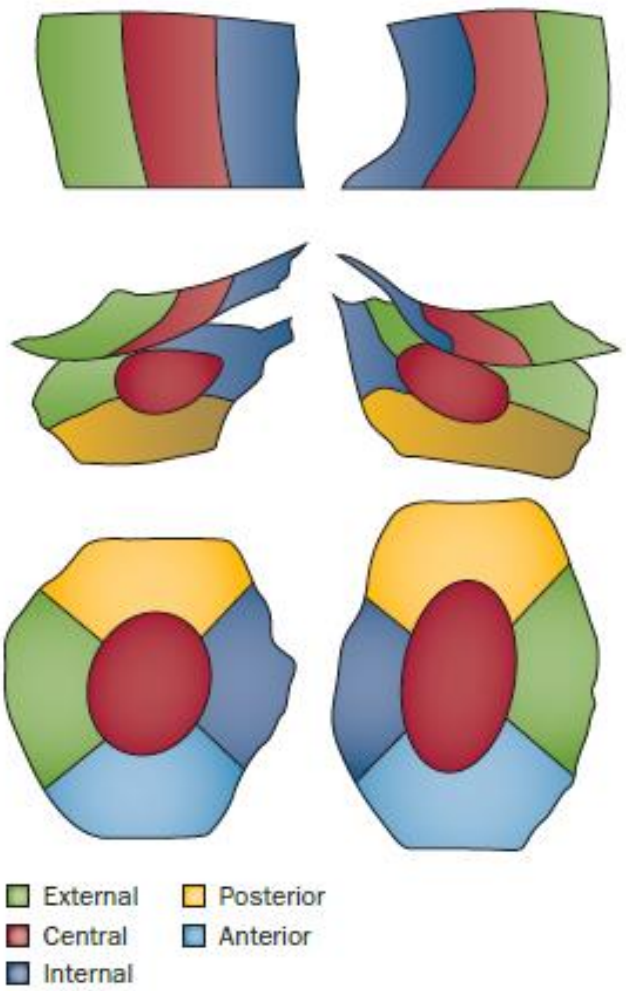

Three-dimensional reconstruction of the tibial and femoral subchondral bone with subregional division. Reprinted by permission from Macmillan Publishers Ltd: Nature Reviews Rheumatology [398] Copyright 2012

Figure 35 Regions and subregions of the knee - Arthrovision

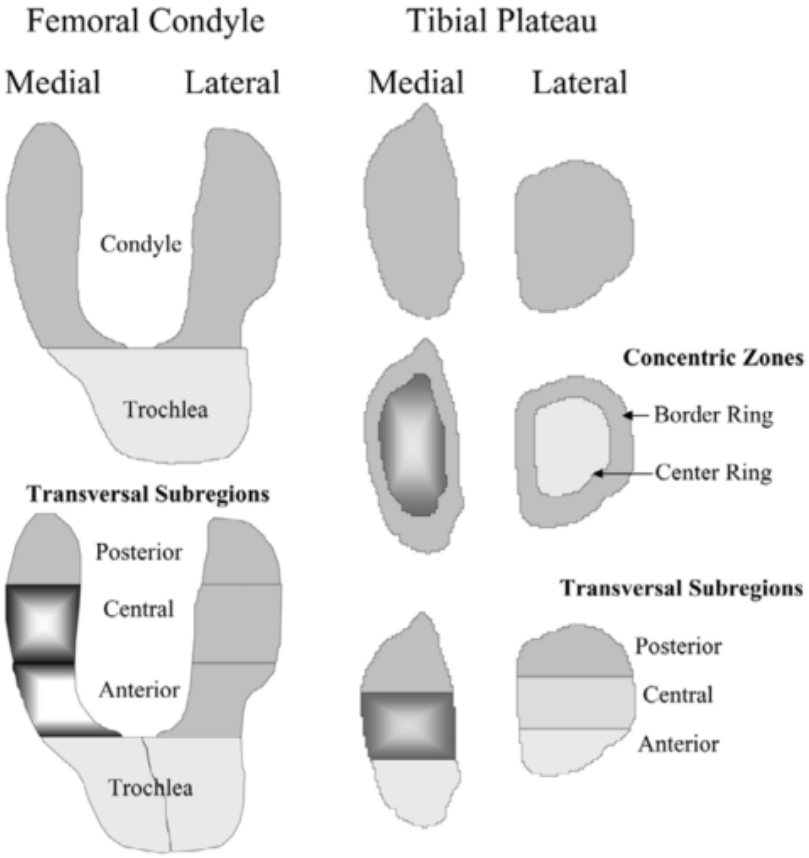

Division of the three-dimensional tibial and femoral subchondral bone into subregions. Reprinted by permission from BioMed Central: Arthritis Research Therapy, Pelletier et al [123]

Pelletier and Arthrovision colleagues have similarly segmented the cartilage plates in order to calculate femoral and tibial cartilage volume by segmenting the tibiofemoral compartment using shape modelling [123](Figure 35). They have also used cartilage thickness and maps of the findings.

In summary there are many examples of 2D and 3D imaging biomarkers that have been described above. The SCB is important in the pathogenesis of OA including SCB shape. The importance of modelling the shape of the knee bones with SSM, ASM and AAM is it may permit the validation of novel imaging biomarkers with improved responsiveness profile than existing imaging biomarkers for prospective use in OA modification trials.

2.11 Imaging biomarkers in OA

Joint imaging has permitted the direct and indirect description of articular tissues and their structural pathology. The quantitative and semi-quantitative descriptions of the imaged articular tissue structural pathology, morphology and composition have provided measures or biomarkers of physiological and pathophysiological processes that are specific to the joint and are these imaging biomarkers are currently the best personalised biomarkers in OA.

Conventional radiography (CR) provides two-dimensional projection images that only directly visualise bone and are insensitive to structural pathology and longitudinal change in this. Therefore imaging biomarkers derived from unstandardised radiographic protocols are typically subject to significant measurement error, poor responsiveness and structural changes are poorly correlated with the clinical syndrome. Nevertheless, with appropriately standardised radiographic protocols the measurement of joint space narrowing from CR is the current standard for determining structural progression in OA.

MRI provides three-dimensional tomographic imaging which greatly improves the sensitivity to detecting structural pathology of all joint tissues and longitudinal change in this. Imaging biomarkers derived from MRI are subject to less measurement error, better responsiveness and structural pathology correlation with the clinical syndrome. MRI measures have greatly contributed to the description of the natural history of knee OA and the identification important structural pathologies of tissues within the ‘whole joint’ that are associated with important clinical and structural outcomes in knee OA.

Imaging biomarkers, unlike systemic biochemical markers (2.8 Biochemical biomarkers), are joint-specific and have been used in longitudinal observational studies to describe the natural history of OA. This process has demonstrated that several of these measures have concurrent and predictive validity regarding clinically important outcomes such as structural progression, pain and joint replacement. The variety, validation, advantages and disadvantages of imaging biomarkers are described here.

2.11.1 Quantitative measures in OA

The structural pathology of OA can be described using quantitative measures. These measures are not used in routine clinical practice but they may be used as a structural outcome measures and for clinically meaningful outcomes like symptoms and joint replacement. These measures are described here.

2.11.1.1 Conventional radiographic quantitative measures

2.11.1.1.1 Continuous joint space width and joint space narrowing

The measurement of joint space width (JSW) and joint space narrowing (JSN) by conventional radiography (CR) quantifies the interbone distance between opposing bones of any diarthrodial (synovial) joint. This section will primarily focus on the knee. JSW for the tibiofemoral joint is between the femur and the tibia. JSW and JSN are considered to be surrogate measures for hyaline articular cartilage thickness or loss respectively. However JSN is in fact a composite of cartilage loss and meniscal degeneration and/or extrusion.

Weight-bearing is necessary to displace synovial fluid, to juxtapose the opposing articular cartilage surfaces and to maintain a similar cartilage compression and hence reproducible joint positioning between examinations. In routine clinical practice knee radiographs are typically weight-bearing in extension. Weight-bearing knee radiographs have a significantly smaller medial minimum JSW than non-weight-bearing radiographs[399].

Any interbone measurement with this protocol may be affected by variation in the degree of knee flexion, rotation (of the femur or tibia), medial tibial plateau alignment and magnification (Figure 36). Magnification is a product of the position of the knee relative to the x-ray beam and x-ray film.

Figure 36 Positioning of the subject for the fixed flexion and Lyon-Schuss radiographs and examples of good and poor alignment of the medial tibial plateau with the X-ray beam

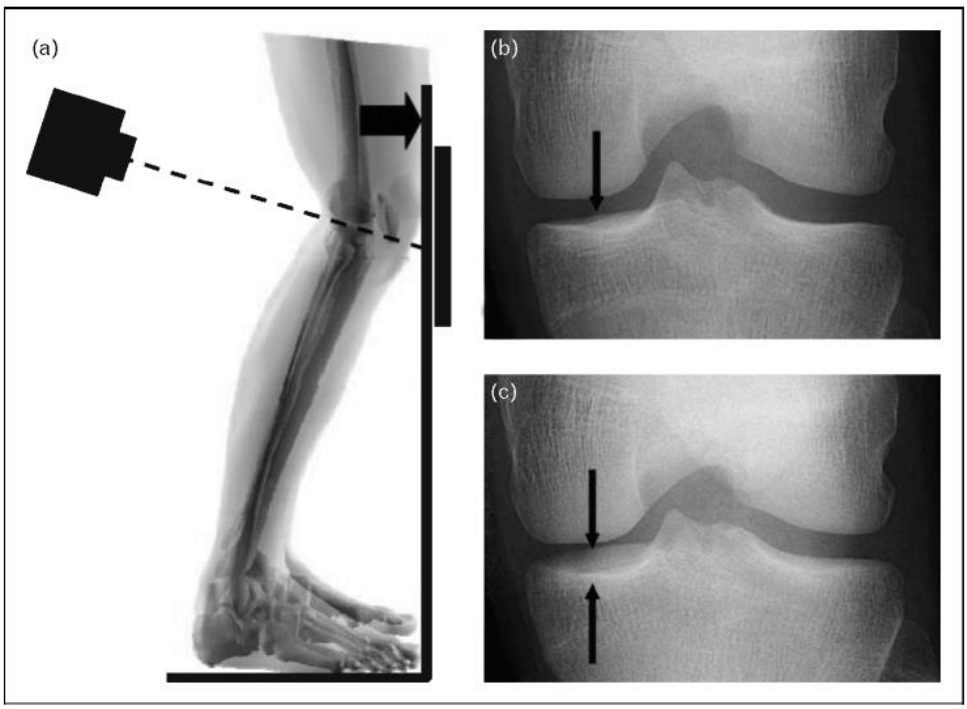

The interbone measurement may be affected by variation in the degree of knee flexion and rotation of the femur or tibia. Reproduced from Annals of Rheumatic diseases, Le Graverand et al, 2008, [94]. with permission from BMJ Publishing Group Ltd.

A full extension knee radiograph can also artificially increase apparent cartilage thickness[400] and is less reproducible than semi-flexed knee views[401, 402]. Therefore in order to improve the measurement noise to signal ratio and minimise the effect of repositioning error or inter-occasion variation (reliability), serial monitoring of JSW should be made by a standardised radiographic positioning with weight-bearing flexion protocols of which there are several;

Fluoroscopic protocols such as

- the Lyon-Schuss protocol takes a posteroanterior view of the knee with the pelvis, thigh and patellae of the patient being flush with the film cassette which is in the same plane as the tips of the great toes and confers an approximate fixed knee flexion of 20 degrees[403].

This method appears to have a better sensitivity to change in JSW because this affords better alignment of the medial tibial plateau (Figure 36) [94, 402, 404] and does not require magnification correction unlike anteroposterior methods[403]. The limitations of this method include increased cost and patient irradiation and hence protocols without fluoroscopic-guidance were developed including the fixed-flexion[402] and metatarsophalangeal[405].

Non-fluoroscopic protocols include:

- A postero-anterior view of the knee with the cassette in the same plane as the 1st metatarsophalangeal joint[406]. However the degree of knee flexion is not standardised.
- A fixed degree of knee flexion and foot rotation and position of the knee relative to the x-ray beam and film can be standardised for each subject using a consistently-placed SynaFlexer plexiglass knee positioning frame[402] (Figure 42).
- Finally a modified Lyon-Schuss protocol combines the positioning of the Lyon-Schuss with the use of the Synaflexer frame without the fluoroscopy[407].

While the sensitivity to change is improved when the medial tibial plateau is parallel to the X-ray beam a suggested alternative without fluoroscopic-guidance is to acquire multiple radiographs of each knee to ensure the best projection image is achieved[408]. A quality control approach for tibial plateau alignment was incorporated in the Osteoarthritis Initiative radiography protocol. Where radiographs of insufficient quality were identified, participants were invited to have multiple knee radiographs (

2.12.4 Knee radiography protocol[409])

Metric JSW can be measured manually from CR with a graduated ruler, calipers, or using semi-automated computer software[410, 411].

Furthermore the minimum interbone distance (mJSW) can also be measured as a measure of greatest JSN[412]. It can also be measured at location-specific locations at or in relation to specific anatomical landmarks[413]. In knees without and with ROA knee, mJSW and location-specific JSW had

optimal responsiveness respectively[413]. However despite the best efforts to minimise repositioning errors, the minimum inter-occasion variation (standard deviation of the difference between test-retest measurements of mJSW) was approximately 0.1mm in the methods with best repeatability[402, 414]. This represents a smallest detectable difference of at least 0.2mm. Considering that the mean rate of annual knee JSN is 0.13 ± 0.15mm/year, with change occurring in only a small group of "progressors"[93, 94], this represents a significant measurement noise to signal ratio and highlights the lack of responsiveness of this measure.

CR JSN is also limited by the fact that JSN is not a specific measure of hyaline cartilage loss but a composite measure of the degeneration of two tissues. JSW is a construct of degeneration and extrusion of the menisci as well as hyaline articular cartilage degeneration[86].

Furthermore a systematic literature review of relevant structural progression defined by JSW identified considerable heterogeneity in definition of loss of metric JSW required to be defined as a 'progressor'[415]. There is no current consensus of opinion on which threshold represents an accurate definition.

Despite these limitations CR continuous JSW or JSN remains the recommended measurement for measuring structural change according to the Osteoarthritis Research Society International Food and Drug Agency (OARSI FDA) OA assessment of structural change working group[367].

The validity of JSN as a clinically and structurally important measure of OA is supported by the following evidence. Knee JSN occurring over five years is predictive of future knee replacements as much as 15-years later[104, 416]. Degenerative meniscal changes at baseline in knees are predictive of JSN two years later[417]. Degenerative changes of knee hyaline articular cartilage, menisci and meniscal extrusion are also predictive of JSN 30 months later[418]. Subchondral bone changes of OA include increased turnover and bone marrow lesions. A bone turnover biomarker is predictive of subsequent JSN in knees with symptomatic and ROA[419]. JSN of hand OA is associated with BMLs[420]. Amongst 942 patients with symptomatic knee OA, a lower baseline metric mJSW and greater JSN over four years was predictive of greater deterioration in pain, function and quality of life

after suitable covariate adjustment[421]. Metric JSW responsiveness (measured using the Synaflexor)[402] has been compared with the responsiveness of cartilage volume in the progressor cohort of the OAI over 12 months in 150 knees. The conclusion from the authors was that the most responsive JSW and MRI cartilage volume measures were comparable at -0.32 and -0.39 respectively (expressed as standardised response means)[413, 422]. This may in part be explained by the slow rate of cartilage progression in conjunction with the equally poor measurement to noise ratio of the cartilage volume measurement method. The greatest rate of cartilage volume loss was -2.5% per annum[422], but the coefficient of the variance (the noise to signal ratio on inter-occasion measurement error) of cartilage volume segmentation ranged from 3 to 5% (see the web appendix of this citation[422]). This is comparable to radiographic JSN coefficient of the variance [412] which may explain the limitations of measurement noise to signal ratio of these methods. A superior coefficient of the variance for the measurement of cartilage volume is quoted by Eckstein et al. of 2.4-3.3%[423] indicating a better method for cartilage volume assessment.

A meta-analysis of the responsiveness of JSW confirmed that this was significantly better with trials with flexed knees with greater than two years of duration (SRM =0.71). The intra-reader and inter-reader intra-class correlation coefficients were excellent and coefficient of the variance estimates were approximately 3%[424].

The implications of this are that trials based on JSW as an outcome measure require follow up periods of at least two years and due to the relative insensitivity to change and poorer reliability, require large numbers of patients per arm to adequately power the study which represents a major barrier to performing trials of prospective disease modifying agents. This highlights the inadequacy of JSN as the current OARSI FDA standard of OA structural progression measurement and the need for better biomarkers.

2.11.1.1.2 Continuous (metric) alignment

Alignment of joints can be assessed using clinical and radiographic methods. This section will focus specifically on the knee. Knee alignment can be measured clinically using a goniometer as it is in the Osteoarthritis

Initiative at baseline or using lower limb conventional radiographs. Radiographic knee alignment can be classified in two ways. The most commonly used method is the mechanical axis which requires a full-length lower limb radiographic image and measures the hip-knee-ankle angle[425]. This is the femur-tibia angle formed by the intersection of a line connecting the centre of the femoral head with the middle of the knee and another line connecting the middle of the ankle joint with the middle of the knee joint. The second method is the anatomic axis which is the angle formed by the intersection of a line through the middle of the tibial shaft and a line through the middle of the femoral shaft[426].

A systematic literature review of the concurrent and predictive validity of knee OA malalignment as a measure of radiographic and MRI structural severity and progression identified that increasing goniometer-measured malalignment was associated with concurrently greater osteophytes and JSN[427]. Continuous varus and valgus malalignment of the knee measured by radiographs was concurrently associated with greater cartilage degeneration on MRI[428]. The systematic review in 2009 also concluded that continuous baseline radiographically-determined alignment was predictive of radiographic and MRI-determined structural progression in longitudinal studies. This along with more recent literature provides evidence of predictive validity of continuous malalignment which will be described here in terms of radiographic followed by MRI structural progression outcomes.

Baseline alignment, in knees with symptomatic ROA, was independently associated with longitudinal progression in medial and lateral JSN with varus and valgus malalignment respectively[429, 430].

Baseline malalignment severity, in 117 knees with symptomatic ROA, was associated with a dose dependent increase in rate of MRI cartilage volume loss (either tibial or femoral) in the medial and lateral compartments, with increasing varus and valgus malalignment respectively over two years[431].

Baseline varus malalignment severity, in 293 knees without evidence of tibiofemoral cartilage defects at baseline, was independently associated with a dose dependent effect on incident medial WORMS cartilage defects (2.11.2.2.2 Knee semi-quantitative measures). Baseline malalignment also

reduced the risk of incident cartilage defects in the compartment receiving less load over 30 months[77]. The same observation that varus and valgus malalignment 'off-loads' the lateral and medial compartments respectively and reduces the odds of cartilage damage over two years, was made amongst knees with ROA[432].

Loss of medial cartilage thickness and volume were both independently associated with continuous varus malalignment in 250 knees with established OA but the valgus deformity was associated but not independently with lateral cartilage loss of the same measures[433].

Sharma and colleagues reported that continuous valgus deformity is not independently associated with lateral cartilage loss[77, 433]. These analyses only included 55 knees with valgus. Felson and Cicuttini and colleagues, included up to 881 knees with valgus deformity and reported independent associations between longitudinal lateral cartilage loss and categorical [76] and continuous [431] valgus malalignment respectively. The risk of incident OA and progression of knee OA utilised ROA and MRI measures and found categorised valgus deformity (in 881 knees) was independently associated with MRI cartilage loss, and increasing severity of radiographic JSN and meniscal degeneration[76]. Therefore there is good evidence that varus and valgus malalignment are independently predictive of structural progression.

Continuous malalignment also has predictive validity regarding future symptoms and total knee replacement. Valgus malalignment at baseline is also independently associated with persistent knee symptoms of OA or total knee replacement after six years [434] and when incorporated in phenotypic stratification, confers a greater risk of structural progression[435].

Varus alignment is associated with pain severity in cross-sectional analysis [436] and malalignment is associated with incident bone marrow lesions in the biomechanically loaded compartment[437].

More recently the femur-tibial angle, obtained from fixed-flexion knee films, with adjustment for sex-specific varus shift was found to be as good as the long-limb radiograph and better than goniometry in predicting change in cartilage thickness over two years[438].

In summary CR quantitative imaging biomarkers have been validated as measures of clinically and structurally important outcome measures. However despite great efforts to optimise the responsiveness of JSN, the current standard for measuring structural progression, the insensitivity of this measure to change represents a significant barrier to discerning the potential for disease modification and advancing the treatment of OA. More responsive biomarkers are therefore required.

2.11.1.2 MRI quantitative measures

There are broadly two strategies for the quantification of MRI OA structural pathology. Quantitative MRI measures are described here and semi-quantitative MRI measures below (2.11.2.2 MRI semi-quantitative measures). While semi-quantitative measures use an ordinal scale, quantitative measures quantify tissue characteristics such as cartilage thickness[439] or volume[440] which typically uses segmentation techniques.

The imaging sequences required for quantitative measures differ from semi-quantitative grading because spatial resolution is more important and the precise distinction of the osteochondral interface and cartilage surface is essential. This is because most quantitative analyses involve the segmentation of tissues which are usually performed manually or using semi-automated methods. These methods can be labour intensive and require expert analysis, specialised computer software, special training of segmenters and quality control procedures[441].

Quantitative measures were found to be more sensitive to change than semi-quantitative measures[442]. As a consequence the measurement of longitudinal structural change with semi-quantitative measures has evolved [443, 444] to offer comparable longitudinal sensitivity to change[366].

2.11.1.2.1 Quantitative morphologic measurement of cartilage thickness & volume

In order to quantitatively measure cartilage thickness or volume, segmentation of the joint tissues on MRI is required. This can be

reconstructed into femoral and tibial cartilage volumes or used to measure cartilage thickness (

Figure 32).The precision and reliability of the different segmentation methods is good[366, 397, 445]. From the segmented cartilage and bone, several measures can be made based upon the division of the joint into regions determined by a panel of experts[271](2.10.2 The two- and three dimensional shape modelling for determining joint shape). Segmentation of the tissues, particularly the cartilage, permits the calculation of the following; the total area of the SCB (tAB), the area of the cartilage surface (AC), the tAB covered by the AC (cAB) and the denuded area of SCB (dAB) which is expressed as percentage of tAB not covered by AC. Finally both volume of cartilage (VC) and cartilage thickness (ThC) can be quantified[446]. These can be calculated for each defined joint region and subregion (Figure 34,Figure 35)[398].

These two measures have excellent reliability as demonstrated by a meta-analysis of studies. This included a coefficient of the variance of 3% for both inter- and intra-reader reliability. Inter- and intra-reader intra-class correlation was excellent[366].

The responsiveness to change of cartilage thickness and volume have been analysed in a broad range of observational studies[95, 431, 447-449]. A meta-analysis of the responsiveness of MRI-determined quantitative cartilage measures to cartilage loss[366] indicated a greater sensitivity to change than an equivalent meta-analysis of radiographic JSW[424]. In direct comparisons of the two methods, MRI-determined cartilage measures were more responsive than CR JSW as well[95, 448].

Cartilage thickness can be described using a thickness map of the femur and tibia..

The rate of cartilage thickness or volume loss is increased in the context of typical OA risk factors and severity measures. This includes obesity[95, 123], meniscal degeneration[123], malalignment[433, 450], frequent pain[448, 451] and evidence of greater radiographic structural severity[123, 451-454].

The validity of cartilage loss as a clinically meaningful biomarker have been reported. Denuded area of SCB (dAB) is associated with knee pain in cross-sectional studies[455, 456] and predictive of incident knee pain in longitudinal studies[456]. Knees with greater rates of tibiofemoral cartilage loss were more likely to subsequently receive total knee replacement than at lower rates[270, 457]. In a nested case-control study within the OAI, the rate of cartilage loss in the two years prior to TKR accelerated[458].

Variable thresholds of cartilage loss have been used to determine significant from insignificant structural progression. This threshold has been determined by the subregional change in healthy joints[459], the precision of cartilage quantification[433] and the smallest detectable change[447] in cartilage quantification.

In summary MRI-determined quantitative measures of cartilage loss are validated biomarkers of clinically important outcomes such as joint replacement, pain and incident pain and are associated with typical risk factors for OA. These measures are more responsive than CR-determined measures.

2.11.1.2.2 Quantitative compositional measurement of cartilage

While morphological MRI sequences permit the three-dimensional measurement of joint tissues, more advanced MRI sequences can be used to characterise and quantify the ultra-structural or biochemical composition of articular cartilage. These assessments of tissue composition may be used to identify and quantify degenerative changes in cartilage that precede morphologically defined cartilage loss of OA.

Healthy cartilage consists of collagen fibres and proteoglycans which are ‘core proteins’ with glycosaminoglycan (GAG) side chains. Collagen fibres are organised in an anisotropic manner in different layers of cartilage (Figure 8) which confers it’s load-dissipating mechanical properties. Early biochemical alterations in the natural history of OA include glycosaminoglycan (GAG) depletion, increased permeability to water[460] and loss of the anisotropy of the extra-cellular matrix network in animals [461, 462] and humans[463, 464]. These alterations can not be detected with standard morphologic magnetic resonance sequences (Figure 37).

Compositional sequences such as diffusion weighted imaging and T2 mapping procedures are sensitive to the loss of anisotropy of the matrix network. Delayed Gadolinium Enhanced MRI of Cartilage (dGEMRIC) [465] and glycosaminoglycan chemical exchange saturation transfer (gagCEST). dGEMRIC are biomarkers of glycosaminoglycan concentration within the cartilage. dGEMRIC has been demonstrated construct validity histologically and biochemically in human and animal cartilage[466-469]. In vivo spatial variation in cartilage signal, in particular circumstances, reflects variations in cartilage GAG concentration[470]. MRI scans are performed 90 minutes after the contrast is administered and dGEMRIC has good reproducibility with an intra-class correlation coefficient (ICC 0.87-0.95)[471].

In case-series analysis of knees undergoing partial meniscectomy, the baseline dGEMRIC values were associated with incident JSN and osteophyte formation[472]. In longitudinal analysis the cartilage thickness change was inversely associated with dGEMRIC[473](Figure 37). Furthermore dGEMRIC is sensitive to weight loss[474]. Therefore dGEMRIC is probably the best-understood compositional sequence with the greatest validation but further validation is required before this can be used as a surrogate measure of OA clinical outcomes such as pain and joint replacement.

Clinical studies for the validation of gagCEST as a biomarker of cartilage degeneration in OA are lacking. Other quantitative compositional imaging biomarkers of cartilage composition lack precision data but include T1-weighted sodium MRI[475], and computed tomography of the knee after intra-articular cationic contrast injection[476].

In summary compositional MRI sequences represent quantitative MRI cartilage measures that have potential to complement the existing and better validated morphological assessments of cartilage

Figure 37 MRI compositional cartilage maps of the tibiofemoral joint

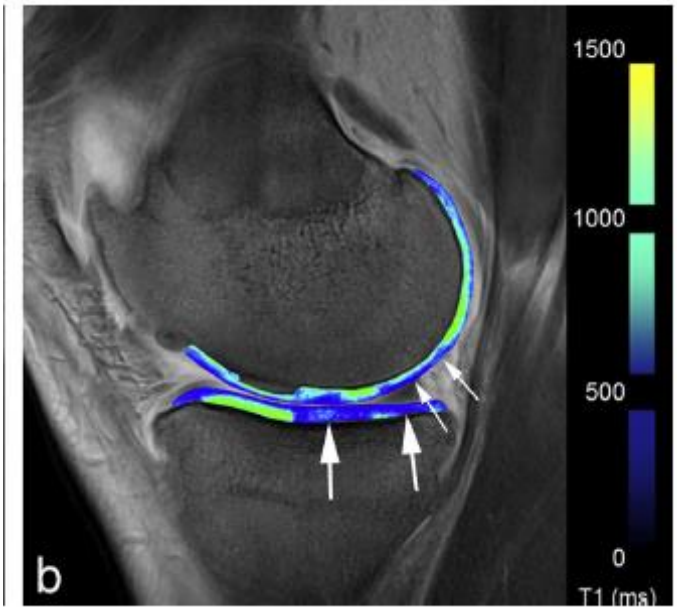

An MRI shows a decrease in the dGEMRIC index particularly in the weight bearing areas at the central and posterior tibia (large white arrows). Reprinted by permission from Elsevier Ltd: Osteoarthritis and cartilage [34]

2.11.1.2.3 Quantitative bone marrow lesions

Bone marrow lesions can be segmented using semi-automated methods that first segment the cartilage-bone interface, the BML itself and then quantify the volume of the BML by using multiple slices of the joint(Figure 38). The importance of segmenting the cartilage bone interface is to ensure the BMLs are within a predefined distance from the bone cortex to ensure they are truly subchondral. The calculated BML volume was associated with adjacent cartilage thickness and full thickness cartilage loss[477]. Bone volume has been quantified using similar methods and found to correlate with increased bone volume fraction[298]. BML volume has also been found to be associated with pain severity and JSN at baseline and to be predictive of JSN progression in longitudinal analyses[100].

Figure 38 Bone marrow lesion segmentation

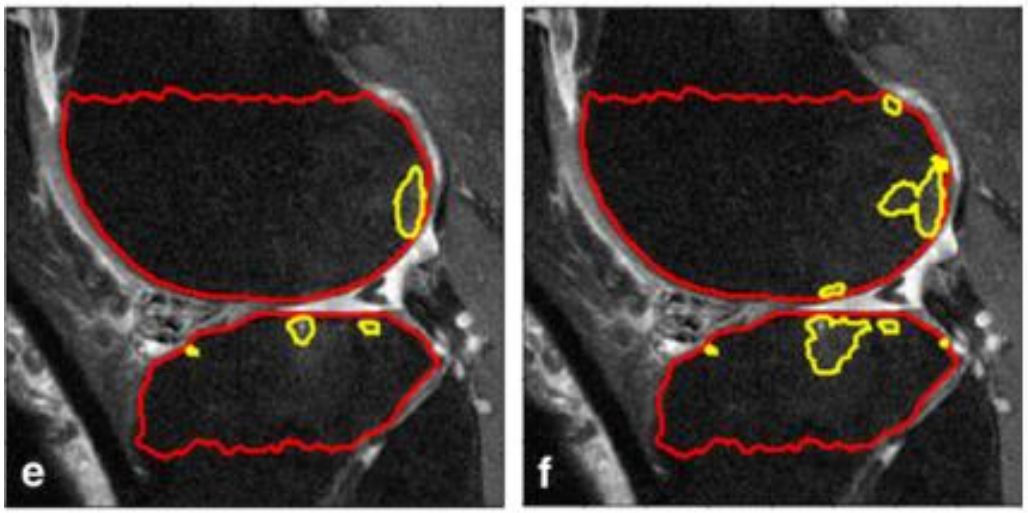

Segmented knee MRI scans. The red lines identify the bone boundary and the yellow lines surround areas of high signal intensity (BMLs). Reprinted by permission from BioMed Central: Arthritis Research Therapy, Driban et a [100]

2.11.1.2.4 Quantitative trabecular morphometry

The structure of bone is complex (2.6 Subchondral bone in OA). Quantitative assessment of macrostructural characteristics, such as geometry and shape of bones are important biomarkers of (OA2.6.3 Bone shape and subchondral bone MRI features in OA). Macrostructural SCB mineral density (BMD) is an important biomarker of OA and this can be quantitatively assessed using conventional radiographs, dual-energy x-ray absorptiometry (DXA) and computed tomography (CT), especially volumetric quantitative (qCT)

Microstructural assessments of the trabecular SCB have greatly improved our understanding of the pathogenesis of OA(2.6.2 Subchondral bone architecture and remodelling in OA). Methods for this microarchitectural assessment include micro- computed tomography (micro-CT), high-resolution computed tomography (hrCT), micromagnetic resonance (micro-MR) and high-resolution magnetic resonance (hrMR). Microarchitectural features can be quantified based on segmentation and three-dimensional methods and the main measurements include bone volume fraction, trabecular thickness, trabecular number, thickness and spacing

Bone volume fraction (BV/TV) or bone mineral density (BMD) is the most important parameter for describing trabecular microarchitecture and is defined as the bone volume divided by its total volume (%). BVF is an approximation of subchondral sclerosis(Figure 20).

Trabecular number (TbN) is a three-dimensional measure calculated from micro-CT images. Trabecular thickness (TbTh) is expressed as the mean trabecular thickness. Trabecular spacing or trabecular separation (TbSp) is calculated as the mean distance between trabeculae (µm). The changes in these measures in OA and their association with clinical OA have been described earlier(2.6.2 Subchondral bone architecture and remodelling in OA).

2.11.1.2.5 Quantitative bone area and three-dimensional bone shape

Bone area (2.6.3.1.1 Knee subchondral bone cross-sectional area) and 3D bone shape (2.6.3.1.2 Three-dimensional knee bone shape) have been discussed earlier.

2.11.1.2.6 Meniscus and effusions

Meniscus and effusions can both be segmented using similar technology to cartilage and bone segmentation. These are in their infancy relative to bone and cartilage.

In summary quantitative measures of OA have been used across a range of imaging modalities. Compared to semi-quantitative measures, quantitative systems use a more complex, technology dependent and time-consuming approach for assessing structural pathology. However the continuous measures may be more sensitive to change making them better outcome measures. The most validated OA quantitative measures are for the knee and include cartilage volume and thickness. The current standard for measuring structural progression in knee OA is radiographic JSN. Regardless of these measures no biomarker demonstrates a strong association with both structural progression and clinically meaningful symptoms. More sensitive and validated biomarkers are therefore desirable.

2.11.2 Semi-quantitative measures of structural OA

The structural pathology of OA can be measured using semi-quantitative scoring systems. These scoring systems are not used in routine clinical practice but are frequently used in longitudinal or cross-sectional observational studies and interventional trials. They may be used as selection criteria to enrich a cohort with a relatively homogenous structural severity of OA (e.g. an identical KL grade)[92] or as a structural outcome for measuring structural progression such as a semi-quantitative cartilage defect score[478].

Conventional radiographic measures whether they are semi-quantitative or quantitative are limited by the fact that they are less responsive, reliable and sensitive to whole-joint structural pathologies and their structural progression than MRI and they are less well correlated with the clinical syndrome. In particular CR is insensitive to the detection of OA structural pathology associated with pain (e.g. BMLs and synovitis)(2.4.3.2 OA pain and its structural associations). Therefore large changes in semi-quantitative structural scoring are often required to represent clinically meaningful change. For example only increases of two more KL grades(Table 1) in knees over 4 to 5 years is associated with increasing pain and dysfunction[98].

Unlike quantitative measures that use continuous scales, semi-quantitative measure use an ordinal scale e.g. 0-3 which may be described as absent, mild, moderate or severe. The structural change required to move from one grade to the next may not be uniform along the scale (e.g the change between zero and one, and between one and two) and therefore these may not be interval variables. Acknowledging these limitations, semi-quantitative measures are more convenient, more rapidly scored and do not require no complex imaging analysis technology. Therefore they are a more feasible and are an approximation of quantitative structural measures. The different forms of semi-quantitative measures of structural OA are described here.

2.11.2.1 Conventional radiographic semi-quantitative measures

2.11.2.1.1 Kellgren Lawrence grade

The most frequently used CR semi-quantitative system to identify and grade OA is the Kellgren–Lawrence (KL) score. This is a widely accepted scale which can be applied to peripheral and axial joints but is most frequently used for the knee[19]. This is a composite measure of JSN, osteophytes, subchondral sclerosis that is described on an ordinal scale (Table 1,Figure 1). The presence or absence of OA is typically defined as grade two or higher. The advantages of KL score are that it incorporates the severity of structural pathology in more than one tissue in this multi-tissue whole joint disorder. The baseline knee KL score is predictive of knee joint replacement in the OAI[479]. Knees demonstrating an increase in KL grade compared to stable KL grade over one year have greater odds of further increases in KL grade in the following year [92], but only increases of 2 more KL grades in knees over 4 to 5 years is associated with increasing pain and dysfunction[98]. However the disadvantages of KL scoring are that it depends upon the presence of osteophytes which can change with minor changes in the rotation of a knee and the standardisation of rotational positioning of the knee is difficult. The KL grade does not represent an interval variable where individual categories are equidistant from each other in severity. Therefore it is important to recognise that the proportion of knees that progress from one grade to the next are not comparable for all starting points in the scale. The OA threshold of KL 2 has been inconsistently defined in longitudinal studies which have led to some heterogeneity in definitions of OA. Almost all definitions of KL 2 require a definite osteophyte, some do not mention JSN, some require JSN while others require the absence of JSN[480]. In the Framingham Osteoarthritis study where X-ray and MRI scores were available for 189 knees, KL grade 2 without JSN (OARSI JSN = 0) and with JSN (OARSI JSN =1) had substantial semi-quantitative WORMS weight-bearing TFJ cartilage loss in 4% and 44% of knees respectively[481]. This highlights the importance of the difference in KL2 definition. It is also noteworthy that KL grade 3 requires definite joint space narrowing but this may range from mild to nearly bone on bone

narrowing. Therefore KL grades may encompass a broad spectrum of pathology and the ordinal KL scale is not an interval variable.

Felson and colleagues analysed a cohort of 842 knees with established ROA in at least one knee from the MOST study. Structural progression was defined after 30 months of follow up using OARSI JSN[84] (with half grades) to define structural progression. Had KL grade been used to define structural progression, less than half of all those determined as having JSN structural progression would have been detected by a change in KL grade. Therefore KL grade is relatively insensitive to structural progression than JSN[481].

This has led to the suggestion from Felson and colleagues that an additional ‘definite osteophyte only’ grade should be distinguished to determine ROA incidence and for structural progression to focus on JSN[482].

In conclusion KL grade is insensitive to clinically meaningful change in symptoms and is less sensitive to structural change than ordinal OARSI JSN but it is still an independent predictor of knee joint replacement. Variations in KL grade definition amongst different studies may represent important and latent differences in structural severity between studies.

2.11.2.1.2 The Osteoarthritis Research Society International (OARSI) atlas classification

The Osteoarthritis Research Society International (OARSI) atlas classification grade ROA of the knee, hip and hand. It provides distinct scoring systems for each joint and describes JSN, osteophytes with a semi-quantitative score (0-3) and the presence or absence of subchondral sclerosis, cysts and attrition but also joint malalignment [84]. In the knee the features are identified by their presence in the medial and lateral tibiofemoral compartments (Figure 39).

Amongst 276 knees in the MOST study, OARSI knee JSN was significantly associated with progressive WORMS cartilage damage, meniscal damage and extrusion after adjusting for age, gender and BMI[418]. Knees with higher OARSI grades of JSN had thinner cartilage in the medial TFJ than those without JSN[483]. This provides evidence of predictive and construct validity of OARSI JSN.

The inter-rater and intra-rater reliability and the sensitivity to change (standardised response mean) was compared between categorised metric JSW, KL grade and OARSI JSN grade for 1759 x-rays from three trials and two cohorts. Categorised metric JSW had better reliabilities and sensitivity to change than the other two ordinal measures[484]. Disease progression may be defined as an increase in KL, JSN or osteophyte grade. However JSN had the lowest inter-observer variability[485].

Cross-sectional analysis of 696 people from the MOST study and 336 people from the Framingham OA cohort examined the association of pain severity and consistency with ROA grade of KL, OARSI JSN and OARSI osteophyte grades. To avoid typical confounders, knees were compared within individuals with discordant pain severity and consistency between knees. All three ROA measures were associated with these pain measures but OARSI JSN grade and KL grade had greater association with OA pain than OARSI osteophyte grade[486].

Other examples of scoring systems utilising atlas scoring systems include Nagaosa and colleagues' for knee OA, the Kallman[487], Verbruggen[488] and Dougados scoring systems[489]. These scoring methods have been compared with KL grade and demonstrated to have similar reliability and sensitivity to change and may be used to detect hand ROA change over time [489].

Therefore OARSI JSN grade has construct validity and offers advantages over KL grade in terms of its reliability and responsiveness and its association with pain relative to OARSI osteophyte grade.

Figure 39 Altman Atlas semi-quantitative scoring

Hand
- Osteophyte
  - DIP (0–3)
  - PIP (0–3)
  - First CMC (0–3)
  - Thumb (IP) (absent/present)
  - Naviculotrapezial joint (NTJ) (absent/present)
- Joint space narrowing
  - DIP (0–3)
  - PIP (0–3)
  - First CMC (0–3)
  - IP (absent/present)
  - NTJ (absent/present)
- Malalignment
  - DIP (absent/present)
  - PIP (absent/present)
  - First CMC (subluxation) (absent/present)
- Erosion
  - DIP (absent/present)
  - DIP central erosion (absent/present)
  - DIP pseudowidening (absent/present)
  - PIP (absent/present)
  - First CMC (absent/present)
- Subchondral sclerosis
  - DIP (absent/present)
  - PIP (absent/present)
  - First CMC (absent/present)
- Subchondral cyst
  - PIP (absent/present)
  - First CMC (absent/present)

Hip
- Marginal osteophytes
  - Superior acetabular (0–3+)
  - Superior femoral (0–3+)
  - Inferior femoral (0–3+)
  - Inferior acetabular (absent/present)
- Joint space narrowing
  - Superior (0–3+)
  - Medial (0–3+)
- Other
  - Acetabular subchondral cyst (absent/present)
  - Acetabular subchondral cyst (absent/present)
  - Femoral subchondral sclerosis (absent/present)
  - Flattening of the femoral head (absent/present)
  - Thickening of the medial femoral calcar (buttressing) (absent/present)

Knee—tibiofemoral
- Marginal osteophytes
  - Medial femoral condyle (0–3+)
  - Medial tibial plateau (0–3+)
  - Lateral femoral condyle (0–3+)
  - Lateral tibial plateau (0–3+)
- Joint space narrowing
  - Medial compartment (0–3+)
  - Lateral compartment (0–3+)
- Other
  - Medial tibial attrition (absent/present)
  - Medial tibial sclerosis (absent/present)
  - Lateral femoral sclerosis (absent/present)

This is the Altman atlas: semi-quantitattive scoring system for radiographic OA [84]

2.11.2.1.3 Categorical Alignment of the knee

A systematic literature review of predictors of radiographic structural progression identified that categorical varus and valgus malalignment of the knee (Figure 40) is independently associated with structural progression[428].

Figure 40 Alignment of the knee

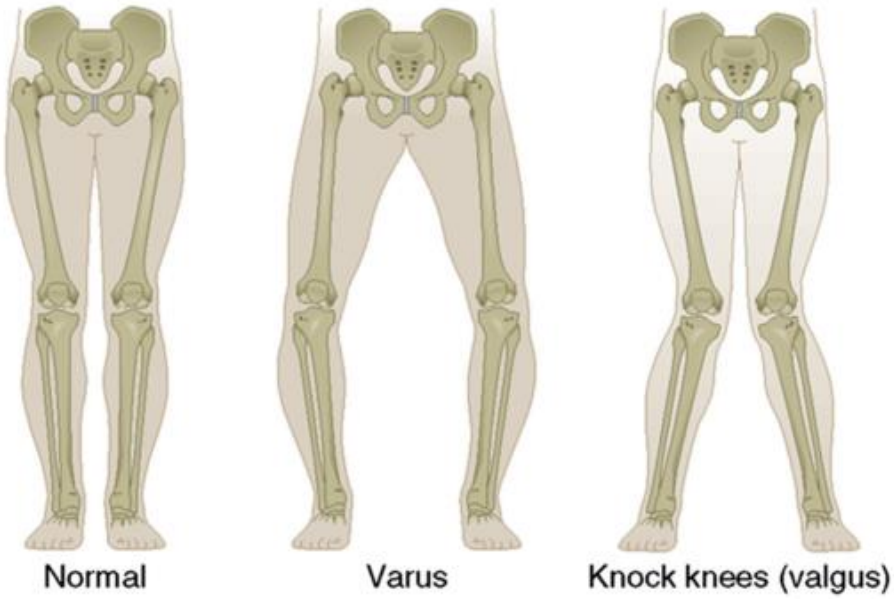

These images explain the different forms of knee malalignment. Reprinted by permission from Elsevier Ltd: Rheum Dis Clin North Am [490]

Incident radiographic OA (KL≥2) was associated with categorical malalignment (varus and valgus) which was specific to obese and overweight individuals and not with normal BMI[491]. Amongst obese women, malalignment (valgus or varus) was associated with greater risk of incident radiographic OA (KL≥2) over 2.5 years [492]. Amongst 315 knees largely without OA and concurrent obesity, the categorised malalignment of the knees was not associated with tibial cartilage volume loss or tibiofemoral chondral defects longitudinally on MRI over 2.4 years after adjustment for confounding factors[268]. This implies that the increased load of malalignment and obesity may contribute to greater risk of incident ROA and these two predictors of OA may interact[493].

In a population of mostly obese individuals at risk of OA, categorised varus but not valgus was associated with incident tibiofemoral ROA after adjusting for age, gender and body mass index [494].

While ROA progression (KL increase ≥1 grade) has been associated with varus but not valgus malalignment [491], this is a relatively insensitive measure of structural progression as previously described (See 2.11.2.1.1 Kellgren Lawrence grade) and therefore the association with valgus malalignment with better structural measures was explored. This included larger studies, of 881 knees using more responsive structural measures, which reported independent associations between categorised valgus deformity and incident knee ROA and progression of knee OA with radiographic JSN and MRI cartilage and meniscal degeneration[76]. Increasing severity of varus and valgus malalignment in ROA knee were also associated with greater risk of progression in the biomechanically loaded compartment[494, 495].

Therefore there is good evidence that categorical varus and valgus malalignment are independently predictive of structural progression and may be involved in structural incidence of knee OA when combined with obesity.

2.11.2.2 MRI semi-quantitative measures

The semi-quantitative strategy for the quantification of MRI OA structural pathology is described below but a comparison with quantitative MRI measures described above (2.11.1.2 MRI quantitative measures) will first be made.

Trained readers can semi-quantitatively describe the severity of OA structural pathology on MRI using an ordinal scale (e.g. 0,1, 2 and 3) without the arduous segmentation, additional image processing and special imaging sequences required for quantitative analysis of joints. The whole joint semi-quantitative scoring systems may take up 50 minutes per knee for a reader and therefore they remain research tools that are not used during routine clinical practice where only qualitative reporting is standard.

Semi-quantitative measures, that may not be interval variables, are designed to approximate the 3D quantitative structural pathology of OA on ordinal scales. The difference in responsiveness of these two measure types was

highlighted when describing changes in BMLs and cartilage in knees over 24 months. Quantitative measures were found to be more sensitive to change than semi-quantitative measures[442]. As a consequence the measurement of longitudinal structural change with semi-quantitative measures has evolved to incorporate 'within-grade' scoring changes to improve longitudinal sensitivity to change [443, 444]. Severe malalignment has since been identified as predictive of 'within grade' but not whole grade progression in cartilage loss supporting this rationale[496].

While 'within-grade' scoring changes are now commonly used, the disadvantage of this is that this process demands that the reader is unblinded to order of serial image acquisition[496] which may introduce bias. Despite these limitations a meta-analysis of the responsiveness and reliability of semi-quantitative and quantitative measures of BMLs and cartilage in knee OA found that the pooled standardised response means for both methods were adequate-to-good and comparable[366]. The random-effects pooling of intrareader and inter-reader intraclass correlation coefficients for each tissue indicated excellent reliability. The intrareader and inter-reader kappa values were also moderate to excellent.

Semi-quantitative measured in cross-section may offer and advantage over metric quantitative measurements. This is because lesion size may vary according to the absolute size of the person whilst semi-quantitative measures are relative to the size of the joint.

The optimum MRI protocol for the purposes of semi-quantitative analysis differs for quantitative MRI analysis. Peterfy for example selected unenhanced pulse-sequences for optimum semi-quantitative evaluation of each component of knee OA[497]. While for quantitative evaluation protocols with better spatial resolution are more important for the precise distinction of the osteochondral interface and cartilage surface for segmentation.

In terms of the validity of semi-quantitative MRI knee scores in relation to pain, two systematic reviews indicated moderate associations of pain with BMLs and synovitis or joint effusion[132, 365]. Felson's BML score was associated with knee pain and incident knee pain was associated with an

increase in BML score. Furthermore a linear positive relationship between BLOKS maximal BML size and WOMAC pain score has been observed[498]

In terms of validity of semi-quantitative MRI knee scores in relation to the prediction of MRI-determined structural progression. Progression of cartilage deterioration is greater in individuals with a raised BMI of 30 or more in a longitudinal observational study[499]. Cartilage deterioration also progresses in longitudinal studies in the context of synovitis[500], BMLs[500], meniscal damage[501] and prevalent cartilage damage[500].

2.11.2.2.2 Knee semi-quantitative measures

The following text describes the semi-quantitative assessment of the knee in OA with scoring systems for individual tissues as well as whole organ assessment .

Individual tissues of the knee can be semi-quantitatively assessed such as the synovium. A precise anatomical description of synovitis of the whole-knee is only possible on contrast enhanced images and Guermazi and colleagues have an example of a synovitis scoring system (0-2) which is assessed at 11 sites to achieve this[502]. On unenhanced MRIs semi-quantitative scoring systems are also described individually for BML size (0-3) [133] the degeneration of cartilage (0-4) [353], meniscus (0-3)[503] and ligaments (0-3)[30].

While OA is a ‘whole organ’ disease the extent of the structural involvement is best captured by ‘whole organ’ scoring systems, of which there are four well-described systems all of which are based on MRI without contrast.

The first comprehensive scoring system was described in 2004 by Peterfy and colleagues[504]. This was named the Whole ORgan Magnetic Resonance iMaging Score (WORMS) and it has been extensively used in MRI studies worldwide. This includes the Framingham Knee Osteoarthritis study[23], the Osteoarthritis Initiative[505] and the Multicenter Osteoarthritis Study (MOST)[307].

This provides a system based upon the division of knees into complex subregions (Figure 41) rather than using a lesion-oriented system. Cumulative scores for each lesion type in each compartment and at a whole

knee level are calculated. One advantage of this is that multiple lesions per subregion are considered together which may simplify analysis and interpretation of data. This is because a lesion based approach may be compromised if lesions coalesce or split during longitudinal observation. Furthermore this is the only whole joint scoring system to include subchondral attrition (Table 9).

Kornaat and colleagues in 2005 introduced the Knee OA Scoring System (KOSS)[506]. This describes similar OA features as the WORMS but with different subregional division and without attrition, bursitides, loose bodies and ligament abnormalities (Table 9). The KOSS scores knees according to the following anatomical areas. The medial and lateral:

- patella facets (divided by the patellar crest)
- femoral trochlear facets
- femoral condyles (excluding the trochlear grove)
- tibial plateaus

The menisci, effusion size, synovitis and Bakers cysts are also included. Unlike WORMS each lesion grade is differentiated by the lesion size. Furthermore subchondral cysts, BMLs and cartilage condition are individually scored for each KOSS subregion unlike the WORMS which scores these cumulatively. KOSS scores meniscal subluxation (unlike WORMS) but both KOSS and WORMS score meniscal morphology.

In 2008 Hunter and colleagues introduced the Boston-Leeds OA Knee Score (BLOKS) which, unlike WORMS, applies a lesion-oriented system to BML scoring[498] which is more conducive to longitudinal analysis of individual lesions. The division into subregions is based upon weight-bearing regions of the knee rather than the patellofemoral joint (Figure 41)

Controversy remains regarding whether the WORMS or BLOKS is a better validated outcome measures in knee OA. When comparing longitudinal changes in BLOKS and WORMS scores in 113 knees, WORMS BML measurements had a stronger association with cartilage loss than BLOKS BML scoring. BLOKS meniscal tear and signal abnormality assessment was

better for predicting cartilage loss than the WORMS meniscal scoring. Neither scoring system was superior at cartilage assessment[507]. However comparison of WORMS and BLOKS scores amongst 71 subjects indicated that unlike BLOKS BML score, WORMS BML score was not associated with pain and was less strongly associated with cartilage loss[498].

In 2011 Hunter and colleagues developed the MOAKs (MRI OA Knee score) system. The design was informed by the relative advantages and disadvantages of the existing scoring system. The MOAKS incorporates a subregional assessment, a refinement of the BML and meniscal scoring and removed redundant features in the scoring of BMLs and cartilage[508]. It is now being used in the Osteoarthritis Initiative.

The WORMS and MOAKs systems similarly divide the femur and tibia into anterior, central and posterior regions while the BLOKS system divides the femoral condyles into trochlear and weight-bearing regions. The WORMS, BLOKS and MOAKS scoring systems share a similar delineation of medial & lateral regions of the femur (Figure 41).

Some of the ordinal measures used in these systems are not interval variables and therefore the structural progression required to progress from one grade to the next may or may not be uniform (Table 8). The acknowledgement that the sensitivity to change of quantitative measures was greater than semi-quantitative measures, led to a change of scoring occurred. This included scoring “within-grade” changes between longitudinal follow up points[496].

Figure 41 Anatomical regions used in WORMS MOAKS & BLOKS

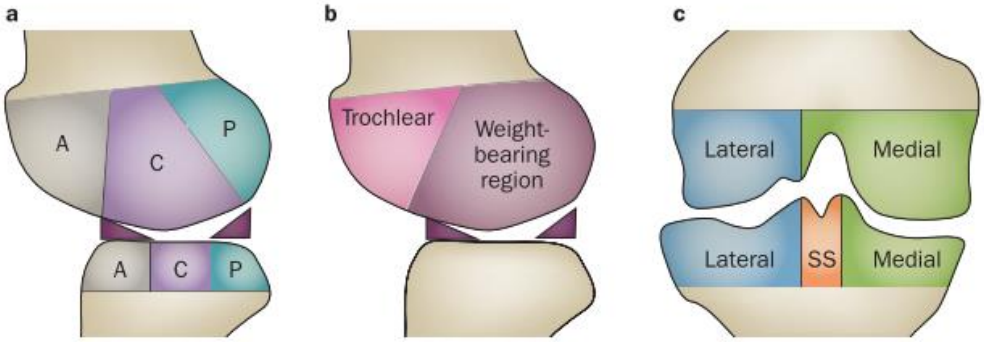

Anatomical subregions used in WORMS, MOAKS and BLOKS semiquantitative scoring systems for knee OA. a | WORMS and MOAKS divide MRI data for the femur and tibia into anterior (A), central (C) and posterior (P) subregions for scoring of knee OA features. b | BLOKS separates assessment of knee OA features of femoral condyle into trochlear and weight-bearing subregions. c | The medio–lateral division of the femur defined for all three scoring systems. Abbreviations: A, anterior; BLOKS, Boston–Leeds Osteoarthritis Knee Score; C, central; MOAKS, MRI Osteoarthritis Knee Score; P, posterior; SS, subspinous; WORMS, Whole Organ Magnetic Resonance Imaging Score. (Reprinted by permission from Macmillan Publishers Ltd: Nat Rev Rheumatol [509], copyright 2013).

Table 8 The ordinal scales of semi-quantitative scoring systems may or may not be interval variables

	Grade 0	Grade 1	Grade 2	Grade 3
BML size scoring – extent of regional involvement				
BLOKS [498]	0%	<25%	25-50%	>50%
MOAKS [508]	0%	<33%	33-66%	>66%
Meniscal extrusion over the edge of the tibial plateau				
KOSS[506]	Absent	<33% width of meniscus	33-66% width of meniscus	>66% width of meniscus
MOAKS [508]	<2mm	2-2.9mm	3-4.9mm	>5mm

Table 9 Comparison of the four knee whole organ semi-quantitative scoring systems

	Cartilage	BMLs	Subchondral cysts	Attrition	Effusion and synovitis	Synovial thickening	Peri-articular cysts	Bursitides	Loose bodies	Osteophyte	Meniscus	Meniscal extrusion	Cruciate and collateral ligaments
WORMS [504]	0-6	0-3	0-3	0-3	0-3		0-3	0-3	0-3	0-7	Tear (0-4)		(0-1) tear Presence or absence
KOSS [506]	Size and depth (0-3)	0-3	0-3		0-3	0-1	Popliteal (0-3)			0-3	Tear (0-3)	0-3	
BLOKS [498]	Size and depth (0-3) % dAB at specified points	For each lesion: size (0-3) % area of adjacent bone surface (0-3)	Proportion of cyst that is BML (0-3)		Effusion size (0-3) Synovial volume in: Hoffa's pad (0-3) 5 other sites (0-1)		0-1	0-1	0-1	(0-3) size in 12 locations	(0-1) for each of: -intrameniscal signal -tears -maceration -cyst	0-3	(0-1) tear Presence or absence
MOAKS [508]	Size and depth (0-3)	For each lesion: size (0-3)			Effusion synovitis (0-3) Hoffa synovitis signal (0-3)		0-1	0-1	0-1	(0-3) size in 12 locations	(0-1) for each of: -intrameniscal signal -tears -maceration -cyst -hypertrophy	0-3	(0-1) tear Presence or absence

BLOKS, Boston–Leeds Osteoarthritis Knee Score; dAB – denuded area of bone; KOSS, Knee OA Scoring System; MOAKS, MRI Osteoarthritis Knee Score; SS, subspinous; WORMS, Whole Organ Magnetic Resonance Imaging Score.,

In conclusion semi-quantitative MRI measures have greatly contributed to the description of the natural history of knee OA and the identification structural pathologies of tissues within the ‘whole joint’ that are associated with important clinical and structural outcomes in knee OA.

Compared to quantitative measures, semi-quantitative systems use a simpler and quicker process for assessing structural pathology than segmentation of tissues but the ordinal scales used may be less sensitive to change and interpretation of change in score progression should acknowledge if the scales are interval variables or not. The most validated OA semi-quantitative measures are for the knee.2.12 The Osteoarthritis Initiative

2.12 Summary of the OAI

2.12.1 Background

Osteoarthritis (OA) is the most common form of arthritis. Its major symptoms are pain and stiffness which negatively impact individuals` ability to perform activities of daily living. There is discordance between symptom and radiographic changes Only 50% of knees with radiographic OA (ROA) have knee OA symptoms[17]. As obesity increases worldwide and coupled with an ageing population, it is anticipated that the burden of OA will become a major problems for health systems.

No proven disease –modifying therapies are available for OA and current treatment is exclusively directed at symptomatic pain relief.

The structural progression measured by radiographic OA of knee, hip and hand OA is typically slow and takes place over several years but can also remain stable over years [89-91]. In knees the mean annual risk of progression of KL grade is 5.6% ± 4.9% and mean rate of joint space narrowing is 0.13 ± 0.15mm/year, with change occurring in only a small group of “progressors”[93, 94]. Radiographic improvement is atypical.

Magnetic resonance imaging provides the ability to visualise joints in three dimensions. The quantification of MRI cartilage volume affords advantages over conventional radiography because structural loss of cartilage can be detected in the pre-radiographic phase of OA[87] and in end-stage OA, after the total loss of joint space width (‘bone on bone’ or Kellgren Lawrence grade 4)[88].

In light of the slow natural history of OA progression, long follow up times are required to study OA and its variable clinical outcomes. It has proven very expensive to conduct trials and the lack of suitable biomarkers of diseases activity have meant that past attempts have been unsuccessful in studying disease progression.

2.12.2 Overview and aims

The broad aims of the OAI are to develop a prospective cohort suitable for investigating the natural history of the entire spectrum of knee OA. This includes those ‘at risk’ of knee OA, with early or pre-clinical knee OA, with established knee OA and those with endstage knee OA. In order to understand this evolution of OA, this cohort will collect imaging, biochemical, genetic and clinical biomarker data from participants representing and progressing through the different stages. This will permit the investigation of the relationship of these biomarkers with the evolution of OA which may identify risk factors for the evolution through each stage. There is also the potential that some of these biomarkers may be validated as surrogate outcome measures of how patient’s joints feel, function and survive in the process.

The OAI also aims to determine the validity of radiographic, magnetic resonance imaging and genetic measurements as potential biomarkers and surrogate endpoints for knee OA. The initial objective was to recruit about 5000 participants with either clinically significant knee OA or those at high risk of developing OA along with a set of ‘normal’ controls for biomarker reference purposes.

In total 4796 participants (age range 45-79) were recruited into the OAI cohort and entered into the study at baseline and were assessed annually thereafter. Each participant was sub-divided into three subcohorts (1) the progression group

(n=1389 (29%)), who had symptomatic and radiographic knee OA on enrolment, (2) the incidence group (n=3285 (68%)), who did not have definite knee OA on enrolment, but were considered at elevated risk of knee OA during the study, and (3) the control group (n=122 (3%), who did not have knee symptoms, knee radiographic OA or any risk factors.

2.12.3 Inclusion criteria

The overall recruitment goal was to obtain approximately equal numbers of males and females, to be aged between 45-79 and at least 23% from ethnic minorities.

Prevalent symptomatic OA definition for OAI encompasses both presence of frequent knee symptoms (FKS) and radiographic features and is similar to the ACR criteria for clinical knee OA[22]. As symptoms of knee OA are often intermittent and many years may elapse before they become monotonic/chronic, there is no clearly defined point of onset. Degenerative changes precede and predict the incidence of radiographic knee OA[122] therefore there are limitations to the existing definition of the OA progression group.

To be in the Progression subcohort participants are required to have in at least one knee both the following:

Frequent knee symptoms (defined as having had had knee pain in the last 12 months for at least one month) and radiographic knee OA defined as a definite tibiofemoral osteophytes (OARSI grade 1-3 equivalent to K-L grade ≥ 2 on a fixed flexion radiograph.

Incident subcohort classification is having no symptomatic OA in either knee but at risk of developing symptomatic OA. Incidence is defined as the first occurrence in either knee of both FKS and radiographic OA in the same knee.

For feasibility of recruitment and to enrich each stratum so that reasonable number of incidents would be recorded age-eligible persons would be classified as high risk depending on age band.

Age 45-79: participants need to have FKS or frequent use of medication for treatment of knee symptoms (use of all types of medication on most days of a

month in the past 12 months), or infrequent knee symptoms (pain, aching or stiffness in or around the knee at any time in the past 12 months but not on moist days for at least one month) and should have at least one eligibility risk factor.

Age 50-69: any of FKS or frequent use of medication as above or be overweight or have 2 or more eligibility risk factors.

Age 70-79: any of FKS, frequent use of medications or at least one risk factor

List of risk factors

- Knee symptoms which can be any of FKS or infrequent and frequent use of medication
- Overweight (greater than 93kg in males and 77kg in females aged 45-69 and greater than 97kg in males and 81kg in females between 70-79 years old)
- Knee injury defined as history of knee injuring causing walking difficulties for at least one week.
- Knee surgery defined as any history of knee surgery
- Family history of total knee replacement in a biological parent or sibling
- Heberden`s nodes
- Repetitive knee bending
- Age 70-79

The control subcohort is defined as those having no pain, aching or stiffness in either knee in the past year, no radiographic OA (OARSI osteophyte grade=0 and JSN grade =0) and no eligibility risk factors.

2.12.4 Knee radiography protocol

For the purposes of the OAI, the non-fluoroscopic fixed flexion SynaFlexer plexiglass knee positioning frame (Figure 42) protocol[402] was adopted as the primary method for serial measurement of JSN in the OAI protocol[510]. This was chosen because a fixed flexion weight-bearing protocol is required for JSW to be a valid indirect measure of cartilage thickness[402, 511] and the chosen method demonstrated comparable repeatability precision for JSW measurement [402, 512] with fluoroscopically-guided protocols[402, 513] (see 2.11.1.1.1 Continuous

joint space width and joint space narrowing) and provides consistency in terms of the image of the knee over time[514].

Fluoroscopic methods were also considered too costly and impractical for the OAI protocol but a subcohort of the progressor subcohort had Lyon Schuss protocols added to test whether there was a difference in sensitivity to the measurement of JSN (pg 20 of protocol [515]).

Figure 42 Non-fluoroscopic fixed flexion SynaFlexer plexiglass knee positioning frame protocol

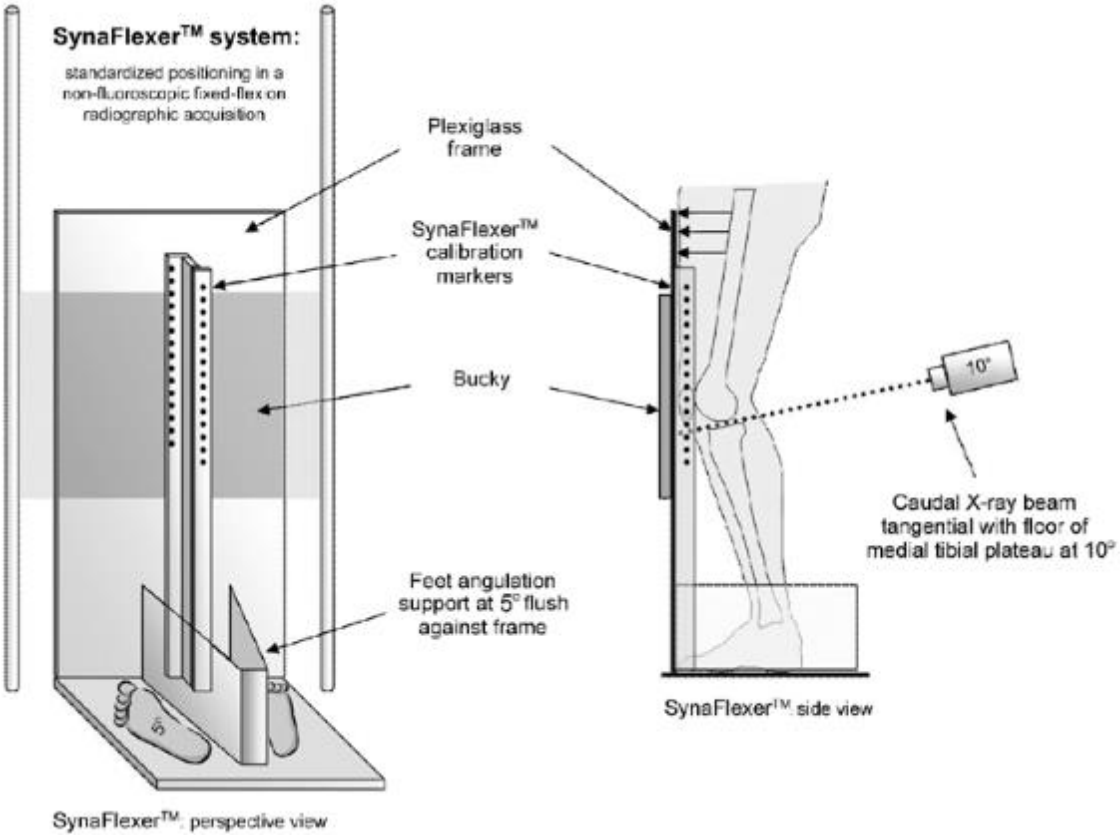

Non-fluoroscopic fixed-flexion radiographic knee protocol with 10° caudal beam angulation to ensure alignment of the beam with the medial tibial plateau. A standardized degree of knee flexion (20°) and external foot rotation (5°) are achieved with use of the SynaFlexer calibration and positioning frame Springer European Radiology, Fixed-flexion radiography of the knee provides reproducible joint space width measurements in osteoarthritis, 2004 Kothari et al, reprinted with permission of Springer[512].

While the majority of knee radiographs were taken without fluoroscopic guidance and the alignment of the tibial plateau is integral to the sensitivity of serial radiographs for measuring joint space narrowing (see 2.11.1 Quantitative measures in OA), a quality control technique was employed to ensure that radiographs failing to meet this and other quality criteria were repeated by inviting participants to return for repeat imaging (page 11 and 18 of the OAI Radiographic operations manual [409])

2.13 Thesis aims

The aim of this thesis was first to describe the association of imaging-detected subchondral bone features of OA with the outcomes of joint replacement, structural progression and pain in the common sites of peripheral OA. The hypothesis underlying this thesis is that subchondral knee bone 3D shape, defined using 3D knee MRI segmentation, would demonstrate association with existing radiographic measures of structural knee OA pathology and with patient-centred knee OA clinical outcomes of total knee replacement and knee OA symptoms. These associations were examined in the largest observational cohort of knee OA in the world, the Osteoarthritis Initiative. By demonstrating these associations, this would potentially provide evidence of construct, predictive and concurrent validity of this novel bone shape biomarker. This may provide a more discriminative biomarker and surrogate measure of important patient-centred outcomes for future therapeutic trials of disease modifying osteoarthritis drugs.

Chapter 3 A systematic review of the relationship between subchondral bone features, pain and structural pathology in peripheral joint osteoarthritis.

3.1 Introduction

It is now well established that OA is a "whole-organ disease" and not a cartilage-centric condition. Hyaline articular cartilage is the most studied of all joint tissues in osteoarthritis (OA) but despite targeting this tissue there are no licensed disease modifying OA drugs (DMOADs). In Chapter 2 the integral role that subchondral bone plays in the pathogenesis of knee osteoarthritis (OA) has been described. The imaging-determined OA subchondral bone features are associated with risk factors of OA, OA severity and pain (described in Table 7). The subchondral bone is intimately associated with hyaline cartilage deterioration and it is therefore a tissue of great interest, however subchondral bone remains relatively understudied in comparison with cartilage.

Conventional radiographs are known to be relatively insensitive to the structural features of OA[23], in part because they do not assess three-dimensional (3D) bone structure[516] (as described in Chapter 4 The relationship between clinical characteristics, radiographic osteoarthritis and 3D bone area). A number of non-conventional radiographic imaging modalities accurately demonstrate *in vivo* SCB pathological changes, including magnetic resonance imaging (MRI), computed tomography (CT), dual-energy X-ray absorptiometry (DXA), scintigraphy and positron emission tomography (PET)[23, 25, 365, 517-521]. Hunter and colleagues found a moderate association between bone marrow lesions BMLs, structural progression and longitudinal change in pain in a systematic review focused on MRI biomarkers and knee OA [365]. In another systematic review Kloppenburg and colleagues examined associations between MRI features and knee pain, but not structural pathology[132].

Therefore a comprehensive review of the literature was performed on subchondral bone structure assessed with all non-conventional radiographic imaging modalities, examining the common sites of peripheral OA and describing the relationships between imaging-detected subchondral bone features and joint replacement, structural progression and pain.

3.2 Aims

A systematic literature review of the association of imaging-detected subchondral bone features of OA with the outcomes of joint replacement, structural progression and pain in the common sites of peripheral OA. Imaging was defined as all non-conventional radiographic imaging modalities.

3.3 Methods

3.3.1 Systematic literature search

A systematic literature search of Medline (from 1950), EMBASE (from 1980) and the Cochrane library databases until September 2014 was performed for original articles reporting relationships of non-radiographic imaging-assessed subchondral bone pathologies with joint replacement, pain or structural progression in knee, hip, hand, ankle and foot OA. The bone pathological changes include bone marrow lesions (BMLs), osteophytes, attrition, cysts, as well as changes in shape, bone mineral density, bone morphometry (bone volume fraction, trabecular number, spacing and thickness), and bone signal from positron emission tomography (PET) and scintigraphy.

Non-conventional radiographic imaging referred to magnetic resonance imaging (MRI), computed tomography (CT), dual-energy x-ray absorptiometry (DXA), scintigraphy and PET. However while this PhD has a major focus on bone shape modelling and conventional radiography is not known to be insensitive to bone shape, the search term ‘bone shape’ was not restricted to non-conventional radiographic imaging.

A full description of the search terms used is recorded in Table 10andTable 11. The final search was restricted to humans. There was no language restriction and abstracts were not excluded. Exclusion criteria included case reports, surgical intervention studies or trials of surgical techniques in OA, imaging technique studies, studies of OA where serum biomarkers are the only structural outcome measure, review articles, editorials and letters, animal studies, studies not meeting the inclusion criteria, studies where the bone feature was not in the subchondral bone adjacent to the joint being analysed and abstracts of any study already included as a formal and full publication. Any analysis of less than 20 patients with confirmed OA was excluded to remove papers at risk of study imprecision. These exclusion criteria are listed in Figure 43. The inclusion criteria were *in vivo* observational studies of a human population with clinical and/or radiographic OA, which included an imaging description of the adjacent subchondral bone pathology to the OA-joint and the relationship of this with pain, structural progression or joint replacement. Analyses describing the relationship between OA bone manifestations and structural severity (cross-sectional) or progression (prospective cohorts) in populations without clinical and radiographic OA were included to incorporate early structural features of joint degeneration. The outcome measures of structural severity or progression included cartilage defects, cartilage thickness, cartilage volume, denuded subchondral bone, Kellgren-Lawrence grade, joint space width and joint space narrowing. Other outcome measures included joint replacement and any pain measures.

The articles identified by the preliminary search were screened by two reviewers (DH, AB) for relevance and for references not identified by the preliminary search, although no additional citations were found. Discordance in opinion was resolved by a third reviewer (SK). We applied the methods for reporting meta-analyses of observational studies in epidemiology that are recommended by the Cochrane collaboration[522, 523].

3.3.2 Data extraction

Data extraction was performed by two reviewers (DH, AB). Papers meeting the inclusion/exclusion criteria were divided into longitudinal and cross-sectional papers. Longitudinal papers included prospective and retrospective cohorts and case-control studies with longitudinal data (i.e. nested case control studies). Extracted data included (a) patient demographics (age, sex and body mass index) (b) OA (clinical, radiographic or diagnostic) classification used, with the definition and prevalence of radiographic OA, (c) subchondral bone pathology feature, (d) joint replacement, pain or structural progression outcome measure (e) presence/absence of a relationship between feature and outcome (f) statistical results with or without adjustment for confounders and (g) the ipsicompartmental or contralateral compartment structural progression in relation to the compartment of the subchondral bone pathology feature for longitudinal studies.

3.3.3 Quality assessment

The quality of each observational study was independently assessed by two reviewers (TC, AB). A standardised quality scoring tool, previously used in other similar systematic reviews[132, 524] was adapted to assess the following components: (a) study population, (b) MRI subchondral bone feature, (c) pain or joint replacement or structural progression outcome, (d) study design and (e) analysis and data presentation (Figure 12). A score of ‘1’ or ‘0’ was allocated for each question according to whether the study fulfilled the criteria or not respectively. Where multiple bone features were assessed per article (e.g. criteria 11) the mean score was used. Any discordance in opinion was recorded and where consensus could not be achieved a third reviewer (PC) was consulted. The total number of criteria applied to each type of study (e.g. cohort n=18 and cross-sectional n=14) varied and therefore scores were compared as percentages of the maximum score. A study was considered to be high quality if it exceeded or equaled the mean score in its class. However quality was not universally considered to be dichotomous. Where inconsistent associations were

observed between studies of high and low quality, the real difference in percentage quality score was acknowledged in drawing conclusions.

Most studies selected patients from existing cohorts rather than from the general population (criteria 1) and patients were selected by a minimum of evidence of OA (e.g. KL≥2) rather than at a uniform stage of OA severity (e.g. KL=2) (criteria 2). Most studies did not provide evidence of assessing the bone image feature before the knee OA outcome (criteria 9) and similarly did not indicate a prospective analysis plan for the relationship between bone image feature and OA outcome (criteria 17)

Table 10 Search terms EMBASE (1980 to September 2014)

1	osteoarthri*	42	25 or 26 or 27 or 28 or 29 or 30 or 31 or 32 or 33 or 34 or 35 or 36 or 37 or 38 or 39 or 40 or 41
2	osteoarthro*	43	"magnetic resonance imag*".ti,ab
3	(arthri* adj2 degenerative)	44	mri.ti,ab
4	exp OSTEOARTHRITIS	45	mr.ti,ab
5	1 or 2 or 3 or 4	46	"magnetic resonance".ti,ab
6	knee*.ti,ab	47	NUCLEAR MAGNETIC RESONANCE IMAGING/
7	KNEE/	48	43 or 44 or 45 or 46 or 47
8	hand*.ti,ab	49	24 AND 42 and 48
9	HAND/	50	DEXA
10	Hip*.ti,ab	51	DXA
11	HIP/	52	DUAL ENERGY X RAY ABSORPTIOMETRY
12	foot*	53	50 OR 51 or 52
13	exp FOOT/	54	"bone mineral density"
14	ankle*	55	BMD
15	exp ANKLE/	56	BONE DENSITY/
16	6 or 7 or 8 or 9 or 10 or 11 or 12 or 13 or 14 or 15	57	54 or 55 or 56
17	5 and 16	58	24 and 53 and 57
18	HAND OSTEOARTHRITIS	59	"Computed tomography"
19	HIP OSTEOARTHRITIS	60	CT
20	coxarthr*.ti,ab	61	COMPUTER ASSISTED TOMOGRAPHY
21	KNEE OSTEOARTHRITIS/	62	"micro-computed tomography"
22	gonarthr*.ti,ab	63	pQCT
23	18 or 19 or 20 or 21 or 22	64	HR-pQCT
24	17 or 23	65	59 or 60 or 61 or 62 or 63 or 64
25	"subchondral bone".ti,ab	66	57 or 42
26	bml.ti,ab	67	24 and 65 and 66
27	"bone marrow lesion*".ti,ab	68	PET
28	"bone marrow oedema".ti,ab	69	24 and 68
29	"bone marrow edema".ti,ab	70	scintigraphy
30	BONE MARROW EDEMA/	71	24 and 70
31	osteophyte*.ti,ab	72	Bone shape
32	OSTEOPHYTE/	73	24 and 72
33	"bone cyst*".ti,ab	74	49 or 58 or 67 or 69 or 71 or 73
34	BONE CYST/	75	74 limit to humans
35	"bone area*".ti,ab		
36	"bone shape".ti,ab		
37	"bone attrition".ti,ab		
38	"trabecular".ti,ab		
39	TRABECULAR BONE/		
40	"volume fraction".ti,ab		
41	"BV/TV".ti,ab		

Table 11 Search Terms Medline (1950 to September 2014)

1	osteoarthri*	40	"magnetic resonance imag*"
2	osteoarthro*	41	mri
3	(arthri* adj2 degenerative)	42	mr
4	exp OSTEOARTHRITIS	43	"magnetic resonance"
5	1 or 2 or 3 or 4	44	MAGNETIC RESONANCE IMAGING/
6	knee*	45	40 OR 41 or 42 OR 43 OR 44
7	knee/ OR exp KNEE JOINT/	46	23 AND 39 and 45
8	hand*	47	DEXA
9	hand/ OR exp HAND joint	48	DXA
10	Hip*	49	Absorbtiometry, photon/
11	hip/ OR exp HIP JOINT	50	47 or 48 or 49
12	foot*.ti,ab	51	"bone mineral density"
13	foot/ OR exp FOOT JOINTS/	52	BMD
14	ankle*.ti,ab	53	BONE DENSITY/
15	ankle / OR exp ANKLE JOINT/	54	51 OR 52 or 53
16	6 or 7 or 8 or 9 or 10 or 11 or 12 or 13 or 14 or 15	55	23 AND 50 and 54
17	5 and 16	56	"Computed tomograph*"
18	osteoarthritis hip	57	CT
19	coxarthr*	58	tomography, X-RAY COMPUTED/
20	osteoarthritis knee	59	**"micro-computed tomography"**
21	gonarthr*	60	pQCT
22	18 or 19 or 20 or 21	61	HR-pQCT
23	17 or 22	62	56 or 57 or 58 or 59 or 60 or 61
24	"subchondral bone"	63	54 or 39
25	bml	64	23 and 62 and 63
26	"bone marrow lesion*"	65	PET
27	"bone marrow oedema"	66	23 and 65
28	"bone marrow edema"	67	Scintigraphy
29	osteophyte*	68	23 and 67
30	OSTEOPHYTE/	69	Bone shape
31	"bone cyst*"	70	23 and 69
32	BONE CYSTS/	71	46 or 55 or 64 or 66 or 68 or 70
33	"bone area*"	72	71 limit to humans
34	"bone shape"		
35	"bone attrition"		
36	trabecular		
37	"volume fraction"		
38	"BV/TV"		
39	24 OR 25 OR 26 OR 27 OR 28 OR 29 OR 30 OR 31 OR 32 OR 33 OR 34 OR 35 OR 36 OR 37 OR 38		

Table 12 Quality scoring tool

Item	Criterion	CC	CH	CS
Study population				
1	Recruitment from the general population	1	1	1
2	Selection occurred before disease onset or at a uniform point. A uniform point was considered to be equal baseline grade of structural progression (e.g. Kellgren Lawrence grade) or an analysis within the same osteoarthritic joint	1	1	1
3	Cases and controls drawn were from the same population	1		
4	Participation rate >80% for cohort studies (retrospective cohort studies score zero automatically)		1	
5	Sufficient description of baseline characteristics - must include age, gender and BMI (or height and weight)	1	1	1
6	Baseline characteristics comparable between cases and controls - must include age, gender and BMI (or height and weight)	1		
Assessment of Imaging-detected subchondral bone risk factor or feature				
7	Risk factor / feature assessed with a standardised method (e.g. WORMS BML scoring or an automated calculation of bone area but not a subjective opinion of a radiologist on the presence of bone attrition)	1	1	1
8	Risk factor / feature assessment was identical (performed the same way) in the studied population(s)	1	1	1
9	Risk factor / feature was assessed prior to the outcome (structural progression or pain). A score of zero was allocated if the methods did not describe this.	1	1	1
Assessment of joint OA outcome (pain or structural progression)				
10	Outcome assessment was identical in the studied population(s)	1	1	1
11	Outcomes were assessed reproducibly (intraclass correlation coefficient > 0.81 with a standardised assessment). If multiple outcomes were measured the mean reproducibility score was used.	1	1	1
12	Outcome classification was standardised (e.g. the WOMAC pain score but not a subjective opinion of a patient's pain)	1	1	1
Study design				
13	Prospective study design used		1	
14	Follow up time > 3 years	1	1	
15	Information provided on completers vs withdrawls in cohorts (without prospective trial data cohorts automatically score zero)		1	
16	Outcome evaluators were blinded to feature (risk factor)	1	1	1
17	Analysis of relationship between feature and outcome was planned prospectively	1	1	1
Analysis and data presentation				
18	The frequency of most important outcomes were given	1	1	1
19	appropriate analysis techniques used (statistical or comparative techniques)	1	1	1
20	adjusted for at least age, BMI and gender	1	1	1
	Maximum Score	17	18	14

CC: case control, CH cohort (prospective and retrospective), CS: cross sectional

3.3.4 Best evidence synthesis

Statistical pooling of the data was considered inappropriate in light of the heterogeneous study populations, methodological quality and bone feature or outcome measurements for OA. For example the feature bone marrow lesions (BMLs) could be described by their crude presence, ordinal size, metric size, volume or change in volume. Therefore a qualitative summary of the evidence for each bone feature (e.g. BML) and its association with pain or structural progression and joint replacement was provided based on the study design, adequacy of adjustment for confounders (age, gender and body mass index) and quality score. An association of a bone feature with a longitudinal OA outcome (i.e. structural progression, longitudinal change in pain, incident pain or joint replacement) was determined from cohort studies only. If a prospective cohort study analysis was of above average quality and found a statistically significant association between a bone feature and a longitudinal outcome after adjustment for at least age, gender and body mass index (referred to in the text as 'well-adjusted'), this association was referred to as an 'independent' association. These three criteria were determined for all longitudinal analyses and if any of these three criteria were not fulfilled, the association was referred to simply as an association. The validity of cross-sectional associations was determined using cross-sectional and case-control studies and establishing whether the analysis of the association of severity was well-adjusted or not. This data is summarized inTable 21.

Studies which investigated the association between multiple bone features and OA pain or structural progression outcomes were considered as a single study for each bone feature. Included studies that established a significant correlation between bone and pain, structural progression or joint replacement were described as positive (+) or negative (-) accordingly. If no association or inconclusive findings were described this was reported as no association (NA) or no conclusion (NC) respectively.

3.4 Results

3.4.1 Systematic literature search and selection

The PRISMA diagram (Figure 43) describes the literature flow. Following exclusion of duplicates and triplicates, 2456 articles met the search criteria. After applying inclusion/exclusion criteria, 139 articles were included for data extraction and quality scoring. In total, 71 papers provided longitudinal data (55 cohorts, 16 case-controls), 70 provided cross-sectional data, and two papers provided both.

3.4.2 Data extraction from selected studies

In only 12 studies did the mean age fall below 50 years[31, 96, 101, 261, 312, 353, 525-531]. Most (n=93) described both genders; two included men only[529, 532], 14 studies included females only [215, 276, 312, 349, 442, 530, 531, 533-539] and there was an undisclosed gender ratio in six[209, 282, 540-546]. Knee OA was defined using clinical and radiographic criteria and is described in Table 16. Radiographic OA was invariably defined as KL grade ≥2 or any radiographic OA abnormality from the Altman atlas[85]. Individual pain or structural progression measures were examined in 88 studies; 52 studies examined multiple features (Table 17,Table 18,Table 19,Table 20). Subchondral bone was analysed with MRI in 113 articles, DXA in eight[206, 208, 209, 532-534, 547, 548], CT in four[214, 215, 539, 549], scintigraphy in eight[216, 526, 536, 537, 550-553] and no articles using PET met the inclusion criteria. Included articles described 116 knee, 15 hip, six hand and two ankle studies. Of these studies 13 described structural associations without clinical or radiographic OA[31, 210, 259, 261, 301, 313, 353, 527, 528, 535, 554-556]. No foot articles met the inclusion criteria.

Figure 43 Search strategy results and article exclusion

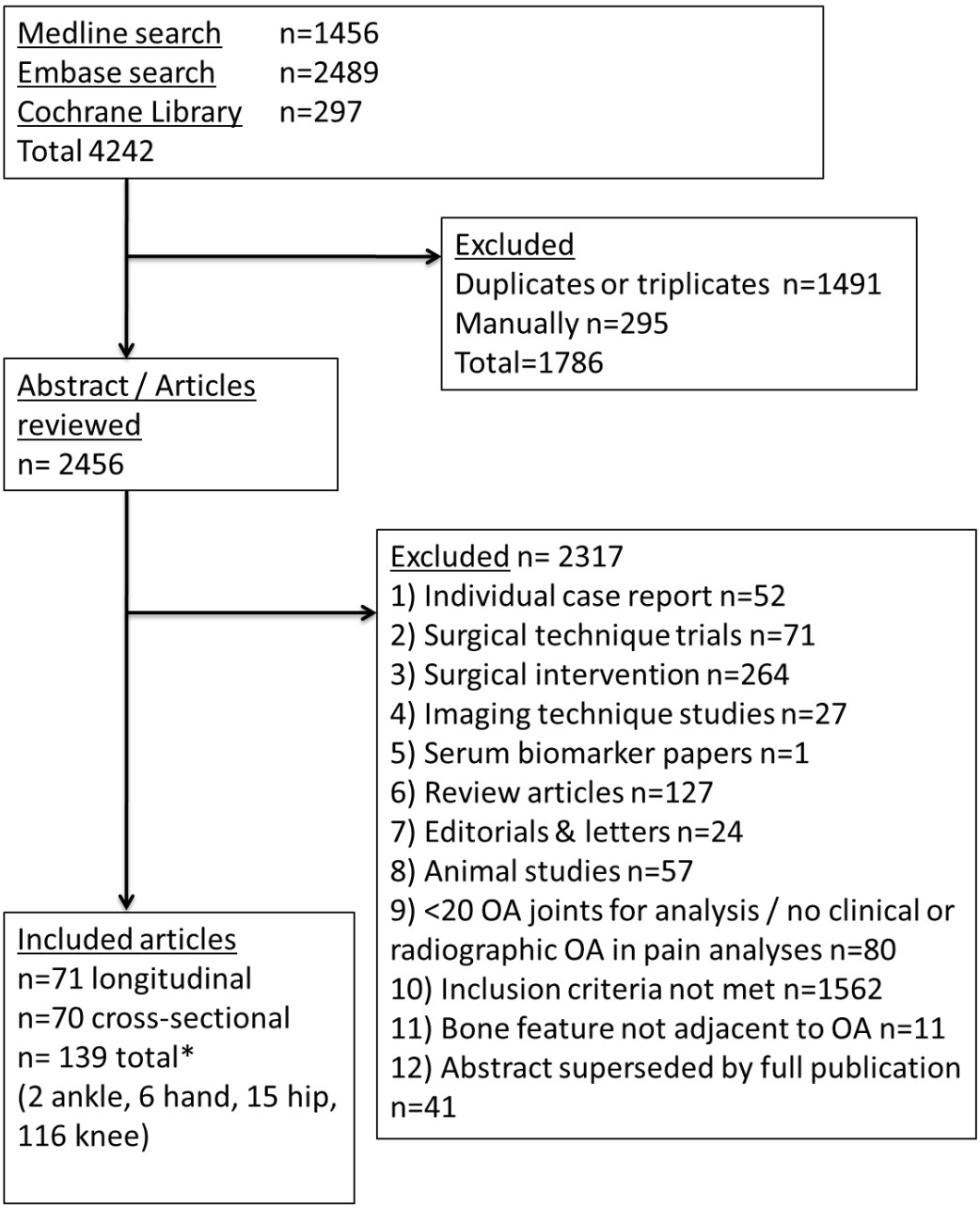

*Two articles included both cross-sectional and longitudinal data.

Longitudinal data included 16 case-control studies and 55 cohort studies

3.4.3 Quality assessment of studies

Concordance of opinion in quality scoring was observed in 2040 (89%) of the 2242 scoring items assessed which are recorded in Table 13, Table 14, Table 15. The majority of discordant scoring was for study design (criteria 17) and data presentation (criteria 18). Quality scores were converted to percentages of the maximum scores for each class of paper. The mean (range) quality score was 59% (29-79), 54% (22-83) and 59% (47-76) for cross-sectional, cohort and case-control studies respectively.

Table 13 Quality scoring results cross-sectional studies

		Quality Scoring Criteria																					
No.	Cross-sectional Study	1	2	3	4	5	6	7	8	9	10	11	12	13	14	15	16	17	18	19	20	Total	%
1	Ai 2010 [557]	0	0			0		1	1	0	1	1	1				1	0	1	1	0	8	57%
2	Akamatsu 2014 [533]	0	0			1		1	1	0	1	0	1				1	0	1	1	0	8	57%
3	Antoniades 2000 [534]	0	0			1		1	1	0	1	1	1				1	0	1	1	0	9	64%
4	Baranyay 2007 [554]	0	1			1		1	1	0	1	1	1				0	0	1	1	1	10	71%
5	Bilgici 2010 [558]	0	0			1		1	1	0	1	1	1				1	0	0	1	0	8	57%
6	Burnett 2012 [549]	0	0			0		1	1	0	1	1	1				1	0	1	1	0	8	57%
7	Chaganti 2010 [532]	0	0			1		1	1	0	1	0	1				1	0	1	1	1	9	64%
8	Chiba 2011[215]	0	0			0		1	1	1	1	0	1				1	0	1	1	0	8	57%
9	Chiba 2012 [349]	0	0			1		1	1	0	1	0	1				1	0	1	1	0	8	57%
10	Crema 2010 [315]	0	0			1		1	1	0	1	1	1				0	0	1	0	0	7	50%
11	Dawson 2013 [556] abstract	0	0			1		0	0	0	0	0	0				0	0	0	0	1	2	14%
12	Ding 2005 [353]	0	0			1		1	1	0	1	1	1				0	0	1	1	1	9	64%
13	Dore [547] 2009	0	0			1		1	1	0	1	1	1				1	0	1	1	1	10	71%
14	Driban [545] 2011	0	0			1		1	1	0	1	1	0				1	0	1	1	1	9	64%
15	Driban [546]2011	0	0			1		1	1	0	1	1	1				1	0	1	1	1	10	71%
16	Eckstein [483] 2010	0	0			1		1	1	0	1	0	1				0	0	1	0	0	6	43%
17	Felson 2001 [133]	0	0			1		1	1	0	1	0.5	1				0	0	1	1	0	7.5	54%
18	Fernandez-Madrid1994 [559]	0	0			1		0	0	0	1	0.5	1				1	0	1	1	0	6.5	46%
19	Frobell 2010 [560]	0	0			1		1	1	0	1	0	1				0	0	1	1	1	8	57%
20	Gosvig 2010 [561]	0	0			0		1	1	0	1	0	1				0	0	1	1	1	7	50%
21	Gudbergsen [562]	0	0			1		1	1	0	1	0	1				0	0	1	1	1	8	57%
22	Guymer 2007 [535]	0	1			1		1	1	0	1	1	1				0	0	1	1	1	10	71%
23	Haugen 2012 [563]	0	0			1		1	1	0	1	1	1				1	0	1	1	0	9	64%
24	Haugen 2013 [564]	0	0			0		1	1	0	1	0	1				0	0	1	1	0	6	43%
25	Haugen 2012 [565]	0	0			1		1	1	0	1	1	1				1	0	1	1	0	9	64%
26	Haverkamp 2011 [276]	0	0			1		1	1	0	1	0	1				0	0	0	1	0.5	6.5	46%
27	Hayashi [566]	0	0			1		0	1	0	1	1	1				1	0	1	1	0	8	57%

No.	Cross-sectional Study	1	2	3	4	5	6	7	8	9	10	11	12	13	14	15	16	17	18	19	20	Total	%
28	Hayes [312]	0	0			1		1	1	0	1	0.5	1				1	0	1	1	0	8.5	61%
29	Hernandez-Molina 2008 [139]	0	0			1		1	1	0	1	1	1				1	0	1	1	1	10	71%
30	Ip [567]	0	0			1		1	1	0	1	0.5	1				1	0	1	1	1	9.5	68%
31	Jones 2004 [31]	0	0			0		1	1	0	1	1	1				0	0	0	1	1	7	50%
32	Kalichman [568] 2007	0	0			1		1	1	0	1	0	1				1	0	1	1	1	9	64%
33	Kalichman [569] 2007	0	0			1		1	1	0	1	0	1				0	0	1	1	1	8	57%
34	Kim [570]	0	0			0		1	1	0	1	1	1				1	0	1	1	1	9	64%
35	Knupp 2009 [526]	0	0			0		1	1	0	1	1	1				1	0	1	1	0	8	57%
36	Kornaat [571] 2006	0	0			1		1	1	0	1	1	1				1	0	1	1	1	10	71%
37	Kornaat [572] 2005	0	0			1		1	1	0	1	1	1				0	0	1	1	0	8	57%
38	Kraus 2009 [550]	0	0			1		1	1	0	1	1	1				1	0	1	1	1	10	71%
39	Kraus 2013 [551]	0	0			1		1	1	0	1	1	1				1	0	1	1	1	10	71%
40	Kumar [573]	1	0			1		1	1	0	1	1	1				1	0	1	1	0	10	71%
41	Lindsey [350]	0	0			1		1	1	0	1	1	1				1	0	1	1	0	9	64%
42	Link [319] 2003	0	0			0		1	1	0	1	0.5	1				1	0	1	1	0	7.5	54%
43	Lo 2005 [574]	0	0			1		1	1	0	1	1	1				0	0	1	0	0	7	50%
44	Lo [575] 2009	0	0			1		1	1	0	1	1	1				1	0	1	1	1	10	71%
45	Lo [206] 2012	0	0			1		1	1	0	1	1	1				1	0	1	1	0	9	64%
46	Lo [208] 2006	0	0			1		1	1	0	1	1	1				1	0	1	1	1	10	71%
47	Macfarlane 1993 [552]	0	0			0		1	1	0	1	1	1				1	0	1	1	0	8	57%
48	Maksymowych 2014 [576]	0	0			1		1	1	0	1	1	1				1	0	1	1	0	9	64%
49	McCauley 2001 [528]	0	0			0		1	1	0	1	0	1				0	0	0	0	0	4	29%
50	McCrae 1992 [553]	0	0			1		1	1	0	1	0	1				0	0	1	1	0	7	50%
51	Meredith 2009 [555]	0	1			0		1	1	0	1	0	1				0	0	1	1	0	7	50%
52	Moisio [456] 2009	0	0			1		1	1	0	1	1	1				1	0	0	1	1	9	64%
53	Neumann 2007 [542]	0	0			0		1	1	0	1	0	1				0	0	1	1	0	6	43%
54	Ochiai [543] 2010	0	0			0		0	1	0	1	1	1				1	0	1	1	0	7	50%
55	Okazaki [539] 2014	0	0			0		1	1	0	1	0	1				1	0	1	1	0	7	50%
56	Ratzlaff [577] 2013	0	0			1		1	1	0	1	1	1				1	0	1	1	1	10	71%
57	Ratzlaff [544] 2014	0	0			1		1	1	0	1	1	1				1	0	1	1	0	9	64%

58	Reichenbach 2008 [306]	0	0			1		1	1	0	1	0	1				0	0	1	0	0	6	43%
No.	Cross-sectional Study	1	2	3	4	5	6	7	8	9	10	11	12	13	14	15	16	17	18	19	20	Total	%
59	Reichenbach 2011 [529]	0	1			1		1	1	0	1	0	1				0	0	1	1	1	9	64%
60	Roemer [578] 2012	0	0			1		1	1	0	1	0	1				0	0	1	1	1	8	57%
61	Scher 2008 [579]	0	0			0		1	1	0	1	0	1				0	0	1	1	0	6	43%
62	Sengupta [580] 2006	0	0			1		1	1	0	1	1	1				1	0	1	1	1	10	71%
63	Sharma [131] 2014	0	0			1		1	1	0	1	1	1				1	0	1	1	1	10	71%
64	Sowers 2003 [531]	0	0			1		1	1	0	1	0.5	1				0	0	1	1	0	7.5	54%
65	Stefanik [581] 2014	0	0			1		1	1	0	1	1.0	1				1	0	1	1	1	10	71%
66	Stefanik [274] 2012	0	0			1		1	1	0	1	0	1				0	0	1	1	1	8	57%
67	Stehling 2010 [313]	0	1			1		1	1	0	1	1	1				0	0	1	1	1	10	71%
68	Torres 2006 [135]	1	0			1		1	1	0	1	0.5	1				0	1	1	1	0	9.5	68%
69	Wang 2005 [259]	0	0			0		1	1	0	1	1	1				0	0	1	1	1	8	57%
70	Zhai 2006 [582]	1	0			1		1	1	0	1	1	1				1	0	1	1	1	11	79%
																				Mean		8.3	59%
																				Max		14	

Table 14 Quality scoring results cohort studies

		Quality Scoring Criteria																					
No.	Cohort Study	1	2	3	4	5	6	7	8	9	10	11	12	13	14	15	16	17	18	19	20	total	%
1	Agricola 2013 [74]	0	1		1	1		1	1	0	1	1	1	0	1	0	0	0	1	1	1	12	67%
2	Agricola 2013 [394]	0	1		1	1		1	1	0	1	1	1	0	1	0	0	0	1	1	1	12	67%
3	Agricola 2013 [583]	0	1		1	1		1	1	0	1	1	1	0	1	0	1	0	1	1	1	13	72%
4	Bruyere[209] 2003	0	0		0	0		1	1	0	1	0	1	0	0	0	1	0	1	1	1	8.0	44%
5	Carnes [584] 2012	0	0		0	1		1	1	0	1	1	1	0	0	0	0	0	1	1	1	9.0	50%
6	Carrino [585] 2006	0	0		0	0		0	1	0	1	0	1	0	0	0	0	0	1	0	0	4.0	22%
7	Cicuttini 2004 [270]	0	0		1	1		1	1	0	1	1	1	1	1	1	1	0	1	1	1	14	78%
8	Crema 2013 [586]	0	0		0	1		1	1	0	1	0	1	0	0	0	0	0	1	1	1	8.0	44%
9	Crema 2014 [587]	1	0		0	1		1	1	0	1	1	1	0	0	0	0	0	1	1	1	10.0	56%
10	Davies-Tuck [588] 2008	0	0		0	1		1	1	0	1	1	1	0	0	1	0	0	1	1	1	10.0	56%
11	Davies-Tuck 2010 [301]	0	1		0	1		1	1	0	1	1	1	0	0	1	0	0	1	1	1	11	61%
12	De-Lange 2014 [589]	0	0		0	1		1	1	0	1	0	1	1	1	0	1	0	1	1	1	11	61%
13	Dieppe 1993 [216]	0	0		0	1		1	1	0	1	0	1	0	1	0	1	0	1	1	0	9.0	50%
14	Ding 2006 [261]	1	0		1	1		1	1	0	1	1	1	0	0	0	0	0	1	1	1	11	61%
15	Ding [96] 2008	1	0		0	1		1	1	0	1	1	1	1	0	1	0	1	1	1	1	13	72%
16	Dore 2010 [99]	1	0		0	1		1	1	0	1	1	1	0	0.5	0	1	0	1	1	1	11.5	64%
17	Dore 2010 [590]	0	0		0	1		1	1	0	1	1	1	0	0	0	0	0	1	1	1	9.0	50%
18	Dore 2010 [210]	0	0		0	1		1	1	0	1	1	1	0	0	0	0	0	1	1	1	9.0	50%
19	Driban[591] 2011	0	0		0	1		1	1	0	1	1	1	0	0	0	0	0	1	1	1	9.0	50%
20	Driban [592] 2012	0	0		0	1		0	1	0	1	0	1	0	0	0	0	0	0	1	0	5.0	28%
21	Driban [100] 2013	0	0		0	1		1	1	0	1	1	1	0	1	0	1	0	1	1	1	11.0	61%
22	Everhart [102] 2014	0	0		0	1		1	1	0	1	1	1	0	1	0	1	0	1	1	1	11.0	61%
23	Felson [294] 2003	0	0		1	1		1	1	1	1	1	1	1	0	1	1	1	1	1	1	15.0	83%
24	Foong [101] 2014	0	0		0	1		1	1	0	1	1	1	0	1	1	1	0	1	1	1	12.0	67%
25	Guermazi [124] 2014	0	0		0	1		1	1	0	1	0	1	0	1	0	1	0	1	1	1	10.0	56%
26	Haugen [39] 2014	0	0		0	1		1	1	0	1	1	1	0	1	0	1	0	1	1	1	11.0	61%
27	Haugen [593] 2014	0	0		0	1		1	1	0	1	1	1	0	1	0	1	0	1	1	1	11.0	61%
28	Hernandez-Molina [594]2008	0	0		0	1		0	1	0	1	1	1	0	0	0	0	0	1	1	1	8.0	44%

No.	Cohort Study	1	2	3	4	5	6	7	8	9	10	11	12	13	14	15	16	17	18	19	20	total	%
29	Hochberg 2014 [540]	0	0		1	0		1	1	0	1	1	1	0	1	0	1	0	1	1	1	11.0	61%
30	Hudelmaier [595] 2013	0	0		0	1		1	1	0	1	1	1	0	0	0	1	0	1	1	0	9.0	50%
31	Hunter [596] 2006	0	0		0	1		1	1	0	1	1	1	0	0	0	0	0	1	1	0	8.0	44%
32	Kornaat [302] 2007	0	0		0	1		1	1	0	1	1	1	0	0	0	1	0	1	1	1	10.0	56%
33	Koster 2011 [527]	0	0		0	1		0	1	0	1	0	1	1	0	1	0	0	1	1	0	8	44%
34	Kothari [478] 2010	1	0		0	1		1	1	0	1	0	1	0	0	0	0	0	1	1	1	9.0	50%
35	Kubota[597] 2010	0	0		0	1		0	1	0	1	0	1	1	0	0	0	0	1	1	0	7.0	39%
36	Liu 2014 [541]	0	1		1	0		1	1	0	1	1	1	1	0	0	0	0	0	1	0	9.0	50%
37	Lo [548] 2012	0	0		0	1		1	1	0	1	0	1	0	0	0	1	0	1	1	1	9.0	50%
38	Madan-Sharma [417] 2008	0	0		0	1		1	1	0	1	0.5	1	0	0	0	0	0	1	1	1	8.5	47%
39	Mazzuca 2004 [536]	0	0		1	1		1	1	0	1	1	1	0	0	0	1	0	1	1	1	11	56%
40	Mazzuca 2005 [537]	0	0		1	1		1	1	0	1	1	1	0	0	0	1	0	1	1	0	10	56%
41	Moisio [456] 2009	0	0		0	1		1	1	0	1	1	1	0	0	0	1	0	1	1	1	10.0	56%
42	Parsons [598] 2014	0	0		0	1		1	1	0	1	0	1	0	0	0	1	0	1	1	1	9.0	50%
43	Pelletier [123] 2007	0	0		0	1		1	1	0	1	1	1	0	0	0	0	0	1	1	1	9.0	50%
44	Raynauld [599] 2008	0	0		0	1		1	1	0	1	1	1	0	0	0	0	0	1	1	1	9.0	50%
45	Raynauld 2011 [457]	0	0		0	1		1	1	0	1	1	1	0	1	0	1	0	1	1	1	11.0	61%
46	Raynauld 2013 [103]	0	0		0	1		1	1	0	1	1	1	0	1	0	1	0	1	1	1	11.0	61%
47	Roemer [443] 2009	0	0		0	1		1	1	0	1	1	1	0	0	0	0	0	1	1	1	9.0	50%
48	Roemer [444] 2009	0	0		0	1		1	1	0	1	0	1	0	0	0	0	0	1	1	1	8.0	44%
49	Roemer [500] 2012	0	0		0	1		1	1	0	1	0	1	0	0	0	0	0	1	1	1	8.0	44%
50	Scher 2008 [579]	0	1		0	1		1	1	0	1	1	1	0	0	0	1	0	1	1	0	10	56%
51	Sowers [530] 2011	0	0		0	1		1	1	0	1	0.5	1	0	1	0	1	0	1	1	0	9.5	53%
52	Tanamas [600] 2010	0	0		0	1		1	1	0	1	1	1	0	0	1	0	0	1	1	0	9.0	50%
53	Tanamas [601] 2010	0	0		0	1		1	1	0	1	1	1	0	0	0	0	0	1	1	0.5	8.5	47%
54	Wildi [602] 2010	0	0		0	1		1	1	0	1	1	1	0	0	0	0	0	1	1	1	9.0	50%
55	Zhang [26] 2011	0	0		0	1		1	1	0	1	1	1	0	0	0	1	0	1	1	0	9.0	50%
																					mean	9.7	54%
																					Max	18.0	

Table 15 Quality scoring results case-control studies

		Quality Scoring Criteria																					
No.	Case control study	1	2	3	4	5	6	7	8	9	10	11	12	13	14	15	16	17	18	19	20	total	%
1	Aitken 2013 [525]	0	0	0		0	0	1	1	0	1	0	1		1		0	0	1	1	1	8	47%
2	Barr 2012 [603]	0	1	1		1	0	1	1	0	1	1	1		1		1	0	1	1	1	13	76%
3	Bennell 2008 [214]	0	0	0		1	0	1	1	0	1	1	1		0		1	0	1	1	1	10	59%
4	Bowes 2012 [604]	0	1	1		1	0	1	1	0	1	0	1		1		1	0	1	1	1	12	71%
5	Doherty 2008 [282]	0	0	0		1	0	1	1	0	1	1	1		0		0	0	1	1	1	9	53%
6	Felson 2007 [134]	0	1	1		1	0	1	1	0	1	1	1		0		1	0	1	1	1	12	71%
7	Hunter 2013 [605]	0	0	1		1	0	1	1	0	1	0	1		1		1	0	1	1	0	10	59%
8	Javaid 2012 [606]	0	0	1		1	1	1	1	0	1	1	1		0		0	0	1	1	0	10	59%
9	Javaid 2010 [607]	0	1	1		1	1	1	1	0	1	1	1		0		1	0	1	1	1	13	76%
10	Neogi 2013 [75]	0	1	1		1	0	1	1	0	1	0	1		0		1	0	1	1	1	11	65%
11	Neogi 2009 [307]	0	0	1		1	1	1	1	0	1	0	1		0		0	0	1	1	1	10	59%
12	Nicholls 2011 [538]	0	0	1		1	1	1	1	0	1	1	1		1		1	0	0	1	1	12	71%
13	Ratzlaff 20148 [608]	0	1	1		0	0	1	1	0	1	1	1		0		1	0	1	1	1	11	65%
14	Stahl 2011 [442]	0	0	1		1	0	1	1	0	1	1	1		0		0	0	1	0	0	8	47%
15	Wluka 2005 [269]	0	0	0		1	0	1	1	0	1	1	1		0		0	0	0	1	1	8	47%
16	Zhao 2010 [609]	1	0	0		1	0	1	1	0	1	0.5	1		0		0	1	1	1	0	9.5	56%
																					mean	10.1	59%
																					max	17	

Table 16 A description of the included studies, the relationships examined and the quality of each paper

Author of longitudinal studies	Patient number (n)	Study demographics	Subchondral bone feature assessed	Structural progression or severity / pain measure	Statistical analysis	Quality (score %)
Knee cohort studies						
Bruyere 2003 [209]	56	Knee OA (ACR criteria), gender distribution unknown, mean age 65 yrs	Subchondral tibial bone BMD (DXA) (C)	Minimum medial JSW TFJ after one year (L)	Multiple regression	Low (44)
Carnes 2012 [584]	395	Randomly selected older adults with over 52% knee ROA. 50% female, mean age 63 yrs. TASOAC	MRI tibial Bone area (C)	Semi-quantitative cartilage defect progression TFJ (L)	Logistic regression	Low (50)
Carrino 2006 [585]	32	Chronic knee pain with MRI features of OA. 63% female, mean age 51 yrs. USA	Crude presence of MRI BML, bone cyst TFJ (C) and (L)	Graded cartilage defect TFJ (L)	Crude comparison	Low (22)
Cicuttini 2004 [270]	113	Symptomatic, clinical (ACR) knee OA with mild to moderate TFJ ROA, mean age 64yrs, mean BMI 29, 58% females. Australia	Baseline Quantitative MRI tibial bone area (C)	TKR incidence (L) over 4 years	Logistic regression	High (78)
Crema 2013 [586]	1351	Knee OA or at high risk of it. 39% ROA, 62% female, mean age 62 yrs. MOST	MRI Incident BML (WORMS) TFJ (L)	Progressive (30 month) semi-quantitative cartilage defect (WORMS) TFJ (L)	Logistic regression	Low (44)
Crema 2014 [587]	163	Clinical knee OA, 37% knee ROA, 54% female, Mean age 58 yrs.	MRI BML (semi-quantitative) (C) (all regions)	Cartilage loss (semi-quantitative) (L) (all regions)	Logistic regression	High (56)
Davies-Tuck 2008 [588]	117	ACR knee OA. 58% female, mean age 64 yrs. Australia	Baseline MRI tibial bone plateau area (C) TFJ	Progressive semi-quantitative cartilage defect score (L) medial and lateral TFJ	Linear regression	High (56)
Davies-Tuck 2010 [301]	271	No clinical knee OA (ACR clinical criteria) and no current or historic	Incident BML (new BML after 2	Progression in semi-quantitative	Logistic regression	High (61)

Author of longitudinal studies	Patient number (n)	Study demographics	Subchondral bone feature assessed	Structural progression or severity / pain measure	Statistical analysis	Quality (score %)
		knee pathology, mean age 58yrs, 65% female, mean BMI 25. Melbourne.	years with no BMLs at baseline) MRI TFJ (L)	MRI cartilage defects score after 2 years. TFJ (L)		
De-Lange 2014 abstract [589]	133	Symptomatic OA knee. ROA Knee (>50%), 80% female, mean age 60 yrs. GARP study	MRI osteophytes (medial or lateral TFJ) (C)	Radiographic JSN progression (OARSI) (L)	Generalised estimation equation models	High (61)
Dieppe 1993 [216]	94	Symptomatic and ROA knee (100%). 96% women, mean age 64 yrs, mean BMI 26. Referrals to hospital rheumatology unit	Baseline late and or early-phase subchondral bone scintigraphy signal (C)	Progression of JSN by ≥2mm or knee operation after 5 years (L)	Pearson Chi squared test	Low (50)
Ding 2006 [261]	325	Mostly no ROA knee (17% ~ KL =1), 58% female, Mean age 45 yrs. Mean BMI 27. Offspring study	Baseline MRI tibial bone area (C) TFJ	Change in semi-quantitative MRI cartilage defect scores over 2.3 yrs (L) TFJ	Logistic regression	High (61)
Ding 2008 [96]	252	Randomly selected adults with 15% knee ROA. 58% female, mean age 45 yrs.	Baseline MRI tibial bone area (C) TFJ	Progressive Cartilage volume loss (L) TFJ	Multivariable linear regression	High (72)
Dore 2010 [99]	395	Symptomatic knee OA, knee ROA (58%). 51% female, mean age 63 yrs, mean BMI 28. TASOAC	MRI BML size (L) regional or whole TFJ over 2.7 years	Change in WOMAC pain (L) over 2.7 years Incident TKR over 5 years (L)	Mixed effects models	High (64)
Dore 2010 [590] 12(6)	405	Prevalent knee OA, 50% female, Mean age 63 yrs. TASOAC	Baseline semi-quantitative BML severity (C) TFJ	Ipsi-compartmental cartilage volume loss (L)	Logistic regression and generalised estimating equations	Low (50)
Dore 2010	341	Older adult cohort. Right knees only.	Baseline	Increase or no	Logistic	Low

Author of longitudinal studies	Patient number (n)	Study demographics	Subchondral bone feature assessed	Structural progression or severity / pain measure	Statistical analysis	Quality (score %)
[210]		Mean age 63 yrs, ~48% female, mean BMI 27. TASOAC	proximal tibial BMD, DXA Baseline tibial bone area MRI (C)	increase in semi-quantitative MRI cartilage defects over 2.7 years (L)	regression	(50)
Driban 2011 [591]	44	ACR knee OA(100%). 100% knee ROA, , 52% female, Mean age 65 yrs. Clinical trial of Vitamin D	Baseline 3D BML volume (C) and 24 month change in 3D BML volume (L) in TFJ compartments	24 month change in ipsicompartmental full thickness cartilage lesion area (L)	Multiple linear regression, Spearman correlations	Low (50)
Driban 2012 [592] Abstract	38	Knee ROA (100%). 66% female, mean age 61 yrs. OAI	MRI BML volume change (L) TFJ over 24 months	Change in cartilage thickness and denuded area of bone (L) TFJ over 24 months	Pearson correlation coefficients	Low (28)
Driban 2013 [100]	404	Prevalent ROA knee (71%) 49% female, mean age 63 yrs. OAI	Knee baseline BML volume (C) BML volume 48 month change (L) (TFJ)	48 month change in WOMAC pain (L) and OARSI JSN grade (L) (TFJ)	Multiple linear regressions & logistic regression	High (61)
Everhart 2014 [102]	1338	Prevalent ROA knee (74%) 60% female, Mean age 62 yrs. OAI	Baseline TFJ subchondral surface ratio of medial and lateral TFJ compartments (C)	Incident frequent knee pain at 48 months or radiographic progression of lateral or medial knee TFJ OA at 48 months (L)	Logistic regression	High (61)
Felson 2003	223	ACR knee OA and 75% ROA. 42%	Baseline	OARSI JSN grade	Generalised	High

Author of longitudinal studies	Patient number (n)	Study demographics	Subchondral bone feature assessed	Structural progression or severity / pain measure	Statistical analysis	Quality (score %)
[294]		female, mean age 66 yrs. BOKS	presence of BML in medial or lateral TFJ (C)	progression of TFJ (L)	estimating equations	(83)
Foong 2014 [101]	198	17% ROA knee, 42% female, Mean age 47 yrs. Offspring study	Change in quantitative BML size (L) and incident BMLs (L) In all three knee compartments over 8 years	WOMAC Knee pain severity over 8 years (L)	Linear regression	High (67)
Guermazi 2014 Abstract [124]	196	Knee ROA (24%), 62% female, mean age 60 yrs	Semi-quantitative BML score WORMS (C) TFJ	Cartilage thickness loss over 30 months (L)	multivariable logistic regression,	High (56)
Hernandez-Molina 2008 [594]	258	ACR knee OA and 77% ROA. 43% female, mean age 67 yrs. BOKS	Crude presence of central BMLs on MRI (C) TFJ	Semi-quantitative cartilage defect (WORMS) (L) TFJ	Logistic regression	Low (44)
Hochberg 2014 Abstract [540]	1024	100% Symptomatic and radiographic knee OA (the 'progressor' arm). OAI	Semi-quantitative MRI baseline femoral condyle BML size (C)	Incident TKR over 6 years (L)	Multivariable Cox proportional hazard models	High (61)
Hudelmaier 2013 [595] abstract	899	Prevalent ROA knee, ROA 60%, 60% women, mean age 62 yrs, OAI	Annual change in Segmented MRI knee bone area (L)	Baseline KL grade (C)	Non-paired t-test	Low (50)
Hunter 2006 [596]	217	ACR knee OA. 44% female, mean age 66 yrs. BOKS	Change in MRI semi-quantitative BML score (L) TFJ	Change in semi-quantitative cartilage defect score (WORMS) (L) TFJ	Generalised estimating equations	Low (44)
Kornaat 2007 [302]	182	OA knee symptoms (38%) and ROA (38%). 80% female, mean age 59 yrs. GARP	Semi-quantitative MRI BML change over 2 years (L) TFJ	Mean WOMAC pain over 2 years	Linear mixed models	High (56)

Author of longitudinal studies	Patient number (n)	Study demographics	Subchondral bone feature assessed	Structural progression or severity / pain measure	Statistical analysis	Quality (score %)
Koster 2011 [527]	117	One year follow up after acute knee trauma in primary care, 12% ROA knee, mean age 41yrs, 43% female, mean BMI 26, HONEUR	Baseline BML presence (C) TFJ	Any progression in KL grade over 1 year (L) TFJ	Logistic regression	Low (44)
Kothari 2010 [478]	177	Some WOMAC dysfunction and >74% ROA knee, 79% female, mean age 66 yrs. MAK-2	Semi-quantitative baseline MRI BML, bone cyst and attrition (WORMS) (C) TFJ	Semi-quantitative cartilage defect score change over 2 years (WORMS) (L) TFJ.	Logistic regression, with generalised estimating equations	Low (50)
Kubota 2010[597]	122	Clinical and ROA (80%) of the knee. >90% female, mean age 68 yrs. Japan	MRI BML semi-quantitative volume score change over 6 months (L) TFJ	KL grade progression over 6 months (L) TFJ	Mann-Whitney U-test	Low (39)
Lo 2012 [548]	497	52% ROA knee, 47% female , Mean age 64 yrs. OAI	DXA measured medial:lateral periarticular BMD and MRI BVF, trabecular number, thickness and spacing (C)	OARSI medial TFJ JSN grade progression between 24 and 48 months (L)	Logistic regression	Low (50)
Liu 2014 S470 Abstract [541]	128	Medial knee OA, KL grade 4. Japan	Baseline Semi-quantitative osteophyte score (WORMS) (C) TFJ	Incident TKR at 6 months follow up (L)	Mann Whitney-U test & ROC curve	Low (50)
Madan-Sharma 2008 [417]	186	Prevalent ROA knee (40%). 81% female, mean age 60 yrs. GARP	Baseline MRI semi-quantitative BML, bone cyst (C) TFJ	OARSI medial TFJ JSN grade progression over 2 years (L) TFJ	Logistic regression	Low (47)
Mazzuca 2004 [536]	86	100% female, mean age 55 yrs, mean BMI 37.	Baseline late-phase bone	Progression of minimum JSN of	Pearson correlation	High (56)

Author of longitudinal studies	Patient number (n)	Study demographics	Subchondral bone feature assessed	Structural progression or severity / pain measure	Statistical analysis	Quality (score %)
			scintigraphy (adjusted for normal bone uptake) of the medial tibia and whole knee (C)	the medial TFJ from baseline to 30 months (L)	coefficients	
Mazzuca 2005 [537]	174	100% female, mean age 56 yrs, mean BMI 36. A placebo controlled trial of doxycycline	Baseline late-phase bone scintigraphy (adjusted for normal bone uptake) of the medial tibia and whole knee (C)	Progression of minimum JSN of the medial TFJ from baseline to 30 months (L)	multiple linear regression	High (56)
Moisio 2009 [456]	168	Some WOMAC dysfunction and 90% ROA knee. 78% female, mean age 66 yrs. MAK-2	Baseline MRI semi-quantitative BML score (C) TFJ and PFJ	Incident frequent knee pain 2 years after baseline (L)	Logistic regression	High (56)
Parsons 2014 Abstract [598]	559	Knee ROA (100%), 73% female, mean age 63 yrs. SEKOIA	Baseline semi-quantitative BML score (C)	Annual TFJ JSN (L)	Linear regression	Low (50)
Pelletier 2007 [123]	107	100% radiographic OA knee, 64% female, Mean age 62 yrs. Bisphosphonate Trial	Regional semi-quantitative baseline BML score (medial or lateral TFJ) (C)	Regional cartilage volume over 24 months (medial or lateral TFJ) (L)	Multivariate regression	Low (50)
Raynauld 2008 [599]	86	64% female, Mean age 61 yrs. Trial of bisphosphonate	Change in BML size (L) at 24 months in TFJ	Medial cartilage volume loss (L) at 24 months in TFJ	Multivariate linear regression	Low (50)
Raynauld 2011 [457]	123	Symptomatic knee OA of the medial TFJ, 65% female, mean age 61 yrs, mean BMI 32.	Baseline semi-quantitative BML score (C) TFJ	Incidence of TKR over 3 years (L)	Logistic regression	High (61)
Raynauld 2013	57	Patients from a chondroitin trial	Baseline semi-	Incident TKR (L) 4	Logistic	High

Author of longitudinal studies	Patient number (n)	Study demographics	Subchondral bone feature assessed	Structural progression or severity / pain measure	Statistical analysis	Quality (score %)
[103]		81% female, mean age 63, mean BMI 31.	quantitative BML WORMS score (C) Medial TFJ	year follow up Time to TKR	regression, Cox regression	(61)
Roemer 2009 [443]	395	Knee OA or at high risk of it. 33% ROA. 68% female, mean age 63 yrs. MOST	Change in MRI semi-quantitative BML size over 30 months (WORMS) (L) TFJ and PFJ	Progression in semi-quantitative cartilage defects in (WORMS) over 30 months (L) TFJ and PFJ	Logistic regression	Low (50)
Roemer 2009 [444]	347	Knee OA or at high risk of it. 14% ROA. 65% female, mean age 64 yrs. MOST	Baseline MRI BML crude presence or absence (WORMS) (L) TFJ	Semi-quantitative cartilage defect progression over 30 months (WORMS) (L) TFJ	Logistic regression	Low (44)
Roemer 2012 [500]	177	Chronic knee pain, 71% knee ROA, 49% female. Mean age 52 yrs. Glucosamine trial	Semi-quantitative BML (WORMS) TFJ and PFJ (C)	Semi-quantitative cartilage score 6-month progression TFJ and PFJ (L)	Logistic regression	Low (44)
Sowers 2011[530]	363	Minor OA symptoms with18% ROA knee. 100% female, median age 45 yrs. SWAN	Semi-quantitative MRI BML, osteophyte, bone cyst size in TFJ (C)	Progression in KL grade and WOMAC pain score (11 years follow up) (L)	Chi-square tests or Fisher exact tests. Logistic regression	Low (53)
Tanamas 2010 [601]	109	ACR knee OA, 73% ROA. 40% female, mean age 63 yrs. Australia	Semi-quantitative change in MRI Bone cyst or BML size (L)	Knee cartilage volume loss over 2 years (L) TFJ Incident TKR over 4 years	Logistic regression	Low (47)
Tanamas 2010 [600]	109	ACR knee OA, 72% ROA. 50% female, mean age 63 yrs, mean BMI 29. Australia	Baseline semi-quantitative MRI BML size (C)	Cartilage volume change over 2 years (L) TFJ	Logistic regression	Low (50)

Author of longitudinal studies	Patient number (n)	Study demographics	Subchondral bone feature assessed	Structural progression or severity / pain measure	Statistical analysis	Quality (score %)
				Annual change in WOMAC pain(L) Incident TKR over 4 years		
Wildi 2010 [602]	161	Symptomatic medial TFJ OA knee (ACR criteria). 100% ROA knee, 66% female, Licofelone trial	24 month change in regional TFJ BML score WORMS (L)	24 months change in WOMAC pain (L) or regional change in cartilage volume (L)	Multivariate regression	Low (50)
Zhang 2011 [26]	570	Patients with knee OA or at high risk of it. 41% ROA knee. 68% female, mean age 62 yrs. MOST	Semi-quantitative change in MRI BML size (L) TFJ over 30 months	Incidence of frequent knee pain, and categorical severity (L) over 30 months	Logistic regression	Low (50)
Knee case-controls studies						
Aitken 2013 [525] Abstract	220	57% female, Mean age 45 yrs. Prevalence of ROA unknown. Offspring	Semi-quantitative BMLs tibia, femur & patella (C)	Cartilage volume and defect score Tibia and femur (L)	Linear regression	Low (47)
Bowes 2012 [604]	2197	Cases of clinical knee OA (100% ROA, n=1312), control healthy knees (0% ROA, n=885). 56% female, mean age 61 yrs. OAI dataset	Change in segmented MRI 3D Bone area over 4 year (L)	KL grade defined ROA knee (C)	ANCOVA model	High (71)
Bennell 2008 [214]	116	Cases of ACR medial knee OA (100% medial TFJ ROA) (n=75), asymptomatic control knees (n=41). 54% female, mean age 64 yrs. Australia	Volumetric BMD of tibial subchondral trabecular bone (qCT) (C)	KL grade (C)	Generalised linear models	Low (59)
Felson 2007 [134]	330	Patients at high risk of knee OA , cases with incident pain (n=110, ROA 30%), controls without pain (n=220,ROA 20%); 66%female, mean age 63 yrs. MOST	Semi-quantitative MRI BML size increase (WORMS) (L) TFJ & PFJ	Incident frequent pain at 15 months (L)	Multiple logistic regression,	High (71)
Hunter 2013	636	636 knees at risk of OA (ROA=0% at	MRI bone area 8	Incident ROA knee	Discrete-time Cox	Low

Author of longitudinal studies	Patient number (n)	Study demographics	Subchondral bone feature assessed	Structural progression or severity / pain measure	Statistical analysis	Quality (score %)
Abstract [605]		baseline). Cases of incident ROA n=318, Controls without incident ROA n=318, 67% female. Mean age 60 yrs. OAI	knee regions (L)	(KL grade ≥2) (TFJ) (L)	Proportional Hazards Regression	(59)
Javaid 2012 [606]	636	Patients with prevalent ROA. Cases have painful knees (n= 546), controls have no knee pain (n=90); 65% female, mean age 73 yrs. Health aging and body composition study	Baseline Semi-quantitative MRI BML, bone cyst and attrition size (WORMS) (C) TFJ & PFJ	Presence of frequent knee pain (C) after 2 years	Conditional and marginal logistic regression	Low (59)
Javaid 2010 [607]	155	Clinical knee OA, cases with incident pain (n=33), controls without pain (n=122); 67% female, mean age 59 yrs. ROA 0%; MOST	Baseline semi-quantitative MRI BML, osteophyte, bone cyst size (WORMS) (C) TFJ & PFJ	Incident frequent knee pain after 15 months (L)	Logistic regression	High (76)
Neogi 2013 [75]	531	Incident knee TFJ ROA cases (n=178), controls did not develop ROA (n=353); 62% female, mean age 61 yrs. OAI dataset	MRI 3D bone shape (Tibia, Femur and patella) (C)	Incident TFJ ROA KL grade ≥2 (L)	Conditional Logistic regression	High (65)
Neogi 2009 [307]	4446	Clinical knee OA. Within-knee subregion cases (n=973) had cartilage loss, controls (n=3473) had not. 64% female, mean age 63 yrs; ROA 59% MOST	Baseline semi-quantitative MRI Bone attrition size (WORMS) (C) TFJ	Cartilage defects progression (WORMS) after 30 months TFJ	Logistic regression	Low (59)
Ratzlaff 2014 [608]	278	59% female, mean age 64, mean BMI 30. 138 cases of TKR and 138 ROA matched controls. OAI	Total tibial BML volume 12 and 24 months before TKR and interval change between 12 and 24 (C) and (L)	Incident TKR (L)	Conditional logistic regression	High (65)
Scher 2008	65	Patients with OA knee based upon	Presence of any	Incident TKR (L)	Generalised	High

Author of longitudinal studies	Patient number (n)	Study demographics	Subchondral bone feature assessed	Structural progression or severity / pain measure	Statistical analysis	Quality (score %)
[579]		radiography (>50% ROA), 54% female, mean age 51 yrs. USA	baseline semi-quantitative MRI BMLs (C)	over 3 years	estimating equations	(56)
Stahl 2011 [442]	60	Clinical and 100% ROA knee cases (n=30) ; controls – healthy knees ROA 0% (n=30); All female, mean age 58 yrs. USA	Semi-quantitative MRI BML size (WORMS) (L) TFJ	Semi-quantitative Cartilage defect size (L) TFJ WOMAC score	Generalised estimating equations	Low (47)
Wluka 2005 [269]	149	ACR knee OA cases (n=68), controls (n=81) without OA; 54% female, mean age 64 yrs. Australia	Change in MRI Tibial bone area (L)	Baseline radiographic JSN (C)	Logistic regression	Low (47)
Zhao 2010 [609]	38	Clinical and ROA cases (n=24), control (n=14) knees (KL=0); 54% female, mean age 52 yrs	MRI BML volume (C) TFJ	Overlying cartilage defect progression after one year (WORMS) (L) TFJ WOMAC pain	Student's t test	Low (56)

Author of studies	Patient number (n)	Study demographics	Subchondral bone feature assessed (method) region	Structural progression / pain outcome (method) region	Statistical analysis	Quality (score%)
Knee cross-sectional studies						
Ai 2010 [557]	28	Clinical knee OA. 55% ROA, 57% female, mean age 61 yrs. China	Semi-quantitative MRI BML and osteophytes (C)	Pain verbal rating scale (Likert) (C)	Fisher exact test	Low (57)
Akamatsu 2014 [533] Abstract	192	Varus ROA Knee 94%, 100% female, mean age 70 yrs. Japan	BMD (DXA) (C) (medial tibia & femoral condyle)	Medial TFJ JSN radiographic (C)	Pearson's Correlation	Low (57)
Baranyay 2007 [554]	297	No clinical knee OA (ACR clinical criteria) and no current or	MRI BML defined as large or not large / absent in the medial	MRI semi-quantitative cartilage defects of medial and lateral	Logistic regression	High (71%)

Author of studies	Patient number (n)	Study demographics	Subchondral bone feature assessed (method) region	Structural progression / pain outcome (method) region	Statistical analysis	Quality (score%)
		historic knee pathology, mean age 58yrs, 63% female, mean BMI 25. Melbourne	and lateral compartments of TFJ (C)	compartments of TFJ Quantitative Cartilage volume medial and lateral TFJ (C)		
Bilgici 2010 [558]	34	ACR knee OA. ROA 65%, 71% female, mean age 50 yrs. Turkey	MRI BML (WORMS) (C)	WOMAC pain & pain VAS (C)	Linear regression	Low (57)
Burnett 2012 [549]	42	Knees with OA awaiting total knee replacement, 100% ROA, 60% Female, mean age 64 yrs. Canada	BMD of patellar facets (qCT) (C)	WOMAC pain – knee pain at rest (C)	Independent t-test	Low (57)
Chiba 2012 [349]	60	Prevalent Knee OA. ROA 50%. 100% female, mean age 68 yrs Japan	MRI Bone volume fraction & trabecular thickness of the medial & lateral femur & tibia. (C)	Metric JSW (radiographic) (C) of the medial and lateral TFJ	Pearson's Correlation	Low (57)
Crema 2010 [315]	1283	Knee OA or at high risk of OA. ROA knee 44%. 60% female, mean age 62 yrs.	MRI Bone cysts (WORMS) (C)	Cartilage defect (WORMS) (C)	Comparison of tabulated data	Low (50)
Ding 2005 [353]	372	Mostly no ROA knee (17% ~ KL =1), 58% female, Mean age 45 yrs. Mean BMI 27. Offspring study	MRI quantitative tibial bone area (C)	Semi-quantitative MRI knee cartilage defect severity scores (C) TFJ	Linear regression	High (64)
Dore 2009 [547]	740	>15% ROA knee, 52% female, Mean age 62 yrs. TASOAC	DXA Tibial subchondral BMD (C)	Radiograph JSN grade and MRI cartilage defect and volume (C)	Multivariable analysis	High (71)
Driban 2011 [545]	421	NR	MRI Bone volume	Radiographic JSN (C)	Multiple linear	High (64)

Author of studies	Patient number (n)	Study demographics	Subchondral bone feature assessed (method) region	Structural progression / pain outcome (method) region	Statistical analysis	Quality (score%)
Abstract			fraction (C)		regression	
Driban 2011 [546] Abstract	285	OAI Progression Cohort. No other demographic data available.	MRI bone volume fraction, trabecular number, spacing & thickness of medial tibia (C)	The presence of any grade of radiographic medial & lateral JSN (C)	Multiple linear regression	High (71)
Eckstein 2010 [483]	73	ROA knee (100%), 63% female with mean age of 61 yrs. OAI	MRI Tibial bone area (segmented) (C)	OARSI JSN grade (C)	Paired t-tests	Low (43)
Felson 2001 [133]	401	Prevalent knee OA (ACR criteria) and assumed ROA knee of 100%. 41% female, and mean age of 67 yrs. BOKS	Semi-quantitative MRI BMLs (C)	KL grade chronic knee pain presence (C)	Chi-square or fisher exact test & logistic regression	Low (54)
Fernandez-Madrid 1994 [559]	90	ACR knee OA, 66% knee ROA, 65% female, mean age 55 yrs. USA	Crude presence of MRI BMLs, osteophytes (C)	KL grade and crude pain presence (C)	Chi-square	Low (46)
Frobell 2010 [560]	891	Three groups; pre-radiographic OA (KL grade <2), ROA and controls without OA, (total ROA knee 89%), 60% female, mean age 61 yrs. OAI	MRI Bone area – manual segmentation (C)	KL grade, OARSI JSN grade (C)	T tests and multivariate analyses	Low (57)
Gudbergsen [562] 2013	192	Obesity and knee OA (ACR criteria). 81% female, mean age 63 yrs. Denmark	Semi-quantitative MRI BML (BLOKS) (C)	KL grade (C)	Spearman correlation analyses	Low (57)
Guymer 2007 [535]	176	No clinical knee OA (ACR clinical criteria) and no current or historic knee pathology,	Presence or absence of MRI BMLs (C) TFJ	Presence or absence of semi-quantitative cartilage defects (C) TFJ	Logistic regression	High (71)

Author of studies	Patient number (n)	Study demographics	Subchondral bone feature assessed (method) region	Structural progression / pain outcome (method) region	Statistical analysis	Quality (score%)
		mean age 52 yrs, 100% female, mean BMI 27. Melbourne.				
Haverkamp 2011 [276]	609	1201 knees with 6% knee ROA and 25% knee pain prevalence, 100% female, and mean age 54 yrs, mean BMI 27. Rotterdam study	2D bone shape knee 1. femur & tibial width 2. elevation of lateral tibial plateau (C)	1.Presence of diffuse cartilage defects semi-quantitative scoring (MRI). 2.Presence of ROA knee (KL≥2) 3.Pain severity VAS (C)	Logistic and linear generalised estimating equation regression models	Low (46)
Hayashi 2012 [566]	40	ROA knee 57% with and without pain, 75% female, mean age 57 yrs. USA	Crude presence of MRI osteophytes, bone cysts (C)	Presence of pain on WOMAC pain subscale (C)	Logistic regression	Low (57)
Hayes 2005 [312]	232	Clinical and ROA knee or healthy patients. 36% ROA knee, 100% female, mean age 46 yrs. Southeast Michigan Cohort.	Semi-quantitative MRI BML, osteophyte, bone cyst (C)	KL grade and chronic pain presence (C)	Fisher Exact Test, Chi-squared test	High (61)
Hernandez-Molina 2008 [139]	1627	Patients >50 yrs of age with and without knee pain. ROA knee 22%, 59% female, mean age 64 yrs. Framingham OA cohort	Semi-quantitative MRI bone attrition (WORMS) (C)	Pain severity and nocturnal pain (WOMAC) (C)	Logistic regression	High (71)
Ip 2011 [567]	255	Knee pain. ROA 38%, 56% female, median age 62 yrs. Canada	Semi-quantitative MRI BML (C)	WOMAC pain, KL grade (C)	Logistic regression & Pearson chi-squared	High (68)
Jones 2004 [31]	372	Mean age 45yrs, right knees, early ROA knee (3-14%), 58% female,	Tibial bone area (MRI) (C)	Radiographic JSN (C)	Linear Regression	Low (50)

Author of studies	Patient number (n)	Study demographics	Subchondral bone feature assessed (method) region	Structural progression / pain outcome (method) region	Statistical analysis	Quality (score%)
		mean BMI 27. Offspring				
Kalichman 2007 [568]	213	Predominantly knee OA (ACR criteria). ROA knee 75%, 41% female, mean age 67 yrs. BOKS	MRI patellar length ratio, trochlea sulcus angle (C)	JSN grade (C)	Logistic regression	High (64)
Kalichman 2007 [569]	213	Predominantly knee OA (ACR criteria). ROA knee 75%, 41% female, mean age 67 yrs. BOKS	MRI patellar length ratio, trochlea sulcus angle (C)	Cartilage defect (WORMS) (C)	Logistic regression	Low (57)
Kim 2013 [570]	358	Aging population with 35% ROA knee. 51% female, mean age 72 yrs. Hallym Aging Study	Summary score and severity of MRI BML (WORMS) (C)	WOMAC pain (C) or presence of knee pain	Logistic regression	High (64)
Kornaat 2006 [571]	205	Symptomatic (35%)and ROA (47%) knee. 80% female, median age 60 yrs. GARP	Semi-quantitative MRI osteophyte bone cyst & BML (C)	Chronic pain presence (C)	Logistic regression	High (71)
Kornaat 2005 [572]	205	Symptomatic (35%)and ROA (47%) knee. 80% female, median age 60 yrs. GARP	Semi-quantitative MRI BML (KOSS) TFJ and PFJ (C)	Semi-quantitative cartilage defects (KOSS) TFJ and PFJ (C)	Odds ratio	Low (57)
Kraus 2009 [550]	159	Unilateral symptomatic and ROA knee (100%);74% female, mean age 63 yrs, mean BMI 32. POP	Ipsicompartmental late phase bone scintigraphy, semi-quantitative retention scoring of TFJ (C)	Ipsicompartmental OARSI scale of TFJ JSN (C)	Bivariate and Multivariable generalised linear modelling	High (71)
Lindsey 2004 [350]	74	Prevalent knee ROA (71%), 53% female, mean age 64 yrs,	MRI bone volume fraction & trabecular spacing (lateral TFJ) (C)	Cartilage volume in (contralateral TFJ) compartment (C)	Spearmans correlation	High (64)
Link 2003 [319]	50	Symptomatic knee OA, ROA 80%, 60% female,	Semi-quantitative MRI BML,	KL grade, WOMAC pain (C)	Fisher Exact Test,	Low (54)

Author of studies	Patient number (n)	Study demographics	Subchondral bone feature assessed (method) region	Structural progression / pain outcome (method) region	Statistical analysis	Quality (score%)
		mean age 64 yrs. USA	osteophytes, and crude presence of bone cysts (C)		Chi-squared test	
Lo 2005 [574]	498	Patients >50 yrs of age with and without knee pain. ROA knee 23%, 59% female, mean age 66 yrs. Framingham OA cohort	Semi-quantitative MRI BML (WORMS≥1) (C)	KL grade≥2 (C)	Crude comparison	Low (50)
Lo 2006 [208]	1612	Prevalent Knee OA, 18% ROA knee, 56% female, mean age 64 yrs. Framingham OA Study Cohort	DXA Medial:lateral BMD ratio at the tibial plateau (C)	Radiographic JSN grade (medial and lateral TFJ) (C)	Logistic regression	High (71)
Lo 2009 [575]	160	Symptomatic OA knee, 100% ROA. 50% female, mean age 61 yrs. OAI	Semi-quantitative MRI BML (BLOKS) (C)	WOMAC pain (C)	Univariate and multivariate cox regressions	High (71)
Lo 2012 [206]	482	Prevalent knee OA, 54% ROA, 47% female, mean age 64 yrs. OAI	MRI bone volume fraction, trabecular thickness, number and DXA BMD of proximal medial tibia (C)	Radiographic medial JSN grade (C)	Kruskal-Wallis and Mann-Whitney U tests	High (64)
McCauley 2001 [528]	193	Knees referred for MRI 43% female, mean age 40 yrs, mean weight 92kg.	MRI central osteophyte presence (C) TFJ	MRI cartilage lesion presence (C) TFJ	Crude association	Low (29)
McCrae 1992 [553]	30	Clinical or ROA knee (100%). 73% female, mean age 66yrs, Overweight or obese (65%). Recruited from	Late phase 'extended bone uptake' pattern bone scintigraphy, presence around the TFJ (C)	Radiographic TFJ JSN presence (C)	Chi squared test	Low (50)

Author of studies	Patient number (n)	Study demographics	Subchondral bone feature assessed (method) region	Structural progression / pain outcome (method) region	Statistical analysis	Quality (score%)
		rheumatology clinic				
Meredith 2009 [555]	140	Knees with MRIs before arthroscopic partial meniscectomy. Median age 61 yrs, 61% female	Sum of semi-quantitative MRI Osteophyte and BML scores in the TFJ and PFJ (C)	Sum of semi-quantitative MRI cartilage defect scores in the TFJ and PFJ (C)	Chi-squared test & Spearman test for non-parametric correlations	Low (50)
Moisio 2009 [456]	305	Patients with some WOMAC dysfunction and 90% ROA knee. 78% female, mean age 66 yrs. MAK-2	Baseline MRI semi-quantitative BML score (C) TFJ and PFJ	Presence of baseline moderate to severe knee pain (C)	Logistic regression	High (64)
Ochiai 2010 [543]	48	Patients with clinical medial knee OA and ROA knee (76%), mean age 73 yrs. Gender distribution unknown. Japan	MRI irregularity of femoral condyle contour (C)	Knee pain VAS (C)	Pearson's correlation	Low (50)
Okazaki 2014 [539]	29	Radiographic knee OA (100%), 100% female, Mean age 65 yrs	Number of CT bone cysts (medial femur and tibia) (C)	Knee KL grade (C)	NR	Low (50)
Ratzlaff 2013 [577]	115	Radiographic knee OA (95%), 48% female, age range 45-79 yrs	Total BML volume in the femur or tibia (C)	Weight bearing knee pain WOMAC subscale (C)	Wilcoxon rank sum test, multivariable analysis,	High (71)
Ratzlaff 2014 [544] abstract	115	Knee ROA (90%)	Median BML volume (PFJ, TFJ) (C)	Stair-climbing knee pain WOMAC (C)	Wilcoxon rank sum test	High (64)
Reichenbach 2008[306]	964	Patients over 50 yrs of age with and without knee pain. ROA knee 18%, 57% female,	Semi-quantitative MRI Bone attrition (WORMS) (C)	KL grade and semi-quantitative cartilage defects (WORMS) (C)	Crude comparison	Low (43)

Author of studies	Patient number (n)	Study demographics	Subchondral bone feature assessed (method) region	Structural progression / pain outcome (method) region	Statistical analysis	Quality (score%)
		mean age 63 yrs. Framingham OA cohort				
Roemer 2012[578]	1248	Patients over 50 yrs of age with and without knee pain. ROA knee 23%, 58% female, mean age 64 yrs. Framingham OA cohort	MRI osteophyte (WORMS) (C)	Cartilage defect (WORMS) (C)	Logistic regression and generalised estimating equations	Low (57)
Scher 2008 [579]	73	Patients with OA knee based upon radiography (>50% ROA), 54% female, mean age 51 yrs. USA	Semi-quantitative MRI BML (C)	Semi-quantitative cartilage defect (modified Noyes) (C)	Univariate comparison (t-tests)	Low (43)
Sengupta 2006 [580]	217	Patients with prevalent knee OA (ACR criteria). ROA knee >75%, 25% female, mean age 67 yrs. BOKS	Semi-quantitative MRI Osteophyte (WORMS) (C)	Pain severity WOMAC, chronic pain (C)	Logistic regression	High (71)
Sharma 2014 [131]	837	At risk of Knee OA but without ROA knee, 0% ROA knee, 57% female, mean age 60 yrs. OAI	Semi-quantitative MRI BML (WORMS) TFJ or PFJ (C)	Prevalent frequent knee symptoms (C)	Multiple logistic regression	High (71)
Sowers 2003 [531]	231	Patients with infrequent OA knee symptoms and 15% ROA knee, 100% female, mean age 47 yrs. SWAN	Semi-quantitative MRI BML (C)	Semi-quantitative cartilage defect, chronic pain presence (C)	Wilcoxon or Maentel–Haenszel test of general association and logistic regression	Low (54)
Stefanik 2012 [274]	881	Patients with knee OA or at high risk of it. (ROA knee % unknown), 63% female,	MRI lateral trochlear inclination and trochlear angle (C)	Semi-quantitative cartilage defect (WORMS) (C)	Logistic regression	Low (57)

Author of studies	Patient number (n)	Study demographics	Subchondral bone feature assessed (method) region	Structural progression / pain outcome (method) region	Statistical analysis	Quality (score%)
		mean age 63 yrs. MOST				
Stefanik 2014 abstract [581]	2087	Prevalent clinical knee OA, 60% female, mean age 67 yrs	BML (WORMS) PFJ (C)	Prevalent knee pain (any pain in last 30 days) and pain VAS (C)	Logistic regression	High (71)
Stehling 2010 [313]	236	Knees without pain and with 6% ROA. Mean age 51yrs, 58% female, mean BMI 24. OAI	Presence of any MRI semi-quantitative BMLs, osteophytes or cysts (C)	Presence of any WORMS MRI cartilage defects (C)	Multi-variate regression	High (71)
Torres 2006 [135]	143	Patients with some WOMAC dysfunction and >55% ROA knee, 78% female, mean age 70 yrs. MAK-2	MRI BML, osteophyte, attrition, bone cyst (WORMS) TFJ & PFJ (C)	Pain VAS, semi-quantitative cartilage (WORMS) TFJ & PFJ (C)	Median quantile regression,	High (68)
Wang 2005 [259]	117	Symptomatic, clinical (ACR) knee OA with mild to moderate TFJ ROA, mean age 64yrs, mean BMI 29, males and females. Australia	Annual % change in tibial bone area (L) 2 yr follow up.	Baseline JSN (C)	Linear regression	Low (57)
Zhai 2006 [582]	500	Randomly selected older adults with over 23% knee ROA. 50% female, mean age 63 yrs. TASOAC	Semi-quantitative MRI BML (C)	WOMAC pain>1 (C)	Multivariable analysis	High (79)
Hip cohort studies						
Agricola 2013 [74]	723	Early symptomatic hip OA, the majority had no ROA hip (with doubtful ROA in 26%), 80% female, mean age 56 yrs, mean BMI 26.1, CHECK	Baseline alpha angle (2D femur shape) dichotomous abnormal >60°, normal ≤60 (C)	Incident ROA hip (KL>1) Incident end-stage ROA hip (KL>2 or THR) at or within 5 yrs (L)	Generalised estimating equations	High (67)

Author of studies	Patient number (n)	Study demographics	Subchondral bone feature assessed (method) region	Structural progression / pain outcome (method) region	Statistical analysis	Quality (score%)
Agricola 2013 [394]	720	Early symptomatic hip OA, the majority had no ROA hip (with doubtful ROA in 24%), 79% female, mean age 56yrs, mean BMI 26.1. CHECK	Baseline 2D Centre edge angle (Acetabular shape): 25°<Normal<40° Undercoverage<25° Overcoverage>40° (C)	Incident ROA hip (KL>1 or THR) at or within 5 yrs (L)	Generalised estimating equations	High (67)
Agricola 2013 [583]	723	Early symptomatic hip OA, the majority had no ROA hip (with doubtful ROA in 24%), 79% women, mean age 56yrs, mean BMI 26.1. CHECK	Baseline 2D femoral and acetabular shape modes (segmented by statistical shape modelling) (C)	Total hip replacement at or within 5 yrs (L)	Generalised estimating equations	High (72)
Hip case-control studies						
Doherty 2008 [282]	2076	Symptomatic radiographic hip OA cases (n=965), asymptomatic controls without radiographic hip OA (n=1111) – GOAL	Non-spherical 2D femoral head shape assessment: 1) Appearance of 'Pistol grip deformity' (C) 2) Maximum femoral head diameter divided by minimum parallel femoral neck diameter (C)	Presence of radiographic hip OA (JSW≤2.5mm) (C)	Multivariable Logistic regression	Low (53)
Barr 2012 [603]	141	First presentation of hip pain to primary care, 32% ACR hip OA criteria, 68% female, mean age 63 yrs, mean BMI 27.	2D Shape measures of centre edge angle (acetabular shape) (C)	THR vs no radiographic progression over 5 years (L)	Logistic regression	High (76)
Nicholls 2011	268	100% women, mean age, 55yrs, mean BMI	2D CAM deformity; mean modified	Total hip replacement (L)	Logistic regression	High (71)

Author of studies	Patient number (n)	Study demographics	Subchondral bone feature assessed (method) region	Structural progression / pain outcome (method) region	Statistical analysis	Quality (score%)
[538]		66. 243 controls, 25 cases of total hip replacement. Chingford Study	triangular index height, alpha angle. Acetabular dysplasia; mean lateral center edge angle (C)			
Hip cross-sectional studies						
Chaganti 2010 [532]	3529	10% ROA hip, 100% male, Mean age 78 years. Cohort of the Study of Osteoporotic Fractures in Men	Femoral neck BMD (C) DXA	Hip ROA Modified croft score (categorical 0-4) (C)	Linear regression	High (64)
Chiba 2011 [215]	47	ROA, 100% female, mean age 69 yrs	Acetabular and femoral head subchondral trabecular morphometry: bone volume fraction, trabecular thickness, number, separation (CT)	Hip joint space volume (CT) (C)	Pearson's correlation test.	Low (57)
Dawson 2013 Abstract [556]	161	142 asymptomatic hips without clinical OA, 19 with hip OA. 56% female, mean age 63yrs, mean BMI 27,	Femoral head BMLs (MRI) (C)	1. Presence of hip OA 2.Femoral head cartilage volume (MRI) (C)	Regression modelling	Low (14)
Gosvig 2010 [561]	3620	Mean age 61yrs, 63% female, ROA hip 10.6% (OA substudy - CCHS III)	2D Categorical Hip deformity: 1) Normal 2)'Pistol grip' 3) Deep acetabular socket (C)	Presence of radiographic hip OA (JSW≤2mm) (C)	Multivariate logistic regression	Low (50)
Maksymowych 2014	40	55% female, mean age	Semi-quantitative	Baseline WOMAC	Univariable	High (64)

Author of studies	Patient number (n)	Study demographics	Subchondral bone feature assessed (method) region	Structural progression / pain outcome (method) region	Statistical analysis	Quality (score%)
[576]		65yrs, symptomatic but not radiographic hip OA	BML HIP (HOAMS) (C)	pain (C)	regression model	
Neumann 2007 [542]	100	Symptomatic hip OA	Semi-quantitative BMLs (C)	Semi-quantitative Cartilage lesions (C)	Spearman's correlations	Low (43)
Reichenbach 2011 [529]	244	Asymptomatic men (100%). Mean age 20 yrs, mean BMI 23, Sumiswald cohort	The presence or absence of any semi-quantitative MRI-defined CAM-deformity (C)	Combined femoral and acetabular cartilage thickness (C)	Multivariable linear regression. & Wald test	High (64)
Antoniades 2000 [534]	1148	White female twins, 29% hip RO A, 100% female, median age 53 yrs. St. Thomas' UK Adult Twin Register (C)	DXA BMD of the femoral neck of left (nondominant) hip with ROA (C)	Radiographic OA (croft Score) (C)	Logistic regression	High (64)
Kumar 2013 [573]	85	Members of the public with 35% ROA hip, 48% female , mean age 56 yrs (C)	Total hip semi-quantitative BML and subchondral cysts score (C)	Self-reported hip pain HOOS score	Non-parametric Spearman's correlations	High (71)
Hand case-series studies						
Haugen 2014 [39]	74	91% female, Mean age 68 yrs	BMLs – semi-quantitative At 2nd to 5th IPJs (C)	Progression of hand ROA (JSN, KL grade or new erosion) (L)	Generalised estimating equations	High (61)
Haugen 2014 Abstract [593]	70	90% female, mean age 68 yrs	Sum scores (0-48) for BMLs (Oslo Hand OA MRI score) (C) IPJS	AUSCAN pain scale (L)	Linear regression	High (61)
Hand cross-sectional studies						
Haugen 2012 Abstract [564]	108	91% women, mean age 69 years, 100% ROA hand Oslo hand osteoarthritis cohort	BML (Oslo MRI hand score) (C) IPJs	Radiographic JSN grade (OARSI atlas) (C) IPJs	logistic regression with generalised estimating equations	Low (43)
Haugen	106	92% women, mean age	BML, cyst, attrition,	Hand KL grade of	Generalised	High (64)

Author of studies	Patient number (n)	Study demographics	Subchondral bone feature assessed (method) region	Structural progression / pain outcome (method) region	Statistical analysis	Quality (score%)
2012 [565]		69 years, 100% ROA Oslo hand osteoarthritis cohort	osteophyte (Oslo MRI hand score) (C) IPJs	IPJs (C)	estimating equations	
Haugen 2012 [563]	85	91% female, mean age 69 years, 100% ROA hand. Oslo hand osteoarthritis cohort	BML, cyst, attrition, osteophyte (Oslo MRI hand score) (C) IPJs sum scores	AUSCAN pain scale (C)	Linear regression	High (64)
Macfarlane 1993 [552]	35	100% ROA Hand, 91% female, mean age 62yrs. Rheumatology clinic attenders	Late phase isotope bone scan small joints of the hand (C)	Hand Pain VAS (C)	Kendall's correlation	Low (57)
Ankle cross-sectional studies						
Knupp 2009 [526]	27	Symptomatic ankle varus or valgus deformities refractory to conservative therapy, 37% female, mean age 49 yrs.	Late phase bone scintigraphy, semi-quantitative retention scoring of tibiotalar joint (C)	Tibiotalar ankle joint JSN. (Modified Takakura score) (C)	Mann-Whitney Rank sum test	Low (57)
Kraus 2013 [551]	138	Symptomatic ankle OA (23%), ROA ankle (79%), 74% female, mean age 64yrs, mean BMI 31. POP	Ipsilateral late phase bone scintigraphy, retention presence in tibiotalar joint (C)	Tibiotalar ROA KL grade and JSN (C)	Generalized estimating equations	High (71)

Australian/Canadian Osteoarthritis Hand Index (AUSCAN); Bone mineral density (BMD); Bone marrow lesion (BML); Boston Osteoarthritis of the Knee Study (BOKS), Boston–Leeds. Osteoarthritis Knee Score (BLOKS); a feature or outcome described in cross-section (C); Copenhagen City Heart Study (CCHS); Cohort hip and cohort knee (CHECK); knee pain on most days for at least the last month (chronic pain); Dual-energy X-ray absorptiometry (DXA); Genetics, Osteoarthritis and Progression study (GARP); GOAL (Genetics of Osteoarthritis and Lifestyle); Hip Osteoarthritis MRI scoring system (HOAMS); Hip dysfunction and Osteoarthritis Outcome Score (HOOS); interphalangeal joint (IPJ); joint space narrowing (JSN); joint space width (JSW); Kellgren Lawrence (KL); Knee Osteoarthritis Scoring System (KOSS); a feature or outcome described longitudinally (L); mechanical factors in arthritis of the knee 2 (MAK-2); patellofemoral joint (PFJ); quantitative

computed tomography (qCT); radiographic osteoarthritis (ROA); Michigan study of Women's Health across the Nation (SWAN); Multicentre Osteoarthritis Study (most); osteoarthritis (OA); Osteoarthritis Initiative (OAI); Osteoarthritis Research Society International (OARSI); Strategies to Predict Osteoarthritis Progression (POP); Tasmanian Older Adult Cohort (TASOAC); tibiofemoral joint (TFJ); Total hip replacement (THR); visual analogue scale (VAS); Western Ontario and McMaster Universities arthritis index (WOMAC); whole-organ magnetic resonance imaging score (WORMS).

3.4.4 Relationship between knee bone feature and structural progression

The association of knee bone features with knee structural progression and joint replacement are described in Table 17, and Table 21.

3.4.4.1 Knee bone marrow lesions:

(31 cohort, 15 cross-sectional, four case-control) MRI

In prospective cohorts with high quality, well-adjusted analyses the presence and increasing size of baseline BMLs and incidence of BMLs conferred greater odds of structural progression [100, 124, 294, 301, 587]. Similarly increasing baseline BML size increased the risk of total knee replacement (TKR) and expedited the outcome of TKR[103, 457, 540, 590]. The association of BMLs with structural progression was maintained in cohorts without clinical features of knee OA[301] and in analyses with poorer quality or statistical adjustment [123, 443, 478, 500, 527, 530, 579, 585, 586, 590-592, 594, 598-601]. Only five low quality cohort analyses did not support these findings[417, 444, 596, 597, 602].

All cross-sectional analyses found positive correlations between BMLs and structural severity[133, 135, 312, 313, 319, 531, 535, 554, 555, 559, 562, 567, 572, 574, 579]. Three case-control analyses found similar associations[525, 608, 609].

Summary: BMLs are independently associated with knee structural progression, and incident TKR.

3.4.4.2 Knee osteophytes:

(Three cohort, eight cross-sectional) MRI

In one prospective cohort with high quality and well-adjusted analysis, the increasing size of osteophytes conferred greater odds of structural

progression[589]. In lower quality inadequately adjusted, prospective cohorts, increasing osteophyte size increased the risk of incident TKR and structural progression[530, 541]. The increasing size and presence of osteophytes was associated with greater structural progression or severity in all included analyses[135, 312, 313, 319, 528, 530, 541, 555, 559, 560, 578, 589].

Summary: Osteophytes are independently associated with knee structural progression and associated with TKR incidence.

3.4.4.3 Knee bone attrition:

(One cohort, two cross-sectional, one case-control) MRI

One prospective, well-adjusted, but below average quality cohort analysis found an association with baseline attrition severity and structural progression that became insignificant after covariate adjustment[478]. The unadjusted cross-sectional analyses and case-control analysis found similar associations with structural severity [135, 306, 307].

Summary: Bone attrition is associated but not independently associated with structural progression.

3.4.4.4 Knee bone shape / dimension:

(Eight cohort, seven cross-sectional, four case-control) MRI

In prospective cohorts with high quality well-adjusted analyses, greater baseline tibial plateau bone area conferred greater odds of structural progression of OA and incidence of TKR [96, 261, 270, 588]. The same association was observed in a lower quality, prospective cohort, well-adjusted analysis[584] and in a study of the knee in patients who predominantly had no radiographic evidence of knee OA[261]. The mismatch ratio of the femoral and tibial articulating areas was not associated with structural progression after adjustment[102], but the trochlear sulcus angle and shape was associated with cross-sectional patellofemoral

structural severity demonstrated on MRI[274, 569]. All cross-sectional [31, 259, 483, 560] and case control [75, 269, 604, 605] analyses of tibial bone area or 3D knee bone shape found association with structural severity [31, 75, 259, 269, 483, 560, 604, 605].

Summary: Tibial bone area is independently associated with knee OA structural progression and incidence of TKR.

3.4.4.5 Knee bone cyst:

(Four cohort, five cross-sectional) MRI & CT

Two prospective cohorts with well-adjusted but below average quality analyses of cysts reported no association with structural progression before or after adjustment[417, 478]. Two prospective cohorts with low quality unadjusted analyses of cysts found an association with structural progression[585, 601]. Cross-sectional well-adjusted [313] and unadjusted [312, 315, 319, 539] cyst analyses found an association with structural severity.

Summary: There is no independent association of cysts with structural progression after covariate adjustment.

3.4.4.6 Knee trabecular bone morphometry:

(One cohort, five cross-sectional) MRI

One prospective cohort, unadjusted, below average quality analysis reported increasing bone volume fraction, trabecular number and thickness and decreasing trabecular spacing were associated with structural progression[548]. The same bone changes were associated with structural severity in cross-sectional unadjusted analyses[206, 349, 350, 545, 546].

Summary: Increasing bone volume fraction, trabecular number, trabecular thickness, and decreasing trabecular spacing are associated with knee structural progression and severity.

3.4.4.7 Knee peri-articular bone mineral density:

(Three cohort, four cross-sectional one case control) DXA and CT

Two prospective cohorts with well-adjusted but below average quality analyses reported increasing tibial subchondral bone mineral density was associated with structural progression[209, 210]. In one prospective cohort with an unadjusted below average quality analysis, the medial to lateral ratio of tibial peri-articular bone mineral density (BMD) was associated with structural progression[548]. All of the cross-sectional analyses[206, 208, 533, 547], including two well-adjusted analyses[208, 547], reported increasing BMD with greater structural severity. One well-adjusted analysis using quantitative CT (qCT) reported higher and lower BMD in the anterior and posterior tibial plateau respectively, of knees with moderate OA relative to asymptomatic controls.

Summary: Increasing peri-articular radiographic BMD is associated with structural progression and severity.

3.4.4.8 Knee scintigraphy:

(Three cohort, two cross-sectional)

Prospective cohorts with high quality analyses found greater late-phase bone signal was associated with structural progression, with no or inadequate covariate adjustment[536, 537], but not after adequate covariate adjustment[536]. A prospective cohort, with below average quality, unadjusted analysis found greater bone signal was associated with structural progression[216]. Bone signal was associated with structural severity in well-adjusted and unadjusted cross-sectional analyses[550, 553].

Summary: Bone scintigraphy signal is associated, but not independently associated, with structural progression.

3.4.4.9 2D knee bone shape

One cross-sectional, well-adjusted analysis identified an association of enlarging femoral and tibial bone width and elevating tibial plateau with greater structural severity[276].

Summary: 2D bone shape is associated with structural severity

3.4.5 Relationship between knee bone features and pain

The association of knee bone features with knee pain are described in Table 18 and Table 21. In all types of study, bone features were compared with the presence, chronicity and severity of pain. In longitudinal studies, features were also compared with change in the presence or severity of pain (e.g. change in WOMAC pain score). Change in the presence of pain included developing new frequent pain, [545], or the resolution of existing pain.

3.4.5.1 Knee bone marrow lesions:

(Nine cohort, 18 cross-sectional, five case-control) MRI

In three prospective cohort, well-adjusted, high quality analyses the baseline or longitudinal increase in size of BMLs was associated with longitudinally increasing knee WOMAC pain severity[99-101]. This association was maintained in one[530] but not two[600, 602] similar prospective cohort, unadjusted, lower quality analyses. Baseline BML size in the lateral but not the medial tibiofemoral joint was associated with incident frequent knee pain in a prospective cohort, well-adjusted, high quality analysis[456]. Longitudinally increasing BML size was associated with incident frequent knee pain in a similar but inadequately adjusted analysis of below average quality[26]. In cross-sectional studies the size or presence of BMLs were inconsistently associated with the presence of a heterogenous range of pain measures, irrespective of adequate covariate adjustment[131, 133, 135, 312, 319, 456, 531, 544, 557-559, 567, 570, 571, 575, 577, 581, 582].

Summary: BMLs are independently associated with longitudinally increasing pain severity and are associated with incident frequent knee pain.

3.4.5.2 Knee osteophytes:

(One cohort, eight cross-sectional, one case-control) MRI

One prospective cohort, unadjusted, below average quality analysis reported increasing baseline osteophyte size was associated with increasing WOMAC pain severity[530]. In well-adjusted cross-sectional analyses, osteophyte size was associated with the presence[571] but not severity of pain[580]. In unadjusted cross-sectional analyses osteophytes were inconsistently associated with a heterogenous range of pain measures[135, 312, 319, 557, 559, 566].

Summary: Osteophytes are associated with longitudinally increasing pain severity and the cross-sectional presence of pain.

3.4.5.3 Knee bone attrition:

(Zero cohort, two cross-sectional, one case-control) MRI

Cross-sectional analyses found greater attrition was associated with greater pain severity, without covariate adjustment[135, 139], but not after adequate covariate adjustment[139]. An unadjusted case-control analysis found an association of attrition and prevalent pain[606].

Summary: Bone attrition is associated but not independently associated with pain severity.

3.4.5.4 Knee bone shape / dimension:

(One cohort, one cross-sectional) MRI

One prospective, well-adjusted, high quality analysis found the femoro-tibial articulating surface mismatch was associated with incident frequent knee

pain[102]. One unadjusted cross-sectional analysis found the irregularity of the femoral condyle surface was associated with knee pain severity[543].

Summary: Specific features of bone shape are independently associated with incident frequent knee pain and also severity.

3.4.5.5 Knee bone cyst:

(One cohort, five cross-sectional, two case-control) MRI

One prospective cohort, unadjusted, low quality analysis found no association between bone cyst size and increasing WOMAC pain[530]. In mostly unadjusted cross-sectional[135, 312, 319, 566, 571] and case control analyses[606, 607] of heterogenous cyst measures and pain measures, an association between cysts and pain was inconsistently found.

Summary: Bone cysts may not be associated with longitudinal pain severity and a cross-sectional association with pain is uncertain.

3.4.5.6 2D knee bone shape:

One inadequately adjusted cross-sectional analysis found an association between the elevation of the lateral tibial plateau and pain severity[276].

Summary: 2D lateral tibial bone shape is associated with cross-sectional pain severity.

3.4.6 Relationship between hand bone feature and structural progression

The association of hand bone features with hand structural progression are described in Table 19 and Table 21.

3.4.6.1 Hand bone marrow lesions:

(One case series, two cross-sectional) MRI

One well-adjusted, high quality analysis of a prospective OA case series, found that increasing BML number and size in the interphalangeal joints at baseline conferred greater odds of structural progression[39]. Two adjusted cross-sectional analyses found increasing BML number and size scores were associated with increasing structural severity[564, 565].

Summary: BMLs are independently associated with hand structural progression.

3.4.6.2 Hand osteophytes bone attrition and cysts:

One cross-sectional, adjusted analysis found greater MRI attrition or MRI osteophyte number and size was associated with greater structural severity[565]. However greater MRI cyst presence was not associated with greater structural severity[565].

Summary: Osteophytes and attrition, but not cysts, are associated with hand structural severity.

3.4.7 Relationship between hand bone feature and pain

The association of hand bone features with hand pain are described in Table 20and Table 21.

3.4.7.1 Hand bone marrow lesions:

(One case series, one cross-sectional) MRI

One well-adjusted, high quality analysis of a prospective OA case series, found that BML number and size at baseline was not associated with longitudinal change in hand pain[593]. One adjusted cross-sectional analysis found no association of BMLs with pain severity[563].

Summary: BMLs are not independently associated with longitudinal or cross-sectional pain severity.

3.4.7.2 Hand osteophytes, bone attrition and cysts:

One cross-sectional, adjusted analysis found no association between the features, MRI osteophytes, attrition or cysts, and pain severity[563].

Summary: Osteophytes, attrition and cysts are not associated with hand pain severity.

3.4.7.3 Hand scintigraphy

(One cross-sectional):

One cross-sectional unadjusted analysis found no significant association between bone signal of the hands and pain severity.

Summary: Bone scintigraphy signal is not associated with hand pain severity

3.4.8 Relationship between hip bone feature and structural progression

The association of hip bone features with hip structural progression and joint replacement are described in Table 19 and Table 21.

3.4.8.1 Hip bone marrow lesions:

(Two cross-sectional) MRI

One well-adjusted [556] and one unadjusted [542] cross-sectional analysis both found that BMLs were associated with greater structural severity.

Summary: BMLs are associated with hip structural severity

3.4.8.2 Hip trabecular bone morphometry:

One unadjusted cross-sectional analysis found greater MRI bone volume fraction, trabecular thickening, trabecular number and lower trabecular spacing were associated with greater structural severity[215].

Summary: Bone volume fraction, trabecular thickening, number and spacing are associated with hip structural severity

3.4.8.3 Hip peri-articular bone mineral density:

(Two cross-sectional) DXA

One well-adjusted [532] and one adjusted[534]cross-sectional analysis found greater BMD was associated with greater structural severity.
Summary: BMD is associated with structural severity of the hip.

3.4.8.4 2D and 3D hip bone shape

(Three cohort, two cross-sectional, three case-control)

In two prospective cohort, well-adjusted, high quality analyses an increasing asphericity of the femoral head (measured as an elevated alpha angle, or in shape modes 11 and 15) was associated with total hip replacement (THR)[583] or with structural progression and THR[74] respectively. In one prospective cohort, well-adjusted, high quality analysis acetabular undercoverage of the femoral head (a low centre edge angle) was associated with structural progression or THR[394].In one well-adjusted cross-sectional analysis, 2D asphericity deformity of the femoral head (cam-type deformities) was associated with structural severity[561]. In one well-adjusted cross-sectional analysis of MRI-determined femoral head asphericity in asymptomatic young men, there was a significantly lower cartilage thickness between those with than those without any detectable asphericity. This became insignificant after covariate adjustment[529]. Case-control analyses identified the same associations as the cohort analyses[282, 538, 603].

Summary: Asphericity of the femoral head and acetabular undercoverage of the femoral head are independently associated with structural progression and THR.

3.4.9 Relationship between hip bone feature and pain

The association of hip bone features with hip pain are described in Table 20 and Table 21.

3.4.9.1 Hip bone marrow lesions:

(Two cross-sectional) MRI

Two cross-sectional, unadjusted analyses found that increasing semi-quantitative BML scores were associated with greater pain severity[573, 576]. Summary: BMLs are associated with hip pain severity.

3.4.9.2 Hip bone cyst:

One cross-sectional, unadjusted analysis found that increasing MRI semi-quantitative cyst scores were associated with greater pain severity[573].

Summary: Cysts are associated with hip pain severity.

3.4.10 Relationship between ankle bone features and structural progression

The association of ankle bone features with ankle structure are described in Table 19 and Table 21.

3.4.10.1 Ankle scintigraphy

(Two cross-sectional)

One well-adjusted[550] and one unadjusted[553] cross-sectional analysis found the presence or semi-quantitative scoring of late phase bone signal in the tibiotalar joint was associated with greater structural severity.

Summary: Bone scintigraphy signal is associated with ankle structural severity.

Table 17 Knee Structural associations by feature and quality grade

Author	Feature (method)	Structural progression outcome	Adjustment for confounders	Association (magnitude) crude	Association (magnitude) adjusted	Association	Quality (score %)
MRI bone marrow lesion – cohorts							
Felson 2003 [294]	Baseline presence of BML in medial or lateral TFJ (C)	OARSI JSN grade progression of TFJ (L)	Age, sex, and BMI	NR	OR 6.5 CI 95%(3.0, 14.0)	+	High (83)
Dore 2010[99]	Baseline semi-quantitative MRI BML size (C) TFJ	Incident TKR over 5 years (L)	Age, sex, BMI, knee baseline pain, leg strength, cartilage defects, tibial bone area, ROA	OR (95% CI) 2.04 (1.55 to 2.69) p<0.01	OR (95% CI) 2.10 (1.13 to 3.90) p=0.019	+	High (64)
Driban 2013 [100]	Knee baseline BML volume (C) BML volume 48 month change (L) (TFJ)	48 month change in OARSI JSN grade (L) (TFJ)	Age, sex, BMI	NR	Baseline BML Volume OR 1.27 (95% CI 1.11 to 1.46) BML volume regression OR 3.36 (95% CI 1.55 to 7.28)	+	High (61)
Davies-Tuck 2010 [301]	Incident BML (new BML after 2 years with no BMLs at baseline) MRI TFJ (L)	Progression in semi-quantitative MRI cartilage defects score after 2 years. TFJ (L)	Age, gender, BMI, baseline cartilage volume	OR (95% CI) Medial TFJ 1.86 (0.70 to 4.93) p=0.21 Lateral TFJ 3.0 (1.01 to 8.93) p=0.05	OR (95% CI) Medial TFJ 2.63 (0.93 to 7.44) p=0.07 Lateral TFJ 3.13 (1.01 to 9.68) p=0.05	+ Association in the lateral TFJ and a trend in the medial TFJ	High (61)
Hochberg 2014 [540]	Semi-quantitative MRI baseline femoral condyle BML size (C)	Incident TKR over 6 years (L)	Age, gender, BMI, race, marital status, depressive symptoms, quality of life, mechanical pain, KL grade,	Medial TFJ p<0.0001	Medial TFJ p=0.02	+	High (61)

Author	Feature (method)	Structural progression outcome	Adjustment for confounders	Association (magnitude) crude	Association (magnitude) adjusted	Association	Quality (score %)
			clinical effusion.				
Raynauld 2011 [457]	Baseline semi-quantitative BML score (C) TFJ	Incidence of TKR over 3 years (L)	Age, sex, BMI, JSW, WOMAC,	NR	OR (95%CI) BML medial plateau 1.81 (1.08 to 2.03) p=0.025	+	High (61)
Raynauld 2013 [103]	Baseline semi-quantitative BML WORMS score (C) medial TFJ	Incident TKR (L) 4 year follow up Time to TKR (L)	Age, BMI, gender WOMAC, CRP	NR	TKR incidence OR (95% CI) 2.107 (1.26 to 3.54) p=0.005 Time to TKR incidence Hazard ratio (95%CI) 2.13 (1.38 to 3.30) p= 0.001	+	High (61)
Crema 2014 [587]	MRI BML (semi-quantitative) (C) all regions	Cartilage loss (semi-quantitative) (L) (all regions)	Age, gender, BMI	NR	β=0.37-0.64 p<0.001	+	High (56)
Guermazi 2014 Abstract [124]	Baseline semi-quantitative BML score WORMS (C)	Cartilage thickness loss over 30 months (L)	Age, sex, body mass index, and anatomical alignment axis (degrees).	NR	Combined BML score in the medial and lateral TFJ compartment OR 1.9 95%CI (1.1-3.3)	+	High (56)
Scher 2008 [579]	Presence of any baseline semi-quantitative MRI BMLs (C)	Incident TKR (L) over 3 years	Age	NR	OR (95% CI) 8.95 (1.49 to 53.68) p=0.02	+	High (56)
Sowers 2011[530]	Semi-quantitative MRI BML, size in TFJ (C)	Progression in KL grade (11 year follow up) (L)	Nil	R (CI 95%) Medial tibia ~ 0.46 (0.35 to 0.55) Lateral tibia ~0.23 (0.13 to 0.33)	NR	+	Low (53)
Kothari	Semi-	Semi-	Age, sex, BMI,	OR 4.04	OR 3.75	+	Low (50)

Author	Feature (method)	Structural progression outcome	Adjustment for confounders	Association (magnitude) crude	Association (magnitude) adjusted	Association	Quality (score %)
2010[478]	quantitative baseline MRI BML, (WORMS) (C) TFJ	quantitative cartilage defect score change over 2 years (WORMS) (L) TFJ.	other bone lesions	CI 95% (2.25 to 7.26)	CI 95% (1.59 to 8.82)		
Raynauld 2008 [599]	Change in BML size (mm) at 24 months in medial TFJ (L)	Medial cartilage volume (L) at 24 months in medial TFJ	Age, gender, BMI, meniscal extrusion and tear, pain and bone lesions at baseline,	NR	Change in BML size with femoral cartilage volume loss β=-0.31 standard error (0.08) p=0.0004	- Larger medial BML size means more cartilage loss in medial compartment	Low (50)
Roemer 2009 [443]	Change in MRI semi-quantitative BML size (WORMS) (L) TFJ and PFJ	Progression in semi-quantitative cartilage defects in (WORMS) over 30 months (L) TFJ and PFJ	Age, sex, BMI, baseline KL grade	NR	OR (95%CI) Incident BML OR 3.5 (2.1 to 5.9) Progression of BML 2.8 (1.5 to 3.2) Resolution of BML OR 0.9 (0.5 to 1.6) Stable BML OR 1.0 (reference)	+	Low (50)
Dore 2010 [590]	Baseline semi-quantitative BML severity (C) (medial and lateral TFJ)	Ipsi-compartmental annual Cartilage volume loss (L)	Age, sex, BMI, meniscal damage	NR	Baseline BML severity β= -22.1 to -42.0, for all regions (p <0.05)	- Bigger BML means bigger volume loss	Low (50)
Parsons 2014 Abstract [598]	Baseline Semi-quantitative BML score (C)	Annual TFJ JSN (L)	Age, sex, baseline KL grade	NR	β=-0.10 (95%CI) (-0.18 to -0.02)	+	Low (50)

Author	Feature (method)	Structural progression outcome	Adjustment for confounders	Association (magnitude) crude	Association (magnitude) adjusted	Association	Quality (score %)
Wildi 2010 [602]	24 month regional change in TFJ BML score WORMS (L)	24 month regional change in cartilage volume (L)	nil	R correlation coefficients all <0.07 p>0.367 for all three compartments at 24 months	NR	NC	Low (50)
Pelletier 2007[123]	Regional Semi-quantitative baseline BML score (medial or lateral TFJ) (C)	Regional Cartilage volume over 24 months (medial or lateral TFJ) (L)	NR	Lateral compartment BML score B=-0.31, p=0.001	NR	-	Low (50)
Driban 2011[591]	Baseline BML volume (C) and 24 month change in BML volume (L) in TFJ compartments	24 month change in full thickness cartilage lesion area (L)	Age, sex, body mass index	NR	Baseline BML volume r = 0.48 (95% CI) (0.20 to 0.69) p < 0.002	+ Baseline femur BML volume with loss in ipsicompartmental full thickness cartilage lesion area.	Low (50)
Tanamas 2010 [600]	Baseline semi-quantitative MRI BML size (C) TFJ	Cartilage volume change over 2 years (L) TFJ Incident TKR over 4 years	Age, sex, BMI, baseline tibial cartilage volume and bone area	R (CI 95%) Total cartilage loss 0.61 (-0.11 to 1.33) OR (CI 95%) Incident TKR 1.55 (1.04 to 2.29) p=0.03	R (CI 95%) Total cartilage loss 1.09 (0.24, 1.93) OR (CI 95%) Incident TKR 1.57 (1.04 to 2.35) p=0.03	+	Low (50)
Madan-Sharma 2008 [417]	Baseline MRI semi-quantitative BML (C) TFJ	OARSI medial TFJ JSN grade progression over 2 years (L) TFJ	Age, sex, BMI, family effect	NR	0.9 RR CI 95% (0.18 to 3.0)	NA	Low (47)

Author	Feature (method)	Structural progression outcome	Adjustment for confounders	Association (magnitude) crude	Association (magnitude) adjusted	Association	Quality (score %)
Tanamas 2010 [601]	Semi-quantitative change in MRI BML severity (C)	Incident TKR over 4 years (L)	Age, gender, KL grade	OR (CI 95%) Medial TFJ 1.72 (0.93 to 3.18) p=0.08 Lateral TFJ 0.95 (0.48 to 1.88) p=0.89	OR (CI 95%) Medial TFJ 1.99 (1.01 to 3.90) p=0.05 Lateral TFJ 0.96 (0.48 to 1.94) p=0.91	+ Association in the medial TFJ but not in the lateral TFJ	Low (47)
Roemer 2012 [500]	Semi-quantitative BML (WORMS) TFJ and PFJ (C)	Semi-quantitative cartilage score 6-month progression TFJ and PFJ (L)	Age, sex, treatment, and BMI.	NR	BML TFJ OR 4.74 95%CI (1.14 to 19.5) p=0.032 BML PFJ OR 1.63 (0.67 to 3.92)	+ BMLs and cartilage score correlate	Low (44)
Crema 2013 [586]	MRI Incident BML (WORMS) TFJ (L)	Progressive (30 month) semi-quantitative cartilage defect (WORMS) TFJ (L)	Age, sex, BMI, malalignment, meniscal disease	NR	OR (CI 95%) Medial TFJ 7.6 (5.1 to 11.3) Lateral TFJ 11.9 (6.2 to 23.0)	+	Low (44)
Hernandez-Molina 2008[594]	Crude presence of central BMLs on MRI (C) TFJ	Semi-quantitative Cartilage defect (WORMS) (L) TFJ	Alignment, BMI, KL grade, sex, and age.	NR	Medial TFJ Cartilage loss OR 6.1 CI 95% (1.0, 35.2)	+	Low (44)
Koster 2011 [527]	Baseline BML presence (C) TFJ	Any progression in KL grade over 1 year (L) TFJ	Age, BMI	OR (95% CI) 6.01 (1.92 to 18.8) p=0.002	OR (95% CI) 5.29 (1.64 to 17.1) p=0.005	+	Low (44)
Hunter 2006[596]	Change in MRI semi-quantitative	Change in semi-quantitative	Limb alignment	Ipsilateral cartilage loss β= 0.65	Ipsilateral cartilage loss β= 0.26 p=0.16	NA after adjustment	Low (44)

Author	Feature (method)	Structural progression outcome	Adjustment for confounders	Association (magnitude) crude	Association (magnitude) adjusted	Association	Quality (score %)
	BML score (L) TFJ	cartilage defect score (WORMS) (L) medial or lateral TFJ		p=0.003 Contralateral cartilage loss β= -0.27 p=0.22	Contralateral cartilage loss β= -0.16 p=0.52		
Roemer 2009 [444]	Baseline MRI BML crude presence or absence (WORMS) (L) TFJ	Semi-quantitative cartilage defect progression over 30 months (WORMS) (L) TFJ	Age, sex, race, BMI, alignment	OR (CI 95%) Slow cartilage loss OR 1.74 (0.85 to 3.55) Fast cartilage loss OR 1.32 (0.37 to 4.78)	OR (CI 95%) Slow cartilage loss OR 1.79 (0.83 to 3.87) Fast cartilage loss OR 1.0 (0.24 to 4.10)	NA	Low (44)
Kubota 2010 [597]	MRI BML semi-quantitative volume score change over 6 months (L) TFJ	KL grade progression over 6 months (L) TFJ	Nil	BML score higher in KL progression group p=0.044	NR	NC	Low (39)
Driban 2012 abstract [592]	MRI BML volume change (L) TFJ over 24 months	Change in cartilage thickness and denuded area of bone (L) TFJ over 24 months	Nil	Cartilage thickness r= -0.34, p=0.04 denuded bone r=0.42, p=0.01 Femoral cartilage indices p>0.05	NR	+	Low (28)
Carrino 2006[585]	Crude presence of MRI BML, TFJ (C) and (L)	Any grade of cartilage defect TFJ (C) & (L)	Nil	NR	NR	+	Low (22)
MRI bone marrow lesion - cross-sectional studies							
Baranyay	MRI BML	MRI semi-	Age, gender, BMI,	OR (95% CI)	OR (95% CI)	+	High (71%)

Author	Feature (method)	Structural progression outcome	Adjustment for confounders	Association (magnitude) crude	Association (magnitude) adjusted	Association	Quality (score %)
2007 [554]	defined as large or not large / absent in the medial and lateral compartments of TFJ (C)	quantitative cartilage defects of medial and lateral compartments of TFJ (C) Quantitative Cartilage volume medial and lateral TFJ (C)	cartilage volume or bone area	Cartilage defect Medial TFJ 1.81 (1.26 to 2.59) p=0.005 Lateral TFJ 1.52 (1.14 to 2.04) p=0.005 No association with ipsicompartmental cartilage volume	Cartilage defect Medial TFJ 1.80 (1.21 to 2.69) p=0.004 Lateral TFJ 1.45 (1.02 to 2.07) p=0.04 No association with ipsicompartmental cartilage volume	Cartilage defects NA Cartilage volume	
Guymer 2007 [535]	Presence or absence of MRI BMLs (C) TFJ	Presence or absence of semi-quantitative cartilage defects (C) TFJ	age, height, weight, and tibial cartilage volume	OR (95% CI) Medial TFJ 6.46 (1.04 to 38.39) p=0.04 Lateral TFJ 1.17 (0.22 to 6.26) p=0.85	OR (95% CI) Medial TFJ 3.51 (1.08 to 11.42) p=0.04 Lateral TFJ 1.02 (0.17 to 6.12) p=0.98	+ A positive association is observed in the medial but not the lateral TFJ	High (71)
Stehling 2010 [313]	Presence of any MRI semi-quantitative BMLs (C)	Presence of any WORMS MRI cartilage defects (C)	age, gender and BMI, KL score, knee injury or knee surgery, family history of TKR and Heberden's nodes	NR	p<0.0001	+	High (71)
Torres 2006[135]	MRI BML (WORMS) (C) TFJ and PFJ	Semi-quantitative cartilage (WORMS) (C)	Nil	R=0.56	NR	+	High (68)
Ip 2011 [567]	Semi-quantitative MRI BML (C)	KL grade (C)	Age, sex, BMI, OA stage, joint effusion, and meniscal damage	NR	Highest BML score p < 0.001	+	High (68)
Hayes	Semi-	KL grade (C)	Nil	p=0.005	NR	+	High (61)

Author	Feature (method)	Structural progression outcome	Adjustment for confounders	Association (magnitude) crude	Association (magnitude) adjusted	Association	Quality (score %)
2005[312]	quantitative MRI BML (C)						
Kornaat 2005 [572]	Semi-quantitative MRI BML (KOSS) TFJ and PFJ (C)	Semi-quantitative cartilage defects (KOSS) TFJ and PFJ (C)	Nil	OR (95% CI) PFJ 17 (3.8 to 72) TFJ 120 (6.5 to 2,221)	NR	+	Low (57)
Gudbergsen 2013 [562]	Semi-quantitative MRI BML (BLOKS) (C)	KL grade (C)	Nil	KL grade p=0.046 lateral p<0.001 medial	NR	+	Low (57)
Link 2003 [319]	Semi-quantitative MRI BML, (C)	KL grade (C)	Nil	p<0.05	NR	+	Low (54)
Sowers 2003 [531]	Semi-quantitative MRI BML (C)	Semi-quantitative cartilage defect (C)	Nil	p for trend p<0.0001	NR	+	Low (54)
Felson 2001 [133]	Semi-quantitative MRI BMLs (C)	KL grade (C)	Nil	NR	NR	+	Low (54)
Lo 2005[574]	Semi-quantitative MRI BML (WORMS≥1) (C)	KL grade≥2 (C)	Nil	NR	NR	+	Low (50)
Meredith 2009 [555]	Sum of semi-quantitative MRI BML scores in the TFJ and PFJ (C)	Sum of semi-quantitative MRI cartilage defect scores in the TFJ and PFJ (C)	Nil	p<0.0003	NR	+	Low (50)

Author	Feature (method)	Structural progression outcome	Adjustment for confounders	Association (magnitude) crude	Association (magnitude) adjusted	Association	Quality (score %)
Fernandez-Madrid 1994 [559]	Crude presence of MRI BMLs (C)	KL grade (C)	Nil	P<0.001	NR	+	Low (46)
Scher 2008[579]	Semi-quantitative MRI BML (C)	Semi-quantitative cartilage defect (modified Noyes) (C)	Nil	p=0.012	NR	+	Low (43)
MRI bone marrow lesion - case control studies							
Ratzlaff 2014 [608]	Total tibial BML volume 12 and 24 months before TKR and interval change between 12 and 24 (C) and (L) TFJ	Incident TKR (L)	NB matched cases and controls	OR (95%CI) 12 mnths (C) 1.68 (1.33 to 2.13) 24 mnths (C) 1.35 (1.02 to 1.78) 12 to 24 mnths change (L) 1.23 (1.03 to 1.46)	NR	+ True of TFJ but not PFJ	High (65)
Zhao 2010 [609]	Baseline crude presence of MRI BMLs at (C) TFJ	Overlying cartilage defect progression after one year (WORMS) (L) TFJ	Nil	Change in cartilage defect scores for areas with and without underlying BMLs p=0.00003	NR	+	Low (56)
Aitken 2013 Abstract [525]	Semi-quantitative BMLs tibia, femur & patella	Cartilage volume and defect score tibia and femur	Age, Sex, BMI	NR	Tibial cartilage volume β=-433mm^3 per unit increase in BML p<0.01	-	Low (47)
Stahl 2011[442]	Semi-quantitative MRI BML	Semi-quantitative cartilage	Nil	NR	p>0.165	NA	Low (47)

Author	Feature (method)	Structural progression outcome	Adjustment for confounders	Association (magnitude) crude	Association (magnitude) adjusted	Association	Quality (score %)
	size (WORMS) (L) TFJ	defect size (L) TFJ					
MRI osteophyte – cohort studies							
De-Lange 2014 abstract [589]	Semi-quantitative osteophyte (KOSS) (C)	Radiographic progression of JSN of TFJ(L)	age, gender, BMI and baseline JSN	NR	OR (95%CI) 1.8(1.1–3.1)	+ Higher OST score, the higher the JSN	High (61)
Liu 2014 Abstract [541]	Baseline Semi-quantitative osteophyte score (WORMS) (C) TFJ	Incident TKR at 6 months follow up (L)	Activity of daily living Disability score	NR	RR (95%CI) 3.01 (1.39 to 6.52)	+	Low (50)
Sowers 2011[530]	Semi-quantitative MRI osteophyte size in TFJ (C)	Progression in KL grade (11 year follow up) (L)	Nil	R (CI 95%) Medial tibia ~ 0.65 (0.59 to 0.71) Lateral tibia ~0.57 (0.49 to 0.63)	NR	+	Low (53)
MRI osteophyte – cross-sectional studies							
Stehling 2010 [313]	Presence of any MRI semi-quantitative osteophytes (C)	Presence of any WORMS MRI cartilage defects (C)	age, gender and BMI, KL score, knee injury or knee surgery, family history of TKR and Heberden's nodes	NR	p=0.0037	+	High (71)
Torres 2006[135]	MRI osteophyte, (WORMS) TFJ & PFJ (C)	Semi-quantitative cartilage (WORMS) TFJ & PFJ (C)	Nil	R=0.73	NR	+	High (68)
Hayes	Semi-	KL grade (C)	Nil	p<0.001	NR	+	High (61)

Author	Feature (method)	Structural progression outcome	Adjustment for confounders	Association (magnitude) crude	Association (magnitude) adjusted	Association	Quality (score %)
2005[312]	quantitative MRI osteophyte (C)						
Meredith 2009 [555]	Sum of semi-quantitative MRI Osteophyte scores in the TFJ and PFJ (C)	Sum of semi-quantitative MRI cartilage defect scores in the TFJ and PFJ (C)	Nil	p<0.0001	NR	+	Low (50)
McCauley 2001 [528]	MRI central osteophyte presence (C) TFJ	MRI cartilage lesion presence (C) TFJ	Nil	Crude association of 32 of 35 central osteophytes having adjacent cartilage lesions	NR	+ Crude, unadjusted	Low (29)
Roemer 2012[578]	MRI osteophyte (WORMS) (C)	Cartilage defect (WORMS) (C)	Age, sex, BMI, race, TFJ radiographic OA	OR 2378.1 CI 95% (249.8, 22,643.4)	OR 108.8 CI 95%(14.2, 834.9) p for trend<0.0001	+	Low (57)
Link 2003 [319]	Semi-quantitative MRI osteophytes (C)	KL grade (C)	Nil	p<0.01	NR	+	Low (54)
Fernandez-Madrid 1994 [559]	Crude presence of MRI osteophytes (C)	KL grade(C)	Nil	P<0.001	NR	+	Low (46)
MRI bone attrition – cohort studies							
Kothari 2010[478]	Semi-quantitative baseline MRI attrition	Semi-quantitative cartilage defect score	Age, sex BMI, other bone lesions	OR 3.17 CI 95%(1.64 to 6.16)	OR 1.85 CI 95% (0.71 to 4.82)	NA	Low (50)

Author	Feature (method)	Structural progression outcome	Adjustment for confounders	Association (magnitude) crude	Association (magnitude) adjusted	Association	Quality (score %)
	(WORMS) (C) TFJ	change over 2 years (WORMS) (L) TFJ.					
MRI bone attrition – cross-sectional studies							
Torres 2006[135]	MRI attrition (WORMS) TFJ & PFJ (C)	Semi-quantitative cartilage (WORMS) TFJ & PFJ (C)	Nil	R=0.75	NR	+	High (68)
Reichenbach 2008[306]	Semi-quantitative MRI Bone attrition (WORMS) (C)	KL grade and semi-quantitative cartilage defects (WORMS) (C)	Nil	NR Crude correlation	NR	+	Low (43)
MRI bone attrition –case control studies							
Neogi 2009[307]	Baseline semi-quantitative MRI Bone attrition size (WORMS) (C) TFJ	Cartilage defects progression (WORMS) after 30 months TFJ	Age, sex, BMI	OR 5.5 CI 95% (3.0, 10.0)	OR 3.0 CI 95% (2.2, 4.2)	+	Low (59)
MRI bone Shape / dimension – cohort studies							
Cicuttini 2004 [270]	Baseline Quantitative MRI tibial bone area (C)	TKR incidence (L) over 4 years	Age, sex, height, weight, BMI, WOMAC, ROA severity	NR	OR (CI 95%) 1.2 (1.0 to 1.4) p=0.02	+	High (78)
Ding 2008[96]	Baseline MRI tibial bone area (C) TFJ	Progressive cartilage volume loss (L) TFJ	Age, sex, BMI, OA family history, muscle strength and ROA.	β (CI 95%) Medial femoral cartilage β=0.17 (0.04 to 0.29) Total femoral cartilage	β (CI 95%) Medial femoral cartilage β=0.35 (0.14 to 0.56) Total femoral cartilage	-	High (72)

Author	Feature (method)	Structural progression outcome	Adjustment for confounders	Association (magnitude) crude	Association (magnitude) adjusted	Association	Quality (score %)
				β =0.07 (0.003 to 0.14)	β=0.13 (0.02 to 0.25)		
Ding 2006 [261]	Baseline MRI tibial bone area (C) TFJ	Change in semi-quantitative MRI cartilage defect scores over 2.3 yrs (L) TFJ	Age, Sex, BMI, Radiographic OA features	NA	OR (95%CI) Medial TFJ 1.24 (1.01 to 1.51) p=0.04 Lateral TFJ 2.07 (1.52 to 2.82) p<0.001	-	High (61)
Everhart 2014 [102]	Baseline TFJ subchondral surface ratio of medial and lateral TFJ compartments(C)	Radiographic progression of lateral or medial TFJ knee OA at 48 months (L)	sex, race, age, BMI, tobacco use, activity level, knee coronal alignment, baseline symptoms, injury history, surgery history, KL grade, and JSW	Unadjusted Medial SSR vs progression of medial JSN OR 1.43 95%CI (1.15 to 1.77) P= 0.0015 Medial SSR vs progression of lateral JSN OR 1.87 95%CI (1.44 to 2.42) P< 0.001	Neither medial nor lateral SSR was associated lateral or medial ROA progression in adjusted analysis P>0.05.	NA	High (61)
Davies-Tuck 2008[588]	Baseline MRI tibial bone plateau area (C) TFJ	Progressive semi-quantitative cartilage defect score (L) medial and lateral TFJ	Age, sex, BMI, baseline cartilage defect score, baseline cartilage volume and baseline tibial plateau area	Lateral TFJ OR (CI 95%) -0.01 (-0.06, 0.03) p=0.59	OR (CI 95%) Lateral TFJ 0.06 (0.004 to 0.11) p=0.03 Medial TFJ 0.07 (0.03 to 0.12) p=0.002	+	High (56)
Carnes 2012[584]	MRI Tibial Bone area (C)	Semi-quantitative cartilage defect progression	Age, sex, BMI, cartilage defects, BML	Lateral tibial bone area OR 1.11 CI 95% (1.0, 1.23)	OR (CI 95%) Bone area Medial 1.12 (1.01 to 1.26) and lateral tibial (1.35	+	Low (50)

Author	Feature (method)	Structural progression outcome	Adjustment for confounders	Association (magnitude) crude	Association (magnitude) adjusted	Association	Quality (score %)
		TFJ (L)			(1.12 to 1.63)		
Dore 2010 [210]	Baseline tibial bone area MRI (C)	Increase or no increase in semi-quantitative MRI tibial cartilage defects over 2.7 years (L)	age, sex, body mass index, baseline cartilage defects, and subchondral bone mineral density	NR	OR (CI 95%) Medial Tibia 1.6 (1.0 to 2.6) p=0.04 Lateral Tibia 2.4 (1.4 to 4.0) p=<0.01	+ Bone area size is associated with increasing cartilage defect scores	Low (50)
Hudelmaier 2013 [595] Abstract	Annual change in segmented MRI knee bone area (L)	Baseline KL grade (C)	Nil	Medial tibia P<0.05	NR	+ The higher the KL grade the larger the increase in bone area	Low (50)
MRI bone shape / dimension – cross-sectional studies							
Ding 2005 [353]	MRI quantitative tibial bone area (C)	Semi-quantitative MRI knee cartilage defect severity scores (C) TFJ	Age, sex, BMI, family history, cartilage volume	β (CI 95%) Medial TFJ 0.06 (0.03 to 0.09) Lateral TFJ 0.09 (0.05 to 0.13)	β (CI 95%) Medial TFJ 0.11 (0.07 to 0.15) Lateral TFJ 0.17 (0.11 to 0.22)	+ Association maintained for the whole TFJ and by compartment	High (64)
Kalichman 2007 [568]	MRI patellar length ratio, trochlea sulcus angle (C)	JSN grade (C)	Age, sex, BMI	NR	Trochlea sulcus angle p for trend Medial JSN p=0.0162 Lateral JSN p= 0.1206	NC	High (64)
Kalichman 2007 [569]	MRI patellar length ratio, trochlea sulcus angle (C)	Cartilage defect (WORMS) (C)	Age, sex, BMI	NR	Trochlea sulcus angle p for trend Medial cartilage loss p=0.0016 Lateral cartilage loss p=0.0009 to	+	Low (57)
Stefanik 2012[274]	MRI lateral trochlear	Semi-quantitative	Age, sex, BMI	NR	Lateral trochlear inclination OR 2.6	+	Low (57)

Author	Feature (method)	Structural progression outcome	Adjustment for confounders	Association (magnitude) crude	Association (magnitude) adjusted	Association	Quality (score %)
	inclination and trochlear angle (C)	cartilage defect (WORMS) (C)			CI 95% (1.9 to 3.7) p<0.0001 trochlear angle OR 2.0 CI 95% (1.2 to 3.5) p<0.0001		
Frobell 2010[560]	MRI Bone area – manual segmentation (C)	KL grade, OARSI JSN grade (C)	Age & BMI	Medial tibia JSN & KL p <0.0125	Medial tibia JSN & KL p <0.0125	+	Low (57)
Wang 2005 [259]	Annual % change in tibial bone area (L) 2 yr follow up.	Baseline JSN (C)	age, sex, BMI, WOMAC score, SF-36 score, physical activity, radiographic OA features, baseline tibial plateau bone area.	β (CI 95%) Medial tibia β=0.35 (-1.10 to 1.80) p=0.63 Lateral tibia -0.87 (-2.35 to 0.61) p=0.25	β (CI 95%) Medial tibia 1.88 (0.43 to 3.33) p=0.01 Lateral tibia -0.42 (-2.31 to 1.48) p=0.66	+ Association with medial tibia but not in the lateral tibia	Low (57)
Jones 2004 [31]	Tibial bone area (MRI) (C)	Radiographic JSN (C)	age, sex, height, weight	β (CI 95%) Medial tibia β=-0.03 (-0.11 to 0.06) Lateral tibia -0.00 (-0.07 to 0.06)	β (CI 95%) Medial tibia β=-0.00 (-0.04 to 0.06) Lateral tibia +0.00 (-0.04 to 0.05)	NA	Low (50)
Eckstein 2010[483]	MRI Tibial bone area (segmented) (C)	OARSI JSN grade (C)	Nil	P<0.01	NR	+	Low (43)
MRI bone shape / dimension – case-control studies							
Bowes 2012	Change in segmented	KL grade defined ROA	Nil	NR Bone area increased	NR	+ Higher KL	High (71)

Author	Feature (method)	Structural progression outcome	Adjustment for confounders	Association (magnitude) crude	Association (magnitude) adjusted	Association	Quality (score %)
[604]	MRI 3D Bone area over 4 year (L)	knee (C) and (L)		significantly faster in ROA vs non-ROA p<0.0001		grades had greater increase in bone area,	
Neogi 2013 [75]	MRI 3D bone shape (Tibia, Femur and patella) (C)	Incident TFJ ROA KL grade ≥2 (L)	Age, sex, BMI	NR	OR 3 CI 95% (1.8-5.0)	+ Developing 3D OA knee shape is associated with increasing ROA knee	High (65)
Hunter 2013 abstract [605]	Change in MRI knee bone area over 24 months (L)	Incident TFJ ROA (KL grade ≥2) (L)	NR	NR	Hazard ratio (CI 95%) range from 1.17 (1.08 to 1.27) to 3.97 (2.38 to 6.63) all highly statistically significant	+ for all bone regions Enlarging bone area associated with increasing ROA knee	Low (59)
Wluka 2005 [269]	Change in MRI tibial bone area (L)	Baseline radiographic JSN (C)	Age, BMI, pain, physical activity	Medial tibial bone area R=160 (CI 95% 120 to 201) P<0.001	Medial tibial bone area R=145 (CI 95% 103 to 186) P<0.001	+	Low (47)
MRI bone cyst – cohort studies							
Kotharii 2010[478]	Semi-quantitative baseline MRI bone Cyst (WORMS) (C) TFJ	Semi-quantitative cartilage defect score change over 2 years (WORMS) (L) TFJ.	Age, sex BMI, other bone lesions	OR 1.66 CI 95% (0.55, 4.99)	OR 0.47 CI 95% (0.11, 2.03)	NA	Low (50)
Tanamas 2010[601]	Semi-quantitative change in MRI Bone	Knee Cartilage volume loss over 2 years (L) TFJ	Nil	β (CI 95%) Lateral tibial cartilage loss in cyst regression relative to stable and	NR	+	Low (47)

Author	Feature (method)	Structural progression outcome	Adjustment for confounders	Association (magnitude) crude	Association (magnitude) adjusted	Association	Quality (score %)
	cyst size (L)			progressive cysts β= -11.81(-16.64 to -6.98)			
Madan-Sharma 2008[417]	Baseline MRI semi-quantitative bone cyst (C) TFJ	OARSI medial TFJ JSN grade progression over 2 years (L) TFJ	Age, sex, BMI and family effect	NR	RR 1.6 CI 95% (0.5, 4.0)	NA	Low (47)
Carrino 2006[585]	Crude presence of MRI bone cyst TFJ (C) and (L)	Any grade of cartilage defect TFJ (C) and (L)	Nil	NR	NR	+	Low (22)
MRI bone cyst – cross-sectional studies							
Stehling 2010 [313]	Presence of any MRI semi-quantitative cyst (C)	Presence of any WORMS MRI cartilage defects (C)	age, gender and BMI, KL score, knee injury or knee surgery, family history of TKR and Heberden's nodes	NR	p=0.0131	+	High (71)
Torres 2006[135]	MRI bone cyst (WORMS) TFJ & PFJ (C)	Semi-quantitative cartilage (WORMS) TFJ & PFJ (C)	Nil	R=0.75		NC	High (68)
Hayes 2005[312]	Semi-quantitative MRI bone cyst (C)	KL grade (C)	Nil	p=0.02	NR	+	High (61)
Link 2003 [319]	Crude presence of MRI Bone cyst (C)	KL grade (C)	Nil	p<0.01	NR	+	Low (54)
Crema 2010[315]	MRI Bone cysts (WORMS)	Cartilage defect (WORMS) (C)	Nil	NR	NR	+	Low (50)

Author	Feature (method)	Structural progression outcome	Adjustment for confounders	Association (magnitude) crude	Association (magnitude) adjusted	Association	Quality (score %)
	(C)						
CT bone cyst – cross-sectional studies							
Okazaki 2014 [539]	Number of CT bone cysts (medial femur and tibia) (C)	Knee KL grade (C)	Nil	p<0.05	Nil	+with KL grade in medial TFJ	Low (50)
MRI subchondral bone morphometry – cohort studies							
Lo 2012 Abstract [548]	MRI BVF, trabecular number, thickness and spacing (C)	OARSI medial TFJ JSN progression between 24 and 48 months (L)	Nil	OR 2.4 95%CI (1.1 – 5.0) p=0.02	NR	BVF, trabecular number and thickness are positively associated with JSN progression but negatively associated with trabecular spacing.	Low (50)
MRI subchondral bone morphometry – cross-sectional studies							
Driban 2011 [546] Abstract	MRI bone volume fraction, trabecular number, spacing & thickness of medial tibia (C)	The presence of any grade of radiographic medial & lateral JSN (C)	Nil	R=0.09-1.77	NR	+ Medial JSN associated with higher BVF, trabecular number, & thickness but lower spacing	High (71)
Driban 2011 [545]	MRI Bone volume fraction (C)	Radiographic JSN (C)	Nil	NR	NR	+ higher JSN score, lower JSW) were associated with higher	High (64)

Author	Feature (method)	Structural progression outcome	Adjustment for confounders	Association (magnitude) crude	Association (magnitude) adjusted	Association	Quality (score %)
						BVF	
Lindsey 2004 [350]	MRI bone volume fraction trabecular and trabecular number (TFJ) (C)	Cartilage volume of tibia or femur in contralateral TFJ compartment (C)	Nil	Medial TFJ cartilage with Lateral TFJ BVF and trabecular number. β =0.29 to 0.36 p=0.0020 to 0.02	NR	+ with contralateral BVF and Trabecular number, but – with trabecular spacing	High (64)
Lo 2012[206]	MRI bone volume fraction, trabecular thickness, number, spacing and DXA BMD of (proximal medial tibia) (C)	Radiographic medial JSN grade (C)	Nil	All p<0.0001	Nil	+ (BV/TV, thickness, number, BMD) - (spacing)	High (64)
Chiba 2012 [349]	MRI Bone volume fraction & trabecular thickness of the medial & lateral femur & tibia. (C)	Metric JSW (radiographic) of the medial and lateral TFJ (C)	Nil	Bone volume fraction -0.48 (p<0.001) Trabecular thickness -0.51 (p<0.001)	NR	-	Low (57)
DXA BMD – cohort studies							
Dore 2010 [210]	Baseline proximal tibial BMD, DXA (C)	Increase or no increase in semi-quantitative MRI tibial cartilage	age, sex, BMI, baseline cartilage defects & subchondral tibial bone area	NR	OR (CI 95%) Medial Tibia 1.6 (1.2 to 2.1) p<0.01 Lateral Tibia 1.2 (0.9, 1.6)	+ Association only observed in medial tibia	Low (50)

Author	Feature (method)	Structural progression outcome	Adjustment for confounders	Association (magnitude) crude	Association (magnitude) adjusted	Association	Quality (score %)
		defects over 2.7 years (L)			p=0.19		
Lo 2012 Abstract [548]	DXA measured medial :lateral periarticular BMD (paBMD) (C)	OARSI medial TFJ JSN progression (L)	Nil	OR 8.4 95%CI (2.8-25.0) p<0.0001	nil	+ JSN association with baseline M:L paBMD	Low (50)
Bruyere 2003 [209]	Subchondral tibial bone BMD (DXA) (C)	Minimum medial JSW TFJ after one year (L)	Age, sex, BMI, minimum JSW	NR	R=-0.43, p=0.02	- Negative correlation i.e. Lower BMD gives bigger JSW or less JSN	Low (44)
DXA BMD – cross-sectional studies							
Dore 2009 [547]	DXA Tibial subchondral BMD (C)	Radiograph JSN grade and MRI cartilage defect and volume (C)	Age, sex BMI	NR	Medial tibial BMD vs JSN R=0.11, p<0.01, defect R=0.16, p<0.01, cartilage volume R=0.12, p=0.01	+ Higher the BMD the greater the JSN and cartilage defects,	High (71)
Lo 2006 [208]	DXA Medial:lateral BMD ratio at the tibial plateau (C)	Radiographic JSN grade (Medial and lateral TFJ) (C)	Age, sex, BMI	P<0.0001	NR	+ with medial JSN, - with lateral JSN	High (71)
Lo 2012 [206]	DXA BMD (proximal medial tibia) (C)	Radiographic medial JSN grade (C)	Nil	P<0.0001	NR	+	High (64)
Akamatsu 2014 [533]	BMD (DXA) (C) (Medial Tibia &	Medial TFJ JSN (radiographic)	Nil	Tibia R=0.571, p<0.001 Femur R=0.550,	NR	+ Medial femoral and tibial	Low (57)

Author	Feature (method)	Structural progression outcome	Adjustment for confounders	Association (magnitude) crude	Association (magnitude) adjusted	Association	Quality (score %)
Abstract	Femoral Condyle)	(C)		p<0.001		condyle BMD correlated with medial JSN	
Volumetric CT BMD – case control studies							
Bennell 2008 [214]	Volumetric BMD in tibial subchondral trabecular bone (C)	KL grade (C)	Age, sex, BMI	NR	P<0.05	NC BMD falls in posterior tibial plateau as KL increases but. Anteriorly increase in BMD noted	Low (59)
Knee scintigraphic subchondral bone cohort studies							
Mazzuca 2004 [536]	Baseline late-phase subchondral bone scintigraphy (adjusted for healthy diaphysis uptake) of the medial tibia and whole knee (C)	Progression of minimum JSN of the medial TFJ from baseline to 30 months (L)	Age, BMI, KL grade (NB all women)	r = 0.22 to 0.30, (p < 0.05)	r= 0 to 0.08 (p>0.05)	NA after adjustment for covariates	High (56)
Mazzuca 2005 [537]	Baseline late-phase subchondral bone scintigraphy (adjusted for healthy diaphysis uptake) of the medial	Progression of minimum JSN of the medial TFJ from baseline to 30 months (L)	Baseline JSW, Treatment group	NR	Coefficient 0.221, 95%CI (0.003 to 0.439), p=0.049	+ The greater the scintigraphic bone signal the greater the JSN	High (56)

Author	Feature (method)	Structural progression outcome	Adjustment for confounders	Association (magnitude) crude	Association (magnitude) adjusted	Association	Quality (score %)
	tibia and whole knee (C)						
Dieppe 1993 [216]	Baseline late and or early-phase subchondral bone scintigraphy signal (C)	Progression of JSN by ≥2mm or knee operation incidence after 5 years (L)	Nil	p<0.005	NR	+	Low (50)
Knee scintigraphic subchondral bone cross-sectional studies							
Kraus 2009 [550]	Ipsilateral late phase bone scintigraphy, semi-quantitative retention scoring of TFJ (C)	Ipsilateral OARSI scale of JSN (C)	Age, gender, BMI, osteophyte OARSI score, knee alignment knee symptoms	Coefficient 0.47 to 0.48 (p<0.0001)	Coefficient 0.26 to 0.29 (p=0.0005 to0.001)	+	High (71)
McCrae 1992 [553]	Late phase 'extended bone uptake' pattern bone scintigraphy, presence around the TFJ (C)	Radiographic JSN presence (C)	Nil	OR 47.3, 95%CI (6.4 to 352) p<0.01	NR	+	Low (50)
2D knee bone shape – cross-sectional studies							
Haverkamp 2011 [276]	2D bone shape knee 1. femur & tibial width 2. elevation of lateral tibial plateau	1.Presence of diffuse cartilage defects semi-quantitative scoring (MRI). 2.Presence of	NB (this is a population of women only) ROA models adjusted for Age, BMI,	OR (95% CI) Bone width vs Knee ROA 2.03 (1.55 to 2.66) p<0.001 Bone width Presence of diffuse cartilage	OR (95% CI) Knee ROA 1.94 (1.44 to 2.62) p<0.001	+ Wider bones & elevated tibial plateau were associated with the presence of ROA knee.	Low (46)

Author	Feature (method)	Structural progression outcome	Adjustment for confounders	Association (magnitude) crude	Association (magnitude) adjusted	Association	Quality (score %)
	(C)	ROA knee (KL≥2) (C)	Cartilage defect models adjusted for KL only	defects p<0.001		Cartilage defects were only associated with bone width	

Positive correlation reported between bone feature and outcome measure (+); Negative correlation reported between bone feature and outcome measure (-); Bone mineral density (BMD); Body mass index (BMI); bone marrow lesion (BML); Boston Osteoarthritis of the Knee Study (BOKS); Boston–Leeds. Osteoarthritis Knee Score (BLOKS); bone volume fraction (BVF); a feature or outcome described in cross-section (C); confidence interval (CI); Computed tomography (CT); Dual-energy X-ray Absorptiometry (DXA); Genetics, Osteoarthritis and Progression Study (GARP); joint space narrowing (JSN); joint space width (JSW); Kellgren Lawrence (KL); knee osteoarthritis scoring system (KOSS); a feature or outcome described longitudinally(L);mechanical factors in arthritis of the knee 2 (MAK-2); No conclusion could be found for an association between bone feature and outcome measure (NC); Michigan study of women's health across the nation (SWAN); multicentre osteoarthritis study (MOST); Magnetic resonance imaging (MRI); No association (NA);No conclusion could be found for an association between bone feature and outcome measure (NC); not reported (NR); osteoarthritis (OA); osteoarthritis initiative (OAI); odds ratio (OR); P value (p); Patellofemoral joint (PFJ); relative risk ratio (RR); Subchondral surface ratio (SSR); Tasmanian Older Adult Cohort (TASOAC); Tibiofemoral joint (TFJ); Visual analogue scale (VAS); Western Ontario and McMaster Universities arthritis index (WOMAC); whole-organ magnetic resonance imaging score (WORMS).

Table 18 Knee Pain associations by feature and quality score

Author	Feature (method)	Knee Pain outcome	Adjustment for confounders	Association (magnitude) crude	Association (magnitude) adjusted	Association	Quality score (%)
MRI bone marrow lesion – Cohort studies							
Foong 2014 [101]	Change in BML size (L) and Incident BMLs (L) In all three knee compartments	WOMAC Knee pain severity at two and ten year visits (L)	age, sex, BMI, leg strength, and the presence of ROA	NR	Incident or change in total BML size β=1.53(95%CI 0.37 to 2.70 Medial tibial change in BML size β = 2.96 (95%CI 0.59-5.34	+ Incidence of BML or increase in size associated with increase in pain in the medial tibia	High (67)
Driban 2013 [100]	Knee baseline BML volume (C) BML volume change (L) (TFJ)	48 month change in WOMAC pain (L),	Age, sex, BMI	NR	β=0.21 (standard error 0.07) p=0.004	+ Longitudinal (L) Changes in BML correlated with (L) changes in pain severity	High (61)
Dore 2010[99]	MRI BML size (L) regional or whole TFJ over 2.7 years	Change in WOMAC pain (L) over 2.7 years	Age, sex, BMI, leg strength, quality of life, and baseline pain, function	β (95% CI) Total BML size change β=1.06 (0.10 to 2.03)	β (95% CI) Total BML size change β= 1.13 (0.28 to 1.98)	+	High (56)
Kornaat 2007[302]	Semi-quantitative MRI BML	Mean WOMAC pain over 2	Age, sex and BMI	NR	β (95% CI) β=2(-8 to 11)	NA	High (56)

Author	Feature (method)	Knee Pain outcome	Adjustment for confounders	Association (magnitude) crude	Association (magnitude) adjusted	Association	Quality score (%)
	change over 2 years (L) TFJ	years					
Moisio 2009[456]	Baseline MRI semi-quantitative BML score (C) TFJ and PFJ	Incident frequent knee pain 2 years after baseline (L)	Age, sex, BMI, BML score, % denuded bone	NR	OR (CI 95%) Medial tibia & femur OR 1.41 (0.86 to 2.33) Lateral tibia & femur OR 1.70 (1.07 to 2.69)	+ Lateral TFJ BML score associated with incident frequent knee pain	High (56)
Sowers 2011[530]	Semi-quantitative MRI BML, size in TFJ (C)	Increasing WOMAC pain (L)	Nil	Medial and lateral TFJ BMLs both p<0.005	NR	+	Low (53)
Zhang 2011 [26]	Semi-quantitative change in MRI BML size (L) TFJ over 30 months	Incidence of frequent knee pain, and categorical severity (L) over 30 months	Synovitis and effusions	OR (CI 95%) Severity of frequent knee pain OR 3.0 (1.5 to 6.0)	OR (CI 95%) Incident frequent knee pain P for trend =0.006 Severity of frequent knee pain OR 2.2 (1.0 to 4.7) p=0.047	+ Ipsilateral association	Low (50)
Wildi 2010	24 month change in	24 months change in	Nil	R<0.15 p>0.067 for all	NR	NA All compartments	Low (50)

Author	Feature (method)	Knee Pain outcome	Adjustment for confounders	Association (magnitude) crude	Association (magnitude) adjusted	Association	Quality score (%)
[602]	regional TFJ BML score WORMS (L)	WOMAC pain (L)		compartments		had no correlation	
Tanamas 2010[600]	Baseline semi-quantitative MRI BML size (C)	Annual change in WOMAC pain (L)	Nil	NR	NR	NA	Low (50)
MRI bone marrow lesion – cross-sectional studies							
Zhai 2006[582]	Semi-quantitative MRI BML (C)	WOMAC pain>1 (C)	Age, BMI, sex, knee strength, chondral defects	NR	OR 1.44 CI 95% (1.04, 2.00)	+	High (79)
Sharma 2014 [131]	Semi-quantitative BML score WORMS TFJ or PFJ (C)	Prevalent frequent knee symptoms (C)	Age, sex, body mass index (BMI), previous knee injury, and previous knee surgery	NR	BMLs in any compartment OR 1.96 (95% CI 1.38 to 2.77	+ BML association with prevalent knee symptoms	High (71)
Kornaat 2006 [571]	Semi-quantitative MRI BML (C)	Chronic pain presence (C)	Age, sex, and BMI	NR	OR, 1.13 CI 99% (0.41, 3.11) p=0.76	NA	High (71)
Lo 2009 [575]	Semi-quantitative MRI BML	WOMAC pain (C)	Synovitis , effusion scores	p for trend p=0.0009	p for trend p=0.006	+	High (71)

Author	Feature (method)	Knee Pain outcome	Adjustment for confounders	Association (magnitude) crude	Association (magnitude) adjusted	Association	Quality score (%)
	(BLOKS) (C)						
Stefanik 2014 abstract [581]	BML (WORMS) (C) (patellofemoral joint)	Prevalent knee pain (any pain in last 30 days) and Pain VAS (C)	Adjusted for age, sex, BMI, depressive symptoms and TFJ BMLs	NR	Isolated BML of the: Lateral PFJ OR (95%CI) 1.4 (0.9-2.0) Medial PFJ OR (95%CI) 1.1 (0.8-1.5) Isolated lateral PFJ BMLs OR 6.6 (1.7 to 11.5)	NC	High (71)
Ratzlaff 2013 [577]	Total BML volume in the femur or tibia (C)	Weight bearing knee pain WOMAC subscale (C)	age, sex, BMI, race, and medial minimum joint space width	NR	Total BML volume femur p= 0.003 Tibia p=0.101	+ Femoral NA Tibial	High (71)
Ip 2011 [567]	Semi-quantitative MRI BML (C)	WOMAC pain (C)	Age, sex, BMI, OA stage, joint effusion, and meniscal damage	NR	Total WOMAC pain R=0.05, CI 95% (-0.04 to 0.14) Stair climbing pain R=0.09 (0.00 to	NC	High (68)

Author	Feature (method)	Knee Pain outcome	Adjustment for confounders	Association (magnitude) crude	Association (magnitude) adjusted	Association	Quality score (%)
					0.18)		
Torres 2006[135]	MRI BML (WORMS) TFJ & PFJ (C)	Pain VAS (C)	Age, BMI	Coefficient 5.00 CI 95% (3.00, 7.00)	Coefficient 3.72 CI 95% (1.76, 5.68)	+	High (68)
Kim 2013 [570]	Summary score and severity of MRI BML (WORMS) (C)	WOMAC pain severity or presence of knee pain (C)	Age, sex, BMI, radiographic OA	NR	BML summary score medial TFJ OR 2.33 CI 95%(1.02, 5.33) p<0.001	+ Severity of BML is proportional to WOMAC in medial compartment after adjustment	High (64)
Moisio 2009[456]	Baseline MRI semi-quantitative BML score (C) TFJ and PFJ	Presence of baseline moderate to severe knee pain (C)	Percent denuded bone, age, sex, BMI	NR	Bone marrow lesion score OR 0.95 CI 95% (0.63, 1.44) Not significant in all compartments	NA found cross-sectionally	High (64)
Ratzlaff 2014 [544] Abstract	Median BML volume (PFJ, TFJ) (C)	Stair-climbing knee pain WOMAC	Nil	TFJ p=0.01 Patellofemoral, p=0.01 Femur p=0.02	NR	+	High (64)

Author	Feature (method)	Knee Pain outcome	Adjustment for confounders	Association (magnitude) crude	Association (magnitude) adjusted	Association	Quality score (%)
		(C)		Tibia p=0.03			
Hayes 2005[312]	Semi-quantitative MRI BML (C)	Chronic pain presence (C)	Nil	p=0.001	NR	+	High (61)
Ai 2010 [557]	Semi-quantitative MRI BML (C)	Pain verbal rating scale (Likert) (C)	Nil	p=0.33	NR	NA	Low (57)
Bilgici 2010[558]	MRI BML (WORMS) (C)	WOMAC pain, pain VAS (C)	Nil	WOMAC r=0.508, p<0.01 Pain VAS r=0.488,p<0.01	NR	+	Low (57)
Sowers 2003 [531]	Semi-quantitative MRI BML (C)	Chronic pain presence (C)	Nil	OR 5.0 CI 95% (2.4, 10.5)	NR	+	Low (54)
Link 2003[319]	Semi-quantitative MRI BML (C)	WOMAC pain (C)	Nil	p>0.05	NR	NA	Low (54)
Felson 2001 [133]	Semi-quantitative MRI BMLs (C)	Chronic knee pain presence (C)	Radiographic severity, age, sex, and effusion score	p<0.001	OR 3.31 CI 95% (1.54 to 7.41)	+	Low (54)

Author	Feature (method)	Knee Pain outcome	Adjustment for confounders	Association (magnitude) crude	Association (magnitude) adjusted	Association	Quality score (%)
Fernandez-Madrid 1994 [559]	Crude presence of MRI BMLs(C)	Crude pain presence (C)	Nil	NR	NR	NA	Low (46)
MRI bone marrow lesion - case control studies							
Javaid 2010 [607]	Baseline semi-quantitative MRI BML size (WORMS) (C) TFJ & PFJ	Incident frequent knee pain after 15 months (L)	Age, sex, race, BMI	NR	Whole knee OR 2.8 CI 95% (1.2, 6.5)	+	High (76)
Felson 2007 [134]	Semi-quantitative MRI BML size increase (WORMS) (L) TFJ & PFJ	Incident frequent pain at 15 months (L)	Age, sex, race, BMI, quadriceps strength, KL score, malalignment, baseline BML score	OR 4.1 CI 95% (2.1, 8.1)	OR 3.2, CI 95% (1.5, 6.8)	+	High (71)
Javaid 2012 [606]	Baseline Semi-quantitative MRI BML, (WORMS) (C) TFJ & PFJ	Presence of frequent knee pain (C) after 2 years	Nil	OR 1.70 CI 95% (1.08, 2.67)	NR	+	Low (59)
Zhao 2010 [609]	Baseline crude presence of MRI BMLs at (C) TFJ	Change in WOMAC Pain (L)	Nil	p=0.60	NR	NA	Low (56)
Stahl 2011	Semi-quantitative	Changes in	Nil	NR	Data not shown	NA	Low (47)

Author	Feature (method)	Knee Pain outcome	Adjustment for confounders	Association (magnitude) crude	Association (magnitude) adjusted	Association	Quality score (%)
[442]	MRI BML size (WORMS) (L) TFJ	WOMAC score (L)					
MRI osteophyte – cohort studies							
Sowers 2011[530]	Semi-quantitative MRI osteophyte, size in TFJ (C)	Increasing WOMAC pain (L)	Nil	Medial and lateral TFJ BMLs Both p<0.001	NR	+	Low (53)
MRI osteophyte - cross-sectional studies							
Kornaat 2006 [571]	Semi-quantitative MRI Osteophyte (C)	Chronic pain presence (C)	Age, sex, and BMI	NR	patellofemoral OR 2.25 CI 95% (1.06 to 4.77)	+	High (71)
Sengupta 2006[580]	Semi-quantitative MRI Osteophyte (WORMS) (C)	Pain severity WOMAC, chronic pain (C)	Age, sex, BMI	NR	OR 0.97 CI 95% (0.86 to 1.10)	NA	High (71)
Torres 2006[135]	MRI osteophyte, (WORMS) TFJ & PFJ (C)	Pain VAS (C)	Nil	Coefficient 1.18 CI 95% (0.63, 1.72)	Coefficient 0.50 CI 95% (0.07, 0.94)	NC	High (68)
Hayes 2005[312]	Semi-quantitative	Chronic pain	Nil	P<0.001	NR	+	High (61)

Author	Feature (method)	Knee Pain outcome	Adjustment for confounders	Association (magnitude) crude	Association (magnitude) adjusted	Association	Quality score (%)
	MRI osteophyte (C)	presence (C)					
Ai 2010 [557]	Semi-quantitative MRI osteophytes (C)	Pain verbal rating scale (Likert) (C)	Nil	p=0.166	NR	NA	Low (57)
Hayashi 2012[566]	Crude presence of MRI Osteophytes (C)	Presence of pain on WOMAC pain subscale (C)	Nil	OR 4.2-6.4, p=0.001-0.011	NR	+	Low (57)
Link 2003[319]	Semi-quantitative MRI osteophytes (C)	WOMAC pain (C)	Nil	p>0.05	NR	NA	Low (54)
Fernandez-Madrid 1994 [559]	Crude presence of MRI osteophytes (C)	Crude pain presence (C)	Nil	NR	NR	NA	Low (46)
MRI osteophyte – case-control studies							
Javaid 2010 [607]	Baseline semi-quantitative MRI osteophyte, size (WORMS)	Incident frequent knee pain after 15	Age, sex, race, BMI	NR	Whole knee Severe osteophyte OR 4.7 CI 95% (1.3 to 18)	+	High (76)

Author	Feature (method)	Knee Pain outcome	Adjustment for confounders	Association (magnitude) crude	Association (magnitude) adjusted	Association	Quality score (%)
	(C) TFJ & PFJ	months (L)					
MRI bone attrition – cross-sectional studies							
Hernandez-Molina 2008 [139]	Semi-quantitative MRI Bone attrition (WORMS) (C)	Pain severity and nocturnal pain (WOMAC) (C)	Age, sex, BMI, BMLs, effusions and KL grade	OR (CI 95%) Pain severity OR 1.6 (1.1 to 2.3) Nocturnal Pain OR 1.1 (0.5 to 2.1)	OR (CI 95%) Pain severity OR 0.9 (0.6 to 1.4) Nocturnal Pain OR 1.0 (0.5 to 2.1).	NA	High (71)
Torres 2006[135]	MRI attrition, (WORMS) TFJ & PFJ (C)	Pain VAS (C)	Nil	Coefficient 3.33 CI 95% (1.79, 4.87)	Coefficient 1.91 CI 95% (0.68 to 3.13)	+	High (68)
MRI bone attrition - case control studies							
Javaid 2012 [606]	Baseline Semi-quantitative MRI attrition size (WORMS) (C) TFJ & PFJ	Presence of frequent knee pain (C) after 2 years	Nil	OR 2.40 CI 95% (1.51, 3.83)	NR	+	Low (59)
MRI bone shape / dimension - cohort studies							
Everhart 2014 [102]	Baseline TFJ subchondral surface ratio of medial and lateral TFJ compartments	Incident frequent knee pain at 48 months,	sex, race, age, BMI, tobacco use, activity level, knee coronal alignment,	NR	Medial SSR OR 0.48 95%CI (0.30, 0.75) p=0.0009	- larger MSSR gets less incident frequent knee pain	High (61)

Author	Feature (method)	Knee Pain outcome	Adjustment for confounders	Association (magnitude) crude	Association (magnitude) adjusted	Association	Quality score (%)
	(C)	(L)	baseline symptoms, injury history, surgery history, KL grade, and JSW		Lateral SSR OR 1.27 95%CI (0.86, 1.88) p=0.19		
MRI Bone Shape / Dimension - Cross-sectional studies							
Ochiai 2010[543]	MRI Irregularity of femoral condyle contour (C)	Knee pain VAS (C)	Nil	Irregularity of femoral condyle contour r= 0.472, p=0.0021	NR	+	Low (50)
MRI Bone Cyst – Cohort studies							
Sowers 2011[530]	Semi-quantitative MRI bone cyst size in TFJ (C)	Increasing WOMAC pain (L)	Nil	NR	NR analysis described as not significant but data not shown	NA	Low (53)
MRI Bone Cyst – cross-sectional studies							
Kornaat 2006 [571]	Semi-quantitative MRI bone cyst(C)	Chronic pain presence (C)	Nil	NR	Patellofemoral OR 1.83 CI 99% (0.80 to 4.16)	NA	High (71)
Torres 2006[135]	MRI bone cyst (WORMS) TFJ	Pain VAS (C)	Age, BMI	Coefficient 2.50	Coefficient 0.82 CI 95%(-0.50 to	NA	High (68)

Author	Feature (method)	Knee Pain outcome	Adjustment for confounders	Association (magnitude) crude	Association (magnitude) adjusted	Association	Quality score (%)
	& PFJ (C)			CI 95% (-0.38, 5.38	2.14)		
Hayes 2005[312]	Semi-quantitative MRI bone cyst (C)	Chronic pain presence (C)	Age, sex, and BMI	P<0.001	NR	+	High (61)
Hayashi 2012[566]	Crude presence of MRI bone cysts (C)	Presence of pain on WOMAC pain subscale (C)	Nil	OR 6.7-17.8 p=0.004 to 0.03	NR	+	Low (57)
Link 2003[319]	Crude presence of MRI bone cyst (C)	WOMAC pain (C)	Nil	p>0.05	NR	NA	Low (54)
MRI Bone cyst – case control studies							
Javaid 2010 [607]	Baseline semi-quantitative MRI bone cyst size (WORMS) (C) TFJ & PFJ	Incident frequent knee pain after 15 months (L)	Nil	NR	NR p>0.1	NA	High (76)
Javaid 2012[606]	Baseline Semi-quantitative MRI bone cyst size (WORMS) (C) TFJ & PFJ	Presence of frequent knee pain (C) after 2 years	Nil	OR 1.61 CI 95% (1.03, 2.52)	NR	+	Low (59)
qCT Bone mineral density – cross-sectional studies							

Author	Feature (method)	Knee Pain outcome	Adjustment for confounders	Association (magnitude) crude	Association (magnitude) adjusted	Association	Quality score (%)
Burnett 2012 [549]	BMD of patellar lateral facet (qCT) (C)	WOMAC – knee pain at rest (C)	Nil	Total lateral patella facet p=0.04, Inferior lateral facet p=0.005	NR	-	Low (57)
2D knee bone shape – cross-sectional studies							
Haverkamp 2011 [276]	2D bone shape knee 1. femur & tibial width 2. elevation of lateral tibial plateau (C)	Pain severity VAS (C)	models adjusted for Age, BMI	NR	Bone width p=0.167 Lateral tibia plateau elevation p=0.002	+ Lateral tibial plateau associated with pain severity NA bone width with pain severity	Low (46)

Positive correlation reported between bone feature and outcome measure (+); Negative correlation reported between bone feature and outcome measure (-); body mass index (BMI); bone marrow lesion (BML); a feature or outcome described in cross-section (C); knee pain on most days for at least the last month (chronic pain) confidence interval (CI); Kellgren Lawrence (KL); a feature or outcome described longitudinally(L); No association (NA); No conclusion could be found for an association between bone feature and outcome measure (NC); not reported (NR); osteoarthritis (OA); Osteoarthritis Initiative (OAI); odds ratio (OR); Patellofemoral joint (PFJ); Subchondral surface ratio (SSR); Tibiofemoral joint (TFJ); visual analogue scale (VAS); Western Ontario and McMaster Universities arthritis index (WOMAC)

Table 19 Hand, hip and ankle structural associations by feature and quality grade

Author	Feature (method)	Structural severity or progression outcome	Adjustment for confounders	Association (magnitude) crude	Association (magnitude) adjusted	Association	Quality (score %)
Hand MRI bone marrow lesion case series							
Haugen 2014 [39]	BMLs – semi-quantitative At 2nd to 5th IPJs (C)	Progression of Hand ROA (JSN, KL grade or new erosion) (L)	Age, sex BMI,	OR 2.73 95% CI (1.29 to 5.78)	NR	+ Bigger the BML, the more the JSN	High (61)
Hand MRI bone marrow lesion cross-sectional studies							
Haugen 2012 Abstract [564] 299	BML (Oslo MRI hand score) (C) IPJs	Radiographic JSN grade IPJ (OARSI atlas.) (C)	Age, sex,	OR 10.0 95%CI (4.2–23)	OR 4.4 95%CI (2.2–9.0)	+ BML score association with more JSN	Low (43)
Haugen 2012 [565]	BML (Oslo MRI hand score) (C) IPJs	Hand KL grade of IPJs (C)	Age, sex	NR	OR (95%CI) BMLs 11(5.5 to 21) p<0.001	+	High (64)
Hand MRI osteophyte cross-sectional studies							
Haugen 2012 [565]	Osteophyte (Oslo MRI hand score) (C) IPJs	Hand KL grade of IPJs (C)	Age, sex	NR	OR (95%CI) Osteophytes 415 (189 to 908) p<0.001	+	High (64)

Author	Feature (method)	Structural severity or progression outcome	Adjustment for confounders	Association (magnitude) crude	Association (magnitude) adjusted	Association	Quality (score %)
Hand MRI attrition cross-sectional studies							
Haugen 2012 [565]	Attrition (Oslo MRI hand score) (C) IPJs	Hand KL grade of IPJs (C)	Age, sex	NR	OR (95%CI) Attrition 87 (37 to 204) p<0.001	+	High (64)
Hand MRI bone cyst cross-sectional studies							
Haugen 2012 [565]	Cyst (Oslo MRI hand score) (C) IPJs	Hand KL grade of IPJs (C)	Age, sex	NR	OR (95%CI) Cysts 2.0 (0.6 to 6.3) P=0.26	nil	High (64)
Hip MRI BML cross-sectional studies							
Neumann 2007 [542]	Semi-quantitative BMLs (C)	Semi-quantitative cartilage lesions (C)	Nil	R=0.44, p≤0.001	NR	+ correlation between BML and cartilage lesions	Low (43)
Dawson 2013 Abstract [556]	Femoral head BMLs (MRI) (C)	1. Presence of hip OA 2.Femoral head cartilage volume (MRI) (C)	Age, sex, BMI	NA	OA hip presence OR (95% CI) 5.32 (1.78 to 15.9) p=0.003 Cartilage volume Regression coefficient (95% CI)	+ BMLs associated with diagnosis of hip OA, - BMLs inversely associated with cartilage volume	Low (14)

Author	Feature (method)	Structural severity or progression outcome	Adjustment for confounders	Association (magnitude) crude	Association (magnitude) adjusted	Association	Quality (score %)
					-245.7mm^3 (-456 to -36) p=0.02		
Hip CT bone morphometry cross-sectional studies							
Chiba 2011 [215]	Acetabular and femoral head subchondral trabecular morphometry: bone volume fraction, trabecular thickness, number, separation (CT) (C)	Hip joint space volume (CT) (C)	Nil	Femoral head Bone volume fraction r=-0.691, p<0.001	NR	Joint space narrowing is associated with increased bone volume fraction, trabecular thickening. Trabecular number and spacing decrease	Low (57)
Hip DXA BMD cross-sectional studies							
Chaganti 2010 [532]	Femoral neck BMD (C) DXA	Hip ROA Modified croft score (categorical 0-4) (C)	Age, BMI, height, activity level, race, 6-m walk pace, Nottingham muscle strength, inability to	NR	p<0.0001	+ Higher BMD for higher grade of OA of hip	High (64)

Author	Feature (method)	Structural severity or progression outcome	Adjustment for confounders	Association (magnitude) crude	Association (magnitude) adjusted	Association	Quality (score %)
			do chair stands, and clinic site				
Antoniades 2000 [534]	DXA BMD of the femoral neck of left (nondominant) hip with ROA (C)	Radiographic OA (Croft Score) (C)	body mass index, lifetime physical activity, menopausal status, use of oestrogen, and smoking	OR 1.63 95%CI(1.06, 2.50)	OR 1.80 95%CI (1.05, 3.12)	+ association between BMD and hip ROA grade in the index hip. Higher OA grade means higher BMD	High (64)
2D hip bone shape longitudinal studies							
Agricola 2013 [583]	Baseline 2D femoral and acetabular shape modes (segmented by statistical shape modelling) (C)	THR at or within 5 yrs (L)	Age, sex, BMI, shape modes	5 modes were associated with THR OR 1.71-2.01 p≤0.001	3 modes were associated with THR OR 1.78-2.10 p≤0.001	+ Increasing femoral head asphericity is associated with THR	High (72)
Agricola 2013 [74]	Baseline alpha angle (2D femur shape) dichotomous abnormal >60°, normal	Incident ROA hip (KL>1) Incident end-stage ROA hip (KL>2 or THR)	Age, sex, BMI, KL grade	OR (95%CI) Incident ROA hip 6.82 (3.55 to 13.10)	OR (95%CI) Incident ROA hip 2.42 (1.15 to 5.06)	+ Elevated alpha angle is associated with incident end-	High (67)

Author	Feature (method)	Structural severity or progression outcome	Adjustment for confounders	Association (magnitude) crude	Association (magnitude) adjusted	Association	Quality (score %)
	≤60 (C)	at or within 5 yrs (L)		p<0.0001	P=0.02 Incident severe ROA or THR 3.67 (1.68-8.01) p<0.0001	stage OA hip	
Agricola 2013 [394]	Baseline 2D Centre edge angle (Acetabular shape): 25°<Normal<40° Undercoverage<25° Overcoverage>40° (C)	Incidence within 5 years of: 1.ROA hip (KL>1) 2.End-stage OA (KL>2 or THR)	Age, sex, BMI, KL grade	OR (95%CI) Overcoverage 0.52 (0.19 to 1.43) p=0.21 Undercoverage 3.64 (1.91 to 6.99) p=0.00	OR (95%CI) Overcoverage 0.34 (0.13 to 0.87) p=0.025 Undercoverage 5.45 (2.40 to 12.34) p=0.00	Overcoverage is protective against OA incidence (-) Undercoverage is associated with greater odds of OA incidence and end-stage OA (+)	High (67)
2D & 3D hip bone shape cross-sectional studies							
Gosvig 2010 [561]	Categorical Hip 2D deformity: 1) Normal 2)'Pistol grip' 3) Deep acetabular socket	Presence of radiographic hip OA (JSW≤2mm) (C)	Age, sex, BMI, other hip deformities	NR	RR (95% CI) Pistol grip 2.2 (1.7 to 2.8) p<0.001 Deep acetabular socket	+	Low (50)

Author	Feature (method)	Structural severity or progression outcome	Adjustment for confounders	Association (magnitude) crude	Association (magnitude) adjusted	Association	Quality (score %)
	(C)				2.4 (2.0 to 2.9) p<0.001 Normal (p>0.05)		
Reichenbach 2011 [529]	The presence or absence of any 3D semi-quantitative MRI-defined cam-deformity (C)	Combined femoral and acetabular cartilage thickness (C)	Age, BMI (NB all participants were young men)	Unadjusted mean cartilage thickness difference with CAM deformity -0.24 mm (95% CI -0.46, -0.03)	Adjusted mean cartilage thickness difference with CAM deformity -0.19 mm (95% CI -0.41, 0.02)	NC	High (64)
2D hip bone shape case control studies							
Doherty 2008 [282]	Non-spherical femoral head 2D shape assessment: 1) Appearance of 'Pistol grip deformity' (C) 2) Maximum femoral head diameter ratio to minimum parallel femoral neck diameter (C)	Presence of radiographic hip OA (JSW≤2.5mm) (C)	age, sex, BMI, BMD, physical activity, history of hip injury, type 3 hand (index finger shorter than ring finger), hand nodes, and center–edge angle	OR (95%CI) Pistol grip deformity 5.75 (4.00 to 8.27) Femoral head-to-neck ratio 10.45 (7.16 to 15.24)	OR (95%CI) Pistol grip deformity 6.95 (4.64 to 10.41) Femoral head-to-neck ratio 12.08 (8.05 to 18.15)	+	Low (53)

Author	Feature (method)	Structural severity or progression outcome	Adjustment for confounders	Association (magnitude) crude	Association (magnitude) adjusted	Association	Quality (score %)
Barr 2012 [603]	2D Shape measures of centre edge angle (acetabular shape) (C)	THR vs no radiographic progression over 5 years (L)	Age, gender, BMI KL grade, use of walking stick, WOMAC function, duration of pain	OR (95%CI) Mode 2 0.74 (0.50 to 1.10) p>0.05	OR (95%CI) Mode 2 0.17 (0.04 to 0.71) p<0.05	- NB, this model association is inverse and correlates with acetabular shape	High (76)
Nicholls 2011 [538]	CAM deformity; mean modified triangular index height, alpha angle. 2D Acetabular dysplasia; mean lateral center edge angle, (C)	Total hip replacement (L)	BMI, age	OR (p value) Triangular index 1.131 (0.021) Alpha angle 1.056 (<0.0005) Centre edge angle 0.906 (0.004)	OR (p value) Triangular index 1.291 (0.011) Alpha angle 1.057 (<0.0005) Centre edge angle 0.887 (0.002)	+ Association of hip replacement with CAM impingement and acetabular dysplasia indicated by these results	High (71)
Ankle scintigraphic subchondral bone cross-sectional studies							
Kraus 2013 [551]	Ipsilateral late phase bone scintigraphy, retention presence in tibiotalar joint (C)	Tibiotalar ROA KL grade and JSN (C)	Age, gender, BMI	NR	KL grade r=0.49 p<0.0001 JSN r=0.35 p<0.0001	+	High (71)

Author	Feature (method)	Structural severity or progression outcome	Adjustment for confounders	Association (magnitude) crude	Association (magnitude) adjusted	Association	Quality (score %)
Knupp 2009 [526]	Late phase bone scintigraphy, semi-quantitative retention scoring of tibiotalar joint (C)	Tibiotalar ankle joint JSN. (Modified Takakura score) (C)	Nil	0.62 to 0.75 ($p<0.01$)	NR	+	Low (57)

Positive correlation was reported between bone feature and outcome measure (+); Negative correlation reported between bone feature and outcome measure (-); bone mineral density (BMD); bone marrow lesion (BML); a feature or outcome described in cross-section (C); Computed tomography (CT); dual-energy X-ray absorptiometry (DXA); Hip Osteoarthritis MRI scoring system (HOAMS); interphalangeal joint (IPJ); joint space narrowing (JSN); joint space width (JSW); Kellgren Lawrence (KL); a feature or outcome described longitudinally(L); No association (NA); magnetic resonance imaging (MRI); patellofemoral joint (PFJ); radiographic osteoarthritis (ROA); osteoarthritis (OA); Osteoarthritis Research Society International (OARSI); odds ratio (OR); relative risk (RR); tibiofemoral joint (TFJ); total hip replacement (THR); total knee replacement (TKR); visual analogue scale (VAS); Western Ontario and McMaster Universities arthritis index (WOMAC); whole-organ magnetic resonance imaging score (WORMS).

Table 20 Hand and Hip Pain associations by feature and quality score

Author	Feature (method)	Pain outcome	Adjustment for confounders	Association (magnitude) crude	Association (magnitude) adjusted	Association	Quality score (%)
Hand MRI bone marrow lesion case series							
Haugen 2014 Abstract [593]	Sum scores (0-48) for BMLs (Oslo Hand OA MRI score) (C)	AUSCAN pain scale (L)	Age, sex, BMI, follow up time	NR	β=-0.26 95%CI (-0.55 to 0.03)	NA	High (61)
Hand MRI bone marrow lesion cross-sectional studies							
Haugen 2012 [563]	BML (Oslo MRI hand score) (C) IPJs sum scores	AUSCAN pain scale (C)	Age, sex	NR	OR (95%CI) 0.96 (0.82 to 1.12)	NA	High (64)
Hand MRI osteophyte cross-sectional studies							
Haugen 2012 [563]	Osteophyte (Oslo MRI hand score) (C) IPJs sum scores	AUSCAN pain scale (C)	Age, sex	NR	OR (95%CI) 1.04 (0.98 to 1.10)	NA	High (64)
Hand MRI attrition cross-sectional studies							
Haugen 2012 [563]	Attrition (Oslo MRI hand score) (C) IPJs sum scores	AUSCAN pain scale (C)	Age, sex	NR	OR (95%CI) 1.15 (0.98 to 1.34)	NA	High (64)

Author	Feature (method)	Pain outcome	Adjustment for confounders	Association (magnitude) crude	Association (magnitude) adjusted	Association	Quality score (%)
Hand MRI subchondral cyst cross-sectional studies							
Haugen 2012 [563]	Cyst (Oslo MRI hand score) (C) IPJs sum scores	AUSCAN pain scale (C)	Age, sex	NR	OR (95%CI) 0.93 (0.56 to 1.55)	NA	High (64)
Hand Scintigraphy subchondral bone cross-sectional studies							
Macfarlane 1993 [552]	Late phase isotope bone scan small joints of the hand (C)	Hand Pain VAS (C)	Nil	Correlation coefficient 0.06, p=0.304	NR	NA	Low (57)
Hip MRI bone marrow lesion cross-sectional studies							
Kumar 2013 [573]	Total hip semi-quantitative BML score (C)	Self-reported hip pain HOOS score (C)	Nil	NR	p correlation -0.29 (p<0.01)	- A higher BML score means a lower or worse HOOS pain score	High (71)
Maksymowych 2014 [576]	Semi-quantitative BML HIP (HOAMS) (C)	Baseline WOMAC pain (C)	Nil	p<0.001	NR	+	High (64)
Hip MRI subchondral cyst cross-sectional studies							
Kumar 2013 [573]	Total hip semi-quantitative subchondral	Self-reported hip pain	Nil	NR	p correlation -0.37 (p<0.001)	- a higher cyst	High (71)

Author	Feature (method)	Pain outcome	Adjustment for confounders	Association (magnitude) crude	Association (magnitude) adjusted	Association	Quality score (%)
	cyst score (C)	HOOS score (C)				score means a lower or worse HOOS pain score	

Positive correlation reported between bone feature and outcome measure (+); Negative correlation reported between bone feature and outcome measure (-); Australian/Canadian Osteoarthritis Hand Index (AUSCAN); bone marrow lesion (BML); a feature or outcome described in cross-section (C); knee pain on most days for at least the last month (chronic pain); Hip Osteoarthritis MRI scoring system (HOAMS); Hip Dysfunction and Osteoarthritis Outcome Score (HOOS); interphalangeal joint (IPJ); a feature or outcome described longitudinally(L); no association (NA); not recorded (NR); osteoarthritis (OA); odds ratio (OR); visual analogue scale (VAS);

Table 21 The summary subchondral bone associations with joint replacement, structural progression and pain in peripheral OA

Subchondral bone feature of OA	Pain and structural associations						
	Knee structure	Knee pain	Hand structure	Hand Pain	Hip structure	Hip Pain	Ankle structure
MRI bone marrow lesions	**Progression (i)** **TKR (i)**	**LPS (i)** **IFP (n)**	**Progression (i)**	No LPS (w) No severity (n)	**Severity (w)**	**Severity (n)**	
MRI osteophytes	**Progression (i)** **TKR (n)**	**LPS (n)**	**Severity (n)**	No severity (n)			
MRI bone attrition	No Progression (0)	No severity (0)	**Severity (n)**	No severity (n)			
MRI bone shape or dimensions	**Progression (i)** **TKR (i)**	**IFP (i)** **Severity (n)**			No severity (0)		
MRI bone cyst	No progression ?severity	No LPS (n)	No severity (n)	No severity (n)		**Severity (n)**	
MRI or CT trabecular morphometry	**Progression (n)**				**Severity (n)**		
DXA or CT Peri-articular BMD	**Progression (n)**				**Severity (w)**		
2D bone shape	**Severity (w)**	**Severity (n)**			**Progression (i)** **THR (i)**		
Scintigraphy	No Progression (0)			No severity (n)			**Severity (w)**

Computed tomography (CT), dual energy X-ray absorptiometry (DXA). independent association (i), incident frequent pain (IFP), association with no or inadequate covariate adjustment (n), total knee replacement (TKR), total hip replacement (THR), mean change in longitudinal pain severity (LPS), well-adjusted association (w), association insignificant after covariate adjustment (0)..

3.5 Discussion

This systematic review is the first to have incorporated quality scoring alongside statistical adjustment in the comprehensive examination of the relationship of subchondral bone pathology with both structural progression of OA and pain for all non-conventional types of radiological imaging of peripheral joints with OA. This systematic review has concluded that there were independent associations between imaging-assessed bone pathologies and structural progression and pain in the knee, hand, and hip.

Subchondral bone pathology may lead to cartilage degeneration by altering the biomechanical force distribution across joint cartilage or disruption of the osteochondral junction and release of soluble biomediators influencing the cartilage[15, 219] (as discussed in 2.6.1 Subchondral bone cellular changes in OA). In OA the homeostatic process of subchondral bone remodelling fails, leading to increased bone turnover, volume and change in stiffness and shock-absorbing capacity[227, 610, 611]. BMLs histologically represent increased bone turnover[297] as discussed in 2.6.3.4 Subchondral bone marrow lesions. Cartilage overlying altered bone demonstrates greater damage than healthy bone in human cadaver knees[226]. That study, and an excluded study[612], concur with the independent association between BMLs, and structural progression of OA in knees and hands and total knee replacement, as concluded by this analysis. Although randomised control trials were not excluded from this review, several such trials were excluded on the basis of failure to formally quantify any correlation between BMLs with structural progression outcomes. These include the strontium[336], intensive weight-loss therapy [613] and glucosamine [614] trials and some of these describe a concordant reduction in BML size and cartilage volume loss.

Osteophytes represent subchondral bone hypertrophy typical of OA as discussed in 2.6.3.6 Osteophytes. They represent endochondral and direct bone formation and create a circumferential increase in bone area around each knee cartilage plate, particularly on the medial side in OA, which

concurs with the independent association of MRI osteophytes with structural progression observed in this analysis.

In terms of bone morphology, knee OA is associated with shallow trochlear patellar grooves in multiple epiphyseal dysplasia[273]. These findings concur with the findings of Stefanik and Kalichman and colleagues in knee OA in this review[274, 568, 569]. Anterior-cruciate ligament (ACL) rupture represents a risk factor for developing knee OA. In cases of ACL tear in previously normal knees of young healthy adults, the 3D shape of the femur, tibia and patella expands more rapidly than controls without radiographic knee OA in the subsequent 5 years[615]. The 3D shape of the same knee bones have also been associated with the outcome of joint replacement[616]. This highlights the importance of bone shape, as discussed in 2.6.3 Bone shape and subchondral bone MRI features in OA, and concurs with the conclusion from this systematic review that 3D knee shape and 2D hip shape are independently associated with structural progression and total joint replacement.

The literature review (in 2.6.3.5 Subchondral bone attrition and 2.6.3.7 Subchondral bone cysts) indicated that bone attrition and cysts were associated with structural severity of OA. However this more rigorous systematic review identified that bone attrition and cysts were associated with structural progression or severity but not after covariate adjustment, which included other OA subchondral bone features. This suggests these bone features are epiphenomenon of the pathogenic process of structural progression rather than a primary cause. This hypothesis is supported by bone cysts and attrition frequently occurring synchronously with BMLs[139, 601] and incident bone attrition has been strongly associated with the presence of BMLs within the same compartment[300].

Increasing bone volume fraction, trabecular number and thickness, but decreasing trabecular spacing on CT and MRI studies were associated with structural progression. These specific associations concur with numerous human histological and histomorphometric analyses of peripheral joint OA subchondral bone samples removed at the time of joint replacement or from

post-mortem joints with early OA and subsequently compared with normal post-mortem joints with age and gender matching [207, 617, 618].

Subchondral bone, particularly BMLs, have been found to be associated with knee, hip and hand OA pain. However some analyses measuring pain with heterogenous pain outcomes, report an absence of a longitudinal or cross-sectional association with BMLs [302, 319, 619]. Furthermore previous systematic reviews have concluded an at-most moderate association of BMLs with knee pain[132, 365]. With the benefit of incorporating more well-adjusted analyses in this systematic review, we have highlighted that BMLs are independently associated with change in longitudinal pain severity but are only associated with incident frequent knee pain. In analyses excluded from the current review, incident knee BMLs predicted incident knee pain in healthy community-based adults at risk of OA[121]. Concurrent trends in reduction of pain and BML size are observed in the zoledronic acid trial[330] and the intensive diet and exercise for arthritis trial [620]. These were not included because they did not make a formal comparison of pain and BMLs. The mechanism by which BMLs may cause pain is unknown but may include subchondral microfractures, angina from a decreased blood supply causing ischaemia and raised intraosseous pressure[136-138].

The independent association of a mismatch of the femoral and tibial articulating surface areas with incident frequent knee symptom indicates that bone shape may predict not only the incidence of radiographic knee OA[75] but also symptomatic OA.

3.6 Limitations

In terms of limitations, stratifying observational studies by quality may artificially create relatively high quality studies from a collection of generally low quality studies. However the distribution and summary statistics of quality scores indicate a suitably broad range of quality, particularly in the influential cohort studies with a mean of 54% and range of 22-83%. The decision to exclude articles with any association analysis of less than 20 patients with OA may seem arbitrary. However several papers report the

presence or absence of pain or structural progression associations based upon small numbers of patients. Our threshold decision reflects the absence of specific guidelines on how to exclude such papers, with inherent risk of imprecision, in the context of heterogenous populations and statistical analyses. Had these papers been included there would have been no change in any of the conclusions in Table 21 (data not shown). The use of joint replacement as an outcome measure has a number of limitations including the effect of patient willingness, orthopaedic variation in opinion, availability of health services and health insurance and therefore may be influenced depending upon which country and context the study is performed in.

Each of the analyses of association of bone features with the outcomes of structural progression, pain or joint replacement include a variety of different covariates for adjustment. For the purposes of this systematic review the persistence of an association after adjustment for age, gender and BMI represented an association that was ‘well-adjusted’ for important covariates of OA. However OA is a multi-tissue disease where the pathology of tissues other than subchondral bone also contribute to structural progression and pain. Therefore when describing bone feature associations with structural progression or joint replacement, the lack of adjustment for other tissue degeneration or the interaction of obesity and alignment may represent residual confounding (2.11.2.1.3 Categorical Alignment of the knee). However the association of BMLs with cartilage loss persists after adjusting for alignment[124], meniscal degeneration[599], baseline cartilage volume and bone area[600], as well as bone attrition and bone cysts[478].

Similarly when describing the association of bone features with pain, the lack of adjustment for synovitis (which is moderately associated with knee OA pain[132]) may represent residual confounding. However the association of BMLs with pain severity and incident frequent knee pain persists after adjustment for synovitis in an analysis performed by Zhang and colleagues[26].

Publication bias could not be assessed with a funnel plot as there were insufficient results for odds and relative risk ratios. The heterogenous nature of the measures of bone features and structural or pain outcomes, precluded a meta-analysis or calculation of an effect size. This was because there were insufficient analyses describing the same association between the same bone feature and outcome measure pair.

Ultrasound represents an important and increasingly accessible imaging modality for use in routine clinical practice. It is a sensitive imaging technique for detecting 3D, early and established structural pathology in OA joints and can directly visualise osteophytes, sclerosis and cysts in the subchondral bone[621]. Therefore this modality could have been included in this review.

3.7 Conclusions

In conclusion subchondral bone plays an integral role in the pathogenesis of OA. BMLs, MRI osteophytes and tibial bone area are independently associated with structural progression of the knee. BMLs and 2D tibial bone area are independently associated with total knee replacement. BMLs are independently associated with hand OA structural progression and 2D hip bone shape is associated with structural hip progression and total hip replacement. BMLs are independently associated with longitudinal change in pain severity and femorotibial articulating area mismatch is independently associated with incident frequent knee pain

The existing standard for measuring structural progression, radiographic joint space narrowing (JSN), poorly correlates with the clinical syndrome and remains a relatively insensitive measure (see 2.11 Imaging biomarkers in OA). When JSN is used as a trial outcome measure this demands that clinical trials are large, long and expensive. Therefore the unmet need for more sensitive and validated imaging biomarkers is huge.

The independent associations of subchondral bone features with important patient-centred outcomes (pain and TKR) and structural progression

suggest they may be valid surrogate measures of these outcomes. While many of these are MRI-derived measures, they are intrinsically more sensitive than radiographic JSN (see 2.11Imaging biomarkers in OA), their use as clinical outcomes may substantially reduce the cost, duration and size of future trials. They may also improve the precision of OA phenotypic stratification to facilitate pathology-specific treatment, prioritisation of individuals most in need of OA modification and measuring treatment response.

This systematic review highlights the need for greater information on the validity of subchondral bone features to be used as surrogate measures of OA patient-centred outcomes in all joints. There was very little evidence describing the validity of 3D bone shape as a surrogate measure. This unmet need was addressed in writing the following chapters.

3.8 Thesis findings and the recent literature

The systematic literature review undertaken here in Chapter 3 was inclusive of studies up to September 2014. However in order to ensure this literature review is up to date, the literature in the intervening period has been reviewed to assess whether it would change the conclusions made in this Chapter. Cohort studies are described separately from cross-sectional and case-control studies in accordance with the methods of this chapter.

3.8.1 The relationship between knee bone feature and structural progression

3.8.1.1 Cohort studies

In total three new cohort studies were identified. Sharma and colleagues identified a subcohort of knees ‘at risk’ of knee OA that did not have radiographic OA within the OAI. Knee BMLs at baseline were independently associated with an increased risk of incident radiographic OA [622]. Wluka

and colleagues described an analysis of knees in a community cohort without knee OA symptoms. Knee BMLs at baseline were associated with medial tibiofemoral cartilage volume loss[623]. Wang and colleagues established a longitudinal cohort of knees of older adults and patellar BMLs at baseline were independently associated with progressive cartilage loss[624]. These associations have already been described as independent associations already and therefore these new reports would not change the conclusions of this chapter.

3.8.1.2 Cross-sectional or case-control studies

In total two new case-control studies were identified and both were nested within the OAI. Roemer and colleagues described an association of incident radiographic knee OA[122] with knee bone marrow lesions. Hunter and colleagues performed a case-control study that identified that longitudinal change in bone shape biomarkers of bone area (tAB) and 3D bone shape were both associated with medial tibiofemoral structural progression [625].

In this chapter, the methods clarify that case-controls cannot be used to describe the independence of an association and therefore the conclusions of this chapter would not change with these new findings.

3.8.2 The relationship between subchondral bone features and pain

3.8.2.1 Cohort studies

In total three new cohort studies were identified. Sharma and colleagues identified a subcohort of knees ‘at risk’ of OA that did not have radiographic OA within the OAI. Within this subcohort knee BMLs at baseline were independently associated with an increased risk of incident persistent knee pain [622]. Wluka and colleagues described an analysis of knees in a community cohort without knee OA symptoms. Knee BMLs at baseline were associated with incident pain [623]. Wang and colleagues established a longitudinal cohort of knees of older adults and patellar BMLs at baseline were independently associated with progressive knee pain[624].

These associations have already been described as independent associations and therefore these new analyses will not change the conclusions within this thesis.

3.8.2.2 Cross-sectional or Case control studies

In total one new case-control study and one cross-sectional study were identified. Hunter and colleagues performed a case-control study nested within the OAI that identified that longitudinal change in bone shape biomarkers of bone area (tAB) and 3D bone shape were both associated with knee pain progression. However the associations with pain progression were less strong compared to structural progression [625].

Stefanik and colleagues described a cross-sectional sample of knees within the MOST and Framingham OA participants. An association between the presence of knee BMLs in the patellofemoral joint and pain was observed[626]. The methods in this chapter clarify that case-controls cannot be used to describe the independence of an association and therefore the these new analyses will not change any previous conclusions.

3.8.3 The relationship between subchondral bone features and joint replacement

3.8.3.1 Cohort studies

In total two new cohort studies were identified. Agricola and colleagues established that in the Cohort Hip and Cohort Knee and Chingford cohorts femoral bone shape based upon hip radiograph segmentation was independently associated with incident joint replacement of the hip[627]. Hafezi-Nejad and colleagues established that in a subcohort of knees within the OAI, baseline semi-quantitative knee BMLs were associated with incident total knee replacement [628]. These associations have already been described as independent associations and therefore these new analyses will not change the conclusions of this chapter.

3.8.3.2 Cross-sectional and case-control studies

In total only one new case-control study was identified. Roemer and colleagues described an association of incident total knee replacement [105] with knee BMLs. This was a case-control study nested within the OAI. This association has previously been described in this chapter and will not change the conclusions in This chapter.

Chapter 4 The relationship between clinical characteristics, radiographic osteoarthritis and 3D bone area

4.1 Introduction

In chapter three the systematic literature review identified the need for evidence of the validity of 3D bone measures as imaging biomarkers. This chapter describes construct validity by exploring the relationship of 3D bone structure of OA with the established constructs of radiographic structural OA severity.

Until recently, structural modification trials have relied upon conventional radiography to define both the OA phenotype for participant inclusion and for measuring structural progression. Conventional radiography is less sensitive and specific in detecting structural pathology and structural progression than magnetic resonance imaging (MRI) [23, 86](2.11 Imaging biomarkers in OA). MRI is therefore increasingly used to provide assessment of OA pathology. Another advantage of MRI is that its three dimensional data can be harnessed to provide quantification of important tissues using manual segmentation [31, 269, 440, 560], or automated analysis techniques such as active appearance modelling (AAM) that enables relatively rapid, accurate quantification of large datasets [629, 630](2.10 Statistical Shape modelling, active shape modelling and active appearance modelling).

Modern imaging approaches recognise that OA is a whole joint disease which may involve multiple tissues which confer different phenotypes[631]; subchondral bone in particular is integral to the pathogenesis and progression of OA [255, 631](2.6 Subchondral bone in OA). In particular, the area of subchondral bone (Figure 23) at the femorotibial articulation is larger in OA knees than healthy controls and correlates with knee joint space narrowing, osteophytes and Kellgren Lawrence (KL) grade after adjusting for

at least age and body mass index in cross-sectional studies[31, 269, 560]. While the severity of conventional radiographic OA may correlate with subchondral bone area expansion, the additional value of bone area expansion of OA and the extent to which radiographic measures explain variation in this is unknown. Height, weight, gender and age are determinants of bone area in healthy knees [256, 257].Therefore the objective of this study was to determine the bone area expansion attributable to OA and then establish what proportion of the variation of this is explained by radiographic measures of knee OA (metric joint space width, osteophyte grade and, subchondral sclerosis grade).

4.2 Methods

Data used in the preparation of this cross-sectional analysis were obtained from the NIH Osteoarthritis Initiative (OAI) database, which is available for public access at http://www.oai.ucsf.edu/ and is described in 2.12 The Osteoarthritis Initiative. This is a database of a multi-centre, prospective, longitudinal observational study of knee OA including approximately 4796 participants [515]. Knee radiographs and knee MRI scans were performed at baseline for all participants.

The main subsample of knees was selected from those with available Kellgren Lawrence (KL) and other radiographic OA measure scoring from the central Boston University reads of plain films in the OAI. The availability of osteophyte and subchondral sclerosis scores was limited to knees of individuals who have had confirmed presence of radiographic OA (KL grade ≥2) in either knee at any time point. Participants without available KL, osteophyte and subchondral sclerosis grade data were excluded and the knee with the highest KL grade for each participant was selected. When the grades for both knees were the same, the right knee was chosen. Baseline MRI, radiographic and clinical data were included. A second subsample of ‘normal’ knees was selected in order to establish a formula for predicting ‘normal’ bone area based upon height, weight, age and gender. From the

whole OAI cohort only knees were included with KL and WOMAC scores of zero at baseline, one, two and four year time points and the absence of any historic OA knee symptoms prior to baseline.

MRI sequences collected in the OAI are described in detail by Peterfy and colleagues [497]. The current study utilised the double-echo-in-steady-state sequence (DESS-we) of the Siemens 3T trio systems [497]. A training set of 96 knee MRIs, using the DESS-we sequence, were used to build active appearance models for the tibia and femur. This training set was selected to contain examples of each stage of OA with approximately equal numbers of knees fulfilling each KL grade. The mean bone shape had anatomical regions outlined as described previously (Figure 44)[632]. We used a definition of the area of subchondral bone or 'tAB' similar to that designated by a nomenclature committee [271]. However this definition was modified to include bone ('peripheral osteophytes') from around the cartilage plate. The boundary between the medial femur (MF) / medial trochlear femur and the lateral femur / lateral trochlear femur boundary in the femur was defined as a line on the bone corresponding to the anterior edge of the medial or lateral meniscus, and extended smoothly to the edge of the tAB. Active appearance models were used for the calculation of tAB from knee MRIs which measured the undulating 3D surface of bone. The surface area of the 3D subchondral bone (tAB) was measured in mm^2.

The medial compartment of the tibiofemoral joint was selected to compare medial femur (MF) tAB and medial tibia (MT) tAB with medial joint radiographic measures on the basis that this compartment is more frequently affected with OA. The following baseline radiographic OA measures are described earlier (2.11.1.1 Conventional radiographic quantitative measures263 and 2.11.2.1 Conventional radiographic semi-quantitative measures). These were selected and divided into three non-KL (OARSI and metric) measures and KL grade: metric minimum joint space width (mJSW) of the medial compartment on continuous scale, subchondral sclerosis score of the medial femur or tibia (OARSI categorical scale 0-3), osteophyte score of the medial femur or tibia (OARSI categorical scale 0-3), KL grade

(categorical scale 0-4). These assessments were provided by the OAI. A semi-automated tool, shown to be as sensitive as manual measures, was used to measure mJSW [424, 633]. Further details of the methodology for these assessments is available [634].

Clinical baseline characteristics, provided by the OAI, included the known important clinical risk factors for knee OA: age, gender, weight, height and ethnicity and goniometer-measured knee alignment [59, 635, 636]. It was this existing clinical knowledge, not a data-driven strategy, that guided the selection of covariates for statistical modelling.

Figure 44 Anatomical Bone areas

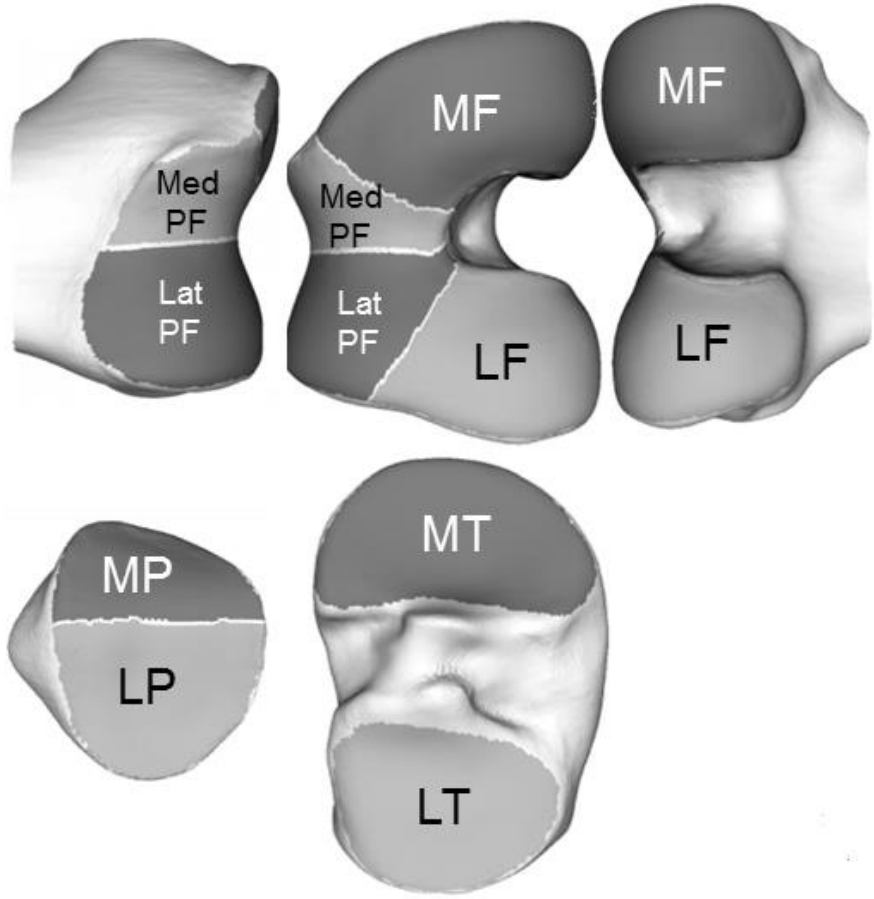

LF (lateral femur), MF (medial femur), MT (medial tibia), LT (lateral tibia), MP (medial patella), LP (lateral patella), LatPF (lateral trochlear), MedPF (medial trochlear)

4.2.1 Statistical analysis

Statistical analysis was conducted using STATA software, version 12 (College Station, TX, 2009). For categorical socio-demographic variables, chi- square tests were performed comparing participants with radiographic OA and those without radiographic OA. Alignment was trichotomised into extreme valgus (<-6°) intermediate alignment (-6° to 6°; reference category) and extreme varus (>6°).

To establish which covariates might operate as potential confounders, mediators or competing exposures in the multivariable regression analyses exploring the amount of variation explained by radiographic measures, a causal path diagram was constructed in the form a Directed Acyclic Graph (DAG) [637].This was drawn from established and hypothesized functional relationships between bone area and each covariate. No non-causal structural association between the radiographic exposure and the bone area outcome was identified (Figure 45).

Figure 45 A directed acyclic graph

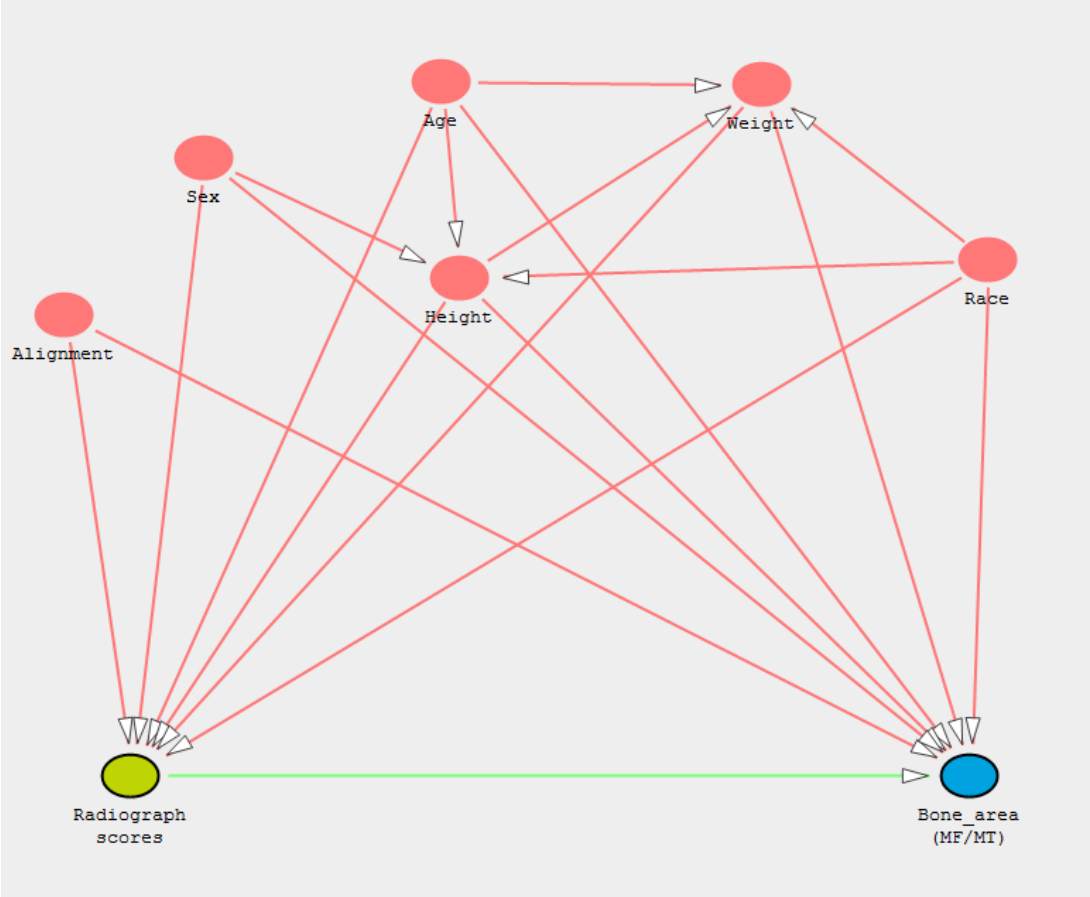

A DAG is used to establish which factors are confounders and mediators to ensure a parsimonious model is achieved and that over-adjustment does not in the statistical analysis.

The benefit of this approach is that it provides an explicit *a priori* model of the postulated relationships between the exposure, outcome variables and each of the available covariates. Such models are invaluable for the specification and verification of the statistical analyses and results in appropriate adjustment and the most parsimonious model being chosen without the risk of over adjustment and thus reduction of statistical power which would otherwise occur.

The first analyses used the ‘normal’ subsample to obtain estimates of what normal bone area should be in the normal population. These estimates were obtained by modelling bone area with height, weight and age, stratified by

sex thereby producing estimates that accounted for the sex differences in bone area (2.6.3.1.1 Knee subchondral bone cross-sectional area). Having obtained the estimates, predicted bone area could be calculated for each of the 2588 knees in the main subsample.

Bone area (MF) =intercept + (A)(HEIGHT) + (B)(WEIGHT) + (C)(AGE) +ε

This was subtracted from the measured bone area (tAB) in each of the 2588 knees to provide the area of bone attributable to OA (OA-tAB)

Multivariable linear regression models were then constructed to determine the proportion of OA-tAB for MF and MT that could be explained by either non-KL measures of radiographic damage (joint space width, sclerosis, osteophytes) or KL grade. Although the methods of scoring non-KL measures of damage are different to that included in the KL scoring system, they measure similar pathology therefore models did not include both to avoid multicollinearity. These models were adjusted for alignment and ethnicity in different combinations and at each stage.

For univariable analyses two-tailed p-values have been presented ($p<0.05$ was considered evidence of association without adjustment for multiplicity); for multivariable analyses 95% confidence intervals have been provided to give an indication of significance at the 5% level. However due to the large sample size we have considered both statistical significance and the associated improvement in R-squared when reporting which variables were associated with tAB to a substantive extent. Normality of residuals and homoscedasticity of errors was assessed using residual diagnostic plots as well as formal tests of heteroscedasticity (White`s test and Breusch-Pagan test) and underlying assumptions of a Gaussian distribution and homoscedasticity were met.

4.3 Results

Of the 4796 participants in the OAI database 131 met the criteria for ‘normal’ knees (Figure 46). Mean age was 60 years and 58 % were female with 12 % being obese (BMI greater than 30kg/m^2). Of the 4796 participants in the OAI

database, 4490 had KL data available. After applying the inclusion criteria for selection of the main subsample, 2588 (57%) knees had radiographic and clinical data available for analysis (Figure 47). Mean age was 61 years and 58% were female with 37% being obese.

Figure 46 Participant flow diagram for the 'normal' knee subsample

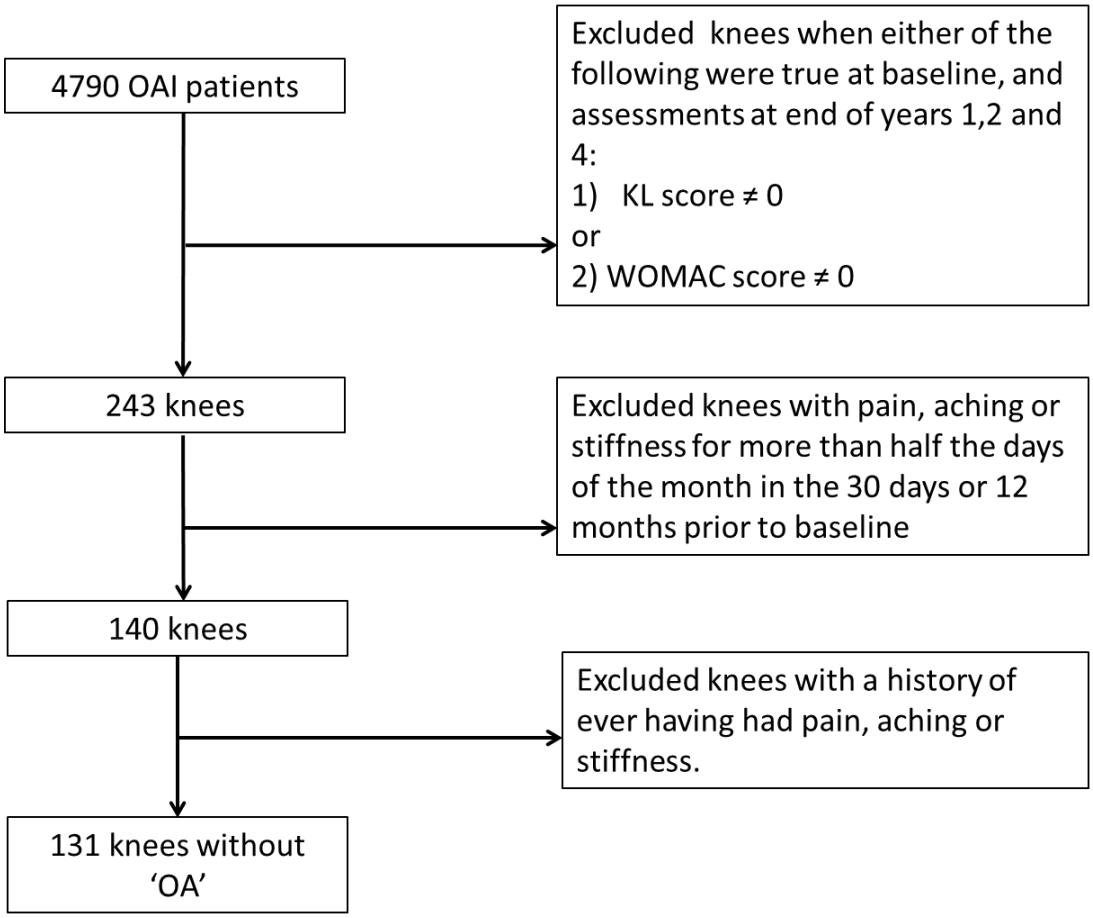

Identifying suitable knees for describing the association of bone area with height, weight and age in knees without OA.

Figure 47 Participant flow diagram

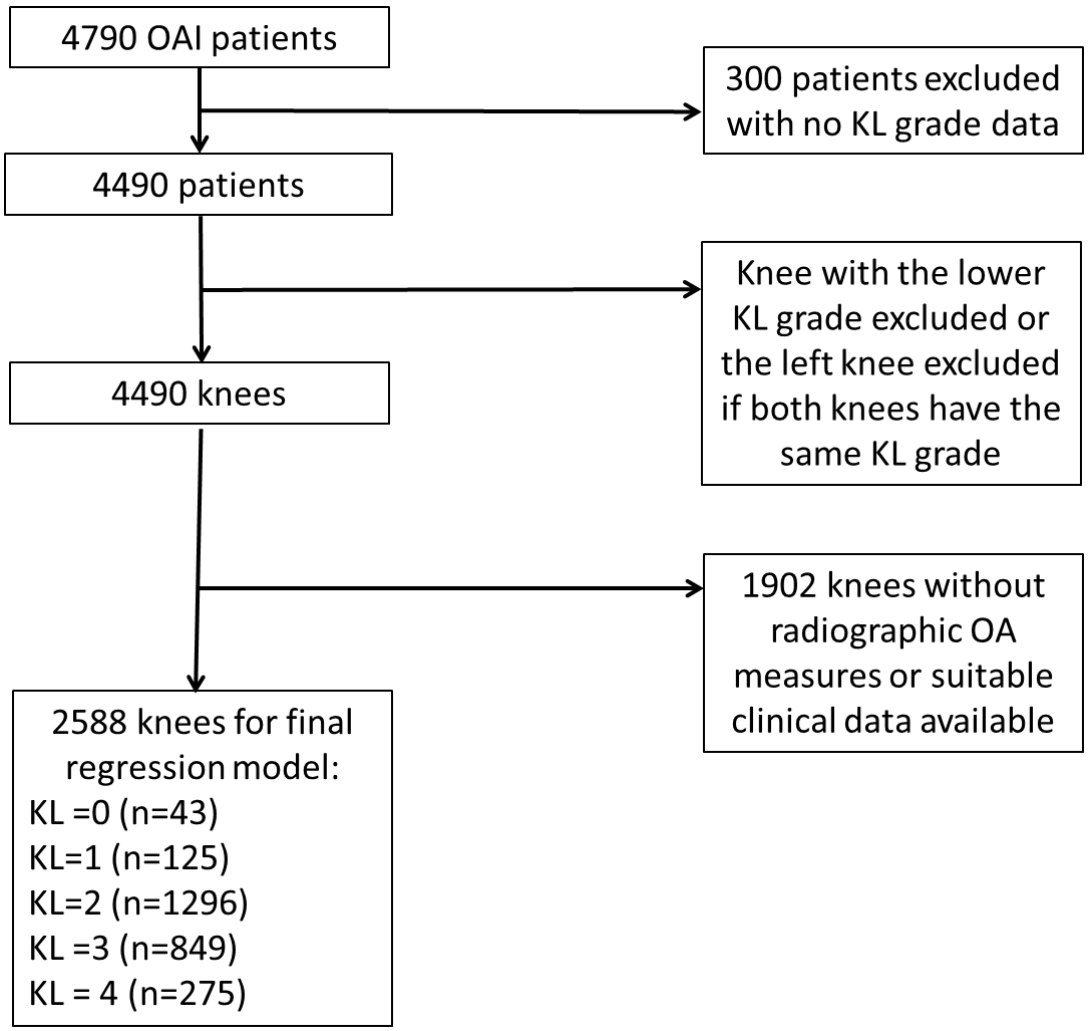

Identifying suitable knees for describing the association of OA-attributable bone area with conventional radiographic measures of OA.

4.3.1 Models of the 'normal' knee subsample with clinical data

When considering the clinical covariates stratified by sex, height, weight, and age in males explained 22.5%, 21.6%, and 3.5% of the MF tAB variance respectively in univariable analyses. In females these clinical covariates explained 43.1%, 32.1% and 0.1% of the MF tAB (Table 22). Similar values were identified for MT tAB (Table 23). The greatest variance in tAB was explained by height in both medial compartment models in both sexes. When all the clinical covariates were entered in the model they explained 26.6% and 28.9% variance in MF and MT tAB respectively for males, while in females they accounted for 54.4% and 53.7% in MF and MT tAB

respectively (Table 24, Table 25). In general, taller and heavier individuals had greater tAB (Figure 48). Females were more likely to have smaller tAB having adjusted for height and weight compared to males (Table 26, Table 27). Considering Table 22 and 23, age was not statistically significantly associated with tAB (p=0.08 in Table 23). However it was included in the non-exposed group models due to existing clinical knowledge that bone expands with age and hence it was included in the DAG.

In order to check whether the linearity assumption held between age and the outcome variable (bone area), a formal statistical test (linktest) was performed for each shape model and this was found to be not significant i.e. the null model is that the model is linear.

The hatsq variable using linktest was found to be not significant (p=0.93) and coupled with linearity plots which suggested a linear relationship, albeit only minimal (Figure 49), there was therefore no evidence of non-linearity or need to use higher order terms for age. Hence it was modelled in its original form. The augmented component-plus-residual plots (Figure 49, Figure 50) suggest mild departure from normality which suggested probably adding a squared version of age, however the model fit and other linearity checks were satisfactory to suggest a linear relationship between age and MF and MT. Therefore the addition of higher order terms (e.g. adding $(age)^2$ for ease of interpretation) was considered unnecessary.

Another non-graphical test, the Breusch –Pagan test was performed to test that the model residuals were homoscedastic. The test was not significant (p=0.60) and therefore the conclusion was drawn that the model residuals were homogenous.

4.3.2 Models with OA-attributable bone area

In univariable analysis both varus and valgus alignment tended to be associated with larger bone area, and explained 2% and 1.2% of the variation in MF OA-tAB and MT OA-tAB respectively (Model 2; Table 30, Table 31). Having adjusted for radiographic measures (models 7 & 8; Table

30, Table 31) extreme valgus alignment was not consistently associated with differences in bone area to a significant degree.

When using the non-KL radiographic variables on a univariable basis, JSW, osteophytes and sclerosis were each significantly associated with MF OA-tAB, however each explained just 5.3%, 14.9% and 10.1% of the variance of MF OA-tAB (Table 28). Higher grades for osteophytes and sclerosis were associated with larger bone areas, whilst wider joint spaces were associated with smaller bone areas. In the univariable MT OA-tAB models, the variance explained by JSW, osteophytes and sclerosis was 6.0%, 10.1% and 8.3% respectively (Table 29).

When entered simultaneously into a model that did not adjust for alignment, the non-KL radiographic variables were associated with OA-tAB independently of each other, but accounted for just 17.4% and 12.9.% of the variance in MF and MT OA-tAB respectively (Model 3: Table 30, Table 31). In the MF OA-tAB model some counter-intuitive trends were observed such as a wider JSW being associated with a larger bone area.

Adjusting for alignment, when entered individually JSW, osteophytes and sclerosis were still independently associated with OA-tAB in the expected direction, and explained an additional 6.7%, 17.2.% and 11.5% of MF OA-tAB variance (Models 4, 5 & 6: Table 30). When entered simultaneously the radiographic variables explained 18.7% of MF OA-tAB variance having adjusted for alignment (Model 7, Table 30). Comparing models 4 and 7, after adjusting, alignment and the non-KL radiographic variables the association between JSW and OA-tAB was reduced in magnitude, to the extent that it did not differ significantly from zero. Similarly in model 7 the differences in OA-tAB between knees with sclerosis grades 1-3 and those without sclerosis were reduced compared to model 6, although grades 2 & 3 still differed from grade 0. The coefficients for osteophyte grades 1, 2 & 3 remained comparatively stable between models 5 & 7.

Adjusting for alignment, JSW, osteophytes and sclerosis explained an 8.3%, 12.8% and 10.4% MT OA-tAB variance individually (models 4, 5 & 6: Table 31); when entered simultaneously they explained approximately 13.5% of

variance in MT OA-tAB (Model 7,Table 31). Similar trends to those found for MF OA-tAB were observed in the differences in the non-KL radiographic variable coefficients between models 4-6 and model 7.

When using the KL grade on a univariable basis, grades 1-4 were associated with greater OA-tAB compared to grade 0; the higher the grade, the greater the difference (Table 28, Table 29). Having adjusted for alignment, (Model 8: Table 30, Table 31) the differences were slightly reduced in magnitude for KL3 and KL4, but KL remained independently associated with both MF and MT OA- tAB. Compared to the model in which the non-KL radiographic variables were entered simultaneously whilst adjusting for clinical variables (Model 7: Table 30, Table 31), the adjusted KL model explained slightly more variance for both MF OA-tAB (adjusted R^2 KL= 0.209 vs non-KL=0.187) and MT OA-tAB (adjusted R^2 KL=0.147 vs non-KL=0.135) but the differences were not substantive.

Table 22 Univariable models between medial femur bone area and selected clinical variables in non-exposed group

Medial femur	Male model		Female model	
	Coefficient (95% CI),significance	R-squared	Coefficient (95% CI),significance	R-squared
Clinical characteristic				
Height (mm)	1.47(0.75,2.18), p<0.001	0.225	2.13(1.55,2.71), p<0.001	0.413
Weight (Kg)	6.57(3.29,9.84), p<0.001	0.216	10.25(6.87,13.63), p<0.001	0.321
Age (yrs)	-4.69(-10.12,0.73), p=0.09	0.035	-0.19(-5.28,4.90),p=0.94	0.013

Table 23 Univariable models between medial tibia bone area and selected clinical variables in non-exposed group

Medial tibia	Male model		Female model	
	Coefficient (95% CI),significance	R-squared	Coefficient (95% CI),significance	R-squared
Clinical characteristic				
Height	0.80(0.41,1.20), p<0.001	0.220	0.98(0.70,1.26), p<0.001	0.394
Weight (Kg)	3.92(2.15,5.69), p<0.001	0.254	4.90(3.31,6.48), p<0.001	0.329
Age (yrs)	-2.68(-5.67,0.32), p=0.08	0.039	0.09(-2.31,2.49),p=0.94	0.013

Table 24 Associations between medial femur bone area and selected clinical variables in non-exposed group

Medial femur	Male model		Female model	
	Coefficient (95% CI),significance	R-squared	Coefficient (95% CI),significance	R-squared
Clinical characteristic				
Height (mm)	1.01(0.14,1.89) p=0.023	0.266	1.79(1.21,2.38) p<0.001	0.544
Weight (Kg)	4.27(0.45,8.10) p=0.029		6.47(3.38,9.58) p<0.001	
Age (yrs)	0.84(-4.55,6.24) p=0.755		2.24(-1.46,5.95)p=0.231	

Table 25 Associations between medial tibia bone area and selected clinical variables in non-exposed group

Medial tibia	Male model		Female model	
	Coefficient (95% CI),significance	R-squared	Coefficient (95% CI),significance	R-squared
Clinical characteristic				
Height (mm)	0.50(0.03,0.98) p=0.039	0.289	0.83(0.55,1.10) p<0.001	0.537
Weight (Kg)	2.79(0.71,4.87) p=0.010		3.14(1.67,4.61) p<0.001	
Age (yrs)	0.44(-2.50,3.38) p=0.767		1.19(-0.57,2.95)p=0.182	

Table 26 Relationship between medial femur bone area and clinical model not stratified by sex

Medial femur	Coefficient (95%CI)	p-value
Height (mm)	1.48 (0.98,1.98)	<0.001
Weight (Kg)	5.08 (2.74,7.42)	<0.001
Age (yrs)	2.28 (-0.76,5.32)	0.14
*Sex (female)	-253.74 (-339.94,-167.54)	<0.001

Table 27 Relationship between medial tibia bone area and clinical model not stratified by sex

Medial tibia	Coefficient (95%CI)	p-value
Height (mm)	0.69 (0.44,0.95)	<0.001
Weight (Kg)	2.89 (1.70,4.08)	<0.001
Age (yrs)	1.03 (-0.51,2.57)	0.19
*Sex (female)	-135.56 (-179.32,-91.80)	<0.001

Figure 48 The relationship between height and weight on medial femur area

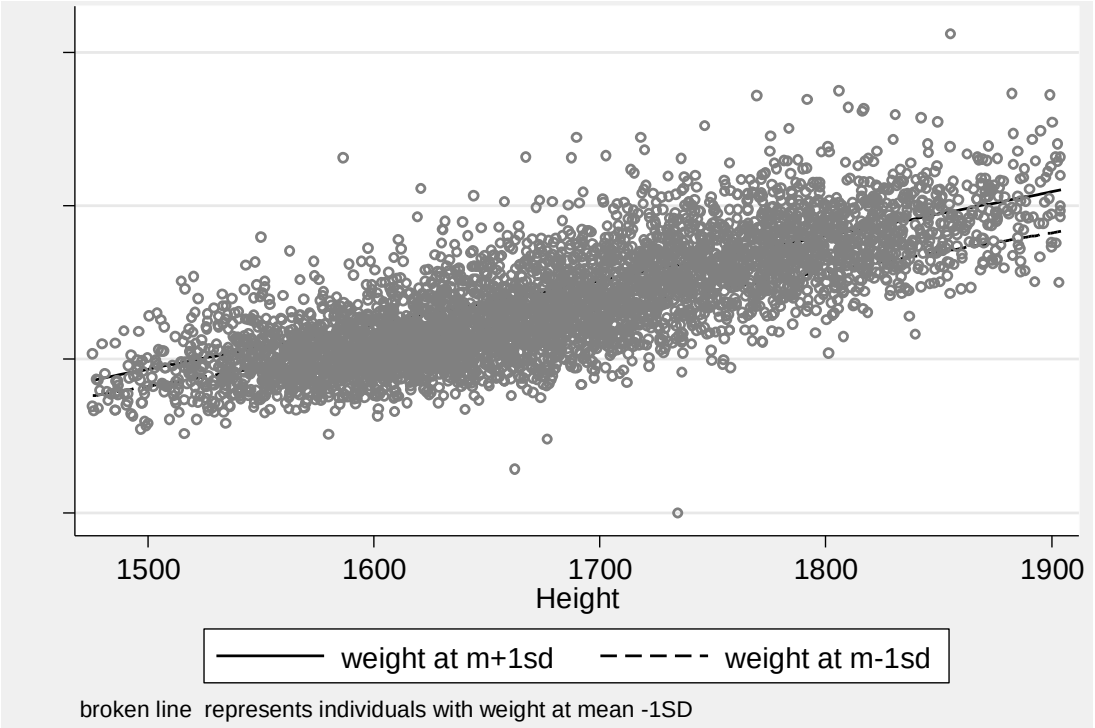

Medial femur area (mm^2), Height (mm)

Figure 49 Augmented component-plus-residual plot of age and MF

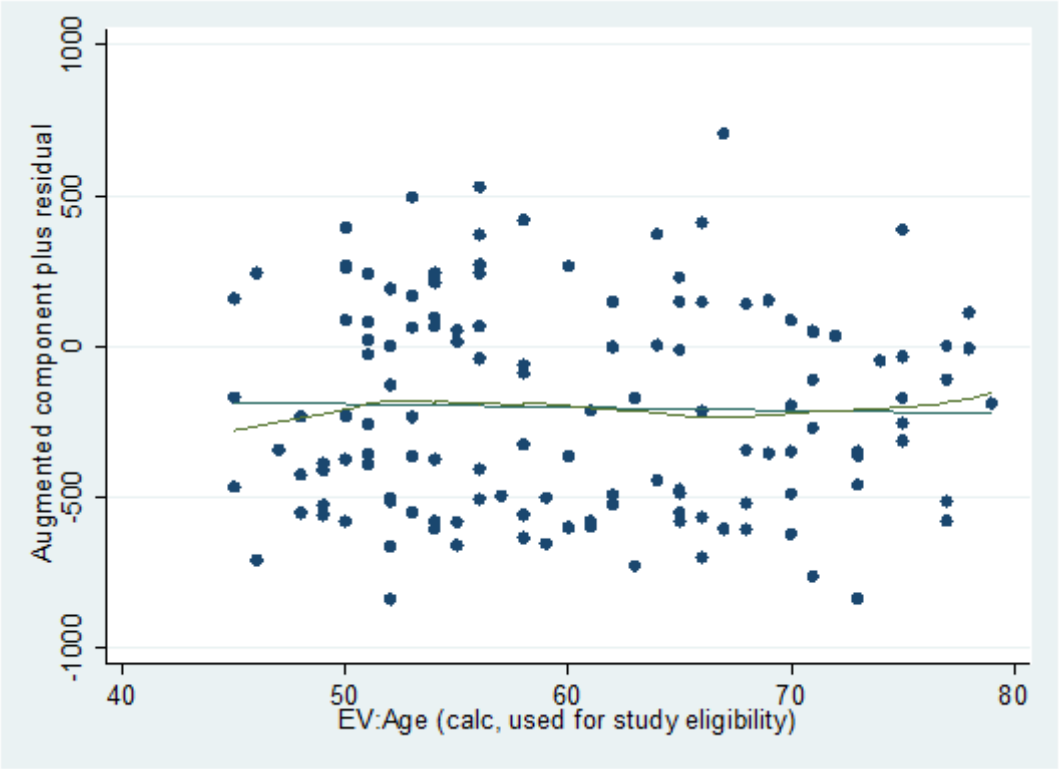

MF – medial femur area (mm^2), Age (yrs)

This augmented component-plus-residual plot suggests a mild departure from normality suggesting a higher order term (i.e. age^2 may be necessary. However the model fit and other linearity checks were satisfactory to suggest a linear relationship between age and MF.

Figure 50 Augmented component-plus-residual plot of age and MT

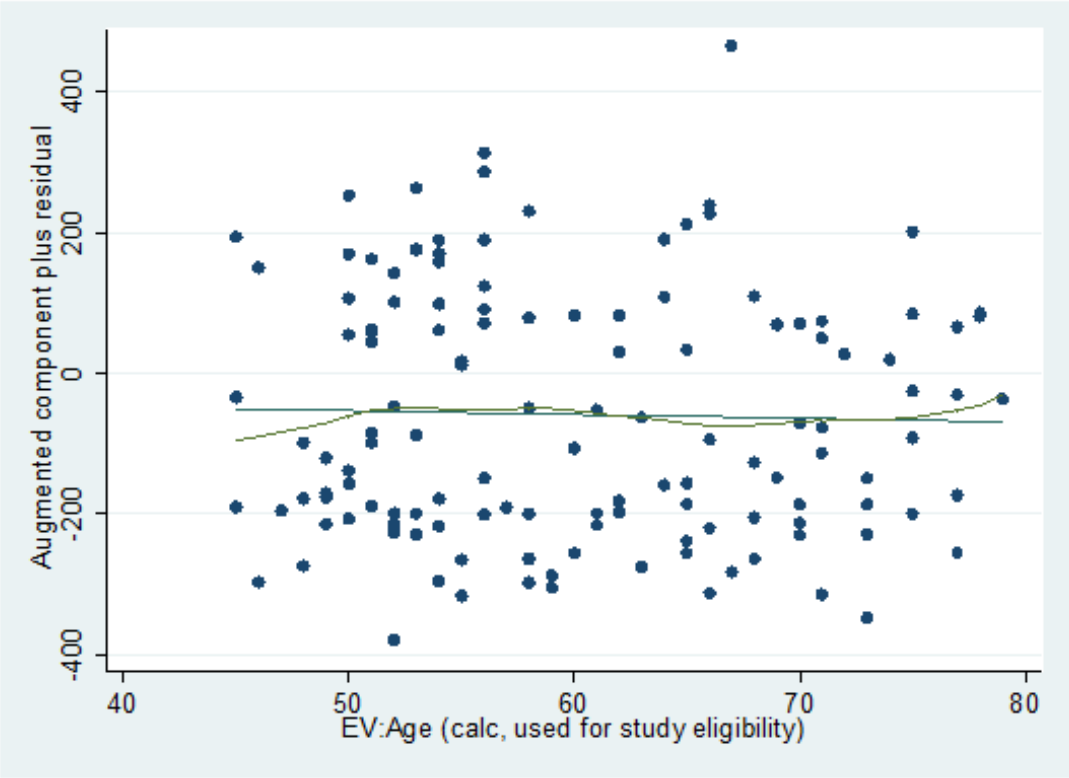

MT- medial tibia area (mm^2), Age (yrs)
This augmented component-plus-residual plot suggests a mild departure from normality suggesting a higher order term (i.e. age^2 may be necessary. However the model fit and other linearity checks were satisfactory to suggest a linear relationship between age and MT

Table 28 Univariable regression analysis of non-KL radiographic variables with medial femur area

Medial femur	Coefficient (95%CI)	p-value	Adjusted r-squared
Osteophytes (ref 0)			
Grade1	23.48 (3.21,43.76)		
Grade2	91.40 (64.28,118.52)		
Grade 3	242.46 (219.71,265.21)	<0.001	0.149
Sclerosis (ref zero)	23.80 (2.33,45.27)		
Grade1	164.02		
Grade2	(141.10,186.94)	<0.001	0.102
Grade 3	301.54 (257.76,352.33)		
Min JSW	-35.46 (-40.87,-30.06)	<0.001	0.053
KL grade(ref zero)			
Grade1	30.89 (12.60,49.19)		
Grade2	63.97 (48.78,79.16)		
Grade3	170.37		
Grade4	(153.36,187.38) 383.64 (358.22,409.06)	<0.001	0.203

Table 29 Univariable regression analysis of non-KL radiographic variables with medial tibia area

Medial tibia	Coefficient (95%CI)	p-value	Adjusted r-squared
Osteophytes (ref 0)			
Grade1	23.18 (13.83,32.53)		0.102
Grade2	69.57 (56.08,83.06)		
Grade 3	133.00 (116.52,149.47)	<0.001	
Sclerosis (ref zero)			
Grade1	22.75 (12.83,32.66)		
Grade2	67.00 (56.17,77.84)		
Grade 3	124.94 (103.13,146.75)	<0.001	0.083
Min JSW	-17.54 (-20.02,-15.06)	<0.001	0.061
KL grade(ref zero)			
Grade1	13.51 (4.71,22.32)		
Grade2	12.47 (5.16,19.78)		
Grade3	60.09 (51.91,68.28)		
Grade4	140.78 (128.55,153.02)	<0.001	0.131

Table 30 Multivariable associations between OA-attributable medial femur area and radiographic variables

Clinical characteristic	Model 2	Model 3	Model 4	Model 5	Model 6	Model 7	Model 8
Alignment **Less than -6º** **Greater than 6º**	 39.58 (6.44, 72..73) 146.53 (111.49, 181.58)		 71.59 (30.84, 112.33) 131.78 (89.61, 173.96)	 8.09 (-30.87, 47.05) 158.18 (116.53, 199.84)	 53.37 (13.06, 93.68) 124.89 (81.09, 168.70)	 17.21 (-22.44, 56.87) 131.39 (88.97, 173.81)	 -3.04 (-32.91, 26.84) 82.54 (50.79, 114.29)
Radiographic variables							
JSW		2.92 (-5.21, 11.06)	-33.17 (-38.69, -27.64)			3.91(-4.24, 12.05)	
Osteophytes* **Grade1** **Grade2** **Grade3**		 12.58 (-8.55, 33.70) 58.89 (29.75, 88.02) 193.38 (166.87, 219.90)		 23.98 (3.90, 44.06) 90.39 (63.44, 117.35) 240.28 (217.65, 262.92)		 13.52 (-7.53, 34.57) 59.56 (30.44, 88.68) 195.92 (169.36, 222.49)	
Sclerosis* **Grade1** **Grade2** **Grade3**		 -0.17 (-24.72, 24.38) 89.53 (55.95, 123.11) 171.52 (109.59, 233.44)			 24.55 (3.12, 45.99) 157.30 (134.30, 180.30) 276.89 (225.62, 328.15)	 -0.23 (-24.66, 24.20) 83.74 (50.32, 117.18) 147.19 (85.14, 209.25)	
KL grade* **Grade1** **Grade2** **Grade3** **Grade4**							 32.20 (13.52, 50.88) 66.42 (50.91, 81.93) 170.33 (153.03,187.63) 375.86 (349.88, 401.74)
R-squared	0.02	0.174	0.067	0.172	0.115	0.187	0.209
Model F (p=)	36 (p<0.001)	70 (p<0.001)	52 (p<0.001)	93(p<0.001)	58 (p<0.001)	60 (p<0.001)	161 (p<0.001)

JSW – joint space width, KL – Kellgren Lawrence. *For all categorical variable models, the reference group is grade zero. ** The alignment reference group is -6 to +6 º

Table 31 Multivariable associations between OA-attributable medial tibia area and radiographic variables

Clinical characteristic	Model 2	Model 3	Model 4	Model 5	Model 6	Model 7	Model 8
Alignment ** **Less than -6º** **Greater than 6º**	 4.25 (-11.07, 19.57) 60.72 (44.52, 76.91)		 20.46 (1.82, 39.09) 52.43 (33.14, 71.72)	 5.80 (-12.71, 24.30) 52.00 (31.97, 72.05)	 12.53 (-6.28, 31.35) 51.54 (30.95, 71.93)	 10.06 (-8.79, 28.91) 44.82 (24.47, 65.17)	 -10.66 (-24.96, 3.65) 37.00 (21.80, 52.20)
Radiographic variables							
JSW		-2.93 (-6.80, 0.93)	-16.69 (-19.22, -14.16)			-2.87 (-6.76, 1.02)	
Osteophytes * **Grade1** **Grade2** **Grade3**		 15.47 (5.37, 25.58) 48.20 (32.61, 63.80) 98.60 (78.49, 118.72)		 22.56 (13.32, 31.81) 67.91 (54.51, 81.32) 128.28 (111.85, 144.72)		 15.26 (5.16, 25.37) 46.65 (31.04, 62.26) 96.14 (76.02, 116.25)	
Sclerosis* **Grade1** **Grade2** **Grade3**		 7.93 (-3.48, 19.35) 26.08 (10.32, 41.84) 45.07 (15.95, 74.20)			 23.28 (13.42, 33.15) 63.20 (52.39, 74.01) 113.66 (91.69, 135.63)	 8.54 (-2.87, 19.97) 24.71 (8.96, 40.46) 38.42 (9.15, 67.68	
KL grade* **Grade1** **Grade2** **Grade3** **Grade4**							 14.76 (5.82, 23.71) 15.56 (8.13, 22.99) 62.04 (53.76, 70.33) 138.47 (126.08, 150.87)
R-squared	0.012	0.129	0.083	0.128	0.104	0.135	0.147
Model F (p=)	27 (p<0.001)	49 (p<0.001)	66 (p<0.001)	66 (p<0.001)	53 (p<0.001)	41 (p<0.001)	106 (p<0.001)

JSW – joint space width, KL – Kellgren Lawrence. *For all categorical variable models, the reference group is grade zero. ** The alignment reference group is -6 to +6 º

4.4 Discussion

This cross-sectional analysis is the first to establish the proportion of OA-attributable tAB variance explained by a comprehensive set of traditional radiographic measures of OA using automated imaging analysis technology in a large OA cohort. The accuracy of the relationship between radiographic OA and tAB is uniquely described with the use of 3D images of knee bones and the lowest coefficient of the variance of tAB measurement, in the published literature, of less than 1%[632].

When considering the regression models of 'normal' knees the largest proportion of variance in tAB in the current study was described by participant height for both MF and MT tAB. This allometric relationship has previously been described in young healthy individuals with normal knee joints using manual segmentation of knee MRIs and multi-linear regression modelling [257]. We similarly observed that this allometric relationship explained a greater proportion of variance in tAB in females.

Tibial tAB has been reported to significantly correlate with increasing age in healthy populations [258, 638]. A similar relationship has been described both in populations with knee OA and in healthy participants, although this correlation significantly reduced in magnitude after adjusting for the presence of radiographic OA, suggesting tAB enlargement is directly relevant to OA [639]. In this analysis of a population with normal knees a linear relationship between tAB and age was also noted. However this association was not considered substantive; age explained only 0.1% of the variance in tAB and thus may only be a minor determinant of tAB.

Gender appeared to explain a large amount of the variance of tAB in this analysis. However the magnitude decreased substantively when adjusted for height. Similar gender differences in height have been observed in patients with healthy knees which accounts for the large proportion of tAB variance explained by gender in unadjusted regression modelling [256].

When considering radiographic data, osteophytes, joint space narrowing and KL grade correlated with tAB in previous cross-sectional analyses of OA knees [31, 269, 483, 560]. These analyses did not adjust for the tAB attributable to OA. This study used OA-attributable tAB and demonstrated the same statistically significant associations, however they did not explain a substantive proportion of OA-attributable tAB variance in uni- and multi-variable models. This may reflect the lack of sensitivity of traditional radiographic measures in detecting structural progression and the additional structural information afforded by the 3D measure we employed. Indeed approximately 80% of the variance of OA-attributable tAB was not explained by radiographic covariates. The apparent lack of substantive association with the radiographic measures may reflect the limitations of 2D projection images of conventional radiography. Semi-quantitative MRI scores (2.11.2.2 MRI semi-quantitative measures) based on similar 3D imaging may prove to be more strongly associated with 3D bone area that is attributable to OA. Unfortunately only 115 OAI knee MRI scans have this scoring available in the public domain which currently precludes an analysis of significant size.

Of the three non-KL radiographic variables, osteophytes explained the largest variance in tAB. This may reflect the expansion of subchondral tAB in OA being largely a product of endochondral and direct bone formation in the medial and lateral peripheral articular cartilage plate [640](2.6.1.2 Subchondral bone and the osteochondral junction).

4.5 Limitations

There are limitations to this study. We have aimed to be cautious in only presenting substantive associations. The OAI is a large cohort and therefore we wanted to demonstrate whether significant statistical associations were substantiated by a significant proportion of tAB variance explained. Although JSW and KL grades were available for 4490 participants in the OAI database, we were limited to approximately 2588 participants by the availability of osteophyte and sclerosis variables.

Bone shape or bone area may be influenced by confounding factors that we did not adjust for, including the use of bisphosphonates.

Magnetic resonance cannot directly identify the presence of calcium. In the segmentation of knee DESS-we MRI sequence the material imaged is assumed to represent bone rather than another tissue type. Confirmation that these surfaces are actually bone requires further work. Finally the automated segmentation used here is both accurate and repeatable however all subtle details of particular diseases may not be identified [259, 267]. The majority of the cohort was Caucasian with smaller numbers of other ethnic groups. Therefore conclusions cannot be readily generalised to non-Caucasian groups

4.6 Conclusions

The analyses within this chapter confirm that radiographic measures, derived from a single radiographic projection, are significantly associated with OA-attributable bone area measured in 3D but do not explain a substantive proportion of OA-attributable bone area. This may reflect the additional 3D MRI structural information, unaccounted for by these 2D radiographic measures. We also confirmed the substantive allometric relationship of bone area with body size. Future analyses of bone area as a measure of structural progression should adjust for OA-attributable bone area.

Chapter 5 The relationship between three-dimensional knee MRI bone shape and total knee replacement – a case control study

5.1 Introduction

In chapter three the systematic literature review identified the need for evidence of the validity of 3D bone measures as imaging biomarkers. In chapter four the significant association of 3D bone structure of OA with conventional radiographic OA measures provided evidence of construct validity but also highlighted the additional structural information provided by 3D bone measures that could not be substantively explained by the 2D projection images of conventional radiography. Conventional radiographic measures of OA are associated with outcomes such as joint replacement. Therefore it is important to know the relationship of the novel bone shape biomarker with important clinical outcomes such as joint replacement, independent of the structural assessment of conventional 2D radiography. This chapter describes evidence of criterion validity by describing the association of 3D bone shape with the patient-centred outcome of total knee replacement.

5.2 Methods

Data used for this nested case-based, case-control analysis, with cumulative incidence sampling, were obtained from the NIH Osteoarthritis Initiative (OAI) database, which is available for public access at http://www.oai.ucsf.edu/ (2.12 Summary of the OAI). This database houses a multi-centre, prospective, longitudinal observational study of knee OA currently including approximately 4,796 participants[515]. Baseline demographic data were collected and MRI scans were performed for all participants. At each site the institutional review board approved the study and informed consent was given by all patients. The OAI study and public use of clinical and imaging data used in this study was approved by the

committee on Human Research, University of California, San Francisco (IRB approval number 10-00532).

During the eight-year period of follow up for the OAI cohort, the MRI systems at all four recruiting centres underwent one hardware upgrade[641]. The timing of this upgrade varied by recruiting centre and by stage of each participant's follow up. This upgrade created a statistically significant difference in the geometric measurement of a phantom[642] that is used to assess reproducibility of MRI scans in the OAI by independent centralized QA analyses[641]. The MRI upgrade conferred a systematic change in 3D bone shape equivalent to about 2-years change. This therefore precluded a longitudinal analysis of 3D bone shape. The decision to use a case-control analysis rather than a time-survival analysis was based upon the following factors. The outcome of TKR is rare and there is significant variation in multiple strong confounding factors for TKR incidence between participants at baseline in the OAI. These include pain, radiographic severity, obesity and previous injury. The primary objective was not to estimate the effect of these well described, strong predictors of TKR but to determine if 3D bone shape vectors were independently associated with the outcome of TKR after effectively adjusting for these confounding factors. Therefore a case-control analysis was chosen

For the current study, definition of case knee or control knee status required baseline records of age, gender, knee numeric pain scale, weight and Kellgren Lawrence (KL) grade. A pre-requisite for eligibility also included having a baseline MRI knee scan and confirmed knee replacement status by the 72 month follow-up visit. Cases were defined as any knee with; confirmed TKR status(patient-reported TKR and adjudicated confirmed status on subsequent radiograph between baseline and the 72 month follow-up visit); confirmed OA indication for TKR or, where this was unrecorded, an OA indication was highly likely (the presence of baseline radiographic and symptomatic evidence of OA) for the replaced knee. Where a participant had both knees replaced during the follow-up (n=69), the first knee to be replaced was included (n=50). Where both knees were replaced on the

same day (n=19) one knee was randomly selected. Knees that ‘survived’ were eligible for selection as controls if they had neither patient-reported nor post-knee replacement adjudicated confirmation on follow-up radiograph at the 6 year follow up point. The OAI cohort has excellent follow up retention rates at 6 years (approximately 88%). Where two ‘control’ knees were available for the same participant, the knee with the highest pain score, or the right side if they reported equal pain, was selected. Control knees were matched 1:1 with case knees using propensity score (PS) matching (described below). With multiple strong confounders (e.g. age, gender and body mass index), PS matching was chosen as an efficient way of creating an unbiased comparison and improving precision.

MRI sequences collected in the OAI are described in detail by Peterfy and colleagues [497]. The current study utilised the double-echo-in-steady-state sequence (DESS-we) of the Siemens 3T trio systems [497].

The quantitative analysis of 3D bone shape was achieved by automated segmentation of the 3D MRI double-echo steady-state water excitation sequences. Active appearance models (AAMs) are statistical shape modelling methods that learn the variation in shape and gray-scale texture (‘appearance’) of objects from a training set (such as the bones from an MRI), and encodes shape and appearance as principal components [629, 630](2.10 Statistical Shape modelling, active shape modelling and active appearance modelling).

The AAM methodology has been previously published [75]. In summary a training set of 96 knees with equal numbers of knees from each KL grade was used to build AAMs for each knee bone so that the trained AAMs can automatically segment bones in MR images. The validation of the accuracy of the knee segmentations has been previously described [630, 643]. For each particular models, the accuracy of the automated segmentations was further assessed using test–retest MRIs for 19 participants (38 images) with no OA to moderate degrees of clinical OA, prepared as a pilot study for the OAI, using the same MRI sequence [644]. The bone surface was manually segmented as previously described[632]. Mean point-to-surface distances

were calculated between the manual and automated segmentations. Mean point-to-surface errors were as follows: for the femur, 0.49 mm; for the tibia, 0.53 mm; and for the patella, 0.57 mm (i.e. each approximately the size of 1 voxel)[75]. The reliability of the automated segmentations has been established [632, 644]. The reliability of the automated segmentations of bone and cartilage has been described [632, 644] While segmentation for cartilage thickness has a coefficient of the variance of over 2%, bone segmentation has a coefficient of the variance of 0.8-1.9%[632]

In order to identify vectors within this shape space that represented average change of the bone with disease we separated the 96 training set cases into OA (KL grade 2-4, n =53) and non-OA groups (KL0-1, n=43)

The shape vector for each bone is calculated by taking the principal components of the mean shape of the OA and non-OA groups, and drawing a straight line through them. Individual bone shapes from knees in this study, represented as principal components following the AAM search, were projected orthogonally onto the vector. The distance along the vector was normalized by treating the mean non-OA shape as -1 and the mean OA shape as +1 (Figure 51, Figure 52).

The reproducibility or test-retest reliability of the method was described in a set of 35 OA knees that underwent magnetic resonance imaging one week apart at one single OAI site, using the same OAI image acquisition sequence [632]. The reproducibility for the OA vector was good, with the smallest detectable difference for the femur, tibia and patella bone shape vectors was 0.22, 0.86 and 0.24 units normalised to the mean non-OA shape respectively[625]. [75].

5.2.1 Statistical analysis

Statistical analysis was conducted using STATA software, version 13 (College Station, TX, 2013). Matching of control knees to case knees 1:1 was performed using PS matching. The PS is the conditional probability of assignment to a particular treatment given a vector of covariates and has been shown to be sufficient in removing bias due to observed covariates in

observational studies [645]. In this analysis the PS is the conditional probability of receiving a TKR given a vector of covariates. The model was based on the probability of having the outcome of TKR conditional on observed covariates. This is stratification score matching which has been previously described [646] and is referred to as PS matching in this retrospective analysis. The propensity model was estimated using logistic regression based on *a priori* known relationships between the outcome TKR, and clinically important risk factors such as age, gender, weight, KL grade, and pain [647], which may influence the surgeon`s decision to operate. We considered whether health insurance could affect the outcome with participants potentially not offered a TKR for financial reasons; however on exploration of the data we found that 98% of participants that had a TKR had some form of health insurance while 96% of those not having a TKR had insurance.

The final logistic regression model included baseline age, gender, weight category, ipsilateral knee pain severity numeric rating scale (Range 0-10), and knee side (right or left) (Table 42). KL grade was deliberately omitted because it directly influences the decision for TKR by the orthopaedic surgeon, resulting in over-matching. Furthermore the KL grade is used to define the scalar 3D bone shape variable and hence the two are moderately correlated (unpublished data).

Age was categorised into 5-year groupings prior to inclusion in the PS model. Weight was categorised using WHO BMI categories, underweight (<18.5kg/m²), normal (18.5-24.9), overweight (25-29.9) and obese (≥30). Underweight and normal categories were subsequently merged because very few patients were underweight (n=10). Control knees were matched to case knees with the nearest PS (nearest neighbour matching) without replacement. Matching between case and control knees was confirmed graphically and by comparing the means or medians for the PS and the distribution of the components of the PS between case and control knees. Age, BMI and pain were analysed as continuous variables and gender kept as dichotomous. The variables were considered well balanced if the

standardised difference percentage (the mean difference as a percentage of the average standard deviation) for continuous variables was less than 10% as values greater than this are reported to represent meaningful imbalance [648], and for dichotomous variables a standardised difference (difference between prevalence in treatment and control group divided by an estimate of with-in group standard deviation) less than 0.1 represented good balance [649].

For simple comparison between the matched groups, Student`s *t*-tests for paired samples were used to compare 3D bone shapes of the femur, tibia and patella between case and control knees. Univariable and multivariable conditional logistic regression analyses were performed to establish the association of each baseline 3D bone shape vector as continuous variables with the outcome of TKR. Multivariable analyses included KL grade and the *Akaike information criterion* (AIC) was used to compare models with and without 3D bone shape, in order to assess any additional association beyond that between KL grade and TKR. Model fit was assessed by examining leverage plots to identify pairs that did not fit the data well, and also observations exerting a strong influence on the estimated coefficients. The model fitted the data well based on diagnostic checks. We also analysed 3-D bone shape vectors categorized into tertiles with the highest tertile containing values closer to mean OA shape and the lowest tertile contained values closer to the mean non-OA shape.

Additional exploratory analyses (conditional logistic regression models) aimed to determine if any association of bone shape with TKR was maintained over all KL grades and to establish if there were any differences in association between 3D bone shape and TKR depending on the time from baseline to TKR date in years.

Figure 51 Scalar continuous vector of 3D bone shape of the femur

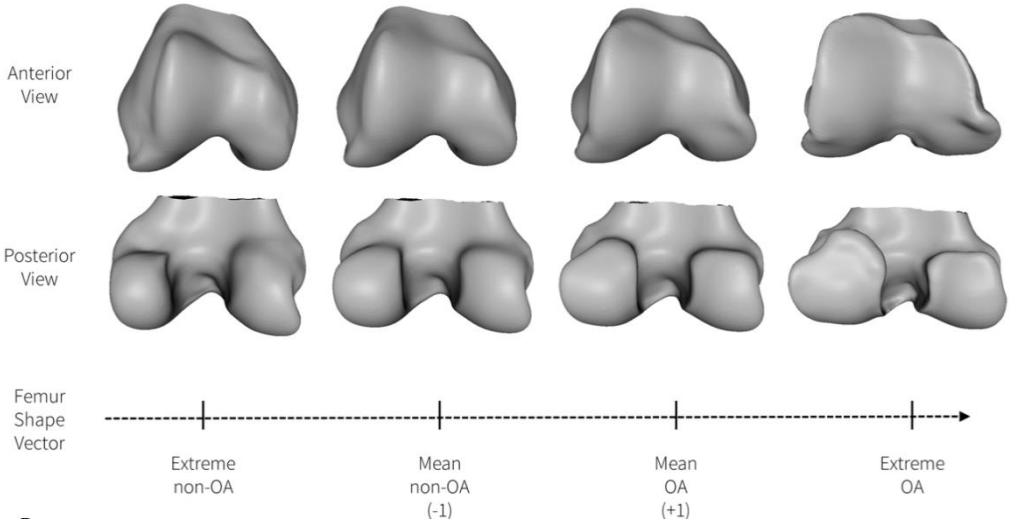

Legend: Anterior and posterior views of right knees. The femoral shape vector is scaled to -1 as the mean shape without radiographic OA and +1 with established radiographic OA

Figure 52 Scaling of the 3D bone shape vectors relative to KL grade

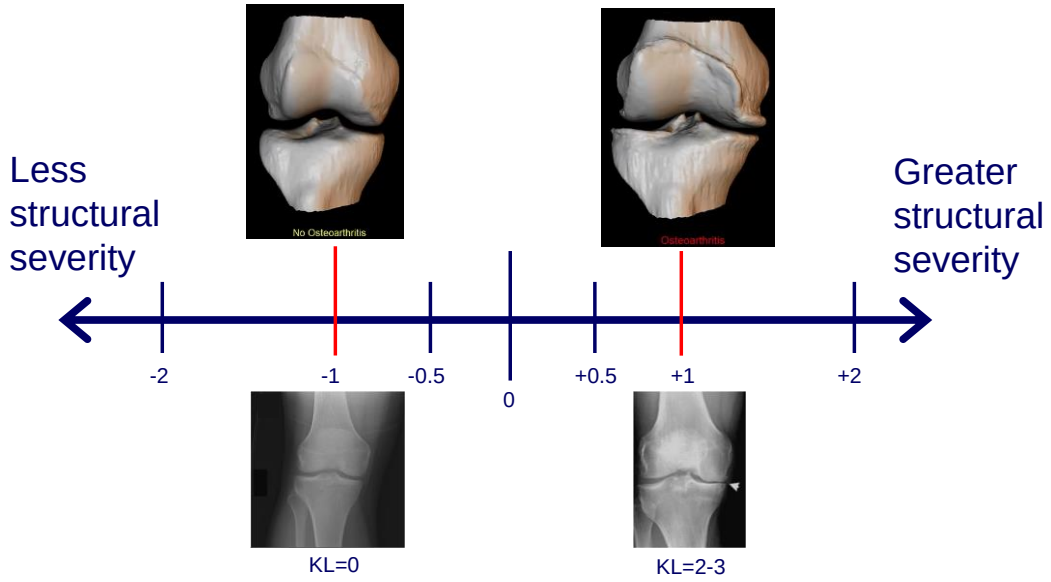

The distance along the vector was normalized by treating the mean non-OA shape as -1 and the mean OA shape as +1

5.3 Results

Of the 4,796 participants in the OAI database, 336 individuals with at least one confirmed knee replacement during follow-up were identified. In total 405 knees had been replaced (right 198, left 207). Of the 69 patients who had both knees replaced; 50 patients' knees were replaced on separate days, and from them 25 right knees and 25 left knees were selected for analysis on the basis that they were replaced first. From the remaining 19 patients whose knees were replaced on the same day; 11 right knees and 8 left knees were randomly selected. Only one knee was excluded by TKR indication which was recorded as rheumatoid arthritis. Having excluded patients with missing MRI data, 310 cases knees met the selection criteria and were suitable for PS matching (Figure 53). The 336 individuals with knee replacements differed from the rest of the OAI cohort in baseline mean age (3 years older), KL grades, obesity and numeric rating scale pain scores (Table 32). The number of exact PS matches was 244 (79%) with all remaining case knees having a PS within 0.01 PS units of their control knee. A minority of case knees had been matched with contralateral control knees (*n*=12[4 %]). There was a concordant gender match in all case-control knee pairs.

There were no substantive differences between the cases and matched controls (Table 33). The distribution of the PSs in the two groups was similar (Figure 54).

Figure 53 Participant flow diagram for the selection of case knees

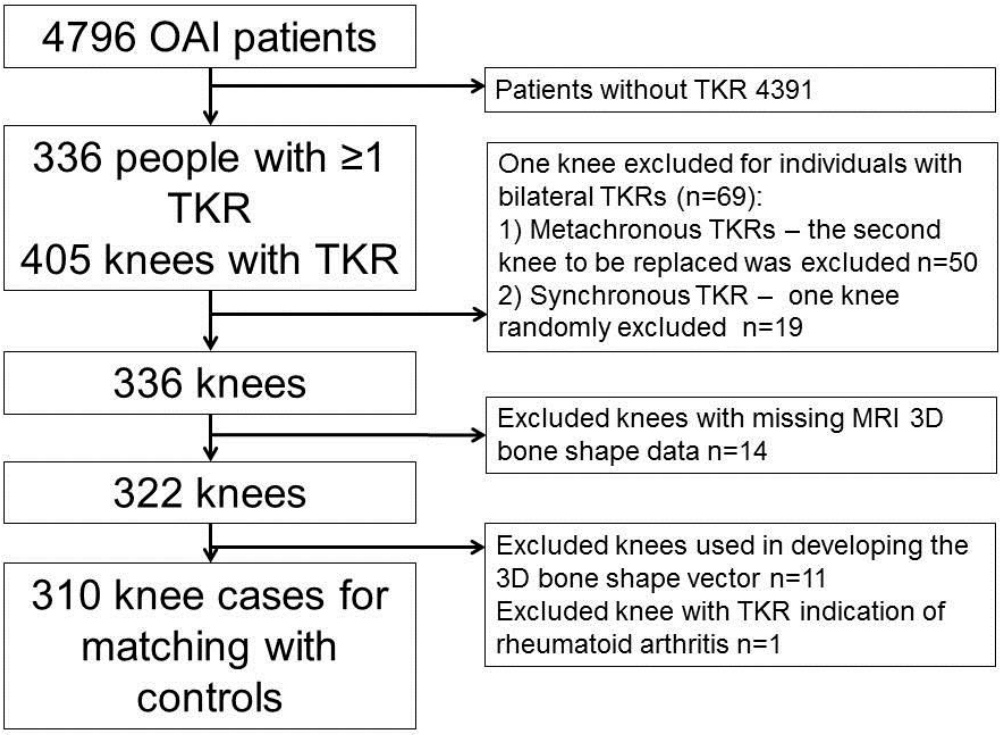

Table 32 Characteristics of 4796 participants according to presence or absence of at least one (1) confirmed, adjudicated total knee replacement (TKR) before matching

	TKR, n=336	No TKR, n=4460
Age, years, mean (SD)	64.1 (8.39)	60.8 (9.19)
Gender ,female,%	60	58
Health insurance,%	98	96
Weight		
Normal/underweight	44 (13)	2004 (25)
Overweight	131 (39)	1746 (39)
Obese	161 (48)	1610(36)
KL grade		
0	11 (3)	1560 (35)
1	15 (5)	715 (16)
2	74 (22)	1112 (25)
3	136 (41)	591 (13)
4	94 (28)	157 (4)
Missing	6 (1)	325 (7)
NRS, median(IQR)	5 (3-7)	3 (1-5)

Figures are n (%) unless stated.

NRS – Numerical Rating Scale for pain

KL - Kellgren Lawrence grade

SD – Standard deviation

IQR – Inter-Quartile Range

TKR – Total Knee Replacement

Table 33 Demographics characteristics of participants with knee replacement and their controls from propensity matching

	TKR cases n=310	Controls n=310
Gender, male	123 (40)	123 (40)
Age categories		
45-49	12 (4)	17 (5)
50-54	34 (11)	35 (11)
55-59	53 (17)	45 (15)
60-64	53 (17)	59 (19)
65-69	64 (21)	59 (19)
70-74	52 (17)	56 (18)
75+	42 (13)	39 (13)
Weight category		
Normal/underweight	165 (53)	157 (51)
Overweight	156 (47)	153 (49)
*Health insurance	301 (98)	292 (95)
Side, right	159 (51)	161 (52)
NRS ,median (IQR)		
Left knee score	5 (3-7)	5 (3-6)
Right knee score	5 (2-7)	5 (3-7)
*KL grade		
0	10 (3)	93 (30)
1	12 (4)	49 (16)
2	69 (22)	85 (27)
3	128 (42)	47 (15)
4	85 (27)	13 (4)
Missing	6 (2)	23 (7)

Figures are n (%) unless stated.

*not used in propensity matching

NRS – Numerical Rating Scale for pain

KL - Kellgren Lawrence grade

SD – Standard deviation

IQR – Inter-Quartile Range

TKR – Total Knee Replacement

Figure 54 The distribution of propensity scores amongst cases and controls

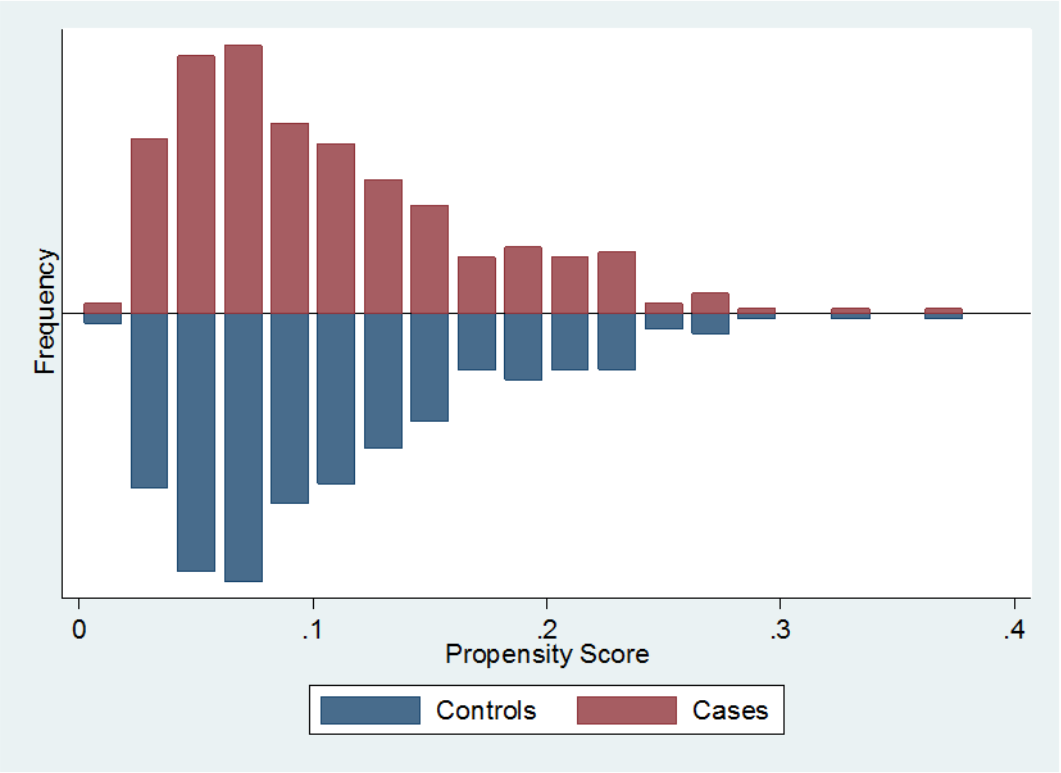

The standardised differences for age, BMI and NRS pain were 3.3%; 0.5% and 1.8% respectively (all within 10%) while gender was matched perfectly.

The mean baseline 3D bone shape scalar variable indicated significantly greater structural severity in cases of TKR than in controls. Mean, (SD) in the femur cases was 0.98 (1.51) compared with controls mean of -0.11 (1.40), with a statistically significant difference of 1.10 (95% CI, 0.89 to 1.31), t (309) =10.31, p<0.001. Mean, (SD) in the patella cases was 0.95 (1.86) compared with controls mean of 0.03 (1.83), with a statistically significant difference of 0.92 (95% CI, 0.65 to 1.20), t (309) =6.61, p<0.001. The femur had the largest mean difference in 3D shape of the three knee bones (Table 34).

The conditional logistic regression models of each individual bone estimated increased odds of TKR with more positive 3D bone shape, indicating greater OA structural severity (Table 35).

Table 34 The mean differences between bone shape vectors of cases and controls

Bone vector	Mean Control	Mean TKR	Mean difference	95% CI	Paired T-test
	(mean, SD)	(mean, SD)			p value
Femur	-0.11, 1.40	0.98, 1.51	1.10	0.88, 1.31	<0.001
Tibia	-0.07, 1.39	0.86, 1.42	0.94	0.72, 1.16	<0.001
Patella	+0.03, 1.83	0.95, 1.84	0.92	0.65, 1.20	<0.001

SD – Standard deviation

Table 35 The associations between 3D bone shape vectors or KL grade with TKR

	Univariable (unadjusted)				Multivariable*			
Imaging variable	OR	95% CI	p value	AIC	OR	95% CI	p value	AIC
Femur vector	1.85	1.59, 2.16	<0.001	341.11	1.24	1.02, 1.51	0.03	241.33
Tibia vector	1.64	1.42, 1.89	<0.001	367.80	1.09	0.90, 1.32	0.40	245.60
Patella vector	1.36	1.22, 1.50	<0.001	390.84	1.06	0.92, 1.23	0.40	245.58
Combined bone vectors								
Femur vector					1.26	1.00, 1.60	0.05	
Tibia vector					0.97	0.78, 1.21	0.80	
Patella vector					1.00	0.85, 1.17	0.96	245.26
KL grade (ref=KL zero)								
1	1.66	0.58, 4.73	0.34					
2	5.66	2.55, 12.55	<0.001					
3	17.18	7.43, 39.72	<0.001					
4	39.77	14.64,108.0	<0.001	244.31				

* Adjusted for KL grade

OR – Odds ratio from conditional logistic regression, KL - Kellgren Lawrence grade, CI – Confidence Interval, AIC – Akaike's Information Criterion, TKR – Total Knee Replacement

Odds ratios (95% confidence intervals) per normalised unit of 3D bone shape vector for the femur, tibia and patella were 1.85 (1.59, 2.16), 1.64 (1.42, 1.89), 1.36 (1.22, 1.50) respectively, all p<0.001. The order of strength of association of bone shape with TKR, from strongest to weakest, was therefore the femur, the tibia and finally the patella. The odds on TKR increased significantly with KL grade. When KL was included in multivariable conditional logistic regression models, the femur remained significantly associated with TKR but the association with the tibia and patella was attenuated. The odds ratios (95% confidence intervals) per normalised unit of 3D bone shape vector were 1.24 (1.02, 1.51), 1.09 (0.90, 1.32), 1.06 (0.92, 1.23) for the femur, tibia and patella respectively. The AIC of the univariable KL model was lower than any of the univariable bone vector models and multivariable tibia and patella models and the strength of association was in the expected direction (OR for KL3 were greater than that of KL2 when compared to KL0 as reference). However the multivariable model of the femur vector had a small improvement in AIC indicating including bone shape contributes to the association with TKR in addition to KL grade.Those in the highest tertile for the femur bone shape vector had 12.7 times higher chance than those in the lowest tertile group of having a TKR (95% CI 6.93-23.40, P<0.001). In all analyses a similar trend was noted with those in the highest tertile having increased chances of having a TKR than both the middle tertile and lowest tertile. After adjusting for KL grade in the tertile model, only the highest tertile of the femur model remained significantly associated with TKR (Table 36). The association between bone shape and TKR was not significantly modified when stratified by KL grade severity (Table 37,Table 38,Table 39).

Table 36 The associations between 3D bone shape vectors TKR using lowest tertile as reference

3-D bone shape vector	Odds ratio (95% CI)	p-value	Adjusted odds (95% CI)	P-value
Femur				
Highest tertile	12.73 (6.93-23.40)		3.47 (1.62-7.47)	0.001
Middle tertile	2.55 (1.60-4.05)		1.17 (0.65-2.08)	0.610
Lowest tertile (ref)	1.0	<0.001		
Tibia				
Highest tertile	6.32 (3.84-10.40)		1.95 (0.99-3.82)	0.052
Middle tertile	2.80 (1.72-4.56)		1.64 (0.85-3.15)	0.140
Lowest tertile(ref)	1.0	<0.001		
Patella				
Highest tertile	3.81 (2.40-6.08)		1.78 (0.92-3.44)	0.088
Middle tertile	2.26 (1.47-3.49)		1.84 (1.01-3.35)	0.046
Lowest tertile(ref)	1.0	<0.001		

Ref = reference

95% CI= 95% confidence interval.

Table 37 The number of propensity score matched pairs of cases and controls with equal KL knee grades

Kellgren Lawrence grade	Pairs of knees	Number of knees
0	2	4
1	4	8
2	14	28
3	18	36
4	3	6
Total	41	82

Table 38 The number of propensity score matched pairs of cases and controls with equal KL knee grades after grouping into KL grade strata

Kellgren Lawrence grade	Pairs of knees	Number of knees
0,1	6	12
2	14	28
3,4	21	42
Total	41	82

Table 39 The difference in mean bone shape vector between propensity score matched cases and controls with equal KL grades after division into strata

Bone	Kellgren Lawrence grade	Mean bone shape vector difference between vectors matched cases and controls with identical KL grade	Standard deviation	Confidence interval	Effect size (Mean/SD)[a]
Femur	0,1	0.78	1.56	-0.85, 2.42	0.50
	2	0.66	1.55	-0.23, 1.56	0.43
	3,4	0.12	2.45	-0.99, 1.23	0.05
Tibia	0,1	0.45	0.99	-0.58, 1.50	0.46
	2	0.59	1.39	-0.21, 1.39	0.42
	3,4	0.38	2.17	-0.61, 1.37	0.18
Patella	0,1	0.07	1.43	-1.43, 1.57	0.05
	2	0.74	2.77	-0.86, 2.35	0.27
	3,4	0.32	2.66	-0.89, 1.53	0.12

The difference in mean bone shape vector between propensity score matched cases and controls with equal KL grades after division into strata. The association between bone shape and TKR was not significantly modified by KL grade severity strata. However this is an exploratory analysis with large confidence intervals, using small numbers of matched case control pairs. [a]The mean bone shape vector difference (column 3) divided by the standard deviation (column 4). TRK: Total Knee Replacement; KL: Kellgren Lawrence grade.

The association between bone shape and TKR was not significantly modified by KL grade severity strata. However this is an exploratory analysis with large confidence intervals, using small numbers of matched case control pairs.

Similarly the association between bone shape and TKR was not significantly modified by the length of the interval between baseline and TKR incidence

(Table 40, Table 41). However these were exploratory analyses which included small numbers in each stratum with large confidence intervals. The cumulative incidence of the 310 TKR cases over approximately seven years is relatively stable over the first seven years (Table 40).

Table 40 The cumulative incidence of the TKR cases used for the case-control analysis

Year of case TKR	Incidence of case TKRs	Cumulative Incidence of case TKRs
0-1	23	23
1-2	37	60
2-3	39	99
3-4	52	151
4-5	54	205
5-6	48	253
6-7	51	304
7-8	6	310
Total	310	310

Table 41 The association of 3D femur bone shape vector with TKR by annual TKR incidence

The year of incidence of case TKR	OR	95% CI	P value
All years combined	1.85	1.59, 2.16	<0.001
0 to 1	1.92	1.17, 3.18	0.010
1 to 2	1.85	1.20, 2.87	0.006
2 to 3	2.68	1.44, 4.99	0.002
3 to 4	1.57	1.12, 2.18	0.008
4 to 5	1.82	1.25, 2.66	0.002
5 to 6	2.30	1.39, 3.81	0.001
6 to 8	1.60	1.15, 2.24	0.006

Table 42 Results from propensity model used to match cases and controls

Outcome -TKR	Coefficient	95% CI	P value
Age category (ref 0)			
1	0.58	-0.05, 1.22	0.072
2	1.15	0.55, 1.76	<0.001
3	1.28	0.68, 1.88	<0.001
4	1.60	1.00, 2.19	<0.001
5	1.47	0.87, 2.08	<0.001
6	1.76	1.13, 2.39	<0.001
Sex (ref male)			
Female	-0.00027	-0.24, 0.24	0.99
NRS	0.17	0.13, 0.21	<0.001
Weight category(ref normal)			
Overweight	0.38	0.14, 0.62	0.002
Side (ref Right)	0.60	0.36, 0.84	<0.001
Constant	-4.87	-5.47, -4.27	<0.001

NRS – numeric rating scale for pain

5.4 Discussion

This is the first study to describe the association between 3D bone shape and TKR. We demonstrated that people having TKR exhibited significantly more advanced 3D shape changes of OA structural progression than controls at baseline. Total knee replacement has been previously associated with age, obesity, pain characteristics, radiographic OA severity and MRI features such as cartilage damage [105, 479, 540, 600, 650]. MRI-determined bone shape is related to OA structural progression[75]. The association of OA subchondral bone pathology with TKR is supported by the association of bone marrow lesions with TKR, though bone shape and BMLs are likely to be measuring a different pathological construct [105, 540, 600].

The odds ratio of TKR per normalised unit of 3D bone shape vector increased with greater baseline 3D shape structural severity for each of the femur, tibia and patella. However femoral bone shape has the strongest association with TKR. It is worth noting that the femoral bone shape had the largest scalar value difference between case and control knees and is the only bone shape that, after adjusting for KL grade, remained significantly associated with the outcome of TKR. These findings concur with the same 3D femur shape having the largest hazard ratio of the three knee bones in predicting incident radiographic knee OA [605].

Furthermore the 3D bone area of femoral trochlear and tibio-femoral articulations were the most responsive and had the greatest percentage change in size of all articulating surfaces in the knee[604]. Cartilage loss from the femur was better than loss from the tibia in distinguishing OA knees requiring and not requiring knee replacement in a previous study [647]. Femoral bone undergoes greater 3D shape change than tibial bone after anterior cruciate ligament rupture[651]. In knee OA the tibial 3D shape changes in a more uniform and symmetric pattern than the femur where the shape change distinctly occurs around the cartilage plates where an increased ridge of “osteophytic” material forms[75]. This may explain why femoral 3D shape has a greater responsiveness and association with TKR. While bone shape readily changes in response to mechanical forces acting upon it (Wolff’s law) [173, 197] it is reasonable that the femur shape should change more than the tibia or patella because the femur receives more load from twice the number of weight bearing surfaces of the tibia and patella.

The association of TKR with femoral, but not tibial or patellar bone shape persists after adjusting for KL grade and is greatest for the femur in the higher tertiles (Table 5). This may reflect the observation that in more advanced structural progression, tibial and patellar shape change is more uniform and symmetrical than the femur [75, 652]. This more readily detectable shape change in the femur may explain the stronger association with TKR in more advanced structural progression (the higher tertiles). The additional structural information provided by 3D bone imaging compared to

conventional radiography[516] may explain why in the exploratory analyses the association with TKR was maintained after stratifying for KL grade severity, indicating the stage of structural severity does not affect this association.

The requirements of biomarker validation have been described [653]. The findings of this study in conjunction with previous data on construct validity, reliability and responsiveness of 3D bone shape, indicates that novel quantitative measures of bone shape are increasingly validated biomarkers of OA structural progression [75, 605, 652]. 3D bone shape has advantages over conventional ordinal and metric radiographic measures of structural progression in that it provides a continuous measurement variable that is a more responsive measure than radiographic measures of knee OA[652] and it is sensitive to pre-radiographic knee OA[75].

5.5 Limitations

There are limitations to this study. Joint arthroplasty is an end-point reflecting symptom and structural damage severity, but many variables influence both the timing and the decision to perform this outcome measure. The surgeon's opinion and the patient's comorbidities and willingness to undergo surgery are examples of these, in addition to local and national health system variations in surgical waiting lists which may cause residual confounding.

There is no consensus on which variables to include in the propensity model with studies showing a similar effect if all measured baseline covariates, all potential confounders or all true confounders are used interchangeably [649]. It has however been demonstrated that in order to maximize the number of matched pairs, the propensity model specified should have only the true or potential confounders [648]. In the final sample 79% of case and control knees were matched exactly. This PS method adjusted for imbalances at baseline but not over time. Body mass index may increase before TKR and this may cause residual confounding conceivably with

greater BMI increases in the TKR cases than in the controls. This may influence the size of the associations described in this analysis.

An alternative study design considered was cox-regression analysis, modelling the time-to-event (in this case TKR) which could have compared different survival times based on the 3D bone vector as well as estimates of covariates using the full cohort. However since the stated objectives did not include estimating the effect of these well described and strong predictors of TKR, and knee replacement satisfied the “rare outcome” assumption (prevalence of 7%), we chose to perform a well-matched case-control analysis instead of a whole cohort survival analysis. Essebag and colleagues highlighted this relative advantage of well-matched case-control analysis where the effect of the confounding factors is ‘not of interest’[654]. A case-control analysis therefore represented a more precise analysis by efficient matching of multiple strong confounding factors to minimise the effect of bias.

We also acknowledge that by effectively matching cases and controls we may inadvertently ‘overmatch’ which may reduce any effect of 3D bone shape on the outcome of TKR and my chosen method was therefore at risk of underestimating the magnitude of the association of bone shape vector with the outcome of TKR.

The multivariable analyses are potentially subject to the effects of multiple collinearity. This is because KL grade is moderately correlated with bone shape vectors and the three bone shape vectors from within the same knee are used in the same multivariable models,

Bone shape or bone area may be influenced by confounding factors that we did not adjust for, including the use of bisphosphonates.

The OAI is predominantly a caucasian cohort with smaller numbers of other ethnic groups. This means that any attempt to match cases and controls based on ethnicity would limit the available pool for matching. We acknowledge that by not matching on ethnicity there may be residual confounding although race was not associated with TKR incidence after

covariate adjustment in the OAI dataset [479]. Health insurance was available for 98% of participants in the study suggesting any differences in ethnicity between cases and controls did not reflect their access to TKR surgery. The associations reported in this analysis should not be generalised to non-caucasian populations due to the lower representation of non-white participants in this analysis.

Additionally, as with any observational study, it is impossible to rule out residual bias from unknown or unmeasured confounders.

Magnetic resonance cannot directly identify the presence of calcium. In the segmentation of knee DESS-we MRI sequence the material imaged is assumed to represent bone rather than another tissue type. Confirmation that these surfaces are actually bone requires further work. Finally the automated segmentation used here is both accurate and repeatable; however some subtle details of particular diseases may not have been identified [259, 267].

5.6 Conclusions

This chapter has demonstrated that 3D bone shape was associated with the important patient-centred outcome of total knee replacement. The femur had the greatest association of the three 3D knee bone shape vectors. This may reflect the superior responsiveness of this bone shape in the structural progression of knee OA. The predictive (criterion) validity demonstrated here further underpins the value of quantitative bone measures in future therapeutic trials of DMOADs.

Chapter 6 The relationship between 3D MRI bone shape and knee osteoarthritis symptoms in knees with and without radiographic knee osteoarthritis.

6.1 Introduction

The systematic literature review in chapter three identified the requirement for evidence of the validity of 3D bone measures as imaging biomarkers. In chapter four the significant association of 3D bone structure of OA with conventional radiographic OA measures provided evidence of construct validity but also highlighted the additional structural information provided by 3D bone measures that could not be substantively explained by the 2D projection images of conventional radiography. This additional structural 'information' appeared to confer an association of 3D bone shape with joint replacement, that is independent of the structural assessment of conventional 2D radiography. This provided evidence of criterion validity, This chapter describes evidence of criterion validity by describing the association of 3D bone shape with the patient-centred outcome of current and incident knee OA symptoms. OA is a major cause of chronic pain and disability and by 2020 is estimated to be the commonest chronic condition seen in primary care [655]. OA is a heterogenous condition characterised by the failure of the whole synovial joint organ[656] (2.4.2 Microscopic). It is widely accepted that OA is present when typical structural pathology is identified by conventional radiography. However the concordance between structural pathology determined by radiographic knee OA (ROA) and knee OA symptoms is poor. Only 50% of knees with ROA have knee OA symptoms [17] and little change is observed in knee pain in knees with ROA over six years [97] except when large increases in radiographic structural severity are observed[98]. However conventional radiography is less sensitive and specific in detecting structural pathology and progression than magnetic resonance imaging (MRI)[23, 86]. MRI-detected OA joint tissue

lesions and structural pathology are prevalent in knees without ROA[23] and these (including bone marrow lesions, cartilage damage and meniscal tears) are associated with incident symptomatic [131] and radiographic OA[75]. As discussed in chapter 5 three dimensional MRI scans can be segmented manually or in an automated manner with methods such as active appearance modelling (AAM) that permit the analysis of large data sets such as the OAI (2.10 Statistical Shape modelling, active shape modelling and active appearance modelling).

Subchondral bone pathology, in particular bone marrow lesions (BMLs), is important in the pathogenesis of knee OA pain in established ROA and in knees at risk of knee OA but without radiographic OA. In cohort studies of knees with prevalent ROA, ranging from 18-71%, longitudinal increase in BML size or baseline BML size are associated with longitudinal increase in knee OA pain severity in the Osteoarthritis Initiative[100], the Tasmanian Older Adult Cohort[99] and the Michigan site of the Study of Women's Health Across the Nation[530]. In cohort studies of knees at risk of OA but without radiographic knee OA, BMLs are also associated with incident frequent knee OA pain. This includes a subcohort study of knees at risk of OA but without any ROA (Kellgren Lawrence zero) within the OAI cohort[131] and the longitudinal structural progression of BMLs in these 'pre-radiographic' OA knees is associated with incident radiographic knee OA and persistence of knee symptoms[622]. This association of BMLs and incident knee pain is also observed in the MOST cohort study where the majority of knees (60%) lacked radiographic knee OA[26]. While much of the relevant OA literature has focussed on MRI-detected BMLs, several recent studies have suggested the importance of bone shape in the structural progression of OA including the pre-radiographic OA stage[75, 197, 604, 605]. The association of OA symptoms with structure in early knee OA represents an important but understudied stage in knee OA. The association of 'pre-radiographic' OA knee bone shape with prevalent frequent knee symptoms (PFKS) and incident persistent knee symptoms (IPKS) in persons

with no evidence of OA anatomical changes on plain radiography has not been previously reported.

The objective of this analysis was to determine the relationship between scalar 3D bone shape with PFKS and IPKS in all knees in the OAI but also in knees without ROA but at risk of OA.

6.2 Methods

Data used for this were obtained from the NIH Osteoarthritis Initiative (OAI) database, which is available for public access at http://www.oai.ucsf.edu/ (2.12 Summary of the OAI). This database houses a multi-centre, prospective, longitudinal observational study of knee OA currently including approximately 4,796 participants[515] . Baseline demographic data were collected and MRI scans were performed for all participants. At each site the institutional review board approved the study and informed consent was given by all patients.

Prevalent frequent knee symptoms (PFKS) was defined as having knee symptoms (pain aching or stiffness) or medication use for knee symptoms most days of one month in the past 12 months which was assessed at baseline and subsequently at every annual review up to the 60-month OAI visit. The outcome of PFKS for the PFKS analysis was defined at the 12-month visit. The outcome of IPKS varied by analysis but universally required the absence of PFKS at enrolment and incident PFKS reported after enrolment at two consecutive annual OAI visits by the 60-month visit. All analyses used 3D bone shape derived from right knee MRIs performed at the 12-month visit to determine its association with PFKS and IPKS.

The inclusion criteria for each analysis is summarised in the figures below (Figure 55, Figure 56). The eligibility for the first subcohort analysis identified all knees within the OAI, with or without radiographic OA, and is referred to as the ‘whole’ OAI subcohort. The eligibility criteria for the PFKS analysis in this subcohort included adequate right knee MRI scans at 12 months with available covariate data at 12 months(see ‘covariate measurement’ below)

along with PFKS status data. Eligibility criteria for the IPKS analysis of all knees in the OAI required adequate right knee MRI scans at 12 months with available covariate data at 12 months and PFKS status data from enrolment up to the 60 month visit. Further enrolment knee symptom data was also required to help identify knees with no previous history of knee pain including any history of previous knee pain, any difficulty walking downstairs or upstairs. This stricter eligibility criteria differed for the subcohort without radiographic OA, in an attempt to more precisely identify knees with early symptomatic OA amongst a subcohort of knees with prevalent radiographic OA that were more likely to have had historic pain. Therefore to be eligible for the IPKS subcohort amongst all knees, this required the lack of any of these previous knee symptoms and PFKS at enrolment (Figure 55).

The eligibility criteria for the second subcohort without radiographic OA but ‘at risk’ of knee OA, were deliberately chosen to replicate (and facilitate comparison of findings with) the dataset used by Sharma and colleagues in their recent study of the association of pre-radiographic structural lesions (e.g. BMLs) with PFKS and IPKS[131]. However unlike Sharma and colleagues we stratified analyses by gender. The eligibility criteria for the subcohort without radiographic OA, for the analysis of the association of 3D bone shape with PFKS and IPKS, required individuals to have the absence of radiographic OA with Kellgren Lawrence (KL) grades available and equal to zero in both knees at the twelve month visit from the OAI. This minimised the risk of the presence of OA in this subcohort because the risk of incident knee OA is increased by contralateral knee OA. Inclusion required both knees had available MRI scans of adequate quality at 12 and 48 months. Finally each participant required appropriate covariate data and PFKS outcome data for defining PFKS and IPKS respectively. The right knees of all eligible individuals were selected for the PFKS subcohort. The right knees with a lack of PFKS at enrolment were eligible for the IPKS subcohort.

6.2.1 Knee radiograph acquisition and assessment.

The OAI protocol utilised postero-anterior fixed-flexion weight-bearing knee radiography with a Plexiglas positioning frame (Syna-Flexer see

2.12.4 Knee radiography protocol). All knee radiographs were assessed by two separate experts that were blinded from each other's assessments and all data. The weighted kappa coefficient for inter-reader K/L grade agreement was 0.79. A third expert resolved pre-specified radiograph assessment discrepancies in a consensus session.

6.2.2 MRI acquisition and assessment

MRI sequences collected in the OAI are described in detail by Peterfy and colleagues [497]. The current study utilised the double-echo-in-steady-state sequence (DESS-we) of the Siemens 3T trio systems [497].

The quantitative analysis of 3D bone shape was achieved by automated segmentation of the 3D MRI double-echo steady-state water excitation sequences and 3D bone shape in a similar manner to chapter 5 (5.2 Methods).

Bone shape varies between males and females and therefore 3D bone shape should be defined separately for men and women. In order to identify gender specific vectors within this shape space that represented average change of the bone with disease we separated training set cases for men and women separately into OA (one knee per individual with KL grade two to four at all time points up to four years) and non-OA groups (KL grade zero at all time points up to four years in both knees and picked one knee from each individual).

The gender-specific shape vector for each bone was calculated by taking the principal components of the mean shape of the OA and non-OA groups, and drawing a straight line through them.

Individual bone shapes from knees used in this analysis, represented as principal components following the AAM search, were projected orthogonally onto the appropriate vector. This raw vector data for every bone in every knee was scaled or normalised. This was achieved by subtracting the gender- and bone-specific mean non-OA shape from the corresponding raw vector data for each bone. The result of this subtraction was then divided by

one standard deviation of the normally distributed gender- and bone-specific non-OA shape raw vector values to provide the final normalised 3D bone shape for use in these analyses. Approximately 400 male and 400 female knees fulfilled the non-OA criteria (KL zero at baseline and for the first 4 years) and were used to scale or normalise the vector. Previous analyses have used bone shape vectors normalised using KL grade. To minimise the dependence on KL grade to define the presence of OA, this latest method was used to normalise the vector based upon mean non-OA shape and hence the absence of radiographic OA.

The reproducibility or test-retest reliability of the method has been described in 5.2 Methods).

6.2.3 Covariate measurement

Body mass index (BMI) was calculated from body weight, measured with a standard balance beam scale, and height, measured with a wall-mounted stadiometer at the 12 months visit. The definition of knee injury was if the study knee was “ever injured badly enough to limit walking ≥2 days” and surgery as “any previous surgery”.

6.2.4 Statistical analysis

Statistical analysis was conducted using STATA software, version 13 (College Station, TX, 2013). All analyses used one right knee per person. For all analyses, BMI was categorized as normal (<25 kg/m²), overweight (≥ 25 to < 30 kg/m²), or obese (≥30 kg/m²), and age as < 60 years, >60 to < 70 years, or >70 years at enrolment into the OAI.

We used separate logistic regression models to estimate the direction and magnitude of association between each 3D bone shape measure and PFKS at 12-month visit and IPKS up to 60-month visit and adjusting for age, sex, BMI, and previous knee injury and previous surgery. The analyses were not adjusted for KL grade in the first ‘whole’ OAI subcohort because the bone shape vectors were derived from KL grade and there was a significant risk of over-adjustment. KL grade adjustment was not required in analyses of the second ‘at-risk’ subcohort because all knees were KL grade zero, None of

the analyses were adjusted for MRI features known to be associated with knee pain (e.g. BMLs or synovitis) because the semi-quantitative scores of these were available in too few knees. Results are reported as unadjusted and adjusted odds ratios (ORs) and 95% confidence intervals (95% CIs).

6.3 Results

6.3.1 PFKS in the 'whole' OAI subcohort

The participant flow chart for this analysis is described in (Figure 55). Of the 4,796 participants in the OAI database, 4048 right knees with and without radiographic knee OA had available bone vector data for PFKS unadjusted analysis. This included 1718 males and 2330 females of which 610 (36%) males and 921 (40%) females had PFKS at the 12-month visit. The distribution of the 3D bone shape vector values is described in (Table 43) for males and females and those with PFKS had generally larger vector values than those without PFKS, indicating greater structural severity.

The unadjusted logistic regression models of each individual male bone estimated increased odds of PFKS with more positive 3D bone shape, indicating greater OA structural severity (Table 44). Odds ratios (95% confidence intervals) per normalised unit of 3D bone shape vector for the femur, tibia and patella were 1.32 (1.23, 1.42), 1.31 (1.20, 1.43), 1.30 (1.19, 1.41) respectively, all $p<0.001$. The strength of association of 3D bone shape with PFKS was similar for all male bones. In logistic regression models the femur, tibia and patella remained significantly associated with PFKS, after adjustment for covariates, with modest attenuation of the association for all bones. The adjusted odds ratios (95% confidence intervals) per normalised unit of 3D bone shape vector were 1.25 (1.16, 1.35), 1.25 (1.14, 1.37), 1.25 (1.14, 1.37) for the femur, tibia and patella respectively, all $p<0.001$.

The same analyses amongst females identified very similar findings (Table 44). Similarly no single bone demonstrated a greater association with PFKS than any other. In both males and female adjusted models, the covariates of

body mass index and previous surgery were both significantly associated with PFKS, all p<0.01 (Table 45, Table 46).

Figure 55 Participant flow diagram for the case selection of knees regardless of the presence of radiographic OA

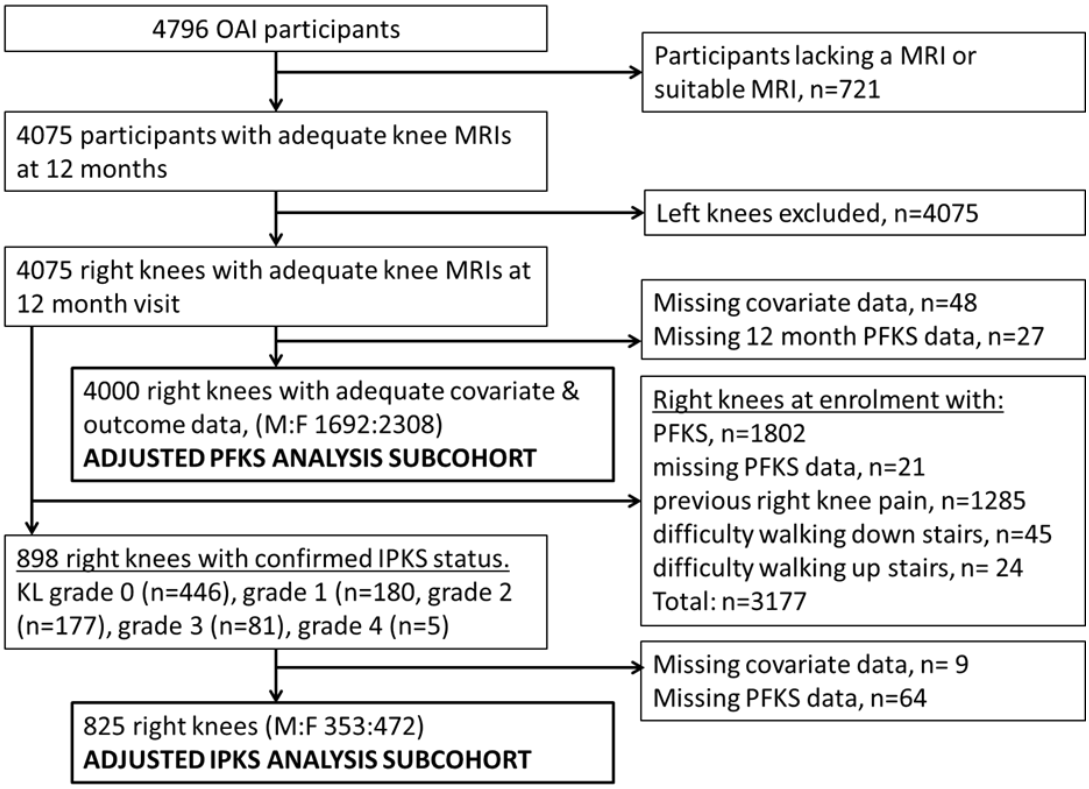

KL – Kellgren Lawrence grade

M:F - male to female ratio

PFKS – Prevalent frequent knee symptoms

IPKS – Incident persistent knee symptoms

Table 43 The distribution of 3D bone shape vectors in male and female participants a) with and without prevalent frequent knee symptoms and b) with and without incident persistent knee symptoms in the 'whole OAI' subcohort of right knees.

	Mean (SD)	Mean (SD)	Mean (SD)
(a) Outcome: prevalent frequent knee symptoms			
3D Bone shape vector(males)	PFKS n=610	No PFKS n=1108	Full group n=1718
Femur	1.09 (1.53)	0.55 (1.28)	0.75 (1.40)
Tibia	0.72 (1.21)	0.36 (1.10)	0.49 (1.16)
Patella	0.79 (1.25)	0.43 (1.14)	0.55 (1.19)
3D Bone shape vector(females)	PFKS n=921	No PFKS n=1409	Full group n=2330
Femur	1.69 (1.82)	0.86 (1.51)	1.18 (1.69)
Tibia	0.39 (1.10)	0.12 (1.09)	0.23 (1.10)
Patella	1.20 (1.43)	0.59 (1.25)	0.83 (1.35)
(b) Outcome: incident persistent knee symptoms			
3D Bone shape vector (males)	IPKS n=42	No IPKS n=316	Full group n=358
Femur	0.80 (1.44)	0.39 (1.17)	0.42 (1.20)
Tibia	0.24 (1.20)	0.12 (1.05)	0.15 (1.06)
Patella	0.50 (0.88)	0.38 (1.18)	0.41 (1.15)
3D Bone shape vector (females)	IPKS n=69	No IPKS n=407	Full group n=476
Femur	0.98 (1.61)	0.53 (1.32)	0.59 (1.37)
Tibia	0.16 (0.99)	-0.01 (1.08)	0.02 (1.06)
Patella	0.59 (1.26)	0.31 (1.22)	0.37 (1.24)

Mean 3D bone shape vectors (SD)

PFKS – persistent frequent knee symptoms

IPKS - incident persistent knee symptoms

Table 44 Associations between 3D bone shape vectors and prevalent frequent knee symptoms at 12 month visit (cross-sectional) and incident persistent knee symptoms by 60-month visit (longitudinal) of all right knees

	OR (95%CI)¥	Adjusted OR (95%CI)†
(a) Outcome: prevalent frequent knee symptoms		
3D Bone shape vector(males)	n=1718 (610 with pain)	n=1692
Femur	**1.32 (1.23, 1.42)****	**1.25 (1.16, 1.35)****
Tibia	**1.31 (1.20,1.43)****	**1.25 (1.14, 1.37)****
Patella	**1.30 (1.19, 1.41)****	**1.25 (1.14, 1.37)****
3D Bone shape vector(females)	n=2330 (921 with pain)	n=2308
Femur	**1.35 (1.28, 1.43)****	**1.29 (1.22, 1.37)****
Tibia	**1.26 (1.17,1.36)****	**1.24 (1.14, 1.34)****
Patella	**1.41(1.32, 1.51)****	**1.33 (1.24, 1.43)****
(b) Outcome: incident persistent knee symptoms		
3D Bone shape vector (males)	n=358 (42 with pain)	n=353
Femur	**1.31 (1.01, 1.69) p=0.04***	1.20 (0.91, 1.59) p=0.20
Tibia	1.11 (0.83, 1.50) p=0.47	1.06 (0.78, 1.44) p=0.71
Patella	1.10 (0.83, 1.45) p=0.52	0.97 (0.71, 1.32) p=0.83
3D Bone shape vector(females)	n=476 (69 with pain)	n=472
Femur	**1.25 (1.05, 1.49) p=0.01***	1.17 (0.97, 1.41) p=0.09
Tibia	1.15 (0.91, 1.46) p=0.24	1.16(0.91, 1.48) p=0.22
Patella	1.20 (0.98, 1.46) p=0.08	1.12 (0.90, 1.38) p=0.30

¥ Right knees with MRIs at 12 months with adequate quality

† Right knees adjusted for age (categorical age (<60, 60-70, >70); BMI (categorical normal <25 kg/m^2, overweight ≥25 to <30kg/m^2, obese ≥30 kg/m^2), previous injury (yes/no), previous surgery (yes/no)

*p<0.05, **p<0.001,

Table 45 The associations between 3D bone shape vectors with prevalent frequent knee symptoms at 12 months – Multivariable models in males.

MALES (n=1692)	OR	95% CI	p-value
Bone – Femur (n=1692)	1.25	1.16, 1.35	<0.01*
Age (ref <60)			
Between 60-70	0.95	0.74, 1.22	0.68
>70 years	1.03	0.80, 1.33	0.83
BMI (ref normal)			
Overweight	1.37	1.03, 1.83	0.03
Obese	1.80	1.34, 2.43	<0.01*
Injury (ref No injury)	1.11	0.88,1.41	0.37
Surgery (ref No surgery)	1.60	1.20, 2.12	<0.01*
Bone – tibia (n=1692)	1.25	1.14, 1.37	<0.01*
Age (ref <60)			
Between 60-70	0.98	0.76, 1.25	0.87
>70 years	1.08	0.84, 1.39	0.56
BMI (ref normal)			
Overweight	1.44	1.08, 1.92	0.01
Obese	1.91	1.42, 2.57	<0.01*
Injury(ref No injury)	1.13	0.90, 1.43	0.30
Surgery(ref No surgery)	1.69	1.27, 2.23	<0.01*
Bone - Patella (n=1692)	1.25	1.14, 1.37	<0.01*
Age (ref <60)			
Between 60-70	0.96	0.75, 1.23	0.75
>70 years	1.02	0.79, 1.31	0.91
BMI (ref normal)			
Overweight	1.36	1.02, 1.81	0.04
Obese	1.81	1.34, 2.44	<0.01*
Injury(ref No injury)	1.14	0.90, 1.44	0.27
Surgery(ref No surgery)	1.76	1.33, 2.33	<0.01*

*p<0.05, **p<0.001, Bone - refers to bone shape vector

Table 46 The associations between 3D bone shape vectors with prevalent frequent knee symptoms at 12 months – Multivariable models in females.

FEMALES (n=2308)	OR	95% CI	p-value
Bone – Femur (n=2308)	1.25	1.16, 1.35	<0.01*
Age (ref <60)			
Between 60-70	0.95	0.74, 1.22	0.68
>70 years	1.03	0.80, 1.33	0.83
BMI (ref normal)			
Overweight	1.37	1.03, 1.83	0.03
Obese	1.80	1.34, 2.43	<0.01*
Injury (ref No injury)	1.11	0.88,1.41	0.37
Surgery (ref No surgery)	1.60	1.20, 2.12	<0.01*
Bone – tibia (n=2308)	1.25	1.14, 1.37	<0.01*
Age (ref <60)			
Between 60-70	0.98	0.76, 1.25	0.87
>70 years	1.08	0.84, 1.39	0.56
BMI (ref normal)			
Overweight	1.44	1.08, 1.92	0.01
Obese	1.91	1.42, 2.57	<0.01*
Injury(ref No injury)	1.13	0.90, 1.43	0.30
Surgery(ref No surgery)	1.69	1.27, 2.23	<0.01*
Bone - Patella (n=2308)	1.25	1.14, 1.37	<0.01*
Age (ref <60)			
Between 60-70	0.96	0.75, 1.23	0.75
>70 years	1.02	0.79, 1.31	0.91
BMI (ref normal)			
Overweight	1.36	1.02, 1.81	0.04
Obese	1.81	1.34, 2.44	<0.01*
Injury(ref No injury)	1.14	0.90, 1.44	0.27
Surgery(ref No surgery)	1.76	1.33, 2.33	<0.01*

*p<0.05, **p<0.001, Bone - refers to bone shape vector

6.3.2 IPKS in the 'whole' OAI subcohort

The participant flow chart for this analysis is described in (Figure 55). Of the 4,796 participants in the OAI database, 834 right knees with and without radiographic knee OA had available bone vector data for IPKS unadjusted analysis. This included 358 males and 476 females of which 42 (12%) males

and 69 (14%) females had IPKS by the 60-month visit. The distribution of the 3D bone shape vector values is described in Table 43)for males and females and those developing IPKS had generally larger vector values than those not developing IPKS, indicating greater structural severity.

The unadjusted logistic regression models of individual male bones estimated increased odds of IPKS with more positive 3D femoral bone shape, indicating greater OA structural severity (Table 44) but there was no association of the tibia or patella with IPKS. Odds ratios (95% confidence intervals) per normalised unit of 3D bone shape vector for the femur, tibia and patella were 1.31 (1.01, 1.69), 1.11 (0.83, 1.50), 1.10 (0.83, 1.45) respectively. The association of femoral 3D bone shape with IPKS was significant (p=0.04). In logistic regression models neither the femur, tibia nor the patella were significantly associated with IPKS, after adjustment for covariates, with attenuation of the unadjusted femoral association. The adjusted odds ratios (95% confidence intervals) per normalised unit of 3D bone shape vector were 1.20 (0.91, 1.59), 1.06 (0.78, 1.44), 0.97 (0.71, 1.32) for the femur, tibia and patella respectively, all p>0.05.

The same analyses amongst females identified very similar findings (Table 44). Similarly no single bone demonstrated a greater association with IPKS than any other.

6.3.3 PFKS in the ‘at-risk’ subcohort without radiographic OA

The participant flow chart for this analysis is described in (Figure 56). Of the 4,796 participants in the OAI database, 858 right knees without radiographic knee OA had available bone vector data for PFKS unadjusted analysis. This included 370 males and 488 females of which 91 (25%) males and 112 (23%) females had PFKS at the 12-month visit. The distribution of the 3D bone shape vector values is described in (Table 47) for males and females and those with and without PFKS had generally similar vector values indicating similar structural severity.

The unadjusted logistic regression models of each individual male bone estimated no association of PFKS with any 3D bone shape (Table 48). Odds ratios (95% confidence intervals) per normalised unit of 3D bone shape vector for the femur, tibia and patella were 1.03 (0.81, 1.32), 1.15 (0.90, 1.46), 1.17 (0.92, 1.48) respectively, all $p>0.05$. In adjusted logistic regression models the femur, tibia and patella remained unassociated with PFKS

The same analyses amongst females identified very similar findings (Table 48) although the unadjusted logistic regression models of only the patella female bone estimated increased odds of PFKS with more positive 3D patellar bone shape, indicating greater OA structural severity (Table 49). Odds ratios (95% confidence intervals) per normalised unit of 3D bone shape vector for the femur, tibia and patella were 1.17 (0.95, 1.43), 1.11 (0.91, 1.37), 1.25 (1.01, 1.55). However the association of the patellar bone shape with PFKS was attenuated after adjustment for covariates (Table 5 & 6) especially BMI and previous injury.

Figure 56 Participant flow diagram for the case selection of knees without radiographic OA

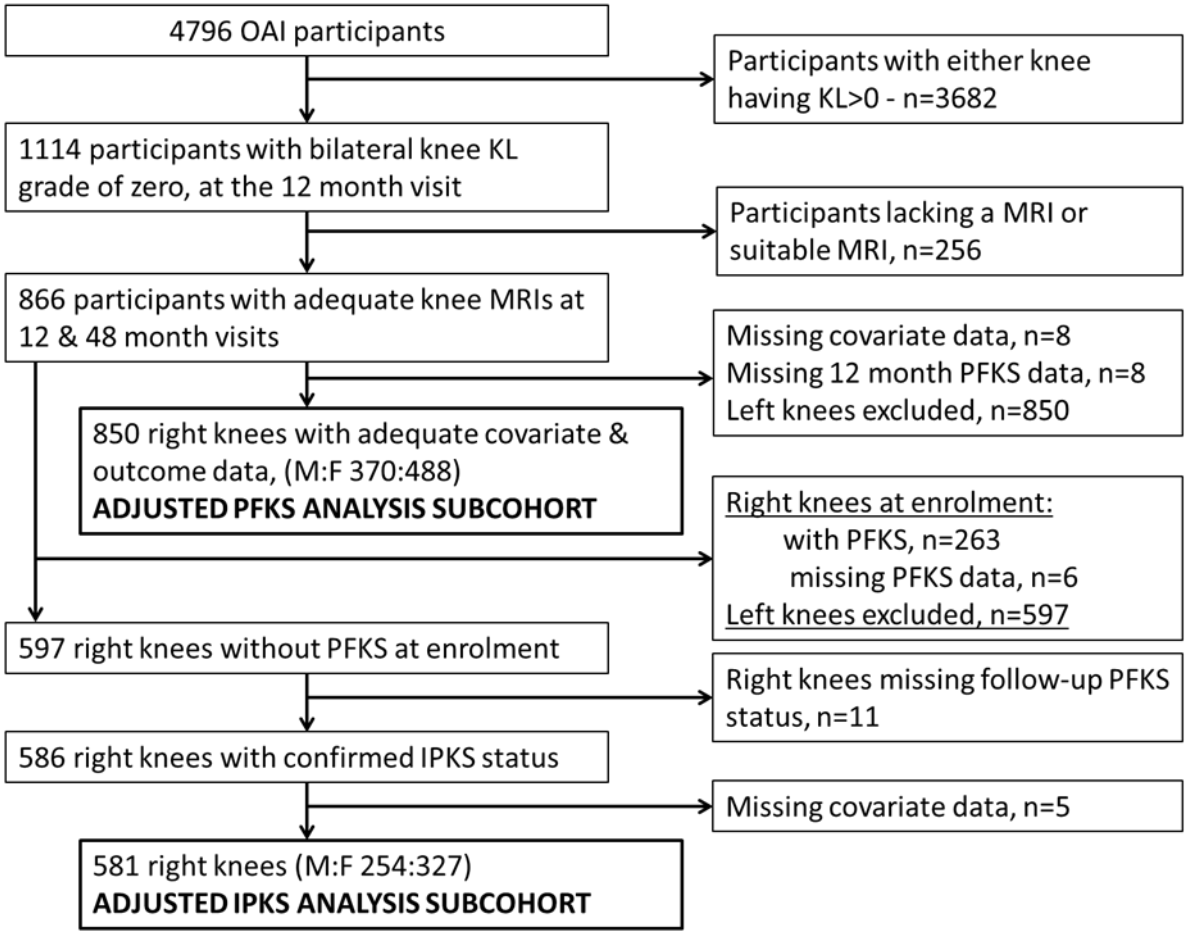

M:F male to female ratio

PFKS – Prevalent frequent knee symptoms

IPKS – Incident persistent knee symptoms

Table 47 The distribution of 3D bone shape vectors in male and female participants a) with and without prevalent frequent knee symptoms and b) with and without incident persistent knee symptoms in all right knees without radiographic knee OA at 12 months.

	Mean (SD)	Mean (SD)	Mean (SD)
(a) Outcome: prevalent frequent knee symptoms			
3D Bone shape vector(males)	PFKS n=91	No PFKS n=279	Full group n=370
Femur	0.09 (0.97)	0.06 (0.98)	0.07 (0.99)
Tibia	-0.01 (1.04)	-0.14 (0.96)	-0.11 (0.98)
Patella	0.21 (1.02)	0.05 (0.99)	0.09 (1.00)
3D Bone shape vector(females)	PFKS n=112	No PFKS n=376	Full group n=488
Femur	0.19 (1.07)	0.02 (1.03)	0.07 (1.04)
Tibia	-0.06 (0.97)	-0.17 (1.04)	-0.14 (1.03)
Patella	0.18 (1.00)	-0.04 (0.99)	0.01 (0.99)
(b) Outcome: incident persistent knee symptoms			
3D Bone shape vector (males)	IPKS n=35	No IPKS n=222	Full group n=257
Femur	-0.04 (0.92)	0.01 (0.98)	0.01 (0.97)
Tibia	0.15 (1.13)	-0.19 (0.96)	-0.14 (0.99)
Patella	-0.01 (0.82)	0.01 (1.00)	0.01 (0.97)
3D Bone shape vector (females)	IPKS n=52	No IPKS n=277	Full group n=329
Femur	0.24 (0.98)	-0.01 (1.00)	0.04 (1.02)
Tibia	0.01 (1.05)	-0.22 (1.00)	-0.18 (1.01)
Patella	0.15 (0.87)	-0.03 (1.01)	-0.01 (0.98)

Mean 3D bone shape vectors (SD)

PFKS – persistent frequent knee symptoms

IPKS - incident persistent knee symptoms

Table 48 Associations between 3D bone shape vectors and prevalent frequent knee symptoms at 12 month visit (cross-sectional) and incident persistent knee symptoms by 60-month visit (longitudinal) of all right knees without radiographic OA at 12 months

	OR (95%CI) ¥	Adjusted OR (95%CI)†
(a) Outcome: prevalent frequent knee symptoms		
3D Bone shape vector (males)	n=370 (91 with pain)	n=365
Femur	1.03 (0.81, 1.32) p=0.81	0.93 (0.72, 1.20) p=0.58
Tibia	1.15 (0.90, 1.46) p=0.27	1.20 (0.93, 1.55) p=0.16
Patella	1.17 (0.92, 1.48) p=0.20	1.08 (0.84, 1.40) p=0.53
3D Bone shape vector (females)	n=488 (112 with pain)	n=485
Femur	1.17 (0.95, 1.43) p=0.13	1.12 (0.91, 1.38) p=0.31
Tibia	1.11 (0.91, 1.37) p=0.30	1.14 (0.92, 1.41) p=0.23
Patella	**1.25 (1.01, 1.55) p=0.04***	1.19 (0.95, 1.49) p=0.12
(b) Outcome: incident persistent knee symptoms		
3D Bone shape vector (males)	n=257 (35 with pain)	n=254
Femur	0.94 (0.65,1.36) p=0.76	0.86 (0.58,1.27) p=0.45
Tibia	1.42 (0.99,2.05) p=0.06	1.47(1.00, 2.17) p=0.05
Patella	0.98(0.68, 1.42) p=0.93	0.90 (0.60, 1.35) p=0.62
3D Bone shape vector (females)	n=329 (52 with pain)	n=327
Femur	1.27 (0.94,1.71) p=0.11	1.21 (0.89,1.64) p=0.23
Tibia	1.26 (0.94,1.69) p=0.13	1.28 (0.94, 1.73) p=0.11
Patella	1.19 (0.88, 1.61) p=0.25	1.14 (0.84, 1.56) p=0.4

¥ Right knees with MRIs at 12 months with adequate quality

† Right knees adjusted for age (categorical age (<60, 60-70, >70); BMI (categorical normal <25 kg/m^2, overweight ≥25 to <30kg/m^2, obese ≥30 kg/m^2), previous injury (yes/no), previous surgery (yes/no)

*p<0.05

Table 49 The associations between patellar 3D bone shape vector with prevalent frequent knee symptoms in right knees without radiographic osteoarthritis at 12 months – Multivariable model

FEMALES (n=488)	OR	95% CI	p-value
Bone - Patella (n=488)	1.19	0.95, 1.49	0.121
Age (ref <60)			
Between 60-70	1.12	0.68, 1.85	0.65
>70 years	0.96	0.52, 1.76	0.89
BMI (ref normal)			
Overweight	1.90	1.17, 3.09	<0.01*
Obese	2.01	1.06, 3.81	0.03
Injury(ref No injury)	2.03	1.19, 3.45	<0.01*
Surgery(ref No surgery)	2.63	0.85, 8.18	0.09

Bone - refers to bone shape vector

6.3.4 IPKS in the 'at-risk' subcohort without radiographic OA

The participant flow chart for this analysis is described in (Figure 56). Of the 4,796 participants in the OAI database, 586 right knees without radiographic knee OA had available bone vector data for IPKS unadjusted analysis. This included 257 males and 329 females of which 35 (14%) males and 52 (16%) females had IPKS by the 60-month visit. The distribution of the 3D bone shape vector values is described in (Table 47) for males and females and those with IPKS had generally no difference in bone shape vector values, than those not developing IPKS.

The unadjusted logistic regression models of each individual male bone estimated no association with PFKS (Table 48). Odds ratios (95% confidence intervals) per normalised unit of 3D bone shape vector for the femur, tibia and patella were 0.94 (0.65, 1.36), 1.42 (0.99, 2.05), 0.98 (0.68, 1.42) respectively, all p>0.05.

In logistic regression models the femur, tibia and patella remained unassociated with the development of IPKS, after adjustment for covariates although the tibia approached borderline significance. The same analyses amongst females identified very similar findings (Table 48).

6.3.5 Diagnostics and linearity checks

In order to check whether the linearity assumption holds between log Incidence pain and outcome variable (bone shape) a formal statistical test was performed for each shape model (linktest) and this was found not to be significant. In other words the null model was that the model is linear.

```
Logistic regression                             Number of obs   =        573
                                                LR chi2(2)      =      14.44
                                                Prob > chi2     =     0.0007
Log likelihood = -235.07716                     Pseudo R2       =     0.0298
```

Incidence	Coef.	Std. Err.	z	P>|z|	[95% Conf.	Interval]
_hat	1.158629	1.223321	0.95	0.344	-1.239036	3.556294
_hatsq	.0524457	.3950597	0.13	0.894	-.7218571	.8267485
_cons	.1077006	.9288484	0.12	0.908	-1.712809	1.92821

P-value for _hatsq=0.89, however linktest alone cannot be used to rule out misspecification therefore a collection of other checks were performed. I have explored the use of Box-Tidwell transformations on bone shape because it is the only one that may have linearity issues to check because the other predictors are categorical (BMI, age, surgery, injury, sex) and I've explored if there are any differences if I have BMI and age maintained as a continuous variable. Results from this suggest that the predictor should be modelled in its current form and there are no misspecification errors in specifying the model in this form and no transformations are needed .Non linearity is related to misspecification.

6.3.5.1Diagnostics plots

Leverage

Figure 57 Leverage Plot 1

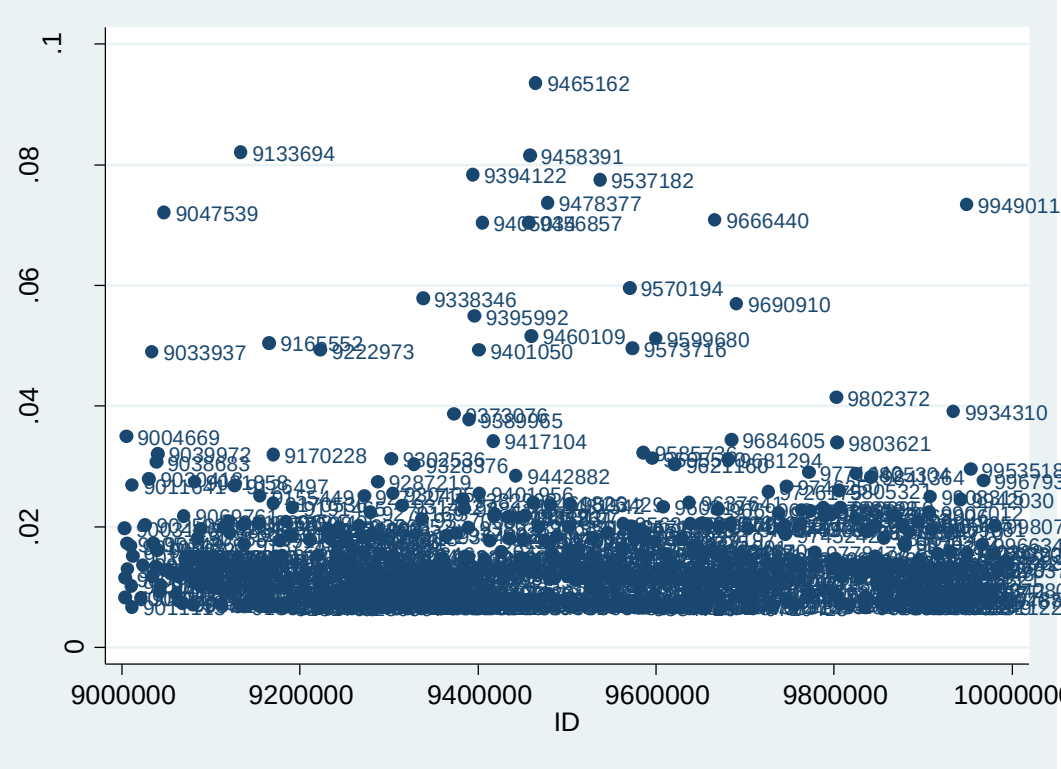

After dropping all the IDs with leverage greater than 0.04 and refitting the model there were no differences hence everyone retained.

-Pregibon`s beta was assessed and not many individuals had values that had undue influence. This is similar to leverage and assesses if there are any individuals with undue influence on covariate estimates.

Figure 58 Leverage Plot 2

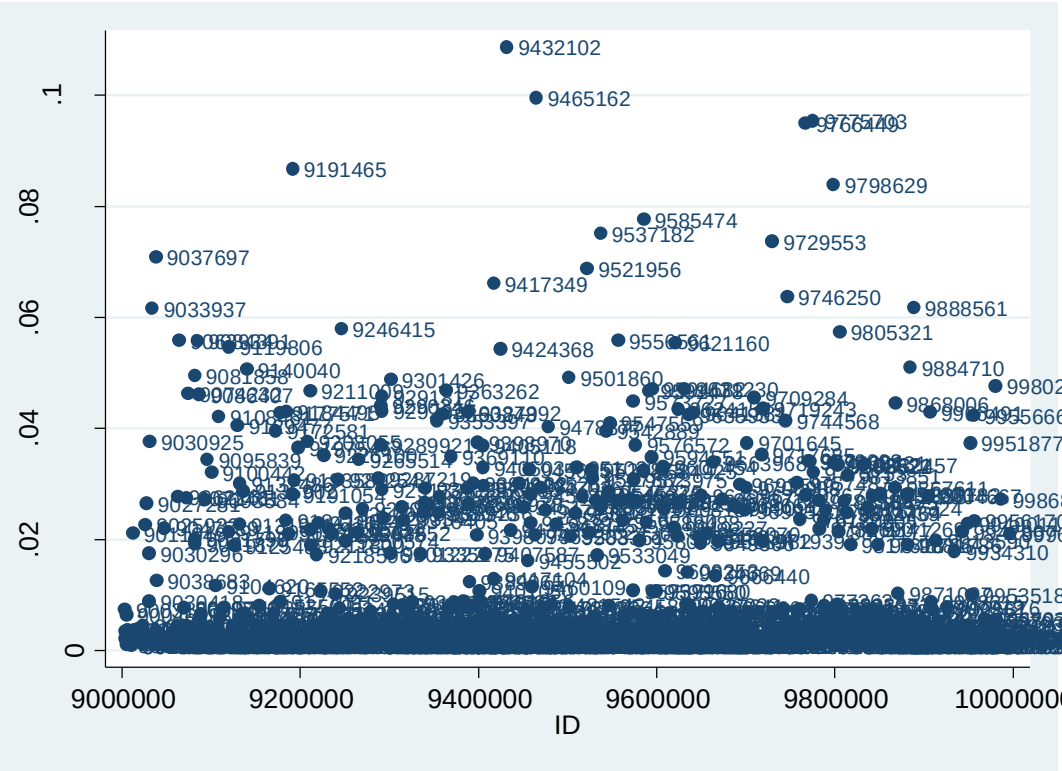

6.3.5.2 Use of polynomials and interactions

From earlier diagnostics there was no suggestion to use any polynomial terms but I just explored these and the results suggested the original form of the variable was sufficient as there was no association seen when the polynomial terms for each bone were included. I have modelled interaction terms separately for the bone measure with BMI and age and no significant interactions were seen and also no change to the odds ratios and therefore the more parsimonious model has been kept in all instances.

6.4 Discussion

This is the first study to describe the relationship of 3D bone shape with PFKS and IPKS in knees with or at risk of OA. This analysis identifies that 3D bone shape is associated with current knee symptoms amongst knees with radiographic OA but not in the ‘at risk’ subcohort without radiographic OA. 3D bone shape is not associated with incident persistent knee OA symptoms regardless of the presence or absence of radiographic knee OA after adjusting for known associations of IPKS. IPKS is associated with female gender, obesity, and knee injury[657].

The analyses within this chapter imply that 3D bone shape is not involved in the pathogenesis of incident knee OA symptoms. Amongst cohorts of knees with prevalent radiographic OA, other subchondral bone pathologies of knee OA have been analysed for their relationship with knee OA symptoms. The best described of these is the bone marrow lesion. BMLs are independently associated with incident frequent knee pain[26, 456] and this has been reported in a recent systematic literature review[658]. However current knee pain in similar cohorts has been reported to have both an association [133, 575, 577] and the absence of a clear association with concurrent BMLs [319, 456, 559, 571]. Systematic literature reviews have identified the association of BMLs with current knee pain in radiographic knee OA as moderate [132] or inconsistent[658]. With appropriate adjustments for important covariates an increasingly larger weight-bearing femoral relative to the tibial subchondral surface area was protective against the incidence of knee OA symptoms in a subcohort of the OAI that included individuals with prevalent knee ROA[102]. Amongst ‘at risk’ subcohorts of knees without radiographic knee OA, PFKS and IPKS in knees at risk of OA have been associated with BMLs, cartilage lesions and meniscal degeneration and these lesions are independently associated with risk of IPKS [131]. In contrast, this study found no clear or consistent evidence that in the same population 3D bone shape vectors for the femur, tibia and patella were related to current frequent knee symptoms or with an increased future risk of the persistence of such symptoms up to 4 years.

The TASmanian Older Adult Cohort examined the relationship between change in BML size and change in ipsilateral knee pain with and without radiographic OA. A change in BML size was associated with changes in ipsilateral pain in those without and not with established ROA implying a greater significance of BMLs in early stage disease [99]

Therefore there is no single knee OA subchondral bone imaging biomarker that has consistently demonstrated both concurrent and predictive criterion validity in relation to knee OA symptoms in knees with and without radiographic OA. However the greatest evidence supporting an association of OA subchondral bone pathology with pain is provided by BMLs and these are likely to be measuring a different pathological construct to bone shape. The pathophysiology by which BMLs may cause pain is unknown but this might include a decreased blood supply causing ischaemia, subchondral microfractures, and raised intraosseous pressure[136-138]. BMLs are and 3D bone shape is not associated with current and future knee symptoms in the ‘at risk’ subcohort without radiographic OA. 3D bone shape is derived from the difference in shape of knees with and without radiographic knee OA. However BMLs are prevalent in knees at risk of OA without radiographic OA and are associated in this group with incident symptoms and radiographic OA[131, 622]. Therefore BMLs may be a more sensitive measure of ‘early’ or pre-radiographic knee OA. The evidence supporting this explanation from my analysis and the association of 3D bone shape with knee OA symptoms is discussed here.3D bone shape change may be involved in the pathogenesis of incident knee symptoms at a more advanced stage of OA, but may be relatively insensitive to knee symptoms in the pre-radiographic phase due to the very narrow distribution of bone vector values at this stage. This is suggested by the fact that the femur, which is the most responsive of the three bone shape vectors[652], was associated with IPKS in univariable analyses in males and females in the ‘whole’ OAI subcohort (Table 2b) but not in the ‘at risk’ subcohort without radiographic OA(Table 5b). It is noteworthy that femoral 3D bone shape changes in a less uniform and symmetric manner in OA progression than the tibia and patella with its

two articulating surfaces and bone expansion occurring around the cartilage plates where increased ridges of “osteophytic” material form[75]. BMLs may represent an early OA focal remodelling that causes future knee symptoms and macroscopic bone remodelling which confers the change in 3D bone shape which is most readily detected in radiographic stages of OA when changes to the bone and joint geometry can adversely affect the congruity of the joint surfaces and impair the effective dissipation of load through the joint tissues. This overloading of the articulating tissues may indirectly cause pain through microfractures and further BMLs or drive cartilage degradation and subsequent synovitis which are both associated with knee pain in a systematic literature review[132].

Amongst knees without radiographic OA BMLs are whilst 3D bone shape is not associated with knee OA symptoms. Amongst knees with established radiographic OA, the association of current knee OA symptoms appears to be more consistent with 3D bone shape than with BMLs after covariate adjustment. This may reflect different mechanisms of pain in radiographic and pre-radiographic OA. 3D bone shape change is closely associated with 3D osteophyte formation (endochondral ossification) which is initiated by vascular invasion of cartilage along with osteoclastogenesis [201-203] which are involved in the innervation and neurovascular invasion of premorbidly aneural cartilage. Therefore 3D bone shape change may correlate with the potential for nociception in cartilage[15]. 3D bone shape change may therefore better reflect the concurrent innervation of cartilage and the potential for concurrent nociception rather than predicting this mechanism of nociception in the future.

3D bone shape was independently associated with TKR in Chapter 5, but the association with knee OA symptoms in this chapter was limited to the presence of radiographic OA. Similarly Waarsing and colleagues[292] identified that 2D bone shape models of the hip correlated well with structural severity but did not correlate well with clinical symptoms and vice-versa.

The validity of 3D bone shape as an outcome measure in clinical trials of knee OA, in light of this chapter's analysis, should be considered. Participants enrolled in all knee OA trials have required symptomatic knee OA and therefore no clinical trial has used incident knee OA symptoms as an outcome. However future clinical trials may attempt to prevent the incidence of knee OA symptoms. If a clinical trial were to attempt to prevent the incidence of knee OA symptoms by targeting the subchondral bone, patients could be selected on the presence of BMLs and incident symptoms would be the primary outcome. However the change in BML size could be a secondary mechanistic outcome[330, 659]. In this context 3D bone shape change could also be used as a sensitive secondary outcome measure of OA structural progression but not for incident symptoms.

6.5 Limitations

There are limitations to this study. Covariates such as BMI may increase between baseline and the onset of IPKS and therefore any association of IPKS may in fact be a consequence of the residual confounding of weight gain. We did not include BML, synovitis, cartilage or meniscal lesion scores because of the limited availability of MOAKs scores in the OAI participants and there could be additional unknown or unmeasured confounders, as with any observational study, that may confer bias. Unmeasured confounders may systematically be different in the subcohorts where we selected right knees only and knees 'at risk' without radiographic OA.

Confounding factors that might influence bone shape could include use of bisphosphonates. Confounding factors for knee OA symptoms could include bone marrow lesions, synovitis, level of activity, muscle strength and increasing BMI after baseline which we did not account for. BMLs and synovitis may reflect failure of the joint to dissipate load effectively and the amount of load put through the joint. Therefore BMLs and synovitis may be on the causal pathway to pain and driven by increased level of activity[660], reduced by pain-related avoidance of activity[661], increased loading of the

joint conferred by increasing BMI or weak muscles which are independently associated with knee OA pain[662, 663].

While the association of 3D bone shape with knee symptoms is conditional to the symptoms being current, and the subcohort including radiographic OA, the limitations of annual pain measurement may confound this analysis. With such large intervening periods between measurement of knee symptoms, these may not be representative of actual knee symptoms. More frequently assessed knee symptoms may be a more precise method for determining pain.

Activity-related pain of OA is typically present in a prodromal phase of ‘early’ OA before the incidence of ROA[18]. This pain in early OA is typically mechanical [128] and pain on stair climbing appears to be the first mechanical symptom to manifest amongst knees with ROA and at risk of ROA[32]. Therefore incident pain might better be assessed more frequently than annually and with more precise symptoms.

The analysis within this chapter relies upon a single time-point measure of 3D bone shape. It remains possible that longitudinal changes in 3D bone shape (within-person pattern of bone shape growth) may confer greater precision, sensitivity to change and association with knee OA symptoms[625].

Magnetic resonance cannot directly identify the presence of calcium. In the segmentation of knee DESS-we MRI sequence the material imaged is assumed to represent bone rather than another tissue type. Confirmation that these surfaces are actually bone requires further work. We are reassured that the automated segmentation used here is both accurate and repeatable.

6.6 Conclusions

This chapter has demonstrated that 3D bone shape vectors are associated with current frequent knee symptoms but not with incident persistent symptoms of knees with radiographic OA. This chapter therefore provides

evidence of concurrent validity of 3D bone shape which is restricted to knees with radiographic knee OA. This chapter also identified that unlike bone marrow lesions, 3D bone shape is not associated with either current knee symptoms or incident persistent knee symptoms in knees without radiographic OA but at risk of knee OA. Therefore 3D bone shape has evidence of validity for use as an outcome measure in interventional clinical trials and may represent and important tissue target for knee OA structural modification. However 3D bone shape is unlikely to be an important tissue target for preventing the onset of symptomatic knee OA.

6.7 Recent evidence for 3D bone biomarker validation

Further validation work has recently been published in parallel with the novel research contained within this PhD. This includes evidence of the reliability and responsiveness and further construct validity of the 3D bone shape biomarkers. This is described here using the domains of the Outcome Measures in Rheumatology (OMERACT) filter[355, 356] which are described in 2.7.2 Validation of biomarkers using the OMERACT filter

6.7.1 Construct validity

Longitudinal change in 3D bone area was described in approximately 1300 knees with established radiographic OA and in 900 knees without radiographic OA. The longitudinal percentage increase in bone area was three fold greater in knees with than those without radiographic OA. Furthermore all bones in the knee increased in 3D bone area, particularly around each cartilage plate in a circumferential pattern, which is likely to represent the 3D characteristics of the 2D osteophytes ‘lip’ seen on conventional radiography. Together this provides evidence of construct validity as bone area correlated with established features of pathology within the same domain of structure[664].

6.7.2 Predictive validity

The association of the longitudinal change in 3D bone shape or bone area with longitudinal medial tibiofemoral radiographic structural progression and pain progression was recently described in a case-control study of knees nested within the OAI [625]. Case knees (n=200) were defined as knees with mild to moderate structural disease with structural and pain progression over 48 months. Controls (n=400) were defined as neither structural or pain progression or only progression in either structure or pain.

Both of the 3D bone biomarkers were independently associated with structural progression but only weakly with pain progression. However this highlights their potential use in prospective DMOAD clinical trials as surrogate measures of these important patient-centred endpoints[625].

A similar hierarchy of strength of association of each of the bones, to the associations identified in this PhD, was observed. The medial femur 3D bone area was most strongly associated with radiographic progression and pain progression. The 3D femoral shape vector was most strongly associated with structural progression but not with pain progression as in the analysis in Chapter 6. It is interesting to note that a similar analysis using change in cartilage thickness instead of bone biomarkers identified similar associations[665].

6.7.3 Reliability

For the active appearance models used in this thesis, the accuracy of the automated segmentations has been further assessed using test–retest MRIs for 19 participants (38 images) with no OA to moderate degrees of clinical OA, that were originally prepared as a pilot study for the OAI, to test the accuracy and precision of knee cartilage qMRI with a fast double echo, steady state (DESS) sequence which is the same as used in the OAI [644]. The bone surface was manually segmented as previously described[632]. Mean point-to-surface distances were calculated between the manual and automated segmentations. Mean point-to-surface errors were as follows: for

the femur, 0.49 mm; for the tibia, 0.53 mm; and for the patella, 0.57 mm (i.e. each approximately the size of 1 voxel)[75].

It is often difficult to obtain inter-occasion reliability data as this involves re-imaging subjects within a short period of time and causes patient inconvenience. The reliability of the method of measuring 3D bone area and 3D bone shape vector was assessed in a set of 35 knees with OA that underwent the same image acquisition as in the OAI on two separate occasions one week apart. The inter-occasion reliability for the 3D bone shape vector was good with the smallest detectable difference (SDD) for the femur, tibia and patella vectors as 0.22, 0.86 and 0.24 units normalised to the mean non-OA shape respectively [625].

The reliability of the tAB or 3D bone area was also good with the SDD (SDD % of baseline bone area) being described in units of area (mm^2) for the medial femur, medial femoral trochlea, medial tibia and medial patella as 24.4 (1.07%), 12.8 (1.98%), 21.6 (1.99%), 20.6 (4.02%)[625].

The root-mean-square coefficient of the variance (CoV) has been calculated to describe the repeatability of bone area within the same test-retest assessment of 35 knees. The CoV of medial femur, medial trochlea femur, medial tibia and medial patella were 0.38%, 0.67%, 0.69%, 1.45% respectively[625]. This compares favourably to a mean CoV of approximately 2-3% for automated segmentations of cartilage thickness in the same test-retest reliability assessment[632].

The reliability of the method of measuring 3D bone area (tAB) and medial joint space (mJSW) width was assessed in a set of 147 knees without radiographic OA that underwent the same image acquisition as in the OAI on two separate occasions one year apart. Considering the absence of radiographic OA, it was therefore expected that little real difference should be expected. The CoV of 3D bone areas and mJSW was <1% and 5.1% respectively[664]. Therefore the reliability of 3D bone shape biomarkers is good and superior to the current standard of measuring structural progression that relies upon JSW. There is substantial measurement error in

JSW and using 3D bone biomarkers may therefore improve the measurement noise to signal ratio.

6.7.4 Responsiveness

The responsiveness of bone area, cartilage thickness and joint space narrowing (JSN) was determined by describing the change in these measures in 350 knees with radiographic OA within the OAI cohort, over two years. Bone area was measured by automated segmentation using active appearance models and cartilage thickness was computed from manual segmentations of the femorotibial joint. JSN was measured using mJSW measures provided by the OAI. The mJSW was measured using a semiautomated tool shown to be as sensitive as manual measures. The responsiveness over two years (standardised response mean) for the medial femur bone area, the most responsive cartilage thickness measure (central medial femorotibial composite) and mJSW was 0.83, 0.38 and 0.35 respectively. The longitudinal changes in bone area in the medial tibiofemoral joint are displayed in (Figure 59). Therefore in comparison to cartilage volume or mJSW, 3D bone area was much more responsive. The responsiveness of 3D bone area is also highlighted by the fact that almost half of all individuals had a change in bone area during the two year period that was greater than the SDD[664].

Figure 59 The longitudinal changes in bone area in the medial tibiofemoral joint

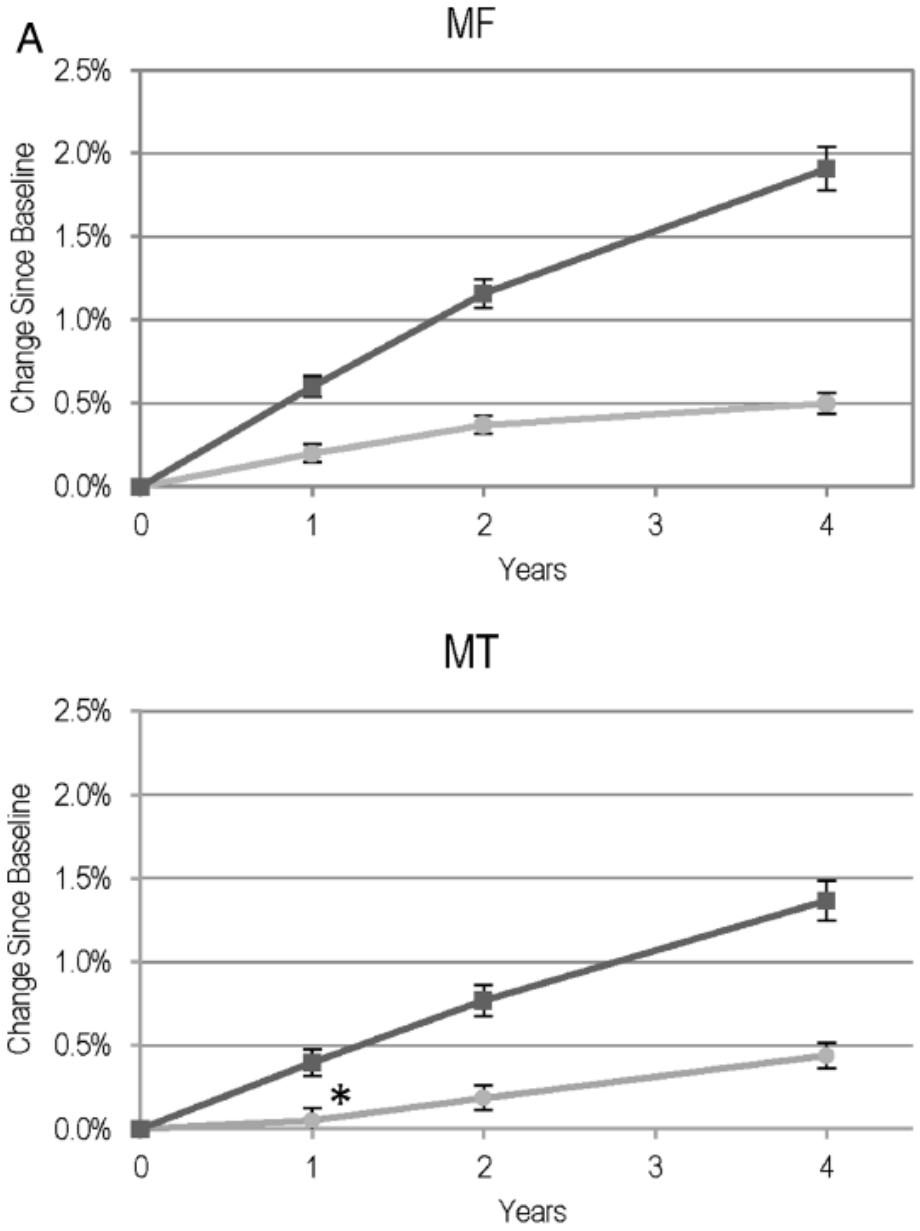

Legend: Percentage change in bone area (tAB) from baseline for medial regions in OA (dark grey) and non-OA groups (light grey) (95% CI). All changes were highly significant ($p<0.0001$) except *

6.7.5 Feasibility

3D bone shape biomarkers require specialised automated segmentation and imaging analysis technology along with technical experts in image analysis and MRI radiographers.

While proprietary software was used for the active appearance models that defined the 3D bone shape biomarkers in this thesis, there are several other research groups that are using similar segmentation methods to define 3D shape of joint structures and the importance of these in OA. These include researchers at Imperial College, London, that have defined the 3D shape of the meniscus and its relationship to cartilage load [666, 667], and researchers at the University of North Carolina that have described the 3D shape of the mandible in temporomandibular joint OA at [668]. Researchers at Parcelsus University have used automated segmentation to describe 3D shape of bone and cartilage[102]. Semi-automated shape recognition technology has been used by researchers at the University of Cambridge to investigate the shape of the femoral head in hip OA[669] and at University of California San Francisco to investigate the shape of the tibia and femur after anterior cruciate ligament injury.[670]. As this technology becomes more readily available, the access to bone shape and joint tissue biomarkers will continue to increase.

The superior responsiveness and reliability of 3D bone shape biomarkers over conventional radiography, should very substantially reduce the number of participants and duration of a clinical trial required, to adequately power a study of a prospective DMOAD[664]. While manual semi-quantitative or quantitative scoring of joint images can be expensive and hugely time consuming for radiologists in clinical and observational trials, the bone shape biomarkers for all 4790 participants in the OAI, in all knees at all time points can be generated using automated active appearance modelling in 24-48 hours. Furthermore a substantial reduction in the number of trial participants required to adequately power a trial, may similarly substantially reduce the burden and practical demands associated with conducting interventional clinical trials in OA. The overall reduction in cost, size and duration of trials

and clinical trial staff labour may substantially facilitate interventional OA researchers in performing vital trials to identify novel therapies in OA.

In the future it remains possible that these bone shape biomarkers and this technology may enter routine clinical practice. Patients at-risk of OA or with OA could be appropriately stratified into those in need of intervention by using bone shape biomarkers. This could be feasible in the clinic setting, if the cost of AAM software becomes cheaper and appropriate decision making tools are developed tool, in a similar manner to the FRAX tool (University of Sheffield) that is used for the management of osteoporosis.

Chapter 7 Discussion, future directions and conclusions

7.1 Thesis synopsis

This thesis is concerned with the role of subchondral bone in knee OA and specifically describes the relationship of 3D knee bone shape with established measures of OA structural severity and important patient-centred outcomes in knee OA including total knee replacement and knee OA symptoms. This provides evidence supporting the validity of bone shape for use as a biomarker in OA clinical trials. The analyses performed in this thesis in Chapters three, four, five and six are summarised as follows:

Chapter 3

The aim of this chapter was to systematically collect all literature pertaining to the relationship between imaging-assessed subchondral bone pathology and the important outcomes of joint replacement, structural progression and pain, with a suitable systematic stratification by quality scoring system and assessment of adequacy of confounder adjustment. This systematic literature review concluded that there were independent associations between imaging-assessed bone pathologies and TKR, structural progression and pain in the knee, hand, and hip. The most substantive evidence for independent associations was for knees:

- MRI BMLs were independently associated with structural progression, TKR and longitudinal change in knee pain severity
- MRI osteophytes were independently associated with knee structural progression only
- MRI 2D tibial bone area was independently associated with structural progression, TKR and the ratio of the medial tibiofemoral articulating bone surface areas was independently associated with incident frequent knee pain
- Trabecular morphometry and bone densitometry were associated with structural progression but this was not independent of confounders

- MRI bone attrition and cysts were not associated with structural progression and may be epiphenomenon of knee OA rather than being on the causal pathway.

2D hip bone shape measures were independently associated with structural progression and total hip replacement. Hand OA structural progression was independently associated with BMLs. The existing standard for measuring structural progression, radiographic (JSN), poorly correlated with the clinical syndrome and remains a relatively insensitive measure (see 2.11 OA biomarkers). When JSN is used as a trial outcome measure this demands that clinical trials are large, long and expensive. Therefore the unmet need for more sensitive and validated imaging biomarkers is huge.

The independent associations of certain subchondral bone features with important patient-centred outcomes (pain and TKR) and structural progression suggest subchondral bone can provide valid surrogate measures of these outcomes. While many of these are MRI-derived measures, they are intrinsically more sensitive than radiographic JSN (see 2.11 OA biomarkers), their use as clinical outcomes may substantially reduce the cost, duration and size of future trials. Bone measures may also improve the precision of OA phenotypic stratification to facilitate pathology-specific treatment, prioritisation of individuals most in need of structure modification and measuring treatment response.

This systematic review highlighted the need for greater information on the validity of subchondral bone features to be used as surrogate measures of OA patient-centred outcomes in all joints. There was very little evidence describing the validity of 3D bone shape as a surrogate measure. This unmet need was addressed in studies presented in the subsequent chapters.

Chapter 4

The aim of this chapter was to describe the association of the 3D bone structure of OA with established constructs of radiographic structural OA.

The objective was to determine if there was evidence of construct validity of the 3D bone structure. The articulating regions of knee bones typically expand in 3D with structural progression of OA. Their physiological 'starting' shape is determined by height, age, weight. The 3D bone structure of OA (described as OA-attributable bone area) was determined by subtracting the actual bone area from the predicted physiological bone area based upon available demographic data. Regression analyses were then performed to establish whether conventional radiographic measures of knee OA were independently associated with corresponding OA-attributable bone area after adjusting for alignment and other conventional radiographic features.

This analysis confirmed metric JSW, osteophyte grade, subchondral sclerosis grade and KL grade all were significantly associated with OA-attributable bone area. None of these measures explained a substantive proportion of the OA-attributable bone area. However the greatest explanation of area variance was provided by osteophyte score. An explanation for this is that OA-attributable bone area is in part a representation of three-dimensional endochondral ossification and osteophyte formation which is less precisely quantified by the 2D projection images of conventional radiography.

The association of OA-attributable 3D bone area with established standards of radiographic OA provides evidence of construct validity. The association of this 3D knee bone shape change of OA with important knee outcomes such as TKR and knee symptoms was subsequently explored and is described in Chapters 5 and 6.

Chapter 5

The aim of this chapter was to establish if 3D bone shape was associated with the important patient-centred outcome of total knee replacement (TKR). A case-control analysis, nested within the OAI, achieved effective matching of multiple strong confounding factors using propensity score matching (without matching for radiographic severity). The 3D bone shape vectors of

the femur, tibia and patella were all significantly associated with the outcome of TKR with the femur having the strongest association which is concordant with other analyses of femur shape. After adjustment for KL grade, the association of TKR with the patella and tibia shape was attenuated but the femur remained associated and improved the model ‘fit’ indicating femoral bone shape has an independent association with TKR after adjustment for KL grade. This was considered to reflect the additional 3D structural information that is not captured by conventional radiography in addition to the observation that femoral bone shape is more responsive and changes in more heterogenous manner with OA structural progression, indicating it may be a more suitable biomarker for use in clinical trials. This provided evidence of predictive validity and further underpinned the value of quantitative bone measures in future therapeutic trials of disease modifying osteoarthritis drugs.

Chapter 6

The aim of this chapter was to establish if 3D bone shape was independently associated with current knee OA symptoms (concurrent validity) and incident persistent knee symptoms (predictive validity). The first analysis was performed upon the ‘whole’ OAI subcohort of knees which included knees with and without radiographic OA with available demographic covariate data and an MRI of suitable quality at the 12 month visit in the OAI. In this analysis 3D bone shape was independently associated with current symptoms but not incident persistent symptoms. The second analysis was performed upon knees ‘at-risk’ of knee OA but without radiographic knee OA. Neither current nor incident knee symptoms were associated with 3D bone shape. In conclusion 3D bone shape was independently associated with current knee OA symptoms when extant radiographic knee OA is present. This provided evidence of conditional concurrent validity. It may be that knee bone shape is more relevant to pain when more advanced structural severity is present, such as when endochondral ossification occurs and the neurovascular invasion of cartilage occurs. However while the

association of 3D bone shape with knee symptoms was conditional, the limitations of annual pain measurement may have confounded this analysis. With such large intervening periods between measurements of knee symptoms, these may not be representative of actual knee symptoms.

Overall Summary

The hypothesis underlying this thesis was that subchondral knee bone 3D shape, defined using 3D knee MRI segmentation and (AAM), would demonstrate validity as a biomarker through association with existing radiographic measures of structural knee OA pathology, TKR and knee OA symptoms as part of the validation of biomarkers for use in knee OA clinical trials. In summary, this thesis has indeed provided evidence supporting the OMERACT biomarker tool validation domain of truth, that 3D knee bone shape biomarkers have construct validity as measures of knee OA radiographic severity, predictive validity by association with total knee replacement (TKR) and concurrent validity by association with knee OA symptoms in knees with radiographic OA. While 3D bone shape is independently associated with knee OA radiographic structural disease and total knee replacement, like many other structural imaging biomarkers, the association with symptoms is weaker.

Evidence for 3D bone shape biomarkers fulfilling the OMERACT domain of discrimination has been provided by the demonstration of good reliability and responsiveness in work performed in parallel to this PhD which is described in full in (6.7.3 Reliability, 6.7.4 Responsiveness).

Finally 3D bone shape biomarkers may fulfil the OMERACT domain of feasibility. The cost and technical demands of performing clinical trials with endpoints defined by conventional radiography and MRI might favour conventional radiography at first glance. However while conventional radiography is inexpensive and easily accessible, the relative insensitivity and poor responsiveness confers the need for relatively large number of participants with long duration compared to MRI bone biomarkers. The

additional expense of MRI and image analysis is very likely to be offset by the substantial reduction in trial size and duration.

7.2 Improving understanding of the relationship between bone features and symptoms

The unmet need for evidence describing the association of 3D bone shape with patient-centred outcomes (e.g. TKR and pain) was highlighted in Chapter 3. In Chapter 3 the only previous analysis of knee bone shape with knee OA symptoms reported an increasingly larger medial weight-bearing femoral relative to tibial subchondral surface area (mSSR) was protective against the incidence of knee OA symptoms in a subcohort of the OAI that included individuals with prevalent knee ROA[102]. This association was independent of important determinants of knee OA symptoms. This applied outcome of incident knee OA symptoms referred to the incidence of these symptoms at one time point in this study which should be distinguished from the definition used in Chapter 6 where the incidence of frequent knee OA symptoms must have been reported at two consecutive annual reviews. Everhart and colleagues used a less strict definition of pain incidence and used bone area measurements focussing on the medial joint space where greater pathological bone shape changes are observed relative to the whole bone shape. These differences in methodology may explain why the vectors of whole 3D bone shape (tibia, femur and patella) used in this thesis were not associated with incident persistent knee OA symptoms in Chapter 6 whilst Everhart and colleagues found an association of mSSR with incident knee OA symptoms in Chapter 3[102].

As described in Chapter 3 BMLs were independently associated with incident frequent knee pain[26, 456, 658] . However in a systematic literature review, BMLs were only moderately associated with knee pain [132]. In cross-sectional analyses BMLs have [133, 575, 577] and have not been found to be associated with current knee pain[319, 456, 559, 571]. However

Sharma and colleagues established that BMLs were associated with current frequent knee symptoms and incident persistent knee symptoms in a subcohort of knees in the OAI that are at risk of knee OA but without radiographic OA knee[131]. By replicating this analysis and replacing BMLs with 3D bone shape, we established that bone shape has neither concurrent nor predictive validity. However by including all knees, including those with radiographic OA, bone shape demonstrated concurrent validity.

The evidence from Chapter 3 and Chapter 6 identified that BMLs and 3D bone shape respectively, are independently associated with future total knee replacement and both have construct validity[516, 671].

There are several possible (non-exclusive) explanations for the variation in association of knee OA symptoms with BMLs and 3D bone shape: firstly the measurement of prevalent frequent knee symptoms in the preceding year is prone to recall bias and fails to distinguish activity-related pain and resting pain which may be measuring different pathologies; secondly knee OA symptoms may be caused by different pathologies at different stages of structural progression; thirdly that unmeasured confounding factors may be responsible for all or some associations observed; fourthly that BMLs cause both knee symptoms and 3D bone shape changes.

In the first explanation it should be acknowledged that self-reported chronic pain assessments are prone to recall biases (e.g. recency and memory effects)[672] particularly where participants are asked to recall frequency of pain over the preceding year as in the methods used by Sharma and colleagues[131] and in Chapter 6. Furthermore by not distinguishing whether the pain described is present whilst resting or on activity, the composite measure of the two of these that is used to describe prevalent knee symptoms may represent residual confounding with a greater association with BMLs rather than bone shape. It is possible that different associations of the BMLs and bone shape may be observed with more precise definitions of pain.

In the second explanation knee OA symptoms may be caused by different pathogenic mechanisms within the subchondral bone and these

predominate at different stages of structural progression. For example BMLs may predominate in the pre-radiographic phase whilst 3D bone shape changes may be the predominant cause of symptoms in the radiographic stages. This is supported by an analysis within the TASmanian Older Adult Cohort which examined the relationship between change in BML size and change in ipsilateral knee pain in knees with and without radiographic OA. A change in BML size was associated with changes in ipsilateral pain in those without and not with established ROA implying a greater significance of BMLs in early stage disease [99]. BMLs are likely to be measuring a different pathological construct to bone shape. The pathophysiology by which BMLs may cause pain is unknown but this might include a decreased blood supply causing ischaemia, subchondral microfractures, and raised intraosseous pressure[136-138].These processes may be more relevant to pain in the pre-radiographic stage of OA.

3D bone shape change is closely associated with 3D osteophyte formation (endochondral ossification) which is initiated by vascular invasion of cartilage along with osteoclastogenesis [201-203] which are involved in the innervation and neurovascular invasion of premorbidly aneural cartilage. Therefore 3D bone shape change may correlate with the potential for nociception in cartilage[15]. 3D bone shape change may therefore better reflect the concurrent innervation of cartilage and the potential for concurrent nociception rather than predicting future nociception. This issue of the change in bone shape is important because this occurs most noticeably in the non-weight bearing regions of the knee which can be described histologically but can also be quantified more specifically using AAMs. This quantitative measure may represent a better biomarker than existing bone shape measures (see 7.4.1.1 Future analyses to elucidate the validity of 3D bone shape as a surrogate measure of knee OA)

3D bone shape, which is in part determined by radiographic severity, may also be relatively insensitive to knee symptoms in the pre-radiographic phase due to the very narrow distribution of bone vector values at this stage. This is suggested by the fact that the femur, which is the most responsive of

the three bone shape vectors[664], was associated with IPKS in univariable analyses in males and females in the ‘whole’ OAI subcohort (Table 2b) but not in the ‘at risk’ subcohort without radiographic OA(Table 5b).

In the third explanation it is important to consider that while we have identified associations of bone features with knee symptoms, these do not imply causation. There may be additional unknown or unmeasured confounders that may directly cause both BMLs and symptoms and future change in 3D bone shape and therefore the subchondral bone features are not on the causal pathway of knee OA symptoms. For example knee OA pain is typically activity-related. The level of activity (or load placed through the joint) is recognised to correlate with BMLs [673], knee OA symptoms and may drive bone remodelling with future 3D change in knee bone shape. Therefore neither BMLs nor 3D bone shape may be independently associated with knee OA symptoms after adjustment for level of activity.

In the fourth explanation bone shape may not be associated with knee OA symptoms but is a consequence of bone remodelling driven by BMLs. In this scenario BMLs may directly cause knee pain and after adjusting the 3D bone shape model for BMLs, 3D bone shape would no longer be independently associated with pain.

7.3 Future Directions

Conventional radiography (CR) is inexpensive and widely available. CR joint space width (JSW) is the traditionally used surrogate for assessing hyaline articular cartilage thickness and is used to define and measure structural progression of OA. Joint space narrowing (JSN) remains the current standard for measuring cartilage loss or structural progression in disease modification trials, where it is used as a primary end point[367]. However there are a number of limitations of using JSN.

Knee JSN lacks tissue-specificity because it reflects a construct of reduction in hyaline articular cartilage thickness along with meniscal extrusion and

degeneration[86]. The measurement of JSN has relatively poor reliability and responsiveness in comparison to MRI-based measures[664] which is in part due to significant repositioning variability (2.11.1.1 Conventional radiographic quantitative measures)[402, 414]. The smallest detectable difference least 0.2mm is large relative to the mean rate of annual knee JSN of 0.13 ± 0.15mm/year, with change occurring in only a small group of “progressors”[93, 94].

There is no consensus on the threshold for defining relevant structural progression using JSN[485], which was highlighted by a systematic literature review describing the heterogeneity of opinion amongst experts [415].

OA is a whole joint disease and can involve a heterogenous combination of joint tissues that are indistinguishable by clinical or conventional radiographic assessment[25]. Participants in clinical trials are typically recruited by the presence of a homogenous clinical and CR phenotype which belies the heterogeneity in tissue pathology. Therefore CR fails to distinguish the variation in OA tissue phenotype. CR is also insensitive to pre-radiographic structural pathology or early OA which is prevalent in individuals at risk of OA with and without symptoms[23]. The presence and changes in tissue pathologies (e.g. BMLs) are relevant to knee OA symptoms and structural progression at this stage but are not detectable by CR[131, 622].

The severity of CR knee OA is also poorly correlated with knee OA symptoms[674], where only 50% of knees with radiographic OA have symptoms and only large changes in conventional radiographic knee OA severity are associated with changes in knee pain[98].

JSN is used by orthopaedic surgeons to determine the need for joint replacement and therefore is associated with TKR[675]. However using JSN as a clinical endpoint in clinical trials confers the need for large numbers of participants for two years or more in order to adequately power the study. This represents a major barrier to performing trials of prospective disease modifying agents. This highlights the need for better biomarkers. This section will discuss further important research required to determine the

validity of 3D bone shape as a surrogate measure of patient-centred outcomes and the potential to segment all of the joint tissues with AAM to provide quantitative measures of whole joint OA-tissue pathology. This section will also describe the potential advantages of using more precisely defined OA phenotypes using multiple modalities in addition to imaging biomarkers and developing improved concepts of early OA. Finally I will discuss the implications of the application of the novel imaging analysis technology used in this thesis in other joints and clinical scenarios beyond the knee.

7.3.1. Further validation and use of bone and multi-tissue biomarkers in clinical research as outcome measures

7.3.1.1 Future analyses to elucidate the validity of 3D bone shape as an outcome for knee OA trials.

While this thesis has provided evidence for the validity of novel imaging bone shape biomarkers towards their use as surrogate measures in future clinical OA trials and parallel work has identified that they 3D bone area is highly responsive and associated with knee OA pain progression, further analyses of their validity will be required.

A better understanding of the relationship between BMLs and bone shape and their relationship with patient centred outcomes such as TKR and OA symptoms is of great interest and relevance to understanding the pathogenesis of OA. With this in mind a number of future analyses should be considered.

The first analysis would be to establish the construct validity of the novel 3D bone shape and tAB (bone area) bone biomarkers in relation to important MRI bone pathologies, including BMLs and osteophytes measured semi-quantitatively using the MOAKs scores (which are publically available for 600 knees in the OAI including knees with both structural and pain progression, knees with structural progression only, knees with pain progression only and knees with neither progression). This could be

performed by establishing the correlation coefficients for corresponding regional tAB and BMLs or osteophytes. For whole 3D bone shape the BMLs and osteophyte scores could be summated for each bone for each region. The objective of this analysis would be to explore the association of these subchondral bone pathologies at various stages of disease.

A second analysis would explore the association of different anatomical regions within the current 3D bone shape with knee OA pain and symptoms. This comes from the observation that knee OA pain progression was associated with change in tAB. I have also observed that the 3D change in knee bone shape occurs in two distinct regions of the bones involved. There is a weight-bearing bone area (A) on each knee bone, and the non-weight-bearing area (B) (Figure 60,Figure 61). I have briefly explored the data and realise the weight-bearing area (A) undergoes minor expansion in area whilst the non-weight-bearing area (B) undergoes significant increase in area. The objective would be to first repeat the case-control analysis conducted by Hunter and colleagues[625] to establish if the change in areas A and B are more strongly associated with pain progression or incidence. A subsequent analysis of interest would also be to repeat analysis of Chapter 6 using areas A and B to establish if the specific changes in bone shape are independently associated with incident and prevalent pain. This analysis should include adjustment for confounding factors for pain such as level of activity. A more precise definition of knee OA symptoms could also be used including the prodromal symptoms of pain that precede radiographic OA[18] and the first symptoms of knee OA pain that appear to occur during weight-bearing activities involving bending of the knee, such as using stairs[32] in addition to pain at rest (7.2 Improving understanding of the relationship between bone features and symptoms). The association of the 3D bone shape biomarkers should also be assessed with these measures.

Future validation of bone biomarkers may also include a composite measure of BMLs and bone shape to enhance the validity of the biomarker. This may draw upon the concurrent and predictive validity against knee OA symptoms in the pre-radiographic phase of BMLs.

Clinical trials of knee OA enrol symptomatic knee OA and therefore no clinical trial has used incident knee OA pain as an outcome. However future clinical trials may attempt to prevent the incidence of knee OA pain. If a clinical trial were to attempt to prevent the incidence of knee OA pain by targeting the subchondral bone, patients could be selected on the presence of BMLs and incident pain would be the primary outcome. However the change in BML size could be a secondary mechanistic outcome[330, 659].

Therapeutic interventions targeting or inhibiting the general expansion of 3D knee bone shape would be unlikely to prevent the onset of knee OA symptoms. However 3D bone shape expansion measures a construct called “OA structural progression” and is the most responsive measure of OA structural progression. Therefore 3D bone shape change could be used as a sensitive secondary outcome measure of OA structural progression in clinical trials attempting to prevent the onset of symptomatic knee OA.

More suitable tissue targets for such a clinical trial would include BMLs and synovitis. This contrasts with the findings of Chapter 5 that indicate that 3D bone shape is associated with TKR and has validity for use as an outcome measure in typical interventional OA trials attempting to modify structural progression. Therapies inhibiting the changes observed in 3D bone shape in knee OA might therefore be targeting an important structural process in the pathogenesis of joint failure and may be an important tissue target in trials attempting to modify structural progression.

Figure 60 Area A – Weight-bearing

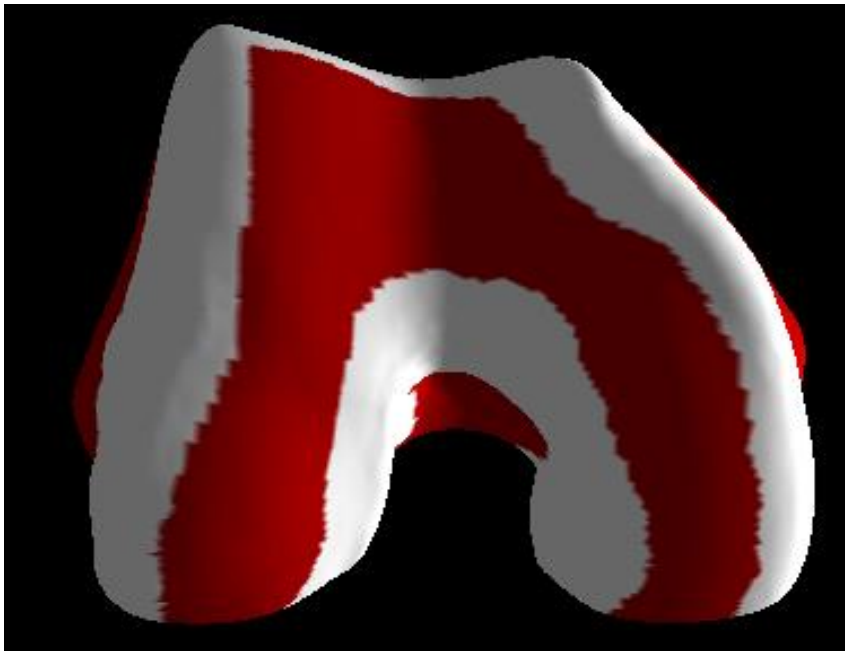

The area of the femur shown in red represents the weight-bearing region

Figure 61 Area B Non-weight-bearing

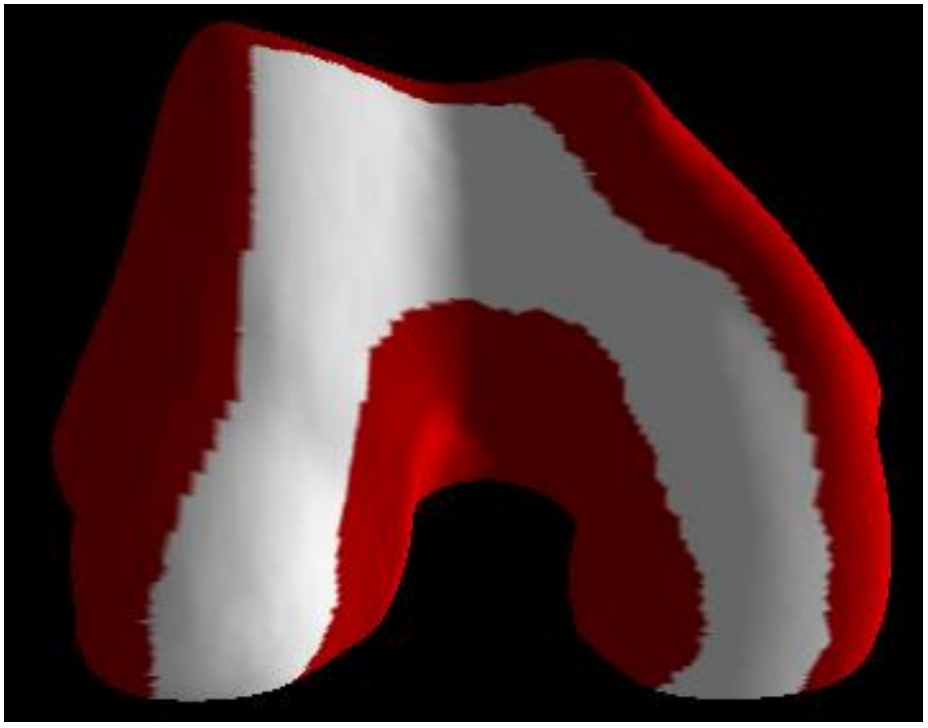

The area of the femur shown in red represents the non-weight-bearing region

7.3.1.2 Future analyses to elucidate the validity of quantitative multi-tissue measures and a whole joint biomarker as a surrogate measure of knee OA.

The technology to automatically segment and quantify the structural status of all the joint tissues represents a unique opportunity to provide highly accurate quantitative biomarkers describing the phenotype and extent of tissue damage in a precise manner. For example, the articular cartilages, subchondral bone and menisci are segmented separately in the image below (Figure 62).

Quantitative measures would be provided more rapidly with an automated segmentation, than semi-quantitative scoring such as the WORMS scores. Multiple quantitative tissue scores could facilitate a more appropriate description of the association of pathology within each of the tissues of the joint in OA. This provides an advantage over semi-quantitative scores which are time-consuming to score and may not represent interval measures.

Finally a composite quantitative measure of whole joint OA pathology may better capture the extent of global structural pathology and in doing so confer greater validity in terms of its association with patient centered variables such as symptoms and TKR which would be re-examined in a similar manner to chapters 5 and 6.

For example BMLs can be subdivided on the basis of their location and association with adjacent tissues. BMLs occurring at the ligament and meniscal attachments may be typical of tractional or repetitive microtrauma whilst ‘kissing’ BMLs may occur where two bones impact as a consequence of meniscal and hyaline cartilage defects are likely a consequence of trauma[671].

In section 7.3, the advantages of using BMLs as surrogate measures of patient-centered outcomes are highlighted. These include construct validity along with predictive and concurrent criterion validity for structural progression and symptoms. One might consider why bone shape should be further pursued as a biomarker. For the purposes of clinical trials, BMLs as

clinical endpoints have several limitations. These included the fact they can change in size over 6 weeks. Any clinical trial without regular monitoring with MRI scans may not capture this rapid variation and false conclusions may be drawn about the trend in BML size or volume based upon two measurements at the beginning and end of the trials. In contrast bone shape and bone area do not reduce in size but continue to increase in OA and therefore are more reliable in considering the underlying trend in structure. Furthermore the identification of the edge of singe, multiple or coalescing BMLs in multiple regions of the knee is a more complex segmentation than bone shape and tAB. This potential error may influence any association with knee pain and highlights the importance of the use of composite measures of joint structure. Bone shape provides a convenient continuous scale which can be measured less frequently to determine the true trend in bone shape.

Figure 62 A whole joint biomarker

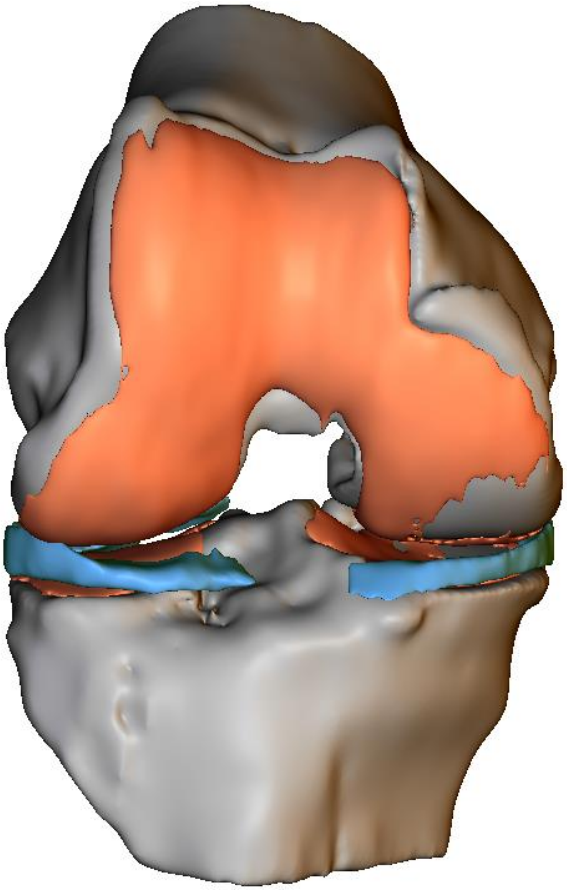

A knee joint with articular cartilage (orange), meniscus (blue) and bone (grey) segmented.

7.3.1.3 The suitability of 3D bone shape biomarkers for use as outcome measures in knee OA trials

To date all clinical knee OA trials have investigated the potential for structural or symptomatic disease modification in established knee OA. The suitability of the two bone shape biomarkers described in this thesis (3D bone shape and bone area) for use as outcome measures in disease modification trials is supported by the predictive validity for TKR described in Chapter 5, the concurrent validity for frequent pain in Chapter 6 and the work done in parallel with this thesis indicating the predictive validity for pain and structural progression[625]. However the lack of predictive validity for incident persistent knee pain reflects the lack of predictive validity for symptomatic disease onset. Therefore clinical trials of prospective structural or symptom disease modification could arguably use these bone shape biomarkers as outcome measures. However the lack of predictive validity for symptom onset indicates these bone shape biomarkers would not be suitable for clinical trials of interventions designed to prevent the onset of symptomatic knee OA. There are other structural biomarkers that have predictive validity for symptom onset including bone marrow lesions and cartilage defects [131, 134, 607] and synovitis [26] and for incident radiographic structural disease including BMLs, cartilage defects and meniscal degeneration and extrusion[622].

7.3.2 Towards a more precisely defined OA phenotype and tissue target

7.3.2.1 The benefits of an improved OA phenotype

The immense burden of OA on a personal, health service and socioeconomic level highlights the need for disease modifying therapies. With each and every failure of prospective DMOADs, the OA research community has attempted to better define the tissue targets and the OA phenotype and this progressive approach may hold future merit with the application of 3D structural biomarkers.

In chondroprotection trials to date, the failure to modify structure and symptoms of knee OA was explained by the chondro-centric approach failing to target non-cartilaginous pathologies in the multi-tissue pathology setting. Thus when oral bisphosphonates failed to modify radiographic structural progression in knee OA in the KOSTAR trial, this was explained by the failure to target individuals with knee OA with confirmed subchondral bone pathology[676]. By selecting an OA subchondral bone phenotype of prevalent BMLs in knee OA, the ZAP trial demonstrated structural modification but not a sustained reduction in symptoms[330]. More recently BMLs are recognised to be phenotypically heterogenous because those appearing on T1 and T2 sequences are more likely to be associated with more cartilage loss and pain[623] than those appearing on T1 alone. This may, in part, explain why treating the acutely painful OA knee with intravenous neridronate or placebo in a randomised placebo controlled trial was able to demonstrate structural modification and sustained reduction in pain[677]. This more recent success in apparently fulfilling the FDA's DMOAD requirement, to improve structure and symptoms, highlights the possible advantages of a more precise definition of OA pathology and phenotype. An imprecise population of knees selected from a population with heterogenous pathologies may represent important confounding factors compared to a more homogenous tissue-pathology-specific cohort. The interaction of different tissue pathologies may establish a non-modifiable and irreversible degeneration trajectory and hence explain the failure of previous DMOAD trials.

Acknowledging the limitations of existing bone biomarkers, I would better define OA phenotypes by using a broad range of potential phenotype determinants. This includes symptom and demographic data, MRI imaging biomarkers, serological soluble biomarkers, along with genetic and epigenetic data. Kerkhof and colleagues have used similar methods[678].

Patients may be better stratified by 'whole joint' quantitative assessments as described above (7.4.1.4). For example, individuals with BMLs and articular cartilage degeneration and pain may be best treated using weight loss and

intravenous bisphosphonates. In the absence of obesity, such individuals should be considered for knee braces to reduce BMLs and symptoms of OA[659] . Knee OA phenotypes and their prognosis have previously been described by stratifying individuals by their trajectories of structural and symptomatic progression as described by Felson and colleagues[92]. Although this phenotyping with greater precision has not been used in clinical trials or in general clinical practice, the broader application of this concept introduces the opportunity for targeted interventions.

A further advantage of improved phenotyping of patients with OA is that the identification of novel genetic associations with these more precise tissue phenotypes is more likely. Currently the known genetic associations are weak, complex, polygenic and are unlikely alone to stratify individuals into those who will or will not develop the generic clinical syndrome of knee OA. However genetic and epigenetic associations exist in OA and these should ideally be incorporated in phenotyping. Should these match the tissue pathology observed, this provides a potentially important tissue target for individual joints[82] and important novel therapeutic targets [83].

7.3.2.2 Improved concepts of early OA

Advances in MRI techniques have facilitated the identification of the pre-radiographic stage of OA, in particular demonstrating pathology of the menisci, synovitis and BMLs[679]. These pathologies play an integral role in the multi-tissue concept of OA pathogenesis. Attempts to define pre-radiographic or ‘early’ OA of the knee using MRI features have been previously described[680]. Should attempts to precisely define ‘early’ OA be enhanced by quantitative bone or whole-joint composite measures, this may significantly improve the prospects of capturing the early interaction of these important tissue pathologies for a more validated ‘whole joint’ clinical staging. This could be used to optimally describe the natural history of structural progression in knee OA and the inter-relationship between tissues in the pathogenesis of OA at early. This may process may also identify potential pathogenic tissue targets of particular interest in ‘early’ OA when

disease modification is more feasible. In summary a validated definition of such a clinical stage would significantly improve the prospects of interventional clinical studies identifying strategies for prevention and modification of structural and symptomatic OA progression.

7.3.3 Implications for novel imaging analysis

This thesis has been concerned with the validation of two novel AAM - derived bone shape biomarkers in the knee. Their validation may substantially reduce the practical and financial barriers to performing clinical trials of prospective DMOADs in the future.

However there is clearly a massive potential for applying the same technology to other weight-bearing as well as non-weight-bearing joints, has the potential to advance our understanding of the pathogenesis of OA, to identify prospective tissue targets and to yield more imaging biomarkers.

7.3.3.1 Other peripheral joints

The limitations of conventional radiography in describing complex 3D structures has been described earlier for knees. These same limitations apply to other joints as well and many other joints are being described using 3D imaging techniques in order to improve the precision of the diagnosis and severity of OA along with identifying patients that may benefit from surgery.

Hip bone shape is known to be integral in the pathogenesis of hip OA. Turmezei and colleagues have established a 3D computerised tomography cortical bone mapping tool of the proximal femur. This is an accurate and reliable novel quantitative grading system for hip OA[681]. Turmezei and colleagues have recently reported evidence of construct validity in relation to radiographic measures of hip OA. Increases in KL grade corresponded with increasing cortical bone thickness which was typically seen at the superolateral femoral head-neck junction and superior subchondral bone plate. Increasing severity of CT-defined osteophytes corresponded to an increase in circumferential cortical thickness and also joint space loss[682, 683]. Further validation of this application of novel AAM technology to

provide apparently superior biomarkers may establish the concurrent and predictive nature of this biomarker and facilitate clinical trials of hip OA as well[669].

Dysplasia of the hip joint is associated with increased risk of hip OA[287]. The structural abnormalities within dysplastic hips are now being more accurately described using 3D CT [684]. The identification of global incongruity of the dysplastic femoro-acetabular joint with 3D imaging, may stratify those in need of earlier surgical intervention and may permit custom made prosthetic joint replacements[685, 686].

Finally 3D imaging of the hip may improve the identification of both cartilage and bone pathology in individuals at risk of OA[687] and this can be used to better determine the suitability of surgical or non-surgical intervention. This may also facilitate pre-operative planning in femoro-acetabular impingement[688].

The relevance of 3D imaging includes other joints including the jaw, shoulder, hand and foot. The relevance to the temporomandibular joint (TMJ) has been described [689] and this is being used to better define the presence of OA of the TMJ[668]. The effect of glenohumeral joint (GHJ) morphology on GHJ movement may be relevant to the pathogenesis of rotator cuff pathology, is of great interest[690] and may lead to a more precise way to predict and treat the pathogenesis of shoulder pathology. Finally 3D imaging of the hand [691] and foot [692] may better stratify patients into those that will or will not benefit from surgery.

7.3.3.2 The spine

Vertebrae can now be segmented from 3D CT and MR imaging. The shape modelling may be more able to discriminate normal vertebral deformities from pathological one. This may improve the diagnosis of vertebral fractures[693] and abnormal shapes in individuals at risk of osteoporotic fracture for suitable osteoporosis prophylaxis[694]

Spinal OA is common and an important cause of chronic back pain. The normal kinematics and articulation of intervertebral joints has been poorly understood. These joints can now be imaged in three dimensions during movement in healthy individuals and individuals with degenerative changes. This may facilitate better understanding of the pathogenesis of discovertebral degeneration and biomechanical interventions to help restore ‘normal’ movement[695]. This may be used before and after surgical interventions to assess the correlation of structural biomechanical changes in relation to symptomatic changes and determine the efficacy of such interventions.[696]

There are also great potential advantages for the use of AAM technology in inflammatory arthritis where shape change is an important feature in the articular and periarticular tissues. This particularly includes axial and peripheral spondyloarthritis and rheumatoid arthritis.

In summary 3D imaging may improve the precision of defining joint pathology, our ability to describe pathogenesis and the potential to measure the success or failure of any intervention in all joints.

7.4 Conclusions

The hypothesis underlying this thesis was that knee OA subchondral bone, defined using 3D knee MRI segmentation with AAMs, would provide novel imaging biomarkers that demonstrate associations with existing radiographic measures of structural knee OA pathology, total knee replacement and knee OA symptoms as part of the validation of biomarkers for use in knee OA clinical trials. A systematic literature review identified the limited validity of existing imaging biomarkers, and hence the need for the work presented in this thesis, but also the potential importance of MRI-assessed bone shape. In conclusion, this thesis has provided good evidence supporting the OMERACT biomarker tool validation domain of truth: 3D knee bone shape biomarkers have construct validity as measures of knee OA radiographic severity, predictive validity by association with total knee replacement and concurrent but not predictive validity by association with knee OA symptoms

in knees with radiographic OA. While 3D bone shape is independently associated with knee OA radiographic structural disease and total knee replacement, like other structural imaging biomarkers, the association with symptoms is weaker.

Evidence for 3D bone shape biomarkers fulfilling the OMERACT domain of discrimination has been provided by the demonstration of good reliability and reproducibility in work performed in parallel to this PhD which is described in. This is the first stage in improving existing biomarkers of OA. Future surrogate measures of patient-centred outcomes are likely to include composite quantitative whole-joint biomarkers along with novel genetic biomarkers. Clinical trials in OA will seek to use these measures to reduce the size, duration and cost of clinical trials that currently hinder progression in interventional clinical trials in OA.

Chapter 8 List of References

1 Care A. OANation Survey 2012 http://www.arthritiscare.org.uk/LivingwithArthritis/oanation-2012.
2 Lawrence RC, Felson DT, Helmick CG, et al. Estimates of the prevalence of arthritis and other rheumatic conditions in the United States. Part II. Arthritis Rheum. 2008;58(1):26-35.
3 Turkiewicz A, Petersson IF, Bjork J, et al. Current and future impact of osteoarthritis on health care: a population-based study with projections to year 2032. Osteoarthritis Cartilage 2014;22(11):1826-32.
4 Jordan JM, Helmick CG, Renner JB, et al. Prevalence of knee symptoms and radiographic and symptomatic knee osteoarthritis in African Americans and Caucasians: the Johnston County Osteoarthritis Project. J. Rheumatol. 2007;34(1):172-80.
5 Jordan JM, Helmick CG, Renner JB, et al. Prevalence of hip symptoms and radiographic and symptomatic hip osteoarthritis in African Americans and Caucasians: the Johnston County Osteoarthritis Project. J. Rheumatol. 2009;36(4):809-15.
6 Murray CJ, Vos T, Lozano R, et al. Disability-adjusted life years (DALYs) for 291 diseases and injuries in 21 regions, 1990-2010: a systematic analysis for the Global Burden of Disease Study 2010. Lancet 2012;380(9859):2197-223.
7 Hubertsson J, Petersson IF, Thorstensson CA, Englund M. Risk of sick leave and disability pension in working-age women and men with knee osteoarthritis. Ann. Rheum. Dis. 2013;72(3):401-5.
8 Hiligsmann M, Cooper C, Arden N, et al. Health economics in the field of osteoarthritis: an expert's consensus paper from the European Society for Clinical and Economic Aspects of Osteoporosis and Osteoarthritis (ESCEO). Semin. Arthritis Rheum. 2013;43(3):303-13.
9 Kingsbury SR, Gross HJ, Isherwood G, Conaghan PG. Osteoarthritis in Europe: impact on health status, work productivity and use of pharmacotherapies in five European countries. Rheumatology (Oxford) 2014;53(5):937-47.
10 Zhang W, Nuki G, Moskowitz RW, et al. OARSI recommendations for the management of hip and knee osteoarthritis: part III: Changes in evidence following systematic cumulative update of research published through January 2009. Osteoarthritis Cartilage 2010;18(4):476-99.
11 Roberts E, Delgado Nunes V, Buckner S, et al. Paracetamol: not as safe as we thought? A systematic literature review of observational studies. Ann. Rheum. Dis. 2015.
12 Patricio JP, Barbosa JP, Ramos RM, Antunes NF, de Melo PC. Relative cardiovascular and gastrointestinal safety of non-selective non-steroidal anti-inflammatory drugs versus cyclo-oxygenase-2 inhibitors: implications for clinical practice. Clin Drug Investig 2013;33(3):167-83.
13 Doherty M, Hawkey C, Goulder M, et al. A randomised controlled trial of ibuprofen, paracetamol or a combination tablet of ibuprofen/paracetamol

in community-derived people with knee pain. Ann. Rheum. Dis. 2011;70(9):1534-41.
14 Guermazi A, Roemer FW, Felson DT, Brandt KD. Motion for debate: osteoarthritis clinical trials have not identified efficacious therapies because traditional imaging outcome measures are inadequate. Arthritis Rheum. 2013;65(11):2748-58.
15 Suri S, Walsh DA. Osteochondral alterations in osteoarthritis. Bone 2012;51(2):204-11.
16 Osteoarthritis Initiative database. http://www.oai.ucsf.edu/.
17 Hannan MT, Felson DT, Pincus T. Analysis of the discordance between radiographic changes and knee pain in osteoarthritis of the knee. J. Rheumatol. 2000;27(6):1513-7.
18 Case R, Thomas E, Clarke E, Peat G. Prodromal symptoms in knee osteoarthritis: a nested case-control study using data from the Osteoarthritis Initiative. Osteoarthritis Cartilage 2015;23(7):1083-9.
19 Kellgren JH, Lawrence JS. Radiological assessment of osteo-arthrosis. Ann. Rheum. Dis. 1957;16(4):494-502.
20 Altman R, Alarcon G, Appelrouth D, et al. The American College of Rheumatology criteria for the classification and reporting of osteoarthritis of the hip. Arthritis Rheum. 1991;34(5):505-14.
21 Altman R, Alarcon G, Appelrouth D, et al. The American College of Rheumatology criteria for the classification and reporting of osteoarthritis of the hand. Arthritis Rheum. 1990;33(11):1601-10.
22 Altman R, Asch E, Bloch D, et al. Development of criteria for the classification and reporting of osteoarthritis. Classification of osteoarthritis of the knee. Diagnostic and Therapeutic Criteria Committee of the American Rheumatism Association. Arthritis Rheum. 1986;29(8):1039-49.
23 Guermazi A, Niu J, Hayashi D, et al. Prevalence of abnormalities in knees detected by MRI in adults without knee osteoarthritis: population based observational study (Framingham Osteoarthritis Study). BMJ 2012;345.
24 Conaghan P. Is MRI useful in osteoarthritis? Best Practice & Research in Clinical Rheumatology 2006;20(1):57-68.
25 Conaghan PG, Felson D, Gold G, Lohmander S, Totterman S, Altman R. MRI and non-cartilaginous structures in knee osteoarthritis. Osteoarthritis Cartilage 2006;14 Suppl A:A87-94.
26 Zhang Y, Nevitt M, Niu J, et al. Fluctuation of knee pain and changes in bone marrow lesions, effusions, and synovitis on magnetic resonance imaging. Arthritis Rheum. 2011;63(3):691-9.
27 Keen HI, Wakefield RJ, Grainger AJ, Hensor EM, Emery P, Conaghan PG. Can ultrasonography improve on radiographic assessment in osteoarthritis of the hands? A comparison between radiographic and ultrasonographic detected pathology. Ann. Rheum. Dis. 2008;67(8):1116-20.
28 Vlychou M, Koutroumpas A, Malizos K, Sakkas LI. Ultrasonographic evidence of inflammation is frequent in hands of patients with erosive osteoarthritis. Osteoarthritis Cartilage 2009;17(10):1283-7.
29 Wenham CY, Conaghan PG. Imaging the painful osteoarthritic knee joint: what have we learned? Nat Clin Pract Rheumatol 2009;5(3):149-58.

30 Crema MD, Guermazi A, Sayre EC, et al. The association of magnetic resonance imaging (MRI)-detected structural pathology of the knee with crepitus in a population-based cohort with knee pain: the MoDEKO study. Osteoarthritis Cartilage 2011;19(12):1429-32.
31 Jones G, Ding C, Scott F, Glisson M, Cicuttini F. Early radiographic osteoarthritis is associated with substantial changes in cartilage volume and tibial bone surface area in both males and females. Osteoarthritis Cartilage 2004;12(2):169-74.
32 Hensor EM, Dube B, Kingsbury SR, Tennant A, Conaghan PG. Toward a clinical definition of early osteoarthritis: onset of patient-reported knee pain begins on stairs. Data from the osteoarthritis initiative. Arthritis Care Res (Hoboken) 2015;67(1):40-7.
33 Binks DA, Hodgson RJ, Ries ME, et al. Quantitative parametric MRI of articular cartilage: a review of progress and open challenges. Br. J. Radiol. 2013;86(1023):20120163.
34 Guermazi A, Alizai H, Crema MD, Trattnig S, Regatte RR, Roemer FW. Compositional MRI techniques for evaluation of cartilage degeneration in osteoarthritis. Osteoarthritis Cartilage 2015;23(10):1639-53.
35 Wenham CY, Conaghan PG. The role of synovitis in osteoarthritis. Ther Adv Musculoskelet Dis 2010;2(6):349-59.
36 Baker K, Grainger A, Niu J, et al. Relation of synovitis to knee pain using contrast-enhanced MRIs. Annals of the Rheumatic Diseases 2010;69(10):1779-83.
37 Conaghan P RL, Hensor EM, Thomas C, Emery P, Grainger AJ. A MRI Study of the Extent of “Gold Standard”-Evaluated Synovitis and its Relationship to Pain in Osteoarthritis of the Knee. American College of Rheumatology 2006;Abstract No 2094

38 Roemer FW, Kassim Javaid M, Guermazi A, et al. Anatomical distribution of synovitis in knee osteoarthritis and its association with joint effusion assessed on non-enhanced and contrast-enhanced MRI. Osteoarthritis Cartilage 2010;18(10):1269-74.
39 Haugen IK, Slatkowsky-Christensen B, Boyesen P, Sesseng S, van der Heijde D, Kvien TK. MRI findings predict radiographic progression and development of erosions in hand osteoarthritis. Ann. Rheum. Dis. 2014.
40 Kortekaas MC, Kwok WY, Reijnierse M, et al. Magnetic Resonance Imaging in Hand Osteoarthritis: Intraobserver Reliability and Criterion Validity for Clinical and Structural Characteristics. J. Rheumatol. 2015;42(7):1224-30.
41 Marshall M, Nicholls E, Kwok WY, et al. Erosive osteoarthritis: a more severe form of radiographic hand osteoarthritis rather than a distinct entity? Ann. Rheum. Dis. 2015;74(1):136-41.
42 Marshall M, Peat G, Nicholls E, van der Windt D, Myers H, Dziedzic K. Subsets of symptomatic hand osteoarthritis in community-dwelling older adults in the United Kingdom: prevalence, inter-relationships, risk factor profiles and clinical characteristics at baseline and 3-years. Osteoarthritis Cartilage 2013;21(11):1674-84.
43 Prieto-Alhambra D, Judge A, Javaid MK, Cooper C, Diez-Perez A, Arden NK. Incidence and risk factors for clinically diagnosed knee, hip and

hand osteoarthritis: influences of age, gender and osteoarthritis affecting other joints. Ann. Rheum. Dis. 2014;73(9):1659-64.
44 Belo JN, Berger MY, Reijman M, Koes BW, Bierma-Zeinstra SM. Prognostic factors of progression of osteoarthritis of the knee: a systematic review of observational studies. Arthritis Rheum. 2007;57(1):13-26.
45 Nelson AE, Smith MW, Golightly YM, Jordan JM. "Generalized osteoarthritis": a systematic review. Semin. Arthritis Rheum. 2014;43(6):713-20.
46 Parsons C, Clynes M, Syddall H, et al. How well do radiographic, clinical and self-reported diagnoses of knee osteoarthritis agree? Findings from the Hertfordshire cohort study. Springerplus 2015;4:177.
47 Knoop J, van der Leeden M, Thorstensson CA, et al. Identification of phenotypes with different clinical outcomes in knee osteoarthritis: data from the Osteoarthritis Initiative. Arthritis Care Res (Hoboken) 2011;63(11):1535-42.
48 Dillon CF, Rasch EK, Gu Q, Hirsch R. Prevalence of knee osteoarthritis in the United States: arthritis data from the Third National Health and Nutrition Examination Survey 1991-94. J. Rheumatol. 2006;33(11):2271-9.
49 Dillon CF, Hirsch R, Rasch EK, Gu Q. Symptomatic hand osteoarthritis in the United States: prevalence and functional impairment estimates from the third U.S. National Health and Nutrition Examination Survey, 1991-1994. Am. J. Phys. Med. Rehabil. 2007;86(1):12-21.
50 Zhang Y, Niu J, Kelly-Hayes M, Chaisson CE, Aliabadi P, Felson DT. Prevalence of symptomatic hand osteoarthritis and its impact on functional status among the elderly: The Framingham Study. Am. J. Epidemiol. 2002;156(11):1021-7.
51 Felson DT, Naimark A, Anderson J, Kazis L, Castelli W, Meenan RF. The prevalence of knee osteoarthritis in the elderly. The Framingham Osteoarthritis Study. Arthritis Rheum. 1987;30(8):914-8.
52 ARUK. http://www.arthritisresearchuk.org/arthritis-information/data-and-statistics/musculoskeletal-calculator/analysis.aspx?ConditionType=1&ChartType=1. 2015.
53 Srikanth VK, Fryer JL, Zhai G, Winzenberg TM, Hosmer D, Jones G. A meta-analysis of sex differences prevalence, incidence and severity of osteoarthritis. Osteoarthritis Cartilage 2005;13(9):769-81.
54 Muthuri SG, McWilliams DF, Doherty M, Zhang W. History of knee injuries and knee osteoarthritis: a meta-analysis of observational studies. Osteoarthritis Cartilage 2011;19(11):1286-93.
55 Roddy E, Thomas MJ, Marshall M, et al. The population prevalence of symptomatic radiographic foot osteoarthritis in community-dwelling older adults: cross-sectional findings from the clinical assessment study of the foot. Ann. Rheum. Dis. 2015;74(1):156-63.
56 Teichtahl AJ, Smith S, Wang Y, et al. Occupational risk factors for hip osteoarthritis are associated with early hip structural abnormalities: a 3.0 T magnetic resonance imaging study of community-based adults. Arthritis Res Ther 2015;17:19.

57 Rossignol M, Leclerc A, Allaert FA, et al. Primary osteoarthritis of hip, knee, and hand in relation to occupational exposure. Occup. Environ. Med. 2005;62(11):772-7.
58 Cooper C, Snow S, McAlindon TE, et al. Risk factors for the incidence and progression of radiographic knee osteoarthritis. Arthritis Rheum. 2000;43(5):995-1000.
59 Bierma-Zeinstra SM, Koes BW. Risk factors and prognostic factors of hip and knee osteoarthritis. Nat Clin Pract Rheumatol 2007;3(2):78-85.
60 Oliveria SA, Felson DT, Reed JI, Cirillo PA, Walker AM. Incidence of symptomatic hand, hip, and knee osteoarthritis among patients in a health maintenance organization. Arthritis Rheum. 1995;38(8):1134-41.
61 Felson DT, Anderson JJ, Naimark A, Walker AM, Meenan RF. Obesity and knee osteoarthritis. The Framingham Study. Ann. Intern. Med. 1988;109(1):18-24.
62 Blagojevic M, Jinks C, Jeffery A, Jordan KP. Risk factors for onset of osteoarthritis of the knee in older adults: a systematic review and meta-analysis. Osteoarthritis Cartilage 2010;18(1):24-33.
63 Muthuri SG, Hui M, Doherty M, Zhang W. What if we prevent obesity? Risk reduction in knee osteoarthritis estimated through a meta-analysis of observational studies. Arthritis Care Res (Hoboken) 2011;63(7):982-90.
64 Zhou ZY, Liu YK, Chen HL, Liu F. Body mass index and knee osteoarthritis risk: a dose-response meta-analysis. Obesity (Silver Spring) 2014;22(10):2180-5.
65 Silverwood V, Blagojevic-Bucknall M, Jinks C, Jordan JL, Protheroe J, Jordan KP. Current evidence on risk factors for knee osteoarthritis in older adults: a systematic review and meta-analysis. Osteoarthritis Cartilage 2015;23(4):507-15.
66 Zhang Y, Niu J, Felson DT, Choi HK, Nevitt M, Neogi T. Methodologic challenges in studying risk factors for progression of knee osteoarthritis. Arthritis Care Res (Hoboken) 2010;62(11):1527-32.
67 Yusuf E, Nelissen RG, Ioan-Facsinay A, et al. Association between weight or body mass index and hand osteoarthritis: a systematic review. Ann. Rheum. Dis. 2010;69(4):761-5.
68 Gelber AC, Hochberg MC, Mead LA, Wang NY, Wigley FM, Klag MJ. Body mass index in young men and the risk of subsequent knee and hip osteoarthritis. Am. J. Med. 1999;107(6):542-8.
69 Mork PJ, Holtermann A, Nilsen TI. Effect of body mass index and physical exercise on risk of knee and hip osteoarthritis: longitudinal data from the Norwegian HUNT Study. J. Epidemiol. Community Health 2012;66(8):678-83.
70 Magnusson K, Slatkowsky-Christensen B, van der Heijde D, Kvien T, Hagen K, Haugen I. Body mass index and progressive hand osteoarthritis: data from the Oslo hand osteoarthritis cohort. Scand. J. Rheumatol. 2015:1-6.
71 Malemud CJ. Biologic basis of osteoarthritis: state of the evidence. Curr. Opin. Rheumatol. 2015;27(3):289-94.
72 Kluzek S, Newton JL, Arden NK. Is osteoarthritis a metabolic disorder? Br. Med. Bull. 2015.

73 Driban JB, Eaton CB, Lo GH, Ward RJ, Lu B, McAlindon TE. Association of knee injuries with accelerated knee osteoarthritis progression: data from the Osteoarthritis Initiative. Arthritis Care Res (Hoboken) 2014;66(11):1673-9.
74 Agricola R, Heijboer MP, Bierma-Zeinstra SM, Verhaar JA, Weinans H, Waarsing JH. Cam impingement causes osteoarthritis of the hip: a nationwide prospective cohort study (CHECK). Ann. Rheum. Dis. 2013;72(6):918-23.
75 Neogi T, Bowes MA, Niu JB, et al. Magnetic Resonance Imaging-Based Three-Dimensional Bone Shape of the Knee Predicts Onset of Knee Osteoarthritis: Data From the Osteoarthritis Initiative. Arthritis Rheum. 2013;65(8):2048-58.
76 Felson DT, Niu J, Gross KD, et al. Valgus malalignment is a risk factor for lateral knee osteoarthritis incidence and progression: findings from the Multicenter Osteoarthritis Study and the Osteoarthritis Initiative. Arthritis Rheum. 2013;65(2):355-62.
77 Sharma L, Chmiel JS, Almagor O, et al. The role of varus and valgus alignment in the initial development of knee cartilage damage by MRI: the MOST study. Ann. Rheum. Dis. 2013;72(2):235-40.
78 arc OC, arc OC, Zeggini E, et al. Identification of new susceptibility loci for osteoarthritis (arcOGEN): a genome-wide association study. Lancet 2012;380(9844):815-23.
79 Panoutsopoulou K, Metrustry S, Doherty SA, et al. The effect of FTO variation on increased osteoarthritis risk is mediated through body mass index: a Mendelian randomisation study. Ann. Rheum. Dis. 2014;73(12):2082-6.
80 Baker-Lepain JC, Lynch JA, Parimi N, et al. Variant alleles of the Wnt antagonist FRZB are determinants of hip shape and modify the relationship between hip shape and osteoarthritis. Arthritis Rheum. 2012;64(5):1457-65.
81 Evangelou E, Kerkhof HJ, Styrkarsdottir U, et al. A meta-analysis of genome-wide association studies identifies novel variants associated with osteoarthritis of the hip. Ann. Rheum. Dis. 2014;73(12):2130-6.
82 Hochberg MC, Yerges-Armstrong L, Yau M, Mitchell BD. Genetic epidemiology of osteoarthritis: recent developments and future directions. Curr. Opin. Rheumatol. 2013;25(2):192-7.
83 Zhang M, Wang J. Epigenetics and Osteoarthritis. Genes Dis 2015;2(1):69-75.
84 Altman RD, Gold GE. Atlas of individual radiographic features in osteoarthritis, revised. Osteoarthritis Cartilage 2007;15 Suppl A:A1-56.
85 Altman RD, Hochberg M, Murphy WA, Jr., Wolfe F, Lequesne M. Atlas of individual radiographic features in osteoarthritis. Osteoarthritis Cartilage 1995;3 Suppl A:3-70.
86 Hunter DJ, Zhang YQ, Tu X, et al. Change in joint space width: hyaline articular cartilage loss or alteration in meniscus? Arthritis Rheum. 2006;54(8):2488-95.
87 Roemer FW GA, Hannon MJ, Hunter DJ, Fujii T, Eckstein F, Boudreau RM, Kwoh CK. Incident MRI features during 4 years prior increase risk for radiographic osteoarthritis development. Osteoarthritis and cartilage / OARS, Osteoarthritis Research Society 2015;23(Suppl 2): A234.

88 Guermazi A, Hayashi D, Roemer F, et al. Severe radiographic knee osteoarthritis - does Kellgren and Lawrence grade 4 represent end stage disease? - the MOST study. Osteoarthritis Cartilage 2015.
89 Dougados M, Gueguen A, Nguyen M, et al. Radiological progression of hip osteoarthritis: definition, risk factors and correlations with clinical status. Ann. Rheum. Dis. 1996;55(6):356-62.
90 Felson DT, Zhang Y, Hannan MT, et al. The incidence and natural history of knee osteoarthritis in the elderly. The Framingham Osteoarthritis Study. Arthritis Rheum. 1995;38(10):1500-5.
91 Paradowski PT, Lohmander LS, Englund M. Natural history of radiographic features of hand osteoarthritis over 10 years. Osteoarthritis Cartilage 2010;18(7):917-22.
92 Felson D, Niu JB, Sack B, Aliabadi P, McCullough C, Nevitt MC. Progression of osteoarthritis as a state of inertia. Annals of the Rheumatic Diseases 2013;72(6):924-9.
93 Brandt KD, Mazzuca SA, Katz BP, et al. Effects of doxycycline on progression of osteoarthritis: results of a randomized, placebo-controlled, double-blind trial. Arthritis Rheum. 2005;52(7):2015-25.
94 Le Graverand MP, Vignon EP, Brandt KD, et al. Head-to-head comparison of the Lyon Schuss and fixed flexion radiographic techniques. Long-term reproducibility in normal knees and sensitivity to change in osteoarthritic knees. Ann. Rheum. Dis. 2008;67(11):1562-6.
95 Raynauld JP, Martel-Pelletier J, Berthiaume MJ, et al. Long term evaluation of disease progression through the quantitative magnetic resonance imaging of symptomatic knee osteoarthritis patients: correlation with clinical symptoms and radiographic changes. Arthritis Res Ther 2006;8(1):R21.
96 Ding C, Martel-Pelletier J, Pelletier JP, et al. Two-year prospective longitudinal study exploring the factors associated with change in femoral cartilage volume in a cohort largely without knee radiographic osteoarthritis. Osteoarthritis Cartilage 2008;16(4):443-9.
97 Collins JE, Katz JN, Dervan EE, Losina E. Trajectories and risk profiles of pain in persons with radiographic, symptomatic knee osteoarthritis: data from the osteoarthritis initiative. Osteoarthritis Cartilage 2014;22(5):622-30.
98 Wesseling J, Bierma-Zeinstra SM, Kloppenburg M, Meijer R, Bijlsma JW. Worsening of pain and function over 5 years in individuals with 'early' OA is related to structural damage: data from the Osteoarthritis Initiative and CHECK (Cohort Hip & Cohort Knee) study. Ann. Rheum. Dis. 2015;74(2):347-53.
99 Dore D, Quinn S, Ding CH, et al. Natural history and clinical significance of MRI-detected bone marrow lesions at the knee: a prospective study in community dwelling older adults. Arthritis Research & Therapy 2010;12(6):R223.
100 Driban JB, Price LL, Lo GH, et al. Evaluation of bone marrow lesion volume as a knee osteoarthritis biomarker - longitudinal relationships with pain and structural changes: Data from the Osteoarthritis Initiative. Arthritis Research and Therapy 2013;15(5).

101 Foong YC, Khan HI, Blizzard L, et al. The clinical significance, natural history and predictors of bone marrow lesion change over eight years. Arthritis Res Ther 2014;16(4):R149.
102 Everhart JS, Siston RA, Flanigan DC. Tibiofemoral subchondral surface ratio (SSR) is a predictor of osteoarthritis symptoms and radiographic progression: data from the Osteoarthritis Initiative (OAI). Osteoarthritis Cartilage 2014;22(6):771-8.
103 Raynauld JP, Martel-Pelletier J, Dorais M, et al. Total Knee Replacement as a Knee Osteoarthritis Outcome: Predictors Derived from a 4-Year Long-Term Observation following a Randomized Clinical Trial Using Chondroitin Sulfate. Cartilage 2013;4(3):219-26.
104 Bruyere O, Richy F, Reginster JY. Three year joint space narrowing predicts long term incidence of knee surgery in patients with osteoarthritis: an eight year prospective follow up study. Ann. Rheum. Dis. 2005;64(12):1727-30.
105 Roemer FW, Kwoh CK, Hannon MJ, et al. Can structural joint damage measured with MR imaging be used to predict knee replacement in the following year? Radiology 2015;274(3):810-20.
106 Dibonaventura MD, Gupta S, McDonald M, Sadosky A, Pettitt D, Silverman S. Impact of self-rated osteoarthritis severity in an employed population: cross-sectional analysis of data from the national health and wellness survey. Health Qual Life Outcomes 2012;10:30.
107 Smith TO, Purdy R, Lister S, Salter C, Fleetcroft R, Conaghan P. Living with osteoarthritis: a systematic review and meta-ethnography. Scand. J. Rheumatol. 2014;43(6):441-52.
108 Gandhi R, Zywiel MG, Mahomed NN, Perruccio AV. Depression and the Overall Burden of Painful Joints: An Examination among Individuals Undergoing Hip and Knee Replacement for Osteoarthritis. Arthritis 2015;2015:327161.
109 Berger A, Hartrick C, Edelsberg J, Sadosky A, Oster G. Direct and indirect economic costs among private-sector employees with osteoarthritis. J. Occup. Environ. Med. 2011;53(11):1228-35.
110 Culliford DJ, Maskell J, Kiran A, et al. The lifetime risk of total hip and knee arthroplasty: results from the UK general practice research database. Osteoarthritis Cartilage 2012;20(6):519-24.
111 Chen A, Gupte C, Akhtar K, Smith P, Cobb J. The Global Economic Cost of Osteoarthritis: How the UK Compares. Arthritis 2012;2012:698709.
112 Nuesch E, Dieppe P, Reichenbach S, Williams S, Iff S, Juni P. All cause and disease specific mortality in patients with knee or hip osteoarthritis: population based cohort study. BMJ 2011;342:d1165.
113 Liu R, Kwok WY, Vliet Vlieland TP, et al. Mortality in osteoarthritis patients. Scand. J. Rheumatol. 2015;44(1):70-3.
114 Hoeven TA, Leening MJ, Bindels PJ, et al. Disability and not osteoarthritis predicts cardiovascular disease: a prospective population-based cohort study. Ann. Rheum. Dis. 2015;74(4):752-6.
115 Barbour KE, Lui LY, Nevitt MC, et al. Hip osteoarthritis and the risk of all-cause and disease-specific mortality in older women: Population-based cohort study. Arthritis & rheumatology 2015.

116 Mow VC, Holmes MH, Lai WM. Fluid transport and mechanical properties of articular cartilage: a review. J. Biomech. 1984;17(5):377-94.
117 Hunziker EB, Quinn TM, Hauselmann HJ. Quantitative structural organization of normal adult human articular cartilage. Osteoarthritis Cartilage 2002;10(7):564-72.
118 Mow VC, Ateshian GA, Spilker RL. Biomechanics of diarthrodial joints: a review of twenty years of progress. J. Biomech. Eng. 1993;115(4B):460-7.
119 Cicuttini F, Ding C, Wluka A, Davis S, Ebeling PR, Jones G. Association of cartilage defects with loss of knee cartilage in healthy, middle-age adults: a prospective study. Arthritis Rheum. 2005;52(7):2033-9.
120 Englund M, Guermazi A, Gale D, et al. Incidental meniscal findings on knee MRI in middle-aged and elderly persons. N. Engl. J. Med. 2008;359(11):1108-15.
121 Davies-Tuck ML, Wluka AE, Wang Y, English DR, Giles GG, Cicuttini F. The natural history of bone marrow lesions in community-based adults with no clinical knee osteoarthritis. Ann. Rheum. Dis. 2009;68(6):904-8.
122 Roemer FW, Kwoh CK, Hannon MJ, et al. What Comes First? Multitissue Involvement Leading to Radiographic Osteoarthritis: Magnetic Resonance Imaging-Based Trajectory Analysis Over Four Years in the Osteoarthritis Initiative. Arthritis & rheumatology 2015;67(8):2085-96.
123 Pelletier JP, Raynauld JP, Berthiaume MJ, et al. Risk factors associated with the loss of cartilage volume on weight-bearing areas in knee osteoarthritis patients assessed by quantitative magnetic resonance imaging: a longitudinal study. Arthritis Res Ther 2007;9(4):R74.
124 Guermazi A, Eckstein F, Hayashi D, et al. Cartilage damage, bone marrow lesions and meniscal lesions predict quantitatively measured loss of cartilage over 30-months: The most study. Osteoarthritis Cartilage 2014;22:S356.
125 Guermazi A, Eckstein F, Hayashi D, et al. Baseline radiographic osteoarthritis and semi-quantitatively assessed meniscal damage and extrusion and cartilage damage on MRI is related to quantitatively defined cartilage thickness loss in knee osteoarthritis: the Multicenter Osteoarthritis Study. Osteoarthritis Cartilage 2015.
126 Kapoor M, Martel-Pelletier J, Lajeunesse D, Pelletier JP, Fahmi H. Role of proinflammatory cytokines in the pathophysiology of osteoarthritis. Nat Rev Rheumatol 2011;7(1):33-42.
127 Felson DT. The sources of pain in knee osteoarthritis. Curr. Opin. Rheumatol. 2005;17(5):624-8.
128 Hawker GA, Stewart L, French MR, et al. Understanding the pain experience in hip and knee osteoarthritis--an OARSI/OMERACT initiative. Osteoarthritis Cartilage 2008;16(4):415-22.
129 Bajaj P, Bajaj P, Graven-Nielsen T, Arendt-Nielsen L. Osteoarthritis and its association with muscle hyperalgesia: an experimental controlled study. Pain 2001;93(2):107-14.
130 Liu A, Kendzerska T, Stanaitis I, Hawker G. The relationship between knee pain characteristics and symptom state acceptability in people with knee osteoarthritis. Osteoarthritis Cartilage 2014;22(2):178-83.

131 Sharma L, Chmiel JS, Almagor O, et al. Significance of preradiographic magnetic resonance imaging lesions in persons at increased risk of knee osteoarthritis. Arthritis & rheumatology 2014;66(7):1811-9.
132 Yusuf E, Kortekaas MC, Watt I, Huizinga TW, Kloppenburg M. Do knee abnormalities visualised on MRI explain knee pain in knee osteoarthritis? A systematic review. Ann. Rheum. Dis. 2011;70(1):60-7.
133 Felson DT, Chaisson CE, Hill CL, et al. The association of bone marrow lesions with pain in knee osteoarthritis. Ann. Intern. Med. 2001;134(7):541-9.
134 Felson DT, Niu J, Guermazi A, et al. Correlation of the development of knee pain with enlarging bone marrow lesions on magnetic resonance imaging. Arthritis Rheum. 2007;56(9):2986-92.
135 Torres L, Dunlop DD, Peterfy C, et al. The relationship between specific tissue lesions and pain severity in persons with knee osteoarthritis. Osteoarthritis Cartilage 2006;14(10):1033-40.
136 Simkin PA. Bone pain and pressure in osteoarthritic joints. Novartis Found. Symp. 2004;260:179-86; discussion 86-90, 277-9.
137 Arnoldi CC, Linderholm H, Mussbichler H. Venous engorgement and intraosseous hypertension in osteoarthritis of the hip. J. Bone Joint Surg. Br. 1972;54(3):409-21.
138 Burr DB. The importance of subchondral bone in the progression of osteoarthritis. J. Rheumatol. Suppl. 2004;70:77-80.
139 Hernandez-Molina G, Neogi T, Hunter DJ, et al. The association of bone attrition with knee pain and other MRI features of osteoarthritis. Ann. Rheum. Dis. 2008;67(1):43-7.
140 Neogi T, Nevitt MC, Yang M, Curtis JR, Torner J, Felson DT. Consistency of knee pain: correlates and association with function. Osteoarthritis Cartilage 2010;18(10):1250-5.
141 Hawker GA, Mian S, Kendzerska T, French M. Measures of adult pain: Visual Analog Scale for Pain (VAS Pain), Numeric Rating Scale for Pain (NRS Pain), McGill Pain Questionnaire (MPQ), Short-Form McGill Pain Questionnaire (SF-MPQ), Chronic Pain Grade Scale (CPGS), Short Form-36 Bodily Pain Scale (SF-36 BPS), and Measure of Intermittent and Constant Osteoarthritis Pain (ICOAP). Arthritis Care Res (Hoboken) 2011;63 Suppl 11:S240-52.
142 Baker PN, van der Meulen JH, Lewsey J, Gregg PJ, National Joint Registry for E, Wales. The role of pain and function in determining patient satisfaction after total knee replacement. Data from the National Joint Registry for England and Wales. J. Bone Joint Surg. Br. 2007;89(7):893-900.
143 Brander VA, Stulberg SD, Adams AD, et al. Predicting total knee replacement pain: a prospective, observational study. Clin Orthop Relat Res 2003(416):27-36.
144 Wylde V, Hewlett S, Learmonth ID, Dieppe P. Persistent pain after joint replacement: prevalence, sensory qualities, and postoperative determinants. Pain 2011;152(3):566-72.
145 Lane NE, Schnitzer TJ, Birbara CA, et al. Tanezumab for the treatment of pain from osteoarthritis of the knee. N. Engl. J. Med. 2010;363(16):1521-31.

146 Zhang W, Doherty M, Leeb BF, et al. EULAR evidence-based recommendations for the diagnosis of hand osteoarthritis: report of a task force of ESCISIT. Ann. Rheum. Dis. 2009;68(1):8-17.
147 Zhang W, Doherty M, Peat G, et al. EULAR evidence-based recommendations for the diagnosis of knee osteoarthritis. Ann. Rheum. Dis. 2010;69(3):483-9.
148 NICE. Osteoarthritis Care and management in adults. http://guidance.nice.org.uk/cg177 2014.
149 Fransen M, McConnell S, Harmer AR, Van der Esch M, Simic M, Bennell KL. Exercise for osteoarthritis of the knee. Cochrane Database Syst Rev 2015;1:CD004376.
150 Fransen M, McConnell S, Hernandez-Molina G, Reichenbach S. Exercise for osteoarthritis of the hip. Cochrane Database Syst Rev 2014;4:CD007912.
151 Hunter DJ, Beavers DP, Eckstein F, et al. The Intensive Diet and Exercise for Arthritis (IDEA) trial: 18-month radiographic and MRI outcomes. Osteoarthritis Cartilage 2015;23(7):1090-8.
152 Messier SP, Mihalko SL, Legault C, et al. Effects of intensive diet and exercise on knee joint loads, inflammation, and clinical outcomes among overweight and obese adults with knee osteoarthritis: the IDEA randomized clinical trial. JAMA : the journal of the American Medical Association 2013;310(12):1263-73.
153 Fernandes L, Hagen KB, Bijlsma JW, et al. EULAR recommendations for the non-pharmacological core management of hip and knee osteoarthritis. Ann. Rheum. Dis. 2013;72(7):1125-35.
154 Machado GC, Maher CG, Ferreira PH, et al. Efficacy and safety of paracetamol for spinal pain and osteoarthritis: systematic review and meta-analysis of randomised placebo controlled trials. BMJ 2015;350:h1225.
155 Fransen M, Agaliotis M, Nairn L, et al. Glucosamine and chondroitin for knee osteoarthritis: a double-blind randomised placebo-controlled clinical trial evaluating single and combination regimens. Ann. Rheum. Dis. 2015;74(5):851-8.
156 Clegg DO, Reda DJ, Harris CL, et al. Glucosamine, chondroitin sulfate, and the two in combination for painful knee osteoarthritis. N. Engl. J. Med. 2006;354(8):795-808.
157 Barr A, Conaghan P.G. Osteoarthritis: recent advances in diagnosis and management. Prescriber 2014;25(21):26-33.
158 Hochberg MC, Altman RD, April KT, et al. American College of Rheumatology 2012 recommendations for the use of nonpharmacologic and pharmacologic therapies in osteoarthritis of the hand, hip, and knee. Arthritis Care Res (Hoboken) 2012;64(4):465-74.
159 Lyons TJ, McClure SF, Stoddart RW, McClure J. The normal human chondro-osseous junctional region: evidence for contact of uncalcified cartilage with subchondral bone and marrow spaces. BMC Musculoskelet Disord 2006;7:52.
160 Li G, Yin J, Gao J, et al. Subchondral bone in osteoarthritis: insight into risk factors and microstructural changes. Arthritis Res Ther 2013;15(6):223.

161 Imhof H, Sulzbacher I, Grampp S, Czerny C, Youssefzadeh S, Kainberger F. Subchondral bone and cartilage disease: a rediscovered functional unit. Invest. Radiol. 2000;35(10):581-8.
162 Pan J, Zhou X, Li W, Novotny JE, Doty SB, Wang L. In situ measurement of transport between subchondral bone and articular cartilage. J. Orthop. Res. 2009;27(10):1347-52.
163 Ogata K, Whiteside LA, Lesker PA. Subchondral route for nutrition to articular cartilage in the rabbit. Measurement of diffusion with hydrogen gas in vivo. J. Bone Joint Surg. Am. 1978;60(7):905-10.
164 Lories RJ, Luyten FP. The bone-cartilage unit in osteoarthritis. Nat Rev Rheumatol 2011;7(1):43-9.
165 Charles JF, Aliprantis AO. Osteoclasts: more than 'bone eaters'. Trends in molecular medicine 2014;20(8):449-59.
166 Herman BC, Cardoso L, Majeska RJ, Jepsen KJ, Schaffler MB. Activation of bone remodeling after fatigue: differential response to linear microcracks and diffuse damage. Bone 2010;47(4):766-72.
167 Collet P, Uebelhart D, Vico L, et al. Effects of 1- and 6-month spaceflight on bone mass and biochemistry in two humans. Bone 1997;20(6):547-51.
168 Vico L, Collet P, Guignandon A, et al. Effects of long-term microgravity exposure on cancellous and cortical weight-bearing bones of cosmonauts. Lancet 2000;355(9215):1607-11.
169 Schaffler MB, Cheung WY, Majeska R, Kennedy O. Osteocytes: master orchestrators of bone. Calcif. Tissue Int. 2014;94(1):5-24.
170 Tatsumi S, Ishii K, Amizuka N, et al. Targeted ablation of osteocytes induces osteoporosis with defective mechanotransduction. Cell Metab 2007;5(6):464-75.
171 Kringelbach TM, Aslan D, Novak I, et al. Fine-tuned ATP signals are acute mediators in osteocyte mechanotransduction. Cell. Signal. 2015.
172 Spatz JM, Wein MN, Gooi JH, et al. The Wnt Inhibitor Sclerostin Is Up-regulated by Mechanical Unloading in Osteocytes in Vitro. J. Biol. Chem. 2015;290(27):16744-58.
173 Chen JH, Liu C, You L, Simmons CA. Boning up on Wolff's Law: mechanical regulation of the cells that make and maintain bone. J. Biomech. 2010;43(1):108-18.
174 Temiyasathit S, Jacobs CR. Osteocyte primary cilium and its role in bone mechanotransduction. Ann. N. Y. Acad. Sci. 2010;1192:422-8.
175 Lewiecki EM. New targets for intervention in the treatment of postmenopausal osteoporosis. Nat Rev Rheumatol 2011;7(11):631-8.
176 Burr DB, Radin EL. Microfractures and microcracks in subchondral bone: are they relevant to osteoarthrosis? Rheum. Dis. Clin. North Am. 2003;29(4):675-85.
177 Burr DB, Schaffler MB. The involvement of subchondral mineralized tissues in osteoarthrosis: quantitative microscopic evidence. Microsc. Res. Tech. 1997;37(4):343-57.
178 Vener MJ, Thompson RC, Jr., Lewis JL, Oegema TR, Jr. Subchondral damage after acute transarticular loading: an in vitro model of joint injury. J. Orthop. Res. 1992;10(6):759-65.

179 Burr DB, Forwood MR, Fyhrie DP, Martin RB, Schaffler MB, Turner CH. Bone microdamage and skeletal fragility in osteoporotic and stress fractures. J. Bone Miner. Res. 1997;12(1):6-15.
180 Lories RJ, Corr M, Lane NE. To Wnt or not to Wnt: the bone and joint health dilemma. Nat Rev Rheumatol 2013;9(6):328-39.
181 Robling AG, Niziolek PJ, Baldridge LA, et al. Mechanical stimulation of bone in vivo reduces osteocyte expression of Sost/sclerostin. J. Biol. Chem. 2008;283(9):5866-75.
182 Gaudio A, Pennisi P, Bratengeier C, et al. Increased sclerostin serum levels associated with bone formation and resorption markers in patients with immobilization-induced bone loss. J. Clin. Endocrinol. Metab. 2010;95(5):2248-53.
183 Power J, Poole KE, van Bezooijen R, et al. Sclerostin and the regulation of bone formation: Effects in hip osteoarthritis and femoral neck fracture. J. Bone Miner. Res. 2010;25(8):1867-76.
184 Xiong J, O'Brien CA. Osteocyte RANKL: new insights into the control of bone remodeling. J. Bone Miner. Res. 2012;27(3):499-505.
185 Nakashima T, Hayashi M, Fukunaga T, et al. Evidence for osteocyte regulation of bone homeostasis through RANKL expression. Nat. Med. 2011;17(10):1231-4.
186 Intema F, Hazewinkel HA, Gouwens D, et al. In early OA, thinning of the subchondral plate is directly related to cartilage damage: results from a canine ACLT-meniscectomy model. Osteoarthritis Cartilage 2010;18(5):691-8.
187 Boyd SK, Matyas JR, Wohl GR, Kantzas A, Zernicke RF. Early regional adaptation of periarticular bone mineral density after anterior cruciate ligament injury. J Appl Physiol (1985) 2000;89(6):2359-64.
188 Batiste DL, Kirkley A, Laverty S, Thain LM, Spouge AR, Holdsworth DW. Ex vivo characterization of articular cartilage and bone lesions in a rabbit ACL transection model of osteoarthritis using MRI and micro-CT. Osteoarthritis Cartilage 2004;12(12):986-96.
189 Walsh DA, McWilliams DF, Turley MJ, et al. Angiogenesis and nerve growth factor at the osteochondral junction in rheumatoid arthritis and osteoarthritis. Rheumatology (Oxford) 2010;49(10):1852-61.
190 Mapp PI, Walsh DA. Mechanisms and targets of angiogenesis and nerve growth in osteoarthritis. Nat Rev Rheumatol 2012;8(7):390-8.
191 Ashraf S, Wibberley H, Mapp PI, Hill R, Wilson D, Walsh DA. Increased vascular penetration and nerve growth in the meniscus: a potential source of pain in osteoarthritis. Ann. Rheum. Dis. 2011;70(3):523-9.
192 Shibakawa A, Yudoh K, Masuko-Hongo K, Kato T, Nishioka K, Nakamura H. The role of subchondral bone resorption pits in osteoarthritis: MMP production by cells derived from bone marrow. Osteoarthritis Cartilage 2005;13(8):679-87.
193 Gray AW, Davies ME, Jeffcott LB. Localisation and activity of cathepsins K and B in equine osteoclasts. Res. Vet. Sci. 2002;72(2):95-103.
194 Logar DB, Komadina R, Prezelj J, Ostanek B, Trost Z, Marc J. Expression of bone resorption genes in osteoarthritis and in osteoporosis. J. Bone Miner. Metab. 2007;25(4):219-25.

195 Pfander D, Cramer T, Weseloh G, et al. Hepatocyte growth factor in human osteoarthritic cartilage. Osteoarthritis Cartilage 1999;7(6):548-59.
196 Sanchez C, Deberg MA, Piccardi N, Msika P, Reginster JY, Henrotin YE. Osteoblasts from the sclerotic subchondral bone downregulate aggrecan but upregulate metalloproteinases expression by chondrocytes. This effect is mimicked by interleukin-6, -1beta and oncostatin M pre-treated non-sclerotic osteoblasts. Osteoarthritis Cartilage 2005;13(11):979-87.
197 Goldring SR. The role of bone in osteoarthritis pathogenesis. Rheum. Dis. Clin. North Am. 2008;34(3):561-71.
198 Suri S, Gill SE, Massena de Camin S, Wilson D, McWilliams DF, Walsh DA. Neurovascular invasion at the osteochondral junction and in osteophytes in osteoarthritis. Ann. Rheum. Dis. 2007;66(11):1423-8.
199 Mackie EJ, Ahmed YA, Tatarczuch L, Chen KS, Mirams M. Endochondral ossification: how cartilage is converted into bone in the developing skeleton. Int. J. Biochem. Cell Biol. 2008;40(1):46-62.
200 Bittner K, Vischer P, Bartholmes P, Bruckner P. Role of the subchondral vascular system in endochondral ossification: endothelial cells specifically derepress late differentiation in resting chondrocytes in vitro. Exp. Cell Res. 1998;238(2):491-7.
201 Kurz B, Lemke AK, Fay J, Pufe T, Grodzinsky AJ, Schunke M. Pathomechanisms of cartilage destruction by mechanical injury. Annals of anatomy = Anatomischer Anzeiger : official organ of the Anatomische Gesellschaft 2005;187(5-6):473-85.
202 Pufe T, Lemke A, Kurz B, et al. Mechanical overload induces VEGF in cartilage discs via hypoxia-inducible factor. Am. J. Pathol. 2004;164(1):185-92.
203 Hashimoto S, Creighton-Achermann L, Takahashi K, Amiel D, Coutts RD, Lotz M. Development and regulation of osteophyte formation during experimental osteoarthritis. Osteoarthritis Cartilage 2002;10(3):180-7.
204 Petersson IF, Boegard T, Svensson B, Heinegard D, Saxne T. Changes in cartilage and bone metabolism identified by serum markers in early osteoarthritis of the knee joint. Br. J. Rheumatol. 1998;37(1):46-50.
205 Messent EA, Buckland-Wright JC, Blake GM. Fractal analysis of trabecular bone in knee osteoarthritis (OA) is a more sensitive marker of disease status than bone mineral density (BMD). Calcif. Tissue Int. 2005;76(6):419-25.
206 Lo GH, Tassinari AM, Driban JB, et al. Cross-sectional DXA and MR measures of tibial periarticular bone associate with radiographic knee osteoarthritis severity. Osteoarthritis Cartilage 2012;20(7):686-93.
207 Li B, Aspden RM. Composition and mechanical properties of cancellous bone from the femoral head of patients with osteoporosis or osteoarthritis. J. Bone Miner. Res. 1997;12(4):641-51.
208 Lo GH, Zhang Y, McLennan C, et al. The ratio of medial to lateral tibial plateau bone mineral density and compartment-specific tibiofemoral osteoarthritis. Osteoarthritis Cartilage 2006;14(10):984-90.
209 Bruyere O, Dardenne C, Lejeune E, et al. Subchondral tibial bone mineral density predicts future joint space narrowing at the medial femoro-tibial compartment in patients with knee osteoarthritis. Bone 2003;32(5):541-5.

210 Dore D, Quinn S, Ding C, Winzenberg T, Cicuttini F, Jones G. Subchondral bone and cartilage damage: a prospective study in older adults. Arthritis Rheum. 2010;62(7):1967-73.
211 Kraus VB, Feng S, Wang S, et al. Trabecular morphometry by fractal signature analysis is a novel marker of osteoarthritis progression. Arthritis Rheum. 2009;60(12):3711-22.
212 Buckland-Wright JC, Lynch JA, Macfarlane DG. Fractal signature analysis measures cancellous bone organisation in macroradiographs of patients with knee osteoarthritis. Ann. Rheum. Dis. 1996;55(10):749-55.
213 Wong AK, Beattie KA, Emond PD, et al. Quantitative analysis of subchondral sclerosis of the tibia by bone texture parameters in knee radiographs: site-specific relationships with joint space width. Osteoarthritis Cartilage 2009;17(11):1453-60.
214 Bennell KL, Creaby MW, Wrigley TV, Hunter DJ. Tibial subchondral trabecular volumetric bone density in medial knee joint osteoarthritis using peripheral quantitative computed tomography technology. Arthritis Rheum. 2008;58(9):2776-85.
215 Chiba K, Ito M, Osaki M, Uetani M, Shindo H. In vivo structural analysis of subchondral trabecular bone in osteoarthritis of the hip using multi-detector row CT. Osteoarthritis Cartilage 2011;19(2):180-5.
216 Dieppe P, Cushnaghan J, Young P, Kirwan J. Prediction of the progression of joint space narrowing in osteoarthritis of the knee by bone scintigraphy. Ann. Rheum. Dis. 1993;52(8):557-63.
217 Radin EL, Parker HG, Pugh JW, Steinberg RS, Paul IL, Rose RM. Response of joints to impact loading. 3. Relationship between trabecular microfractures and cartilage degeneration. J. Biomech. 1973;6(1):51-7.
218 Radin EL, Ehrlich MG, Chernack R, Abernethy P, Paul IL, Rose RM. Effect of repetitive impulsive loading on the knee joints of rabbits. Clin Orthop Relat Res 1978(131):288-93.
219 Radin EL, Rose RM. Role of subchondral bone in the initiation and progression of cartilage damage. Clin Orthop Relat Res 1986(213):34-40.
220 Fazzalari NL, Parkinson IH. Fractal properties of subchondral cancellous bone in severe osteoarthritis of the hip. J. Bone Miner. Res. 1997;12(4):632-40.
221 Grynpas MD, Alpert B, Katz I, Lieberman I, Pritzker KP. Subchondral bone in osteoarthritis. Calcif. Tissue Int. 1991;49(1):20-6.
222 Mansell JP, Bailey AJ. Abnormal cancellous bone collagen metabolism in osteoarthritis. J. Clin. Invest. 1998;101(8):1596-603.
223 Pugh JW, Radin EL, Rose RM. Quantitative studies of human subchondral cancellous bone. Its relationship to the state of its overlying cartilage. J. Bone Joint Surg. Am. 1974;56(2):313-21.
224 Day JS, Van Der Linden JC, Bank RA, et al. Adaptation of subchondral bone in osteoarthritis. Biorheology 2004;41(3-4):359-68.
225 Ding M. Microarchitectural adaptations in aging and osteoarthrotic subchondral bone issues. Acta Orthop Suppl 2010;81(340):1-53.
226 Day JS, Ding M, van der Linden JC, Hvid I, Sumner DR, Weinans H. A decreased subchondral trabecular bone tissue elastic modulus is associated with pre-arthritic cartilage damage. J. Orthop. Res. 2001;19(5):914-8.

227 Burr DB. Anatomy and physiology of the mineralized tissues: role in the pathogenesis of osteoarthrosis. Osteoarthritis Cartilage 2004;12 Suppl A:S20-30.
228 Li B, Aspden RM. Mechanical and material properties of the subchondral bone plate from the femoral head of patients with osteoarthritis or osteoporosis. Ann. Rheum. Dis. 1997;56(4):247-54.
229 Matsui H, Shimizu M, Tsuji H. Cartilage and subchondral bone interaction in osteoarthrosis of human knee joint: a histological and histomorphometric study. Microsc. Res. Tech. 1997;37(4):333-42.
230 Klose-Jensen R, Hartlev LB, Boel LW, et al. Subchondral bone turnover, but not bone volume, is increased in early stage osteoarthritic lesions in the human hip joint. Osteoarthritis Cartilage 2015.
231 Marijnissen AC, van Roermund PM, TeKoppele JM, Bijlsma JW, Lafeber FP. The canine 'groove' model, compared with the ACLT model of osteoarthritis. Osteoarthritis Cartilage 2002;10(2):145-55.
232 Mastbergen SC, Marijnissen AC, Vianen ME, van Roermund PM, Bijlsma JW, Lafeber FP. The canine 'groove' model of osteoarthritis is more than simply the expression of surgically applied damage. Osteoarthritis Cartilage 2006;14(1):39-46.
233 Sniekers YH, Intema F, Lafeber FP, et al. A role for subchondral bone changes in the process of osteoarthritis; a micro-CT study of two canine models. BMC Musculoskelet Disord 2008;9:20.
234 Intema F, Sniekers YH, Weinans H, et al. Similarities and discrepancies in subchondral bone structure in two differently induced canine models of osteoarthritis. J. Bone Miner. Res. 2010;25(7):1650-7.
235 Botter SM, van Osch GJ, Waarsing JH, et al. Quantification of subchondral bone changes in a murine osteoarthritis model using micro-CT. Biorheology 2006;43(3-4):379-88.
236 Sniekers YH, Weinans H, van Osch GJ, van Leeuwen JP. Oestrogen is important for maintenance of cartilage and subchondral bone in a murine model of knee osteoarthritis. Arthritis Res Ther 2010;12(5):R182.
237 Botter SM, van Osch GJ, Waarsing JH, et al. Cartilage damage pattern in relation to subchondral plate thickness in a collagenase-induced model of osteoarthritis. Osteoarthritis Cartilage 2008;16(4):506-14.
238 Botter SM, Glasson SS, Hopkins B, et al. ADAMTS5-/- mice have less subchondral bone changes after induction of osteoarthritis through surgical instability: implications for a link between cartilage and subchondral bone changes. Osteoarthritis Cartilage 2009;17(5):636-45.
239 Hayami T, Pickarski M, Wesolowski GA, et al. The role of subchondral bone remodeling in osteoarthritis: reduction of cartilage degeneration and prevention of osteophyte formation by alendronate in the rat anterior cruciate ligament transection model. Arthritis Rheum. 2004;50(4):1193-206.
240 Boyd SK, Muller R, Leonard T, Herzog W. Long-term periarticular bone adaptation in a feline knee injury model for post-traumatic experimental osteoarthritis. Osteoarthritis Cartilage 2005;13(3):235-42.
241 Pastoureau PC, Chomel AC, Bonnet J. Evidence of early subchondral bone changes in the meniscectomized guinea pig. A densitometric study

using dual-energy X-ray absorptiometry subregional analysis. Osteoarthritis Cartilage 1999;7(5):466-73.
242 Christiansen BA, Anderson MJ, Lee CA, Williams JC, Yik JH, Haudenschild DR. Musculoskeletal changes following non-invasive knee injury using a novel mouse model of post-traumatic osteoarthritis. Osteoarthritis Cartilage 2012;20(7):773-82.
243 Lavigne P, Benderdour M, Lajeunesse D, et al. Subchondral and trabecular bone metabolism regulation in canine experimental knee osteoarthritis. Osteoarthritis Cartilage 2005;13(4):310-7.
244 Bolbos RI, Zuo J, Banerjee S, et al. Relationship between trabecular bone structure and articular cartilage morphology and relaxation times in early OA of the knee joint using parallel MRI at 3 T. Osteoarthritis Cartilage 2008;16(10):1150-9.
245 van Meer BL, Waarsing JH, van Eijsden WA, et al. Bone mineral density changes in the knee following anterior cruciate ligament rupture. Osteoarthritis Cartilage 2014;22(1):154-61.
246 Davies-Tuck ML, Martel-Pelletier J, Wluka AE, et al. Meniscal tear and increased tibial plateau bone area in healthy post-menopausal women. Osteoarthritis Cartilage 2008;16(2):268-71.
247 Antony B, Ding C, Stannus O, Cicuttini F, Jones G. Association of baseline knee bone size, cartilage volume, and body mass index with knee cartilage loss over time: a longitudinal study in younger or middle-aged adults. J. Rheumatol. 2011;38(9):1973-80.
248 Mrosek EH, Lahm A, Erggelet C, et al. Subchondral bone trauma causes cartilage matrix degeneration: an immunohistochemical analysis in a canine model. Osteoarthritis Cartilage 2006;14(2):171-8.
249 Muraoka T, Hagino H, Okano T, Enokida M, Teshima R. Role of subchondral bone in osteoarthritis development: a comparative study of two strains of guinea pigs with and without spontaneously occurring osteoarthritis. Arthritis Rheum. 2007;56(10):3366-74.
250 Hulet C, Sabatier JP, Souquet D, Locker B, Marcelli C, Vielpeau C. Distribution of bone mineral density at the proximal tibia in knee osteoarthritis. Calcif. Tissue Int. 2002;71(4):315-22.
251 Wada M, Maezawa Y, Baba H, Shimada S, Sasaki S, Nose Y. Relationships among bone mineral densities, static alignment and dynamic load in patients with medial compartment knee osteoarthritis. Rheumatology (Oxford) 2001;40(5):499-505.
252 Lo GH, Niu J, McLennan CE, et al. Meniscal damage associated with increased local subchondral bone mineral density: a Framingham study. Osteoarthritis Cartilage 2008;16(2):261-7.
253 Ledingham J, Regan M, Jones A, Doherty M. Factors affecting radiographic progression of knee osteoarthritis. Ann. Rheum. Dis. 1995;54(1):53-8.
254 Wirth WEF. A technique for regional analysis of femorotibial cartilage thickness based on quantitative magnetic resonance imaging. IEEE Trans. Med. Imaging 2008;27:737-44.
255 Ding C, Cicuttini F, Jones G. Tibial subchondral bone size and knee cartilage defects: relevance to knee osteoarthritis. Osteoarthritis Cartilage 2007;15(5):479-86.

256 Otterness IG, Eckstein F. Women have thinner cartilage and smaller joint surfaces than men after adjustment for body height and weight. Osteoarthritis Cartilage 2007;15(6):666-72.
257 Otterness IG, Le Graverand MP, Eckstein F. Allometric relationships between knee cartilage volume, thickness, surface area and body dimensions. Osteoarthritis Cartilage 2008;16(1):34-40.
258 Wang Y, Wluka AE, Davis S, Cicuttini FM. Factors affecting tibial plateau expansion in healthy women over 2.5 years: a longitudinal study. Osteoarthritis Cartilage 2006;14(12):1258-64.
259 Wang Y, Wluka AE, Cicuttini FM. The determinants of change in tibial plateau bone area in osteoarthritic knees: a cohort study. Arthritis Res Ther 2005;7(3):R687-93.
260 Ding C, Cicuttini F, Scott F, Cooley H, Jones G. Knee structural alteration and BMI: a cross-sectional study. Obes. Res. 2005;13(2):350-61.
261 Ding C, Cicuttini F, Scott F, Cooley H, Boon C, Jones G. Natural history of knee cartilage defects and factors affecting change. Arch. Intern. Med. 2006;166(6):651-8.
262 Bloecker K, Englund M, Wirth W, et al. Revision 1 size and position of the healthy meniscus, and its correlation with sex, height, weight, and bone area- a cross-sectional study. BMC Musculoskeletal Disorders 2011;12:248.
263 Ding C, Martel-Pelletier J, Pelletier JP, et al. Knee meniscal extrusion in a largely non-osteoarthritic cohort: association with greater loss of cartilage volume. Arthritis Res Ther 2007;9(2):R21.
264 Ding C, Martel-Pelletier J, Pelletier JP, et al. Meniscal tear as an osteoarthritis risk factor in a largely non-osteoarthritic cohort: a cross-sectional study. Journal of Rheumatology 2007;34(4):776-84.
265 Wang Y, Wluka AE, Pelletier JP, et al. Meniscal extrusion predicts increases in subchondral bone marrow lesions and bone cysts and expansion of subchondral bone in osteoarthritic knees. Rheumatology (Oxford) 2010;49(5):997-1004.
266 Stein V, Li L, Lo G, et al. Pattern of joint damage in persons with knee osteoarthritis and concomitant ACL tears. Rheumatol. Int. 2012;32(5):1197-208.
267 Eckstein F, Hudelmaier M, Cahue S, Marshall M, Sharma L. Medial-to-lateral ratio of tibiofemoral subchondral bone area is adapted to alignment and mechanical load. Calcif. Tissue Int. 2009;84(3):186-94.
268 Zhai G, Ding C, Cicuttini F, Jones G. A longitudinal study of the association between knee alignment and change in cartilage volume and chondral defects in a largely non-osteoarthritic population. J. Rheumatol. 2007;34(1):181-6.
269 Wluka AE, Wang Y, Davis SR, Cicuttini FM. Tibial plateau size is related to grade of joint space narrowing and osteophytes in healthy women and in women with osteoarthritis. Ann. Rheum. Dis. 2005;64(7):1033-7.
270 Cicuttini FM, Jones G, Forbes A, Wluka AE. Rate of cartilage loss at two years predicts subsequent total knee arthroplasty: a prospective study. Ann. Rheum. Dis. 2004;63(9):1124-7.
271 Eckstein F, Ateshian G, Burgkart R, et al. Proposal for a nomenclature for magnetic resonance imaging based measures of articular cartilage in osteoarthritis. Osteoarthritis Cartilage 2006;14(10):974-83.

272 Nakamura M, Sumen Y, Sakaridani K, Exham H, Ochi M. Relationship between the shape of tibial spurs on X-ray and meniscal changes on MRI in early osteoarthritis of the knee. Magn. Reson. Imaging 2006;24(9):1143-8.
273 Miura H, Noguchi Y, Mitsuyasu H, et al. Clinical features of multiple epiphyseal dysplasia expressed in the knee. Clin Orthop Relat Res 2000(380):184-90.
274 Stefanik JJ, Roemer FW, Zumwalt AC, et al. Association between measures of trochlear morphology and structural features of patellofemoral joint osteoarthritis on MRI: the MOST study. Journal of Orthopaedic Research 2012;30(1):1-8.
275 Matsuda S, Miura H, Nagamine R, et al. Anatomical analysis of the femoral condyle in normal and osteoarthritic knees. J. Orthop. Res. 2004;22(1):104-9.
276 Haverkamp DJ, Schiphof D, Bierma-Zeinstra SM, Weinans H, Waarsing JH. Variation in joint shape of osteoarthritic knees. Arthritis Rheum. 2011;63(11):3401-7.
277 Bredbenner TL, Eliason TD, Potter RS, Mason RL, Havill LM, Nicolella DP. Statistical shape modeling describes variation in tibia and femur surface geometry between Control and Incidence groups from the osteoarthritis initiative database. Journal of Biomechanics 2010;43(9):1780-6.
278 Tanamas SK, Teichtahl AJ, Wluka AE, et al. The associations between indices of patellofemoral geometry and knee pain and patella cartilage volume: a cross-sectional study. BMC Musculoskelet Disord 2010;11:87.
279 Lievense A, Bierma-Zeinstra S, Verhagen A, Verhaar J, Koes B. Influence of work on the development of osteoarthritis of the hip: a systematic review. J. Rheumatol. 2001;28(11):2520-8.
280 Gelber AC, Hochberg MC, Mead LA, Wang NY, Wigley FM, Klag MJ. Joint injury in young adults and risk for subsequent knee and hip osteoarthritis. Ann. Intern. Med. 2000;133(5):321-8.
281 MacGregor AJ, Antoniades L, Matson M, Andrew T, Spector TD. The genetic contribution to radiographic hip osteoarthritis in women: results of a classic twin study. Arthritis Rheum. 2000;43(11):2410-6.
282 Doherty M, Courtney P, Doherty S, et al. Nonspherical femoral head shape (pistol grip deformity), neck shaft angle, and risk of hip osteoarthritis: a case-control study. Arthritis Rheum. 2008;58(10):3172-82.
283 Glyn-Jones S, Palmer AJ, Agricola R, et al. Osteoarthritis. Lancet 2015;386(9991):376-87.
284 Agricola R, Waarsing JH, Arden NK, et al. Cam impingement of the hip: a risk factor for hip osteoarthritis. Nat Rev Rheumatol 2013;9(10):630-4.
285 Jacobsen S, Sonne-Holm S, Soballe K, Gebuhr P, Lund B. Hip dysplasia and osteoarthrosis: a survey of 4151 subjects from the Osteoarthrosis Substudy of the Copenhagen City Heart Study. Acta Orthop 2005;76(2):149-58.
286 Sandell LJ. Etiology of osteoarthritis: genetics and synovial joint development. Nat Rev Rheumatol 2012;8(2):77-89.

287 Reijman M, Hazes JM, Pols HA, Koes BW, Bierma-Zeinstra SM. Acetabular dysplasia predicts incident osteoarthritis of the hip: the Rotterdam study. Arthritis Rheum. 2005;52(3):787-93.
288 Lane NE, Lin P, Christiansen L, et al. Association of mild acetabular dysplasia with an increased risk of incident hip osteoarthritis in elderly white women: the study of osteoporotic fractures. Arthritis Rheum. 2000;43(2):400-4.
289 Cootes TF, Taylor CJ, Cooper DH, Graham J. Active Shape Models - Their Training and Application. Comput Vis Image Und 1995;61(1):38-59.
290 Gregory JS, Waarsing JH, Day J, et al. Early identification of radiographic osteoarthritis of the hip using an active shape model to quantify changes in bone morphometric features: can hip shape tell us anything about the progression of osteoarthritis? Arthritis Rheum. 2007;56(11):3634-43.
291 Lynch JA, Parimi N, Chaganti RK, Nevitt MC, Lane NE, Study of Osteoporotic Fractures Research G. The association of proximal femoral shape and incident radiographic hip OA in elderly women. Osteoarthritis Cartilage 2009;17(10):1313-8.
292 Waarsing JH, Rozendaal RM, Verhaar JA, Bierma-Zeinstra SM, Weinans H. A statistical model of shape and density of the proximal femur in relation to radiological and clinical OA of the hip. Osteoarthritis Cartilage 2010;18(6):787-94.
293 Zanetti M, Bruder E, Romero J, Hodler J. Bone marrow edema pattern in osteoarthritic knees: correlation between MR imaging and histologic findings. Radiology 2000;215(3):835-40.
294 Felson DT, McLaughlin S, Goggins J, et al. Bone marrow edema and its relation to progression of knee osteoarthritis. Ann. Intern. Med. 2003;139(5 Pt 1):330-6.
295 Lo GH, Hunter DJ, Nevitt M, Lynch J, McAlindon TE, Group OAII. Strong association of MRI meniscal derangement and bone marrow lesions in knee osteoarthritis: data from the osteoarthritis initiative. Osteoarthritis Cartilage 2009;17(6):743-7.
296 Hovis KK, Alizai H, Tham SC, et al. Non-traumatic anterior cruciate ligament abnormalities and their relationship to osteoarthritis using morphological grading and cartilage T2 relaxation times: Data from the Osteoarthritis Initiative (OAI). Skeletal Radiology 2012;41(11):1435-43.
297 Hunter DJ, Gerstenfeld L, Bishop G, et al. Bone marrow lesions from osteoarthritis knees are characterized by sclerotic bone that is less well mineralized. Arthritis Research and Therapy 2009;11(1).
298 Driban JB, Tassinari A, Lo GH, et al. Bone marrow lesions are associated with altered trabecular morphometry. Osteoarthritis Cartilage 2012;20(12):1519-26.
299 Kazakia GJ, Kuo D, Schooler J, et al. Bone and cartilage demonstrate changes localized to bone marrow edema-like lesions within osteoarthritic knees. Osteoarthritis and cartilage / OARS, Osteoarthritis Research Society 2013;21(1):94-101.
300 Roemer FW, Neogi T, Nevitt MC, et al. Subchondral bone marrow lesions are highly associated with, and predict subchondral bone attrition longitudinally: the MOST study. Osteoarthritis Cartilage 2010;18(1):47-53.

301 Davies-Tuck ML, Wluka AE, Forbes A, et al. Development of bone marrow lesions is associated with adverse effects on knee cartilage while resolution is associated with improvement--a potential target for prevention of knee osteoarthritis: a longitudinal study. Arthritis Res Ther 2010;12(1):R10.
302 Kornaat PR, Kloppenburg M, Sharma R, et al. Bone marrow edema-like lesions change in volume in the majority of patients with osteoarthritis; associations with clinical features. European Radiology 2007;17(12):3073-8.
303 Crema MD, Roemer FW, Marra MD, Guermazi A. MR imaging of intra- and periarticular soft tissues and subchondral bone in knee osteoarthritis. Radiologic Clinics of North America 2009;47(4):687-701.
304 Neogi T, Nevitt M, Niu J, et al. Subchondral bone attrition may be a reflection of compartment-specific mechanical load: the MOST Study. Ann. Rheum. Dis. 2010;69(5):841-4.
305 Hunter DJ, Zhang Y, Niu J, et al. Structural factors associated with malalignment in knee osteoarthritis: the Boston osteoarthritis knee study. Journal of Rheumatology 2005;32(11):2192-9.
306 Reichenbach S, Guermazi A, Niu J, et al. Prevalence of bone attrition on knee radiographs and MRI in a community-based cohort. Osteoarthritis Cartilage 2008;16(9):1005-10.
307 Neogi T, Felson D, Niu J, et al. Cartilage Loss Occurs in the Same Subregions as Subchondral Bone Attrition: A Within-Knee Subregion-Matched Approach From the Multicenter Osteoarthritis Study. Arthrit Rheum-Arthr 2009;61(11):1539-44.
308 van der Kraan PM, van den Berg WB. Osteophytes: relevance and biology. Osteoarthritis Cartilage 2007;15(3):237-44.
309 Panzer S, Augat P, Atzwanger J, Hergan K. 3-T MRI assessment of osteophyte formation in patients with unilateral anterior cruciate ligament injury and reconstruction. Skeletal Radiol. 2012;41(12):1597-604.
310 Mazzuca SA, Brandt KD, Lane KA, Chakr R. Malalignment and subchondral bone turnover in contralateral knees of overweight/obese women with unilateral osteoarthritis: implications for bilateral disease. Arthritis Care Res (Hoboken) 2011;63(11):1528-34.
311 Lerer DB, Umans HR, Hu MX, Jones MH. The role of meniscal root pathology and radial meniscal tear in medial meniscal extrusion. Skeletal Radiol. 2004;33(10):569-74.
312 Hayes CW, Jamadar DA, Welch GW, et al. Osteoarthritis of the knee: comparison of MR imaging findings with radiographic severity measurements and pain in middle-aged women. Radiology 2005;237(3):998-1007.
313 Stehling C, Lane NE, Nevitt MC, Lynch J, McCulloch CE, Link TM. Subjects with higher physical activity levels have more severe focal knee lesions diagnosed with 3T MRI: Analysis of a non-symptomatic cohort of the osteoarthritis initiative. Osteoarthritis Cartilage 2010;18(6):776-86.
314 Pouders C, De M, Van P, Gielen J, Goossens A, Shahabpour M. Prevalence and MRI-anatomic correlation of bone cysts in osteoarthritic knees. AJR. American Journal of Roentgenology 2008;190(1):17-21.

315 Crema MD, Roemer FW, Marra MD, et al. Contrast-enhanced MRI of subchondral cysts in patients with or at risk for knee osteoarthritis: the MOST study. European Journal of Radiology 2010;75(1):e92-6.
316 Chen Y, Wang T, Guan M, et al. Bone turnover and articular cartilage differences localized to subchondral cysts in knees with advanced osteoarthritis. Osteoarthritis Cartilage 2015.
317 Chiba K, Burghardt AJ, Osaki M, Majumdar S. Three-dimensional analysis of subchondral cysts in hip osteoarthritis: an ex vivo HR-pQCT study. Bone 2014;66:140-5.
318 Crema MD, Roemer FW, Zhu Y, et al. Subchondral cystlike lesions develop longitudinally in areas of bone marrow edema-like lesions in patients with or at risk for knee osteoarthritis: detection with MR imaging--the MOST study. Radiology 2010;256(3):855-62.
319 Link TM, Steinbach LS, Ghosh S, et al. Osteoarthritis: MR imaging findings in different stages of disease and correlation with clinical findings. Radiology 2003;226(2):373-81.
320 Reid IR. Bisphosphonates: new indications and methods of administration. Curr. Opin. Rheumatol. 2003;15(4):458-63.
321 Jones MD, Tran CW, Li G, Maksymowych WP, Zernicke RF, Doschak MR. In vivo microfocal computed tomography and micro-magnetic resonance imaging evaluation of antiresorptive and antiinflammatory drugs as preventive treatments of osteoarthritis in the rat. Arthritis Rheum. 2010;62(9):2726-35.
322 Kadri A, Funck-Brentano T, Lin H, et al. Inhibition of bone resorption blunts osteoarthritis in mice with high bone remodelling. Ann. Rheum. Dis. 2010;69(8):1533-8.
323 Moreau M, Rialland P, Pelletier JP, et al. Tiludronate treatment improves structural changes and symptoms of osteoarthritis in the canine anterior cruciate ligament model. Arthritis Res Ther 2011;13(3):R98.
324 Strassle BW, Mark L, Leventhal L, et al. Inhibition of osteoclasts prevents cartilage loss and pain in a rat model of degenerative joint disease. Osteoarthritis Cartilage 2010;18(10):1319-28.
325 Muehleman C, Green J, Williams JM, Kuettner KE, Thonar EJ, Sumner DR. The effect of bone remodeling inhibition by zoledronic acid in an animal model of cartilage matrix damage. Osteoarthritis Cartilage 2002;10(3):226-33.
326 Hellio Le Graverand-Gastineau MP. OA clinical trials: current targets and trials for OA. Choosing molecular targets: what have we learned and where we are headed? Osteoarthritis Cartilage 2009;17(11):1393-401.
327 Garnero P, Aronstein WS, Cohen SB, et al. Relationships between biochemical markers of bone and cartilage degradation with radiological progression in patients with knee osteoarthritis receiving risedronate: the Knee Osteoarthritis Structural Arthritis randomized clinical trial. Osteoarthritis Cartilage 2008;16(6):660-6.
328 Buckland-Wright JC, Messent EA, Bingham CO, 3rd, Ward RJ, Tonkin C. A 2 yr longitudinal radiographic study examining the effect of a bisphosphonate (risedronate) upon subchondral bone loss in osteoarthritic knee patients. Rheumatology (Oxford) 2007;46(2):257-64.

329 Spector TD, Conaghan PG, Buckland-Wright JC, et al. Effect of risedronate on joint structure and symptoms of knee osteoarthritis: results of the BRISK randomized, controlled trial [ISRCTN01928173]. Arthritis Res Ther 2005;7(3):R625-33.
330 Laslett LL, Dore DA, Quinn SJ, et al. Zoledronic acid reduces knee pain and bone marrow lesions over 1 year: a randomised controlled trial. Ann. Rheum. Dis. 2012;71(8):1322-8.
331 Neogi T, Nevitt MC, Ensrud KE, Bauer D, Felson DT. The effect of alendronate on progression of spinal osteophytes and disc-space narrowing. Ann. Rheum. Dis. 2008;67(10):1427-30.
332 Carbone LD, Nevitt MC, Wildy K, et al. The relationship of antiresorptive drug use to structural findings and symptoms of knee osteoarthritis. Arthritis Rheum. 2004;50(11):3516-25.
333 Cauley JA, Black D, Boonen S, et al. Once-yearly zoledronic acid and days of disability, bed rest, and back pain: randomized, controlled HORIZON Pivotal Fracture Trial. J. Bone Miner. Res. 2011;26(5):984-92.
334 Koivisto K, Kyllonen E, Haapea M, et al. Efficacy of zoledronic acid for chronic low back pain associated with Modic changes in magnetic resonance imaging. BMC Musculoskelet Disord 2014;15:64.
335 Reginster JY, Badurski J, Bellamy N, et al. Efficacy and safety of strontium ranelate in the treatment of knee osteoarthritis: results of a double-blind, randomised placebo-controlled trial. Ann. Rheum. Dis. 2013;72(2):179-86.
336 Pelletier JP, Roubille C, Raynauld JP, et al. Disease-modifying effect of strontium ranelate in a subset of patients from the Phase III knee osteoarthritis study SEKOIA using quantitative MRI: reduction in bone marrow lesions protects against cartilage loss. Ann. Rheum. Dis. 2015;74(2):422-9.
337 Bruyere O, Delferriere D, Roux C, et al. Effects of strontium ranelate on spinal osteoarthritis progression. Ann. Rheum. Dis. 2008;67(3):335-9.
338 Pelletier JP, Kapoor M, Fahmi H, et al. Strontium ranelate reduces the progression of experimental dog osteoarthritis by inhibiting the expression of key proteases in cartilage and of IL-1beta in the synovium. Ann. Rheum. Dis. 2013;72(2):250-7.
339 Kyrkos MJ, Papavasiliou KA, Kenanidis E, Tsiridis E, Sayegh FE, Kapetanos GA. Calcitonin delays the progress of early-stage mechanically induced osteoarthritis. In vivo, prospective study. Osteoarthritis Cartilage 2013;21(7):973-80.
340 Behets C, Williams JM, Chappard D, Devogelaer JP, Manicourt DH. Effects of calcitonin on subchondral trabecular bone changes and on osteoarthritic cartilage lesions after acute anterior cruciate ligament deficiency. J. Bone Miner. Res. 2004;19(11):1821-6.
341 Esenyel M, Icagasioglu A, Esenyel CZ. Effects of calcitonin on knee osteoarthritis and quality of life. Rheumatol. Int. 2013;33(2):423-7.
342 Manicourt DH, Azria M, Mindeholm L, Thonar EJ, Devogelaer JP. Oral salmon calcitonin reduces Lequesne's algofunctional index scores and decreases urinary and serum levels of biomarkers of joint metabolism in knee osteoarthritis. Arthritis Rheum. 2006;54(10):3205-11.

343 Chang JK, Chang LH, Hung SH, et al. Parathyroid hormone 1-34 inhibits terminal differentiation of human articular chondrocytes and osteoarthritis progression in rats. Arthritis Rheum. 2009;60(10):3049-60.
344 Sampson ER, Hilton MJ, Tian Y, et al. Teriparatide as a chondroregenerative therapy for injury-induced osteoarthritis. Sci Transl Med 2011;3(101):101ra93.
345 Bellido M, Lugo L, Roman-Blas JA, et al. Improving subchondral bone integrity reduces progression of cartilage damage in experimental osteoarthritis preceded by osteoporosis. Osteoarthritis Cartilage 2011;19(10):1228-36.
346 Lane NE, Gore LR, Cummings SR, et al. Serum vitamin D levels and incident changes of radiographic hip osteoarthritis: a longitudinal study. Study of Osteoporotic Fractures Research Group. Arthritis Rheum. 1999;42(5):854-60.
347 McAlindon TE, Felson DT, Zhang Y, et al. Relation of dietary intake and serum levels of vitamin D to progression of osteoarthritis of the knee among participants in the Framingham Study. Ann. Intern. Med. 1996;125(5):353-9.
348 McAlindon T, LaValley M, Schneider E, et al. Effect of vitamin D supplementation on progression of knee pain and cartilage volume loss in patients with symptomatic osteoarthritis: a randomized controlled trial. JAMA : the journal of the American Medical Association 2013;309(2):155-62.
349 Chiba K, Uetani M, Kido Y, et al. Osteoporotic changes of subchondral trabecular bone in osteoarthritis of the knee: a 3-T MRI study. Osteoporos. Int. 2012;23(2):589-97.
350 Lindsey CT, Narasimhan A, Adolfo JM, et al. Magnetic resonance evaluation of the interrelationship between articular cartilage and trabecular bone of the osteoarthritic knee. Osteoarthritis Cartilage 2004;12(2):86-96.
351 Wu H, Webber C, Fuentes CO, et al. Prevalence of knee abnormalities in patients with osteoarthritis and anterior cruciate ligament injury identified with peripheral magnetic resonance imaging: a pilot study. Can. Assoc. Radiol. J. 2007;58(3):167-75.
352 Reichenbach S, Dieppe PA, Nuesch E, Williams S, Villiger PM, Juni P. Association of bone attrition with knee pain, stiffness and disability: a cross-sectional study. Annals of the Rheumatic Diseases 2011;70(2):293-8.
353 Ding C, Garnero P, Cicuttini F, Scott F, Cooley H, Jones G. Knee cartilage defects: association with early radiographic osteoarthritis, decreased cartilage volume, increased joint surface area and type II collagen breakdown. Osteoarthritis Cartilage 2005;13(3):198-205.
354 Lassere MN, Johnson KR, Boers M, et al. Definitions and validation criteria for biomarkers and surrogate endpoints: development and testing of a quantitative hierarchical levels of evidence schema. J. Rheumatol. 2007;34(3):607-15.
355 Boers M, Brooks P, Strand CV, Tugwell P. The OMERACT filter for Outcome Measures in Rheumatology. J. Rheumatol. 1998;25(2):198-9.
356 Boers M KJ, Tugwell P, et al. The Omeract Handbook. OMERACT 2015;www.omeract.org/pdf/OMERACT_Handbook.pdf.
357 van Spil WE, DeGroot J, Lems WF, Oostveen JC, Lafeber FP. Serum and urinary biochemical markers for knee and hip-osteoarthritis: a

systematic review applying the consensus BIPED criteria. Osteoarthritis Cartilage 2010;18(5):605-12.
358 Bauer DC, Hunter DJ, Abramson SB, et al. Classification of osteoarthritis biomarkers: a proposed approach. Osteoarthritis Cartilage 2006;14(8):723-7.
359 Blumenfeld O, Williams FM, Hart DJ, Spector TD, Arden N, Livshits G. Association between cartilage and bone biomarkers and incidence of radiographic knee osteoarthritis (RKOA) in UK females: a prospective study. Osteoarthritis Cartilage 2013;21(7):923-9.
360 Golightly YM, Marshall SW, Kraus VB, et al. Biomarkers of incident radiographic knee osteoarthritis: do they vary by chronic knee symptoms? Arthritis Rheum. 2011;63(8):2276-83.
361 Reijman M, Hazes JM, Bierma-Zeinstra SM, et al. A new marker for osteoarthritis: cross-sectional and longitudinal approach. Arthritis Rheum. 2004;50(8):2471-8.
362 Lotz M, Martel-Pelletier J, Christiansen C, et al. Value of biomarkers in osteoarthritis: current status and perspectives. Ann. Rheum. Dis. 2013;72(11):1756-63.
363 Arden N, Richette P, Cooper C, et al. Can We Identify Patients with High Risk of Osteoarthritis Progression Who Will Respond to Treatment? A Focus on Biomarkers and Frailty. Drugs Aging 2015.
364 Chan WP, Lang P, Stevens MP, et al. Osteoarthritis of the knee: comparison of radiography, CT, and MR imaging to assess extent and severity. AJR. American Journal of Roentgenology 1991;157(4):799-806.
365 Hunter DJ, Zhang W, Conaghan PG, et al. Systematic review of the concurrent and predictive validity of MRI biomarkers in OA. Osteoarthritis Cartilage 2011;19(5):557-88.
366 Hunter DJ, Zhang W, Conaghan PG, et al. Responsiveness and reliability of MRI in knee osteoarthritis: a meta-analysis of published evidence. Osteoarthritis Cartilage 2011;19(5):589-605.
367 Conaghan PG, Hunter DJ, Maillefert JF, Reichmann WM, Losina E. Summary and recommendations of the OARSI FDA osteoarthritis Assessment of Structural Change Working Group. Osteoarthritis Cartilage 2011;19(5):606-10.
368 Hutton TJ, Cunningham S, Hammond P. An evaluation of active shape models for the automatic identification of cephalometric landmarks. Eur. J. Orthod. 2000;22(5):499-508.
369 Heimann T, Meinzer HP. Statistical shape models for 3D medical image segmentation: a review. Med. Image Anal. 2009;13(4):543-63.
370 Deligianni F, Chung AJ, Yang GZ. Nonrigid 2-D/3-D registration for patient specific bronchoscopy simulation with statistical shape modeling: phantom validation. IEEE Trans. Med. Imaging 2006;25(11):1462-71.
371 King AP, Blackall JM, Penney GP, Hawkes DJ. Tracking liver motion using 3-D ultrasound and a surface based statistical shape model. Ieee Workshop on Mathematical Methods in Biomedical Image Analysis, Proceedings 2001:145-52.
372 Lee SL, Horkaew P, Caspersz W, Darzi A, Yang GZ. Assessment of shape variation of the levator ani with optimal scan planning and statistical shape modeling. J. Comput. Assist. Tomogr. 2005;29(2):154-62.

373 Andresen PR, Bookstein FL, Conradsen K, Ersboll BK, Marsh JL, Kreiborg S. Surface-bounded growth modeling applied to human mandibles. IEEE Trans. Med. Imaging 2000;19(11):1053-63.
374 Miller NA, Gregory JS, Aspden RM, Stollery PJ, Gilbert FJ. Using active shape modeling based on MRI to study morphologic and pitch-related functional changes affecting vocal structures and the airway. J. Voice 2014;28(5):554-64.
375 Rueckert D, Frangi AF, Schnabel JA. Automatic construction of 3-D statistical deformation models of the brain using nonrigid registration. IEEE Trans. Med. Imaging 2003;22(8):1014-25.
376 Ferrarini L, Olofsen H, Palm WM, van Buchem MA, Reiber JH, Admiraal-Behloul F. GAMEs: growing and adaptive meshes for fully automatic shape modeling and analysis. Med. Image Anal. 2007;11(3):302-14.
377 Cates J MA, Bieging E, Kholmovski E, Bengali S, MacLeod R, McGann C. TOWARDS A PRACTICAL CLINICAL WORKFLOW FOR CARDIAC SHAPE MODELING, WITH APPLICATION TO ATRIAL FIBRILLATION AND STROKE. http://www.shapesymposium.org/2014/Proceedings.pdf 2014;(Abstract):15.
378 Roberts MG, Oh T, Pacheco EM, Mohankumar R, Cootes TF, Adams JE. Semi-automatic determination of detailed vertebral shape from lumbar radiographs using active appearance models. Osteoporos. Int. 2012;23(2):655-64.
379 Roberts MG, Pacheco EM, Mohankumar R, Cootes TF, Adams JE. Detection of vertebral fractures in DXA VFA images using statistical models of appearance and a semi-automatic segmentation. Osteoporos. Int. 2010;21(12):2037-46.
380 Bansal R, Staib LH, Xu D, Zhu H, Peterson BS. Statistical analyses of brain surfaces using Gaussian random fields on 2-D manifolds. IEEE Trans. Med. Imaging 2007;26(1):46-57.
381 McClure RK, Styner M, Maltbie E, et al. Localized differences in caudate and hippocampal shape are associated with schizophrenia but not antipsychotic type. Psychiatry Res. 2013;211(1):1-10.
382 Styner M, Lieberman JA, McClure RK, Weinberger DR, Jones DW, Gerig G. Morphometric analysis of lateral ventricles in schizophrenia and healthy controls regarding genetic and disease-specific factors. Proc. Natl. Acad. Sci. U. S. A. 2005;102(13):4872-7.
383 Wang YM, Peterson BS, Staib LH. 3D Brain surface matching based on geodesics and local geometry. Comput Vis Image Und 2003;89(2-3):252-71.
384 Fritscher KD, Peroni M, Zaffino P, Spadea MF, Schubert R, Sharp G. Automatic segmentation of head and neck CT images for radiotherapy treatment planning using multiple atlases, statistical appearance models, and geodesic active contours. Med. Phys. 2014;41(5):051910.
385 Viswanath S, Bloch BN, Genega E, et al. A comprehensive segmentation, registration, and cancer detection scheme on 3 Tesla in vivo prostate DCE-MRI. Med Image Comput Comput Assist Interv 2008;11(Pt 1):662-9.

386 Sierra R, Zsemlye G, Szekely G, Bajka M. Generation of variable anatomical models for surgical training simulators. Med. Image Anal. 2006;10(2):275-85.
387 Jolesz FA, Nabavi A, Kikinis R. Integration of interventional MRI with computer-assisted surgery. J. Magn. Reson. Imaging 2001;13(1):69-77.
388 Barratt DC, Chan CS, Edwards PJ, et al. Instantiation and registration of statistical shape models of the femur and pelvis using 3D ultrasound imaging. Med. Image Anal. 2008;12(3):358-74.
389 Chan CSK, Edwards PJ, Hawkes DJ. Integration of ultrasound based registration with statistical shape models for computer assisted orthopaedic surgery. Medical Imaging 2003: Image Processing, Pts 1-3 2003;5032:414-24.
390 Fleute M, Lavallee S. Building a complete surface model from sparse data using statistical shape models: Application to computer assisted knee surgery. Lect Notes Comput Sc 1998;1496:879-87.
391 Fleute M, Lavallee S, Julliard R. Incorporating a statistically based shape model into a system for computer-assisted anterior cruciate ligament surgery. Med. Image Anal. 1999;3(3):209-22.
392 Paulsen RR, Nielsen C, Laugesen S, Larsen R. Using a shape model in the design of hearing aids. P Soc Photo-Opt Ins 2004;5370:1304-11.
393 Toth R, Bloch BN, Genega EM, et al. Accurate prostate volume estimation using multifeature active shape models on T2-weighted MRI. Acad. Radiol. 2011;18(6):745-54.
394 Agricola R, Heijboer MP, Roze RH, et al. Pincer deformity does not lead to osteoarthritis of the hip whereas acetabular dysplasia does: acetabular coverage and development of osteoarthritis in a nationwide prospective cohort study (CHECK). Osteoarthritis Cartilage 2013;21(10):1514-21.
395 Cicuttini FM, Wluka AE, Stuckey SL. Tibial and femoral cartilage changes in knee osteoarthritis. Ann. Rheum. Dis. 2001;60(10):977-80.
396 Jones G, Glisson M, Hynes K, Cicuttini F. Sex and site differences in cartilage development: a possible explanation for variations in knee osteoarthritis in later life. Arthritis Rheum. 2000;43(11):2543-9.
397 Eckstein F, Burstein D, Link TM. Quantitative MRI of cartilage and bone: degenerative changes in osteoarthritis. NMR Biomed. 2006;19(7):822-54.
398 Eckstein F, Wirth W, Nevitt MC. Recent advances in osteoarthritis imaging--the osteoarthritis initiative. Nat Rev Rheumatol 2012;8(10):622-30.
399 Marsh M, Souza RB, Wyman BT, et al. Differences between X-ray and MRI-determined knee cartilage thickness in weight-bearing and non-weight-bearing conditions. Osteoarthritis Cartilage 2013;21(12):1876-85.
400 Buckland-Wright C. Which radiographic techniques should we use for research and clinical practice? Best Pract Res Clin Rheumatol 2006;20(1):39-55.
401 Buckland-Wright JC, Macfarlane DG, Williams SA, Ward RJ. Accuracy and precision of joint space width measurements in standard and macroradiographs of osteoarthritic knees. Ann. Rheum. Dis. 1995;54(11):872-80.

402 Peterfy C, Li J, Zaim S, et al. Comparison of fixed-flexion positioning with fluoroscopic semi-flexed positioning for quantifying radiographic joint-space width in the knee: test-retest reproducibility. Skeletal Radiol. 2003;32(3):128-32.
403 Vignon E, Piperno M, Le Graverand MP, et al. Measurement of radiographic joint space width in the tibiofemoral compartment of the osteoarthritic knee: comparison of standing anteroposterior and Lyon schuss views. Arthritis Rheum. 2003;48(2):378-84.
404 Radiography Working Group of the O-OIW, Le Graverand MP, Mazzuca S, et al. Assessment of the radioanatomic positioning of the osteoarthritic knee in serial radiographs: comparison of three acquisition techniques. Osteoarthritis Cartilage 2006;14 Suppl A:A37-43.
405 Buckland-Wright JC, Wolfe F, Ward RJ, Flowers N, Hayne C. Substantial superiority of semiflexed (MTP) views in knee osteoarthritis: a comparative radiographic study, without fluoroscopy, of standing extended, semiflexed (MTP), and schuss views. J. Rheumatol. 1999;26(12):2664-74.
406 Buckland-Wright JC, Ward RJ, Peterfy C, Mojcik CF, Leff RL. Reproducibility of the semiflexed (metatarsophalangeal) radiographic knee position and automated measurements of medial tibiofemoral joint space width in a multicenter clinical trial of knee osteoarthritis. J. Rheumatol. 2004;31(8):1588-97.
407 Mazzuca SA, Hellio Le Graverand MP, Vignon E, et al. Performance of a non-fluoroscopically assisted substitute for the Lyon schuss knee radiograph: quality and reproducibility of positioning and sensitivity to joint space narrowing in osteoarthritic knees. Osteoarthritis Cartilage 2008;16(12):1555-9.
408 Le Graverand MPH, Clemmer RS, Brunell RM, Hayes CW, Miller CG, Vignon E. Considerations when designing a disease-modifying osteoarthritis drug (DMOAD) trial using radiography. Seminars in Arthritis and Rheumatism 2013;43(1):1-8.
409 Manual OO. Radiographic Procedure Manual for Examinations of the Knee, Hand, Pelvis and Lower Limbs. http://www.oai.ucsf.edu/datarelease/OperationsManuals.asp 2006.
410 Ravaud P, Chastang C, Auleley GR, et al. Assessment of joint space width in patients with osteoarthritis of the knee: a comparison of 4 measuring instruments. J. Rheumatol. 1996;23(10):1749-55.
411 Hellio Le Graverand MP, Mazzuca S, Duryea J, Brett A. Radiographic grading and measurement of joint space width in osteoarthritis. Rheum. Dis. Clin. North Am. 2009;35(3):485-502.
412 Duryea J, Zaim S, Genant HK. New radiographic-based surrogate outcome measures for osteoarthritis of the knee. Osteoarthritis Cartilage 2003;11(2):102-10.
413 Duryea J, Neumann G, Niu J, et al. Comparison of radiographic joint space width with magnetic resonance imaging cartilage morphometry: analysis of longitudinal data from the Osteoarthritis Initiative. Arthritis Care Res (Hoboken) 2010;62(7):932-7.
414 Conrozier T, Favret H, Mathieu P, et al. Influence of the quality of tibial plateau alignment on the reproducibility of computer joint space

measurement from Lyon schuss radiographic views of the knee in patients with knee osteoarthritis. Osteoarthritis Cartilage 2004;12(10):765-70.
415 Ornetti P, Brandt K, Hellio-Le Graverand MP, et al. OARSI-OMERACT definition of relevant radiological progression in hip/knee osteoarthritis. Osteoarthritis Cartilage 2009;17(7):856-63.
416 Bruyere O, Cooper C, Pavelka K, et al. Changes in structure and symptoms in knee osteoarthritis and prediction of future knee replacement over 8 years. Calcif. Tissue Int. 2013;93(6):502-7.
417 Madan-Sharma R, Kloppenburg M, Kornaat PR, et al. Do MRI features at baseline predict radiographic joint space narrowing in the medial compartment of the osteoarthritic knee 2 years later? Skeletal Radiology 2008;37(9):805-11.
418 Crema MD, Nevitt MC, Guermazi A, et al. Progression of cartilage damage and meniscal pathology over 30 months is associated with an increase in radiographic tibiofemoral joint space narrowing in persons with knee OA--the MOST study. Osteoarthritis Cartilage 2014;22(10):1743-7.
419 Huebner JL, Bay-Jensen AC, Huffman KM, et al. Alpha C-telopeptide of type I collagen is associated with subchondral bone turnover and predicts progression of joint space narrowing and osteophytes in osteoarthritis. Arthritis & rheumatology 2014;66(9):2440-9.
420 Haugen IK, Boyesen P, Slatkowsky-Christensen B, Sesseng S, Van DH, Kvien T. Radiographic joint space narrowing, malalignment and clinical soft tissue swelling are associated with mridefined bone marrow lesions in hand osteoarthritis. Osteoarthritis Cartilage 2012;20:S14-S5.
421 Oak SR, Ghodadra A, Winalski CS, Miniaci A, Jones MH. Radiographic joint space width is correlated with 4-year clinical outcomes in patients with knee osteoarthritis: data from the osteoarthritis initiative. Osteoarthritis Cartilage 2013;21(9):1185-90.
422 Hunter DJ, Niu J, Zhang Y, et al. Change in cartilage morphometry: a sample of the progression cohort of the Osteoarthritis Initiative. Ann. Rheum. Dis. 2009;68(3):349-56.
423 Eckstein F, Buck RJ, Burstein D, et al. Precision of 3.0 Tesla quantitative magnetic resonance imaging of cartilage morphology in a multicentre clinical trial. Ann. Rheum. Dis. 2008;67(12):1683-8.
424 Reichmann WM, Maillefert JF, Hunter DJ, Katz JN, Conaghan PG, Losina E. Responsiveness to change and reliability of measurement of radiographic joint space width in osteoarthritis of the knee: a systematic review. Osteoarthritis Cartilage 2011;19(5):550-6.
425 Cooke TD, Sled EA, Scudamore RA. Frontal plane knee alignment: a call for standardized measurement. J. Rheumatol. 2007;34(9):1796-801.
426 Felson DT, Cooke TD, Niu J, et al. Can anatomic alignment measured from a knee radiograph substitute for mechanical alignment from full limb films? Osteoarthritis Cartilage 2009;17(11):1448-52.
427 van der Esch M, Steultjens M, Wieringa H, Dinant H, Dekker J. Structural joint changes, malalignment, and laxity in osteoarthritis of the knee. Scand. J. Rheumatol. 2005;34(4):298-301.
428 Tanamas S, Hanna FS, Cicuttini FM, Wluka AE, Berry P, Urquhart DM. Does knee malalignment increase the risk of development and

progression of knee osteoarthritis? A systematic review. Arthritis Rheum. 2009;61(4):459-67.
429 Cerejo R, Dunlop DD, Cahue S, Channin D, Song J, Sharma L. The influence of alignment on risk of knee osteoarthritis progression according to baseline stage of disease. Arthritis Rheum. 2002;46(10):2632-6.
430 Felson DT, Gale DR, Elon Gale M, et al. Osteophytes and progression of knee osteoarthritis. Rheumatology (Oxford) 2005;44(1):100-4.
431 Cicuttini F, Wluka A, Hankin J, Wang Y. Longitudinal study of the relationship between knee angle and tibiofemoral cartilage volume in subjects with knee osteoarthritis. Rheumatology (Oxford) 2004;43(3):321-4.
432 Moisio K, Chang A, Eckstein F, et al. Varus-valgus alignment: reduced risk of subsequent cartilage loss in the less loaded compartment. Arthritis Rheum. 2011;63(4):1002-9.
433 Sharma L, Eckstein F, Song J, et al. Relationship of meniscal damage, meniscal extrusion, malalignment, and joint laxity to subsequent cartilage loss in osteoarthritic knees. Arthritis Rheum. 2008;58(6):1716-26.
434 Kastelein M, Luijsterburg PA, Belo JN, Verhaar JA, Koes BW, Bierma-Zeinstra SM. Six-year course and prognosis of nontraumatic knee symptoms in adults in general practice: a prospective cohort study. Arthritis Care Res (Hoboken) 2011;63(9):1287-94.
435 Waarsing JH, Bierma-Zeinstra SM, Weinans H. Distinct subtypes of knee osteoarthritis: data from the Osteoarthritis Initiative. Rheumatology (Oxford) 2015;54(9):1650-8.
436 Shimura Y, Kurosawa H, Sugawara Y, et al. The factors associated with pain severity in patients with knee osteoarthritis vary according to the radiographic disease severity: a cross-sectional study. Osteoarthritis Cartilage 2013;21(9):1179-84.
437 Hayashi D, Englund M, Roemer FW, et al. Knee malalignment is associated with an increased risk for incident and enlarging bone marrow lesions in the more loaded compartments: the MOST study. Osteoarthritis Cartilage 2012;20(11):1227-33.
438 Moyer R, Wirth W, Duryea J, Eckstein F. Anatomical Alignment, But Not Goniometry, Predicts Femorotibial Cartilage Loss as well as Mechanical Alignment: data from the Osteoarthritis Initiative. Osteoarthritis Cartilage 2015.
439 Wirth W, Hellio Le Graverand MP, Wyman BT, et al. Regional analysis of femorotibial cartilage loss in a subsample from the Osteoarthritis Initiative progression subcohort. Osteoarthritis Cartilage 2009;17(3):291-7.
440 Reichenbach S, Yang M, Eckstein F, et al. Does cartilage volume or thickness distinguish knees with and without mild radiographic osteoarthritis? The Framingham Study. Ann. Rheum. Dis. 2010;69(1):143-9.
441 Eckstein F, Guermazi A, Roemer FW. Quantitative MR imaging of cartilage and trabecular bone in osteoarthritis. Radiol. Clin. North Am. 2009;47(4):655-73.
442 Stahl R, Jain SK, Lutz J, et al. Osteoarthritis of the knee at 3.0 T: comparison of a quantitative and a semi-quantitative score for the assessment of the extent of cartilage lesion and bone marrow edema pattern in a 24-month longitudinal study. Skeletal Radiology 2011;40(10):1315-27.

443 Roemer FW, Guermazi A, Javaid MK, et al. Change in MRI-detected subchondral bone marrow lesions is associated with cartilage loss: the MOST Study. A longitudinal multicentre study of knee osteoarthritis. Ann. Rheum. Dis. 2009;68(9):1461-5.
444 Roemer FW, Zhang Y, Niu J, et al. Tibiofemoral joint osteoarthritis: Risk factors for MR-depicted fast cartilage loss over a 30-month period in the multicenter osteoarthritis study. Radiology 2009;252(3):772-80.
445 Schneider E, Nevitt M, McCulloch C, et al. Equivalence and precision of knee cartilage morphometry between different segmentation teams, cartilage regions, and MR acquisitions. Osteoarthritis Cartilage 2012;20(8):869-79.
446 Buck RJ, Wyman BT, Graverand MPHL, Wirth W, Eckstein F. An efficient subset of morphological measures for articular cartilage in the healthy and diseased human knee. Magnetic Resonance in Medicine 2010;63(3):680-90.
447 Eckstein F, Mc Culloch CE, Lynch JA, et al. How do short-term rates of femorotibial cartilage change compare to long-term changes? Four year follow-up data from the osteoarthritis initiative. Osteoarthritis Cartilage 2012;20(11):1250-7.
448 Raynauld JP, Martel-Pelletier J, Berthiaume MJ, et al. Quantitative magnetic resonance imaging evaluation of knee osteoarthritis progression over two years and correlation with clinical symptoms and radiologic changes. Arthritis Rheum. 2004;50(2):476-87.
449 Wluka AE, Forbes A, Wang Y, Hanna F, Jones G, Cicuttini FM. Knee cartilage loss in symptomatic knee osteoarthritis over 4.5 years. Arthritis Res Ther 2006;8(4):R90.
450 Eckstein F, Wirth W, Hudelmaier M, et al. Patterns of femorotibial cartilage loss in knees with neutral, varus, and valgus alignment. Arthritis Rheum. 2008;59(11):1563-70.
451 Saunders J, Ding C, Cicuttini F, Jones G. Radiographic osteoarthritis and pain are independent predictors of knee cartilage loss: a prospective study. Intern Med J 2012;42(3):274-80.
452 Eckstein F, Le Graverand MP, Charles HC, et al. Clinical, radiographic, molecular and MRI-based predictors of cartilage loss in knee osteoarthritis. Ann. Rheum. Dis. 2011;70(7):1223-30.
453 Eckstein F, Nevitt M, Gimona A, et al. Rates of change and sensitivity to change in cartilage morphology in healthy knees and in knees with mild, moderate, and end-stage radiographic osteoarthritis: results from 831 participants from the Osteoarthritis Initiative. Arthritis Care Res (Hoboken) 2011;63(3):311-9.
454 Wirth W, Nevitt M, Hellio Le Graverand MP, et al. Lateral and medial joint space narrowing predict subsequent cartilage loss in the narrowed, but not in the non-narrowed femorotibial compartment--data from the Osteoarthritis Initiative. Osteoarthritis Cartilage 2014;22(1):63-70.
455 Cotofana S, Wyman BT, Benichou O, et al. Relationship between knee pain and the presence, location, size and phenotype of femorotibial denuded areas of subchondral bone as visualized by MRI. Osteoarthritis Cartilage 2013;21(9):1214-22.

456 Moisio K, Eckstein F, Chmiel JS, et al. Denuded subchondral bone and knee pain in persons with knee osteoarthritis. Arthritis Rheum. 2009;60(12):3703-10.
457 Raynauld JP, Martel-Pelletier J, Haraoui B, et al. Risk factors predictive of joint replacement in a 2-year multicentre clinical trial in knee osteoarthritis using MRI: Results from over 6 years of observation. Annals of the Rheumatic Diseases 2011;70(8):1382-8.
458 Eckstein F, Boudreau RM, Wang Z, et al. Trajectory of cartilage loss within 4 years of knee replacement--a nested case-control study from the Osteoarthritis Initiative. Osteoarthritis Cartilage 2014;22(10):1542-9.
459 Buck RJ, Wyman BT, Le Graverand MP, et al. Osteoarthritis may not be a one-way-road of cartilage loss--comparison of spatial patterns of cartilage change between osteoarthritic and healthy knees. Osteoarthritis Cartilage 2010;18(3):329-35.
460 Buckwalter JA, Mankin HJ. Articular cartilage: degeneration and osteoarthritis, repair, regeneration, and transplantation. Instr. Course Lect. 1998;47:487-504.
461 Dunham J, Chambers MG, Jasani MK, Bitensky L, Chayen J. Changes in the orientation of proteoglycans during the early development of natural murine osteoarthritis. J. Orthop. Res. 1990;8(1):101-4.
462 Dunham J, Shackleton DR, Nahir AM, et al. Altered orientation of glycosaminoglycans and cellular changes in the tibial cartilage in the first two weeks of experimental canine osteoarthritis. J. Orthop. Res. 1985;3(3):258-68.
463 Mori Y, Kubo M, Okumo H, Kuroki Y. A scanning electron microscopic study of the degenerative cartilage in patellar chondropathy. Arthroscopy 1993;9(3):247-64.
464 Muir H, Bullough P, Maroudas A. The distribution of collagen in human articular cartilage with some of its physiological implications. J. Bone Joint Surg. Br. 1970;52(3):554-63.
465 Burstein D, Gray M, Mosher T, Dardzinski B. Measures of molecular composition and structure in osteoarthritis. Radiol. Clin. North Am. 2009;47(4):675-86.
466 Allen RG, Burstein D, Gray ML. Monitoring glycosaminoglycan replenishment in cartilage explants with gadolinium-enhanced magnetic resonance imaging. J. Orthop. Res. 1999;17(3):430-6.
467 Bashir A, Gray ML, Boutin RD, Burstein D. Glycosaminoglycan in articular cartilage: in vivo assessment with delayed Gd(DTPA)(2-)-enhanced MR imaging. Radiology 1997;205(2):551-8.
468 Bashir A, Gray ML, Burstein D. Gd-DTPA2- as a measure of cartilage degradation. Magn. Reson. Med. 1996;36(5):665-73.
469 Bashir A, Gray ML, Hartke J, Burstein D. Nondestructive imaging of human cartilage glycosaminoglycan concentration by MRI. Magn. Reson. Med. 1999;41(5):857-65.
470 Burstein D, Velyvis J, Scott KT, et al. Protocol issues for delayed Gd(DTPA)(2-)-enhanced MRI (dGEMRIC) for clinical evaluation of articular cartilage. Magn. Reson. Med. 2001;45(1):36-41.
471 Vandecasteele J, De Deene Y. On the validity of 3D polymer gel dosimetry: I. reproducibility study. Phys. Med. Biol. 2013;58(1):19-42.

472 Owman H, Ericsson YB, Englund M, et al. Association between delayed gadolinium-enhanced MRI of cartilage (dGEMRIC) and joint space narrowing and osteophytes: a cohort study in patients with partial meniscectomy with 11 years of follow-up. Osteoarthritis Cartilage 2014;22(10):1537-41.
473 Crema MD, Hunter DJ, Burstein D, et al. Association of changes in delayed gadolinium-enhanced MRI of cartilage (dGEMRIC) with changes in cartilage thickness in the medial tibiofemoral compartment of the knee: a 2 year follow-up study using 3.0 T MRI. Ann. Rheum. Dis. 2014;73(11):1935-41.
474 Anandacoomarasamy A, Leibman S, Smith G, et al. Weight loss in obese people has structure-modifying effects on medial but not on lateral knee articular cartilage. Ann. Rheum. Dis. 2012;71(1):26-32.
475 Newbould RD, Miller SR, Upadhyay N, et al. T1-weighted sodium MRI of the articulator cartilage in osteoarthritis: a cross sectional and longitudinal study. PLoS One 2013;8(8):e73067.
476 Stewart RC, Bansal PN, Entezari V, et al. Contrast-enhanced CT with a high-affinity cationic contrast agent for imaging ex vivo bovine, intact ex vivo rabbit, and in vivo rabbit cartilage. Radiology 2013;266(1):141-50.
477 Pang J, Driban JB, Destenaves G, et al. Quantification of bone marrow lesion volume and volume change using semi-automated segmentation: data from the osteoarthritis initiative. BMC musculoskeletal disorders 2013;14:3.
478 Kothari A, Guermazi A, Chmiel JS, et al. Within-subregion relationship between bone marrow lesions and subsequent cartilage loss in knee osteoarthritis. Arthritis Care Res. 2010;62(2):198-203.
479 Hochberg M, Favors, KJ., Sorkin, D. Quality of life and radiographic severity of knee osteoarthritis predict total knee arthroplasty: Data from the osteoarthritis initiative. Osteoarthritis Cartilage 2013;21:S11.
480 Schiphof D, Boers M, Bierma-Zeinstra SM. Differences in descriptions of Kellgren and Lawrence grades of knee osteoarthritis. Ann. Rheum. Dis. 2008;67(7):1034-6.
481 Felson DT, Nevitt MC, Yang M, et al. A new approach yields high rates of radiographic progression in knee osteoarthritis. J. Rheumatol. 2008;35(10):2047-54.
482 Felson DT, Niu J, Guermazi A, Sack B, Aliabadi P. Defining radiographic incidence and progression of knee osteoarthritis: suggested modifications of the Kellgren and Lawrence scale. Ann. Rheum. Dis. 2011;70(11):1884-6.
483 Eckstein F, Wirth W, Hunter DJ, et al. Magnitude and regional distribution of cartilage loss associated with grades of joint space narrowing in radiographic osteoarthritis - data from the Osteoarthritis Initiative (OAI). Osteoarthritis Cartilage 2010;18(6):760-8.
484 Gossec L, Jordan JM, Mazzuca SA, et al. Comparative evaluation of three semi-quantitative radiographic grading techniques for knee osteoarthritis in terms of validity and reproducibility in 1759 X-rays: report of the OARSI-OMERACT task force. Osteoarthritis Cartilage 2008;16(7):742-8.
485 Guermazi A, Hunter DJ, Li L, et al. Different thresholds for detecting osteophytes and joint space narrowing exist between the site investigators

and the centralized reader in a multicenter knee osteoarthritis study-data from the Osteoarthritis Initiative. Skeletal Radiology 2012;41(2):179-86.
486 Neogi T, Felson D, Niu JB, et al. Association between radiographic features of knee osteoarthritis and pain: results from two cohort studies. Br. Med. J. 2009;339.
487 Kallman DA, Wigley FM, Scott WW, Jr., Hochberg MC, Tobin JD. New radiographic grading scales for osteoarthritis of the hand. Reliability for determining prevalence and progression. Arthritis Rheum. 1989;32(12):1584-91.
488 Verbruggen G, Veys EM. Numerical scoring systems for the anatomic evolution of osteoarthritis of the finger joints. Arthritis Rheum. 1996;39(2):308-20.
489 Maheu E, Cadet C, Gueneugues S, Ravaud P, Dougados M. Reproducibility and sensitivity to change of four scoring methods for the radiological assessment of osteoarthritis of the hand. Ann. Rheum. Dis. 2007;66(4):464-9.
490 Felson DT, Hodgson R. Identifying and treating preclinical and early osteoarthritis. Rheum. Dis. Clin. North Am. 2014;40(4):699-710.
491 Brouwer GM, van Tol AW, Bergink AP, et al. Association between valgus and varus alignment and the development and progression of radiographic osteoarthritis of the knee. Arthritis Rheum. 2007;56(4):1204-11.
492 Runhaar J, van Middelkoop M, Reijman M, Vroegindeweij D, Oei EH, Bierma-Zeinstra SM. Malalignment: a possible target for prevention of incident knee osteoarthritis in overweight and obese women. Rheumatology (Oxford) 2014;53(9):1618-24.
493 Yusuf E, Bijsterbosch J, Slagboom PE, Rosendaal FR, Huizinga TW, Kloppenburg M. Body mass index and alignment and their interaction as risk factors for progression of knees with radiographic signs of osteoarthritis. Osteoarthritis Cartilage 2011;19(9):1117-22.
494 Sharma L, Song J, Dunlop D, et al. Varus and valgus alignment and incident and progressive knee osteoarthritis. Ann. Rheum. Dis. 2010;69(11):1940-5.
495 Sharma L, Song J, Felson DT, Cahue S, Shamiyeh E, Dunlop DD. The role of knee alignment in disease progression and functional decline in knee osteoarthritis. JAMA : the journal of the American Medical Association 2001;286(2):188-95.
496 Roemer FW, Nevitt MC, Felson DT, et al. Predictive validity of within-grade scoring of longitudinal changes of MRI-based cartilage morphology and bone marrow lesion assessment in the tibio-femoral joint--the MOST study. Osteoarthritis Cartilage 2012;20(11):1391-8.
497 Peterfy CG, Schneider E, Nevitt M. The osteoarthritis initiative: report on the design rationale for the magnetic resonance imaging protocol for the knee. Osteoarthritis Cartilage 2008;16(12):1433-41.
498 Hunter DJ, Lo GH, Gale D, Grainger AJ, Guermazi A, Conaghan PG. The reliability of a new scoring system for knee osteoarthritis MRI and the validity of bone marrow lesion assessment: BLOKS (Boston Leeds Osteoarthritis Knee Score). Ann. Rheum. Dis. 2008;67(2):206-11.
499 Laberge MA, Baum T, Virayavanich W, et al. Obesity increases the prevalence and severity of focal knee abnormalities diagnosed using 3T MRI

in middle-aged subjects--data from the Osteoarthritis Initiative. Skeletal Radiol. 2012;41(6):633-41.
500 Roemer FW, Kwoh CK, Hannon MJ, et al. Risk factors for magnetic resonance imaging-detected patellofemoral and tibiofemoral cartilage loss during a six-month period: the joints on glucosamine study. Arthritis Rheum. 2012;64(6):1888-98.
501 Crema MD, Guermazi A, Li L, et al. The association of prevalent medial meniscal pathology with cartilage loss in the medial tibiofemoral compartment over a 2-year period. Osteoarthritis Cartilage 2010;18(3):336-43.
502 Guermazi A, Roemer FW, Hayashi D, et al. Assessment of synovitis with contrast-enhanced MRI using a whole-joint semiquantitative scoring system in people with, or at high risk of, knee osteoarthritis: the MOST study. Ann. Rheum. Dis. 2011;70(5):805-11.
503 Berthiaume MJ, Raynauld JP, Martel-Pelletier J, et al. Meniscal tear and extrusion are strongly associated with progression of symptomatic knee osteoarthritis as assessed by quantitative magnetic resonance imaging. Ann. Rheum. Dis. 2005;64(4):556-63.
504 Peterfy CG, Guermazi A, Zaim S, et al. Whole-Organ Magnetic Resonance Imaging Score (WORMS) of the knee in osteoarthritis. Osteoarthritis Cartilage 2004;12(3):177-90.
505 Lynch JA, Roemer FW, Nevitt MC, et al. Comparison of BLOKS and WORMS scoring systems part I. Cross sectional comparison of methods to assess cartilage morphology, meniscal damage and bone marrow lesions on knee MRI: data from the osteoarthritis initiative. Osteoarthritis Cartilage 2010;18(11):1393-401.
506 Kornaat PR, Ceulemans RY, Kroon HM, et al. MRI assessment of knee osteoarthritis: Knee Osteoarthritis Scoring System (KOSS)--inter-observer and intra-observer reproducibility of a compartment-based scoring system. Skeletal Radiol. 2005;34(2):95-102.
507 Felson DT, Lynch J, Guermazi A, et al. Comparison of BLOKS and WORMS scoring systems part II. Longitudinal assessment of knee MRIs for osteoarthritis and suggested approach based on their performance: data from the Osteoarthritis Initiative. Osteoarthritis Cartilage 2010;18(11):1402-7.
508 Hunter DJ, Guermazi A, Lo GH, et al. Evolution of semi-quantitative whole joint assessment of knee OA: MOAKS (MRI Osteoarthritis Knee Score). Osteoarthritis Cartilage 2011;19(8):990-1002.
509 Guermazi A, Roemer FW, Haugen IK, Crema MD, Hayashi D. MRI-based semiquantitative scoring of joint pathology in osteoarthritis. Nat Rev Rheumatol 2013;9(4):236-51.
510 OAI. https://oai.epi-ucsf.org/datarelease/operationsManuals.asp. Osteoarthritis Initiaitive.
511 Buckland-Wright JC, Macfarlane DG, Lynch JA, Jasani MK, Bradshaw CR. Joint space width measures cartilage thickness in osteoarthritis of the knee: high resolution plain film and double contrast macroradiographic investigation. Ann. Rheum. Dis. 1995;54(4):263-8.
512 Kothari M, Guermazi A, von Ingersleben G, et al. Fixed-flexion radiography of the knee provides reproducible joint space width measurements in osteoarthritis. Eur. Radiol. 2004;14(9):1568-73.

513 Buckland-Wright JC, Bird CF, Ritter-Hrncirik CA, et al. X-ray technologists' reproducibility from automated measurements of the medial tibiofemoral joint space width in knee osteoarthritis for a multicenter, multinational clinical trial. J. Rheumatol. 2003;30(2):329-38.
514 Nevitt MC, Peterfy C, Guermazi A, et al. Longitudinal performance evaluation and validation of fixed-flexion radiography of the knee for detection of joint space loss. Arthritis Rheum. 2007;56(5):1512-20.
515 OAI Study Protocol. https://oai.epi-ucsf.org/datarelease/docs/StudyDesignProtocol.pdf.
516 Barr AJ, Dube B, Hensor EM, et al. The relationship between clinical characteristics, radiographic osteoarthritis and 3D bone area: data from the osteoarthritis initiative. Osteoarthritis Cartilage 2014;22(10):1703-9.
517 Betancourt MC, Linden JC, Rivadeneira F, et al. Dual energy x-ray absorptiometry analysis contributes to the prediction of hip osteoarthritis progression. Arthritis Res Ther 2009;11(6):R162.
518 Boegard T. Radiography and bone scintigraphy in osteoarthritis of the knee--comparison with MR imaging. Acta Radiol. Suppl. 1998;418:7-37.
519 Boegard T, Rudling O, Dahlstrom J, Dirksen H, Petersson IF, Jonsson K. Bone scintigraphy in chronic knee pain: comparison with magnetic resonance imaging. Ann. Rheum. Dis. 1999;58(1):20-6.
520 Temmerman OP, Raijmakers PG, Kloet R, Teule GJ, Heyligers IC, Lammertsma AA. In vivo measurements of blood flow and bone metabolism in osteoarthritis. Rheumatol. Int. 2013;33(4):959-63.
521 Johnston JD, Masri BA, Wilson DR. Computed tomography topographic mapping of subchondral density (CT-TOMASD) in osteoarthritic and normal knees: methodological development and preliminary findings. Osteoarthritis Cartilage 2009;17(10):1319-26.
522 Stroup DF, Berlin JA, Morton SC, et al. Meta-analysis of observational studies in epidemiology: a proposal for reporting. Meta-analysis Of Observational Studies in Epidemiology (MOOSE) group. JAMA : the journal of the American Medical Association 2000;283(15):2008-12.
523 van Tulder M, Furlan A, Bombardier C, Bouter L. Updated method guidelines for systematic reviews in the cochrane collaboration back review group. Spine 2003;28(12):1290-9.
524 Lievense AM, Bierma-Zeinstra SM, Verhagen AP, van Baar ME, Verhaar JA, Koes BW. Influence of obesity on the development of osteoarthritis of the hip: a systematic review. Rheumatology (Oxford) 2002;41(10):1155-62.
525 Aitken D, Khan HI, Ding C, et al. Structural predictors of ten year knee cartilage volume loss. Arthritis Rheum. 2013;65:S97-S8.
526 Knupp M, Pagenstert GI, Barg A, Bolliger L, Easley ME, Hintermann B. SPECT-CT compared with conventional imaging modalities for the assessment of the varus and valgus malaligned hindfoot. Journal of Orthopaedic Research 2009;27(11):1461-6.
527 Koster IM, Oei EHG, Hensen JHJ, et al. Predictive factors for new onset or progression of knee osteoarthritis one year after trauma: MRI follow-up in general practice. European Radiology 2011;21(7):1509-16.

528 McCauley TR, Kornaat PR, Jee WH. Central osteophytes in the knee: prevalence and association with cartilage defects on MR imaging. AJR. American Journal of Roentgenology 2001;176(2):359-64.
529 Reichenbach S, Leunig M, Werlen S, et al. Association between cam-type deformities and magnetic resonance imaging-detected structural hip damage: a cross-sectional study in young men. Arthritis Rheum. 2011;63(12):4023-30.
530 Sowers M, Karvonen-Gutierrez CA, Jacobson JA, Jiang Y, Yosef M. Associations of anatomical measures from MRI with radiographically defined knee osteoarthritis score, pain, and physical functioning. Journal of Bone and Joint Surgery - Series A 2011;93(3):241-51.
531 Sowers MF, Hayes C, Jamadar D, et al. Magnetic resonance-detected subchondral bone marrow and cartilage defect characteristics associated with pain and X-ray-defined knee osteoarthritis. Osteoarthritis Cartilage 2003;11(6):387-93.
532 Chaganti RK, Parimi N, Lang T, et al. Bone mineral density and prevalent osteoarthritis of the hip in older men for the Osteoporotic Fractures in Men (MrOS) Study Group. Osteoporos. Int. 2010;21(8):1307-16.
533 Akamatsu Y, Kobayashi H, Kusayama Y, Kumagai K, Mitsugi N, Saito T. Does subchondral sclerosis protect progression of joint space narrowing in patients with varus knee osteoarthritis? Osteoarthritis Cartilage 2014;22:S362.
534 Antoniades L, MacGregor AJ, Matson M, Spector TD. A cotwin control study of the relationship between hip osteoarthritis and bone mineral density. Arthritis Rheum. 2000;43(7):1450-5.
535 Guymer E, Baranyay F, Wluka AE, et al. A study of the prevalence and associations of subchondral bone marrow lesions in the knees of healthy, middle-aged women. Osteoarthritis Cartilage 2007;15(12):1437-42.
536 Mazzuca A, Brandt D, Schauwecker S, et al. Bone scintigraphy is not a better predictor of progression of knee osteoarthritis than Kellgren and Lawrence grade. J. Rheumatol. 2004;31(2):329-32.
537 Mazzuca A, Brandt D, Schauwecker S, et al. Severity of joint pain and Kellgren-Lawrence grade at baseline are better predictors of joint space narrowing than bone scintigraphy in obese women with knee osteoarthritis. J. Rheumatol. 2005;32(8):1540-6.
538 Nicholls AS, Kiran A, Pollard TC, et al. The association between hip morphology parameters and nineteen-year risk of end-stage osteoarthritis of the hip: a nested case-control study. Arthritis Rheum. 2011;63(11):3392-400.
539 Okazaki N, Chiba K, Kidera K, Yonekura A, Osaki M. Relationship between subchondral bone cysts, the severity of knee osteoarthritis, and alignments of lower extremities. Osteoarthritis Cartilage 2014;22:S370-S1.
540 Hochberg MC, Yip A, Favors K, Sorkin J, Martel-Pelletier J, Pelletier JP. Features assessed on magnetic resonance images improve prediction of total knee arthroplasty in subjects with symptomatic radiographic knee osteoarthritis: Data from the osteoarthritis initiative. Osteoarthritis Cartilage 2014;22:S175.
541 Liu L, Kaneko H, Sadatsuki R, et al. MRI-detected osteophyte is a predictor for receiving total knee arthroplasty in patients with end-stage knee osteoarthritis. Osteoarthritis Cartilage 2014;22:S470-S1.

542 Neumann G, Mendicuti AD, Zou KH, et al. Prevalence of labral tears and cartilage loss in patients with mechanical symptoms of the hip: evaluation using MR arthrography. Osteoarthritis Cartilage 2007;15(8):909-17.
543 Ochiai N, Sasho T, Tahara M, et al. Objective assessments of medial osteoarthritic knee severity by MRI: new computer software to evaluate femoral condyle contours. International Orthopaedics 2010;34(6):811-7.
544 Ratzlaff C, Russell R, Duryea J. Quantitatively-measured bone marrow lesions in the patellofemoral joint: Distribution and association with pain. Osteoarthritis Cartilage 2014;22:S247-S8.
545 Driban JB, Price LL, Tassinari AM, Lo GH, McAlindon TE. Peri-articular apparent bone volume fraction is associated with numerous patient characteristics in knees with osteoarthritis: Data from the osteoarthritis initiative. Arthritis Rheum. 2011;63(10 SUPPL. 1).
546 Driban JB, Price LL, Tassinari AM, Lo GH, Schneider E, McAlindon TE. Trabecular morphology is associated with numerous patient characteristics in knees with osteoarthritis: Data from the osteoarthritis initiative (OAI). Osteoarthritis Cartilage 2011;19:s169.
547 Dore D, Quinn S, Ding C, Winzenberg T, Jones G. Correlates of subchondral BMD: a cross-sectional study. J. Bone Miner. Res. 2009;24(12):2007-15.
548 Lo GH, Schneider E, Price L, et al. Periarticular bone density and trabecular morphology predict knee OA structural progression. Osteoarthritis Cartilage 2012;20:S76.
549 Burnett WK, SA. McLennan, CE. Wheaton, D. Talmo, C. Hunter, DJ. Wilson, DR. Johnston, JD. Patella Bone density is lower in knee osteoarthritis patients experiencing pain at rest. Osteoarthritis Cartilage 2012;20(S200-S201).
550 Kraus VB, McDaniel G, Worrell TW, et al. Association of bone scintigraphic abnormalities with knee malalignment and pain. Annals of the rheumatic diseases 2009;68(11):1673.
551 Kraus VB, Worrell TW, Renner JB, Coleman RE, Pieper CF. High prevalence of contralateral ankle abnormalities in association with knee osteoarthritis and malalignment. Osteoarthritis and cartilage / OARS, Osteoarthritis Research Society 2013;21(11):1693.
552 Macfarlane DG, Buckland-Wright JC, Lynch J, Fogelman L. A study of the early and late 99technetium scintigraphic images and their relationship to symptoms in osteoarthritis of the hands. Br. J. Rheumatol. 1993;32(11):977-81.
553 McCrae F, Shouls J, Dieppe P, Watt I. Scintigraphic assessment of osteoarthritis of the knee joint. Annals of the rheumatic diseases 1992;51(8):938.
554 Baranyay FJ, Wang Y, Wluka AE, et al. Association of bone marrow lesions with knee structures and risk factors for bone marrow lesions in the knees of clinically healthy, community-based adults. Semin. Arthritis Rheum. 2007;37(2):112-8.
555 Meredith DS, Losina E, Neumann G, Yoshioka H, Lang PK, Katz JN. Empirical evaluation of the inter-relationship of articular elements involved in

the pathoanatomy of knee osteoarthritis using magnetic resonance imaging. BMC Musculoskeletal Disorders 2009;10:133.
556 Dawson L, Bennell, K., Wluka, A., Wang, Y., Cicuttini, F. Hip bone marrow lesions in asymptomatic and osteoarthritic adults: Prevalence, risk factors and significance. Osteoarthritis and cartilage / OARS, Osteoarthritis Research Society 2013;21(Suppl):S241.
557 Ai F, Yu C, Zhang W, Morelli JN, Kacher D, Li X. MR imaging of knee osteoarthritis and correlation of findings with reported patient pain. Journal of Huazhong University of Science and Technology - Medical Science 2010;30(2):248-54.
558 Bilgici A, Dogan C, Cil E, Sakarya S, Kuru O, Selcuk MB. Relationship between pain severity and magnetic resonance imaging features in patients with osteoarthritis of the Knee [Turkish]. Turkish Journal of Rheumatology 2010;25(4):184-90.
559 Fernandez-Madrid F, Karvonen RL, Teitge RA, Miller PR, Negendank WG. MR features of osteoarthritis of the knee. Magn. Reson. Imaging 1994;12(5):703-9.
560 Frobell RB, Nevitt MC, Hudelmaier M, et al. Femorotibial subchondral bone area and regional cartilage thickness: a cross-sectional description in healthy reference cases and various radiographic stages of osteoarthritis in 1,003 knees from the Osteoarthritis Initiative. Arthritis Care Res. 2010;62(11):1612-23.
561 Gosvig KK, Jacobsen S, Sonne-Holm S, Palm H, Troelsen A. Prevalence of malformations of the hip joint and their relationship to sex, groin pain, and risk of osteoarthritis: a population-based survey. J. Bone Joint Surg. Am. 2010;92(5):1162-9.
562 Gudbergsen H, Lohmander LS, Jones G, et al. Correlations between radiographic assessments and MRI features of knee osteoarthritis - a cross-sectional study. Osteoarthritis Cartilage 2013;21(4):535-43.
563 Haugen IK, Boyesen P, Slatkowsky-Christensen B, Sesseng S, van der Heijde D, Kvien TK. Associations between MRI-defined synovitis, bone marrow lesions and structural features and measures of pain and physical function in hand osteoarthritis. Ann. Rheum. Dis. 2012;71(6):899-904.
564 Haugen IK. BP, Slatkowsky-Christensen B., Sesseng S., van der Heijde D., Kiven TK. Associations between radiographic and clinical osteoarthritis features and mri-defined bone marrow lesions in the finger joints. Annals of the Rheumatic Diseases 2012;71(Suppl 3):299.
565 Haugen IK, Boyesen P, Slatkowsky-Christensen B, et al. Comparison of features by MRI and radiographs of the interphalangeal finger joints in patients with hand osteoarthritis. Ann. Rheum. Dis. 2012;71(3):345-50.
566 Hayashi D, Xu L, Roemer FW, et al. Detection of osteophytes and subchondral cysts in the knee with use of tomosynthesis. Radiology 2012;263(1):206-15.
567 Ip S, Sayre EC, Guermazi A, et al. Frequency of bone marrow lesions and association with pain severity: results from a population-based symptomatic knee cohort. J. Rheumatol. 2011;38(6):1079-85.
568 Kalichman L, Zhang Y, Niu J, et al. The association between patellar alignment on magnetic resonance imaging and radiographic manifestations of knee osteoarthritis. Arthritis Research & Therapy 2007;9(2).

569 Kalichman L, Zhang Y, Niu J, et al. The association between patellar alignment and patellofemoral joint osteoarthritis features - An MRI study. Rheumatology 2007;46(8):1303-8.
570 Kim IJ, Kim DH, Jung JY, et al. Association between bone marrow lesions detected by magnetic resonance imaging and knee pain in community residents in Korea. Osteoarthritis Cartilage 2013;21(9):1207-13.
571 Kornaat PR, Bloem JL, Ceulemans RY, et al. Osteoarthritis of the knee: association between clinical features and MR imaging findings. Radiology 2006;239(3):811-7.
572 Kornaat PR, Watt I, Riyazi N, Kloppenburg M, Bloem JL. The relationship between the MRI features of mild osteoarthritis in the patellofemoral and tibiofemoral compartments of the knee. European Radiology 2005;15(8):1538-43.
573 Kumar D, Wyatt CR, Lee S, et al. Association of cartilage defects, and other MRI findings with pain and function in individuals with mild-moderate radiographic hip osteoarthritis and controls. Osteoarthritis Cartilage 2013;21(11):1685-92.
574 Lo GH, Hunter DJ, Zhang Y, et al. Bone marrow lesions in the knee are associated with increased local bone density. Arthritis Rheum. 2005;52(9):2814-21.
575 Lo GH, McAlindon TE, Niu J, et al. Bone marrow lesions and joint effusion are strongly and independently associated with weight-bearing pain in knee osteoarthritis: data from the osteoarthritis initiative. Osteoarthritis Cartilage 2009;17(12):1562-9.
576 Maksymowych WP, Cibere J, Loeuille D, et al. Preliminary validation of 2 magnetic resonance image scoring systems for osteoarthritis of the hip according to the OMERACT filter. J. Rheumatol. 2014;41(2):370-8.
577 Ratzlaff C, Guermazi A, Collins J, et al. A rapid, novel method of volumetric assessment of MRI-detected subchondral bone marrow lesions in knee osteoarthritis. Osteoarthritis Cartilage 2013;21(6):806-14.
578 Roemer FW, Guermazi A, Niu J, Zhang Y, Mohr A, Felson DT. Prevalence of magnetic resonance imaging-defined atrophic and hypertrophic phenotypes of knee osteoarthritis in a population-based cohort. Arthritis Rheum. 2012;64(2):429-37.
579 Scher C, Craig J, Nelson F. Bone marrow edema in the knee in osteoarthrosis and association with total knee arthroplasty within a three-year follow-up. Skeletal Radiology 2008;37(7):609-17.
580 Sengupta M, Zhang YQ, Niu JB, et al. High signal in knee osteophytes is not associated with knee pain. Osteoarthritis Cartilage 2006;14(5):413-7.
581 Stefanik J, Gross K, Felson D, et al. Does medial patellofemoral osteoarthritis matter? the relation of mri-detected structural damage in the medial and lateral patellofemoral joint to knee pain: the most and framingham osteoarthritis studies. Osteoarthritis Cartilage 2014;22:S54-S5.
582 Zhai G, Blizzard L, Srikanth V, et al. Correlates of knee pain in older adults: Tasmanian Older Adult Cohort Study. Arthritis Rheum. 2006;55(2):264-71.
583 Agricola R, Reijman M, Bierma-Zeinstra SM, Verhaar JA, Weinans H, Waarsing JH. Total hip replacement but not clinical osteoarthritis can be

predicted by the shape of the hip: a prospective cohort study (CHECK). Osteoarthritis Cartilage 2013;21(4):559-64.
584 Carnes J, Stannus O, Cicuttini F, Ding C, Jones G. Knee cartilage defects in a sample of older adults: natural history, clinical significance and factors influencing change over 2.9 years. Osteoarthritis Cartilage 2012;20(12):1541-7.
585 Carrino JA, Blum J, Parellada JA, Schweitzer ME, Morrison WB. MRI of bone marrow edema-like signal in the pathogenesis of subchondral cysts. Osteoarthritis Cartilage 2006;14(10):1081-5.
586 Crema MD, Felson DT, Roemer FW, et al. Prevalent cartilage damage and cartilage loss over time are associated with incident bone marrow lesions in the tibiofemoral compartments: the MOST study. Osteoarthritis and cartilage / OARS, Osteoarthritis Research Society 2013;21(2):306-13.
587 Crema MD, Cibere J, Sayre EC, et al. The relationship between subchondral sclerosis detected with MRI and cartilage loss in a cohort of subjects with knee pain: the knee osteoarthritis progression (KOAP) study. Osteoarthritis Cartilage 2014;22(4):540-6.
588 Davies-Tuck ML, Wluka AE, Wang Y, et al. The natural history of cartilage defects in people with knee osteoarthritis. Osteoarthritis Cartilage 2008;16(3):337-42.
589 de_Lange BJ, Ioan-Facsinay A, Bijsterbosch J, et al. The patellofemoral and femorotibial joints are related based on patterns of MRI features and their association with radiologic progression. Osteoarthritis Cartilage 2014;22:S254-S5.
590 Dore D, Martens A, Quinn S, et al. Bone marrow lesions predict site-specific cartilage defect development and volume loss: a prospective study in older adults. Arthritis Res Ther 2010;12(6):R222.
591 Driban JB, Lo GH, Lee JY, et al. Quantitative bone marrow lesion size in osteoarthritic knees correlates with cartilage damage and predicts longitudinal cartilage loss. BMC Musculoskelet Disord 2011;12:217.
592 Driban JB, Pang J, Miller E, et al. Quantitative bone marrow lesion changes relate to cartilage parameter changes. Osteoarthritis Cartilage 2012;20:S217-S8.
593 Haugen IK. KE, Slatkowsky-Christensen B., Sesseng S., Kiven TK. Predictive value of mri-defined synovitis, bone marrow lesions and central erosions on pain and physical function in hand osteoarthritis. Osteoarthritis Cartilage 2014;22:S386.
594 Hernandez-Molina G, Guermazi A, Niu J, et al. Central bone marrow lesions in symptomatic knee osteoarthritis and their relationship to anterior cruciate ligament tears and cartilage loss. Arthritis Rheum. 2008;58(1):130-6.
595 Hudelmaier M, Wirth W, Nevitt M, Eckstein F. Longitudinal rates of change in subchondral bone size in healthy knees and knees with radiographic osteoarthritis. Osteoarthritis Cartilage 2013;21(April Suppl):S242.
596 Hunter DJ, Zhang Y, Niu J, et al. Increase in bone marrow lesions associated with cartilage loss: a longitudinal magnetic resonance imaging study of knee osteoarthritis. Arthritis Rheum. 2006;54(5):1529-35.

597 Kubota M, Ishijima M, Kurosawa H, et al. A longitudinal study of the relationship between the status of bone marrow abnormalities and progression of knee osteoarthritis. Journal of Orthopaedic Science 2010;15(5):641-6.
598 Parsons C. EMH, Bruye`re O., Belissa P., Genant H.K., Guermazi A., Roemer F., Zaim S., Reginster J.-Y., Dennison E.M., Cooper C. Impact of bone marrow lesion on the progression of knee osteoarthritis in the sekoia study. Rheumatology 2014;53(Suupl 1):i130.
599 Raynauld JP, Martel-Pelletier J, Berthiaume MJ, et al. Correlation between bone lesion changes and cartilage volume loss in patients with osteoarthritis of the knee as assessed by quantitative magnetic resonance imaging over a 24-month period. Annals of the Rheumatic Diseases 2008;67(5):683-8.
600 Tanamas SK, Wluka AE, Pelletier JP, et al. Bone marrow lesions in people with knee osteoarthritis predict progression of disease and joint replacement: a longitudinal study. Rheumatology 2010;49(12):2413-9.
601 Tanamas SK, Wluka AE, Pelletier JP, et al. The association between subchondral bone cysts and tibial cartilage volume and risk of joint replacement in people with knee osteoarthritis: a longitudinal study. Arthritis Res Ther 2010;12(2):R58.
602 Wildi LM, Raynauld JP, Martel-Pelletier J, Abram F, Dorais M, Pelletier JP. Relationship between bone marrow lesions, cartilage loss and pain in knee osteoarthritis: results from a randomised controlled clinical trial using MRI. Ann. Rheum. Dis. 2010;69(12):2118-24.
603 Barr RJ, Gregory JS, Reid DM, et al. Predicting OA progression to total hip replacement: can we do better than risk factors alone using active shape modelling as an imaging biomarker? Rheumatology (Oxford) 2012;51(3):562-70.
604 Bowes MA, Wolstenholme CB, Hopkinson D, Vincent GR, Conaghan PG. Changes in subchondral bone provide a sensitive marker for osteoarthritis and its progression: Results from a large osteoarthritis initiative cohort. Arthritis Rheum. 2012;64.
605 Hunter DJ, Bowes M, Boudreau RM, Hannon MJ, Kwohx KC. Does bone shape predict the development of incident knee oa? Osteoarthritis Cartilage 2013;21.
606 Javaid MK, Kiran A, Guermazi A, et al. Individual magnetic resonance imaging and radiographic features of knee osteoarthritis in subjects with unilateral knee pain: The health, aging, and body composition study. Arthritis Rheum. 2012;64(10):3246-55.
607 Javaid MK, Lynch JA, Tolstykh I, et al. Pre-radiographic MRI findings are associated with onset of knee symptoms: the most study. Osteoarthritis Cartilage 2010;18(3):323-8.
608 Ratzlaff C. RLR, K. Kwoh, M. Hannon, J. Grago, A. Guermazi, F. Roemer, M. Jarraya, D. Hunter, J. Duryea. Quantitative MRI measures of bone marrow lesion volume predict total knee replacement. Osteoarthritis Cartilage 2014;22:S238-S9.
609 Zhao J, Li X, Bolbos RI, Link TM, Majumdar S. Longitudinal assessment of bone marrow edema-like lesions and cartilage degeneration

in osteoarthritis using 3 T MR T1rho quantification. Skeletal Radiol. 2010;39(6):523-31.
610 Hayami T, Pickarski M, Zhuo Y, Wesolowski GA, Rodan GA, Duong le T. Characterization of articular cartilage and subchondral bone changes in the rat anterior cruciate ligament transection and meniscectomized models of osteoarthritis. Bone 2006;38(2):234-43.
611 Bettica P, Cline G, Hart DJ, Meyer J, Spector TD. Evidence for increased bone resorption in patients with progressive knee osteoarthritis: longitudinal results from the Chingford study. Arthritis Rheum. 2002;46(12):3178-84.
612 Roemer F, Felson DT, Wang K, et al. Co-localization of non-cartilaginous articular pathology and cartilage damage in regard to subsequent cartilage loss in subjects with or at risk for knee osteoarthritis - The most study. Annals of Rheumatic Diseases 2013;72(6):942-8.
613 Henriksen M, Christensen R, Hunter DJ, et al. Structural changes in the knee during weight loss maintenance after a significant weight loss in obese patients with osteoarthritis: a report of secondary outcome analyses from a randomized controlled trial. Osteoarthritis Cartilage 2014;22(5):639-46.
614 Kwoh CK, Roemer FW, Hannon MJ, et al. Effect of oral glucosamine on joint structure in individuals with chronic knee pain: a randomized, placebo-controlled clinical trial. Arthritis & rheumatology 2014;66(4):930-9.
615 Bowes M, Lohmander S, Wolstenholme C, Vincent G, Frobell R. Significant change of bone shape occur over the first five years after acl injury. Osteoarthritis Cartilage 2013;21(April Suppl):S220.
616 Barr A DB, Hensor E, Kingsbury S, Peat G, Sharples L, Bowes M, Conaghan P.G. . Three-Dimensional Magnetic Resonance Imaging Knee Bone Shape Predicts Total Knee Replacement: Data from the Osteoarthritis Initiative. Annals of Rheumatic Diseases 2015;74(Suppl 2):185.
617 Bobinac D, Spanjol J, Zoricic S, Maric I. Changes in articular cartilage and subchondral bone histomorphometry in osteoarthritic knee joints in humans. Bone 2003;32(3):284-90.
618 Ding M, Odgaard A, Hvid I. Changes in the three-dimensional microstructure of human tibial cancellous bone in early osteoarthritis. J. Bone Joint Surg. Br. 2003;85(6):906-12.
619 Phan CM, Link TM, Blumenkrantz G, et al. MR imaging findings in the follow-up of patients with different stages of knee osteoarthritis and the correlation with clinical symptoms. European Radiology 2006;16(3):608-18.
620 Hunter DJ, Beavers D, Eckstein F, et al. The intensive diet and exercise for arthritis trial (IDEA): 18-month radiographic and MRI outcomes. Arthritis Rheum. 2012;64(Suppl S10):S1070.
621 Iagnocco A, Ceccarelli F, Perricone C, Valesini G. The role of ultrasound in rheumatology. Semin. Ultrasound. CT MR 2011;32(2):66-73.
622 Sharma L, Nevitt M, Hochberg M, et al. Clinical significance of worsening versus stable preradiographic MRI lesions in a cohort study of persons at higher risk for knee osteoarthritis. Ann. Rheum. Dis. 2015.
623 Wluka AE, Teichtahl AJ, Maulana R, et al. Bone marrow lesions can be subtyped into groups with different clinical outcomes using two magnetic resonance imaging (MRI) sequences. Arthritis Res Ther 2015;17:270.

624 Wang J, Antony B, Zhu Z, et al. Association of patellar bone marrow lesions with knee pain, patellar cartilage defect and patellar cartilage volume loss in older adults: a cohort study. Osteoarthritis Cartilage 2015;23(8):1330-6.
625 Hunter D, Nevitt M, Lynch J, et al. Longitudinal validation of periarticular bone area and 3D shape as biomarkers for knee OA progression? Data from the FNIH OA Biomarkers Consortium. Ann. Rheum. Dis. 2015.
626 Stefanik JJ, Gross KD, Guermazi A, et al. The relation of MRI-detected structural damage in the medial and lateral patellofemoral joint to knee pain: the Multicenter and Framingham Osteoarthritis Studies. Osteoarthritis Cartilage 2015;23(4):565-70.
627 Agricola R, Leyland KM, Bierma-Zeinstra SM, et al. Validation of statistical shape modelling to predict hip osteoarthritis in females: data from two prospective cohort studies (Cohort Hip and Cohort Knee and Chingford). Rheumatology (Oxford) 2015.
628 Hafezi-Nejad N, Zikria B, Eng J, Carrino JA, Demehri S. Predictive value of semi-quantitative MRI-based scoring systems for future knee replacement: data from the osteoarthritis initiative. Skeletal Radiol. 2015.
629 Cootes TF EG, Taylor CJ. Active Appearance Models. IEEE Trans Patt Anal Mach Intell 2001;23(6):681-85.
630 Williams TG VG, Bowes M, et al. Automatic segmentation of bones and inter-image anatomical correspondence by volumetric statistical modelling of knee MRI. Proceedings of the 2010 IEEE international conference on Biomedical imaging: from nano to Macro. 2010:Rotterdam, Netherlands: IEEE Press, 2010:432-35.
631 Karsdal MA, Bay-Jensen AC, Lories RJ, et al. The coupling of bone and cartilage turnover in osteoarthritis: opportunities for bone antiresorptives and anabolics as potential treatments? Annals of the Rheumatic Diseases 2014;73(2):336-48.
632 Hunter DJ, Bowes MA, Eaton CB, et al. Can cartilage loss be detected in knee osteoarthritis (OA) patients with 3-6 months' observation using advanced image analysis of 3T MRI? Osteoarthritis Cartilage 2010;18(5):677-83.
633 Duryea J, Li J, Peterfy CG, Gordon C, Genant HK. Trainable rule-based algorithm for the measurement of joint space width in digital radiographic images of the knee. Med. Phys. 2000;27(3):580-91.
634 OAI imaging assessment. https://oai.epi-ucsf.org/datarelease/docs/ImageAssessments/ImageAssessmentDataOverview.pdf.
635 Felson DT, Lawrence RC, Dieppe PA, et al. Osteoarthritis: new insights. Part 1: the disease and its risk factors. Annals of Internal Medicine 2000;133(8):635-46.
636 Zhang W, McWilliams DF, Ingham SL, et al. Nottingham knee osteoarthritis risk prediction models. Ann. Rheum. Dis. 2011;70(9):1599-604.
637 Shrier I, Platt RW. Reducing bias through directed acyclic graphs. BMC medical research methodology 2008;8:70.

638 Russo CR, Lauretani F, Bandinelli S, et al. Aging bone in men and women: beyond changes in bone mineral density. Osteoporosis International 2003;14(7):531-8.
639 Ding C, Cicuttini F, Scott F, Cooley H, Jones G. Association between age and knee structural change: a cross sectional MRI based study. Annals of the Rheumatic Diseases 2005;64(4):549-55.
640 Felson DT, Neogi T. Osteoarthritis: is it a disease of cartilage or of bone? Arthritis Rheum. 2004;50(2):341-4.
641 Schneider E, Nessaiver M. The Osteoarthritis Initiative (OAI) magnetic resonance imaging quality assurance update. Osteoarthritis Cartilage 2013;21(1):110-6.
642 Price RR, Axel L, Morgan T, et al. Quality assurance methods and phantoms for magnetic resonance imaging: report of AAPM nuclear magnetic resonance Task Group No. 1. Med. Phys. 1990;17(2):287-95.
643 Solloway S, Hutchinson CE, Waterton JC, Taylor CJ. The use of active shape models for making thickness measurements of articular cartilage from MR images. Magn. Reson. Med. 1997;37(6):943-52.
644 Eckstein F, Hudelmaier M, Wirth W, et al. Double echo steady state magnetic resonance imaging of knee articular cartilage at 3 Tesla: a pilot study for the Osteoarthritis Initiative. Ann. Rheum. Dis. 2006;65(4):433-41.
645 Rosenbaum PR, Rubin DB. The Central Role of the Propensity Score in Observational Studies for Causal Effects. Biometrika 1983;70(1):41-55.
646 Epstein MP, Duncan R, Broadaway KA, He M, Allen AS, Satten GA. Stratification-score matching improves correction for confounding by population stratification in case-control association studies. Genet. Epidemiol. 2012;36(3):195-205.
647 Eckstein F, Kwoh CK, Boudreau RM, et al. Quantitative MRI measures of cartilage predict knee replacement: a case-control study from the Osteoarthritis Initiative. Ann. Rheum. Dis. 2013;72(5):707-14.
648 Austin PC, Grootendorst P, Anderson GM. A comparison of the ability of different propensity score models to balance measured variables between treated and untreated subjects: a Monte Carlo study. Stat. Med. 2007;26(4):734-53.
649 Austin PC. An Introduction to Propensity Score Methods for Reducing the Effects of Confounding in Observational Studies. Multivariate Behav Res 2011;46(3):399-424.
650 Pelletier JP, Cooper C, Peterfy C, et al. What is the predictive value of MRI for the occurrence of knee replacement surgery in knee osteoarthritis? Annals of the Rheumatic Diseases 2013;72(10):1594-604.
651 Hunter DJ, Lohmander LS, Makovey J, et al. The effect of anterior cruciate ligament injury on bone curvature: exploratory analysis in the KANON trial. Osteoarthritis Cartilage 2014;22(7):959-68.
652 Bowes MA, Wolstenholme CB, Souza KD, Vincent GR, Conaghan P. The responsiveness of 3D bone shape compared with radiographic joint space width and MR cartilage thickness. Osteoarthritis Cartilage 2013;21:S177-S8.
653 D'Agostino MA, Boers M, Kirwan J, et al. Updating the OMERACT filter: implications for imaging and soluble biomarkers. J. Rheumatol. 2014;41(5):1016-24.

654 Essebag V, Platt RW, Abrahamowicz M, Pilote L. Comparison of nested case-control and survival analysis methodologies for analysis of time-dependent exposure. BMC medical research methodology 2005;5(1):5.
655 Woolf AD, Pfleger B. Burden of major musculoskeletal conditions. Bull. World Health Organ. 2003;81(9):646-56.
656 Loeser RF, Goldring SR, Scanzello CR, Goldring MB. Osteoarthritis: a disease of the joint as an organ. Arthritis Rheum. 2012;64(6):1697-707.
657 Ingham SL, Zhang W, Doherty SA, McWilliams DF, Muir KR, Doherty M. Incident knee pain in the Nottingham community: a 12-year retrospective cohort study. Osteoarthritis Cartilage 2011;19(7):847-52.
658 Barr AJ, Campbell TM, Hopkinson D, Kingsbury SR, Bowes MA, Conaghan PG. A systematic review of the relationship between subchondral bone features, pain and structural pathology in peripheral joint osteoarthritis. Arthritis Res Ther 2015;17(1):228.
659 Callaghan MJ, Parkes MJ, Hutchinson CE, et al. A randomised trial of a brace for patellofemoral osteoarthritis targeting knee pain and bone marrow lesions. Ann. Rheum. Dis. 2015;74(6):1164-70.
660 Lo GH, McAlindon TE, Hawker GA, et al. Symptom Assessment in Knee Osteoarthritis Needs to Account for Physical Activity Level. Arthritis & rheumatology 2015;67(11):2897-904.
661 Holla JF, van der Leeden M, Knol DL, et al. Predictors and outcome of pain-related avoidance of activities in persons with early symptomatic knee osteoarthritis: a five-year followup study. Arthritis Care Res (Hoboken) 2015;67(1):48-57.
662 Reid KF, Price LL, Harvey WF, et al. Muscle Power Is an Independent Determinant of Pain and Quality of Life in Knee Osteoarthritis. Arthritis & rheumatology 2015;67(12):3166-73.
663 Oiestad BE, Juhl CB, Eitzen I, Thorlund JB. Knee extensor muscle weakness is a risk factor for development of knee osteoarthritis. A systematic review and meta-analysis. Osteoarthritis Cartilage 2015;23(2):171-7.
664 Bowes MA, Vincent GR, Wolstenholme CB, Conaghan PG. A novel method for bone area measurement provides new insights into osteoarthritis and its progression. Ann. Rheum. Dis. 2015;74(3):519-25.
665 Eckstein F, Collins JE, Nevitt MC, et al. Cartilage thickness change as an imaging biomarker of knee osteoarthritis progression - data from the fnih OA biomarkers consortium. Arthritis & rheumatology 2015.
666 Zhang KY, Kedgley AE, Donoghue CR, Rueckert D, Bull AM. The relationship between lateral meniscus shape and joint contact parameters in the knee: a study using data from the Osteoarthritis Initiative. Arthritis Res Ther 2014;16(1):R27.
667 Zhang KY, Wiktorowicz-Conroy A, Hutchinson JR, et al. 3D Morphometric and posture study of felid scapulae using statistical shape modelling. PLoS One 2012;7(4):e34619.
668 Gomes LR, Gomes M, Jung B, et al. Diagnostic index of three-dimensional osteoarthritic changes in temporomandibular joint condylar morphology. J Med Imaging (Bellingham) 2015;2(3):034501.

669 Turmezei TD, Treece GM, Gee AH, Fotiadou AF, Poole KE. Quantitative 3D analysis of bone in hip osteoarthritis using clinical computed tomography. Eur. Radiol. 2015.
670 Pedoia V, Lansdown D, Zaid M, Jung P, Ma C, Li X. Longitudinal analysis of the shape changes of the knee in patients with anterior cruciate ligament injuries. Osteoarthritis Cartilage 2014;22:S248-S9.
671 Bowes MA, McLure SW, Wolstenholme CB, et al. Osteoarthritic bone marrow lesions almost exclusively colocate with denuded cartilage: a 3D study using data from the Osteoarthritis Initiative. Ann. Rheum. Dis. 2015.
672 Patel KV, Dansie EJ, Turk DC. Impact of chronic musculoskeletal pain on objectively measured daily physical activity: a review of current findings. Pain Manag 2013;3(6):467-74.
673 Beckwee D, Vaes P, Shahabpour M, Muyldermans R, Rommers N, Bautmans I. The Influence of Joint Loading on Bone Marrow Lesions in the Knee: A Systematic Review With Meta-analysis. Am. J. Sports Med. 2015;43(12):3093-107.
674 Bedson J, Croft PR. The discordance between clinical and radiographic knee osteoarthritis: a systematic search and summary of the literature. BMC Musculoskelet Disord 2008;9:116.
675 Maillefert JF, Gueguen A, Nguyen M, et al. Relevant change in radiological progression in patients with hip osteoarthritis. I. Determination using predictive validity for total hip arthroplasty. Rheumatology (Oxford) 2002;41(2):142-7.
676 Bingham CO, 3rd, Buckland-Wright JC, Garnero P, et al. Risedronate decreases biochemical markers of cartilage degradation but does not decrease symptoms or slow radiographic progression in patients with medial compartment osteoarthritis of the knee: results of the two-year multinational knee osteoarthritis structural arthritis study. Arthritis Rheum. 2006;54(11):3494-507.
677 Varenna M, Zucchi F, Failoni S, Becciolini A, Berruto M. Intravenous neridronate in the treatment of acute painful knee osteoarthritis: a randomized controlled study. Rheumatology (Oxford) 2015;54(10):1826-32.
678 Kerkhof HJ, Bierma-Zeinstra SM, Arden NK, et al. Prediction model for knee osteoarthritis incidence, including clinical, genetic and biochemical risk factors. Ann. Rheum. Dis. 2014;73(12):2116-21.
679 Roemer FW, Eckstein F, Hayashi D, Guermazi A. The role of imaging in osteoarthritis. Best Pract Res Clin Rheumatol 2014;28(1):31-60.
680 Hunter DJ, Arden N, Conaghan PG, et al. Definition of osteoarthritis on MRI: Results of a Delphi exercise. Osteoarthritis Cartilage 2011;19(8):963-9.
681 Turmezei TD, Fotiadou A, Lomas DJ, Hopper MA, Poole KE. A new CT grading system for hip osteoarthritis. Osteoarthritis Cartilage 2014;22(10):1360-6.
682 Turmezei T.D. DJL, M.A. Hopper, K.E. Poole. 3D FEATURE SEVERITY MAPPING OF THE HIP WITH COMPUTED TOMOGRAPHY REVEALS PATTERNS OF RADIOLOGICAL OSTEOARTHRITIS. Osteoarthritis Cartilage 2013;21:S189.

683 Turmezei TD, Lomas DJ, Hopper MA, Poole KE. Severity mapping of the proximal femur: a new method for assessing hip osteoarthritis with computed tomography. Osteoarthritis Cartilage 2014;22(10):1488-98.
684 van Bosse H, Wedge JH, Babyn P. How are dysplastic hips different? A three-dimensional CT study. Clin Orthop Relat Res 2015;473(5):1712-23.
685 Popov I, Onuh SO. Reverse engineering of pelvic bone for hip joint replacement. J. Med. Eng. Technol. 2009;33(6):454-9.
686 Xuyi W, Jianping P, Junfeng Z, Chao S, Yimin C, Xiaodong C. Application of three-dimensional computerised tomography reconstruction and image processing technology in individual operation design of developmental dysplasia of the hip patients. Int. Orthop. 2015.
687 Link TM, Schwaiger BJ, Zhang AL. Regional Articular Cartilage Abnormalities of the Hip. AJR. Am. J. Roentgenol. 2015;205(3):502-12.
688 Kuhn AW, Ross JR, Bedi A. Three-dimensional Imaging and Computer Navigation in Planning for Hip Preservation Surgery. Sports Med Arthrosc 2015;23(4):e31-8.
689 Relvas C, Ramos A, Completo A, Simoes JA. The influence of data shape acquisition process and geometric accuracy of the mandible for numerical simulation. Comput Methods Biomech Biomed Engin 2011;14(8):721-8.
690 Park HJ, Lee SY, Rho MH, Kwon HJ, Kim MS, Chung EC. The usefulness of the three-dimensional enhanced T1 high-resolution isotropic volume excitation MR in the evaluation of shoulder pathology: comparison with two-dimensional enhanced T1 fat saturation MR. Br. J. Radiol. 2015;88(1054):20140830.
691 Shahabpour M, Staelens B, Van Overstraeten L, et al. Advanced imaging of the scapholunate ligamentous complex. Skeletal Radiol. 2015;44(12):1709-25.
692 Jamal B, Pillai A, Fogg Q, Kumar S. The metatarsosesamoid joint: an in vitro 3D quantitative assessment. Foot Ankle Surg 2015;21(1):22-5.
693 Stern D, Likar B, Pernus F, Vrtovec T. Parametric modelling and segmentation of vertebral bodies in 3D CT and MR spine images. Phys. Med. Biol. 2011;56(23):7505-22.
694 Stern D, Njagulj V, Likar B, Pernus F, Vrtovec T. Quantitative vertebral morphometry based on parametric modeling of vertebral bodies in 3D. Osteoporos. Int. 2013;24(4):1357-68.
695 Aiyangar AK, Zheng L, Tashman S, Anderst WJ, Zhang X. Capturing three-dimensional in vivo lumbar intervertebral joint kinematics using dynamic stereo-X-ray imaging. J. Biomech. Eng. 2014;136(1):011004.
696 Svedmark P, Berg S, Noz ME, et al. A New CT Method for Assessing 3D Movements in Lumbar Facet Joints and Vertebrae in Patients before and after TDR. Biomed Res Int 2015;2015:260703.